OCS Study
BOEM 2017-032

# Arctic Nearshore Impact Monitoring in Development Area III (ANIMIDA): Contaminants, Sources, and Bioaccumulation

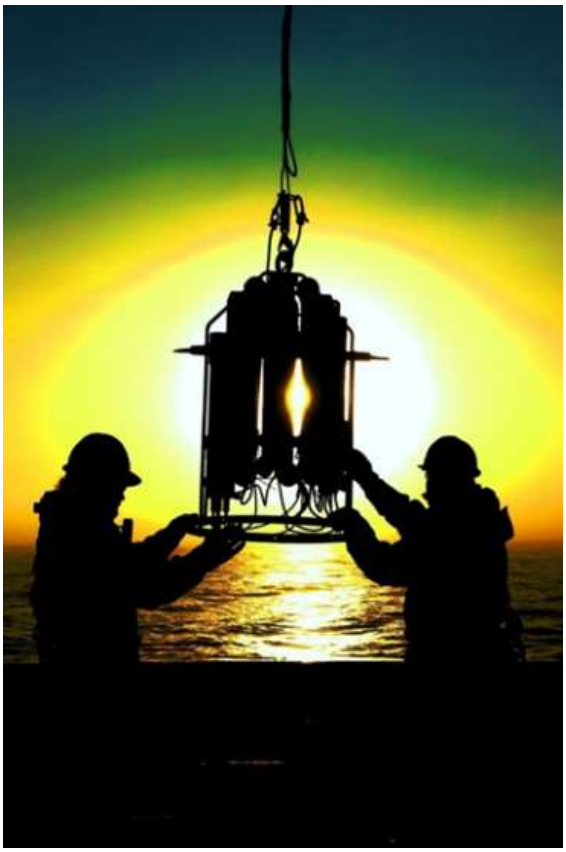

**U.S. Department of the Interior**
**Bureau of Ocean Energy Management**
**Alaska OCS Region**

BOEM
Bureau of Ocean Energy Management

OCS Study
BOEM 2017-032

# Arctic Nearshore Impact Monitoring in Development Area III (ANIMIDA): Contaminants, Sources, and Bioaccumulation

Authors

Jeremy Kasper
Kenneth Dunton
Susan Schonberg
John Trefry
Bodil Bluhm
Greg Durell

Prepared under BOEM Contract
M13PC00019
by
Olgoonik Fairweather, LLC
3201 C Street, Suite 700
Anchorage, Alaska 99503

Published by

**U.S. Department of the Interior**
**Bureau of Ocean Energy Management**
**Alaska OCS Region**

**Anchorage, AK**
**August 2017**

## DISCLAIMER

This report was prepared under contract between the Bureau of Ocean Energy Management (BOEM) and Olgoonik Fairweather, LLC. This report has been technically reviewed by BOEM, and it has been approved for publication. Approval does not necessarily signify that the contents reflect the views and policies of BOEM, nor does mention of trade names or commercial products constitute endorsement or recommendation for use.

## REPORT AVAILABILITY

To download a PDF file of this Alaska OCS Region report, go to the U.S. Department of the Interior, Bureau of Ocean Energy Management, Environmental Studies Program Information System website and search on OCS Study BOEM 2017-032.

This report can be viewed at select Federal Depository Libraries. It can also be obtained from the National Technical Information Service; the contact information is below.

U.S. Department of Commerce
National Technical Information Service
5301 Shawnee Rd.
Springfield, Virginia 22312
Phone: (703) 605-6000, 1(800)553-6847
Fax: (703) 605-6900
Website: http://www.ntis.gov/

## CITATION

Kasper J., Dunton K.H., Schonberg S.V., Trefry J., Bluhm B., Durell G., Wisdom S., and Blank J. 2017. Arctic Nearshore Impact Monitoring in Development Area (ANIMIDA) III: Contaminants, Sources, and Bioaccumulation. U.S. Dept. of the Interior, Bureau of Ocean Energy Management, Alaska OCS Region, Anchorage, AK. OCS Study BOEM 2013-032. 280 pp.

# Contents

# List of Figures

# List of Tables

## Contributors

| | | |
|---|---|---|
| Chapter 1 | Jeremy L. Kasper | Institute of Northern Engineering, University of Alaska Fairbanks |
| | John Trefry | Department of Marine & Environmental Systems, Florida Institute of Technology |
| | Gregory S. Durell | NewFields LLC |
| | Scott Libby | Battelle |
| | Ken Dunton | University of Texas Marine Science Institute, University of Texas at Austin |
| | Susan Schonberg | |
| | Bodil Bluhm | The Arctic University of Norway and University of Alaska Fairbanks |
| | Sheyna Wisdom | Olgoonik Fairweather LLC |
| | Justin Blank | Olgoonik Fairweather LLC |
| | | |
| Chapter 2 | Jeremy L. Kasper | Institute of Northern Engineering, University of Alaska Fairbanks |
| | Sookmi Moon | Institute of Marine Science, University of Alaska Fairbanks |
| | Peter Shipton | Institute of Marine Science, University of Alaska Fairbanks |
| | | |
| Chapter 3 | John H. Trefry | Department of Marine & Environmental Systems, Florida Institute of Technology |
| | Robert P. Trocine | |
| | Austin L. Fox | |
| | Stacey L. Fox | |
| | | |
| Chapter 4 | Gregory S. Durell | New Fields LLC |
| | Scott Libby | Battelle |
| | | |
| Chapter 5 | Ken Dunton | University of Texas Marine Science Institute, University of Texas at Austin |
| | Susan Schonberg | |
| | | |
| Chapter 6 | Bodil Bluhm | The Arctic University of Norway and University of Alaska Fairbanks |
| | Alex Ravelo | University of Alaska Fairbanks |
| | Katrin Iken, Lauren Bell, Kyle Dilliplaine, Lorena Edenfield, Tanja Schollmeier, Kelly Wal | Field support, University of Alaska Fairbanks |

## Acronyms and Abbreviations

| | |
|---|---|
| µg | microgram |
| µL | microliter |
| µm | micrometer |
| µM | microMolar |
| AAS | atomic absorption spectrometer |
| ADCP | Acoustic Doppler Current Profiler |
| ADNR | Alaska Department of Natural Resources |
| Ag | silver |
| Al | aluminum |
| AMBON | Arctic Marine Biodiversity Observing Network |
| ANIMIDA | Arctic Nearshore Monitoring in Development Area |
| ANISOM | Analysis of Similarities |
| AOOS | Alaska Ocean Observing System |
| As | arsenic |
| Ba | barium |
| $BaSO_4$ | barite |
| Battelle | Battelle Memorial Institute |
| Be | beryllium |
| BIO-ENV | Biota-Environmental |
| BOEM | Bureau of Ocean Energy Management |
| BREA | Beaufort Regional Environmental Assessment |
| BSMP | Beaufort Sea Monitoring Program |
| BVSTEP | Biological Variables Stepwise Procedure |
| C | carbon |
| C:N | carbon to nitrogen molar ratio |
| cANIMIDA | Arctic Nearshore Monitoring in Drilling Area |
| CBR | critical body residue |
| cc | cubic centimeters |
| Cd | cadmium |
| chl:pyro | ratio of chlorophyll to total pheopigments |
| CI | confidence interval |
| cm | centimeter |
| cm/s | centimeter per second |
| $CO_2$ | carbon dioxide |
| COMIDA | Chukchi Sea Offshore Monitoring in Drilling Area |
| CPI | carbon preference index |
| Cr | chromium |
| CRM | Certified Reference Material |
| CTD | Conductivity Temperature Depth |
| Cu | copper |
| DBO | Distributed Biological Observatory |

| | |
|---|---|
| DCM | dichloromethane |
| DIW | deionized water |
| DOC | dissolved organic carbon |
| d. wt. | dry weight |
| ECM | electronics control module |
| EIP | extracted ion profiles |
| EPA | U.S. Environmental Protection Agency |
| ER50 | effects body residue for 50% mortality |
| ERL | effects range low |
| ERM | effects range median |
| ESB | equilibrium partitioning sediment |
| F1 | petroleum biomarker fraction |
| F2 | aromatic hydrocarbon fraction |
| Fe | iron |
| FIT | Florida Institute of Technology |
| g | gram |
| GC/FID | gas chromatography/flame ionization detection |
| GC/MS | gas chromatography/mass spectrometry |
| GFF | glass fiber filters |
| gww | gram wet weight |
| $H_2O_2$ | hydrogen peroxide |
| HCl | hydrochloric acid |
| Hg | mercury |
| HMW | high molecular weight |
| $HNO_3$ | nitric acid |
| HPLC | High Performance Liquid Chromatography |
| Hz | Hertz |
| ICP-MS | inductively coupled plasma mass spectrometer |
| ind | individuals |
| IS | internal standards |
| kHz | kiloHertz |
| kg | kilogram |
| KLI | Kinnetic Laboratories Inc. |
| km | kilometer |
| $km^2$ | square kilometer |
| $km^3$ | kilometers cubed |
| L | liter |
| LALK | lower molecular weight alkines |
| LCS | laboratory control sample |
| LMW | low molecular weight |
| LR50 | lethal body residue 50% mortality |
| m | meter |
| $m^2$ | square meter |

| | |
|---|---|
| m/s | meters per second |
| MB | method blank |
| MDL | method detection limits |
| MFB | microphytobenthos |
| mg | milligram |
| mi | mile |
| min | minute |
| mL | milliliter |
| mm | millimeter |
| mM | milliMolar |
| MMHg | monomethyl mercury |
| MMS | Minerals Management Service |
| Mn | magnesium |
| MQO | measurement quality objectives |
| MS | matrix spike |
| MSD | matrix spike duplicate |
| nMDS | non-metric multidimensional scaling |
| $NH_4$ | ammonium |
| Ni | nickel |
| NIST | National Institute of Standards and Technology |
| ng | nanogram |
| nm | nanometer |
| $NO_2$ | nitrite |
| $NO_3$ | nitrate |
| NODC | National Oceanographic Data Center |
| NRC | National Research Council |
| NSC | North Slope crude |
| OCS | Outer Continental Shelf |
| OCSEAP | Outer Continental Shelf Environmental Assessment Program |
| OF | Olgoonik Fairweather |
| OM | organic matter |
| OMterr | terrigeneous organic matter |
| PAH | polycyclic aromatic hydrocarbons |
| PAR | photosynthetically available radiation |
| Pb | lead |
| PSBT-A | plumb-staff beam trawl |
| PCA | principal component analysis |
| PEL | probable effects level |
| PFTBA | perfluorotributlyamine |
| PI | Principle Investigator |
| $PO_4$ | phosphate |
| POC | particulate organic carbon |
| POM | particulate organic matter |

| | |
|---|---|
| ppb | parts per billion |
| ppm | parts per million |
| QA | quality assurance |
| QAM | Quality Assurance Manual |
| QAAP | Quality Assurance Project Plan |
| QAU | Quality Assurance Unit |
| QC | quality control |
| QMP | Quality Management Plan |
| RDW | random tessellated |
| Re | rhenium |
| RF | response factors |
| RL | reporting limits |
| rpm | revolutions per minute |
| s | seconds |
| S | salinity |
| Sb | antimony |
| SBE | Seabird Electronics |
| SD | standard deviation |
| Se | selenium |
| SHC | saturated hydrocarbons |
| SIM | selected ion monitoring |
| SIMPER | similarity percentage |
| SIMPROF | Similarity Profile |
| $SiO_4$ | silicate |
| SIS | surrogate internal standard |
| Sn | tin |
| SOM | sediment organic matter |
| SOP | Standard Operating Procedures |
| SPOM | suspended particulate organic matter |
| SRM | standard reference material |
| S/T | sterane and triterpane petroleum biomarkers |
| T | temperature |
| TALK | total alkines |
| TBA | tetrabuyl ammonium acetate |
| TDR | time-depth recorder |
| TEL | threshold effects level |
| TEO | total extractable organics |
| Tl | thallium |
| TL | trophic levels |
| TN | total nitrogen |
| TOC | total organic carbon |
| TON | total organic nitrogen |
| TPH | total petroleum hydrocarbons |

| | |
|---|---|
| TS | temperature - salinity |
| TSG | thermosalinograph |
| TSS | total suspended solids |
| UAF | University of Alaska Fairbanks |
| UPI | upper prediction level |
| UTA | University of Texas Austin |
| UTMSI | University of Texas Marine Science Institute |
| V | vanadium |
| WEBSEC | Western Beaufort Sea Ecological Cruises |
| WHOI | Woods Hole Oceanographic Institution |
| Zn | zinc |

# Chapter 1 Overview

The Arctic Nearshore Impact Monitoring in Development Area III (ANIMIDA III) Project was designed to update previous evaluations of impacts that may have resulted from offshore oil and gas exploration and production in the coastal Beaufort Sea. The Bureau of Ocean Energy Management (BOEM), Alaska Outer Continental Shelf (OCS) Region previously sponsored the following three major environmental monitoring programs in the Development Area: (1) the Beaufort Sea Monitoring Program (BSMP, 1984–1989), (2) the ANIMIDA Project (1999–2002), and (3) the continuation of the Arctic Nearshore Impact Monitoring in the Drilling Area (cANIMIDA) Project (2004–2007). As part of this four-year ANIMIDA III, Olgoonik Fairweather (OF), in conjunction with a team of scientists, conducted two seasons of offshore in open water and one season of spring sampling field collection in ice programs. A team of scientists from the University of Alaska-Fairbanks (UAF), The University of Texas at Austin (UTA), Florida Institute of Technology (FIT), Battelle Memorial Institute (Battelle), Kinnetic Laboratories Inc. (KLI), and OF comprise the project team.

Sampling was undertaken during the open-water periods in 2014 and 2015 (late July through early August in both years) and during the 2015 spring-freshet. This report describes observations of (1) physical oceanography, (2) the distributions of trace metals in bottom sediments, suspended sediments, and biota, (3) the characteristics of petroleum hydrocarbons in the sediments and benthic organisms, (4) benthic infauna, carbon resources, and trophic structure, and (5) epibenthic communities and demersal fish communities in the central portion of the U.S. Beaufort Sea.

Most of the metals and hydrocarbons found in sediments and biota from the ANIMIDA III study are introduced naturally by river runoff and coastal erosion (Boehm et al., 2001; Trefry et al., 2003; Rember and Trefry, 2004; Neff et al., 2009; Brown et al., 2010, Ping et al., 2011; Neff and Durell, 2011; Trefry et al., 2013). Very few instances of metal or hydrocarbon contamination have been identified in the coastal Beaufort Sea (e.g., ANIMIIDA III Final Report plus all previous reports and references listed above) because most of the $2.7 \times 10^{12}$ liters (L, 17 billion barrels) of oil produced in the Alaskan Arctic have been recovered from land or nearshore gravel islands (Alyeska, 2017). When limited instances of contamination have been identified, sources include the following: (1) discharged drilling mud and cuttings within 25-100 meters (m) of exploratory drilling sites (~30 Federal or Federal/State lease sites in the ANIMIDA III study area), (2) activities at coastal locations including West Dock, Endicott, Kaktovik, Northstar, and Liberty, and (3) a few other unidentified sources.

## 1.1 Field Sampling Summary

### 1.1.1 2014 Offshore Field Season Summary

The team conducted a 7-day sampling cruise in the Beaufort Sea during August 1-7, 2014. The cruise originally intended to use two vessels, an offshore vessel (R/V *Norseman II*) for water depths between ~ 12-60 m and a nearshore vessel (R/V *Launch 1273*) for water depths less than ~20 m, in the immediate vicinity of the coastline. However, due to mechanical difficulties and foul weather, the nearshore vessel was not able to conduct any sampling this year.

Forty-three stations were originally slated for sampling as per the ANIMIDA sampling plan. Forty-three stations were sampled, in addition to 13 (totaling 56 stations) other secondary and /or opportunistic stations where various samples were collected, depending on the particular discipline (Figure 1). Some of the intended stations were replaced by secondary or opportunistic stations as a result

of challenges experienced with the nearshore vessel. Samples collected include sediment for physical, chemical, and biological analysis, water for physical and chemical analysis, biota for chemical and taxonomic analysis, and water column sensor data for physical oceanographic analysis (e.g., conductivity, temperature, current velocity; an Acoustic Doppler Current Profiler [ADCP] was used only on the offshore vessel).

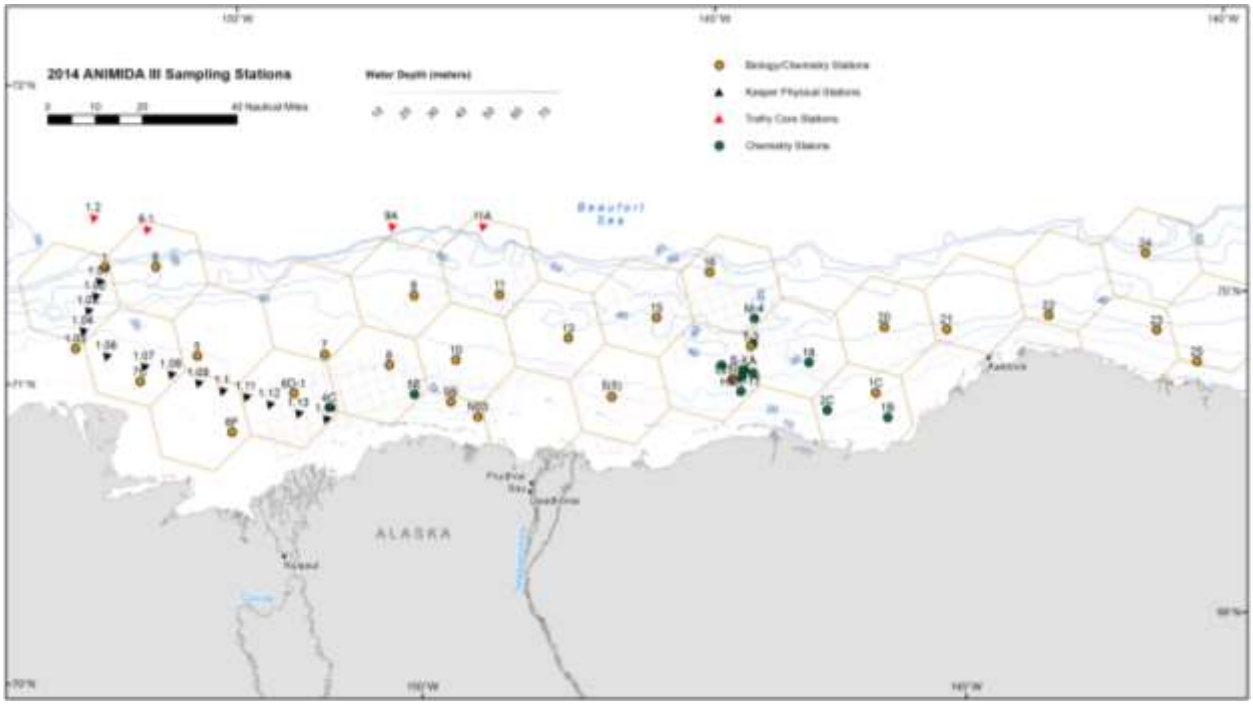


**Figure 1. Map indicating ANIMIDA 2014 station locations and type.**

### 1.1.3 2015 Spring Sampling Field Season Summary

A team of scientists from KLI, UAF, and FIT sampled and documented the under ice spreading of the Colville River spring freshet from May 15-29, 2015. The study was designed to delineate and quantify the offshore dispersion of river runoff and suspended sediments during the spring melt as well as trace the dispersion of suspended sediments into deeper, outer shelf water (Figure 2).

The following tasks were completed:

- Collected water samples for dissolved and particulate organic carbon (POC) and metals daily from the Colville River, Kuparuk, and Sagavanirktok Rivers over a ~3-week period starting with the onset of the spring meltwater event; a subset of the samples has been submitted for hydrocarbon analysis. Data for river stage, conductivity, pH, total suspended solids, and other properties were obtained.
- Collected under-ice water samples at multiple stations from 10-12 offshore sites in Harrison Bay.
- Installed temporary moorings for temperature (T) and salinity (S) at as many under-ice locations as possible. Made water velocity measurements utilizing through ice moored ADCPs (4) and point current meters (2).

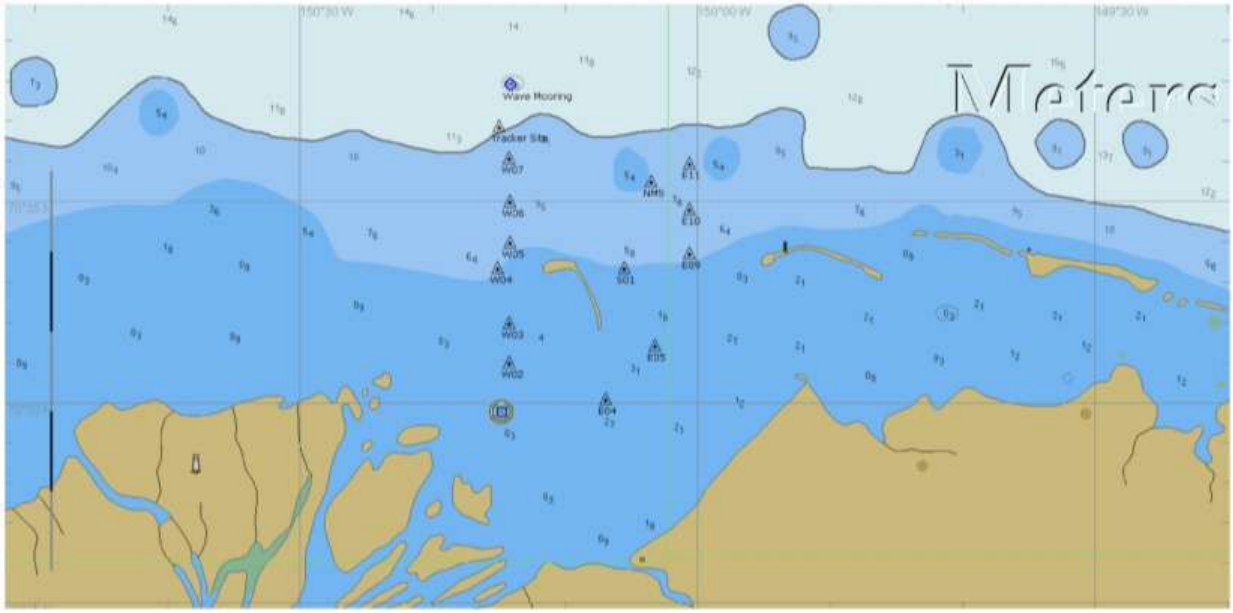


**Figure 2. Spring Sampling Through-Ice Locations.**

### 1.1.3 2015 Offshore Field Season Summary

The second and final ANIMIDA III cruise began on July 31, 2015 with the attempted recovery of a physical oceanography mooring and ended on August 8, 2015 with the completion of all sampling activities. Sampling was only conducted from the offshore vessel (R/V *Norseman II*), as the nearshore vessel (R/V *Launch 1273*) not used in 2015.

Stations were selected following numerous team Principle Investigator (PI) discussions and were iteratively modified based on availability and content of historic data at specific locations (e.g., BSMP and Camden Bay stations) as well as extensive expertise of the PIs, study area geospatial spread (east to west across the coastal Beaufort Sea), locations relative to current BOEM lease blocks, and transit timing aspect of the research vessel. The breakdown of the sampling included four main location types: (1) historic BSMP, (2) historic Camden Bay, (3) Random Tessellated (RDW) stations, and new 8 stations from areas identified as lacking in data (Figure 3).

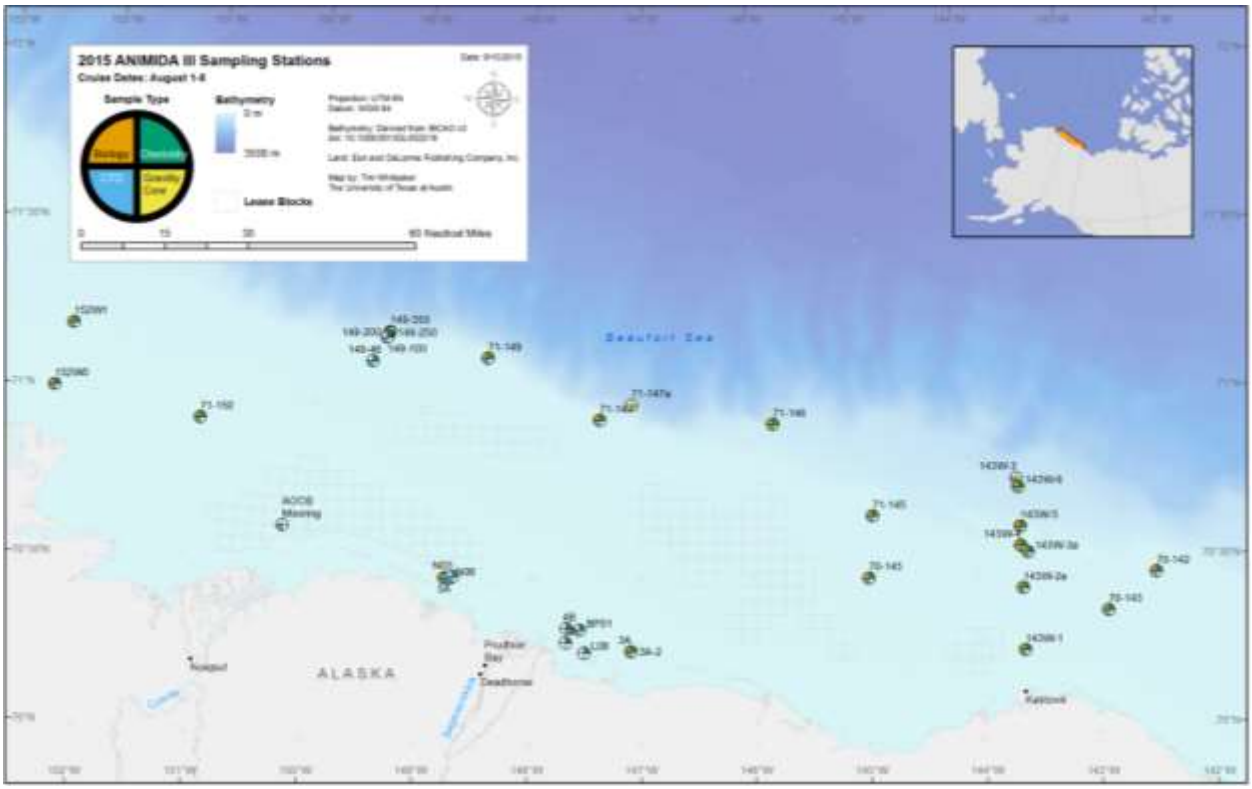


**Figure 3. Map indicating ANIMIDA 2015 station locations and type.**

## 1.1 Physical Oceanography

The central and eastern portions of the U.S. Beaufort Sea are essentially estuarine in character and are characterized by the presence of low nutrient, river-influenced water masses at the surface. Nutrient concentrations and salinities increase with increasing distance from the coast and with depth. Temperatures vary with winds and depth; strong stratification can result in surface water temperatures up to 7 °C. The presence of ice that accompanies persistent downwelling favorable winds (winds from the West) generally leads to temperatures <2 °C and the concentration of fresh water against the coast. The trend toward increasing nutrient concentrations with depth and distance from the coast is a result of the influence of shelfbreak water masses. These water masses are advected in an eastward flowing shelfbreak jet, a narrow and swift, bottom intensified current that forms the northern boundary of this shelf. Many of these shelfbreak water masses are derived from Pacific waters which are modified as they flow northward on the Chukchi Sea shelf and eventually form the core of the Beaufort Sea shelfbreak jet. Frequent upwelling favorable winds (winds from the East) in the region reverse the eastward flowing jet and upwell these water masses onto the Beaufort shelf along the bottom. As a result, nutrient concentrations along the outer Beaufort Sea shelf are comparable to values from the northeastern Chukchi Sea shelf. At the surface, the presence of numerous seasonally frozen rivers along the coast means that during the summer, surface waters are typically very fresh with salinities seasonally ranging from 0 to 30. Note, salinity, derived from conductivity is unitless so no units are reported for measured salinities reported herein. Because surface waters can be strongly stratified, temperatures can exceed 6 °C and winds readily move these surface water masses across and along the shelf.

As a result of differences in winds during the two ANIMIDA field seasons, surface water properties and sea ice conditions were very different between years. A moored record of water level (pressure), temperature, and salinity from ~13 m of water, within Harrison Bay, captures the extremes in hydrographic conditions that characterize the shelf, especially the nearshore, where temperatures at the bottom ranged from the freezing point to 5 °C. Salinities at the mooring ranged from 25 to >35. The latter occurred during an episode in mid-winter when brine rejection from freezing was likely taking place near the mooring. Density currents that result from such extreme events are one mechanism nearshore water masses and their dissolved and suspended materials can be transported across the shelf and eventually into the shelfbreak jet. The pressure record from the mooring shows extremes in water levels due to differences in winds: water level deviations of +0.71 m (storm surge due to downwelling favorable winds) and -2.85 m (sea level set down due to upwelling favorable winds) were recorded during the year-long record. In addition to illustrating the strong effect of winds on the shelf, such large fluctuations in sea level mean that low-lying coastal ecosystems, which support numerous bird species, are subject to extremes in conditions, as well. Measurements from the Colville Delta during the spring freshet in 2015 showed that surface waters in the nearshore are essentially fresh (S=0). Thus, conditions in the nearshore are extreme with salinities ranging from 0 to periods of hypersaline water with S>35.

## 1.2 Trace Metals in Bottom Sediments, Suspended Sediments and Biota

Data for trace metals in bottom sediments, suspended particles, and marine biota were used to identify any recent spatial or temporal changes in concentrations of potentially toxic metals in the coastal Beaufort Sea. Concentrations of 17 trace metals (silver [Ag], arsenic [As], Barium [Ba], beryllium [Be], cadmium [Cd], chromium [Cr], copper [Cu], mercury [Hg], magnesium [Mn], nickel [Ni], lead [Pb], antimony [Sb], selenium [Se], tin [Sn], thallium [Tl], vanadium [V], and zinc [Zn]) in 63 surface sediment and 300 sediment core samples collected during 2014 and 2015 as part of ANIMIDA III were essentially all at natural, baseline values. Previously-established background ratios of metals/aluminum [Al] in sediments were used to identify any sediment metal values that were anomalous. Four anomalies (concentrations above baseline) were observed for Ba and single anomalies were identified for Be, Hg, Sb, V, and Zn during ANIMIDA III. All concentrations of the potentially toxic metals Ag, Cd, Hg, Pb, and Zn were below published sediment quality criteria. At offshore locations (water depths >200 m), concentrations of As, Mn, and Hg were very high in some surface sediments from offshore at water depths of ~200-800 m; these deviations were linked to subsurface, diagenetic remobilization of these metals with subsequent reprecipitation and enrichment in surface sediments. Concentrations of total suspended solids during August 2014 ranged from 0.13-6.1 milligrams per liter (mg/L) and averaged 1.1 mg/L. Particulate Ba/Al ratios in these particles were within 2% of values for bottom sediments and provide a well-defined marker for tracing dispersion of discharged drilling fluids in the water column. In contrast with Ba, particulate iron [Fe]/Al ratios were ~80% greater than in bottom sediments in support of sorption of iron oxides and scavenged metals on suspended particles. Concentrations of the same 19 metals were determined for clams (*Astarte* sp.) and amphipods (*Anonyx* sp.) collected during 2014 and 2015. Results showed a variety of patterns and are presented and discussed here to provide a baseline for future assessments.

## 1.3 Characteristics of Petroleum Hydrocarbons in the Sediments and Benthic Organisms

Hydrocarbons (polycyclic aromatic hydrocarbons [PAH], saturated hydrocarbons [SHC], and sterane and triterpene [S/T] petroleum biomarkers) were measured in sediment and marine animal samples collected from the nearshore environment to the continental shelf 50 miles (mi) offshore. Most of the nearshore stations had been sampled in earlier phases of ANIMIDA, and the offshore stations were new. The methods that were used were the same as those used in earlier phases of ANIMIDA.

Though several classes of hydrocarbons were measured, PAH are the class that are of greatest environmental interest. The surface sediment Total PAH concentration generally ranged from 100 to 1,000 nanograms per gram (ng/g), dry weight (d. wt.), and averaged 532 (2014) and 707 (2015) ng/g for the two survey years. These concentrations were comparable to what had been measured in ANIMIDA I and II; the mean concentration for each year in those programs ranged from 380 to 570 ng/g. The hydrocarbon concentrations were also similar to what has been measured in the sediments in other studies in the Beaufort and Chukchi Seas, and other marine regions of Alaska. The surface sediment concentrations were slightly higher at the offshore stations than nearshore, possibly as a result of transport of fine-grained material that tends to have higher hydrocarbon concentrations than coarser material. A sediment core, collected well offshore, had uniform hydrocarbon concentrations at all depths, also in sediments representing deposition from many centuries ago; the amount and source of the hydrocarbons has remained constant for a long time and does not seem to have been altered by human activities. The hydrocarbons in the Beaufort Sea sediments are primarily from non-oil petrogenic and biogenic sources, with small amounts of pyrogenic hydrocarbons. Most of the hydrocarbons are carried to the Beaufort Sea through coastal erosion and river input of hydrocarbon rich materials, such as peat and shale. The concentrations of PAH in the sediments are low, at natural background levels, below concentrations that could cause harm to marine animals.

The concentrations of PAH, and other hydrocarbons, were more variable in the tissue of marine animals than in the sediment; there are seasonal and annual fluctuations with aspects of the animal's life and feeding. The mean Total PAH concentration ranged from 25 to 30 ng/g, d. wt., in the amphipods collected in 2014 and 2015, from 44 to 380 ng/g in the clams (a few values above 100 ng/g were attributed to analytical challenges, and do not represent actual field concentrations), and from 24 to 94 ng/g in the Arctic cod. The concentrations did not correlate well with the lipid content of the animals, demonstrating that many factors influence the accumulation of hydrocarbons by marine animals. There was no clear geographic pattern in the hydrocarbon concentrations of these marine animals. The tissue hydrocarbon concentrations were comparable to what had been measured during ANIMIDA I and II, and in other studies in the Arctic. The concentrations of the PAH that have accumulated in the marine animals are low, at natural background levels, and well below concentrations that could cause toxic effects or other harm to those animals.

## 1.4 Benthic Infauna, Carbon Resources, and Trophic Structure

A quantitative assessment of the biomass, abundance, and community structure of benthic populations of the Beaufort Sea Shelf along with a detailed characterization of food web dynamics were carried out as part of ANIMIDA III. Our analysis documented a benthic species inventory of 353 taxa collected from 126 individual van Veen grab samples (0.1 meters squared [$m^2$]) at 42 stations. Infaunal abundance was dominated by polychaetes, bivalves, and amphipods; bivalves, echinoderms, and

polychaetes constituted the greatest fractions by biomass. Shannon Diversity Index values of the infaunal community at different stations (by abundance) was between 1.5 and 4.1 (mean = 3.3 ± standard deviation [SD] 0.02), out of a possible range of 0-5. Thirty of the 42 stations had high diversity values, between 3.1 and 3.9, and two stations had higher values, 4.0 and 4.1. Pielou's Evenness Index values ranged from 0.86 to 0.98 (mean = 0.96 ± SD 0.52) out of a range of 0-1, demonstrating balanced contributions from all collected species at many but not all stations.

We used a Biota and Environment matching routine to examine the relationships between infaunal distributions of all collected taxa with the physical environment. A combination of water depth, TOC, and salinity correlated with infaunal abundance distribution ($\rho = 0.54$). We also noted that stations exhibiting the highest levels of both pyropheophorbide and pheophorbide *a* (chlorophyll degradation products that are markers for metazoan grazing) were characterized by the highest infaunal abundance. These stations contained polychaetes and crustaceans that constituted >75% of all organisms present and were located in three "hotspots" along the Beaufort shelf. The three hotspots include mid-shelf locations in the western Beaufort in Harrison Bay, the central Beaufort, including Stefansson Sound, and the eastern Beaufort from Barter Island east to Icy Reef. Our results imply a strong correlation between infaunal abundance and a deposited sediment pool that may include ice algae, bacteria, and other benthic microalgae. Preliminary data on the stable nitrogen isotopic composition of benthic organisms reveal complex food webs dominated by decidedly omnivorous consumers that occupy up to four trophic levels. Stable carbon isotopic composition of these benthic organisms, along with isotopic analyses of suspended particulate organic matter (SPOM) and zooplankton, reveal a primary mixture of terrestrial and phytoplankton carbon, but an additional benthic microalgal subsidy appears to play a role at moderate depths that correspond to the three hotspots of infaunal abundance. Half the genera examined also displayed a distinct eastward depletion in $\delta^{13}C$ values that likely reflects the influence of the Mackenzie and other sources of freshwater runoff in the Eastern U.S. Beaufort Sea, which transport allochthonous inputs of terrestrial organic carbon that become available as a food source to the benthos. These results provide compelling evidence for the important role of terrestrial carbon in Beaufort Sea food webs. Aside from the nearshore Sagavanirktok and Colville Rivers' deltas, the U.S. Beaufort Sea shelf overall supports a rich benthic infauna community, particularly in the region around Kaktovik, where repeated upwelling events have been reported.

## 1.5 Epibenthic Communities and Demersal Fish Communities

The dynamic physical and biological gradients of the Beaufort Sea shelf have a distinctive influence on epibenthic and demersal fish standing stocks. Epibenthos and demersal fish community structure vary both along and across shelf. Epifaunal communities shallower than approximately 20 m, sampled primarily in the western part of the study area near the Colville and Sagavanirktok Rivers, were relatively depauperate in species richness and abundance and biomass, likely related to a combination of bottom fast ice, scour by deep-draft ice, and extreme salinity changes during spring break-up. Dominant epibenthos in this zone included mobile crustaceans. Shelf areas outside such chronic perturbations were more species rich with largely overlapping character species in several community clusters. Shelf break and upper slope fauna formed distinct clusters, with typical deep-water species were only found at the deepest stations. Dominant fauna on the shelf and upper slope included echinoderms and mollusks. While demersal fish were less abundant and diverse than epibenthic invertebrates, fish communities were also distinct between nearshore and offshore areas, though less bound to the 20 m isobath and grouped in fewer clusters. Sculpins (*Cottidae*) generally dominated by abundance; while snail fishes (*Liparidae*),

cods (*Gadidae*), and eel pouts (*Zoarcidae*) also contributed almost equally to the species inventory. Along the shelf, the decreasing influence of Pacific-origin water along the continental slope resulted in lower epibenthic stocks east of approximately 150° W compared to previous studies conducted further west. A shift in taxonomic composition also aligned with this longitude.

In summary, the ANIMIDA III results document that epibenthic communities reflected the physically very dynamic nature of the Beaufort Sea shelf, characterized by strong land-ocean interactions in its nearshore zone, and its interaction across a steep slope that reaches into Atlantic-origin waters. The areas off the Colville and Sagavanirktok Rivers contained less rich epibenthic communities than the Chukchi-influenced western Beaufort Sea and also somewhat less rich communities than the shelf region off Barter Island.

## References


Alyeska Pipeline Service Company. 2017. http://www.alyeska-pipe.com/TAPS/PipelineFacts .

Boehm P.D., Brown J., Camp H., Cook L., Trefry J., Trocine R.P., Rember R.D., and Shepard G. 2001. ANIMIDA Phase I: Arctic Nearshore Characterization and Monitoring of the Physical Environment in the Northstar and Liberty Development Areas. OCS Study MMS-2001-104. Minerals Management Service, Alaska OCS Region, Anchorage, AK.194 p.

Brown J., Boehm P., Cook L., Trefry J., Smith W., and Durell G. 2010. cANIMIDA Task 2: Hydrocarbon and metal characterization of sediments in the cANIMIDA study area. OCS Study MMS 2010-004. US Dept. of the Interior, Minerals Management Service, Alaska OCS Region, Anchorage, Alaska. 241 p.

Neff J.M., Trefry J., and Durell G. 2009. Task 5. Integrated Biomonitoring and Bioaccumulation of Contaminants in Biota of the cANIMIDA Study Area. Final Report. OCS Study MMS 2009–037. U.S. Dept. of the Interior, Minerals Management Service, Alaska OCS Region, Anchorage, AK. 186 p.

Neff J.M. and Durell G. 2011. Bioaccumulation of petroleum hydrocarbons in arctic amphipods in the oil development area of the Alaskan Beaufort Sea. Integr. Environ. Assess. Manage. 8:301-319.

Ping C-L., Michaelson G.M., Guo L., Jorgenson M.T., Kanevskiy M., Shur Y., Dou F., and Liang J. 2011. Soil carbon and material fluxes across the eroding Alaska Beaufort Sea coastline. J. Geophys. Res., 116, G02004, doi:10.1029/2010JG001588.

Rember R.D. and Trefry J. 2004. Increased concentrations of dissolved trace metals and organic carbon during snowmelt in rivers of the Alaskan Arctic. Geochim Cosmochim Acta 68:477–489.

Trefry J., Rember R.D., Trocine R.P., and Brown J.S. 2003. Trace metals in sediments near offshore oil exploration and production sites in the Alaskan Arctic. Environ Geol 45:149-160.

Trefry J., Dunton K.H., Trocine R.P., Schonberg S.V., McTigue N.D., Hersh E.S., and McDonald T.J. 2013. Chemical and biological assessment of two offshore drilling sites in the Alaskan Arctic. Mar Environ Res 86:35-45.

# Chapter 2 Physical Oceanography

## Abstract

The central and eastern portions of the U.S. Beaufort Sea are characterized by the presence of low nutrient, river-influenced water masses at the surface. Nutrient concentrations and salinities increase with increasing distance from the coast and with depth. Temperatures vary with winds and depth; strong stratification can result in surface water temperatures up to 7 °C. The presence of ice that accompanies persistent downwelling favorable winds (winds from the West) generally leads to temperatures <2 °C and the concentration of fresh water against the coast. The trend toward increasing nutrient concentrations with depth and distance from the coast is a result of the influence of shelfbreak water masses. These water masses are advected in an eastward flowing shelfbreak jet, a narrow and swift, bottom intensified current that forms the northern boundary of this shelf. Many of these shelfbreak water masses are derived from Pacific waters which are modified as they flow northward on the Chukchi Sea shelf and eventually form the core of the Beaufort Sea shelfbreak jet. Frequent upwelling favorable winds (winds from the East) in the region reverse the eastward flowing jet and upwell these water masses onto the Beaufort shelf along the bottom. As a result, nutrient concentrations along the outer Beaufort Sea shelf are comparable to values from the northeastern Chukchi Sea shelf. At the surface, the presence of numerous seasonally frozen rivers along the coast means that during the summer surface waters are typically very fresh with salinities seasonally ranging from 0 to 30. Note, salinity, derived from conductivity is unitless so no units are reported for measured salinities reported herein. Because surface waters can be strongly stratified, temperatures can exceed 6 °C and winds readily move these surface water masses across and along the shelf.

As a result of differences in winds during the two ANIMIDA field seasons, surface water properties and sea ice conditions were very different between years. A moored record of water level (pressure), temperature and salinity from ~13 m of water captures the extremes in hydrographic conditions that characterize the shelf, especially the nearshore, where temperatures at the bottom ranged from the freezing point to 5 °C. Salinities at the mooring ranged from 25 to >35. The latter occurred during an episode in mid-winter when brine rejection from freezing was likely taking place near the mooring. Density currents that result from such extreme events are one mechanism nearshore water masses and their dissolved and suspended materials can be transported across the shelf and eventually into the shelfbreak jet. The pressure record from the mooring shows extremes in water levels due to differences in winds: water level deviations of +0.71 m (storm surge due to downwelling favorable winds) and -2.85 m (sea level set down due to upwelling favorable winds) were recorded during the year long record. In addition to illustrating the strong effect of winds on the shelf, such large fluctuations in sea level mean that low lying coastal ecosystems, which support numerous bird species, are subject to extremes in conditions as well. Measurements from the Colville Delta during the spring freshet in 2015 (discussed in a separate section) showed that surface waters in the nearshore are essentially fresh (S=0). Thus, conditions in the nearshore are extreme with salinities ranging from 0 to periods of hypersaline water with S>35.

## 2.1 Introduction

In the western U.S. Beaufort Sea, high nutrient Pacific origin water masses are upwelled onto the outer shelf and influence the planktonic, benthic, and pelagic food web communities here (e.g., Rand and Logerwell, 2011; Pickart et al., 2013; Ravelo et al., 2015). Upwelling peaks during the "partial ice coverage" season (Schulze and Pickart, 2012) and nutrients depleted during the summer months are replenished during the stormy, partial ice season (Pickart et al., 2013). In the central and eastern U.S. Beaufort Sea shelf where biomass and species diversity are comparatively low (Ravelo et al., 2015), the connections between seasonal water masses, upwelling and productivity are currently an area of active research (e.g., Logerwell et al., 2011; Kasper et al., 2012; Bell et al., 2013). Overall, because there are so few physical oceanographic measurements from the central and eastern U.S. Beaufort Sea (Weingartner et al., 2009; Kasper et al., 2012), it is difficult to assess the fidelity of numerical model results in these regions and thus it is difficult to understand the possible impacts of drilling in the region. Because offshore activities can precipitate increases in suspended sediments and decreases in light penetration, such activities have the potential to impact biological productivity and disperse contaminants across the shelf.

The objectives of this component of the ANIMIDA III Project were to provide information to the other disciplines about hydrographic conditions (e.g., water mass presence and absence, characteristics of water masses, temporal variability in hydrography) with the goal of improving our understanding of how the hydrography impacts distributions of species diversity, biomass, trace metals, etc. The hydrographic data can also be used to improve regional modeling efforts used in regional spill modeling and prediction.

## 2.2 Methods

### 2. 2.1 Data Collection

The *Norseman II* was equipped with a Teledyne Workhorse Mariner 300 kiloHertz (kHz) ADCP for measuring water column velocity. Velocities were averaged over 4-m bins. With these settings, the uncertainty in the ADCP velocities is 6.7 centimeters per second (cm/s).

The *Norseman II* was also equipped with Seabird Electronics SBE-21 pumped flow through, thermosalinograph (TSG) for measuring conductivity and temperature of the top ~1 m of the water column. The *Norseman II* TSG system was equipped with an additional, remote SBE 38 temperature sensor to eliminate thermal contamination due to the TSG's plumbing system on the temperature measurement. Comparison with pre- and post- cruise calibration values indicate that the temperature data were accurate to better than 0.1 °C and that the salinity data were accurate to 0.01.

In addition to supplying the vessel mounted sensors, UAF also supplied each vessel with a SBE-25 Conductivity-Temperature-Depth (CTD) system. Each CTD package was equipped with external photosynthetically available radiation (PAR; Biospherical Instruments QSP 2300), Transmissivity (WET Labs ECO FLNTURT), Fluorometry (WET Labs ECO FLNTURT), and Altimetry sensors for making water column measurements of conductivity (Salinity), temperature, pressure as well as PAR, transmissivity, and chlorophyll *a* (fluorometer), and elevation above the bottom (altimeter). The CTD used on the *Norseman II* was equipped with 6-bottle carousel equipped with 4-L bottles (an SBE 55), a deck unit (SBE 33), and an electronics control module (ECM, SBE 55) to allow for real time read out of the measurements. Bottles were used for taking discrete water column samples for nutrients and trace metals as well as other parameters of interest.

Samples for nutrient analysis were collected in 50 milliliter (mL) polyethylene bottles. Bottles were triple rinsed with seawater before the samples were collected. Samples were immediately frozen for later processing at UAF. Concentrations of phosphate ($PO_4$), silicate ($SiO_4$), ammonium ($NH_4$), Nitrite ($NO_2$), and Nitrate ($NO_3$) were determined using colorimetric techniques on Technicon AutoAnalyzer II and Alpkem model 300 continuous nutrient analyzers (Whitledge et al., 1981)

The SBE-25 sampled at 16 Hertz (Hz) and was lowered through the water column at a rate of ~3 m/s so that 5 samples/m were collected. Measured variables include pressure, temperature, conductivity, beam transmission, fluorescence, and PAR. Derived variables include depth, salinity, potential temperature, density, and speed of sound. The data were processed according to the manufacturer's recommended procedures (provided in the SBE Data Processing Manual) and were screened further for anomalous spikes, dropouts, and density inversions. Post-season calibrations of the temperature and conductivity cells were conducted at the manufacturer's calibration facility. Comparison of the pre- and post-calibration values indicate that the temperature data are accurate to better than 0.05 °C and that the salinity data are accurate to 0.005.

**2014:** Approximately 57 CTD stations (Figure 1) were occupied between July 30 and August 7, 2014 on the eastern and central sections of the U.S. Beaufort Sea shelf. The stations included a mix of full, partial, and physical oceanography only stations. The latter generally consisted of a CTD cast with no water samples (Figure 1, Table 1). The physical oceanography-only stations were carried out in rapid succession along a track line to create a "quasi-synoptic" section (stations 1.01-1.05 and 1.05-1.14). Full CTD stations included bottle samples collected at discrete depths (surface, bottom, and chlorophyll max) and sampled for nutrients, chlorophyll *a*, as well as chemical analysis.

A total of 101 samples were collected for analysis of major and trace nutrients (Whitledge et al., 1981). An additional 45 samples were collected, filtered, and analyzed for water column Ba (e.g., Rember and Trefry, 2004). Samples were vacuum filtered through polycarbonate filters (Poretics, 47-millimeter [mm] diameter, 0.4-micrometer [µm] pore size) in a laminar flow hood aboard ship immediately after collection. Filters had been pre-washed in nitric acid (5N $HNO_3$) and rinsed three times using 18 MΩ-cm deionized water (DIW) and then weighed three times to the nearest micrograms (µg) under cleanroom conditions at FIT. Fifty mL polyethylene bottles were triple rinsed with filtered seawater before the sample was capped. Samples were refrigerated for analysis at UAF.

Ba is an effective tracer for the presence of Mackenzie River water (e.g., Guay and Falkner, 1998). The collection of Ba samples was concentrated on the eastern portion of the U.S. Beaufort Sea and near the shelfbreak where we expect Mackenzie River water to be present. In addition to the CTD stations, data from the vessel mounted ADCP were logged for the duration of the cruise as well as the "flow through" TSG that sampled at approximately 1 m below the surface at 1 Hz during the cruise.

**Table 1. Summary of stations occupied during the 2014 ANIMIDA cruise.**

| Station ID | Station Type[1] | Latitude (ºW) | Longitude (ºN) | Nutrient Samples | Water Column Barium |
|---|---|---|---|---|---|
| 6D | B/C | 70.749 | 150.475 | 3 | |
| 4C | C | 70.672 | 150.155 | | |
| 7 | B/C | 70.850 | 150.061 | 3 | |
| 8 | B/C | 70.757 | 149.440 | 3 | |
| 10 | B/C | 70.713 | 148.765 | 3 | |
| 5E | C | 70.638 | 149.272 | | |
| 5(5) | B/C | 70.437 | 147.344 | 3 | |
| HEX-1 | C | 70.422 | 146.182 | | |
| L250-5 | B/C | 70.365 | 146.118 | 3 | |
| HEX-17 | C | 70.316 | 146.081 | | |
| HEX-12 | C | 70.360 | 145.906 | | |
| HH1-5 | C | 70.363 | 146.018 | | |
| S-XA | C | 70.382 | 145.985 | | |
| T-3 | B/C | 70.451 | 145.837 | 3 | |
| T-XA | C | 70.456 | 145.810 | | |
| M-4 | C | 70.537 | 145.710 | | |
| 18 | C | 70.332 | 145.336 | | |
| 20 | B/C | 70.358 | 144.495 | 3 | 3 |
| 21 | B/C | 70.275 | 143.910 | 3 | 3 |
| 22 | B/C | 70.192 | 142.905 | 3 | 3 |
| 23 | B/C | 70.004 | 141.963 | 3 | 3 |
| 24 | B/C | 70.260 | 141.763 | 3 | 3 |
| 25 | B/C | 69.851 | 141.718 | 3 | 3 |
| 1B | C | 70.065 | 144.778 | | |
| 1C | B/C | 70.158 | 144.805 | 3 | 3 |
| 2C | C | 70.159 | 145.322 | | |
| 16 | B/C | 70.734 | 145.992 | 3 | 3 |
| 15 | B/C | 70.646 | 146.661 | 3 | 3 |
| 12 | B/C | 70.672 | 147.591 | 3 | 3 |

[1]BC = Biology and Chemistry, C = Chemistry. CTD = CTD sensor only (no bottles)

**Table 2. Summary of stations occupied during the 2015 ANIMIDA cruise.**

| Station ID | Station Type[1] | Latitude (ºN) | Longitude (ºW) | Depth |
|---|---|---|---|---|
| 152W0 | ACWPVTBA | 71.0042 | 152.38 | 15.9 |
| 152W1 | ACWPVTBA | 71.1939 | 152.25 | 38 |
| 71-150 | CWPVT | 70.9404 | 151.03 | 18.2 |
| AOOS Mooring | C | 70.6331 | 150.23 | 13 |
| 5A | ACWPVTBA | 70.4947 | 148.76 | 11.8 |
| NO6 | CV | 40.4924 | 148.72 | 11.9 |
| NO3 | DV | 70.4991 | 148.69 | 13.0 |
| 3A-1 | C | 70.2829 | 147.09 | 6.4 |
| 3A-2a | ACWPVTBA | 70.2824 | 147.09 | 6.4 |
| 143W-1 | ACWPVTBA | 70.2573 | 143.61 | 38.8 |
| 143W-2A | ACWPVTBA | 70.4425 | 143.60 | 48.0 |
| 143W-3 | CTD only | 70.7714 | 143.61 | 198 |
| 143W-6 | CWPGT | 70.7445 | 143.59 | 502 |
| 143W-5 | CWPVGT | 70.6260 | 143.59 | 303 |
| 143W-4 | CWPVT | 70.5691 | 143.60 | 154 |
| 143W-3A | CWPVT | 70.5482 | 143.54 | 103 |
| 70-142 | ACWPVTBA | 70.4658 | 142.40 | 65.5 |
| 70-143 | ACWPVTBA | 70.3614 | 142.85 | 57 |
| 70-145 | ACWPVTBA | 70.4912 | 144.97 | 45.8 |
| 71-145 | ACWPVTBA | 70.6753 | 144.92 | 103 |
| 71-146 | CWPVGT | 70.9569 | 145.80 | 395 |
| 71-147A | G | 71.0181 | 147.09 | -- |
| 71-147 | CWPVTB | 70.9716 | 147.38 | 104 |
| 71-149 | ACWPVTBA | 71.1525 | 148.41 | 68.4 |
| 149-350 | CVG | 71.2236 | 149.33 | 325 |
| 149-250 | C | 71.2199 | 149.33 | 265 |
| 149-200 | CWPVT | 71.2123 | 149.34 | 207 |
| 149-100 | CW | 71.2058 | 149.35 | 108 |
| 149-46 | CW | 71.1340 | 149.47 | 48.1 |

[1]A=amphipod, C = CTD, W = Niskin water samples, P = plankton net, V = van Veen grab, T = trawl, B = Bivalve rake

**2015:** A total of 29 CTD casts were taken (Figure 3, Table 2) between July 31 and August 8, 2015 on the eastern and central sections of the U.S. Beaufort Sea shelf. Stations include a mix of full, partial, and physical oceanography only stations. The latter generally consisted of a CTD cast with no water samples. Full CTD stations included bottle samples collected at discrete depths (surface, bottom, and chlorophyll max) and sampled for nutrients, chlorophyll *a* as well as chemical analysis. Approximately 110 samples were collected for analysis of nutrients.

CTD casts provide a snapshot of the hydrographic conditions. The analysis of salinity and potential temperature from these transects provides information on water masses on the shelf including whether nutrient rich "Pacific Water Masses" are present. Note that since times between stations were generally long because of long sampling times and the sampling was spatially random by design, hydrographic sections can only be constructed for a limited number of transects: the Kaktovik Distributed Biological Observatory (DBO) line in 2015 and a physical oceanography-only transect occupied along ~152 ºW in 2014 are the only quasi synoptic cross-shelf transects occupied during the program.

In addition, a bottom mounted mooring was deployed on the first day of the 2014 cruise on July 30. The mooring consisted of a bottom mounted "Sea Spider" fiberglass mooring frame, an Alaska Ocean Observing System (AOOS)-funded ADCP as well as a Seabird 16+ CTD and transmissometer (Figure 4). The Sea Spider, CTD, and transmissometer were contributed to the project from the UAF equipment pool. The ADCP failed two days after deployment so no ADCP data are available for the deployment. The CTD recorded temperature, conductivity, and pressure for the entire year long deployment. Salinity, depth, and density are derived from the mooring data. The mooring was recovered in 2015 by scientists aboard the *Norseman II* for the Arctic Marine Biodiversity Observing Network (AMBON) project. Finally, hourly surface winds from the Prudhoe Bay airport were used in this study.


**Figure 4. Physical oceanographic mooring deployed in Harrison Bay.**

## 2.3 Results

### 2.3.1 Sample Data

Maps of surface salinity and temperature from the flow through thermosalinograph are shown in Figure 5 through Figure 10. Potential Temperature (°C) versus S for 2014 and 2015 are shown in Figure 11. There are several features of note in the S and T maps: in 2014 offshore of the Colville River Delta

(~150 ºW) there is distinct band of warm water nearshore that extends west of the delta and visible in Figure 7. This plume of warm river water is present in 2015 as well. Though in contrast to 2014, in 2015 this band of fresh, river influenced water is not continuous along the coast and is likely characterized by strong frontal systems (regions where density varies over short distances). The presence of a strong front is suggested by distinct bands of temperature and salinity visible near 152º W (Figure 5 and Figure 8) as well as in the eastern portion of the survey region where 7 °C is present. This nearshore water is part of riverine coastal domain described by Carmack et al. (2015). It is noteworthy that this "contiguous" band of river influenced water varies considerably with winds and freshwater input (e.g., Okkonen et al., 2016). Also, note that in both years, there is very warm water, Mackenzie River influenced water, present in the eastern reaches of the survey region (7 °C). This water mass is advected into the study area from the Mackenzie shelf of the Beaufort Sea by easterly winds. There are also differences visible in the property-property plots: in 2014 surface waters largely consisted of a narrow range of temperature-salinity (TS) between -1 and 5 °C with mixing taking place along two lines originating at -1 °C and S of ~27.5 and 30. The source water masses in both cases are river influenced shelf water. In contrast, in 2015, there are three mixing lines originating at 0 °C and 26, 0 °C and 29, and 1 °C and 30. While the water mass for these first two mixing lines is river influenced shelf water, the water mass for the third line is a shelfbreak water mass: Bering Sea Water (e.g., von Appen and Pickart, 2012).

Though not shown, winds during the two cruise years were markedly different: in 2014 winds were upwelling favorable (easterly). Upwelling winds distribute river influenced shelf water masses westward and offshore. As a result, the ice was concentrated seaward of the shelfbreak during the 2014 cruise. In contrast, in 2015, Prudhoe Bay winds during the cruise were downwelling favorable (westerly) with the result that pack ice covered the shelf in 2015 and shelfbreak water masses were moved onto the shelf via Ekman transport. Note that the cruise took place during the first week of August in both years.

Plots of salinity, temperature, and nutrient concentrations at the bottom in 2014 are shown in Figure 12 through Figure 18. Plots of these same variables in 2015 are shown in Figure 19 through Figure 24. In both years, nutrient concentrations generally increase with increasing depth as a result of the upwelling of nutrient rich shelfbreak water masses in the bottom boundary layer. As a consequence, at the bottom, nutrient concentrations increase with salinity and temperature towards the shelfbreak. Grebmeier and Cooper (2014) report $PO_4$ between 1.1–1.6 microMolar (µM) and $NH_4$ between 1.9–2.8 µM on the northern Chukchi shelf and $NO_3$+$NO_2$ of 5.5 µM and $SiO_4$ values of 15.1 µM. Concentrations of these same nutrients on the outer Beaufort Sea shelf are comparable in magnitude to the northeastern Chukchi Sea shelf. In contrast, nearshore water masses are depleted in nutrients compared to these offshore water masses.

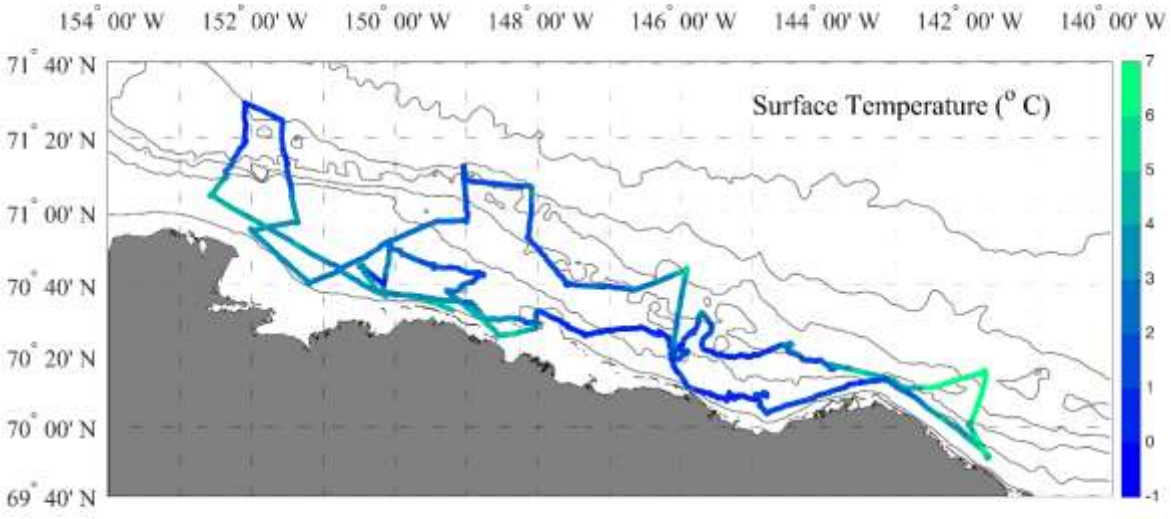


**Figure 5. 2014 surface temperature (°C).**

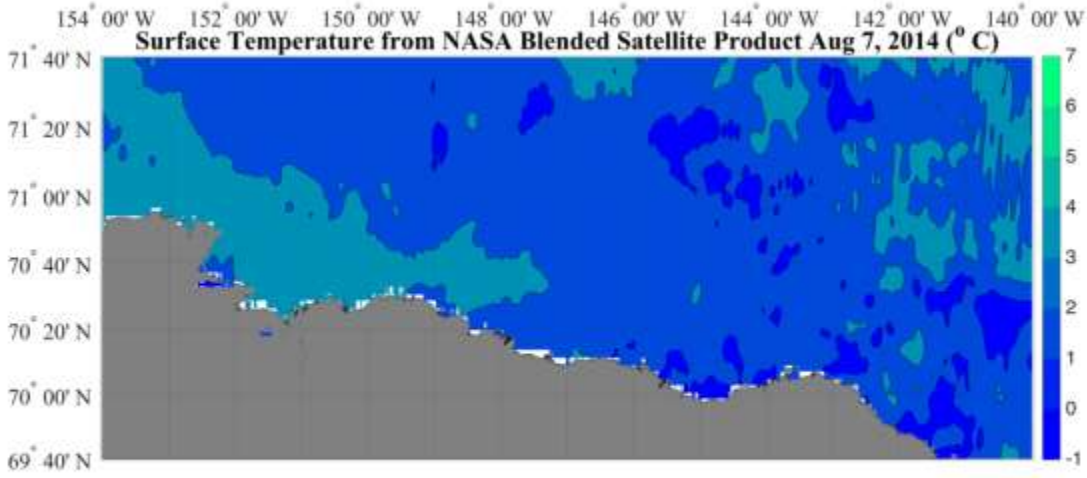


**Figure 6. 2014 surface temperature (°C) from MODIS.**

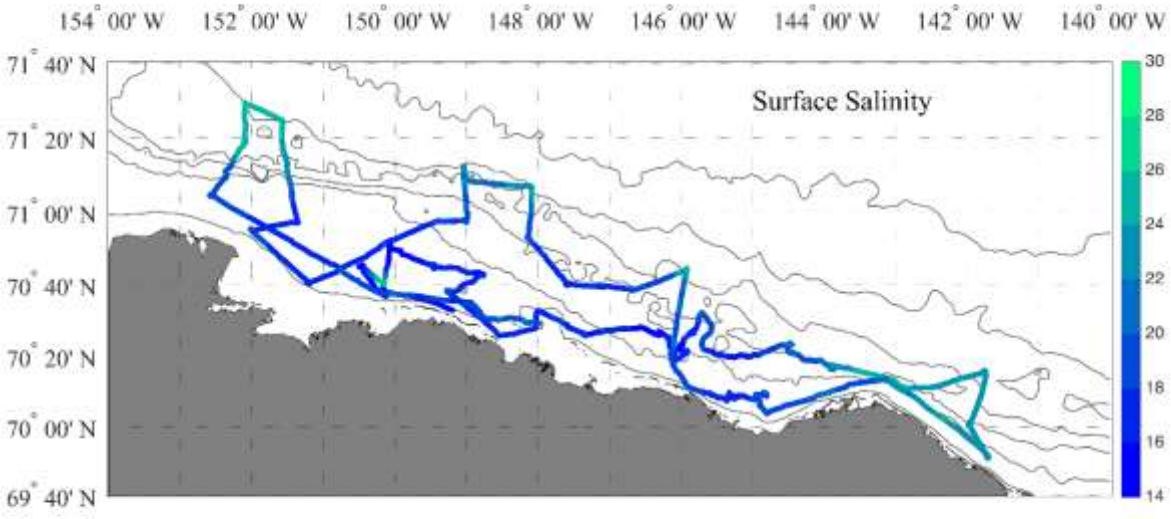


**Figure 7. 2014 surface salinity.**

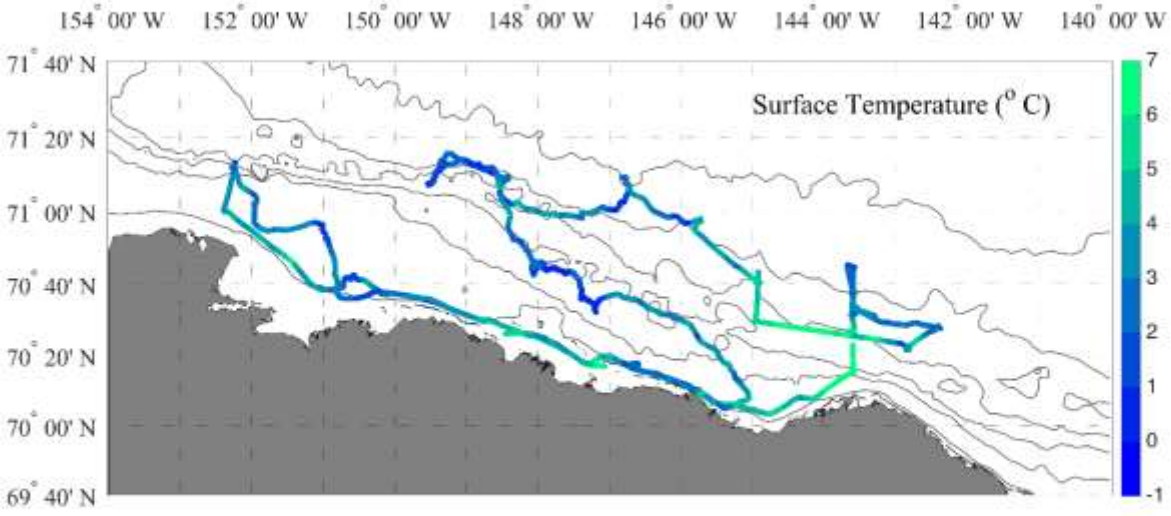


**Figure 8. 2015 surface temperature (°C).**

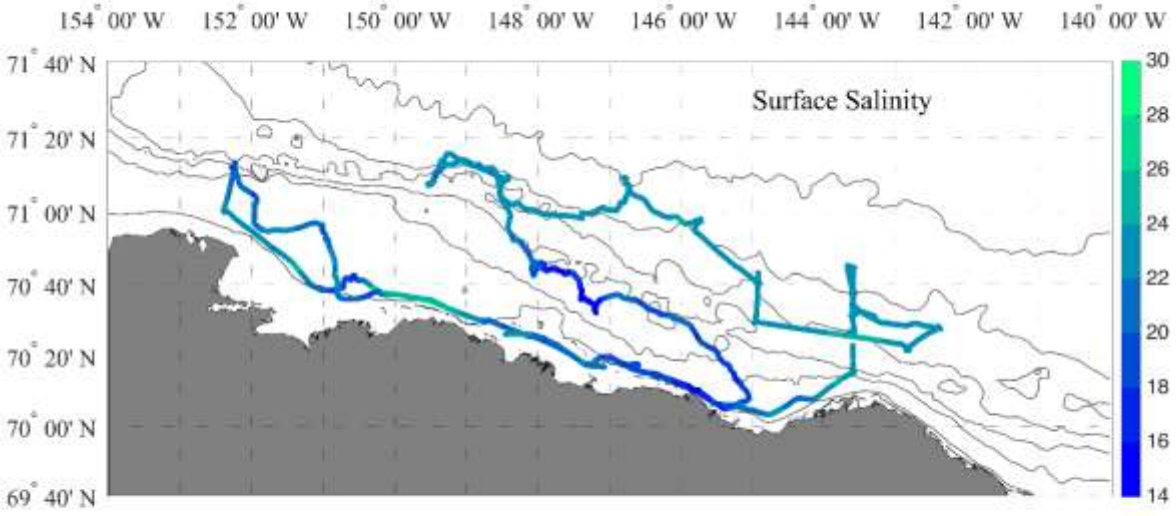


**Figure 9. 2015 surface salinity.**

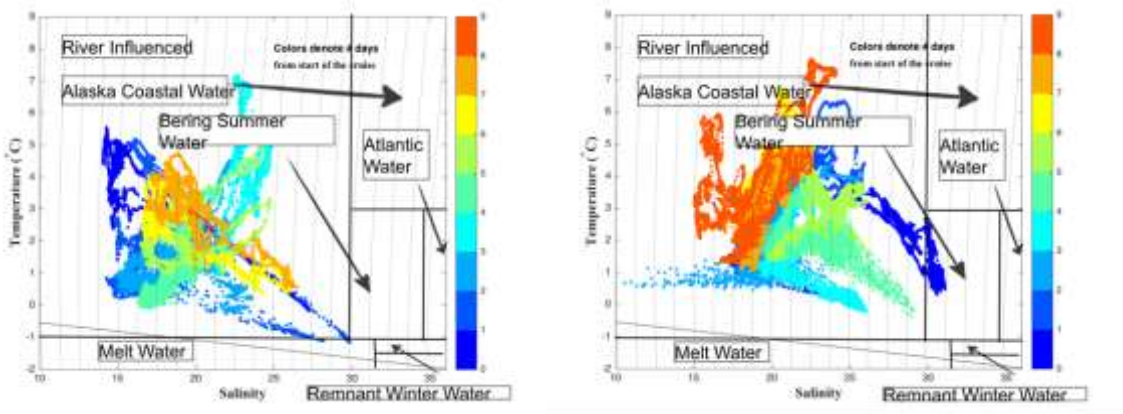


**Figure 10. Surface temperature (°C) vs. salinity from 2014 (left) and 2015 (right) with water masses labeled. The freezing point is indicated by the dashed line.**

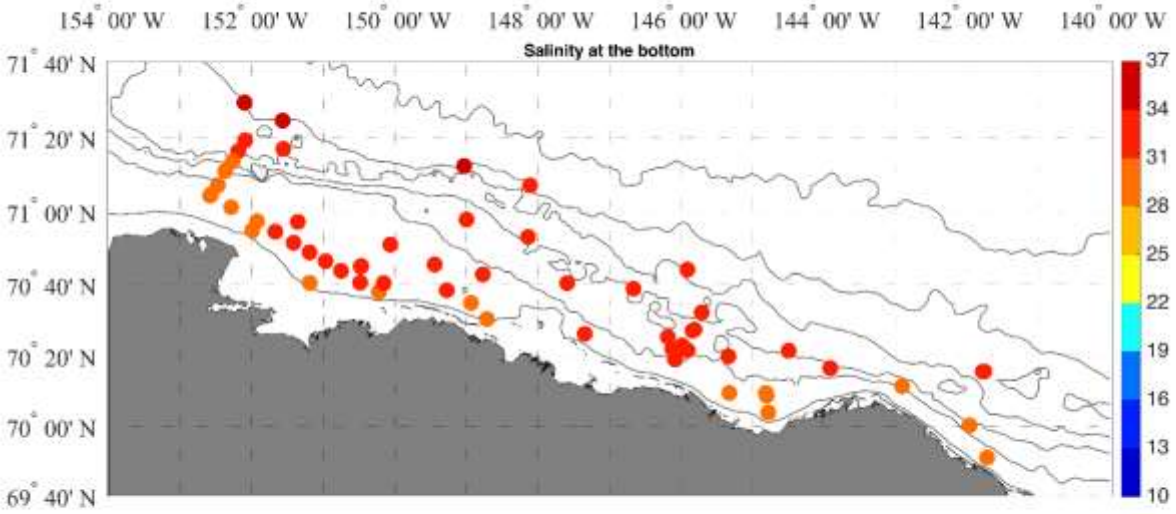


**Figure 11. Salinity at the bottom from 2014.**

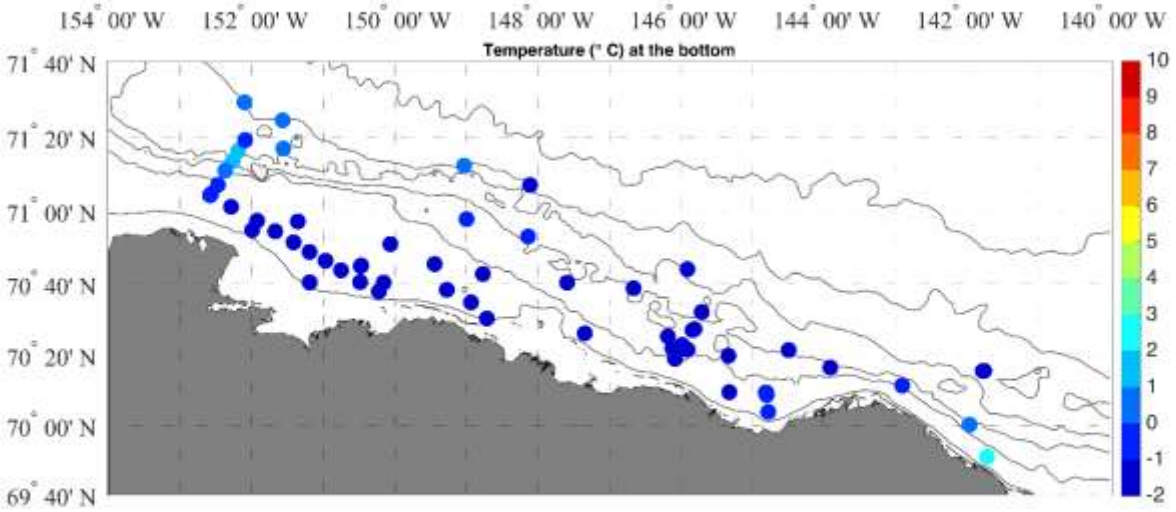


**Figure 12. Temperature at the bottom (°C) from 2014.**

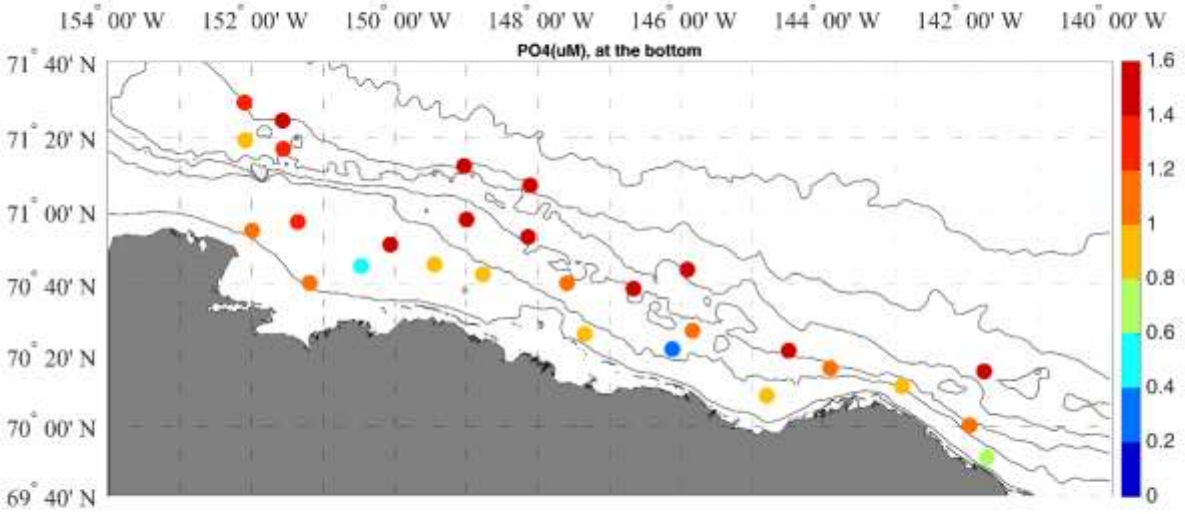


**Figure 13. Concentration of phosphate ($PO_4$, µM) at the bottom from 2014.**

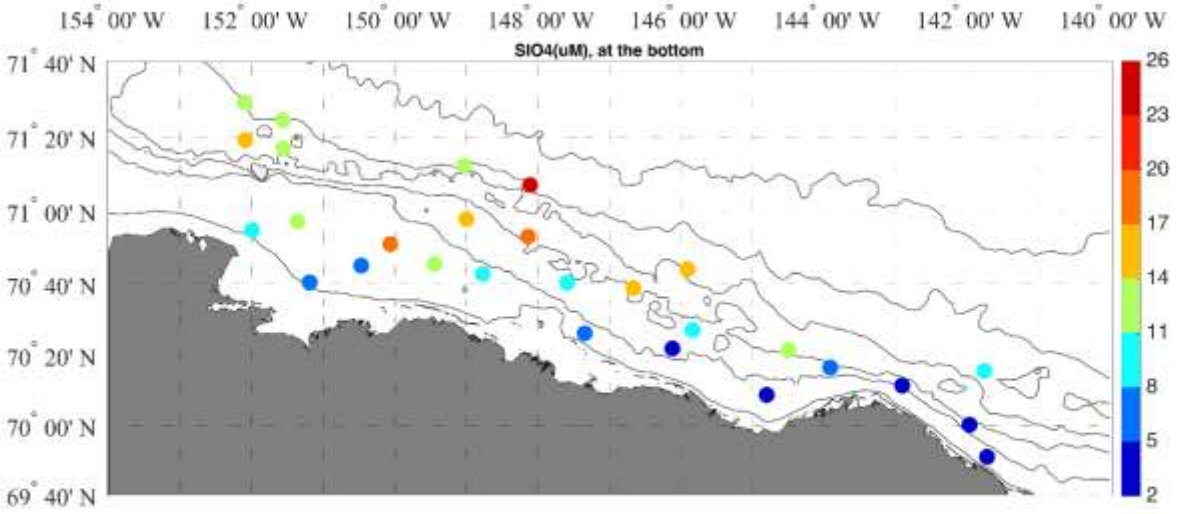


**Figure 14. Concentration of silicate ($SiO_4$, µM) at the bottom from 2014.**

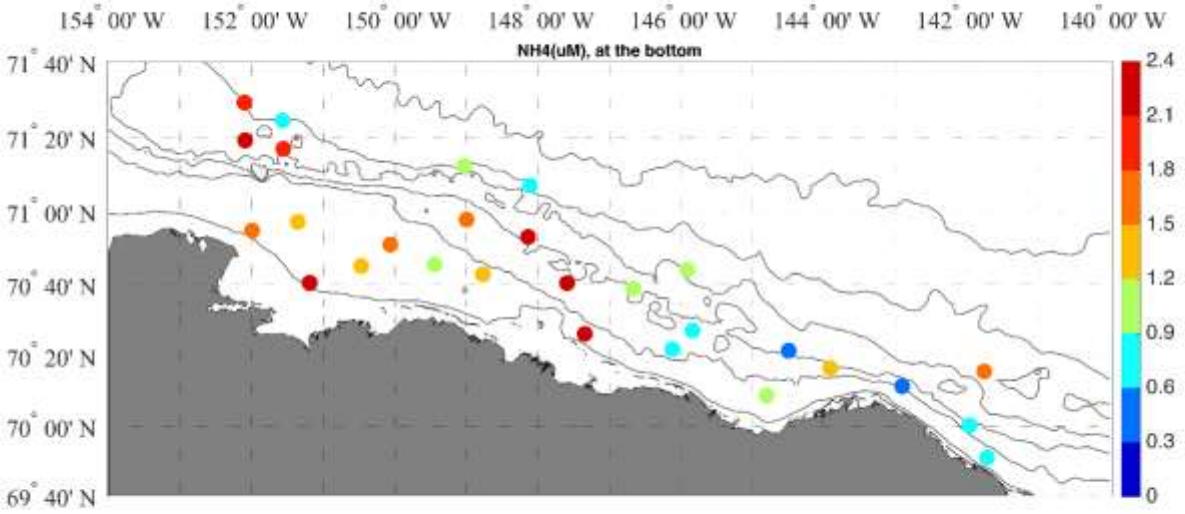


**Figure 15. Concentration of ammonium ($NH_4$, µM) at the bottom from 2014.**

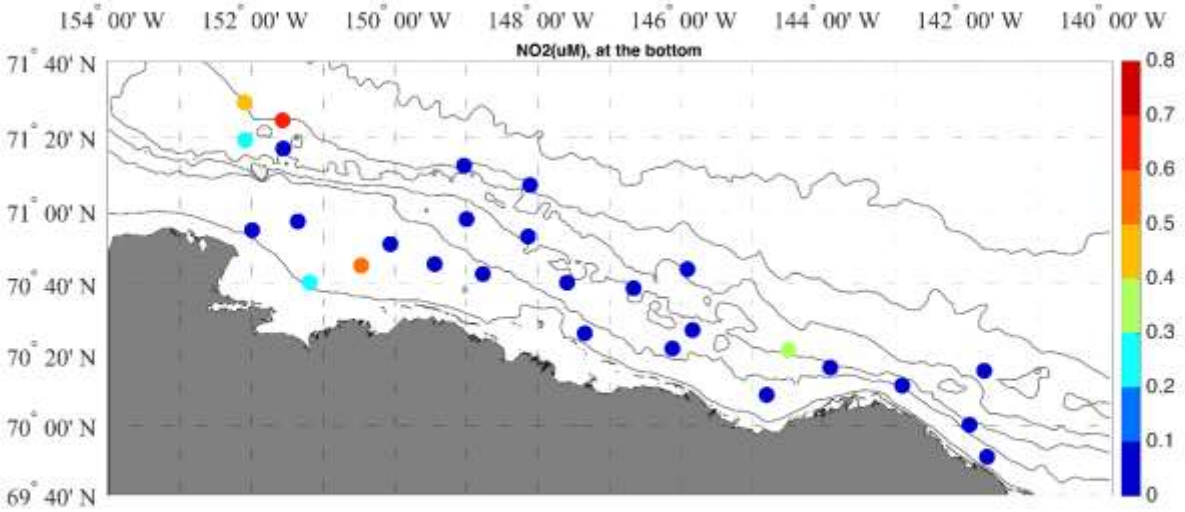


**Figure 16. Concentration of nitrite ($NO_2$, µM) at the bottom from 2014.**

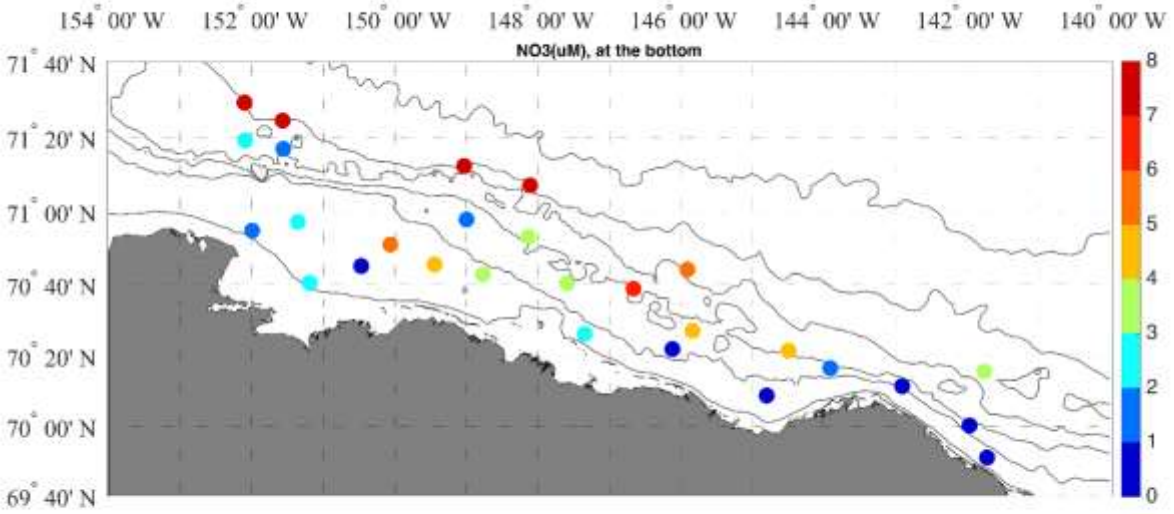


**Figure 17. Concentration of nitrate ($NO_3$, µM) at the bottom from 2014.**

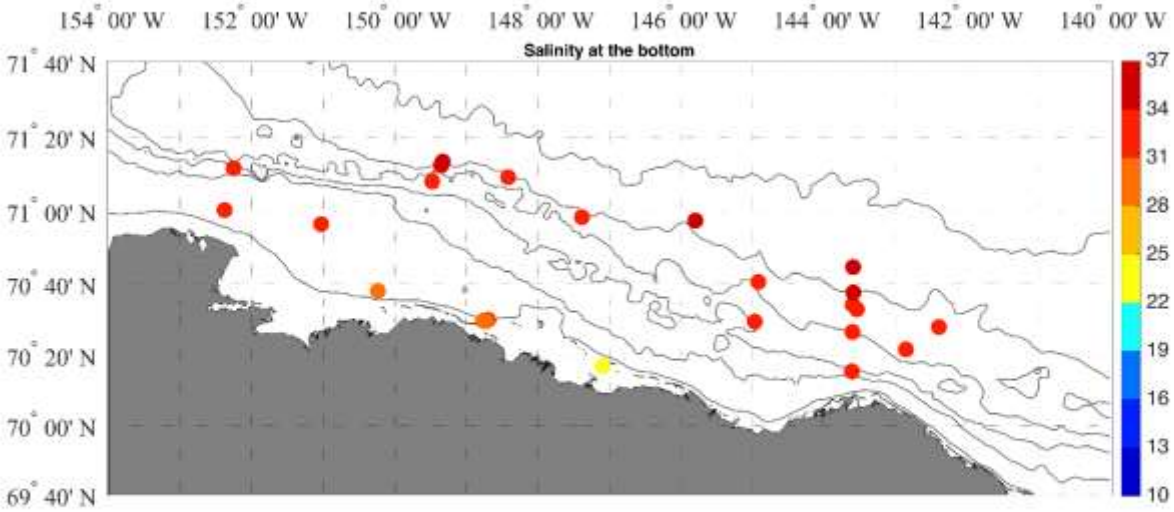


**Figure 18. Salinity at the bottom 2015.**

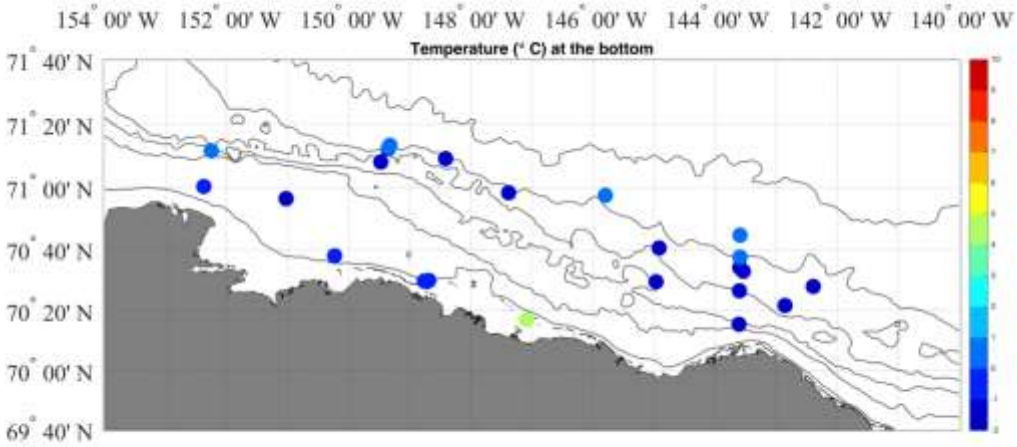


**Figure 19. Temperature (°C) at the bottom 2015.**

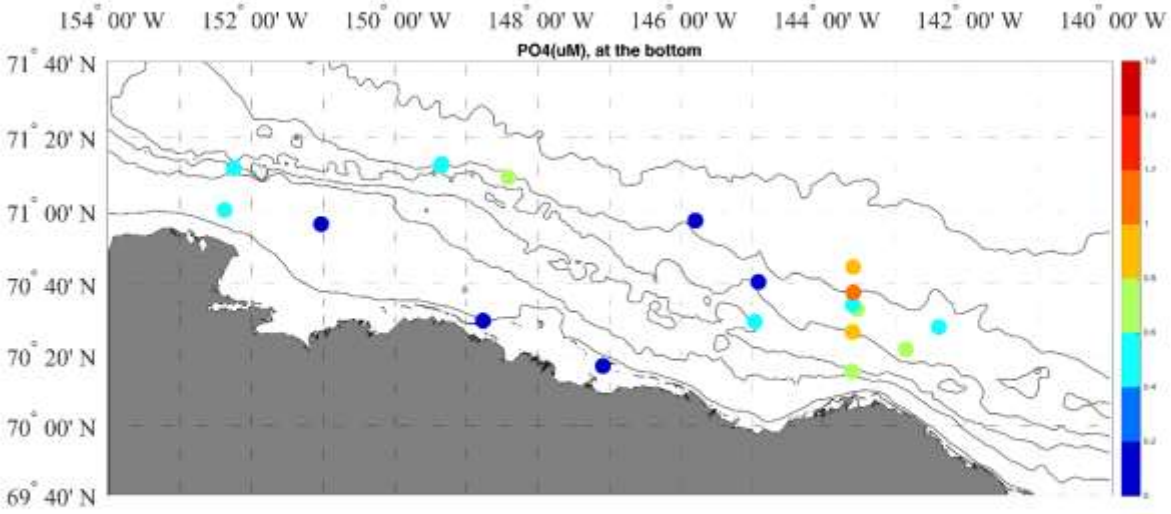


**Figure 20. Phosphate ($PO_4$, µM) at the bottom from 2015.**

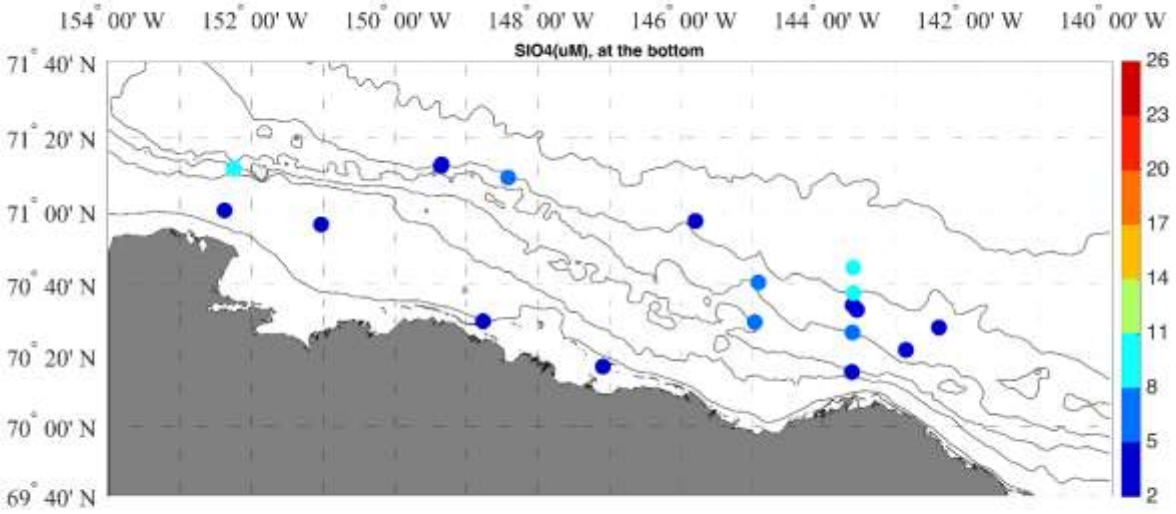


**Figure 21. Concentration of silicate ($SiO_4$, µM) at the bottom from 2015.**

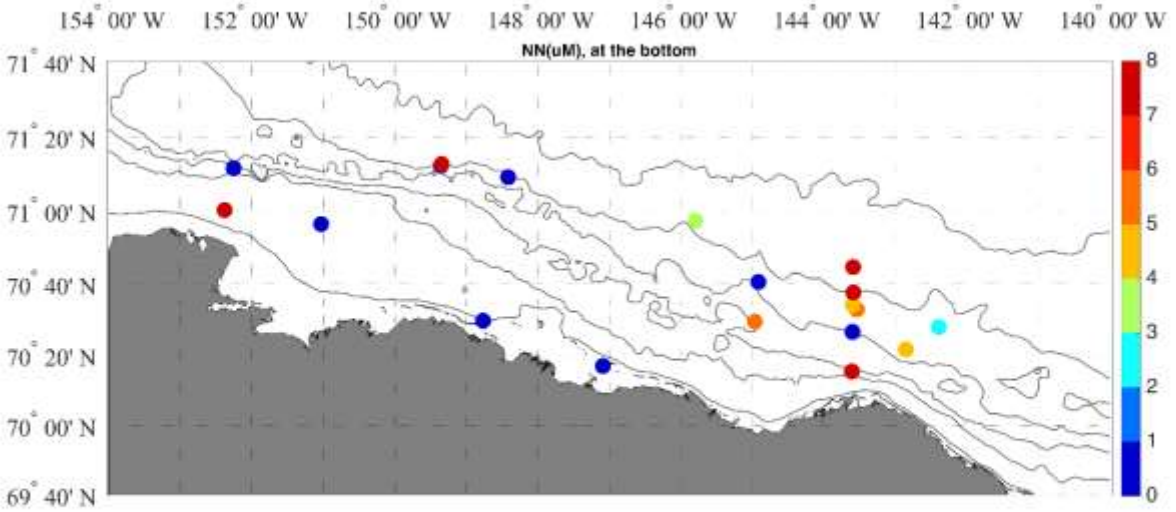


**Figure 22. Concentration of nitrite plus nitrate ($NO_2$ + $NO_3$, µM) at the bottom 2015.**

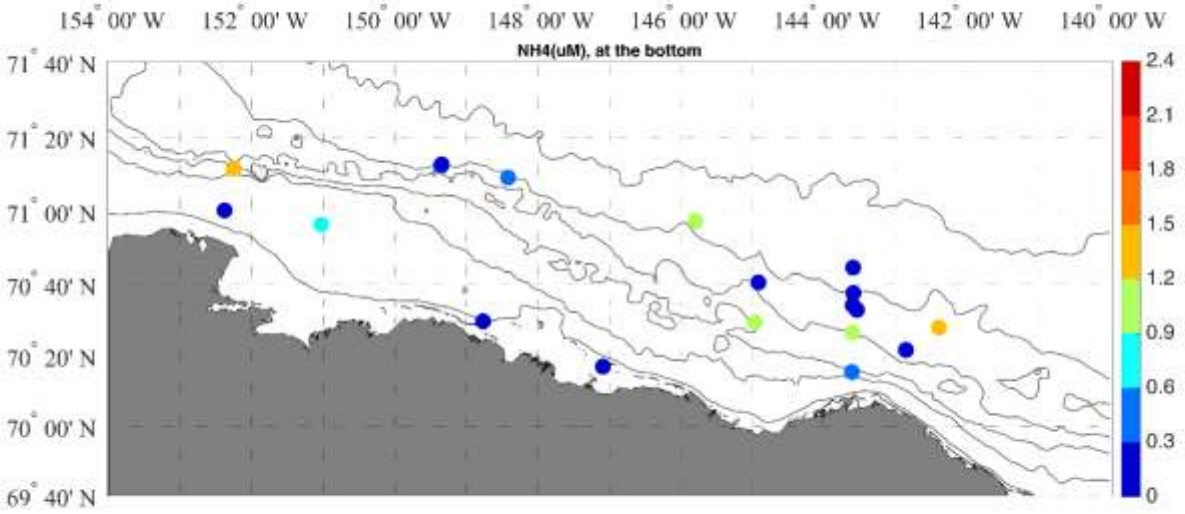


**Figure 23. Concentration of ammonium ($NH_4$, µM) at the bottom 2015.**

TS plots at the bottom for 2014 and 2015 are shown in Figure 24 through Figure 25. The color scale indicates the concentration of the nutrients. Black dots are the full temperature and salinity values from all the CTD casts. Major regional water masses are labeled. The bottom water masses are clustered around the Bering summer water and remnant winter water masses that originate in the Bering Sea, are modified over the Chukchi and that are then advected by the Beaufort Sea shelfbreak jet (e.g., von Appen and Pickart, 2012; Gong and Pickart, 2015).

Figure 26 through Figure 38 show the salinity, temperature, and nutrient concentrations at the chlorophyll max for 2014 and 2015. Salinities range from 13 in the very nearshore to 34 in 2014. In 2015, the salinity range is slightly smaller and lies between ~19 and 34. Temperatures in both years are less than 2 °C except at the shallowest stations. Nutrients concentrations are slightly less than at the bottom at all stations.

TS plots from the chlorophyll max are shown in Figure 39 for 2014 and Figure 40 for 2015. Compared to the bottom TS plots, the water at the chlorophyll max is fresher and slightly warmer with more variability in temperature and salinity than at the bottom. The water masses at the chlorophyll max are mixture of river influenced water and shelfbreak water masses (Bering summer water and remnant winter water).

Salinity, temperature, and nutrient concentrations at the surface (~2 m) for 2014 are shown in Figure 41 through Figure 47 and for 2015 in Figure 48 through Figure 53. Salinities in 2014 strongly reflect the presence of river water with salinities in the nearshore as low as 10. Surface temperatures in 2014 ranged from 7 to -1 °C with higher temperatures generally associated with strongly stratified river influenced water. In 2015, salinities are markedly different and they ranged between 19 and 22. Surface temperatures in 2015 are also less variable than in 2014 and they generally are <3 °C and show less variability than in 2014.

TS plots from the surface for 2014 and 2015 are shown in Figure 54 and Figure 55. The TS plots show that nutrients are depleted compared to lower depths at these same sites. Also, in 2015 the salinity range is much smaller than in 2014 and temperature and salinity in 2015 is clustered around over a smaller range than in 2014.

The differences in surface salinity and temperature are likely a result of differences in winds between the two years. In 2015, the downwelling favorable winds during the cruise meant that the shelf remained ice covered for the entire cruise and pushed shelfbreak, surface water masses onto the shelf. In contrast, upwelling favorable winds in 2014 meant there was no ice on the shelf during the cruise and strongly stratified, river influenced coastal waters were spread along- and off-shore.

A TS plot that includes all the data from the CTD casts for both 2014 and 2015 is shown in Figure 56. 2014 data are shown in blue and 2015 data are shown in red. The figure illustrates the differences between the years: in 2014 river influenced water is much more prevalent than in 2015 and salinities in 2014 are markedly fresher than 2015.

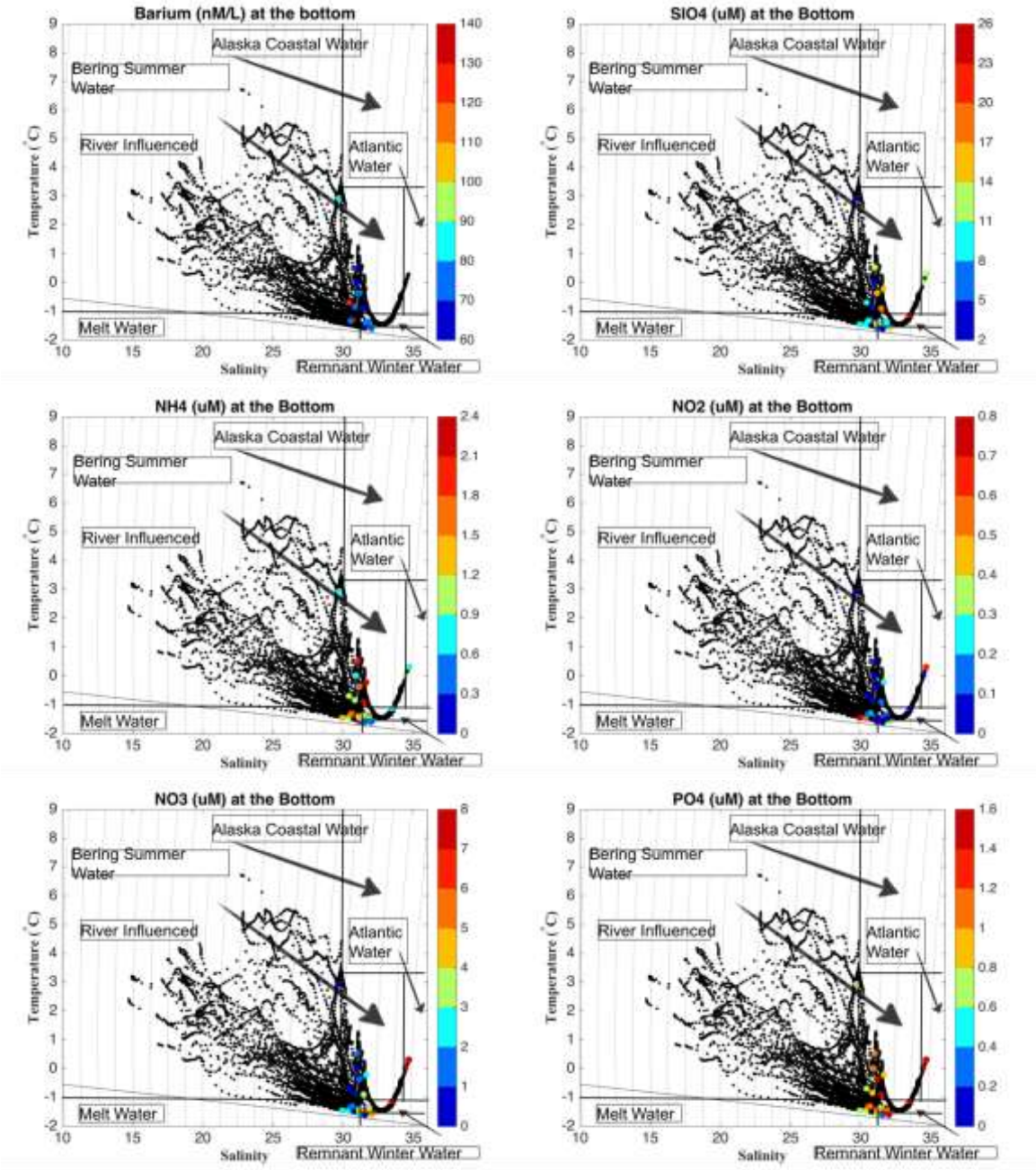


**Figure 24. Barium and nutrients at the bottom from 2014.**

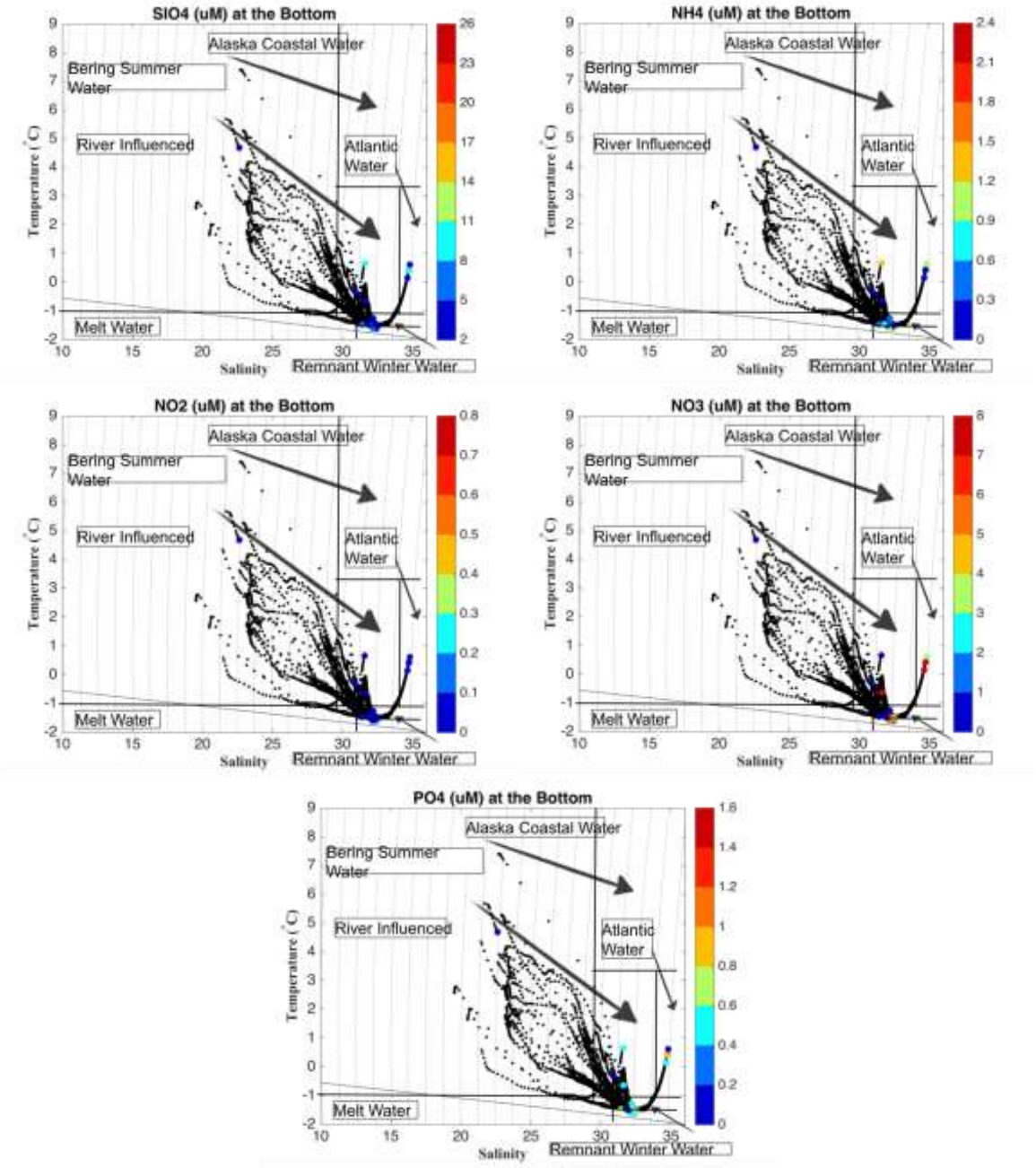


**Figure 25. Nutrients at the bottom from 2015.**

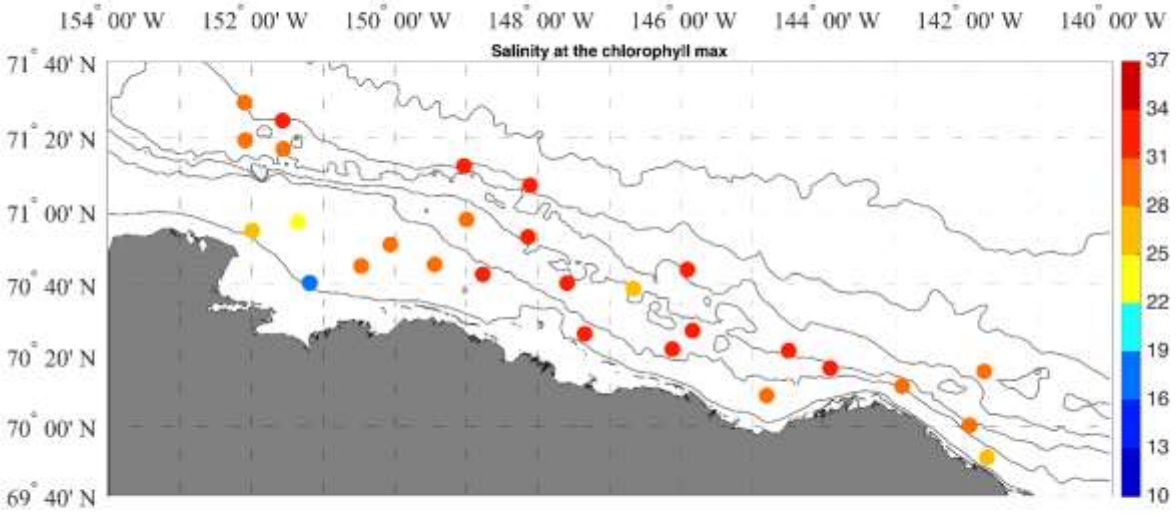


**Figure 26. Salinity at the chlorophyll max from 2014.**

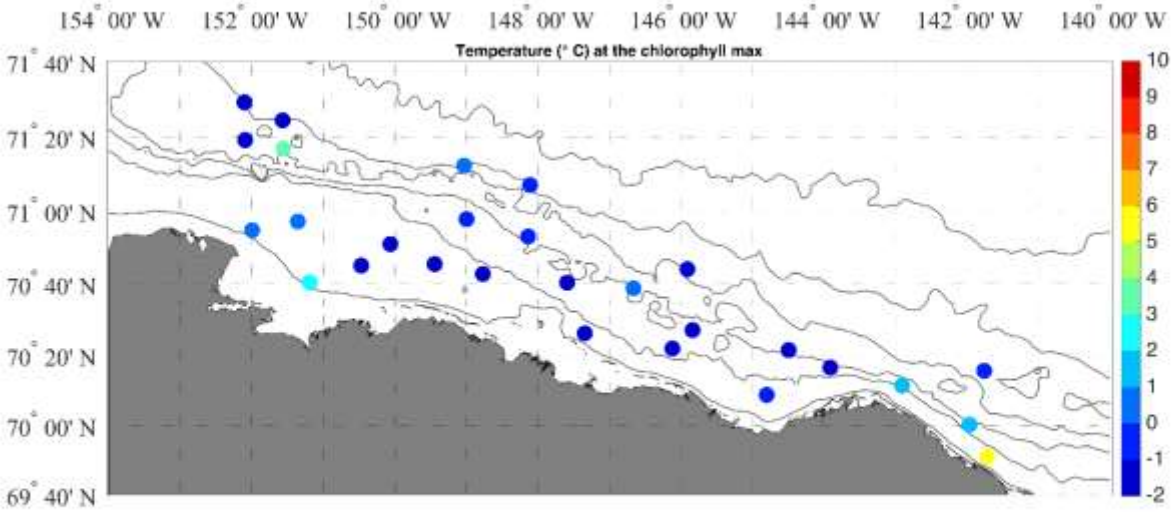


**Figure 27. Temperature (°C) at the chlorophyll max from 2014.**

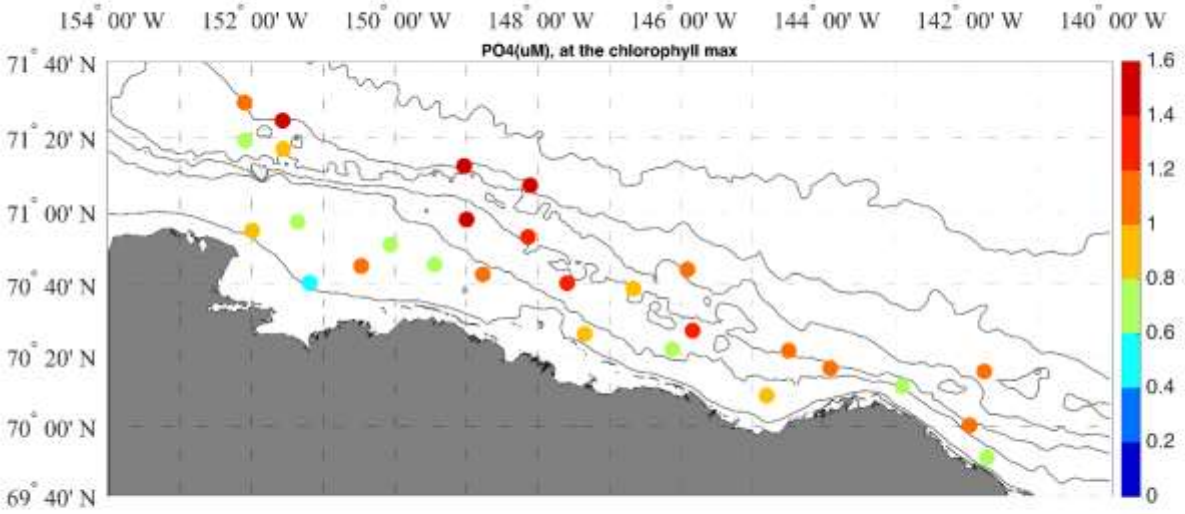


**Figure 28. Phosphate ($PO_4$, µM) at the chlorophyll max from 2014.**

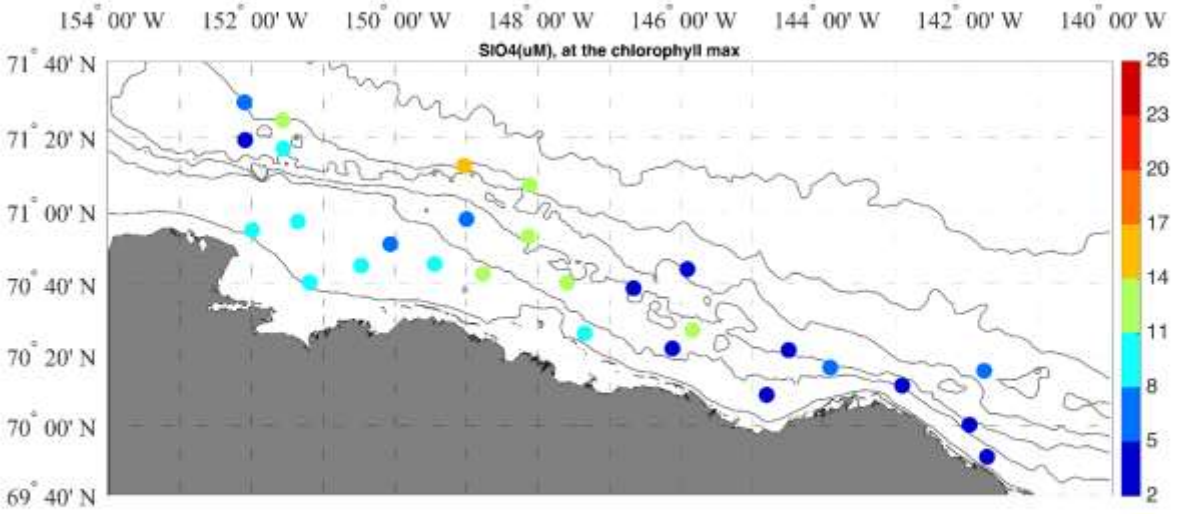


**Figure 29. Silicate ($SiO_4$, µM) at the chlorophyll max from 2014.**

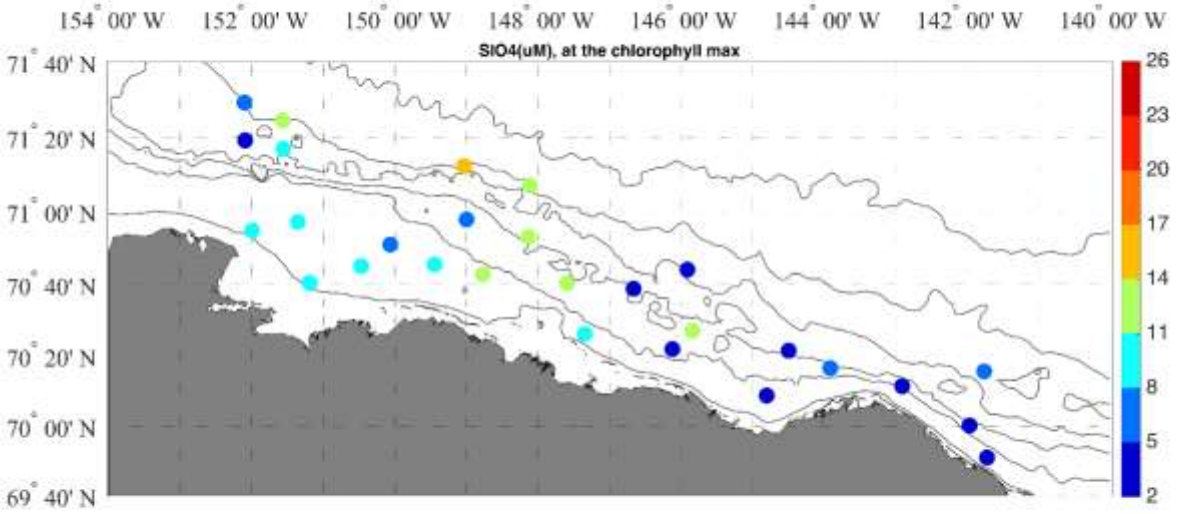


**Figure 30. Ammonium ($NH_4$, µM) at the chlorophyll max from 2014.**

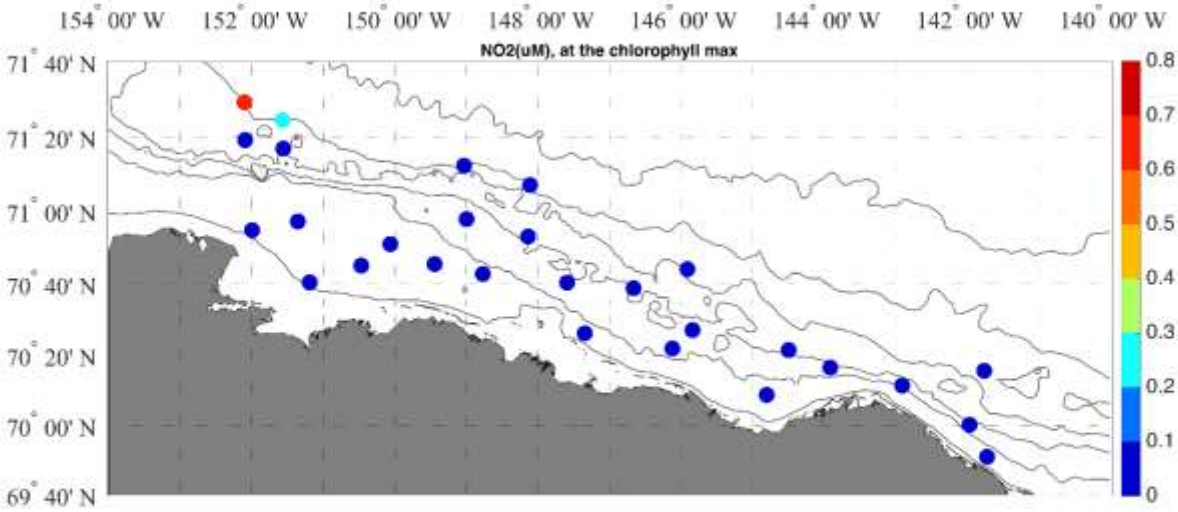


**Figure 31. Nitrite ($NO_2$, µM) at the chlorophyll max from 2014.**

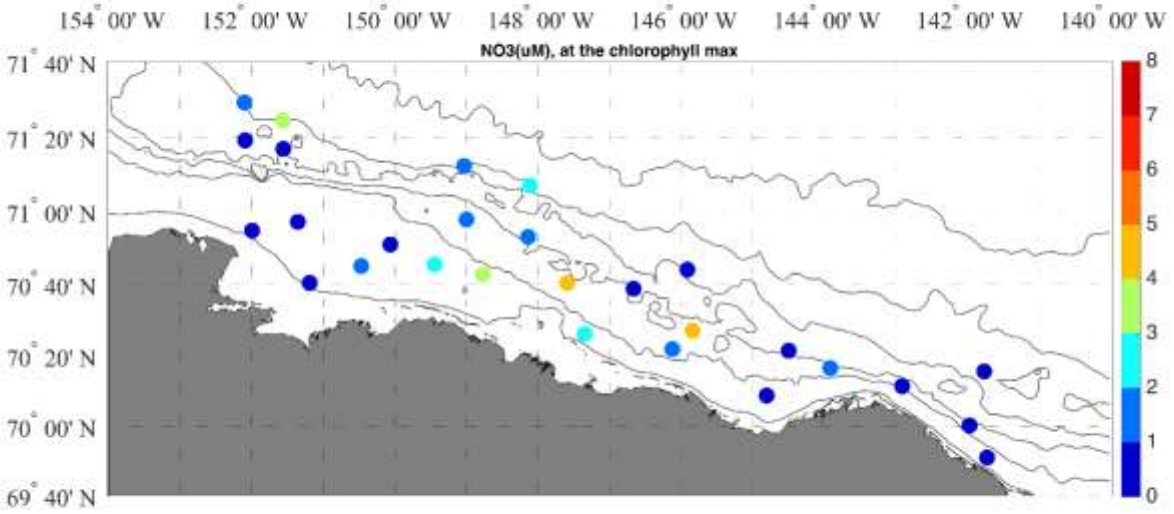


**Figure 32. Nitrate ($NO_3$, µM) at the chlorophyll max from 2014.**

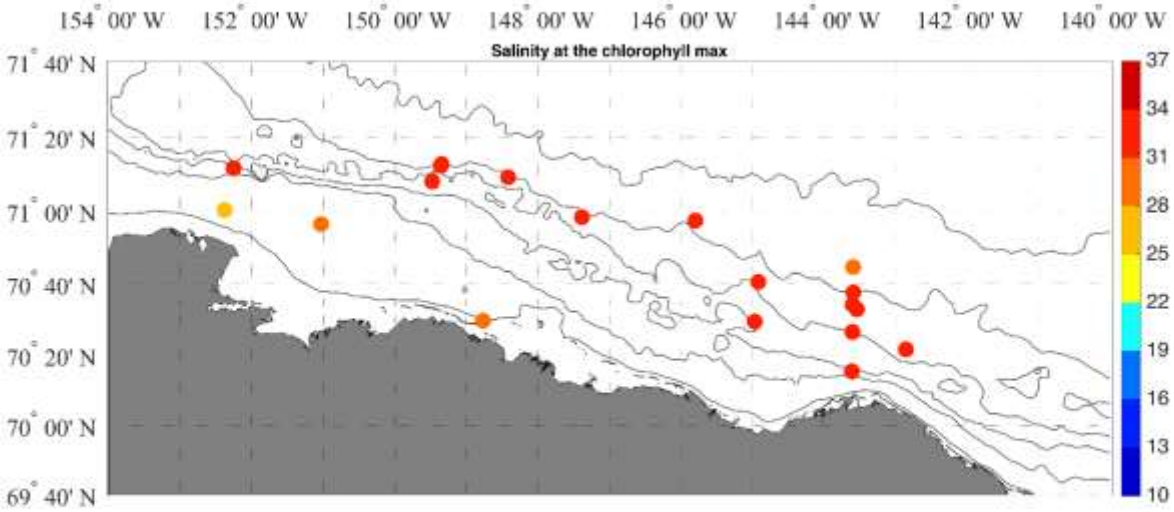


**Figure 33. Salinity at the chlorophyll max from 2015.**

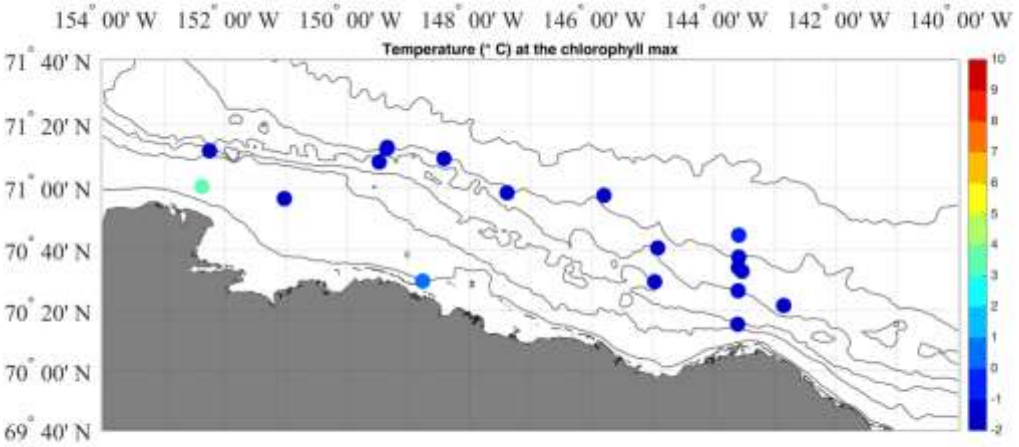


**Figure 34. Temperature (°C) at the chlorophyll max from 2015.**

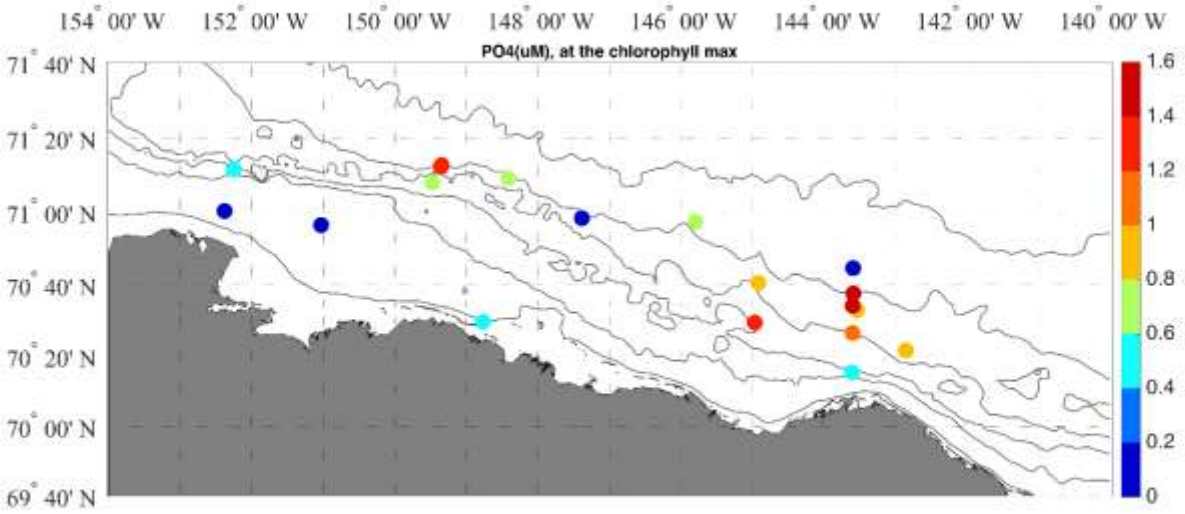


**Figure 35. Phosphate ($PO_4$, µM) at the chlorophyll max from 2015.**

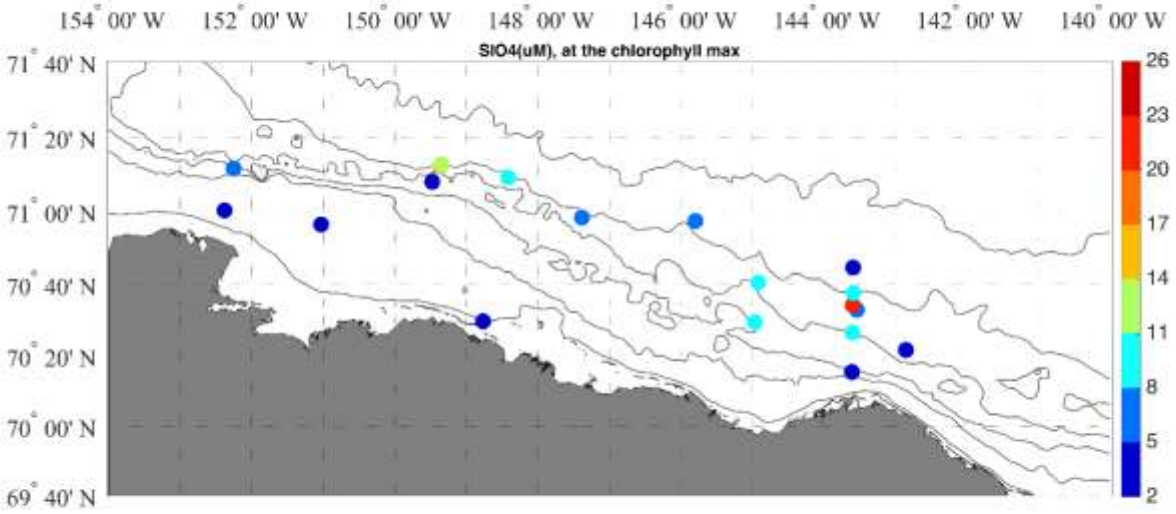


**Figure 36. Silicate ($SiO_4$, µM) at the chlorophyll max from 2015.**

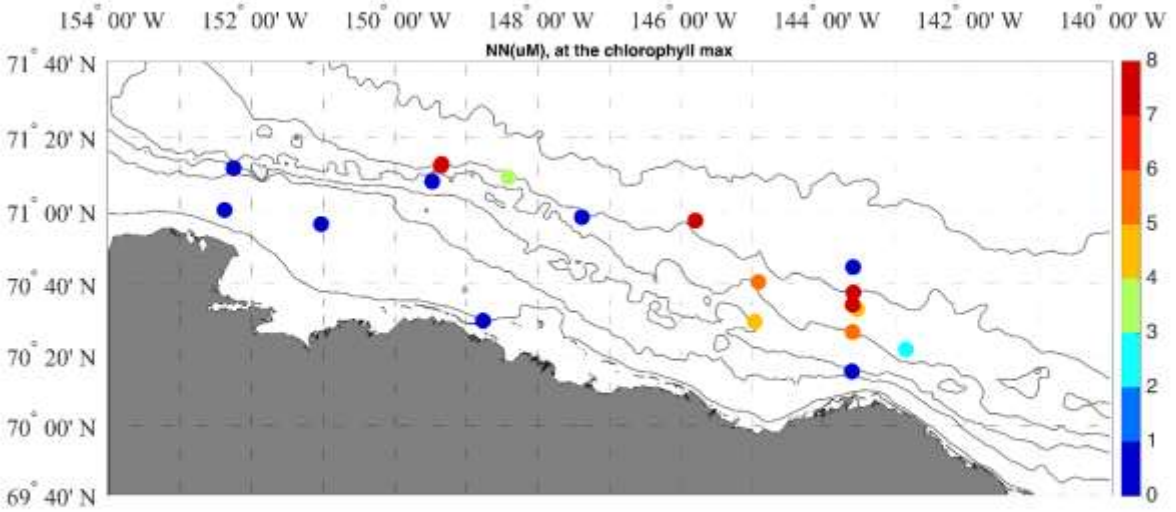


**Figure 37. Nitrite + nitrate ($NO_2$ + $NO_3$, µM) at the chlorophyll max from 2015.**

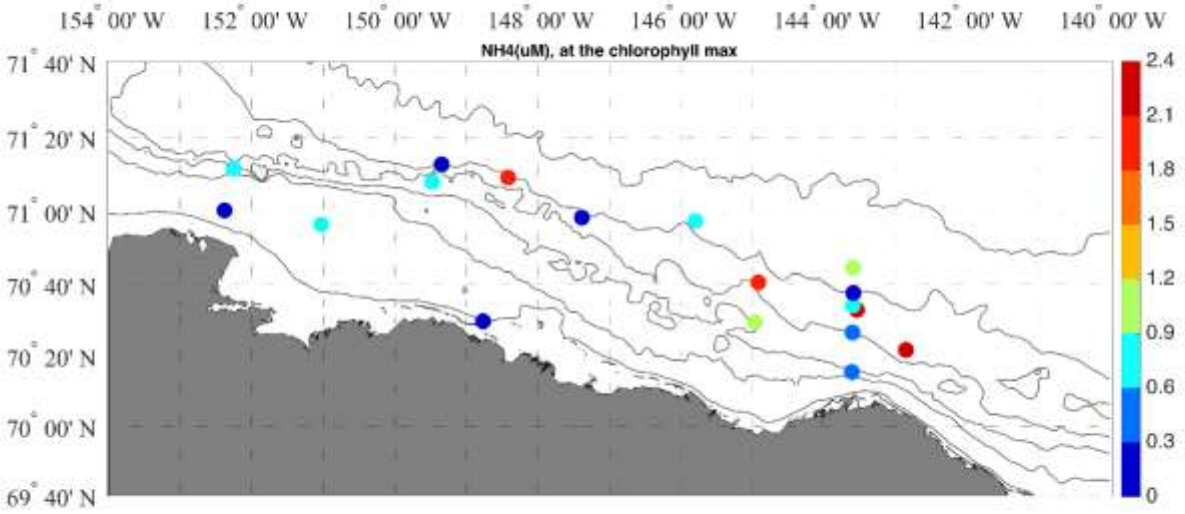


**Figure 38. Ammonium ($NH_4$, µM) at the chlorophyll max from 2015.**

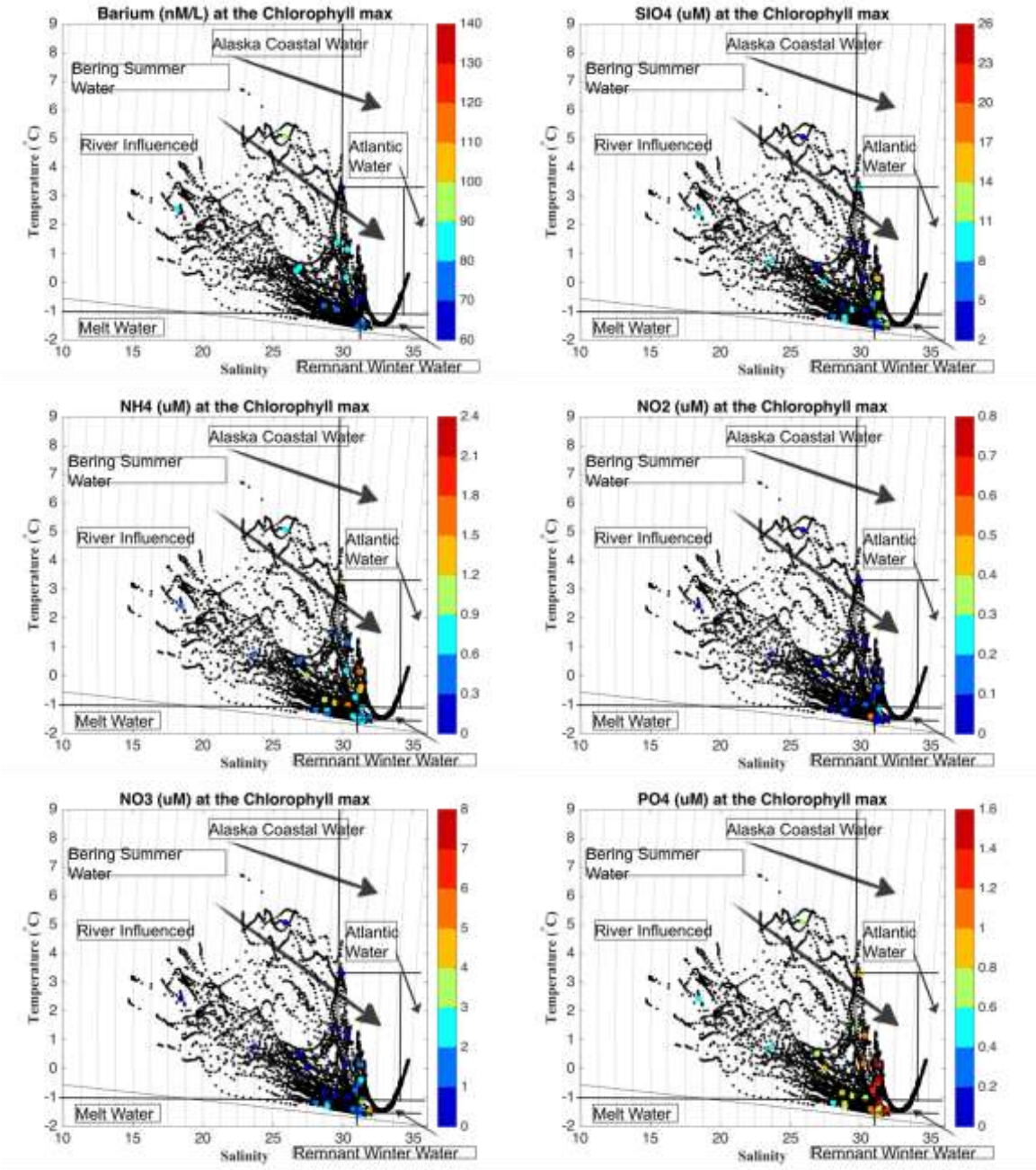


**Figure 39. Barium and nutrients at the chlorophyll max from 2014.**

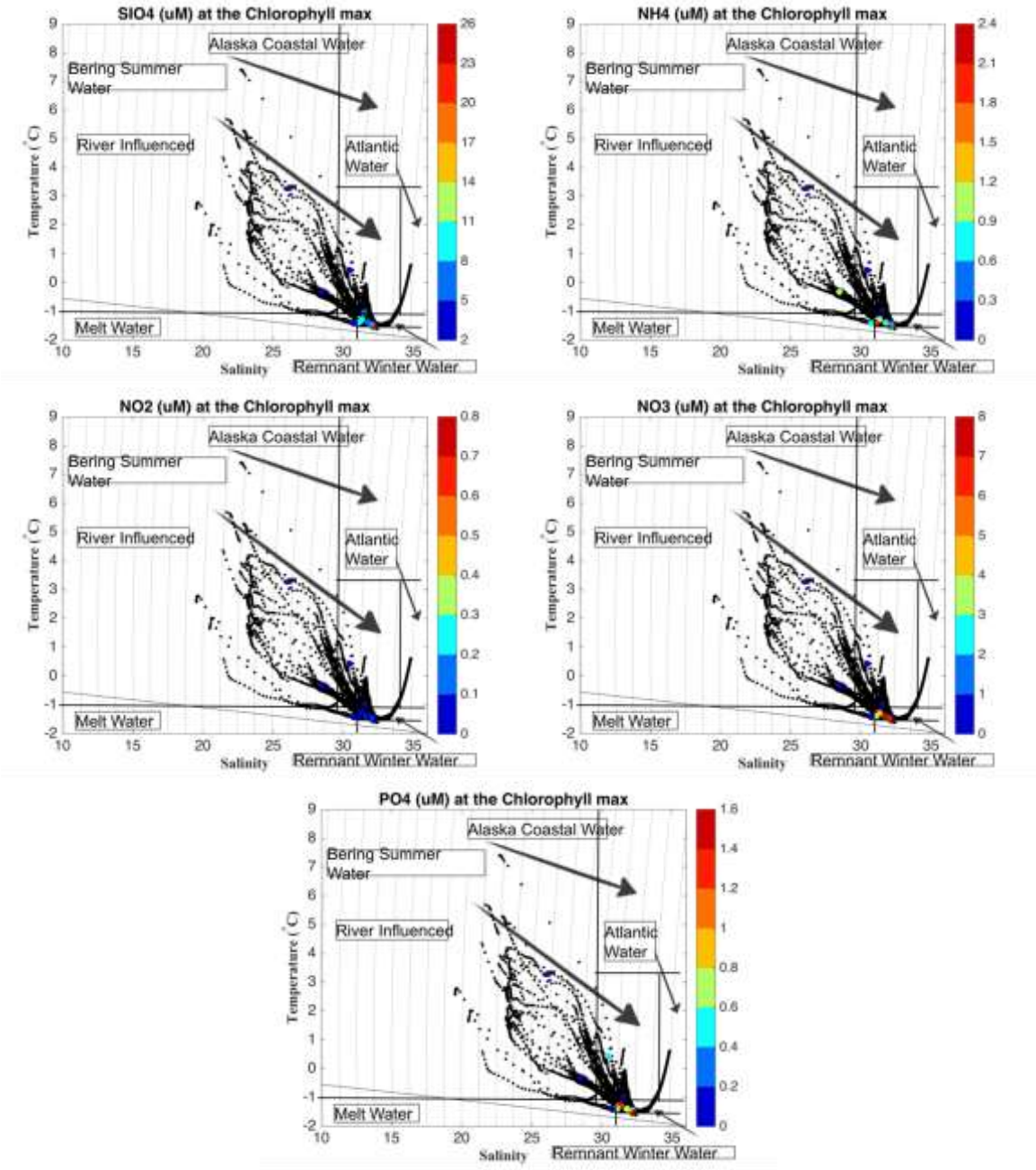


**Figure 40. Nutrients at the chlorophyll max from 2015.**

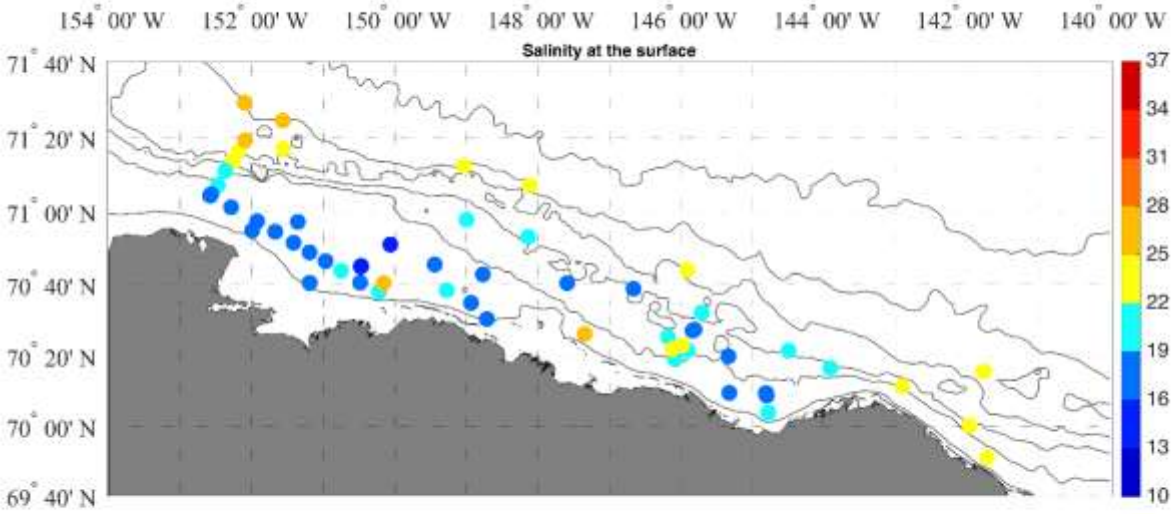


**Figure 41. Salinity at the surface from 2014.**

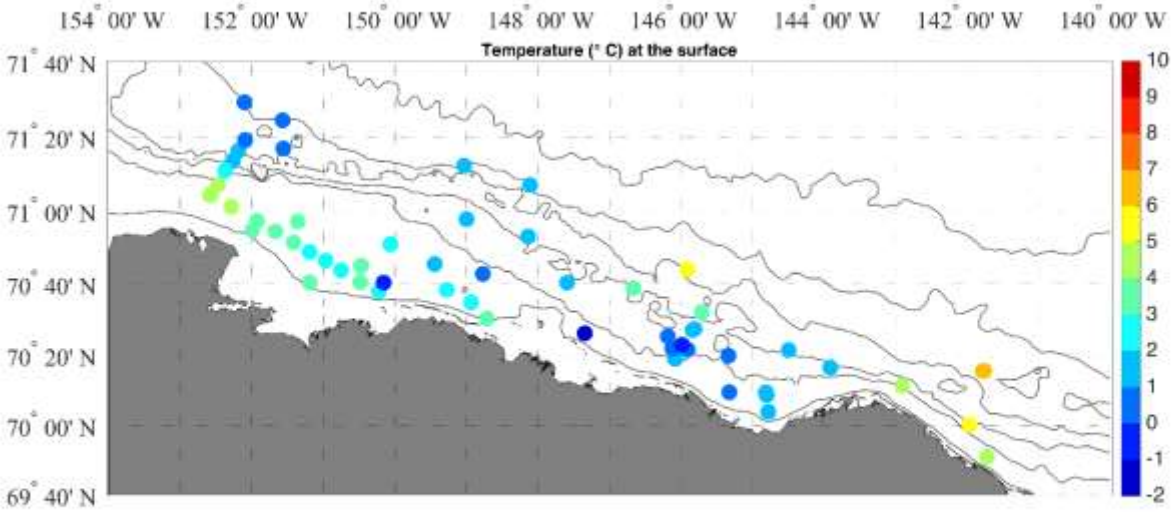


**Figure 42. Temperature (°C) at the surface from 2014.**

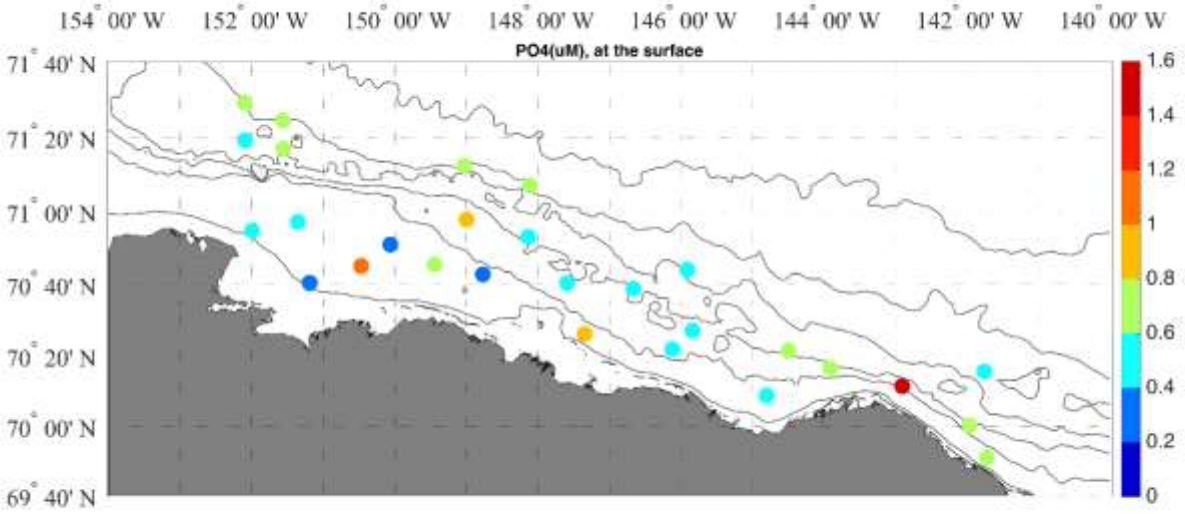


**Figure 43. Phosphate ($PO_4$, µM) at the surface from 2014.**

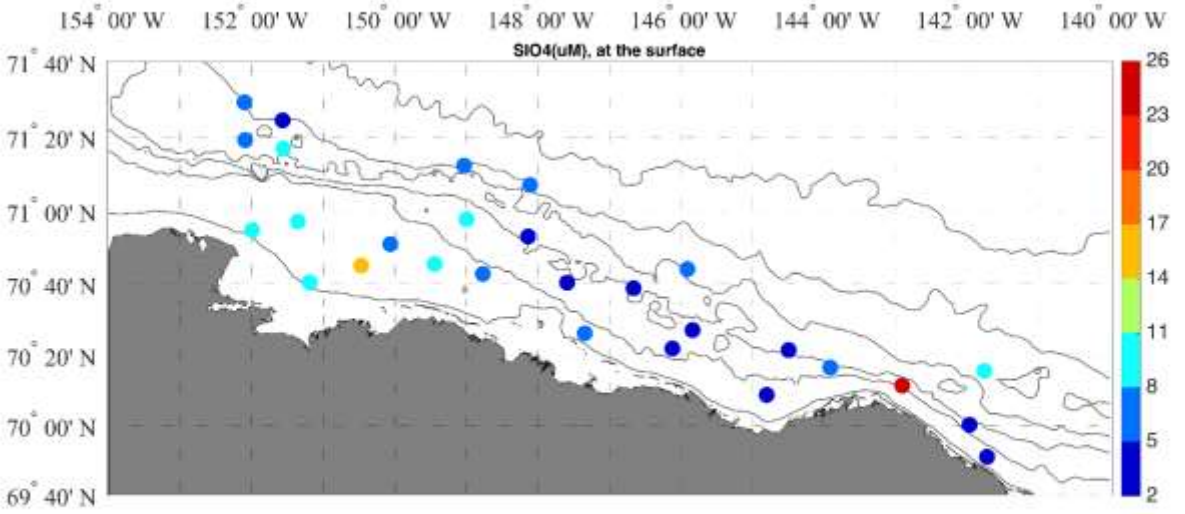


**Figure 44. Silicate ($SiO_4$, µM) at the surface from 2014.**

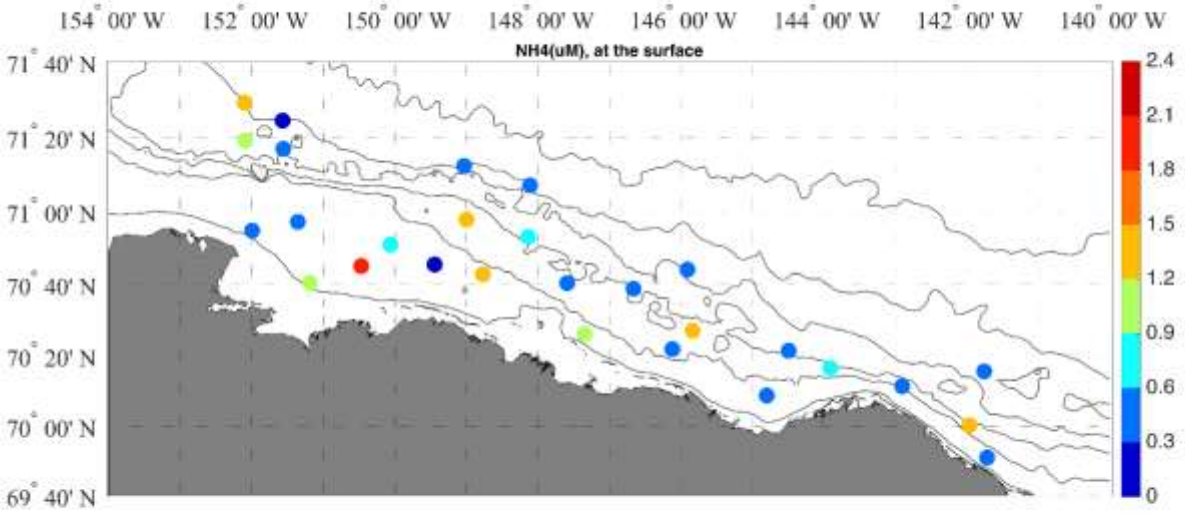


**Figure 45. Ammonium ($NH_4$, µM) at the surface from 2014.**

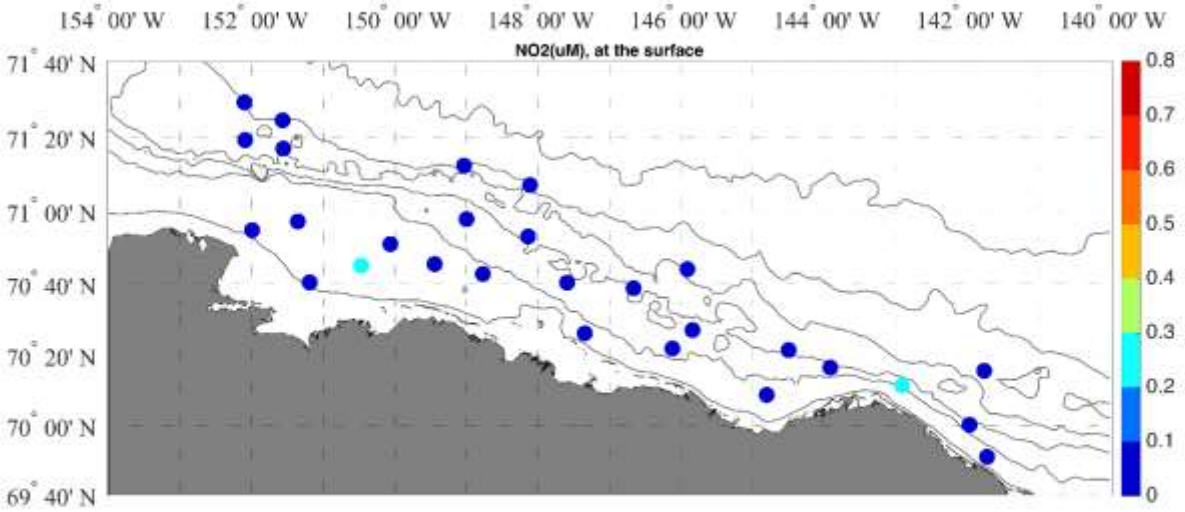


**Figure 46. Nitrite ($NO_2$, µM) at the surface from 2014.**

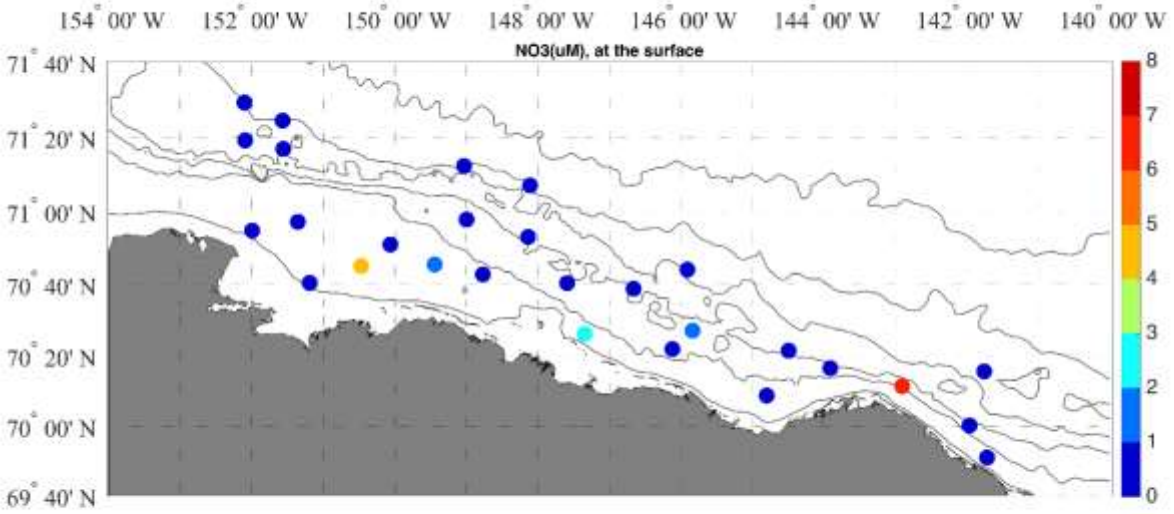


**Figure 47. Nitrate ($NO_3$, µM) at the surface from 2014.**

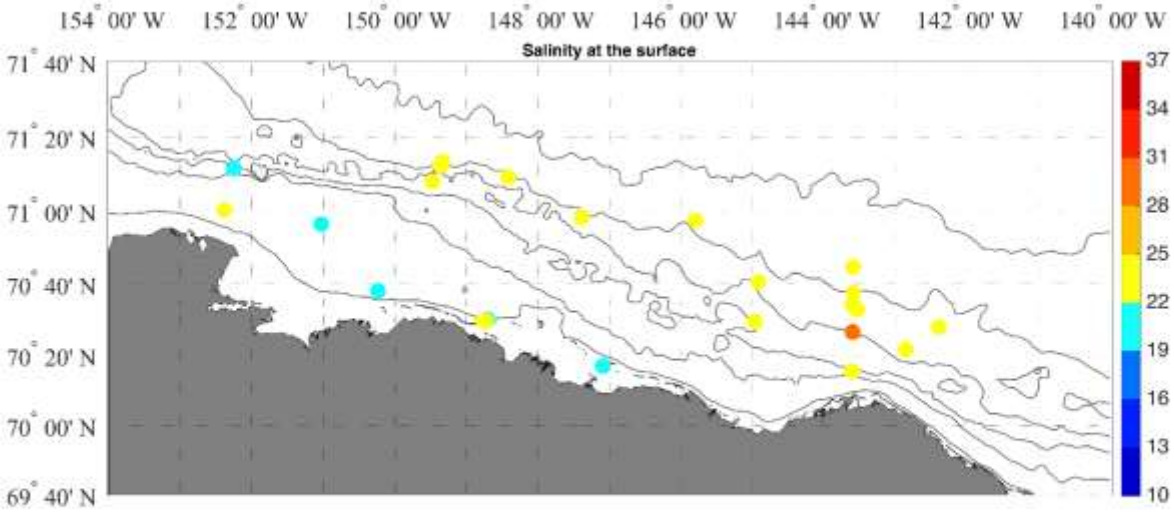


**Figure 48. Salinity at the surface from 2015.**

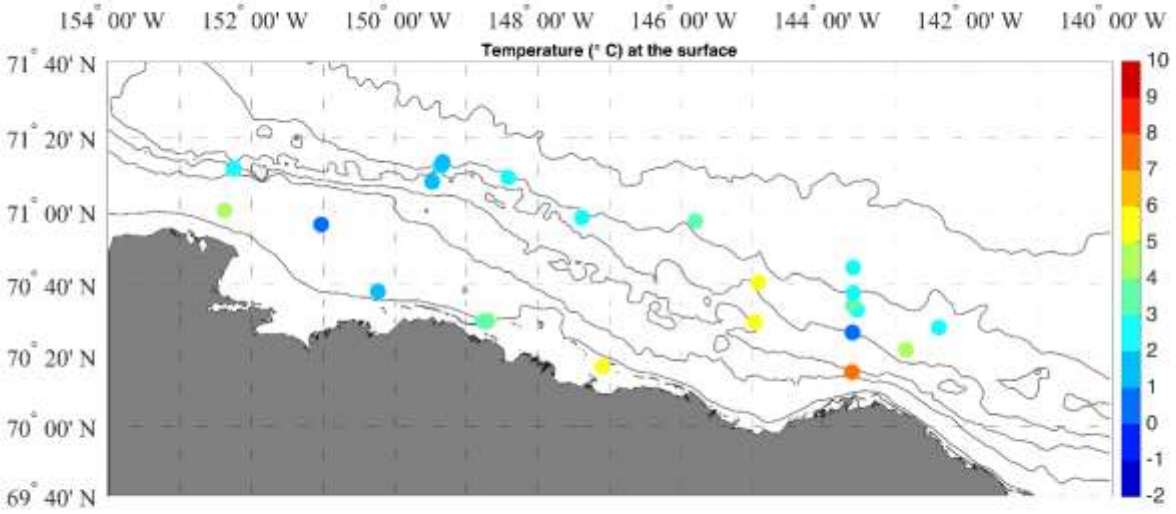


**Figure 49. Temperature (°C) at the surface from 2015.**

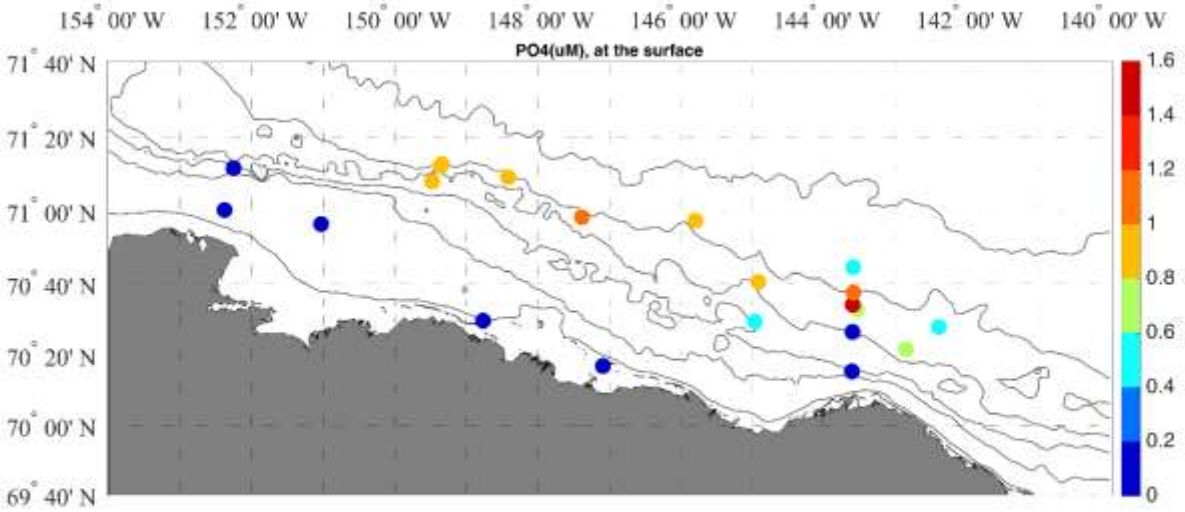


**Figure 50. Phosphate ($PO_4$, µM) at the surface from 2015.**

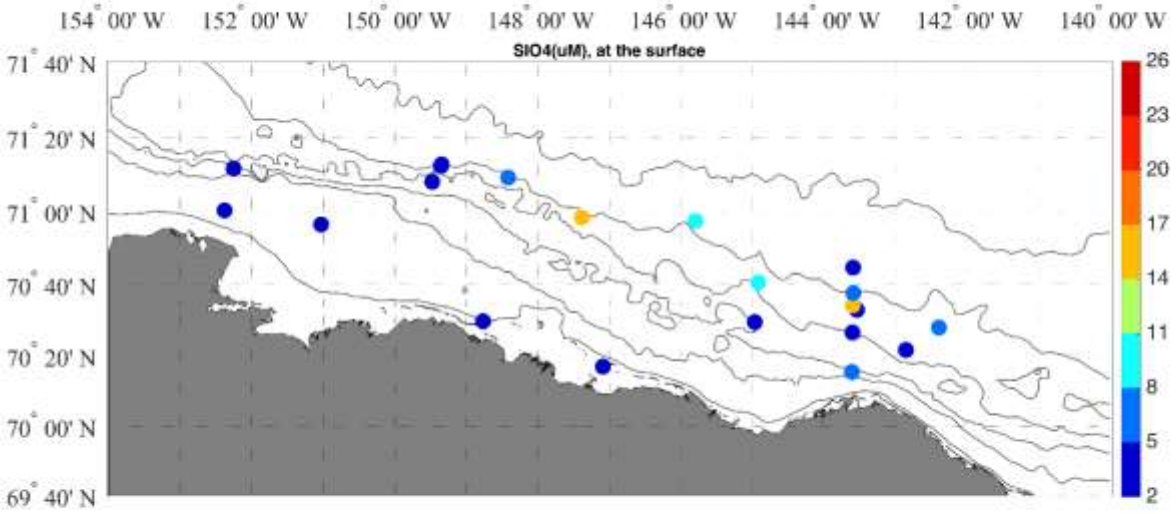


**Figure 51. Silicate ($SiO_4$, µM) at the surface from 2015.**

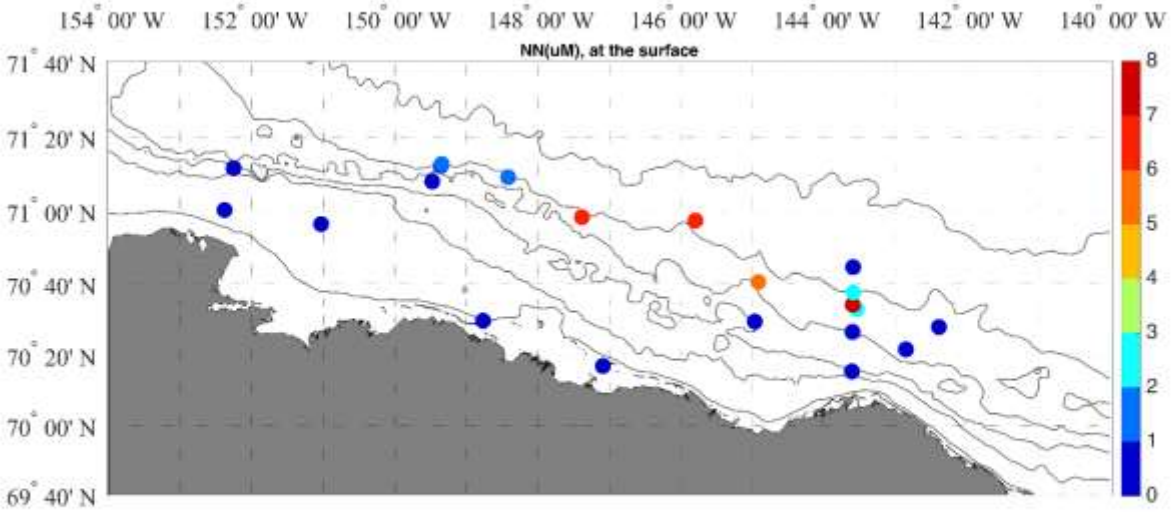


**Figure 52. Nitrite + nitrate ($NO_2$ + $NO_3$, µM) at the surface from 2015.**

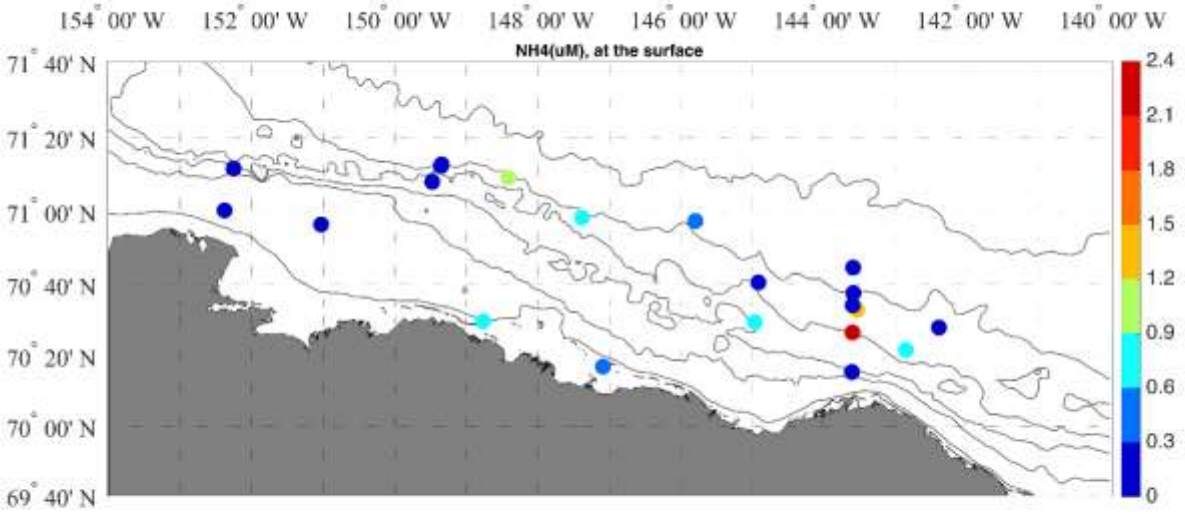


**Figure 53. Ammonium ($NH_4$, µM) at the surface from 2015.**

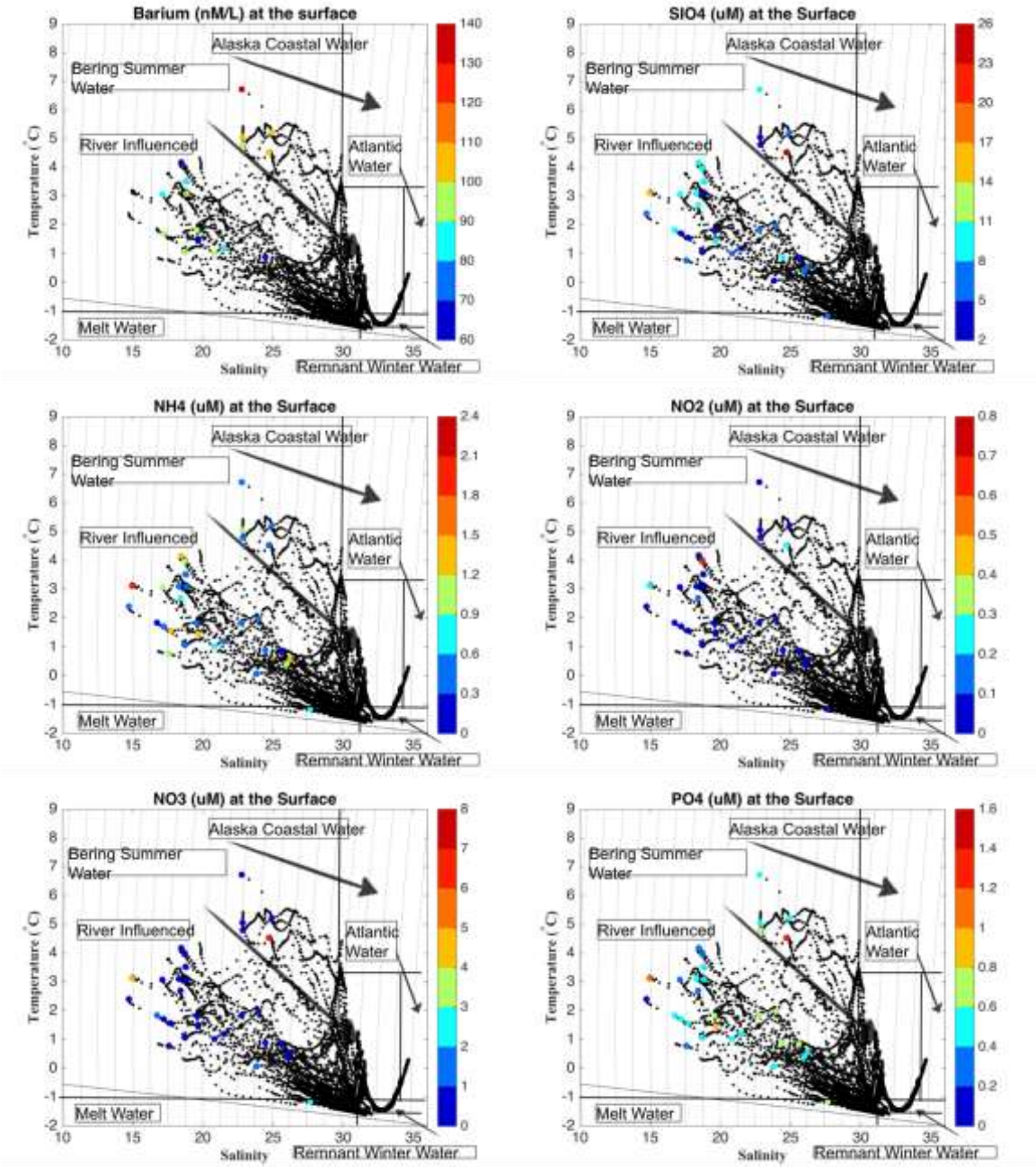


**Figure 54. Barium and nutrients at the surface from 2014.**

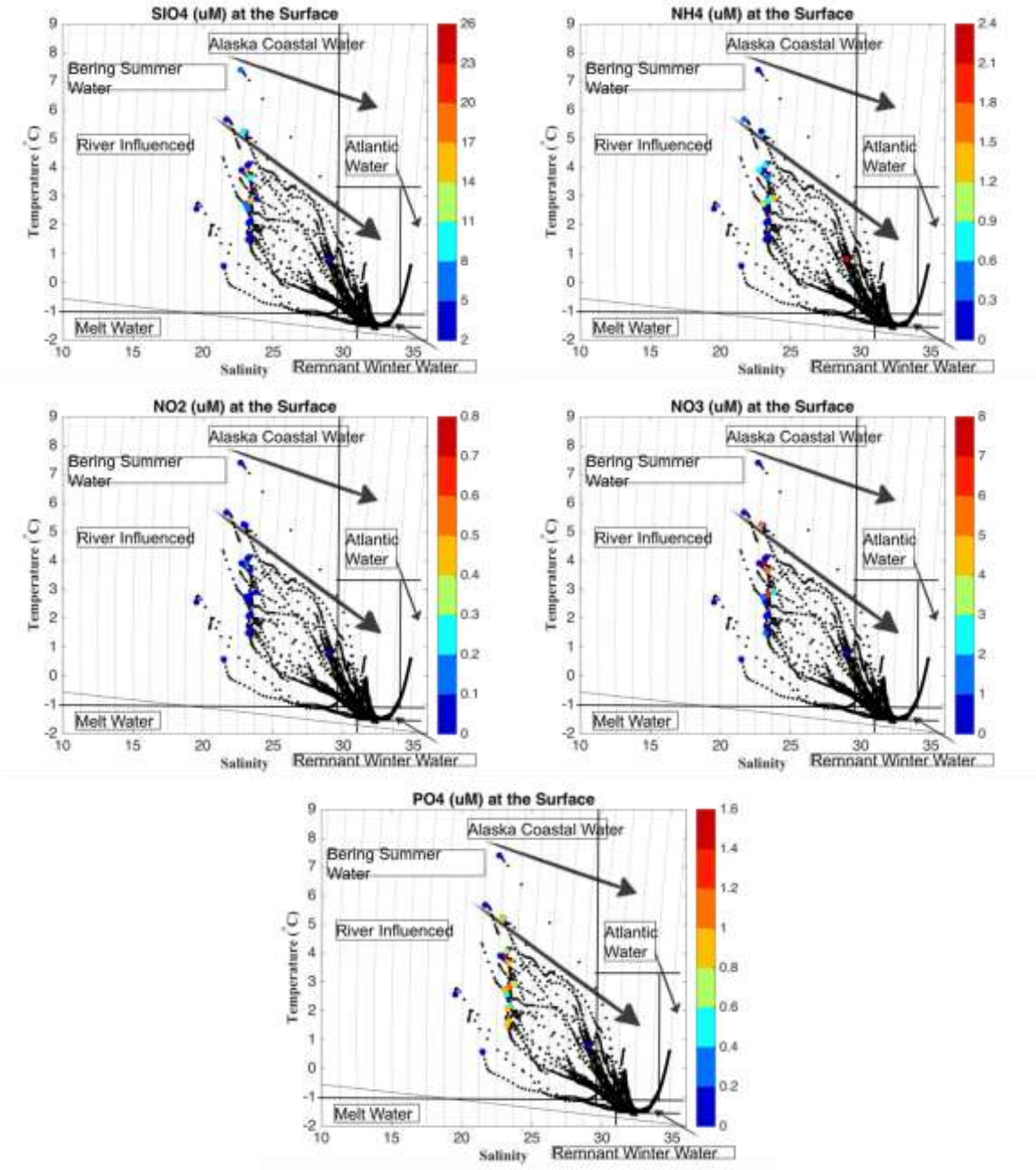


**Figure 55. Nutrients at the surface from 2015.**

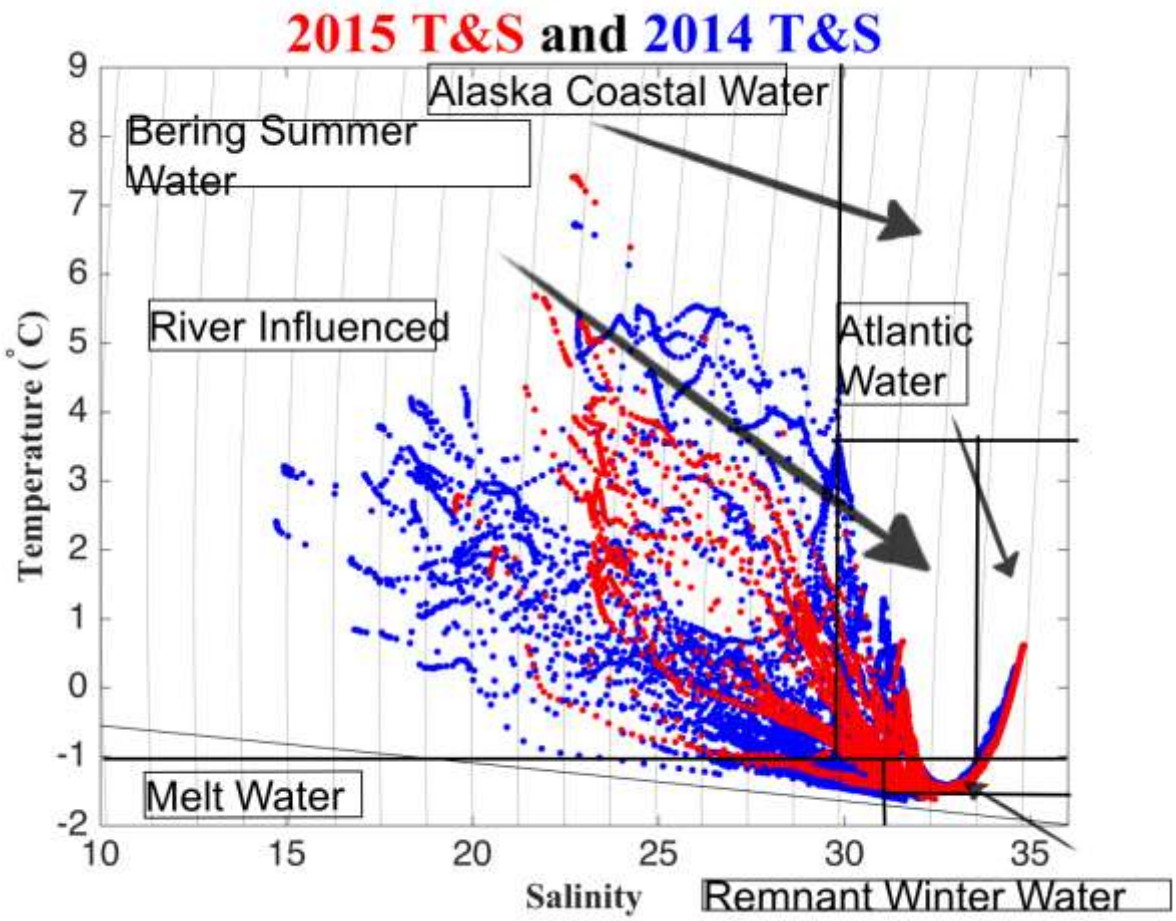


**Figure 56. Temperature (°C) and salinity from 2014 (blue) and 2015 (red).**

## 2.4 Mooring Data

Pressure, temperature, and salinity from the moored CTD are shown in Figure 57. Figure 58 is a TS plot from the moored record overlaid on the 2014 and 2015 CTD cast data. The pressure (sea level) varies with wind stress such that upwelling favorable, easterly winds lead to lowered sea level over the mooring. The average height of the water column over the mooring is 12.85 m with deviations of +0.71 m (surge due to downwelling favorable winds) and -2.85 m (sea level set down due to upwelling favorable winds). The largest deviations in sea level occur in the fall, when strong storms pass through the region (e.g., Pickart, 2004) and sea level fluctuations are on the same order of water level fluctuations associated with the passage of hurricanes (Yankovsky, 2009). Note that in August of 2014 (start of the record), there is an extended period of low sea levels over the mooring (approaching -0.5 m of sea level change). This is a result of the persistent upwelling favorable winds that marked the 2014 cruise. In contrast in July 2015, the sea level record over the mooring is marked by several episodes of high sea level associated with downwelling favorable winds which helped push sea ice onto the shelf and elevated water levels along the coast.

TS show a strong seasonal cycle with maximum values of temperature in Sept. 2014 and August, 2015). Temperatures drop to the freezing point in ~November and remain at the freezing point until June, 2015. Salinities gradually increase throughout the record until they reach maximum, >35, values in March and April 2015. Salinities gradually decrease after this. Measurements are consistent with previous observations from the region (e.g., Weingartner et al., 2009).

The TS plot of the mooring data shows a mix of water masses at the site with river influenced shelf water dominating the record. Consistent with the episodes of high salinity water noted in the time series, newly ventilated water is also clearly forming locally; water with S>32 and at the freezing point, generated by brine rejection during sea ice formation, is clearly present at the mooring site. This water is most likely transported towards deeper water and the shelfbreak through density induced currents (e.g., Gawarkiewicz et al., 1998). This cross-shelf exchange mechanism is a means by which nearshore waters including their dissolved and suspended materials can be transported offshore.

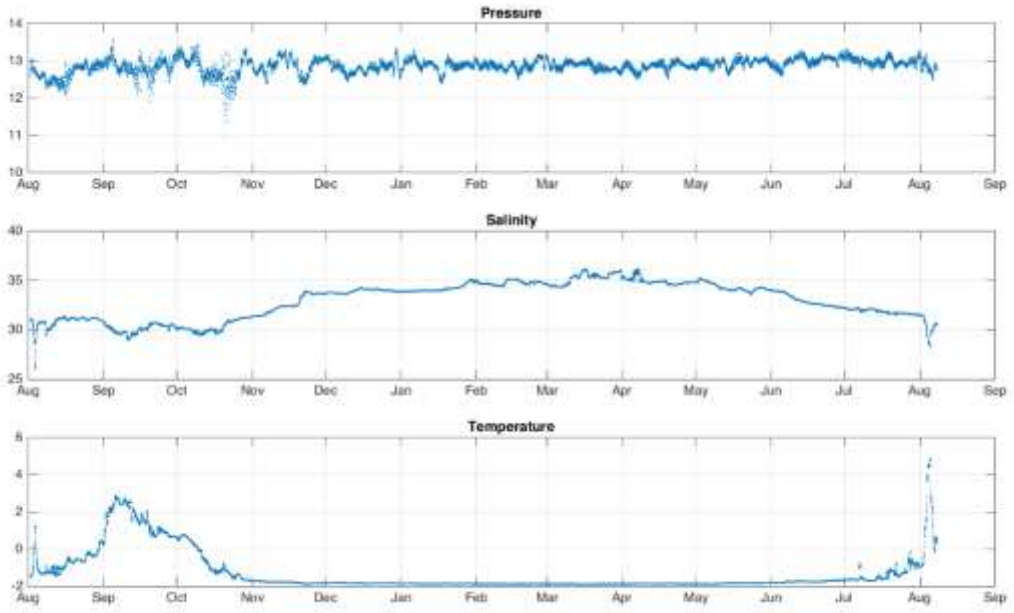


**Figure 57. Time series of pressure (water level), salinity, and temperature from the mooring record versus time.**

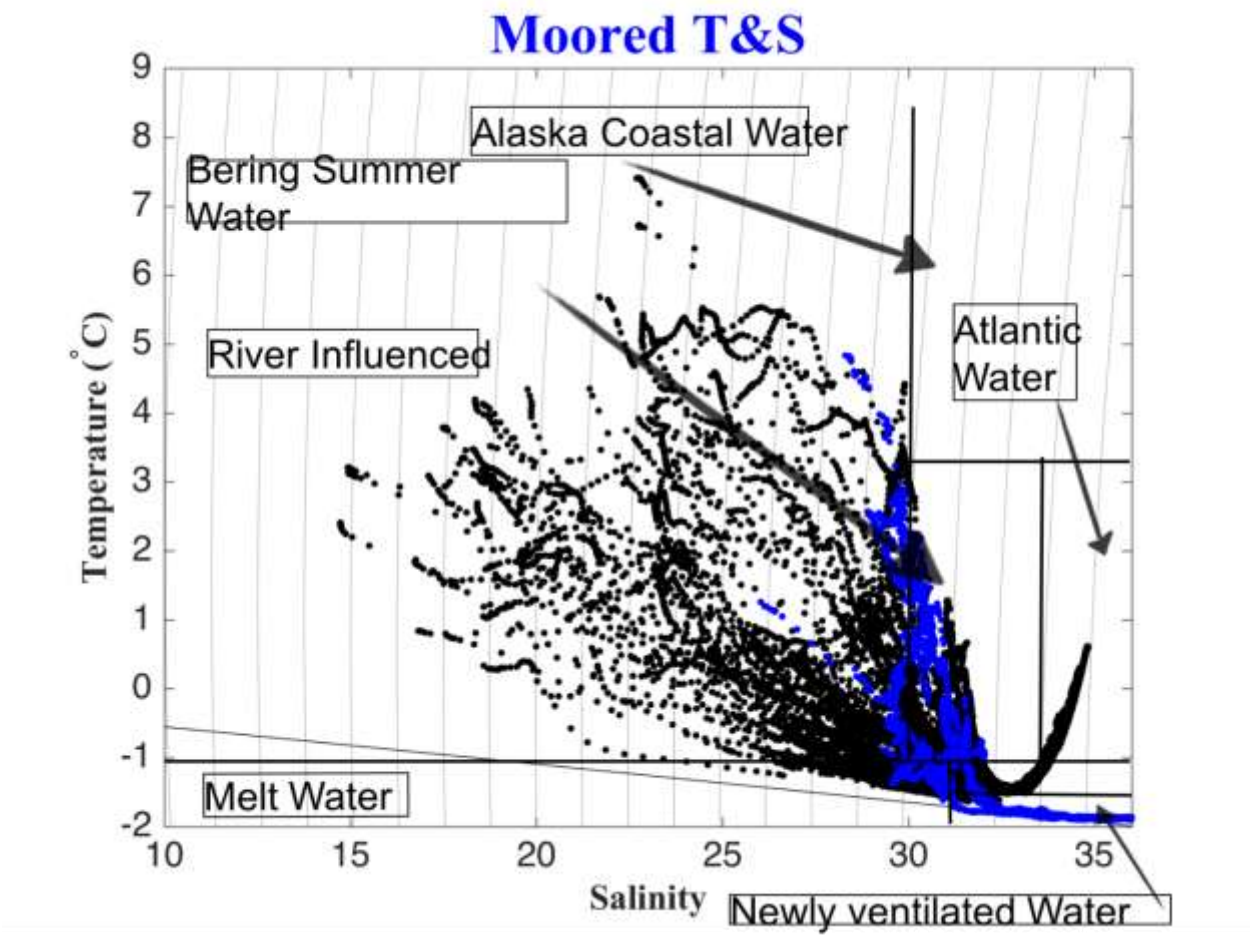


**Figure 58. Temperature (°C) versus salinity from the mooring record (blue) overlaid on 2014 and 2015 ANIMIDA CTD cast data.**

**The freezing point is indicated by the solid line between ~0.5 and 2 ºC.**

## 2.5 Summary and Conclusions

The central and eastern portions of the U.S. Beaufort Sea are essentially estuarine in character and are characterized by the presence of low nutrient, river influenced water masses at the surface. Nutrient concentrations and salinities increase with increasing distance from the coast and with depth. Temperatures vary with winds and depth; strong stratification can result in surface water temperatures up to 7 °C. The presence of ice that accompanies persistent downwelling favorable winds (winds from the West) generally leads to temperatures <2 °C and the concentration of fresh water against the coast. In both field years, Mackenzie River water was noted in the eastern portion of the sampling region; characterized by strong stratification and warm temperatures as well as elevated Ba levels.

The trend toward increasing nutrient concentrations with depth and distance from the coast is a result of the influence of shelfbreak water masses. These water masses are advected in an eastward flowing shelfbreak jet, a narrow and swift, bottom intensified current that forms the northern boundary of this shelf. Many of these shelfbreak water masses are derived from Pacific waters which are modified as they flow northward on the Chukchi shelf and eventually form the core of the Beaufort Sea shelfbreak jet. Frequent upwelling favorable winds (winds from the East) in the region reverse the eastward flowing jet (see Pickart et al., 2009) and upwell these water masses onto the Beaufort shelf along the bottom. As a result, nutrient concentrations along the outer Beaufort Sea shelf are comparable to values from the northern Chukchi shelf.

At the surface, the presence of numerous seasonally frozen rivers along the coast means that during the summer, surface waters are typically very fresh with salinities seasonally ranging from 0 to 30. Because surface waters can be strongly stratified, temperatures can exceed 6 °C and winds readily move these surface water masses across and along the shelf. As a result of differences in winds during the two ANIMIDA field seasons, surface water properties and sea ice conditions were very different between sampling years.

A moored record of water level (pressure), temperature, and salinity from ~13 m of water captures the extremes in hydrographic conditions that characterize the shelf, especially the nearshore, where temperatures at the bottom ranged from the freezing point to 5 °C. Salinities at the mooring ranged from 25 to >35. Measurements from the Colville Delta during the spring freshet in 2015 showed that surface waters in the nearshore are essentially fresh (S=0). Thus, conditions in the nearshore are extreme with salinities ranging from 0 to periods of hypersaline water with S>35.

The most saline conditions recorded by the mooring occurred in mid-winter likely during an episode when brine rejection from freezing was taking place near the mooring. Density currents that result from such extreme events are one mechanism nearshore water masses and their dissolved and suspended materials can be transported across the shelf and eventually into the shelfbreak jet. The Stamukhi zone (ridges of ice that become grounded during winter and remain attached to the ocean bottom through summer) is porous so does not prevent cross-shelf exchange of shelf waters (Kasper et al., 2012; Kasper unpub.).The pressure record from the mooring shows extremes in water levels due to differences in winds: water level deviations of +0.71 m (storm surge due to downwelling favorable winds) and -2.85 m (sea level set down due to upwelling favorable winds) were recorded during the year long record. In addition to illustrating the strong effect of winds on the shelf, such large fluctuations in sea level mean that low lying coastal ecosystems, which support numerous bird species, are subject to extremes in

conditions as well. Overall, the extreme variability in hydrography on the Beaufort Sea shelf defines the character of the shelf ecosystem.

These summer hydrographic measurements are a snapshot of shelf conditions and help illustrate the variability while the mooring record provides annual context. While chemical and biological studies in the summer provide important integrative measures of the fate and effects of terrestrial material and/or contaminants and their distribution across this shelf ecosystem, overall, the physical mechanisms and their variability remain poorly quantified. Measurements from this ANIMIDA campaign, as well as past efforts in the region, show that there is significant year to year to variability but seasonal variations remain unquantified because of limited, focused physical oceanographic sampling in the region. While the importance of freshwater to the shelf is well established, the frontal systems between fresh-river influenced water masses and offshore water masses are not understood at present. Frontal systems and the strong currents due to cross frontal density differences are ubiquitous mechanisms for rapidly moving suspended and dissolved materials across shelf ecosystems (O'Donnell, 2009; Winsor et al., 2014) though such processes have not been studied in the Beaufort Sea.

Cross-shelf transport of terrigenous material likely peaks during the fall storm period (e.g., Pickart et al., 2013) and there are very few physical measurements from this important period in the central and eastern regions of the shelf (e.g., Weingartner et al., 2009; Nikolopolous et al., 2009). There is also very strong evidence that physical conditions are changing rapidly with the decrease in sea ice. For example, surface gravity waves at lower latitudes are an important component of nearshore momentum balances (Lentz and Fewings, 2012), and mixing of river plumes (Thomson et al., 2014) and they play a critical role in the transport of material on lower latitude shelves. However, there are only limited wave measurements from the shallow Beaufort Sea shelf and regional modeling efforts do not currently include wave forcing. Surface gravity waves also play an important role in eroding the Beaufort Sea coast (Barnhart et al., 2014) which poses threats to coastal infrastructure but also affects the delivery of carbon to the nearshore. There is also increasing evidence that surface gravity waves are becoming increasingly important in the Beaufort Sea (Thomson et al., 2016). Since waves strongly affect mixing of freshwater, cross-shore transport of material and erosion, without an understanding of waves it is difficult to make accurate predictions about the fate and transport of material in the region.

## Acknowledgments

We thank Dan Holiday and Catherine Coon of BOEM, U.S. Department of Interior, for their interest and enthusiasm for the long-term monitoring of the Beaufort Sea. We also thank the crew, officers, and commanding officer of *Norseman II* for logistical and sampling support. This field and laboratory study was funded by the U.S. Department of the Interior, BOEM, Alaska Outer Continental Shelf Region, Anchorage, Alaska under Contract M13PC00019 as part of the ANIMIDA III project and the BOEM Alaska Environmental Studies Program.

## References


Barnhart K.R., Overeem I., and Anderson R.S. 2014. The effect of changing sea ice on the physical vulnerability of Arctic coasts. The Cryosphere, 8: 1777-1799. DOI: 10.5194/tc-8-1777-2014.

Bell L., Iken K., and Bluhm B. 2013. Trophic structure of benthic primary consumers on the U.S. Eastern Beaufort Sea shelf. Poster, Alaska Marine Science Symposium, January 2013, Anchorage, AK.

Carmack E., Winsor P., and Williams W. 2015. The contiguous panarctic Riverine Coastal Domain: A unifying concept. Progress in Oceanography, http://dx.doi.org/10.1016/j.pocean.2015.07.014.

Gawarkiewicz G., Weingartner, T., and Chapman D.C. 1998. Sea-ice processes and water mass modification and transport over Arctic Shelves. In: The Sea, Vol. 10, The Global Coastal Ocean: Processes and Methods , K. H. Brink and A. R. Robinson, editors, Wiley Interscience, New York, 171-190.

Gong D. and Pickart R.S. 2015. Summertime circulation in the Eastern Chukchi Sea. Deep-Sea Research II 105, 53-73.

Grebmeier J. and Cooper L. 2014. PacMARS Bottom Water Nutrients (1988–2012), Version 1.0. http://dx.doi.org/10.5065/D6MW2F69; available at the PacMARS EOL data archive site <http://pacmars.eol.ucar.edu>.

Guay C. K. and Falkner K.K. 1998. A survey of dissolved barium in the estuaries of major Arctic rivers and adjacent seas, Continental Shelf Research, 18, 859-882.

Kasper J., Pickart R., and Weingartner T., 2012 Impact of ice cover on wind-forced exchange in the Alaskan Beaufort Sea, Ocean Sciences Meeting Abstracts.

Lentz S. J. and Fewings M.R. 2012, The wind-and wave-driven inner-shelf circulation. Annual Review of Marine Science, 4, 317-343, doi: 10.1146/annuvrev-marine-120709-142745.

Logerwell E., Rand K., and Weingartner, T.J. 2011. Oceanographic characteristics of the habitat of benthic fish and invertebrates in the Beaufort Sea. Polar Biol 34: 1783. doi:10.1007/s00300-011-1028-8

Okkonen S., Clarke J., and Potter R. 2016. Relationships among high river discharges, upwelling events, and bowhead whale (*Balaena mysticetus*) occurrence in the central Alaskan Beaufort Sea, Deep Sea Research, in press, http://dx.doi.org/10.1016/j.dsr2.2016.11.015

O'Donnell J. 2009. The Dynamics of Estuary Plumes and Fronts. In "Contemporary Issues in Estuarine Physics, A. Valle Levinson, (Edt). Cambridge University Press.

Nikolopoulos A., Pickart R.S., Fratantoni P.S., Shimada K., Torres D.J., and Jones E.P. 2009. The western arctic boundary current at 152◦W: Structure, variability, and transport. Deep Sea Res. II , 56, 1164–1181.

Pickart R. S. 2004. Shelfbreak circulation in the Alaskan Beaufort Sea: Mean structure and variability. Journal of Geophysical Research, 109, (C4), C04024 10.1029/2003JC001912.

Pickart R.S, Schulze L.M., Moore G.W.K., Charette M.A, Arrigo K., van Dijken G., and Danielson S. 2013. Long–term trends of upwelling and impacts on primary productivity in the Alaskan Beaufort Sea Deep Sea Research I, 79, 106-121.

RD Instruments. 1989. Acoustic Doppler Current Prolers Principles of Operation: A Practical Primer. Available from RD Instruments, 9855 Businesspark Av., San Diego, CA 92131.

Rand K.M. and Logerwell E.A. 2011. The first demersal trawl survey of benthic fish and invertebrates in the Beaufort Sea since the late 1970s. Polar Biol. 34:475-488

Ravelo A.M., Konar B., and Bluhm B.A. 2015. Spatial variability of epibenthic communities on the Alaska Beaufort Shelf Polar Biology. doi: DOI 10.1007/s00300-015-1741-9

Rember R.D. and Trefry J. H. 2004 Increased concentrations of dissolved trace metals and organic carbon during snowmelt in rivers of the Alaskan Arctic. Geochimica et Cosmochimica Acta, 68, doi:10.1016/S0016-7037(03)00458-7

Schulze L. M. and Pickart R. S. 2012. Seasonal variation of upwelling in the Alaskan Beaufort Sea: Impact of sea ice cover. J. Geophys. Res., 117, C06022, doi:10.1029/2012JC007985.

Thomson J., Horner-Devine A. R., Zippel S., Rusch C., and Geyer W. 2014. Wave breaking turbulence at the offshore front of the Columbia River Plume, Geophys. Res. Lett., 41, 8987–8993, doi:10.1002/2014GL062274.

Thomson J., Fan Y., Stammerjohn S., Stopa J., Rogers W.E., Girard-Ardhuin F., Ardhuin F., Shen H., Perrie W., Shen H., Ackley S., Babanin A, Liui Q., Guestk P., Maksym T., Wadhams P., Fairall C., Persson O., Doble M., Graber H., Lund B., Squires V., Gemmrich G., Lehner S., Holt B., Meylan M., Brozena J., and Bidlot J. 2016: Emerging trends in the sea state of the Beaufort and Chukchi Seas. Ocean Modell., 105, 1–12, doi:10.1016/j.ocemod.2016.02.009.

von Appen, Wilken-Jon and Pickart R. S. 2012: Two Configurations of the Western Arctic Shelfbreak Current in Summer. Journal of Physical Oceanography, 42.

Weingartner T. J., Danielson S., Kasper J., and Okkonen, S., 2009. Circulation and water property variations in the nearshore Alaskan Beaufort Sea (1999–2007). U.S. Dept. of Interior, Minerals Management Service, Alaska Outer Continental Shelf Region, Anchorage, AK, 154 pp.

Whitledge T.E., Malloy S.C., Patton C.J., and Wirick C.D. 1981. Automated nutrient analyses in seawater. Brookhaven National Laboratory Technical Report BNL 51398.

Winsor P., Weingartner T.J., Kasper J.L., Statscewich H., and Potter R.A. 2014 High-Resolution Hydrography of The Northeastern Chukchi Sea from AUV Gliders and Towed CTD Surveys – The Alaska Coastal Current, Upwelling and Fronts. Ocean Sciences Meeting, Oral presentation.

Yankovsky A. E., 2009. Large-scale edge waves generated by hurricane landfall, J. Geophys. Res., 114, C03014, doi:10.1029/2008JC005113.

# Chapter 3 Trace Metals in Bottom Sediments, Suspended Sediments and Biota


## Abstract

As part of the ANIMIDA III Project, data for trace metals in bottom sediments, suspended particles, and marine biota were used to identify any recent spatial or temporal changes in concentrations of potentially toxic metals in the coastal Beaufort Sea. Concentrations of 17 trace metals (Ag, As, Ba, Be, Cd, Cr, Cu, Hg, Mn, Ni, Pb, Sb, Se, Sn, Tl, V, and Zn) in 63 surface sediment and 300 sediment core samples collected during 2014 and 2015 were essentially all at natural, baseline values. Previously established background ratios of metals/Al in sediments were used to identify any sediment metal values that were anomalous. Four anomalies (concentrations above baseline) were observed for Ba and single anomalies were identified for Be, Hg, Sb, V, and Zn during ANIMIDA III. All concentrations of the potentially toxic metals Ag, Cd, Hg, Pb, and Zn were below published sediment quality criteria. At offshore locations (water depths >200 m), concentrations of As, Mn, and Hg were very high in some surface sediments from offshore at water depths of ~200-800 m; these deviations were linked to subsurface, diagenetic remobilization of these metals with subsequent reprecipitation and enrichment in surface sediments. Concentrations of total suspended solids during August 2014 ranged from 0.13-6.1 mg/L and averaged 1.1 mg/L. Particulate Ba/Al ratios in these particles were within 2% of values for bottom sediments and provide a well-defined marker for tracing dispersion of discharged drilling fluids in the water column. In contrast with Ba, particulate Fe/Al ratios were ~80% greater than in bottom sediments in support of sorption of iron oxides and scavenged metals on suspended particles. Concentrations of the same 19 metals were determined for clams (*Astarte* sp.) and amphipods (*Anonyx* sp.) collected during 2014 and 2015. Results showed a variety of patterns and are presented and discussed here to provide a baseline for future assessments.


## 3.1 Introduction

Trace metals are effective indicators of impacts from industrial activity because they are generally enriched in the raw and finished materials used by modern industry. Barite ($BaSO_4$), for example, is a primary component of fluids used during petroleum drilling operations; concentrations of Ba in these fluids are often 100–500 times greater than baseline Ba values in Beaufort Sea sediments (Trefry et al., 2003, 2013). Other metals from industrial and other human activities also can be concentrated in bottom sediments where they are often sensitive indicators of cumulative inputs from a variety of anthropogenic sources.

Thirty exploratory wells were drilled in State/Federal and Federal lease tracts managed by the Minerals Management Service (MMS) in the Beaufort Sea Program Area between 1981 and 2002; most of them were in the Development Area at water depths of 5.5 to 51 m (BOEM, 2016). Several hundred exploratory and development wells also were drilled in State lease tracts on the shore, on barrier islands, and in shallow waters along the central Beaufort Sea coast (Alaska Department of Natural Resources [ADNR], 2009). Construction of Northstar began in 1999, oil production commenced in 2001; no drilling fluid or other discharges from Northstar were permitted.

Earlier studies of metals in sediments from the coastal Beaufort Sea showed that concentrations were quite variable, but generally at natural levels with minimal localized inputs from development (Sweeney and Naidu, 1989; Snyder-Conn et al., 1990; Crecelius et al., 1991; Naidu et al., 2001, 2012; Valette-Silver et al., 1999; Trefry et al., 2003). Snyder-Conn et al. (1990), for example, identified elevated concentrations of Ba, Cr, Pb, and Zn in areas adjacent to one or more disposal sites for drilling effluent. Crecelius et al. (1991) found elevated Ba values at a few sites in western Harrison Bay and Cr enrichment near the mouth of the Canning River, but no other indications of metal contamination. Within 250 m of two historic (1985-86) drill sites in Camden Bay, Trefry et al. (2013) found numerous stations with elevated concentrations of Ba in sediment, plus a few instances of anomalous Cr, Cu, Hg, and Pb values.

The objectives of this component of the ANIMIDA III Project were as follows: (1) to determine concentrations of trace metals in sediments and identify any recent inputs of anthropogenic origin, (2) expand the geographical database for metals in surface and subsurface sediments farther offshore where future drilling may occur, (3) determine concentrations of Ba and other selected elements in suspended particles with a focus on using data for suspended particles to trace of discharges of drilling fluids and other components, and (4) test for any significant changes in metals in marine biota while continuing to build a database for future use.

## 3.2 Methods

### 3.2.1 Study Area

The study area for this project was the coastal Beaufort Sea (Figure 59) from western Harrison Bay (~152 ˚W) to east of Kaktovik at ~142 ˚W. This region overlaps with the area previously studied as part of the BSMP (1984–1989), ANIMIDA (1999–2003), and continuation of ANIMIDA (cANIMIDA, 2004-2007) Projects. The provenance of sediments in the study area includes the Colville, Kuparuk, and Sagavanirktok Rivers as well as coastal erosion. The Brooks Range, 100 to 150 kilometer (km) south of the Beaufort Sea, and the broad coastal plain are a major source for river-borne sediments that include Cretaceous and Tertiary sandstones, conglomerates and siltstones, shale from Triassic to Pennsylvanian Ages, and Quaternary riverine and marine sediments that underlie the coastal plain (Payne et al., 1951). The Colville River is the largest river in northern Alaska with a drainage basin of ~50,000 square kilometers ($km^2$) and an annual sediment load of 5–10 million metric tons (Arnborg et al., 1967; Naidu and Mowatt, 1974).

The inner shelf of the Beaufort Sea descends gradually from the shoreline to a water depth of 30 m and is interrupted nearshore by sandbars and narrow gravel and sand barrier islands. The sediments in the study area are a patchwork of sand, silty-sand, and silty-clay (Naidu et al., 2001; Trefry et al., 2003; Brown et al., 2010). Clay size (<2 μm) sediments make up an average of 13 ± 9% of the sediments on the inner shelf (Crecelius et al., 1991). The sand- and silt-rich sediment on the shelf is generally <5 m thick (Reimnitz and Barnes, 1974). Sediment deposition is patchy (Weiss and Naidu 1986; Naidu et al., 2001, Trefry et al., 2003); Reimnitz and Wolf (1998) suggest that the entire area is a net erosional environment during the Holocene.

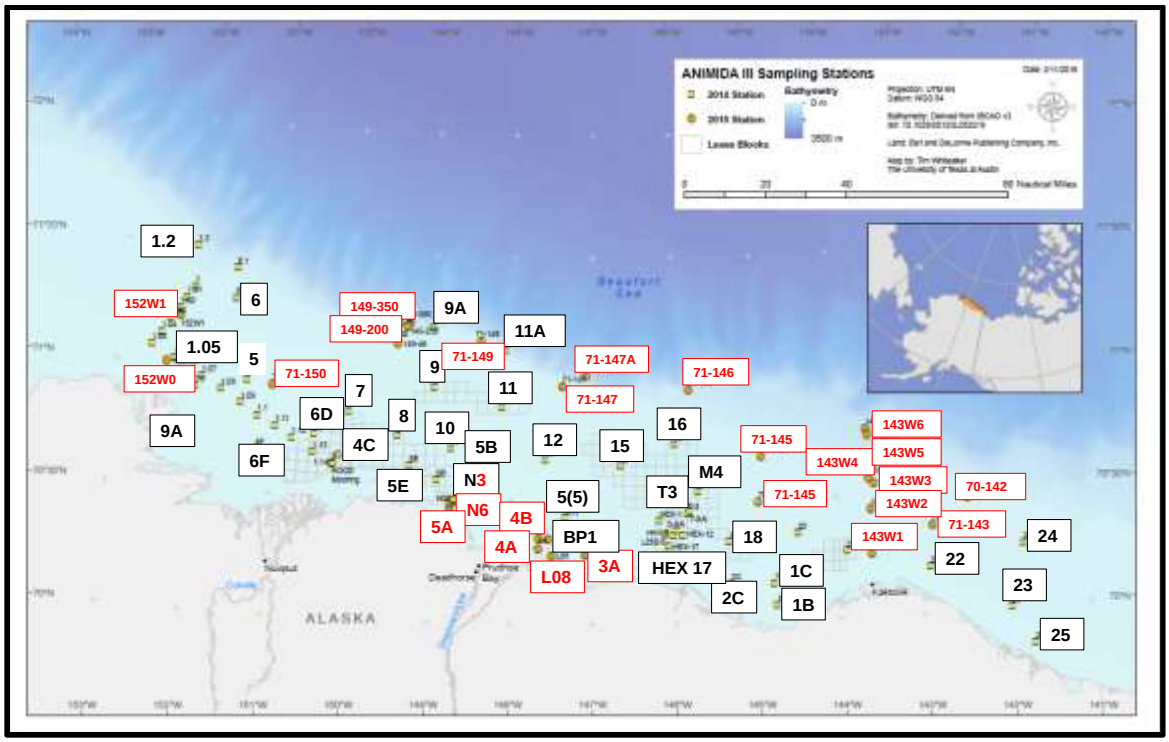


**Figure 59. Sampling stations for field surveys during 2014 (in black font) and 2015 (in red font) for the ANIMIDA III Project in the Beaufort Sea.**

**Inset map shows location of study area along the northern coast of Alaska. The following six stations from the 2014 survey were located between stations T3 and HEX 17: HH1-5, HEX 1, HEX 12, S-XA, T-XA and L250-5). N3 was sampled both years.**

### 3.2.2 Sample Collection

Sampling for sediment and biota were carried out during August 2014 and 2015 using the R/V *Norseman II*. Stations were selected by (1) returning to stations previously sampled during the ANIMIDA (1999–2003) and cANIMIDA (2004–2006) Projects and (2) choosing new locations using a probability-based, hexagonal grid approach of White et al. (1992) to ensure random selection with an even distribution of sites. Sediment sampling was conducted at 43 stations in 2014 and 20 stations in 2015 (Figure 59, Table 3). Sediment cores were collects at 5 different locations in 2014 and 2015 (for 10 total cores, Figure 59, Table 3). Surface sediments were collected using a pre-cleaned, double van Veen grab that obtained two side-by-side samples, each with a surface area of 0.1 $m^2$ and a depth of ~15 cm. Samples (top 1 cm) were carefully collected from one of the two grabs and placed in separate containers for metals, organic carbon (C), and grain size. The companion grab was used for sampling benthic biota. A Benthos gravity core with a 1-m long barrel and 7.5-cm diameter plastic liner was deployed for sediment coring. Cores were split into 1- to 2-cm thick layers aboard ship under clean conditions. All sediments samples, except those for grain size analysis, were frozen shipboard.

**Table 3. Summary of sediment, water and biota samples collected for metals.**

| 2014 | Surface Sediments | Sediment Cores with (# sections) | Water Samples (# stations) | Biota (# stations) |
|---|---|---|---|---|
| # of samples | 43 (0-1 cm) | 5 (150) | 77 (23) | 26 (20) |
| Stations sampled | 1B, 1C, 1.05, 1.2, 2C, 4, 4C, 5, 5B, 5E, 5(5), 6, 6.1, 6D, 6F, 7, 7C, 8, 9, 9A, 10, 11, 11A, 12, 15, 16, 18, 20, 21, 22, 23, 24, 25, HEX-1, L250-5, HEX-17, HEX-12, HH1-5, M-4, N03, S-XA, T-3, T-XA | 1C, 1.2, 6.1, 9A, 11A | 5, 6, 6D, 6F, 7, 7C, 8, 9, 10, 11, 5(5), L250-5, T3, 20, 21, 22, 23, 24, 25, 1C, 1.05, 16, 15, 12 | 1.05, 5, 5B, 5(5), 6, 6D, 7, 7C, 8, 10, 12, 15, 16, 20, 21, 22, 23, 24, 25, T-3 |
| **2015** | **Surface Sediments** | **Sediment Cores with (# sections)** | **Water Samples** | **Biota (# stations)** |
| # of samples | 20 (0-1 cm) | 5 (150) | None | 12 (9) |
| Stations sampled | N03, N06, 3A, 5A, 70-142, 70-143, 70-145, 71-145, 71-146, 71-147, 71-149, 71-149-350, 71-150, 143-W1, 143-W2, 143-W4, 143-W5, 149-200, 152-W0, 152-W1 | 71-146, 71-147A, 143-W5, 143-W6, 149-350 | None | 3A, 70-143, 70-145, 71-147, 71-148, 71-149, 143-W1, 152-W0, 152-W1 |

Water column samples for suspended particles were collected at 23 stations (77 samples) in 2014 (Figure 59, Table 3). These samples were collected using a 5-L Teflon-lined Niskin bottle with external closure. Samples were vacuum filtered through polycarbonate filters (Poretics, 47-mm diameter, 0.4-µm pore size) in a laminar flow hood aboard ship immediately after collection. Filters had been pre-washed in 5N $HNO_3$ and rinsed three times using 18 MΩ-cm DIW and then weighed three times to the nearest µg under cleanroom conditions at FIT. Precision for replicate filtrations averaged <4% (i.e., <0.04 mg/L). Particle-bearing filters were sealed in acid-washed petri dishes, labeled and then double-bagged in plastic and stored until dried and re-weighed at FIT. Samples for POC were filtered through pre-combusted Gelman Type A/E glass fiber filters mounted on acid-washed filtration glassware within a Class-100 laminar-flow hood.

Clams and amphipods were collected by rake and baited traps, respectively. Whole clams and amphipods were rinsed with deionized water immediately after collection and stored frozen until laboratory analysis.

### 3.2.3 Laboratory Methods

Total concentrations of Ag, Al, As, Ba, Be, Cd, Cr, Cu, Fe, Hg, Mn, Ni, Pb, Re, Sb, Se, Sn, Tl, V, Zn and organic carbon were determined for 63 surface sediments and 300 samples from 10 sediment cores (Figure 59, Table 3). Sediment samples for metal analysis were homogenized and a wet portion was set aside for Hg analysis. The remaining sediment was freeze-dried to provide percent water content and dry sediment for acid digestion for other metals. A separate, wet sediment sample from each location was used for grain size analysis.

Sediment samples for metal analysis, except Hg, were homogenized, completely digested in Fisher Trace Metal Grade HF, $HNO_3$, and hydrochloric acid (HCl) and analyzed for Al, Cr, Cu, Fe, Mn, V, and Zn using a Perkin-Elmer Model 4000 atomic absorption spectrometer (AAS) and for Ag, As, Ba, Be, Cd, Ni, Pb, Sb, Se, Sn, and Tl using a Varian Model 820-MS inductively coupled plasma mass spectrometer (ICP-MS) according to established laboratory methods (Trefry et al., 2003, 2013). Standard reference material (SRM) #2709 (soil with certified Ba value) from the National Institute of Standards and Technology (NIST) was processed with each batch of samples; all concentrations were within the

95% confidence intervals for certified values. Analytical precision ranged from 1% (Al, Cu, Fe, and Pb) to 4% (Hg). Method detection limits were 25 (Cu) to >5,000 (Ba, Pb) times lower than the lowest value obtained for field samples.

Sediment digestion for Hg was carried out using high-purity $HNO_3$ and $H_2SO_4$ (Trefry et al., 2007). The sediment Certified Reference Material (CRM) MESS-3 from the National Research Council of Canada (NRC) was digested and analyzed with each group of sediment samples. The sediment digestions included MESS-3 and the SRM #2709 from the NIST. Analysis was by cold-vapor AAS (Trefry et al., 2007).

Sediment total organic carbon (TOC) concentrations were determined by treating freeze-dried sediment with 10% HCl to remove inorganic carbon, followed by high-temperature combustion and infra-red carbon dioxide ($CO_2$) quantification using a Leco TruMac Analyzer© and following methods provided by the manufacturer. All values obtained for the CRM (Leco CRM 502-309©) were within the 95% confidence interval for certified values. Laboratory precision for TOC was 6%. Grain size analyses of surface sediment samples were carried out using the classic method of Folk (1974) that includes a combination of wet sieving and pipette techniques.

Suspended sediments were analyzed for metals following the sample preparation and analysis techniques of Trefry and Trocine (1991). The POC content was determined using acid-treated samples of filtered particles that were combusted in ceramic boats at 900ºC using the Leco TruMac© as described above. Precision was 1.6% and results for the CRM MESS-2, marine sediment issued by the NRC were within the 95% confidence limits for the certified value.

Freeze-dried tissue samples were homogenized and completely digested in Fisher Trace Metal Grade $HNO_3$ and hydrogen peroxide ($H_2O_2$) and analyzed for Cu, Fe, Mn, and Zn using a Perkin-Elmer Model 4000 AAS, for THg using a Laboratory Data Control cold vapor AAS and for other metals by ICP-MS according to established laboratory methods (Trefry et al., 2007, 2013; Fox et al., 2014). SRM #1566b (oyster tissue) from the NIST was processed with each batch of samples; all values were within the 95% confidence intervals for the certified values. Analytical precision was better than 6% for all analytes.

Tissue samples for monomethyl mercury (MMHg, no dimethyl mercury was detected) analysis were digested using an acid bromide/methylene chloride extraction. The aqueous phase was analyzed using ethylation, isothermal gas chromatography separation and detection by cold vapor atomic fluorescence spectrometry based on methods from Bloom and Crecelius (1983) and Bloom (1989). The certified reference material DORM-3 from the NRC was processed with each batch of samples and all values were within the 95% confidence interval for the certified value. Analytical precision was better than 7% for lab replicates. Concentration data for metals in biota are reported on a d. wt. basis to account for variability in water content among species.

## 3.3 Results and Discussion

### 3.3.1 Metal Distributions in Sediments

Data from 63 stations along the coastal Beaufort Sea show that sediments were a patchwork of sands, silty-sands, and silty-clays (Table 4). Concentrations of TOC also were variable with a range from 0.25% nearshore (e.g., station 5E) to ~2.4% in nearshore peat-bearing sediments (e.g., station 3A, Table 5, Table 6). In deeper (>200 m) offshore sediments, TOC was typically ~1.2-1.3%. Concentrations of

sediment Al, a proxy for clay minerals, were as low as 1.4% nearshore (e.g., station 5B) to 7.8% offshore (e.g., station 71-146 at a water depth of 400 m, Table 5, Table 6).

Data for metals from the present study (Table 5, Table 6) agree well with and complement previous results (Trefry et al., 2003, 2013; Brown et al., 2010). Large ranges in concentrations for each metal were found throughout the study area with maximum/minimum values that varied from ~3 for Be to 17 for Mn (Table 5, Table 6). Concentrations of Al and other trace metals correlated well with concentrations of silt + clay because concentrations of both Al and most metals are very low in coarse-grained quartz sand or carbonate shell material and much higher in fine-grained aluminosilicates. Concentrations of sediment Al have been previously shown to correlate strongly ($r = 0.7–0.9$) or very strongly ($r > 0.9$) with clay content and concentrations of selected trace metals in the coastal Beaufort Sea (Trefry et al., 2003, 2013; Brown et al., 2010). Aluminum is rarely introduced by anthropogenic activities and is present at percent levels in most sediment relative to part per million (ppm or µg/g) for trace metals. Thus, concentrations of trace metals were normalized to Al (i.e., use of metal/Al ratios) as a proxy for the metal controlling variables of grain size, organic carbon content and mineralogy.

All concentrations of Cr, Ni, and Pb for sediment samples collected during 2014 and 2015 plotted within the 99% prediction intervals developed during the ANIMIDA Project with data from 1999-2001 (Figure 60). Previous outlying data points for Cr, Ni, and Pb were linked with the presence of trace amounts of metal-rich sulfides and other heavy minerals in nearshore sand and gravel or anthropogenic contamination (Brown et al., 2010). No anomalous data points on metal versus Al graphs from the 2014 and 2015 surveys were found for Ag, Cd, Cu, and Tl (Table 7).

Barium concentrations plotted well above the upper prediction interval on the Ba versus Al plot for stations 70-145 and 143-W2 (Figure 61A). These two stations are located in the eastern area of Camden Bay (Figure 59). One previous study in Camden Bay found Ba concentrations as high as 140,000 µg/g near the location of a 1985 oil drilling site (Trefry et al., 2013). The two stations sampled in 2015 with elevated Ba values (stations 70-145 and 143-W2) were ~20 and 50 km east of the drill site from the 1980s. Sediment transport of Ba-rich sediment from western Camden Bay is one possible explanation for the higher Ba values. No sediments cores were collected at either location; therefore, the vertical extent of the Ba enrichment in unknown. Barium values also were above baseline values for stations 71-147 and 71-149 (Figure 61A); these anomalies may be due to diagenetic remobilization of Ba as reported by numerous authors (e.g., Riedinger et al., 2006).

**Table 4. Grain size for surface sediments from ANIMIDA III Project for 2014 and 2015.**

| Surface Sediment | Statistic | Gravel (%) | Sand (%) | Silt (%) | Clay (%) | Silt + Clay (%) |
|---|---|---|---|---|---|---|
| **2014** | | | | | | |
| Cumulative (0-1 cm) | Mean | 5.4 | 43.1 | 27.9 | 23.1 | 51.0 |
| | Standard Deviation | 12.5 | 25.6 | 15.1 | 11.9 | 25.1 |
| | n | 43 | 43 | 43 | 43 | 43 |
| | Maximum | 61.9 | 96.3 | 60.7 | 47.1 | 97.0 |
| | Minimum | 0.0 | 0.7 | 1.1 | 2.4 | 3.7 |
| | Median | 0.5 | 36.9 | 29.2 | 25.1 | 57.3 |
| **2015** | | | | | | |
| Cumulative (0-1 cm) | Mean | 9.3 | 33.1 | 31.1 | 26.5 | 57.5 |
| | Standard Deviation | 20.8 | 28.9 | 20.0 | 15.0 | 32.9 |
| | n | 23 | 23 | 23 | 23 | 23 |
| | Maximum | 75 | 94 | 66 | 50 | 100 |
| | Minimum | 0 | 0 | 2 | 3 | 6 |
| | Median | 0 | 28 | 32 | 26 | 63 |

**Table 5. Concentrations of metals and total organic carbon (TOC) in surface sediments from ANIMIDA III Project for 2014.**

| Surface Sediment | Statistic | Ag (µg/g) | Al (µg/g) | As (µg/g) | Ba (µg/g) | Be (µg/g) | Cd (µg/g) | Cr (µg/g) | Cu (µg/g) | Fe (µg/g) | Hg (µg/g) |
|---|---|---|---|---|---|---|---|---|---|---|---|
| Cumulative (0-1 cm) | Mean | 0.16 | 5.04 | 15.4 | 537 | 1.26 | 0.22 | 73.7 | 18.9 | 2.94 | 0.040 |
| | Standard Deviation | 0.04 | 1.42 | 6.9 | 130 | 0.27 | 0.05 | 19.1 | 6.2 | 0.75 | 0.016 |
| | n | 43 | 43 | 43 | 43 | 43 | 43 | 43 | 43 | 43 | 43 |
| | Maximum | 0.28 | 7.07 | 50.6 | 810 | 1.56 | 0.32 | 103 | 30.0 | 4.88 | 0.090 |
| | Minimum | 0.05 | 1.44 | 7.3 | 162 | 0.51 | 0.06 | 20.1 | 4.8 | 1.16 | 0.006 |
| | Median | 0.16 | 5.51 | 14.7 | 574 | 1.35 | 0.23 | 77.1 | 20.0 | 30.2 | 0.043 |
| **Surface Sediment** | **Mean** | **Mn (µg/g)** | **Ni (µg/g)** | **Pb (µg/g)** | **Sb (µg/g)** | **Se (µg/g)** | **Sn (µg/g)** | **Tl (µg/g)** | **Va (µg/g)** | **Zn (µg/g)** | **TOC (%)** |
| Cumulative (0-1 cm) | Standard Deviation | 417 | 30.7 | 12.1 | 0.51 | 0.93 | 1.85 | 0.43 | 119 | 79.9 | 1.07 |
| | n | 43 | 43 | 43 | 43 | 43 | 43 | 43 | 43 | 43 | 43 |
| | Maximum | 797 | 45.8 | 16.2 | 0.76 | 1.60 | 3.67 | 0.57 | 174 | 115 | 2.28 |
| | Minimum | 172 | 10.5 | 4.82 | 0.21 | 0.38 | 0.46 | 0.13 | 30.8 | 26.4 | 0.25 |
| | Median | 383 | 32.0 | 12.9 | 0.52 | 0.92 | 1.91 | 0.47 | 125 | 86.3 | 1.07 |

**Table 6. Concentrations of metals and total organic carbon (TOC) in surface sediments from ANIMIDA III Project for 2015.**

| Surface Sediment | Statistic | Ag (µg/g) | Al (µg/g) | As (µg/g) | Ba (µg/g) | Be (µg/g) | Cd (µg/g) | Cr (µg/g) | Cu (µg/g) | Fe (µg/g) | Hg (µg/g) |
|---|---|---|---|---|---|---|---|---|---|---|---|
| Cumulative (0-1 cm) | Mean | 0.10 | 5.51 | 25.1 | 734 | 1.60 | 0.18 | 79.5 | 21.9 | 3.38 | 0.050 |
| | Standard Deviation | 0.03 | 1.60 | 24.0 | 417 | 0.40 | 0.005 | 17.9 | 7.2 | 1.2 | 0.018 |
| | n | 20 | 20 | 20 | 20 | 20 | 20 | 20 | 20 | 20 | 20 |
| | Maximum | 0.15 | 7.78 | 116 | 2210 | 2.64 | 0.30 | 106 | 36.9 | 6.94 | 0.077 |
| | Minimum | 0.05 | 2.03 | 9.21 | 405 | 0.74 | 0.11 | 43.5 | 6.4 | 1.69 | 0.011 |
| | Median | 0.11 | 5.12 | 17.0 | 644 | 1.58 | 0.18 | 73.9 | 22.0 | 2.97 | 0.049 |
| **Surface Sediment** | **Statistic** | **Mn (µg/g)** | **Ni (µg/g)** | **Pb (µg/g)** | **Sb (µg/g)** | **Se (µg/g)** | **Sn (µg/g)** | **Tl (µg/g)** | **Va (µg/g)** | **Zn (µg/g)** | **TOC (%)** |
| Cumulative (0-1 cm) | Mean | 802 | 33.5 | 15.2 | 0.62 | 0.93 | 1.54 | 0.50 | 140 | 96.4 | 1.20 |
| | Standard Deviation | 891 | 8.8 | 3.8 | 0.17 | 0.42 | 0.42 | 0.14 | 42 | 21.5 | 0.51 |
| | n | 20 | 20 | 20 | 20 | 20 | 20 | 20 | 20 | 20 | 20 |
| | Maximum | 3990 | 48.2 | 20.6 | 1.17 | 1.88 | 2.12 | 0.74 | 211 | 130 | 2.36 |
| | Minimum | 231 | 17.0 | 8.06 | 0.40 | 0.39 | 0.64 | 0.17 | 64 | 53.6 | 0.30 |
| | Median | 532 | 32.3 | 14.6 | 0.58 | 0.78 | 1.50 | 0.49 | 133 | 89.9 | 1.11 |

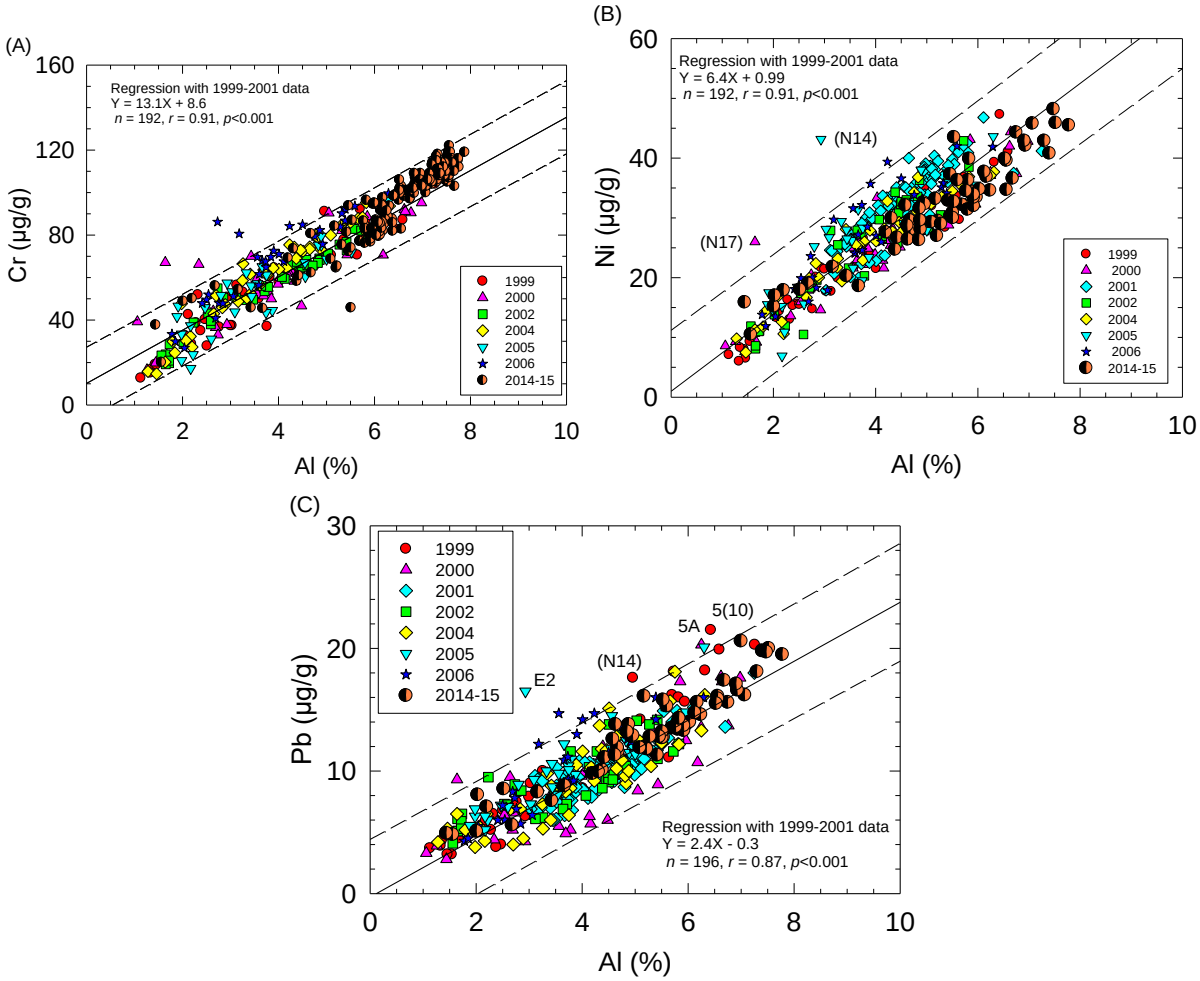


**Figure 60. Concentrations of Al versus (A) Cr, (B) Ni, and (C) Pb for surface sediments collected during 2014 and 2015 (ANIMIDA III) and previous surveys in the coastal Beaufort Sea.**

**Solid lines and equations show linear regression fit to data from 1999-2001 (ANIMIDA Project, Trefry et al., 2003), dashed lines show 99% prediction intervals, *r* is the correlation coefficient, and *p* is the statistical *p* value.**

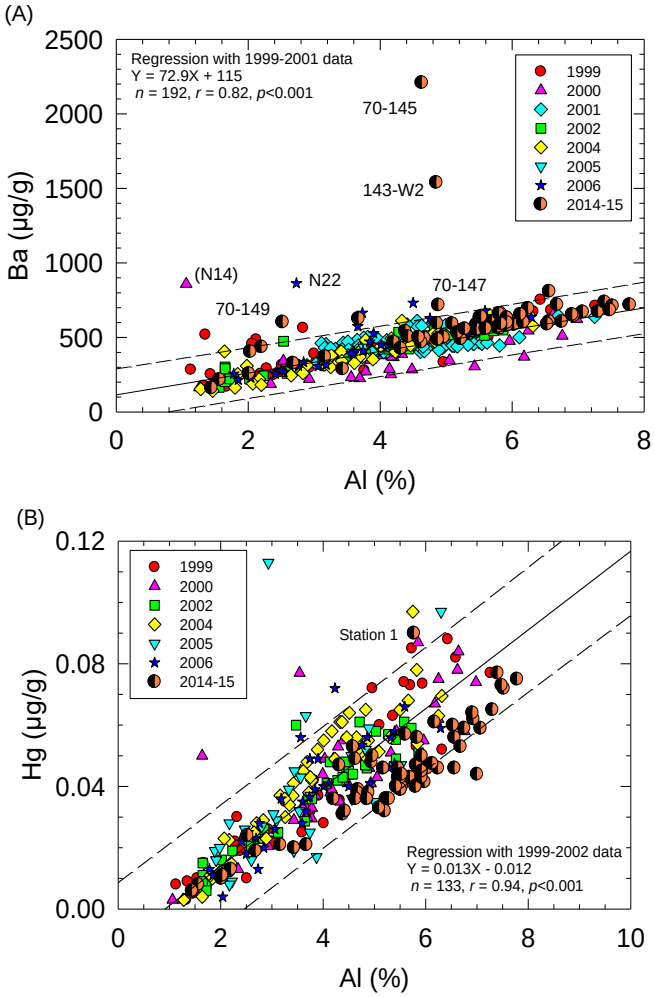


**Figure 61. Concentrations of Al versus (A) Ba and (B) Hg for surface sediments collected during 2014 and 2015 (ANIMIDA III) and previous surveys in the coastal Beaufort Sea.**

**Solid lines and equations show linear regression fit to data from 1999-2001 (ANIMIDA Project, Trefry et al., 2003), dashed lines show 99% prediction intervals, *r* is the correlation coefficient, and *p* is the statistical *p* value.**

Single point anomalies from the 2014-15 (ANIMIDA III) sampling were observed for Be, Hg, Sb, V, and Zn (Table 7; Hg in Figure 61) sources of these anomalies are unknown and may be due to diagenesis or anthropogenic inputs. More numerous exceptions to the anomalies described above were observed for As and Mn (Figure 62) due to diagenetic remobilization of these metals followed by enrichment in the surface sediment layers due to oxidative precipitation (Trefry et al., 2014); these anomalies are described in more detail below with introduction of vertical profiles for sediment metals. All concentrations of the potentially toxic metals (Ag, Cd, Cu, Hg, Pb, and Zn) were below published sediment quality criteria (Table 7).

Vertical profiles for metals in sediment in the Beaufort Sea study area showed two trends. The most common trend was essentially straight vertical profiles for the metal/Al ratio with very little variation (Figure 63). Uniform metal/Al ratios throughout the cores were found for most metals, including Ba (Figure 63D, G), Pb (Figure 63B, E, H), and most Hg profiles (Figure 63I). This same observation was previously described for the coastal Beaufort Sea (Trefry et al., 2003; Brown et al., 2010). These sediment cores likely record decades to centuries of uniform metal/Al ratios with no detectable anthropogenic or diagenetic modification. Although mixing can mute anthropogenic or diagenetic anomalies, such alteration, if any, must be small to support the uniform metal/Al ratios observed.

The second trend was greatly elevated As and Mn values in the surface layers (0-5 cm) of sediment from selected stations on the outer shelf and slope cores (Figure 64). Higher As concentrations (and As/Al ratios) in the surface layers of sediment (Figure 64D, G) are caused by diagenetic remobilization of As in subsurface, reducing sediments. Subsequent upward diffusion moves dissolved As toward the oxic, sediment-water interface where it can precipitate with Fe oxides (Figure 64E, H) or diffuse into the overlying seawater (Farmer and Lovell, 1986; Linge and Oldham, 2002). Very large diagenetic enrichments of As (values >30 µg/g) were observed to occur at 7 of 66 stations during 2014 and 2015 (Figure 65). Water depths at these stations ranged 200-823 m.

Manganese remobilization and surface enrichment also was observed in many of the cores where As values were elevated with Mn concentrations as high as 16,000 µg/g (e.g., Figure 64C, F, I). The process is similar to that described above for As and previously observed in many studies (e.g., Lynn and Bonatti, 1965; Trefry and Presley, 1982). Remobilization of Fe also was observed in cores with diagenetic impacts for As and Mn (Figure 64B, E, H). The magnitude of enrichment for Fe appears somewhat diminished in the profiles that show Fe values in %. However, the highest Fe value for station 71-146 (57,500 µg/g at 2-3 cm in Figure 64E) is 12,500 µg/g greater than down core where Fe concentrations average ~45,000 µg/g. Therefore, the diagenetically induced Fe enrichment is on par or greater than observations for Mn.

**Table 7. Stations with metal values for surface sediments collected during 2014 and 2105 (ANIMIDA III) that are greater than (A) the upper prediction interval (UPI) on metal versus aluminum plots and (B) values for Effects Range Low (ERL) and Effects Range Median (ERM) based on sediment quality guidelines from Long et al. (1995).**

| Metal | 2014-15 samples with Values>UPI (n = 63) | Maximum (this study) (µg/g) | ERL (µg/g) | ERM (µg/g) | Sites with Values>UPI and >ERL |
|---|---|---|---|---|---|
| Ag | None | 0.28 | 1.0 | 3.7 | None |
| As | Many due to natural diagenesis | 116 | (8.2)1 | 70 | Many due natural diagenesis |
| Ba | 70-145, 143-W2 20 24, 71-147, 71-149 | 2210 | None | None | (N/A)[2] |
| Be | 71-145 | 2.6 | None | None | (N/A)[2] |
| Cd | None | 0.32 | 1.2 | 9.6 | None |
| Cr | None | 106 | (81)1 | 370 | None |
| Cu | None | 37 | (70)3 | 270 | None |
| Hg | 1 | 0.090 | 0.150 | 0.710 | None |
| N | None | 45.8 | (20.9)1 | 51.6 | None |
| Pb | None | 21 | 46.7 | 218 | None |
| Sb | 149-200 | 1.2 | None | None | (N/A)[2] |
| Tl | None | 0.74 | None | None | (N/A)[2] |
| V | 149-200 | 211 | None | None | (N/A)[2] |
| Zn | 71-149 | 130 | 150 | 410 | None |

[1]ERL is lower than natural concentrations of this metal in the coastal Beaufort Sea.
[2]No ERL or ERM available.
[3]ERL from O'Connor (2004).

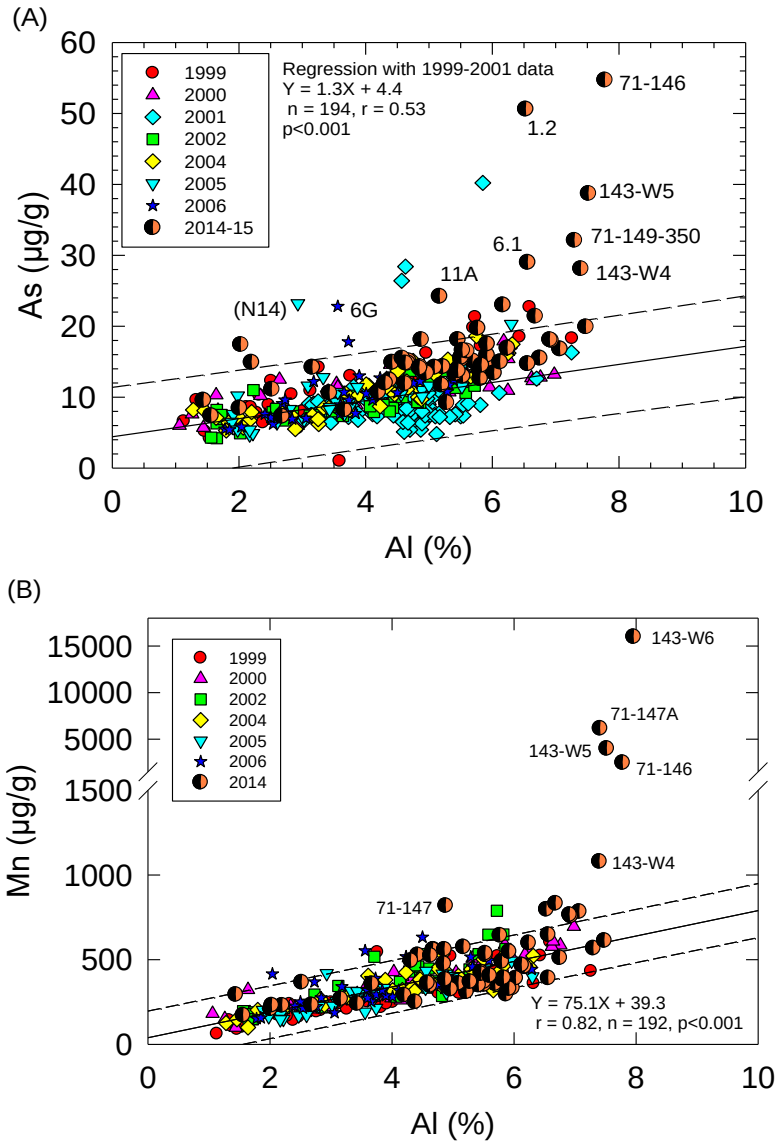


**Figure 62. Concentrations of Al versus (A) As and (B) Mn for surface sediments collected during 2014 and 2015 from the coastal Beaufort Sea.**

**Solid lines and equations show linear regression fit to data from 1999-2001 (ANIMIDA Project, Trefry et al., 2003), dashed lines show 99% prediction intervals, r is the correlation coefficient, and p is the statistical p value.**

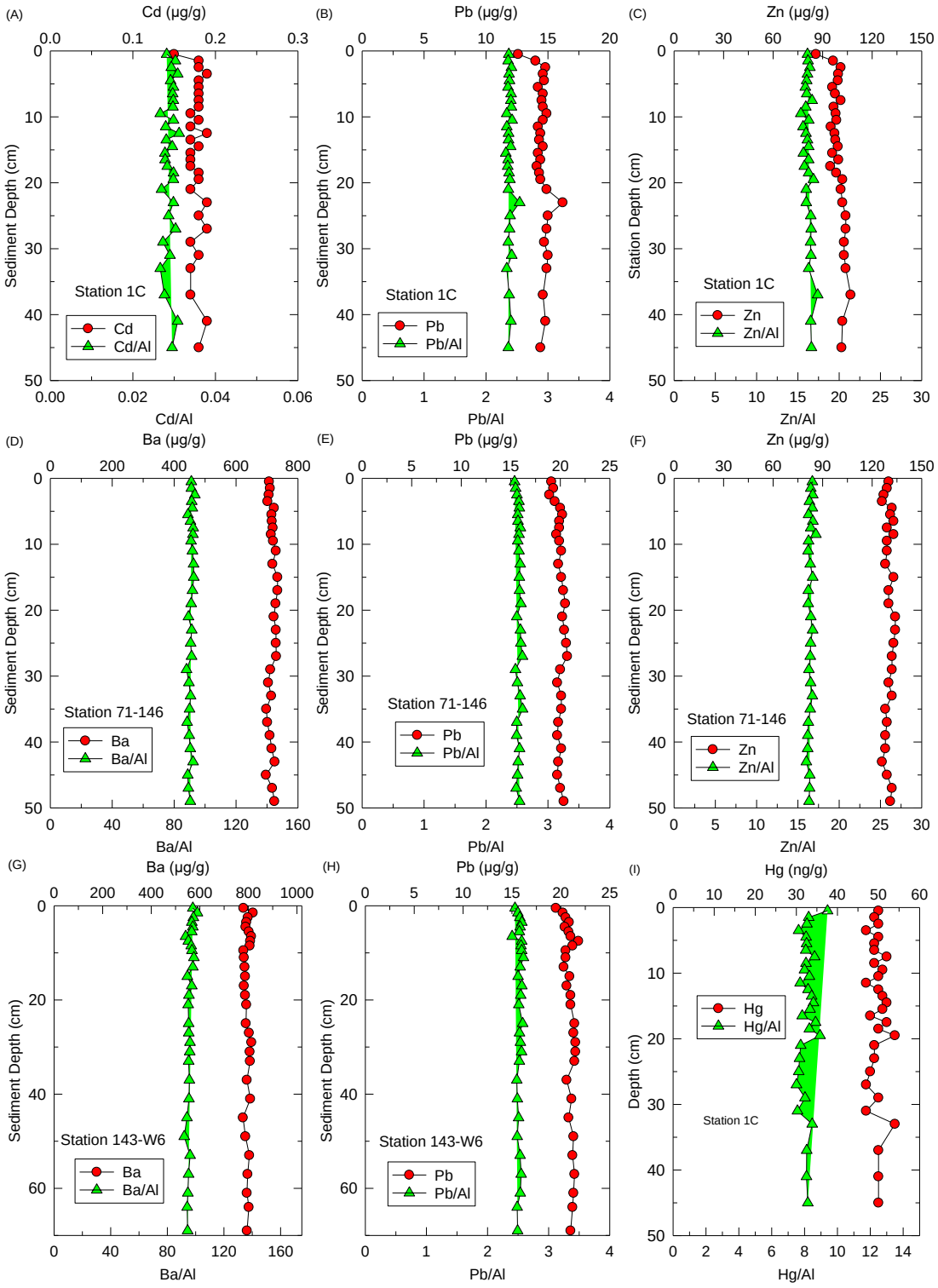


**Figure 63. Vertical profiles for (A) Cd, (B) Pb, (C) Zn, (D) Ba, (E) Pb, (F) Zn, (G) Ba, (H) Pb, and (I) total Hg in sediment from selected stations in the coastal Beaufort Sea with their ratios to Al.**

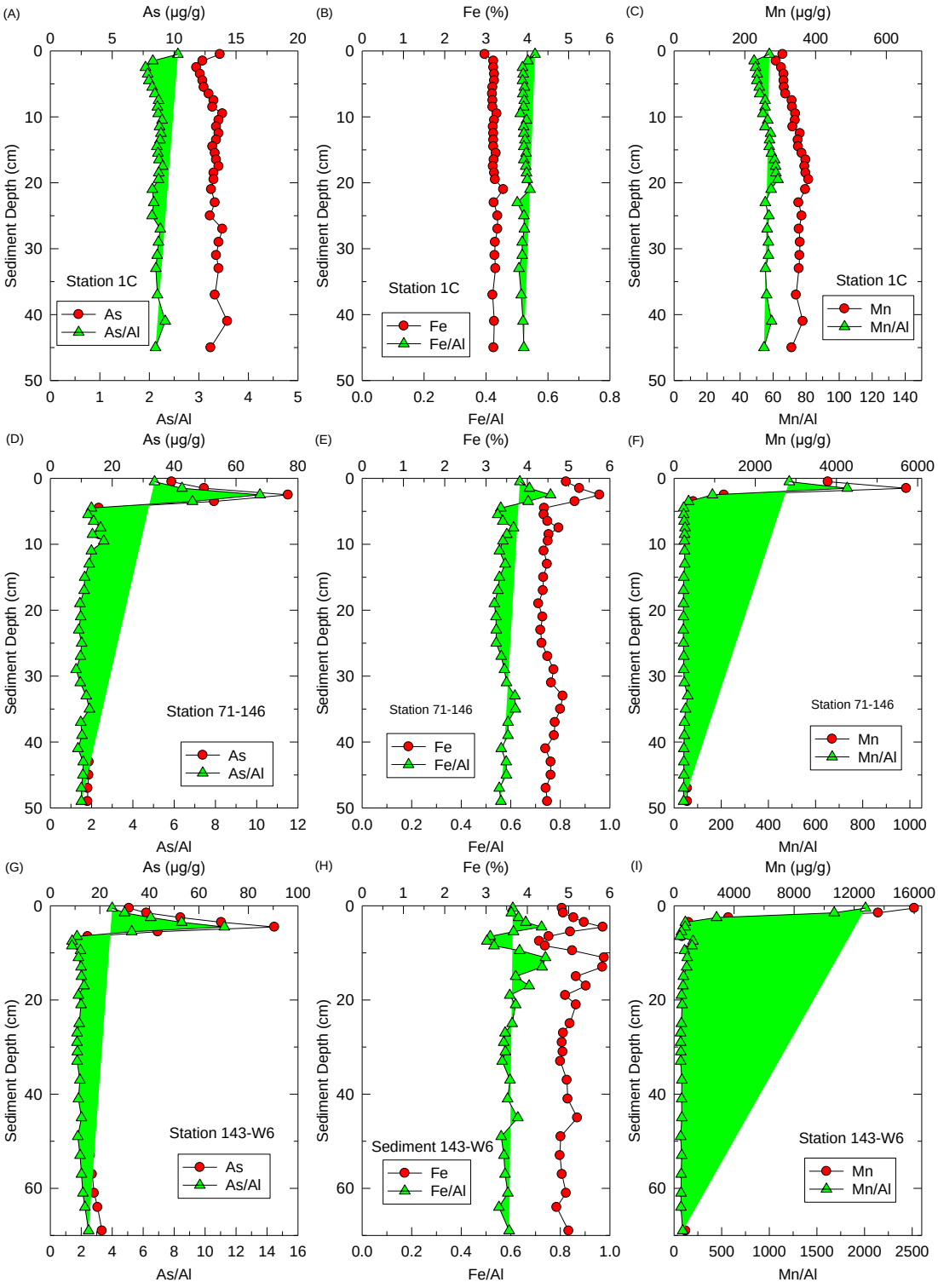


**Figure 64. Vertical profiles for (A) As, (B) Fe, (C) Mn, (D) As, (E) Fe, (F) Mn, (G) As, (H) Fe, and (I) Mn in sediment from selected stations in the coastal Beaufort Sea with their ratios to Al.**

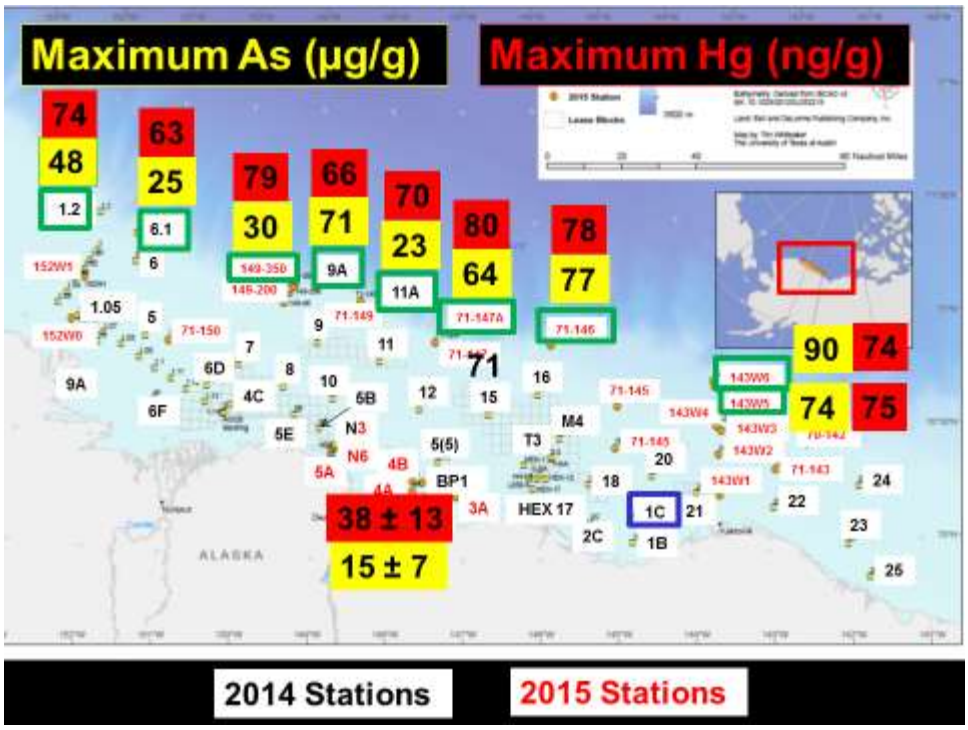


**Figure 65. Maximum concentrations of mercury (Hg, upper value in red box) and arsenic (As, lower number in yellow box) for offshore stations (numbers in green rectangles) in the coastal Beaufort Sea.**

**Mean values for Hg and As in sediments without any diagenetic influence were 38 ± 13 ng/g for Hg and 15 ± 7 µg/g for As (number shown on lower portion of map).**

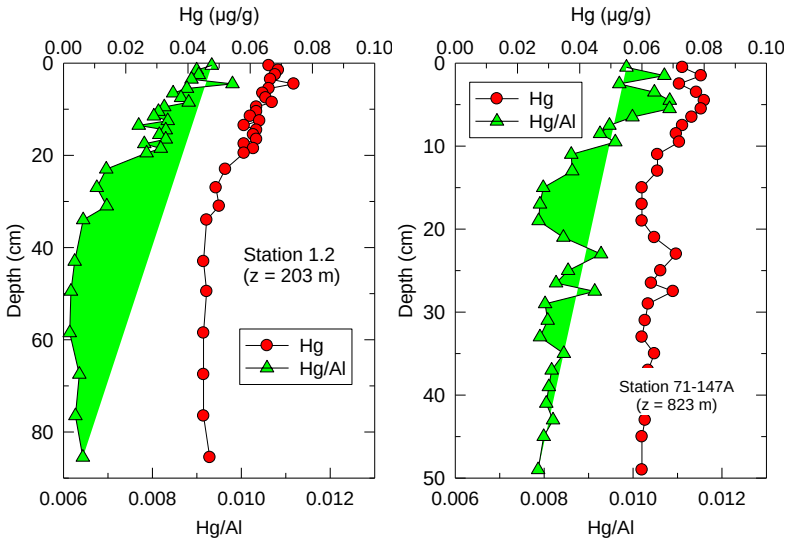


**Figure 66. Vertical profiles for total Hg in sediment cores from (A) station 1.2 at a water depth (z) of 203 m and (B) station 71-147A (z = 823 m) in the coastal Beaufort Sea with their ratios to Al.**

Mercury values greater than 0.064 µg/g (64 ng/g, which is 2 SD above the mean ± SD of 0.038 ± 0.013 µg/g (38 ± 18 ng/g) were observed in the surface layers of eight offshore cores (water depths of 203-823 m; Figure 66 for stations 1.2 and 71-147A). The Hg/Al ratio was 25-50% higher in the surface layers of these cores. Similar Hg profiles were observed by Gobeil et al. (1999) in some of the major basins of the Arctic Ocean at water depths of 2,265-4,230 m. The magnitude of Hg enrichment observed by Gobeil et al. (1999) was equal to and as much as 2 times greater than observed in this ANIMIDA III study. A key paper is being developed from this ANIMIDA III study that focuses on the diagenetic processes that lead to remobilization and enrichment of As, Mn, and Hg in surface sediments from the outer shelf and slope of the coastal Beaufort Sea.

### 3.3.2 Metals in Suspended Sediments

Concentrations of trace metals, especially Ba, have been used to trace of discharges of drilling fluids and cuttings from exploration platforms in the marine environment (Trocine and Trefry, 1983; Trefry et al., 1985). Samples of suspended particles were collected from the coastal Beaufort Sea during the open-water period in August 2014 (Table 8, ANIMIDA III) to expand the data set for particulate metals obtained during 2000–2002 (ANIMIDA) and 2004-2006 (cANIMIDA, Table 9). These cumulative data from 320 samples provide a useful baseline for assessing future discharges of drilling fluid and cuttings (Table 9). Concentrations of particulate Ba ranged from 63-504 µg/g during August 2014 with higher values in samples with abundant Al-rich clay particles (aluminosilicates) and lower values in organic-rich, clay-poor particles (Figure 67A). A strong correlation between Ba and Al for the 2014 samples (Figure 67A) shows a well-defined baseline for concentrations of particulate Ba as a function of particulate Al values. The slope of the line for particulate Ba versus Al is within 2% of the slope for natural bottom sediments (Figure 67B), showing the strong link between the Ba/Al ratio in suspended particles and bottom sediments (Table 9and Figure 67A, B). Therefore, using Ba to identify barite from drilling fluid in the water column will provide a sensitive tracer of drilling discharges, if permitted, relative to sediment resuspension or other sediment event.

**Table 8. Concentrations of metals, particulate organic carbon (POC), total suspended solids (TSS) for suspended particles from the coastal Beaufort Sea during August 2014.**

| Statistic | Al (%) | Ba (µg/g) | Cu (µg/g) | Fe (µg/g) | Mn (µg/g) | Si (µg/g) | POC (%) | TSS mg/L |
|---|---|---|---|---|---|---|---|---|
| Mean | 3.45 | 327 | 53.1 | 3.07 | 1311 | 18.5 | 12.2 | 1.18 |
| Standard Deviation | 1.07 | 89 | 18.1 | 1.04 | 740 | 4.3 | 6.5 | 0.92 |
| n | 70 | 70 | 70 | 70 | 70 | 70 | 67 | 70 |
| Maximum | 5.13 | 504 | 118 | 4.67 | 3170 | 24.8 | 37.8 | 6.11 |
| Minimum | 0.51 | 63 | 16.6 | 0.18 | 25 | 2.4 | 2.8 | 0.13 |
| Median | 3.68 | 335 | 49.4 | 3.23 | 1250 | 19.4 | 10.6 | 1.01 |

**Table 9. Concentrations of metals and total suspended solids (TSS) for suspended particles from the coastal Beaufort Sea during the open-water season in 2000-2002, 2004-2006 and 2014 and for baseline bottom sediments. Data for suspended particles (2000-2006) from Trefry et al. (2009) and bottom sediments from Trefry et al. (2003).**

| Year | n | Al (%) | Ba (µg/g) | Ba/AL (x $10^4$) | Fe (%) | Fe/AL | TSS mg/L |
|---|---|---|---|---|---|---|---|
| 2000 | 51 | 7.4 | 738 | 100 | 4.3 | 0.58 | 8.2 |
| 2001 | 34 | 8.0 | 775 | 97 | 4.8 | 0.60 | 5,1 |
| 2002 | 32 | 5.9 | 564 | 96 | 4.1 | 0.69 | 2.1 |
| 2004 | 42 | 6.9 | 680 | 99 | 4.0 | 0.58 | 13 |
| 2005 | 65 | 4.9 | 507 | 103 | 3.6 | 0.73 | 1.7 |
| 2006 | 26 | 5.7 | 574 | 101 | 3.9 | 0.68 | 1.3 |
| 2014 | 70 | 3.4 | 327 | 96 | 3.1 | 0.91 | 1.2 |
| Bottom Sediments | 192 | 3.9 | 394 | 101 | 2.3 | 0.58 | - |

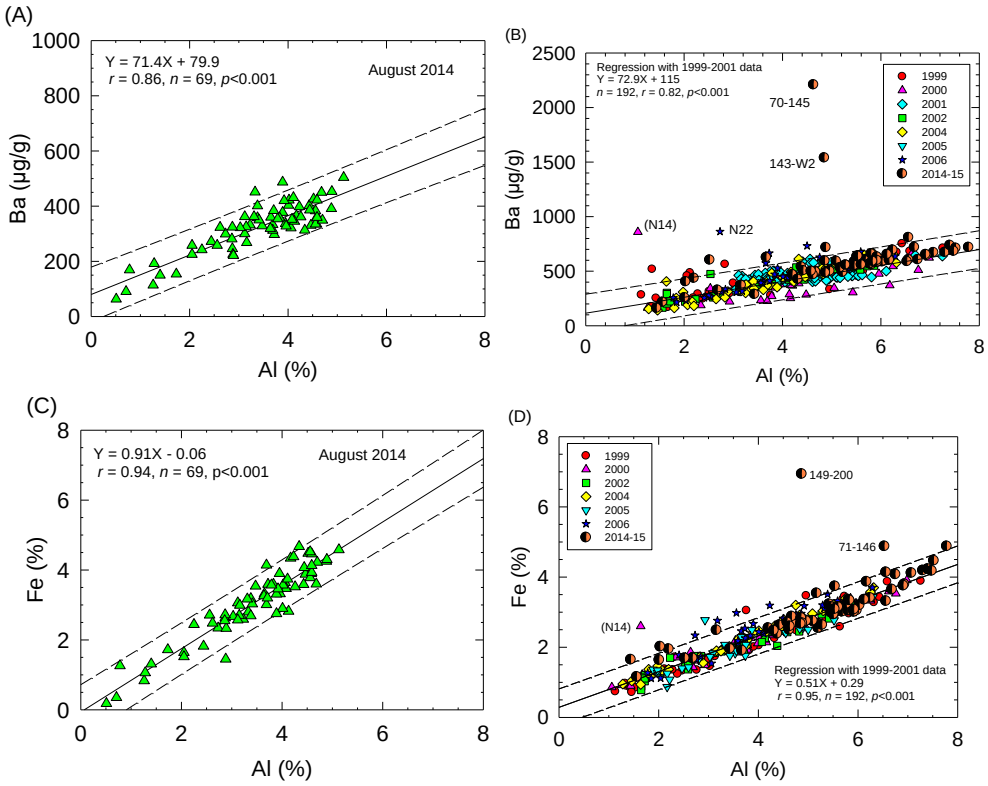


**Figure 67. Concentrations of Ba versus Al for (A) suspended particles and (B) bottom sediments and Fe versus Al for (C) suspended particles and (D) bottom sediments from the coastal Beaufort Sea.**

**Solid lines and equations show linear regression fit to data, dashed lines show 99% prediction intervals, *r* is the correlation coefficient and *p* is the statistical *p* value.**

Similar to results for Ba, strong correlations were found for Fe versus Al in both suspended particles and bottom sediments (Figure 67C, D). In contrast, the slope of the linear regression line for suspended particles was ~80% greater than found for bottom sediments (Figure 67C, C). This observation is consistent with adsorption of Fe on clay-rich particles. The total suspended solids (TSS) versus Fe relationship was not significant (p = 0055); therefore, Fe enrichment of particles is not a likely function of the mass of TSS, but rather the clay content. As discussed previously, diagenetic remobilization enriches surface sediments with Fe.

### 3.3.3 Metals in Biota

Concentrations of Ag, As, Ba, Cd, Cr, Cu, Fe, Total Hg, MMHg, Mn, Ni, Sb, Se, Sn, V, and Zn were determined for clams (*Astarte* sp.) and amphipods (*Anonyx* sp.) from the coastal Beaufort Sea during 2014 and 2015. These most recent data are compared with previous results for the BSMP (1986–1989), ANIMIDA (1999–2002), and cANIMIDA (2004–2007) Projects. One long-term goal of this effort was to develop a data base for trace metals in these two organisms that enables scientists and managers to monitor changes in metal concentrations over time and space. Complications in this process result from (1) large standard deviations in concentrations of some metals both temporally and spatially, (2) possible combined species for the groups collected as clams or amphipods, (3) inclusion of sediment in samples, the largest impact is for metals with low values in biota and higher values in sediment (e.g., Cr, Ni), and (4) limited repeat station locations over the 30-year period of data collection due to the absence of amphipods and clams at a specific station during any given year. Nevertheless, useful data (relative SD: <30%) have been acquired for a variety metals.

Concentrations of Zn and Cu in clams from the coastal Beaufort Sea have been relatively uniform over time (Table 10 and Figure 68) because both metals are regulated biochemically by the clams. Iron and Mn values for clams are sometimes impacted by the presence of sediment in the samples; this leads to more variability in the data (Table 10 and Figure 68). The impact of sediment inclusion in the samples also impacts concentrations of metals that are very low in biota relative to sediments. For example, higher average concentrations of Cr and Ni in the 1999 samples most likely were caused by sediment incorporation in the samples. Among the other metals, no significant variations ($\alpha = 0.05$) were observed over time for Pb, As, Ag, Sb, Hg, and Tl, partially because of the large standard deviations. Clams from this study contained 30–40 % of the total Hg as MMHg; this is a typical range for bivalves in the Arctic (Fox et al., 2014). Significantly higher Cd values were found for clams from 2014–2015; we believe that this observation is partly explained by inclusion of a few individuals of a different species in the pooled samples.

More variability and shifts in metal concentrations have been found for amphipods relative to clams (Table 11, Figure 69). Concentrations of Zn show likely biochemical regulation; however, a shift in Cu values was found for 2014 and 2105 relative to previous years (Figure 69). In amphipods, such shifts can be related to changes in diet as well as differences in samples from farther offshore we had not sampled previously. The trend observed for Cu is also seen for Mn, Ag, Ba, and Sb (Figure 69). In contrast, the opposite trend of higher concentrations in the 2014 and 2015 samples was observed for As, Cd, and Hg. About 50% of the total Hg in amphipods was present as MMHg, again a typical value for the Arctic (Fox et al., 2014). Overall, the ANIMIDA III data help meet the goal of establishing a baseline for contaminants in clams and amphipods.

**Table 10. Concentrations of trace metals in clams (*Astarte* sp.) collected in the coastal Beaufort Sea during August 2014 and 2015.**

| Statistic | Water Content (%) | Ag (µg/g) | Al (µg/g) | As (µg/g) | Ba (µg/g) | Be (µg/g) | Cd (µg/g) | Cr (µg/g) | Cu (µg/g) | Fe (µg/g) | |
|---|---|---|---|---|---|---|---|---|---|---|---|
| **2014** | | | | | | | | | | | |
| Mean | 78.7 | 0.077 | 99.3 | 10.5 | 47.6 | 0.028 | 24.8 | 1.26 | 12.2 | 1877 | |
| Standard Deviation | 1.3 | 0.095 | 610 | 1.0 | 29.7 | 0.005 | 8.8 | 0.66 | 2.3 | 456 | |
| n | 6 | 6 | 6 | 6 | 6 | 6 | 6 | 6 | 6 | 6 | |
| Maximum | 80.8 | 0.264 | 2200 | 12.1 | 102 | 0.036 | 36.5 | 2.15 | 16.3 | 2710 | |
| Minimum | 76.8 | 0.022 | 610 | 9.22 | 14.5 | 0.022 | 14.4 | 0.73 | 9.9 | 1510 | |
| Median | 78.7 | 0.030 | 717 | 10.6 | 43.7 | 10.28 | 25.7 | 0.90 | 11.3 | 1750 | |
| **2014** | | | | | | | | | | | |
| **Statistic** | **Hg (µg/g)** | **MMHg (µg/g)** | **Mn (µg/g)** | **Ni (µg/g)** | **Pb (µg/g)** | **Sb (µg/g)** | **Se (µg/g)** | **Sn (µg/g)** | **Tl (µg/g)** | **V (µg/g)** | **Zn (µg/g)** |
| Mean | 0.078 | 0.026 | 178 | 5.42 | 0.573 | 0.018 | 5.39 | 0.027 | 0.016 | 3.71 | 66.8 |
| Standard Deviation | 0.14 | 0.004 | 84 | 1.16 | 0.210 | 0.004 | 0.60 | 0.017 | 0.007 | 13.5 | 6..8 |
| n | 6 | 5 | 6 | 6 | 6 | 6 | 6 | 6 | 6 | 6 | 6 |
| Maximum | 0.101 | 0.092 | 314 | 7.44 | 0.881 | 1.022 | 6.42 | 0.059 | 0.029 | 5.57 | 75.9 |
| Minimum | 0.059 | 0.299 | 68.7 | 4.32 | 0.317 | 0.012 | 4.74 | 0.012 | 0.010 | 2.38 | 57.5 |
| Median | 0.077 | 0.026 | 158 | 4.92 | 0.528 | 0.020 | 5.31 | 0.023 | 0.12 | 3.20 | 66.9 |
| **Statistic** | **Water Content (%)** | **Ag (µg/g)** | **Al (µg/g)** | **As (µg/g)** | **Ba (µg/g)** | **Be (µg/g)** | **Cd (µg/g)** | **Cr (µg/g)** | **Cu (µg/g)** | **Fe (µg/g)** | |
| **2015** | | | | | | | | | | | |
| Mean | 84.8 | 0.054 | 1174 | 14.2 | 22.2 | 0.024 | 21.2 | 1.28 | 13.0 | 2393 | |
| Standard Deviation | 3.2 | 0.062 | 774 | 4.0 | 10.8 | 0.006 | 13.9 | 0.15 | 4.7 | 1637 | |
| n | 5 | 5 | 5 | 5 | 5 | 5 | 5 | 5 | 5 | 5 | |
| Maximum | 88.0 | 0.164 | 2240 | 20.6 | 40.1 | 0.030 | 42.9 | 1.45 | 18.1 | 4220 | |
| Minimum | 79.5 | 0.014 | 793 | 9.8 | 12.4 | 0.017 | 8.8 | 1.07 | 9.3 | 601 | |
| Median | 85.6 | 0.032 | 926 | 13.1 | 20.4 | 0.28 | 22.4 | 1.28 | 10.0 | 2450 | |
| **Statistic** | **Hg (µg/g)** | **MMHg (µg/g)** | **Mn (µg/g)** | **Ni (µg/g)** | **Pb (µg/g)** | **Sb (µg/g)** | **Se (µg/g)** | **Sn (µg/g)** | **Tl (µg/g)** | **V (µg/g)** | **Zn (µg/g)** |
| **2015** | | | | | | | | | | | |
| Mean | 0.052 | 0.023 | 212 | 8.56 | 0.81 | 0.033 | 5.21 | 0.178 | 0.018 | 6.7 | 73.2 |
| Standard Deviation | 0.018 | 0.003 | 140 | 3.41 | 0.38 | 0.023 | 1.14 | 0.116 | 0.009 | 3.8 | 12.0 |
| n | 5 | 4 | 5 | 5 | 5 | 5 | 5 | 5 | 5 | 5 | 5 |
| Maximum | 0.075 | 0.025 | 409 | 13.20 | 1.25 | 0.070 | 6.47 | 0.378 | 0.033 | 12.7 | 92.9 |
| Minimum | 0.028 | 0.018 | 45 | 5.06 | 0.44 | 0.016 | 3.97 | 0.080 | 0.009 | 3.8 | 64.0 |
| Median | 0.049 | 0.024 | 161 | 9.19 | 0.75 | 0.024 | 5.14 | 0.138 | 0.017 | 4.7 | 66.5 |

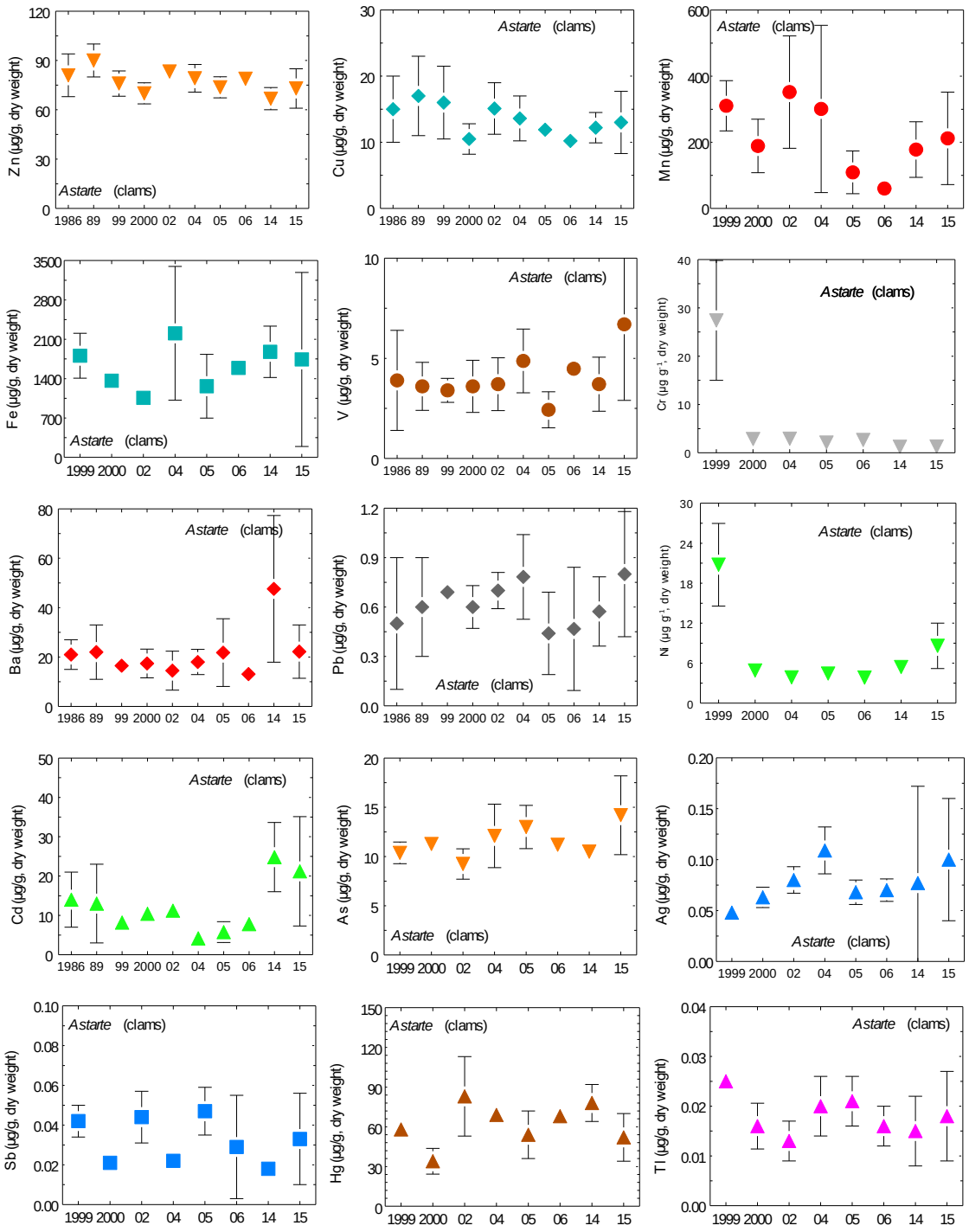


**Figure 68. Concentrations of trace metals in clams (*Astarte* sp.) from the coastal Beaufort Sea during the BSMP (1986-–989), ANIMIDA (1999–2002), cANIMIDA (20042007), and ANIMIDA III (2014–2015) projects.**

**Table 11. Concentrations of trace metals in amphipods (*Anonyx* sp.) collected in the coastal Beaufort Sea during August 2014 and 2015.**

| Statistic | Water Content (%) | Ag (µg/g) | Al (µg/g) | As (µg/g) | Ba (µg/g) | Be (µg/g) | Cd (µg/g) | Cr (µg/g) | Cu (µg/g) | Fe (µg/g) | |
|---|---|---|---|---|---|---|---|---|---|---|---|
| **2014** | | | | | | | | | | | |
| Mean | 75.0 | 1.50 | 273 | 17.2 | 9.91 | 0.005 | 3.39 | 1.37 | 64.6 | 240 | |
| Standard Deviation | 1.8 | 0.48 | 251 | 8.5 | 3.95 | 0.004 | 1.83 | 1.22 | 28.8 | 163 | |
| n | 20 | 20 | 20 | 20 | 20 | 20 | 20 | 20 | 20 | 20 | 20 |
| Maximum | 78.7 | 2.44 | 1280 | 40.9 | 22.6 | 0.020 | 6.78 | 4.76 | 154 | 865 | |
| Minimum | 71.5 | 0.38 | 47 | 6.75 | 3.05 | 0.001 | 0.41 | 0.11 | 30.4 | 55.1 | |
| Median | 74.4 | 1.44 | 211 | 15.6 | 9.19 | 0.004 | 2.87 | 1.14 | 56.8 | 217 | |
| **2014** | | | | | | | | | | | |
| **Statistic** | **Hg (µg/g)** | **MMHg (µg/g)** | **Mn (µg/g)** | **Ni (µg/g)** | **Pb (µg/g)** | **Sb (µg/g)** | **Se (µg/g)** | **Sn (µg/g)** | **Tl (µg/g)** | **V (µg/g)** | **Zn (µg/g)** |
| Mean | 0.148 | 0.068 | 15.2 | 3.13 | 0.109 | .009 | 2.50 | 0.010 | 0.006 | 2.82 | 140 |
| Standard Deviation | 0.89 | 0.044 | 7.2 | 1.12 | 0.083 | 0.008 | 0.65 | 0.004 | 0.002 | 2.16 | 35 |
| n | 20 | 20 | 20 | 20 | 20 | 20 | 20 | 20 | 20 | 20 | 20 |
| Maximum | 0.411 | 0.145 | 36.1 | 5.37 | 0.356 | 0.040 | 3.77 | 0.017 | 0.15 | 9.64 | 191 |
| Minimum | 0.021 | 0.047 | 5.6 | 1.07 | 0.012 | 0.002 | 1.06 | 0.003 | 0.002 | 0.77 | 50.1 |
| Median | 0.131 | 0.086 | 13.2 | 2.99 | 0.097 | 0.007 | 2.44 | 0.011 | 0.006 | 1.96 | 149 |
| **Statistic** | **Water Content (%)** | **Ag (µg/g)** | **Al (µg/g)** | **As (µg/g)** | **Ba (µg/g)** | **Be (µg/g)** | **Cd (µg/g)** | **Cr (µg/g)** | **Cu (µg/g)** | **Fe (µg/g)** | |
| **2015** | | | | | | | | | | | |
| Mean | 76.0 | 1.41 | 221 | 20.9 | 8.98 | 0.003 | 5.19 | 1.76 | 63.4 | 142 | |
| Standard Deviation | 2.7 | 0.030 | 50 | 11.3 | 1.00 | 0.001 | 2.15 | 1.38 | 19.1 | 94 | |
| n | 6 | 6 | 6 | 6 | 6 | 6 | 6 | 6 | 6 | 6 | |
| Maximum | 79.3 | 1.90 | 303 | 41.8 | 10.5 | 0.005 | 7.83 | 4.05 | 99.5 | 303 | |
| Minimum | 72.2 | 1.05 | 164 | 9.47 | 7.87 | 0.002 | 2.47 | 0.35 | 46.1 | 54.4 | |
| Median | 75.5 | 1.35 | 207 | 18.7 | 8.87 | 0.003 | 5.20 | 1.46 | 60.1 | 122 | |
| **Statistic** | **Hg (µg/g)** | **MMHg (µg/g)** | **Mn (µg/g)** | **Ni (µg/g)** | **Pb (µg/g)** | **Sb (µg/g)** | **Se (µg/g)** | **Sn (µg/g)** | **Tl (µg/g)** | **V (µg/g)** | **Zn (µg/g)** |
| **2015** | | | | | | | | | | | |
| Mean | 0.210 | 0.146 | 13.5 | 3.22 | 0.118 | 0.007 | 2.84 | 0.016 | 0.009 | 5.69 | 156 |
| Standard Deviation | 0.103 | 0.021 | 2.6 | 1.00 | 0.032 | 0.007 | 0.61 | 0.008 | 0.002 | 2.40 | 10 |
| n | 6 | 3 | 6 | 6 | 6 | 6 | 6 | 6 | 6 | 6 | 6 |
| Maximum | 0.384 | 0.167 | 18.3 | 4.54 | 0.165 | 0.21 | 3.61 | 0.025 | 0.011 | 8.66 | 173 |
| Minimum | 0.101 | 0.125 | 11.0 | 2.14 | 0.078 | 0.001 | 1.97 | 0.003 | 0.007 | 2.68 | 146 |
| Median | 0.188 | 0.146 | 13.2 | 2.99 | 0.120 | 0.004 | 2.82 | 0.016 | 0.008 | 5.49 | 155 |

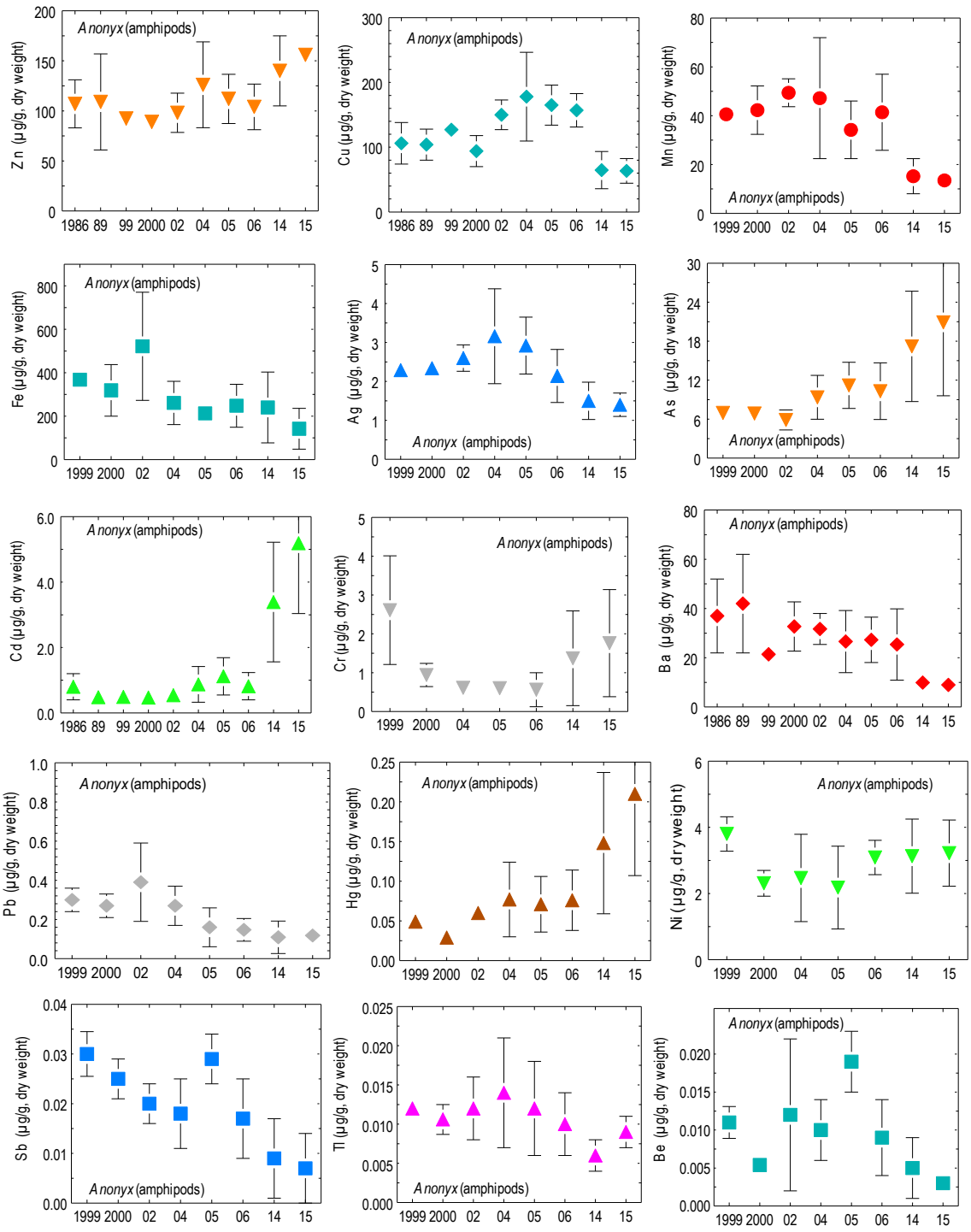


**Figure 69. Concentrations of trace metals in amphipods (*Anonyx* sp.) from the coastal Beaufort Sea during the BSMP (1986–1989), ANIMIDA (1999–2002), cANIMIDA (2004–2007), and ANIMIDA III (2014–2015) projects.**

## 3.4 Conclusions

Interpretation of the results for the trace metals portion of the ANIMIDA III Project yields the following conclusions.

- Sediments from the coastal Beaufort Sea are essentially uncontaminated with respect to trace metals.
- No evidence was found that showed metal concentrations that exceeded sediment quality criteria.
- Long-term records from sediment cores show uniform concentrations of most metals including Pb, Ag, Cd, and Zn.
- Surface sediments from the outer shelf and upper slope have greatly elevated concentrations of As, Mn, and Hg that result from post-depositional remobilization of these metals under reducing conditions. No anthropogenic inputs are indicated.
- Suspended particles are a valuable tracer of discharges of drilling fluids and other substances to the water column as shown by Ba/Al ratios.
- Metal concentrations in clams and amphipods provide a baseline for future reference; however, for some metals, considerable variability in concentrations has been observed.

## Acknowledgments

We thank Dan Holiday and Catherine Coon of BOEM, U.S. Department of Interior, for their interest and enthusiasm for studies of metals in biota. We also thank the crew and captains of *Norseman II* for their amazing efforts to ensure that we were successful at sea. Logistical and collegial support from Sheyna Wisdom and Justin Blank of Olgoonik Fairweather were first class. Our scientific colleagues in this program were a joy to work with at sea and team meetings. This field and laboratory study was funded by the U.S. Department of the Interior, BOEM, Alaska Outer Continental Shelf Region, Anchorage, Alaska under Contract Number Operative Agreement No. M13PC00019 as part of the ANIMIDA III Project.

## References


ADNR (Alaska Dept. of Natural Resources). 2009. Proposed Beaufort Sea area wide oil and gas lease sale: Preliminary finding of the Director. April 2, 2009. ADNR Division of Oil and Gas, Anchorage, AK. 412 p.

Arnborg L., Walker H.J., and Peippo J. 1967. Suspended load in the Colville River, Alaska, 1962. Geog Annaler 49A: 131-144.

Bloom N.S. and Crecelius E.A. 1983. Determination of mercury in seawater at sub-nanogram per liter levels. Mar. Chem. 14, 49-59.

Bloom N. 1989. Determination of picogram levels of methylmercury by aqueous phase ethylation, followed by cryogenic gas-chromatography with cold vapor atomic fluorescence detection. Can. J. Fish. Aquat. Sci. 46, 1131-1140.

BOEM (Bureau of Ocean Energy Management). 2016. Beaufort Sea exploratory wells. BOEM Alaska OCS Region, Anchorage, AK. 2 p. Brown J., Boehm P., Cook, Trefry J., Smith W., and Durell G. 2010. Hydrocarbon and metal characterization of sediments in the cANIMIDA study area. OCS Study MMS 2010-004. US Department of Interior, Anchorage.

Crecelius E.A., Trefry J.H., Steinhauer M.S., and Boehm P.D. 1991. Trace metals in sediments from the inner continental shelf of the western Beaufort Sea. Environ. Geol. Water Sci. 18: 71-79

Farmer, J.G. and Lovell M.A. 1986. Natural enrichment of arsenic in Lock Lomond sediments. Geochim. Cosmochim. Acta 50, 2059–2067.

Folk, R.L. 1974. Petrology of Sedimentary Rocks. Hemphill Publishing Co., Austin.

Fox, A.L., Hughes E.A., Trocine R.P., Trefry J.H., Schonberg S.V., McTigue N.D., Lasorsa B.K., Konar B., and Cooper L.W. 2014. Mercury in the northeastern Chukchi Sea: Distribution patterns in seawater and sediments and biomagnification in the benthic food web. Deep-Sea Res. II, 102, 56-67.

Gobeil C., Macdonald R.W., and Smith J.N. 1999. Mercury profiles in sediments of the Arctic Ocean basins. Environ. Sci. Technol. 33, 4194-4198.

Linge K.L. and Oldham C.E. 2002. Arsenic remobilization in a shallow lake: The role of sediment resuspension. J. Environ. Qual. 31, 822–828.

Long E.R., Macdonald D.D., Smith S.L., and Calder F.D. 1995. Incidence of adverse biological effects with ranges of chemical concentrations in marine and estuarine sediments. Environ. Manage. 19:81-97.

Lynn D.C. and Bonatti E. 1965. Mobility of manganese in diagenesis of deep sea sediments. Mar. Geol. 3, 457–474.

Naidu A.S. and Mowatt T.C. 1974. Depositional environments and sediment characteristics of the Colville and adjacent deltas, north Arctic Alaska. In: Broussard MLS (ed.) Deltas for subsurface exploration. Houston Geol. Soc., pp. 283-309.

Naidu A.S., Goering J.J., Kelley J.J., and Venkatesan, M.I. 2001. Historical changes in trace metals and hydrocarbons in the inner shelf sediments, Beaufort Sea: prior and subsequent to petroleum-related industrial developments. Final Rept US Dept. Int., MMS 2001-061.

Naidu A.S., Blanchard A.L., Misra D., Trefry J.H., Dasher D.H., Kelley J.J., and Venkatesan M.I. 2012. Historical changes in trace metals and hydrocarbons in nearshore sediments, Alaskan Beaufort Sea, prior and subsequent to petroleum-related industrial development: Part I. Trace metals. Mar. Poll. Bull. 64, 2177–2189.

O'Connor T.P. 2004. The sediment quality guideline, ERL, is not a chemical concentration at the threshold of sediment toxicity. Mar. Poll. Bull. 49, 383-385.

Payne T.G., Dana S.W., Fischer W.A., Yuster S.T., Krynine P.D., Morris R.H., Lanthram E., and Tappan H. 1951. Geology of the arctic slope of Alaska. USGS Oil Gas Invest. Map OM-126.

Riedinger N., Kasten S., Groger J., Franke C., and Pfeifer K. 2006. Active and buried authigenic barite fronts in sediments from the Eastern Cape Basin. Earth, Planet. Sci. Lett. 241, 876–887.

Reimnitz E. and Barnes, P.W. 1974. Sea ice as a geologic agent on the Beaufort Sea shelf of Alaska. In: Reed, J.C., Sater, J.E. (eds.) The coast and shelf of the Beaufort Sea. Arctic Inst. No. Am., Arlington, Virginia, pp. 301-353

Reimnitz E. and Wolf S.C. 1998 Are north slope surface alluvial fans pre-Holocene relicts? USGS Prof. Paper 1605.

Snyder-Conn E., Densmore D., Moitoret C., and Stroebele J. 1990. Persistence of trace metals in shallow arctic marine sediments contaminated by drilling effluents. Oil & Chem. Poll. 7, 225-247.

Sweeney M.D. and Naidu A.S. 1989. Heavy metals in sediments of the inner shelf of the Beaufort Sea, Northern Arctic Alaska. Mar. Poll. Bull. 20, 140-143.

Trefry J.H. and Presley B.J. 1982. Manganese fluxes from Mississippi delta sediments. Geochim. Cosmochim. Acta. 46, 1715–1726.

Trefry J.H., Trocine R.P., and Proni J.R. 1985. Drilling-fluid discharges into the northwestern Gulf of Mexico. In: Duedall, I.W., Kester, D.R., Park, P.K., Ketchum, B.H. (eds.) Wastes in the ocean, Vol. 4. John Wiley, NY, pp 195-222.

Trefry J.H. and Trocine R.P. 1991. Collection and analysis of marine particles for trace elements. In: Hurd DC, Spencer DW (eds) Marine particles: Analysis and characterization. Am Geophys Union Monograph 63, pp 311-315.

Trefry J.H., Rember R.D., Trocine R.P., and Brown J.S. 2003. Trace metals in sediments near offshore oil exploration and production sites in the Alaskan Arctic. Environ. Geol. 45, 149-160.

Trefry J.H., Trocine R.P., McElvaine M.L., Rember R.D., and Hawkins L.T. 2007. Total mercury and methylmercury in sediments near offshore drilling sites in the Gulf of Mexico. Environ. Geol. 53, 375-385.

Trefry J.H., Trocine R.P., Alkire M.B., Semmler C.M., Savoie M., and Rember R.D. 2009. Sources, concentrations, composition, partitioning and dispersion pathways for suspended sediments and

potential metal contaminants in the coastal Beaufort Sea. OCS Study MMS 2009-014. US Department of Interior, Anchorage.

Trefry J.H., Dunton K.H., Trocine R.P., Schonberg S.V., McTigue N.D., Hersh E.S., and McDonald T.J. 2013. Chemical and biological assessment of two offshore drilling sites in the Alaskan Arctic. Mar. Environ. Res. 86, 35-45.

Trefry J.H., Trocine R.P., Cooper L.W., and Dunton K.H. 2014. Trace metals and organic carbon in sediments of the northeastern Chukchi Sea. Deep-Sea Res. II, 102, 18-31.

Trocine R.P. and Trefry J.H. 1983. Particulate metal tracers of petroleum drilling mud dispersion in the marine environment. Environ. Sci. Technol. 17, 507-512.

Valette-Silver N., Hameed M.J., Efurd D.W., and Robertson A. 1999. Status of the contamination in sediments and biota from the western Beaufort Sea (Alaska). Mar. Poll. Bull. 38: 702-722.

Weiss H.V. and Naidu A.S. 1986. 210Pb flux in an arctic coastal region. Arctic 39: 59-64.

White, D. Kimerling J. A., and Overton W. S. 1992. Cartographic and geometric components of a global sampling design for environmental monitoring. Cartogr. Geogr. Inform. 19, 5–22.

# Chapter 4 Characteristics of Petroleum Hydrocarbons in the Sediments and Benthic Organisms of the Beaufort Sea Continental Shelf.

## Abstract

The ANIMIDA III project, described in this report, extended the original ANIMIDA field program with additional surveys in 2014 and 2015; field surveys were conducted between 1999 and 2006 for earlier phase of ANIMIDA. The ANIMIDA III project was performed to further characterize the lease areas and surrounding environs of the Beaufort Sea, to help understand how oil and gas activities may impact the environment. This chapter describes the hydrocarbon component of ANIMIDA III, which included measuring aliphatic hydrocarbons, PAH, and petroleum biomarkers and determining the concentrations and distribution of those chemicals in the Beaufort Sea sediments and in selected benthic organisms and fish. The information was used to gain an overall understanding of the hydrocarbon characteristics of the sediments and animals, the possible sources and mobility of the hydrocarbons, and the environmental importance of the measured hydrocarbons.

Hydrocarbons (PAHs, SHC, and S/T petroleum biomarkers) were measured in surface sediment (and one sediment core) and marine animal (amphipods, clams, and fish) samples collected at stations in less than 25 m deep water in the nearshore environment to the edge of the continental shelf 50 mi off shore in water depths of 500 m. Most of the nearshore stations were stations that had been sampled in earlier phases of ANIMIDA, while the offshore stations were new to the program. The sample collection and analysis methods that were used were the same as those used in earlier phases of ANIMIDA, to ensure data comparability.

Though several classes of hydrocarbons were measured and the data analyzed, PAH are the class that are of greatest environmental interest. The surface sediment Total PAH concentration ranged from a little under 100 to a little over 1,000 ng/g, d. wt., and averaged 532 (2014) and 707 (2015) ng/g for the two survey years. These concentrations were comparable to those that had been measured in ANIMIDA I and II; the mean concentration for each year ranged from 380 to 570 ng/g. The hydrocarbon concentrations (PAH, SHC, and S/T) were also similar to what has been measured in the sediments in other studies in the Beaufort and Chukchi Seas, and other marine regions of Alaska that have not been impacted by anthropogenic activities (Harvey et al., 2014; Trefry et al., 2013; Brown et al., 2010; Neff and Durell, 2010). The surface sediment concentrations were slightly higher at the offshore stations than nearshore, potentially as a result of seaward transport of fine-grained material that tends to have higher hydrocarbon concentrations than coarser material. The sediment core, collected well offshore, had uniform hydrocarbon concentrations at all depths, including in sediment strata representing deposition from many centuries ago; the amount and source of the hydrocarbons has remained constant for a long time and does not seem to have been altered by human activities. The hydrocarbons in the Beaufort Sea sediments are primarily from non-oil petrogenic and biogenic sources, with minimal amounts of pyrogenic hydrocarbons. Most of the hydrocarbons are carried to the Beaufort Sea through coastal erosion and river input of hydrocarbon rich materials, such as peat and shale. The concentrations of PAH in the sediments are low, at natural background levels, and well below concentrations that could cause harm to marine animals.

The concentrations of PAH, and other hydrocarbons, were more variable in the tissue of marine animals than in the sediment; there are seasonal and annual fluctuations with many aspects of the animal's life and feeding. The mean Total PAH concentration ranged from 25 to 30 ng/g, d. wt., in the amphipods collected in 2014 and 2015, from 44 to 380 ng/g in the clams (a few values above 100 ng/g were attributed to analytical challenges, and do not represent actual field concentrations), and from 24 to 94 ng/g in the Arctic cod. The concentrations did not correlate well with the lipid content of the animals, demonstrating that many factors influence the accumulation of hydrophobic compounds by marine animals. There was no clear geographic pattern in the hydrocarbon concentrations of these marine animals. The tissue hydrocarbon concentrations were comparable to what had been measured during ANIMIDA I and II, and in other studies in the Arctic (Harvey et al., 2014; Neff and Durell, 2012; Neff and Durell, 2010; Neff et al., 2009). The concentrations of the PAH that have accumulated in the marine animals are low, at natural background levels, and well below concentrations that could cause toxic effects or other harm to those animals.

The ANIMIDA III project has built on and expanded the knowledge base from earlier phases of ANIMIDA. The project has extended the monitoring from mainly nearshore environments to the continental slope to gain a better understanding of the Beaufort Sea environment and system as a whole, and also to study some areas well off shore that may be of interest for future development. ANIMIDA III has provided additional hydrocarbon monitoring information that can be used as valuable reference data should new oil and gas development occur, and for environmental management.

## 4.1 Introduction

During ANIMIDA I and II the monitoring was performed in near-shore potential development areas from Harrison Bay in the west to just beyond Camden Bay in the east (Neff and Durell, 2010; Brown et al., 2004; Neff et al., 2009). The stations were within 25 mi of the shore and in less than 25 m water depth. These were the near-shore areas of the Beaufort Sea where there, at the time, was the greatest interest in potentially developing for oil and gas production. They also included monitoring pre- and post-development at the Northstar production facility. ANIMIDA I and II also included studying the major rivers of the Beaufort Sea, including their significance sources of the water, sediment, organic matter, and other substances.

For ANIMIDA III, the geographical area was expanded significantly. Survey stations were located as far as 50 mi off-shore, at the edge of the continental shelf and the beginning of the slope, in water depths of up to 500 m. The study area was expanded to include new offshore areas where development may potentially occur and to also obtain a better understanding of the physical, chemical, and biology characteristics of the Beaufort Sea. ANIMIDA III also included resampling at a series of stations sampled during ANIMIDA I and II to gain an understanding of the current conditions and trends at these stations.

Specifically, this chapter addresses the hydrocarbon chemistry component of ANIMIDA III, including the concentrations and distribution of hydrocarbons in the Beaufort Sea sediments monitored during ANIMIDA III, the accumulation of hydrocarbons by selected benthic organisms and fish, the potential sources and fate of the hydrocarbons, the geochemical history of hydrocarbons in the Beaufort Sea, and the environmental relevance of the measured hydrocarbons. The hydrocarbon information produced during ANIMIDA III, together with the ANIMIDA I and II data, provides a comprehensive characterization of the hydrocarbons in the sediment and benthic environment of the Beaufort Sea,

emphasizing the oil and gas lease areas. This information is useful for also understanding the dynamics of the hydrocarbons in these same areas, and can be valuable for understanding and managing future potential impact of oil and gas activities in the Beaufort Sea.

## 4.2 Methods

This section summarizes the methods used to collect and analyze the ANIMIDA III samples. The field work is only briefly summarized. The field work was more thoroughly documented the Field Sampling Plan and the Field Reports from the two cruises (OF, 2014a, 2014b, and 2015), including the navigation and specific sampling locations, sample collection procedures, sample types collected, navigation, equipment decontamination and field quality control, and sample handling and storage and shipping. Similarly, the laboratory sample analysis procedures that were used, including the quality assurance and quality control, were described in detail in laboratory Quality Assurance Project Plans (QAPPs).

### 4.2.1 Field Sampling

The stations that were sampled are shown in Figure 70. ANIMIDA III stations sampled in 2014 and 2015.; the yellow squares indicate the stations sampled in 2014 and the orange circles those sampled in 2015. The sampling design is described in detail in the Field Sampling Plan (OF, 2014a), and specific information on each sampling location and the conduct of the field activities is summarized in the Field Reports (OF, 2014b and 2015).

The number of samples, in total and by sample type, is summarized in Table 12 for both 2014 and 2015. The ANIMIDA III sampling included (1) 18 nearshore stations at locations previously sampled in ANIMIDA I and/or II, (2) 35 new generally farther off-shore stations, 25 of which were randomly located within 25 hexagons placed over the study area and 10 of which were strategically located to ensure sufficient coverage of the study area and to obtain sampling on the slope, (3) 9 new ANIMIDA Program stations within the parts of Camden Bay where there has been recent interest in oil and gas development, and (4) 7 stations, in total, from two DBO lines located in the study area (152 ºW and 143 ºW lines, Figure 70).

**Table 12. Total number of stations sampled for hydrocarbon analysis by sample type and year.**

| | Sediment Stations[b] | | Biota Stations | | | | | |
|---|---|---|---|---|---|---|---|---|
| | | | Amphipods | | Clams | | Arctic cod | |
| | 2014 | 2015 | 2014 | 2015 | 2014 | 2015 | 2014 | 2015 |
| BSMP/cANIMIDA/Nearshore | 10 | 8 | 5 | | 2 | 1 | 3 | |
| Random/Offshore | 24 | 11 | 15 | 4 | 5 | 3 | 7 | 3 |
| Camden Bay | 9 | | 1 | | | | 1 | |
| DBO Line (2 lines) | | 7 | | 3 | | 3 | | 3 |
| Total | *43* | *26* | *21* | *7* | *7* | *7* | *11* | *6* |

a The numbers represent the number of discrete stations that were sampled, not the number of samples that were collected; some station replicates were also collected and analyzed.
b The sediment stations represent surface sediments. Sediment cores were also collected at a subset of the stations, and hydrocarbons were analyzed in 11 segments from a core collected at Station 1.2 in 2014.

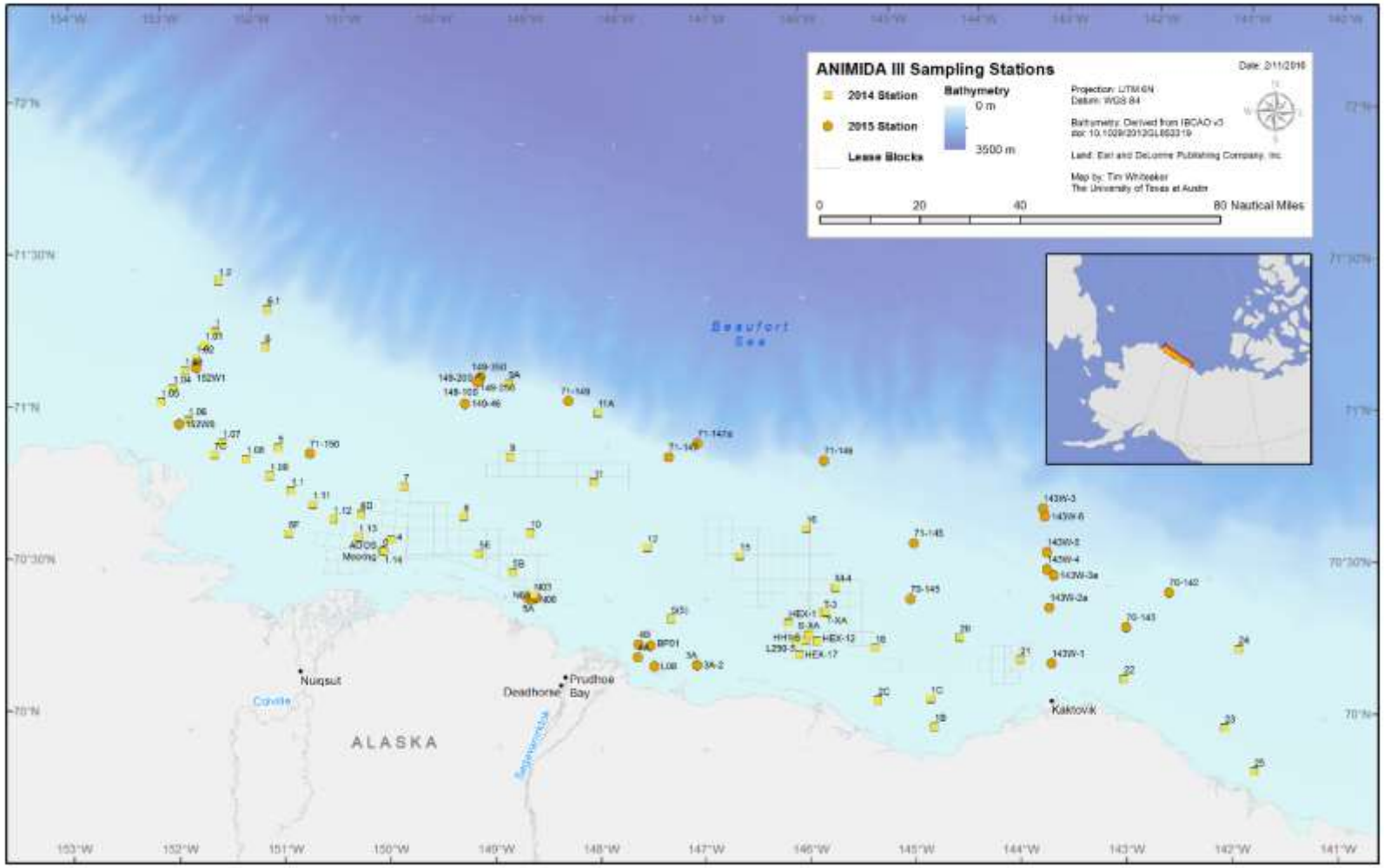


**Figure 70. ANIMIDA III stations sampled in 2014 and 2015.**

The majority of the samples were surface sediments. A few sediment cores were also collected, and one of those (from Station 1.2 in 2014) was selected for hydrocarbon analysis of selected segments, after the sediment integrity and depositional stability had been verified through radiochemical analysis. Biological samples were collected for different purposes and different ANIMIDA III technical disciplines, including for hydrocarbon analysis of amphipods (*Anonyx* sp.), clams (*Astarte* sp.), and Arctic cod (*Boreogadus saida*) to understand the presence and accumulation of hydrocarbons in those animals. Additionally, while not part the ANIMIDA III scope of work, sub-samples were taken from the surface sediments collected at 14 stations in 2014 and 20 stations in 2015 as samples of opportunity, and provided for *Alexandrium* cyst analysis.

Surface sediment samples were collected using a modified double van Veen grab sampler (Figure 71). Care was taken throughout the subsampling process to avoid contact with hydrocarbon and metals sources; samples for analysis were taken from the center of the grab and away from the sides of the grab using non-contaminating materials (e.g., stainless steel, glass, Teflon®, Kynar®). Sediment samples were collected from the top 2 cm of the grab to represent recent accumulation. Sediment cores were collected at 12 locations (7 in 2014 and 5 in 2015) using a gravity coring system; one core was, subsequently, used for hydrocarbon analysis.

Amphipods were collected in Nytex mesh-lined plastic minnow traps baited with sardines (Figure 72), and deployed over several hours. Clams were collected using a clam rake (Figure 73). The amphipods and the clams were gently rinsed with site-seawater. Adult *Astarte* sp. were subsequently used for chemical analysis both because they were found in greatest amounts and to ensure comparability to relevant historical data. Fish were collected with a benthic trawl, and Arctic cod (*Boreogadus saida*) collected at several locations were removed for hydrocarbon analysis. The benthic (clams), epibenthic (amphipods), and pelagic (Arctic cod) animals were included in the monitoring to gain an understanding of current hydrocarbon body-burden conditions and potential bioaccumulation assessment.

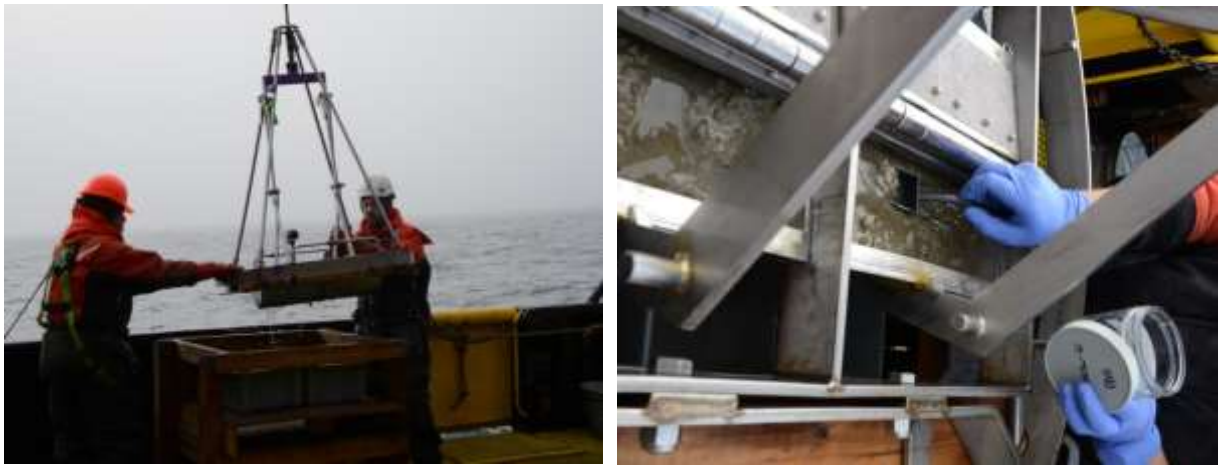

**Figure 71. Double van Veen surface sediment sampler.**

**Figure 72. Amphipod traps and amphipods.**

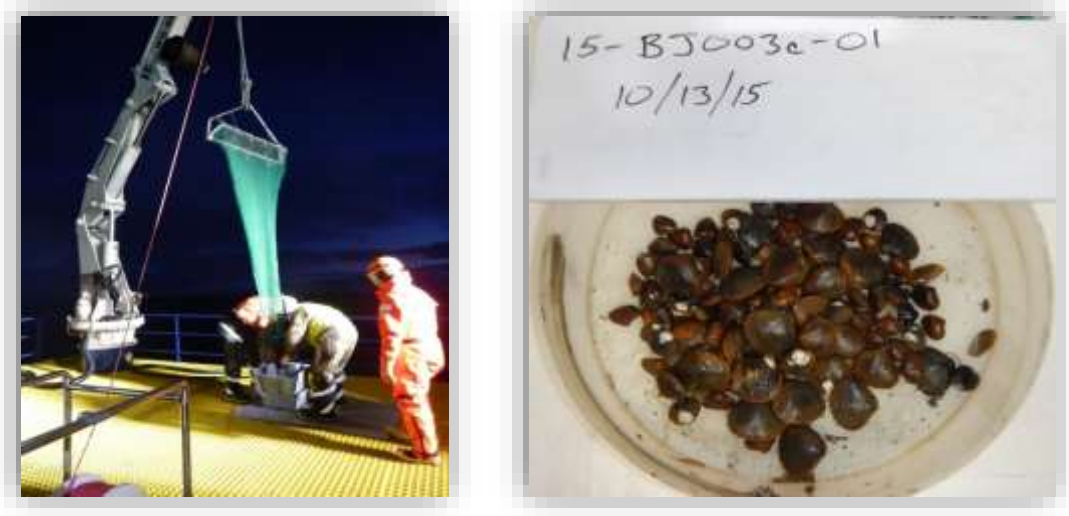


**Figure 73. Clam collection and clams collected from the seafloor.**

### 4.2.2 Analytical Methods

The chemical classes of greatest environmental interest associated with offshore oil and gas exploration, development, and production are metals and hydrocarbons (Neff, 1987, 2010). Petroleum also may enter the environment in accidental discharges or spills from vessels during exploration. The chemical constituents of primary environmental concern in petroleum are PAH. The sediment and biological tissue samples were analyzed for several classes of hydrocarbons (Table 13), including PAH. The approximate method detection limits and reporting limits are summarized in Table 14. A detailed listing of the individual hydrocarbon compounds that were measured, including the analytical limits of detection, are presented in appendix Tables A-1 through A-3.

The analysis of hydrocarbons in sediment and marine invertebrate tissue samples was performed at Battelle. Samples were analyzed for PAH, S/T, TPH, and SHC (Table 13). The PAH analyses captured 45 parent PAH compounds and alkyl-PAH isomer groups (including the 16 priority pollutant PAH), the SHC analysis included 37 alkanes and isoprenoids, and the petroleum biomarker analysis included 47 S/T

compounds (including the 15 base S/T compounds monitored during ANIMIDA I and II). Selected sums of these compounds were also calculated and reported. The list of analytes included hydrocarbons that are expected to be present in permitted or accidental discharges during oil and gas development and production. Additionally, these analyses are useful in identifying potential sources of hydrocarbons in marine environments. Tissue samples were also analyzed for total lipid concentration, and grain size and TOC was measured on the sediment samples (by FIT).

The analytical methods that were employed were developed, refined, and validated specifically for reliable trace-level analysis of the target parameters in marine sediment and biological tissue. The analytical protocols have been used extensively for baseline hydrocarbon characterization and monitoring of potential impact from offshore oil and gas activities in Alaska, including in the previous phases of the ANIMIDA Program, ensuring data comparability.

**Table 13. Summary of chemical analyses of sediment, marine invertebrate, and fish samples.**

| Parameter | Sediment | Invertebrate Tissue | Fish Tissue |
|---|---|---|---|
| **Hydrocarbons** | | | |
| Parent and alkylated polycyclic aromatic hydrocarbons (PAH) | X | X | X |
| Petroleum Biomarkers (S/T) | X | X | X |
| Saturated Hydrocarbons (SHC) | X | X | X |
| **Ancillary Measurements** | | | |
| Total organic carbon (TOC) | X | | |
| Total Lipids | | X | X |

**Table 14. Approximate method detection limits (MDLs) and reporting limits (RLs) for petroleum hydrocarbons in sediment and marine invertebrate and fish tissues.**

**Water MDLs are in ng/L and sediment and tissue MDLs in ng/g, d. wt.**

| Compound Class | MDL | RL |
|---|---|---|
| **PAH and Alkylated PAH** | | |
| Sediment | 0.087–0.50 | 1.2–2.5 |
| Biological tissue | 0.43–1.3 | 2.4–4.7 |
| **Petroleum Biomarkers (S/T compounds)** | | |
| Sediment | 0.17–0.20 | 0.62–1.9 |
| Biological tissue | 0.46–1.5 | 2.4–7.1 |
| **Individual SHC Compounds** | | |
| Sediment | 5.4–10 | 50 |
| Biological tissue | 17–120 | 240 |

#### 4.2.2.1 Analysis of Hydrocarbons

The sediment and biological tissue samples were analyzed for a large suite of parent and alkylated PAH, S/T petroleum biomarker compounds, SHC compounds, and TPH/tSHC. The TPH analysis, like all analyses, was performed in accordance with the QAPP but was not a TPH analysis. This is because TPH analysis is usually performed to assess the contamination associated with petroleum releases, or other samples with high concentrations of petroleum. The extract for TPH analysis of samples from this type of monitoring generally includes significant amounts of interference and false positive contributions from biogenic materials, and does not produce useful data. Even with the TPH analysis for this study being performed on a partially purified SHC extract fraction (F1-fraction from a silica-gel fractionation), and thus referred to as "Total SHC", notable interference was observed at the low concentrations measured in these samples, and the TPH/tSHC data are not considered representative of the actual concentrations and are of limited value. TPH analysis is often not a useful measurement when monitoring near-background environmental conditions and the individual target SHC compound measurements provide a better assessment of the overall hydrocarbon situation.

The sediment and tissue samples were frozen shortly after collection, and stored frozen at approximately -20 ºC, until laboratory processing could begin. The samples were processed in laboratory analytical batches of no more than 20 field samples, with each batch containing a set of laboratory quality control (QC) samples that included a method blank (MB), laboratory control sample (LCS), matrix spike (MS), and a matrix spike duplicate (MSD). A SRM was also analyzed with the sediment and tissue samples, for those parameters that have certified values. In addition, an Alaska North Slope crude (NSC) reference oil was analyzed to monitor instrument performance and compare to a historical database for this material of more than 25 years. The QC program was designed to monitor the potential for laboratory contamination, and accuracy and precision in the presence and absence of a sample matrix. The QC results indicate that the data are of high quality and that the results are representative of the samples and can be used with confidence.

#### 4.2.2.2 Sediment Sample Preparation for Analysis

Sediment samples were extracted as described in Battelle Standard Operating Procedure (SOP) 5-192, Soil/Sediment Extraction Using an Orbital Shaker Table Method for Trace Level Semi-Volatile Organic Contaminant Analysis. The sample preparation procedures are modifications of the Environmental Protection Agency (EPA) SW846 methods. Approximately 30 grams of well mixed sediment was spiked with the appropriate amount of SHC, PAH, and S/T surrogate internal standard (SIS) compounds and serially extracted with dichloromethane (DCM) using orbital shaker table techniques. The combined extracts were dried over anhydrous sodium sulfate and concentrated by Kuderna-Danish or TurboVap and N2 evaporation techniques. Activated copper was added to the sample extracts to remove residual sulfur. The extracts were then purified using a combination of alumina clean up column and silica gel column fractionation, isolating the saturated hydrocarbon and petroleum biomarker fraction (F1) from the aromatic hydrocarbon fraction (F2). The F1 and F2 fractions were collected, concentrated, and spiked with internal standards (IS) compounds and analyzed as described below.

Some of the surface sediment samples collected in 2014 and 2015 were subsampled and submitted to the Woods Hole Oceanographic Institution (WHOI) for *Alexandrium* cyst analysis (Figure 74). For cyst enumeration, a homogenized 5 mL sediment sample was removed from each sample, resuspended with filtered seawater, sonicated, and sieved to yield a clean, 20-100 µm size fraction (Anderson et al., 2003). Cysts were then concentrated, stained with primulin, and enumerated in each sample as described in Anderson et al. (2003).

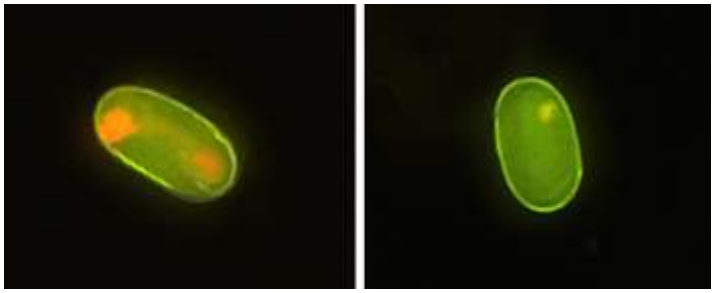

**Figure 74. *Alexandrium fundyense* cysts in sediment samples collected in 2015 from station 149-350 in the Beaufort Sea.**

**Micrographs of primulin-stained cells viewed using epifluorescence microscopy.**

#### 4.2.2.3 Tissue Sample Preparation for Analysis

The amphipod, clam, and fish tissue were partially thawed and the clams shucked with a pre-cleaned titanium knife to remove soft tissues from shell. The overlying water was poured off and the samples were homogenized in a glass jar by maceration with a Tissuemizer™ equipped with Teflon™ gaskets and titanium probes, prior to analysis. Marine tissue samples were extracted as described in Battelle SOP 5-190, Tissue Extraction for Trace Level Semi-Volatile Organic Contaminant Analysis. Approximately 20 g of homogenized tissue was spiked with the SIS compounds and serially extracted three times with DCM using a Tissuemizer™ technique. Between extractions, the samples were centrifuged to facilitate solvent removal. The combined extract was dried over anhydrous sodium sulfate and concentrated by Kuderna-Danish or TurboVap and N2 evaporation techniques. A portion of the extract was removed to determine the total extractable organics (TEO), as a measure of total lipid weight,

by a gravimetric analysis. The extracts were processed through alumina column and fractionated on silica gel column to isolate the hydrocarbon fractions. The F1 and F2 fractions were collected, concentrated, and spiked with IS compounds and analyzed as described below.

#### 4.2.2.4 Instrumental Analysis of Hydrocarbons in Sediment and Tissues

The instrumental analysis was conducted following methods that have been modified from EPA Methods 8015 (SHC compounds and TPH) and 8270 (PAH and S/T compounds), to obtain improved sensitivity and specificity, to include a number of additional key target parameters, and to ensure that the analysis is appropriate for low level detections in marine sediment and tissue samples.

Sediment and marine tissue samples were analyzed for PAH as described in Battelle SOP 5-157, Identification and Quantification of Semi-Volatile Organic Compounds by Gas Chromatography/Mass Spectrometry. This protocol was also used for petroleum biomarker analysis of sediment and tissue samples. The method described in the SOP is a modification of EPA Method 8270, modified to include additional target compounds (e.g., alkyl PAHs and S/Ts), and to obtain lower detection limits and better specificity by operating the mass spectrometer detector in the selected ion monitoring (SIM) mode. The target parent and alkylated PAH are summarized in Table A-1 and target petroleum biomarkers are summarized in Table A-2 (the 15 base S/T compounds from prior phases of ANIMIDA are listed first).

The F1 fraction was analyzed for petroleum biomarkers, and the F2 fraction for PAH, by gas chromatography/mass spectrometry (GC/MS). Prior to the analysis of analytical standards and samples, the mass spectrometer was tuned with perfluorotributlyamine (PFTBA) to maximize the sensitivity of the instrument. The GC/MS was calibrated with at least a 5-point calibration consisting of target compounds to demonstrate the linear range of the analysis. Typically, the calibration for this method ranges from 0.010 to 10 ng per microliter (µL). Calibration verification was performed at the beginning and end of each 24 hour period.

Concentrations of the individual PAH and S/T compounds were calculated by the internal standard method. Target PAH and S/T concentrations were quantified using average response factors (RF) generated from the multi-level calibration. Alkyl homologue PAH concentrations were determined using the average RF for the corresponding parent compound, hopanes were assigned the RF of hopane, and all other biomarkers were assigned the RF of cholestane. Well established alkyl homologue pattern recognition and integration techniques were used to determine alkyl homologues. S/Ts were identified based on characteristic elution patterns. Final concentrations were determined versus the appropriate SIS (i.e., corrected for SIS recovery).

Sediment and marine animal tissue samples were also analyzed for SHC and TPH, as described in Battelle SOP 5-202, Determination of Low Level Total Petroleum Hydrocarbon and Individual Hydrocarbon Concentrations in Environmental Samples by gas chromatography/flame ionization detection (GC/FID). The SOP is a modification of EPA Method 8015, modified to obtain improved sensitivity and specificity, to include a number of additional key target parameters, and to ensure that the analysis is appropriate for marine samples. The target SHC analytes are summarized in Table A-3.

The F1 fraction was analyzed for SHC compounds and TPH (as Total SHC) by GC/FID. Prior to sample analysis, the GC was calibrated using, at a minimum, a 5-point calibration consisting of the target compounds to demonstrate the linear range of the analysis. The concentration of the calibration solutions typically ranged from 1 to 100 µg/mL. The low calibration standard was selected at a concentration near,

but above the method detection limit (MDL). Calibration verification was performed at the beginning and end of each 24-hour period in which samples were analyzed.

Concentrations of SHC and TPH were calculated by the internal standard method. Normal alkanes were quantified using the RF generated from the initial calibration. Isoprenoid hydrocarbon concentrations were quantified using the RF of the n-alkane immediately preceding each target isoprenoid. TPH concentrations were quantified using the average RF of C8 through C40. TPH was measured by integrating the resolved and unresolved peaks in a sample extract in the n-C8 through n-C40 range and subtracting out the response generated from baseline drift attributed by the GC column bleed. The baseline drift was determined by analyzing a solvent blank spiked with IS and quantifying the response generated in the same manner as the sample extracts. Final concentrations were determined versus the appropriate surrogate compound.

#### 4.2.2.5 Notes on Hydrocarbon Summations for Reporting

The concentrations have been determined and reported for each of the individual compounds listed in Tables A-1 through A-3. Sediment and tissue concentrations were reported as ng/g (kilogram [kg]; parts-per-billion [ppb]) on a d. wt. basis. In addition, selected summations of target compounds were produced for data review and analysis, and for comparison to historical data. These include:

- Total PAH: the sum of all PAH compounds that were determined, including alkyl homologues, except retene, C4-dibenzothiphene, and C4-fluroanthene/pyrene, to ensure comparability to ANIMIDA I and II.
- LMW PAH: Low-molecular weight PAH. 2- and 3-ring PAH, including alkyl homologues (Naphthalene through C4-dibenzothiophene), excluding retene.
- HMW PAH: High-molecular weight PAH. 4-, 5-, and 6-ring PAH, including alkyl homologues (fluoranthene through benzo(g,h,i)perylene).
- Sum PAH16 (sometimes referred to as Total PAH16): the sum of the 16 priority pollutant PAHs (EPA Method 610), as shown in bold in Table A-1.
- TPH (total SHC): the concentration based on the total resolved compounds and unresolved complex mixture in the SHC (F1) fraction (C9 – C40).
- Sum SHC: the sum of the individual resolved SHC target compounds (C9 – C40)
- Total S/T: sum of all 47 S/T compounds measured.
- Sum S/T15: sum of the base 15 S/T compounds.

All summations reported use a zero value for non-detects.

### 4.2.3 Quality Assurance/Quality Control

The laboratory work, including the analytical measurements and quality assurance (QA) and QC program, was implemented in accordance with the Program objectives. Laboratory procedures, including QA/QC procedures, were also documented in the laboratory's SOPs and the QAPPs. The following sections present key elements of the laboratory QA/QC Program.

The laboratory analysis for organic compounds was performed by Battelle, and the work adhered to a Quality System described in Battelle's Quality Management Plan (QMP). Battelle's Quality Assurance Manual (QAM) details the application of the Quality System specifically to Battelle's Analytical and Environmental Chemistry Laboratory. Specific project activities were defined in a laboratory QAPP that was prepared by the Project's Laboratory Task Leader and reviewed by the Project

Manager. The Quality Assurance Unit (QAU) at Battelle monitored the analytical components of the project according to existing Battelle SOPs to ensure accuracy, integrity, and completeness of the data. All sample receipt, storage, preparation, analysis, and reporting procedures followed written SOPs. Project staff members were responsible for following these procedures and ensuring that measurement quality objectives (MQOs) were achieved. In the event that an MQO was not met, the analytical staff documented all corrective actions taken related to that exceedance. The Task Leader reviewed and approved corrective actions. The Task Leader was responsible for ensuring that project objectives were met and that the data were traceable and defensible.

#### 4.2.3.1 Field Quality Control

All field personnel (including boat crew members) were briefed on the potential for contamination and cross-contamination of samples and were given guidance on techniques to avoid such problems (e.g., no cigarette smoking in the vicinity of scientific gear or during sampling activities). This included the use of pre-cleaned sample containers, the use of clean sampling equipment, the use of the decontamination protocol described above, and good field practices in general. It also included the following specified sampling procedures and protocols in accordance with the Field Sampling Plan (OF, 2014a).

#### 4.2.3.2 Laboratory Quality Control

A set of QC samples accompanied all field samples processed and analyzed at the laboratory. The following QC samples were analyzed with each batch of field samples:

- MB: A procedural blank is a combination of solvents, surrogates, and all reagents used during sample processing, extracted and analyzed concurrently with the field samples. It is intended to monitor purity of reagents and potential laboratory background contamination.
- LCS: An LCS sample is a contaminant-free matrix-specific sample [e.g., Ottawa sand or sodium sulfate (sediment) and clean Tilapia (tissue)] that is prepared with each analytical batch. It is spiked with the analytes of interest and processed identically to the field samples to assess the analyte recovery and method accuracy in the absence of a field sample matrix.
- MS: A matrix spike is a field sample spiked with the analytes of interest at approximately 10 × the MDL, processed concurrently with the field samples. It is intended to monitor the analyte recovery and method accuracy in the presence of a field sample matrix.
- MSD: A duplicate is a matrix spike sample. It is intended to provide an additional measure of recovery and method accuracy in the presence of a field sample matrix, and also to assess precision by comparing the results to the MS results.
- (SRM: A standard reference material is a field sample with certified and naturally incurred analyte concentrations. An SRM is prepared and analyzed to assess the accuracy of the analytical procedures.
- (NSC Reference Oil: A NSC oil sample is used to evaluate the instrumental accuracy and also provides petroleum pattern information, aiding in the qualitative identification of target analytes.
- SIS: (1 to 3 per sample for organic analyses) SIS compounds are spiked into each field and quality control sample prior to organic compound extraction and analysis. The surrogate recoveries provide a measure of the overall sample extraction and processing efficiency.

A set of MQOs were established to ensure that the analytical data would be of the quality necessary to achieve the project objectives. The MQO for each QC parameter listed above is presented in Table A-4 and the data qualifiers that were used are summarized in Table A-5.

#### 4.2.3.3 Method Detection Limits

The MDL is defined as the minimum concentration that can be measured and reported with 99% confidence that the analyte concentration is greater than zero. Reporting limits (RL) are defined by the sample concentration of a compound that is equivalent to the final extract concentration based on the low calibration standard concentration. Target compounds confidently detected below the RL (typically down to a concentration using a signal-to-noise ratio criteria of approximately 3-5:1) were reported and qualified appropriately, regardless of how it compares to the calculated MDL. Approximate MDLs and RLs for each matrix for hydrocarbons are summarized in Table 14, and actual MDLs for each compound are included in Tables A-1 through A-3.

## 4.3 Results

Sediment and marine animal (clams, amphipods, and Arctic cod) samples were collected in August 2014 and 2015. The number of samples that were collected and analyzed are summarized in Table 12. The locations of the 2014 and 2015 stations are illustrated in Figure 70.

Samples were analyzed for four types of hydrocarbons: total petroleum hydrocarbons (represented by the Total SHC), individual SHC, individual S/T, and PAHs; the individual target hydrocarbon compounds that were measured are presented in Tables A-1 through A-3. This section summarizes the results of the analyses of hydrocarbons in environmental samples collected in 2014 and 2015 during the ANIMIDA III Program summer surveys.

The presentations and discussions in this report are focused on the summations of hydrocarbon data (e.g., Total PAH, Total SHC), to represent the hydrocarbon chemistry. The information is in particular focused on the PAH chemistry; PAH being the hydrocarbon chemical constituents of primary environmental concern in petroleum and activities associated with oil and gas development (Neff and Durell, 2012; Neff, 2010; Neff, 1987). Summaries across the two survey years are presented in this section. The results for each sample are presented in Tables A-6 through A-8 (sediment), and Tables A-11 and A-12 (biological tissue). The detailed data for each sample and each of the 129 individual hydrocarbon parameters (45 PAH, 37 SHC, and 47 S/T) has been delivered to BOEM, and was used as the basis for this report. ANIMIDA III data are archived at the National Centers for Environmental Information (NCEI) at https://doi.org/10.7289/V5VQ30R3.

The sediment and biological tissue data in this report are presented on a d.wt. basis. The use of d. wt. to report chemical concentrations reduces data variability caused by variations in the amounts of water retained by the sample matrix, and provides for a more reliable data comparison. All hydrocarbon concentration data are presented as surrogate corrected data. Target compounds are corrected for the recovery of a representative surrogate compound added to the sample during laboratory analysis. The main purpose of this data correction is to account for sample loss that may have occurred during sample processing, and to more accurately represent the actual hydrocarbon concentration in the original field sample.

### 4.3.1 Sediment Monitoring

Concentrations of individual PAH, S/T, and SHC compounds, as well as TPH (as tSHC), were measured in sediments collected in 2014 and 2015 during the ANIMIDA III surveys. The sediment hydrocarbon concentrations, and summary statistics, using key parameter summations, and TPH, are summarized in Table 15. Table 15 includes both the surface sediment data from 2014 and 2015, and the data for the single sediment core that was collected in 2014 and analyzed for hydrocarbon concentrations.

As discussed, TPH analysis of sediments such as these is susceptible to interference from biogenic and other non-petroleum organic compounds and is not useful for trace-level environmental monitoring or to assess small potential changes over low environmental background concentrations. Therefore, the TPH data (as Total SHC) should not be used in this data assessment; the sum of the target SHC compound concentrations provides a better measure of the general hydrocarbon levels. Furthermore, it is important to consider the variability in the data when, for instance, comparing mean 2014 and 2015 concentration or when comparing these data to data from any future potential development and production years, to determine if there are significant differences.

**Table 15. Summary of concentrations of hydrocarbons in sediment samples collected during ANIMIDA III.**

**All concentrations are ng/g dry wt (µg/kg; parts per billion).**

| Hydrocarbon Type | 2014 | | | | 2015 | | | |
|---|---|---|---|---|---|---|---|---|
| | Mean | SD | Min | Max | Mean | SD | Min | Max |
| ***Surface Sediment (n=43 in 2014 and n=26 in 2015)*** | | | | | | | | |
| Total PAH | 532 | 331 | 22.6 | 1,300 | 707 | 450 | 96.0 | 1,470 |
| Sum SHCs | 3,010 | 1,800 | 200 | 7,950 | 3,340 | 1,820 | 410 | 7,340 |
| Total SHC | 5,510 | 3,650 | 490 | 13,700 | 8,300 | 5,580 | 130 | 17,700 |
| Sum S/T | 85.1 | 39.9 | 8.41 | 154 | 108 | 62.3 | 16.2 | 212 |
| % TOC | 1.07 | 0.40 | 0.25 | 2.28 | 1.17 | 0.45 | 0.30 | 2.36 |
| **Sediment Core (n=11 segments from one core in 2014)** | | | | | | | | |
| Total PAH | 1,320 | 102 | 1,150 | 1,490 | | | | |
| Sum SHCs | 7,630 | 870 | 6,190 | 8,470 | | | | |
| Total SHC | 14,800 | 3,960 | 10,200 | 23,500 | | | | |
| Sum S/T | 165 | 11.7 | 141 | 179 | | | | |
| % TOC | 1.57 | 0.07 | 1.45 | 1.67 | | | | |

#### 4.3.1.1 Polycyclic Aromatic Hydrocarbons (PAH)

Concentrations of Total PAH in the 2014 surface sediment samples range from 22.6 to 1,300 ng/g with 36 of the 43 samples having Total PAH concentrations less than 1,000 ng/g (Table 15, Table A-6), and the remaining having concentrations only slightly above 1,000 ng/g. The 2015 surface sediment Total PAH concentrations were similar, ranging from 96 to 1,470 ng/g. The mean Total PAH concentrations were 532 ± 331 ng/g (one SD) and 707 ± 450 ng/g in the surface sediments collected in 2014 and 2015, respectively. The 11 segments from the sediment core collected at Station 1.2, about 50 mi offshore, had higher and rather consistent PAH concentrations, with a mean Total PAH concentration of 1,320 ± 102 ng/g (and a range of 1,150 to 1,490 ng/g for the 11 segments). Though not consistently so, the lower PAH (and other hydrocarbon) concentrations were generally in the sediments with lower total organic carbon (%TOC) and higher sand content that other samples, and often from closer to the shore than far offshore.

#### 4.3.1.2 Saturated Hydrocarbons (TPH and SHC)

The surface sediment TPH (as Total SHC; tSHC) concentrations showed a somewhat higher degree of variability than other hydrocarbon measurements, which can, as discussed earlier, be attributed to challenges in reliably measuring an overall hydrocarbon value (as opposed to discrete compounds) in environmental samples at trace-level concentrations. The measured TPH/tSHC concentrations are likely, in part, contributed by biogenic (both plant and animal based) and other organic compounds, and not only hydrocarbons of petroleum nature, even following sample extract purification; the measurement is therefore of less value for samples such as these. TPH analysis is primarily intended for characterization of sites with significant petroleum contamination and not for low-level environmental monitoring of un-impacted locations. The analysis of the individual target SHC compounds, as represented by the sum of the concentrations of the SHC compounds, is a more reliable method for assessing the general petroleum hydrocarbon concentrations in these samples than TPH or TSHC analysis, and for comparing the overall hydrocarbon levels.

Sediment Sum SHC concentrations (the sum of the individual alkane and isoprenoid compound concentrations) ranged from 200 ng/g to 7,950 ng/g in the 2014 samples and from 410 to 7,340 ng/g in 2015. The mean Sum SHC concentrations were 3,010 ± 1,800 ng/g (one SD) and 3,340 ± 1,820 ng/g in the surface sediments collected in 2014 and 2015, respectively. The mean Sum SHC concentration for the sediment core samples from Station 1.2 (2014) was 7,630 ± 870 ng/g so, like for PAH, somewhat higher and much more uniform concentrations than the surface sediments. The most abundant resolved alkanes in all sediment samples were the higher molecular weight n-alkanes (above n-C20), and particularly the odd-numbered alkanes, with the most abundant n-alkane in all sediment samples generally being n-C27, indicating significant contributions from terrestrial plant material sources.

#### 4.3.1.3 Petroleum Biomarkers - Steranes and Triterpanes (S/T)

(S/T are generally present at substantially lower concentrations than SHCs and PAH in both petroleum materials and environmental samples, and are not considered to be environmental contaminants. They are, however, a component of petroleum and because of their stability and unique composition in different petroleum and hydrocarbon materials are often very useful for identifying and differentiating sources of petroleum, including spilled materials and if petrogenic or biogenic. S/T data can therefore be important to include when establishing baseline hydrocarbon conditions, and when conducting potential impact monitoring.

The Sum S/T15 concentration has been used and reported based on the 15 S/T parameters used in earlier ANIMIDA phases. Those have also been reported for ANIMIDA III, and a total of 32 additional S/T compounds were included in the analysis of these samples (Table A-2), many of which can be useful for identifying subtle differences in hydrocarbon sources.

Concentrations of Sum S/T (based on all 47 S/T compounds) in the 2014 and 2015 surface sediment samples ranged from 8.41 to 154 ng/g and 16.2 to 212 ng/g, respectively (Table 15). The S/T concentrations were generally quite uniform, with the majority of the samples having Sum S/T concentrations that were within a factor of three of each other (generally between 50 and 150 ng/g). The mean Sum S/T concentrations were 85.1 ± 39.9 ng/g and 108 ± 62.3 ng/g in the 2014 and 2015 surface sediments, respectively. The mean S/T concentration for the Station 1.2 sediment core was 165 ± 11.7 ng/g (ranging from 141 to 179 ng/g, with the concentration tending to decrease with depth); so, again, slightly higher and more uniform concentrations than the surface sediments.

#### 4.3.1.4 Alexandrium Cyst Measurements

There have been several recent reports of this bloom-forming toxic alga in the Arctic and adjacent seas, including the discovery of extremely large accumulations of dormant *Alexandrium fundyense* cysts in the eastern Chukchi Sea (Gu et al., 2013; Natsuike et al., 2013). The origin or history of *A. fundyense* cysts in the Arctic and their current role in the population dynamics of *Alexandrium* in the region and prevalence in Arctic food webs are unknown. However, the high cyst accumulations observed in the Chukchi Sea could represent a significant and sustained seedbed for future outbreaks and species dispersal as Arctic waters continue to warm.

Sediment samples of opportunity were collected during the 2014 and 2015 ANIMIDA III survey in support of a WHOI study investigating the prevalence of the cyst-forming, toxin-producing dinoflagellate *A. fundyense* in the Beaufort Sea (Figure 75). The effort focused on delineating the geographic extent of cyst seedbeds and determining the magnitude of blooms in this region. This analysis complements ongoing research at WHOI to examine the origin and transport of *A. fundyense* in Arctic waters, characterize the physical and physiological processes that determine the extent of cyst germination and vegetative cell growth in the Arctic, and identify favorable habitat areas for bloom initiation.

A total of 34 sediment samples were processed and analyzed. *A. fundyense* resting cysts were observed in five of the 14 samples collected in 2014, and six of the 20 samples collected in 2015 (Figure 75). Concentrations at stations where cysts were observed ranged from 3 to 18 cysts/mL (mean ± SD: 5.4 ± 4.8 cysts/mL).

Analysis of sediments collected from the Beaufort Sea in 2014 and 2015 showed that *A. fundyense* cysts were present at low densities in approximately one-third of the samples examined. Cyst abundances in Beaufort Sea sediments were significantly lower than those observed in the Chukchi Sea. The Beaufort Sea may represent the leading edge of this species' distribution in the region, with the major seedbed located to the west in the Chukchi Sea.

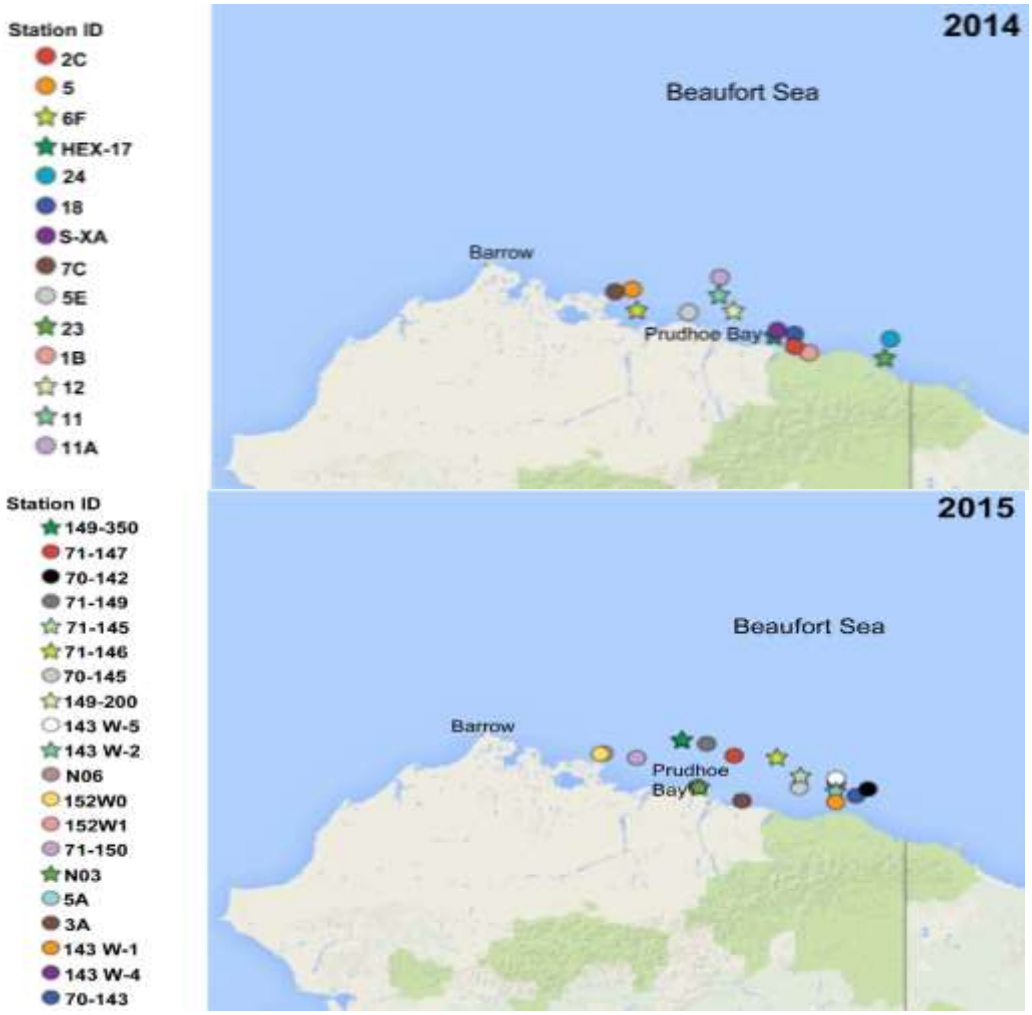


**Figure 75. Maps showing sediment sampling locations in 2014 (top panel) and 2015 (bottom panel).**

**Stars indicate stations where *Alexandrium* cysts were detected. Circles indicate no cysts observed. Unpublished results provided by Don Anderson and Mindy Richlen, WHOI.**

### 4.3.2 Biota Monitoring

Concentrations of individual PAH, S/T, and SHC compounds, and TPH (as Total SHC), were also measured in tissue of marine invertebrates (clams and amphipods) and fish (Arctic cod) collected during ANIMIDA III. The tissue hydrocarbon concentrations, and summary statistics, are summarized in Table 16, and the results for each individual sample are presented in Tables A-11 and A-12. The Total PAH and Sum SHC data are described in this report; the S/T and TPH/tSHC data have also been reported, but are of limited value for biological tissue evaluation. The lipid content (as a percentage (%), on a d. wt. basis) was also determined on all tissue samples, and is also reported.

When evaluating biological tissue hydrocarbon concentrations, it is important to remember the animal mobility and the contaminant accumulation mechanisms; station-specific results are less meaningful than for sediment (particularly for the mobile amphipods and fish). Additionally, fairly small

numbers of biological tissue samples were collected, making it difficult to perform reliable statistics on the data. Also, it is important to consider the variability in the data when, for instance, comparing mean 2014 and 2015 (and future) concentrations, or when performing areal comparisons, to determine if there are differences.

**Table 16. Summary of hydrocarbon concentrations in amphipod, clam, and fish tissue samples collected during ANIMDA III.**

**All concentrations are ng/g dry wt (µg/kg; parts per billion); lipid is % dry wt.**

| Hydrocarbon Type | 2014 | | | | 2015 | | | |
|---|---|---|---|---|---|---|---|---|
| | Mean | SD | Min | Max | Mean | SD | Min | Max |
| ***Amphipods (n=21 in 2014 and n=7 in 2015)*** | | | | | | | | |
| Total PAH | 30.4 | 25.2 | 12.4 | 109 | 25.1 | 3.80 | 20.4 | 30.7 |
| Sum SHC | 61,000 | 60,200 | 4,020 | 296,000 | 47,600 | 53,600 | 15,500 | 164,000 |
| % Lipid | 5.46 | 1.35 | 2.60 | 7.71 | 5.11 | 1.02 | 3.91 | 7.03 |
| **Clams (n=7 in 2014 and n=7 in 2015)** | | | | | | | | |
| Total PAH | 380 | 694 | 55.6 | 1,930 | 44.0 | 22.6 | 17.2 | 69.9 |
| Sum SHC | 3,690 | 4,130 | 1,130 | 12,900 | 2,700 | 1,510 | 1,320 | 6,100 |
| % Lipid | 2.82 | 0.72 | 1.83 | 4.00 | 1.08 | 0.46 | 0.66 | 2.09 |
| **Fish (n=11 in 2014 and n=6 in 2015)** | | | | | | | | |
| Total PAH | 94.3 | 21.5 | 63.9 | 131 | 23.9 | 9.58 | 11.3 | 37.0 |
| Sum SHC | 80,100 | 105,000 | 1,930 | 314,000 | 978,000 | 1,190,000 | 15,600 | 3,080,000 |
| % Lipid | 3.40 | 1.15 | 1.51 | 4.80 | 5.50 | 1.14 | 4.06 | 6.85 |

#### 4.3.2.1 Polycyclic Aromatic Hydrocarbons (PAH)

The Total PAH concentrations in the clam, amphipod, and Arctic cod tissue samples are summarized in Table 16. The Total PAH d. wt. concentrations were rather uniform for amphipods, more variable for clams, while the fish Total PAH concentrations were quite uniform for a given year. The amphipod Total PAH concentrations ranged from 12.4 to 109 ng/g in 2014 and from 20.4 to 30.7 ng/g in 2015 (most were between 20 and 30 ng/g), and the lipid content ranged from 2.60 to 7.71% across the two years. The mean Total PAH concentrations in the amphipods were 30.4 ± 25.2 ng/g in 2014 and 25.1 ± 3.80 ng/g in 2015; a few apparently elevated concentrations in 2014 clearly impacted the summary statistics.

Concentrations of Total PAH in clam tissue ranged from 55.6 to 1,930 ng/g in 2014 and from 17.2 to 69.9 ng/g in 2015 (Table 16); most clam samples had Total PAH concentrations under 100 ng/g, and the one sample with a reported concentration of 1,930 ng/g was likely the result of an analytical artifact. The lipid content of the clams ranged from 0.66 to 4.36%, d. wt. for the 2014 and 2015 samples. The amphipods had about two to three times higher lipid content than the clam samples. The mean Total PAH concentrations in the clams were 380 ± 694 ng/g in 2014 and 44.0 ± 22.6 ng/g in 2015; one dramatically elevated, and likely erroneous, concentrations reported in 2014 clearly impacted the summary statistics.

Concentrations of Total PAH in Arctic cod tissue ranged from 63.9 to 131 ng/g in 2014 and from 11.3 to 37.0 ng/g in 2015 (Table 16). The mean Total PAH concentrations in the fish were 94.3 ± 21.5 ng/g in 2014 and 23.9 ± 9.58 ng/g in 2015. The fish Total PAH concentrations were quite uniform within a given year, but the 2014 concentrations were, on average, four times higher than in 2015. The lipid

content of the Arctic cod ranged from 1.51 to 6.85%, d. wt. for the 2014 and 2015 samples and, surprisingly, the lipid content was higher in the 2015 fish, that had lower Total PAH concentrations.

#### 4.3.2.2 Saturated Hydrocarbons (SHC)

As discussed for the sediment TPH results, the tissue TPH/tSHC analysis is susceptible to interference contributions from non-petroleum hydrocarbons in complex sample matrices, and that is even more the case for tissue samples than sediment samples. Additionally, the tissue TPH/tSHC concentrations were generally near the limit of detection, when detectable, which further confounds those results. Again, the resolved SHC compound analysis (including Sum SHC) is a more reliable method for assessing the overall petroleum hydrocarbon concentrations in these samples, and for comparing the hydrocarbon data, and that is what is presented below.

Tissue Sum SHC concentrations range from 4,020 to 296,000 ng/g in the amphipod samples in 2014 and from 15,500 to 164,000 ng/g in 2015; the concentrations were quite variable (Table 16). The saturated hydrocarbon concentrations in the amphipod are dominated by the isoprenoid pristane that is, naturally produced by some marine plants and animals as part of their metabolic processes, and bioaccumulated by amphipods and Arctic cod from their food. The mean Sum SHC concentrations in the amphipods were 61,000 ± 60,200 ng/g in 2014 and 47,600 ± 53,600 ng/g in 2015; the concentrations clearly had a large amount of variability.

The Sum SHC concentrations in clam tissue range from 1,130 to 12,900 ng/g in 2014 and from 1,320 to 6,100 ng/g in 2015; most clam sampled had Sum SHC concentrations under 5,000 ng/g. The mean Sum SHC concentrations in the clams were 3,690 ± 4,130 ng/g in 2014 and 2,700 ± 1,510 ng/g in 2015.

The Sum SHC concentrations in Arctic cod tissue range from 1,930 to 314,000 ng/g in 2014 and from 15,600 to 3,080,000 ng/g in 2015 (Table 16). The mean Sum SHC concentrations in the fish were 80,100 ± 105,000 ng/g in 2014 and 978,000 ± 1,190,000 ng/g in 2015. As in amphipods, most of the Sum SHC was pristine. The fish Sum SHC concentrations were highly variable, and a few fish samples with more than 100,000 ng/g (in 2014) and more than 1,000,000 ng/g (in 2015) clearly impact the summary statistics.

## 4.4 Discussion

The results that were presented in Section 4.3 are further described and discussed in this section. Information related to the surface sediment hydrocarbon concentrations that were measured, including how those vary geographically and how they compare to results obtained in other relevant studies, are presented and discussed. The composition of the measured hydrocarbon compounds is also described, and the potential sources of the hydrocarbons in the Beaufort Sea is discussed. The potential ecological implications of the measured surface sediment hydrocarbon concentrations are also discussed. Hydrocarbon concentrations in sediment core samples are described, to gain an understanding of the history of hydrocarbon loadings.

Hydrocarbon concentrations in the tissue of amphipods, clams, and Arctic cod are also discussed, to understand the levels of those chemicals in selected key marine animals. Additionally, the potential ecological implications of the accumulated hydrocarbons are described.

The focus will be on discussing the PAH data in this document; PAH being the class of hydrocarbons related to oil and gas activities that are of greatest interest from an environmental impact

perspective. The SHC, and S/T chemical biomarker data will be included when those add useful information. The sum of the compound concentrations by compound class (e.g., Total PAH) will be discussed as an overall representation of the hydrocarbons, and individual compound data will be described when useful. TPH analysis is, as discussed, not a useful measurement in near-background environmental monitoring such as this, and it is recommended that it not be included in future monitoring.

### 4.4.1 Sediment Monitoring

#### 4.4.1.1 Surface Sediments

##### *4.4.1.1.1 Hydrocarbon Characteristics: Concentrations and Distribution*

The sediment hydrocarbon concentrations, and summary statistics, using key parameter summations, and TPH, are summarized in Table 15. The data for each individual station are presented in Tables A-6 through A-8, and the individual compound data have been reported to BOEM and were used to generate the information in this document.

The Total PAH concentrations range from a little under 100 ng/g (d. wt.) to a little over 1,000 ng/g for the surface sediment samples collected during ANIMIDA III (Table 17 and Figure 76); most samples had concentrations between 200 and 800 ng/g. The sediments at the historic BSMP and ANIMIDA stations that were re-sampled during ANIMIDA III had mean Total PAH concentration of 336 ng/g (2014) and 390 ng/g (2015), while the new stations had mean Total PAH concentrations of 590 and 810 ng/g in 2014 and 2015, respectively. The SHC and S/T concentrations were, on average, also higher in the sediments from the new stations than the historic stations. The TOC concentrations, on the other hand, were quite similar and slightly higher, on average, for the historic stations even though the sediments from the new stations were finer grained (Table 17).

**Table 17. Mean and range of concentrations of TPAH, TSHC, TStTr, TOC, and silt+clay in surface sediments collected in 2014 and 2015 in ANIMIDA III and between 2000 and 2006 in ANIMIDA I and II.**

**Hydrocarbon concentrations are ng/g dry wt (parts per billion) and TOC and silt+clay (mud) are % dry wt. ANIMIDA I and II data from Neff and Durell (2010).**

| Year | Total PAH (ng/g) | Total SHC (ng/g) | Total St/Tr[a] (ng/g) | TOC (%) | Silt+Clay (%) |
|---|---|---|---|---|---|
| ***ANIMIDA III - New Stations (n=33 in 2014 and n=18 in 2015)*** | | | | | |
| 2014 | 590 (51 – 1,300) | 6,200 (490 – 14,000) | 95 (9.7 – 150) | 1.0 (0.29 – 1.8) | 55 (4.8 – 97) |
| 2015 | 810 (96 – 1,400) | 9,100 (480 – 17,000) | 130 (16 – 210) | 1.0 (0.30 – 1.5) | 62 (5.9 – 100) |
| **ANIMIDA III - Historical BSMP and ANIMIDA Stations (n=10 in 2014 and n=8 in 2015)** | | | | | |
| 2014 | 336 (23 – 1,100) | 3,000 (500 – 8,900) | 51 (8.4 – 120) | 1.2 (0.25 – 2.3) | 34 (3.7 – 68) |
| 2015 | 390 (120 – 630) | 5,400 (130 – 9,400) | 58 (17 – 100) | 1.5 (0.84 – 2.4) | 54 (17 – 81) |
| **ANIMIDA I and II - Historical BSMP and ANIMIDA Stations** | | | | | |
| 2000 (n=51) | 560 (26 – 1,800) | 11,000 (1,000 – 27,000) | 56 (2.9 – 180) | 0.99 (<0.1 – 4.4) | 53 (1.2 – 94) |
| 2002 (n=43) | 380 (12 - 940) | 7,500 (440 – 22,000) | 39 (1.5 – 110) | 0.75 (0.14 – 1.8) | 49 (0.9 – 92) |
| 2004 (n=47) | 440 (13 – 1,100) | 13,000 (1,000 – 85,000) | 45 (1.8 – 110) | 0.61 (0.05 – 2.4) | 48 (0.1 – 100) |
| 2005 (n=39) | 520 (45 – 1,400) | 12,000 (230 – 100,000) | 60 (2.1 – 660) | 0.91 (0.05 – 6.4) | 39 (3.1 – 92) |
| 2006 (n=30) | 570 (25 – 1,800) | 10,000 (1,100 – 27,000) | 46 (3.3 – 170) | 0.91 (0.08 – 2.8) | 47 (1.2 – 95) |

a TotalSt/Tr is based on all 46 compounds measured in 2014 and 2015 for ANIMIDA III, and the 15 compounds measured in 2000-2006 for ANIMIDA I and II; the sum of the 46 compounds averaged 1.99 (Std. dev = 0.11) times the sum of the 15 compounds in 2014 and 2015.

Hydrophobic organic compounds, like PAH, SHC, and S/T, tend to adhere to organic matter and fine-grained material in sediment, and there is often a relationship of increasing hydrocarbon concentration with increasing TOC concentration, when other factors are constant. A similar relationship is often also observed with the % fines and % Al in the sediment, because most of the TOC is absorbed to the clay (aluminosilicate) fraction; the smaller the particle size is of the sediments the more hydrocarbons are often measured, for a given general environment. Aluminum, the most abundant mineral in sediment, increases in concentration as the grain size decreases. As a result, the TOC concentration also tends to positively correlate with the % fines and % Al in the sediment; Figure 77 illustrates the Total PAH concentration vs %TOC, %fines, and %Al in all the ANIMIDA III surface sediment samples. The hydrocarbon concentrations do not correlate well overall with the TOC content in these sediments (Figure 77), although the graph suggests there may be subsets of samples with a more consistent relationship, possibly from different parts of the study area with differing organic compound characteristics. Eroded peat particles (part of TOC) have a wide range of particle sizes. The hydrocarbon concentrations correlate better with the % fines and % Al, and this may be useful to help understand if the concentration in a sample is greater than what would be expected naturally, and could be the result of anthropogenic activities.

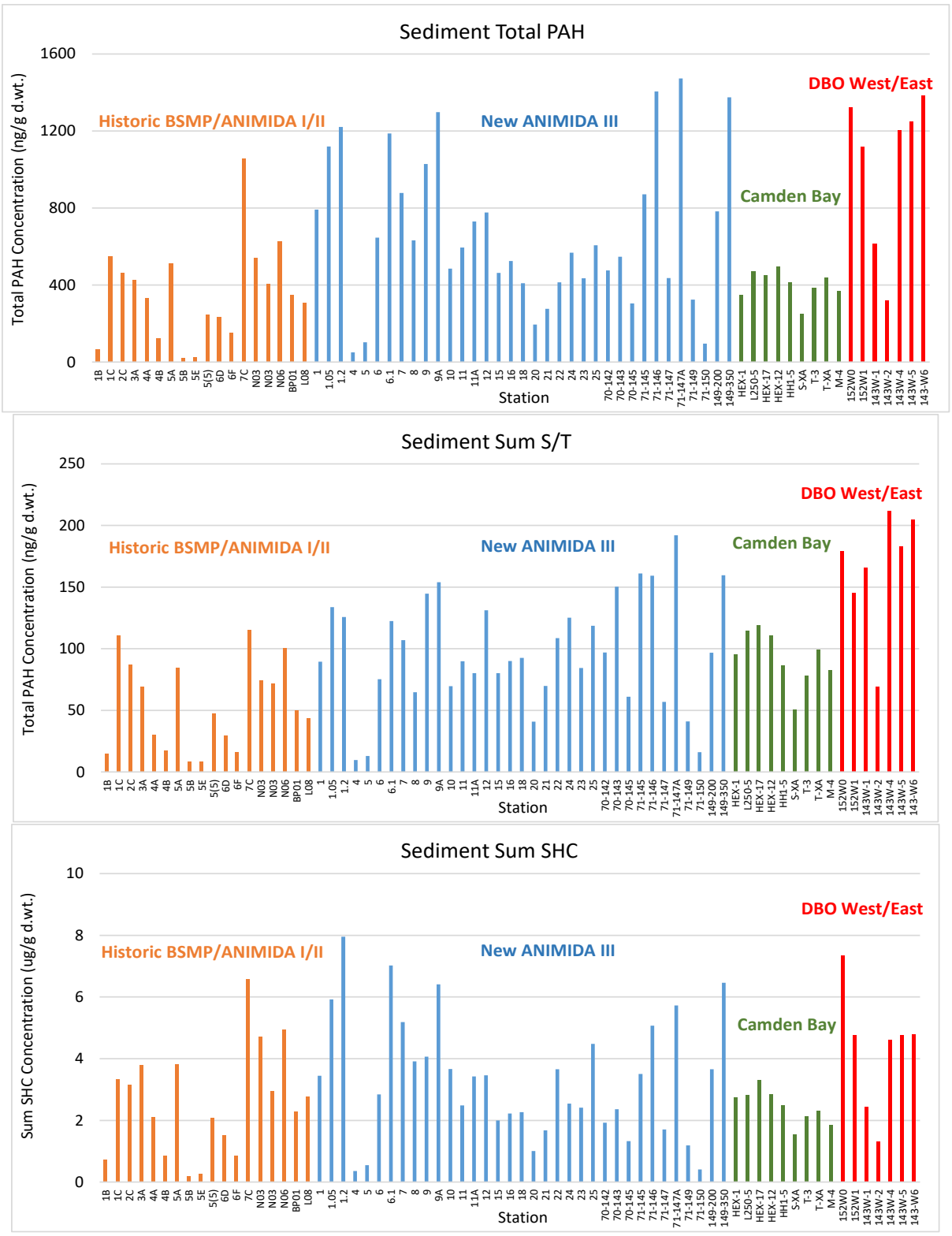


**Figure 76. Sediment Total PAH, Sum S/T, and Sum SHC concentrations in the sediment samples collected during in 2014 and 2015 as part of ANIMIDA III.**

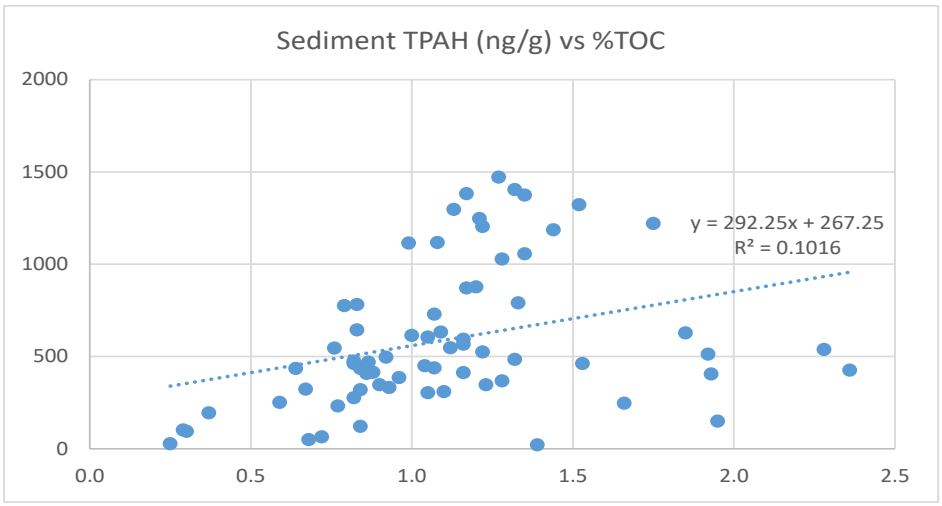


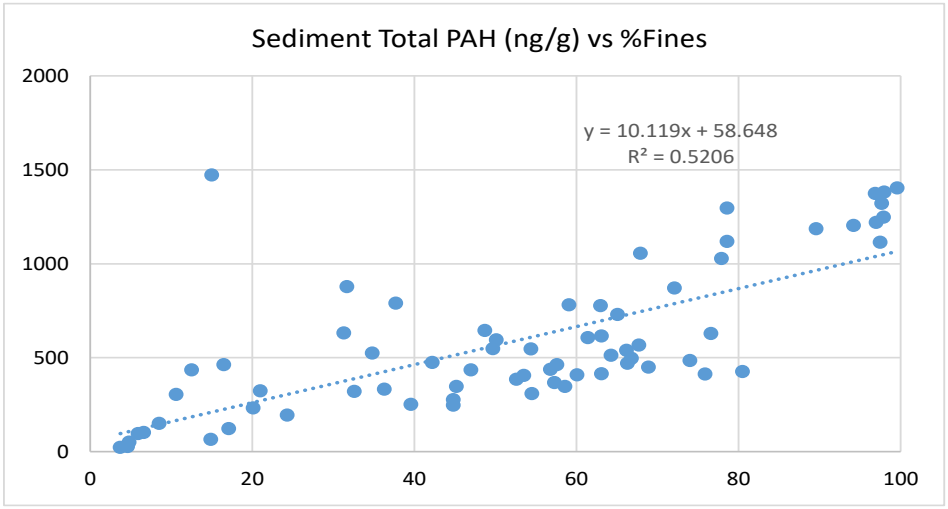


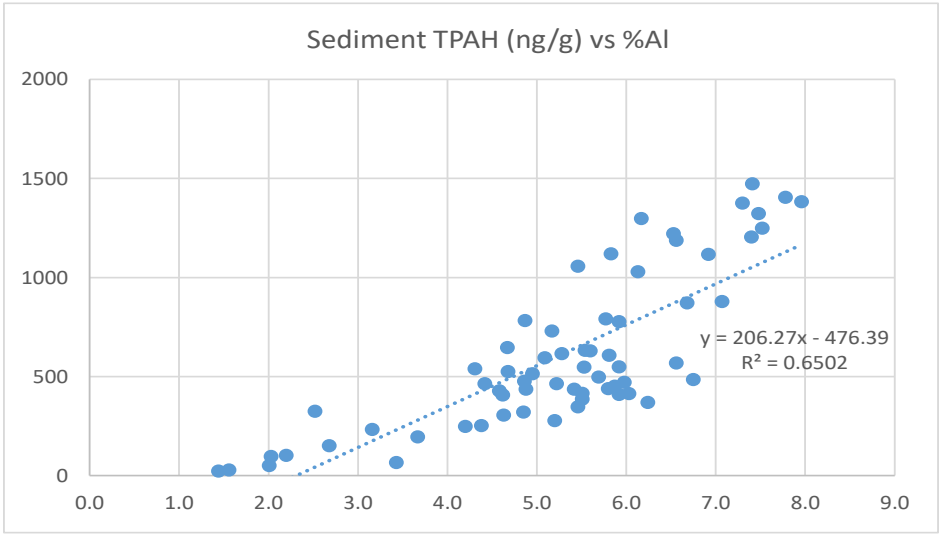


**Figure 77. Sediment Total PAH concentrations vs sediment geochemical parameters (%TOC, % fines, and %aluminum).**

Hydrocarbon concentrations measured during ANIMIDA I and II are also summarized in Table 17 and Table 18, and such data from other studies of Alaskan marine sediment are also shown in Table 18. The Total PAH, Total SHC, and S/T concentrations were, in general, comparable for the ANIMIDA III surface sediment samples and samples collected during BSMP, ANIMIDA I and II, sediments collected in Cook Inlet, Shelikof Strait, and other parts of the Alaska marine environment. The surface sediment Total PAH concentrations that were measured in ANIMIDA III were generally between 200 and 800 ng/g. The sediment Total PAH concentrations measured during BSMP and ANIMIDA I and II were generally in the 300 to 600 ng/g range, and concentrations measured in other Alaskan' studies varied more widely. The ANIMIDA III sediment hydrocarbon concentrations compare particularly well for the samples collected at historical BSMP and ANIMIDA stations, and the ANIMIDA I and II stations from those same general areas, as would be expected. The hydrocarbon data are also quite comparable on a station-specific basis, for stations that have been monitored over many years. For instance, Liberty Station L08 had a measured surface sediment Total PAH concentration of 310 ng/g in ANIMIDA III (2015), and in the three ANIMIDA II survey years (2004-2006) it was 740, 310, and 360 ng/g. The sediments at Northstar Station N06 had 629 ng/g in ANIMIDA III (2015), and between 410 and 830 ng/g during ANIMIDA II. Nearby Station N03 (within 1 km of the Northstar production island) had a Total PAH concentration of 540 (2014) and 407 ng/g (2015) during ANIMIDA III, and somewhat higher 1,110 (2004), 950 (2005), and 1,110/1,000 (duplicates from 2006) ng/g Total PAH during ANIMIDA II; it may be that slightly elevated hydrocarbon concentrations from the development if the production island have now dissipated to background levels.

**Table 18. Mean Concentrations of key hydrocarbons in surficial sediments from ANIMIDA I and II study area, Alaska marine sediments, and Cook Inlet and Shelikof Strait sediments.**

| | Total PAH (ng/g) | Total PHC[g] (ng/g) | Total S/T (ng/g) |
|---|---|---|---|
| Concentrations in Alaska Marine Sediments[a] | 16–2,400 | 470–38,000 | NA |
| Concentrations in Cook Inlet and Shelikof Strait Sediments[b] | 1–1,100 | 900–69,000 | 9–87 |
| Average (Range) Concentrations for ANIMIDA Study Area Sediment Cores[c] | 540 (280–2,000) | 9,000 (3,200–31,000) | 59 (21–220) |
| Average (Range) Concentrations for Phase I ANIMIDA I Study Area Surficial Sediments[d] | 390 (7–2,700) | 6,600 (210–50,000) | 25 (1–82) |
| Average (Range) Concentrations for Phase II ANIMIDA I Study Area Surficial Sediments[e] | 490 (12–2,000) | 9,500 (440–27,000) | 49 (2–180) |
| Average (Range) Concentrations for ANIMIDA II Study Area Surficial Sediments[f] | 460 (13–1,600) | 13,000 (390–104,000) | 50 (2–660) |
| Average (Range) Concentrations for ANIMIDA II Study Area Sediment Cores[f] | 820 (300–1,600) | 15,000 (3,800–42,000) | 66 (13–190) |

a Prince William Sound subtidal and Beaufort Sea (Bence et al., 1996; Boehm et al., 1991).
b ENRI - UAA, 1995, Hyland, et al.,1995; KLI, 1996; KLI, 1997; Boehm et al., 2001a.
c Brown et al., 2003.
d Boehm et al. 2001b.
e Brown et al., 2005.
f Results from this study.
g Total PHC concentrations for the ANIMIDA I and II studies included saturated hydrocarbons only, while Total PHC concentrations for the other studies included saturated and aromatic hydrocarbons.
NA – not applicable.
From Brown et al., 2010.

The S/T concentrations compare similarly as the PAH concentrations. However, comparisons of S/T data to historical data is less meaningful than for PAH data, because S/T compounds are present at only trace levels and not considered a contaminant with common anthropogenic sources. S/T data are generated primarily to be able to characterize the different types of hydrocarbon materials that may be present, and for source identification (e.g., from terrestrial sources, seeps, accidental spills, etc.); the *relative* S/T compounds concentration are what is of greatest interest, not absolute concentrations. The Total SHC and PHC concentrations show more fluctuation across different studies and years, as this analysis is highly susceptible to natural non-target compound matrix contributions and interferences influenced by subtle differences in the analytical methodologies, and reliable comparisons across projects can often not be made.

There appears to be a slight difference in the hydrocarbon concentrations in the sediments from the new stations and the historical stations sampled during ANIMIDA III, with the new stations, on average, having nearly twice as high hydrocarbon concentrations (Table 17 and Figure 76). The historical BSMP and ANIMIDA station samples had quite variable concentrations, while it was somewhat more uniform for the new stations; particular those collected within the more uniform environment of Camden Bay (Figure 76). An important factor influencing the surface sediment hydrocarbon concentration seems to be the distance the sample is collected from the shore. The new ANIMIDA III stations are mostly farther offshore, and in deeper waters, than the BSMP and historical ANIMIDA stations (Figure 70, Figure 76, Figure 78).

Although the stations within 10 mi of the shore have variable PAH concentrations, the concentrations are clearly lower for that set of stations than at the stations more than 10 mi offshore (Figure 78). The TOC-normalized PAH concentrations are also higher for the offshore than nearshore stations, so the difference cannot be attributed to differences in the organic carbon content of the sediments. The sediments are slightly more fine than coarse grained offshore, which could help explain some of the differences in the hydrocarbon concentrations. The lower hydrocarbon concentrations closer to the shore may, in part, be attributed to the somewhat coarser grain sediment in this higher energy environment near the shore. The fine grain material, with higher hydrocarbon concentrations, is more readily carried offshore, settling in a lower energy location.

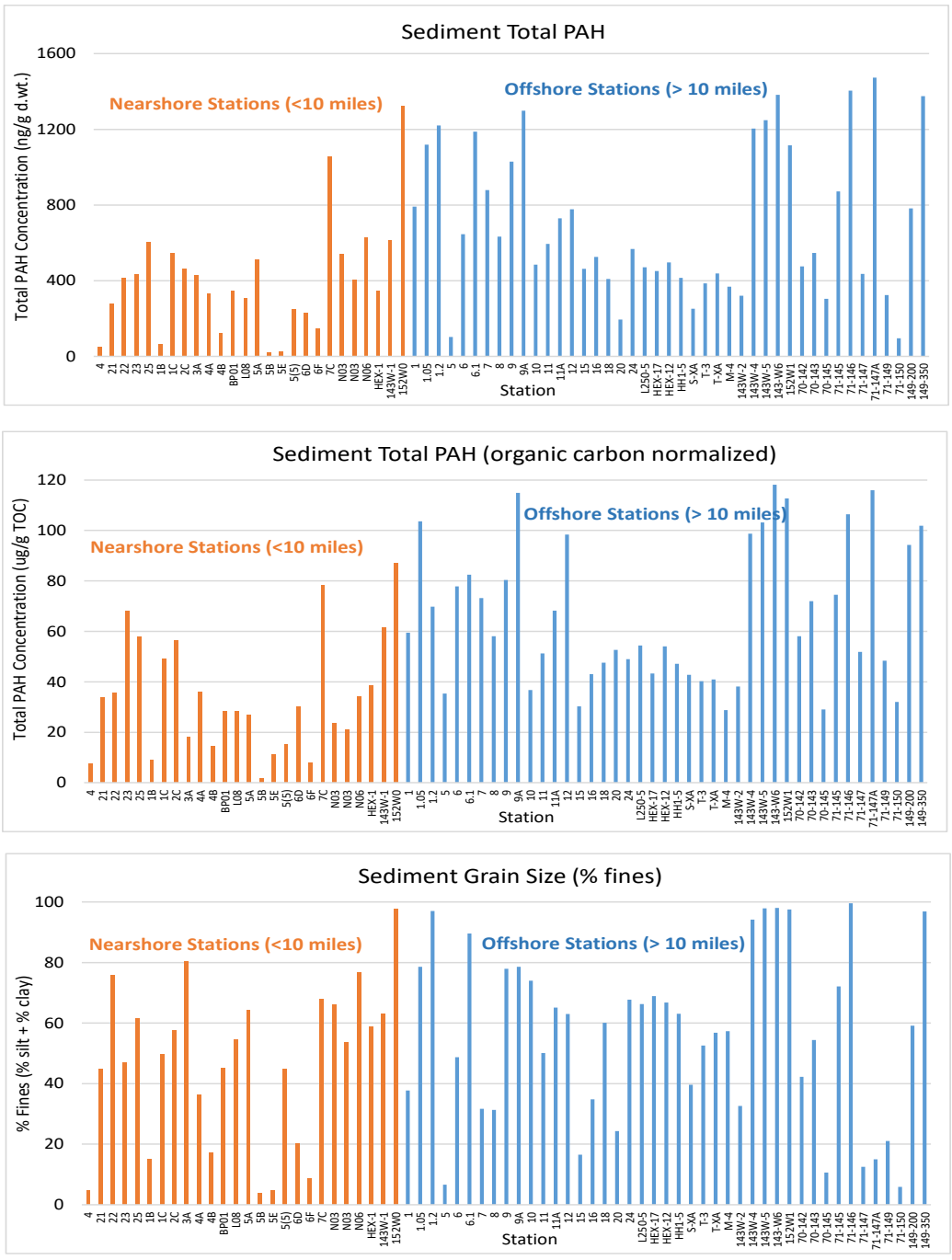


**Figure 78. Sediment Total PAH concentrations un-normalized (top), Total PAH concentrations normalized to % TOC, and the % fines (silt + clay) of the sediment samples collected during ANIMIDA III, separated by nearshore and offshore stations.**

#### *4.4.1.1.2 Hydrocarbon Characteristics: Composition and Potential Sources*

Studying the relative concentrations (i.e., composition) of the hydrocarbons, and different summations and diagnostic ratios of hydrocarbon compound concentrations, is useful for understanding similarities and differences in the sources of the hydrocarbons. Concentrations of the isoprenoid hydrocarbons, (e.g., pristane and phytane, measured as part of the SHC analysis), for instance, can be used as a general indicator of the types of sources of the hydrocarbon mixture (Wang et al., 2009), as can many of the PAH and S/T petroleum biomarkers. The following are commonly used compound summations and calculations for better understanding the types and sources of the hydrocarbons; the hydrocarbon data that have been generated provide many options for different data analyses.

- Lower Molecular Weight Alkanes (LALK): sum of the lower molecular weight n-alkanes (n-C9 to n-C20) generally associated with fresh petroleum
- Total Alkanes (TALK): sum total alkanes (n-C9 to n-C40)
- LALK/TALK: diagnostic ratio to assess relative abundance of petroleum originating alkanes.
- Pristane/Phytane: Petroleum is the primary source of phytane while pristine is derived from both biogenic and petrogenic sources. High ratios of pristane to phytane, may reflect source material of terrestrial or other biogenic origin.
- Carbon Preference Index (CPI): carbon preference index; the relative amount of odd- and even-chain alkanes within a specific carbon range. CPI = (n-C27+n-C29+n-C31)/(n-C26+n-C28+n-C30). A CPI of >2 indicates primarily terrestrial plant based sources of the alkanes, and a CPI of 1 indicates mainly oil sources.
- Petro (low molecular weight [LMW]) PAH, Pyro (high molecular weight [HMW]) PAH, and Pyro/Petro PAH ratio. Petrogenic PAH are primarily the 2- and 3-ring lower molecular weight PAH and the pyrogenic PAH are primarily the 4-, 5-, and 6-ring higher molecular weight PAH. A high Pyro/Petro PAH ration suggests primarily pyrogenic sources.
- Retene+Perylene/TPAH. Retene and perylene are PAH that primarily originate with plant-based biogenic sources, and are rarely (or only at very low concentrations) found in petroleum. A high proportion of retene and perylene indicates biogenic sources.

The saturated hydrocarbons pristane and phytane often are abundant in crude oil, coal, and peat. Phytane is rare in living organisms, but pristane is biosynthesized in large amounts by some marine animals, particularly calanoid copepods (Avigan and Blumer, 1968), which are important components of the Beaufort Sea pelagic food web. Pristane and phytane also biodegrade more slowly than n-alkanes of similar molecular weight, making them useful indicators of the weathering state of petroleum hydrocarbon mixtures in sediments. Thus, the pristane/phytane ratio can also be used to help differentiate among sources of hydrocarbons in sediments, the degree of weathering, and the sources of saturated hydrocarbons in tissues of marine animals. The chemical biomarker data (i.e., S/T) are particularly useful for associating the hydrocarbons to petroleum sources, as they are highly resistant to degradation and changes in their compositional signature due to environmental weathering processes. Table A-9 presents a set of hydrocarbon diagnostic measures for the sediment samples, as well as peat and oil samples that were analyzed during ANIMIDA III. Additionally, concentrations of Total PAH, Total SHC, and Total S/T15 in coastal peat samples collected during ANIMIDA I, II, and III are presented in Table 19, as reference information.

**Table 19. Concentrations of TPAH, TSHC, TStTr, and TOC in river or coastal peat collected in 2015 in ANIMIDA III and between 1985 and 2006 in BSMP and ANIMIDA I and II. 1985-2006**

**Data from Neff and Durell (2010).**

| River | Year | Total PAH (ng/g) | Total SHC (ng/g) | Total $StTr_{15}$ (ng/g) | TOC (%) |
|---|---|---|---|---|---|
| Sagavanirktok River | 2015 | 490 | 7,700 | 59 | --- |
| | 2006 | 290 | 25,000 | 41 | --- |
| | 2002 | 160 | 41,000 | 38 | --- |
| Kuparuk River | 2015 | 160 | 15,000 | 42 | --- |
| | 2006 | 110 | 57,000 | 35 | --- |
| | 2002 | 140–450 | 71,000–72,000 | 92–390 | --- |
| | 2000 | 100 | 18,000 | 51 | 2.4 |
| Colville River | 2002 | 360 | 50,000 | 110 | --- |
| | 2006 | 740 | 47,000 | 83 | --- |
| Canning River | 1985 | 410 | 84,000 | --- | 1.7 |
| Arey Lagoon | 1985 | 620 | 260,000 | --- | 0.95 |
| Flaxman Island | 1985 | 170 | 39,000 | --- | 0.42 |
| Tigvariak Island | 1985 | 180 | 230,000 | --- | 2.3 |
| Heald Point | 1985 | 50 | 83,000 | --- | 0.93 |
| Milne Point | 1985 | 200 | 240,000 | --- | 2.6 |
| Cape Halkett | 1985 | 710 | 41,000 | --- | 0.23 |
| Kogru Island | 1985 | 50 | 600,000 | --- | 3.0 |
| Eskimo Island | 2006 | 120 | 230,000 | 87 | --- |
| Pingok Island | 2006 | 13 | 8700 | 3.0 | --- |

The composition of the hydrocarbon compounds was quite consistent for the surface sediment samples, indicating that the source(s) of the hydrocarbons in these Beaufort Sea sediments is, for the most part, the same, or very similar. There were more of the low molecular weight (petrogenic) PAH than high molecular weight (pyrogenic) PAH in these sediments. The Pyro/Petro PAH ratio was mostly in the 0.1-0.2 range, indicating that there were 80% or more petrogenic PAH, and the proportions did not fluctuate much between samples (Table A-9). The Petro PAH frequently are associated with refined and unrefined petroleum materials and a variety of natural petrogenic source materials, and the Pyro PAH are primarily derived from the combustion of fossil fuels or as principal components of pyrogenic tars (e.g., creosote- and coal tar-type formulations). Retene and perylene together represented between 8 and 17%, and on average a little more than 10%, of the PAH in the surface sediments, indicating a significant contribution from biogenic sources. Although most crude oils contain some perylene (and retene), much of what is found in sediments is derived from the anaerobic diagenesis of recent plant materials (Venkatesan and Kaplan, 1982).

The composition of the PAH assemblage in the ANIMIDA III sediments show, as expected, little among-station variability. Figure 79 shows the PAH compound composition of a typical sediment sample (from Station N03), as well as the composition of regional oil (Northstar) and peat sample (from the Kuparuk River). The compounds commonly attributed to primarily petrogenic, pyrogenic, and biogenic sources are also indicated. The PAH assemblage in all sediment samples is composed of a full suite of both parent and alkyl PAH, indicative of a mixture of pyrogenic (from pyrolysis and incomplete

combustion of organic matter), petrogenic (from fossil fuels or their precursors), and biogenic (e.g., from recent anaerobic diagenesis of certain natural organic chemicals) hydrocarbon sources. The alkylated naphthalenes and phenanthrenes/anthracenes, generally associated with petroleum, were the most abundant PAH in the sediment. Perylene and retene, PAH from primarily biogenic sources, were also usually present at high relative concentrations. Selected pyrogenic PAH (e.g., the benzofluoranthenes and benzopyrenes) were present at lower relative concentrations. This PAH assemblage is typical for the region, and indicates a mixture of fossil fuel (petroleum, peat, and coal) PAH, with notable contributions of biogenic PAH, and less pyrogenic PAH.

The composition of saturated hydrocarbons (e.g., n-alkanes) also shows evidence of a combination of petroleum and biogenic sources of the hydrocarbons in sediment (Figure 80), with easily measurable concentrations of alkanes from n-C10 through n-C35, and higher concentrations in the n-C20 to n-C30 range. The higher relative concentrations of the odd-alkane compounds in the C23 to C31 range (n-C27 was generally the alkane with the highest concentration) are indicative of a significant contribution of hydrocarbons from biogenic sources, most likely from plant-based terrestrial sources. The LALK/TALK ratio of the alkanes in the surface sediment samples was mostly in the 0.2 to 0.4 range, which is more similar to the ratio found in peat samples than in crude oil (Table A-9). Additionally, the CPI was mostly in the 3 to 5 range and quite similar to that for peat from the Kuparuk and Sagavanirktok rivers, and substantially higher than the 0.8 to 0.9 measured for the regional crude oils, indicating primarily terrestrial plant based sources of the alkanes.


**Figure 79. PAH compound composition of a representative North Slope crude oil (Northstar), a representative river peat sample (from the Kuparuk River), and a representative surface sediment sample (from Station N03).**

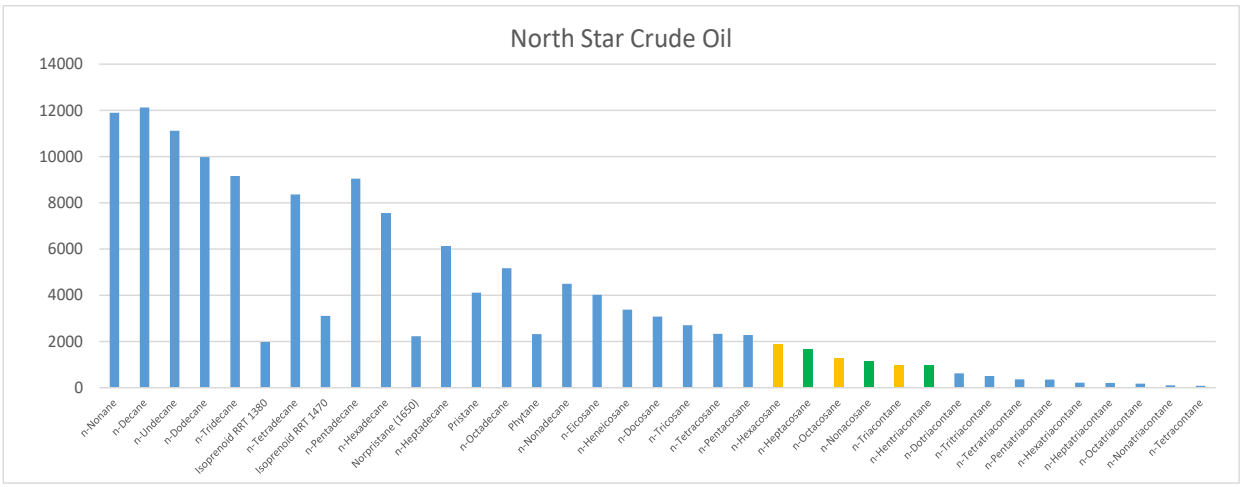


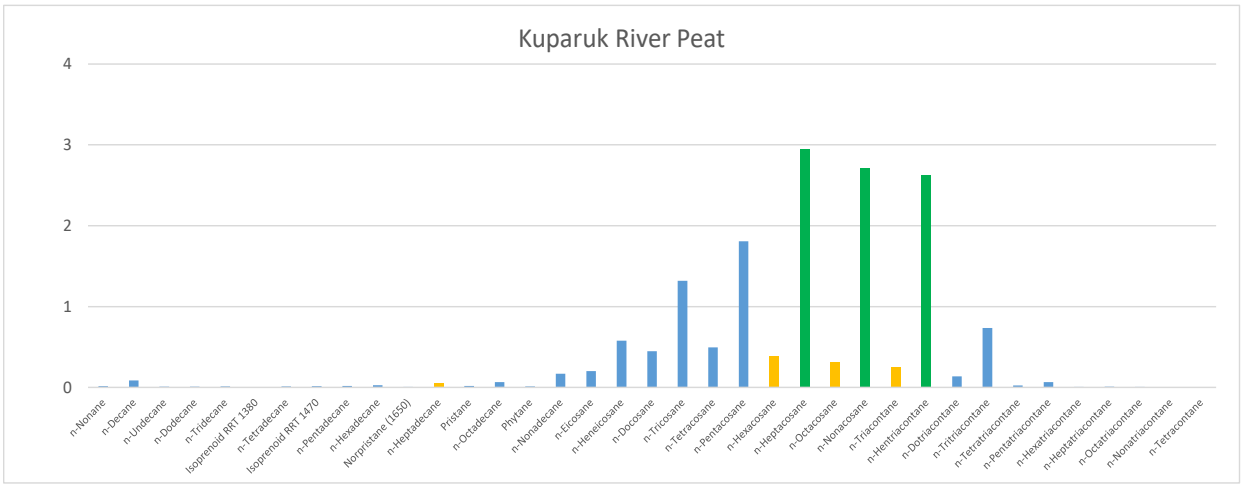


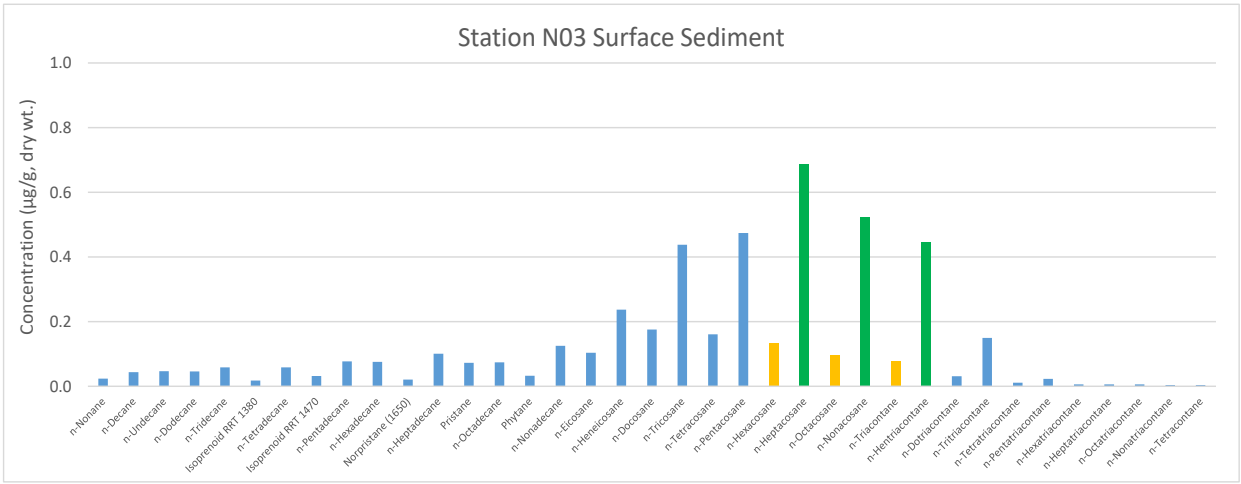


**Figure 80. Saturated hydrocarbon (alkane and isoprenoid) compound composition of a representative North Slope crude oil (Northstar), a representative river peat sample (from the Kuparuk River), and a representative surface sediment sample (from Station N03).**

**See Figure 79 for color descriptions.**

The majority of the sterane and triterpane data and extracted ion profiles (EIPs) for the sediment samples from throughout the study area show little variation and are similar to the biomarker distributions observed previously in Beaufort Sea sediments (Brown et al., 2010). Triterpane distributions suggest that the hydrocarbons present in these samples are primarily a mixture of petrogenic and biogenic hydrocarbons, including possibly from peat, kerogens from organic-rich shales, and coal (Venkatesan and Kaplan, 1982; Anders and Magoon, 1985).

Principal component analysis (PCA) and double ratio plots were produced using the PAH and S/T data to further analyze the characteristics of the hydrocarbon composition, and possible source links. The PCA analysis indicates that the PAH composition of the surface sediment samples are uniform and similar to each other, and quite comparable to what is found in peat samples collected from the major rivers that empty in to the Beaufort Sea. (Figure 81). The PAH composition is dissimilar to that of crude oil samples from the North Slope. Double ratio analysis was performed using several diagnostic PAH and S/T ratios, to confirm and complement the findings of the PAH PCA analysis. Figure 82 contains two double ratio plots based on the data for two sets of PAH and two sets of S/T compounds often used for this analysis. This is a good illustration of how PAH double ratio analysis is not always sufficient to differentiate sources; the Northstar crude oil sample plots along with the surface sediment, even though, as it turns out, there is no link between the hydrocarbons in the sediments and the Northstar oil, or the oil as a source material. The double ratio plot based on the two key sterane (S25 and S28) and triterpane (T21 and T22) compounds, on the other hand, clearly shows how the sediment and peat sample cluster together as having similar composition, and different from all the crude oil samples confirming the findings of the PCA.

The hydrocarbon compositional data and the analyses of those data indicate that the hydrocarbons in the sediments of the Beaufort Sea are primarily from terrestrial sources with significant biogenic and non-oil petrogenic character, including peat and shale materials, and much less from seeps or other oil-based petroleum sources on the shelf. The majority of hydrocarbons are carried from coastal and inland land-sources to the Beaufort Sea during the spring ice melt and breakup, when most of the annual suspended solids enter the coastal Beaufort Sea during a few weeks in May and June (Trefry et al., 2009; Rember and Trefry, 2004).

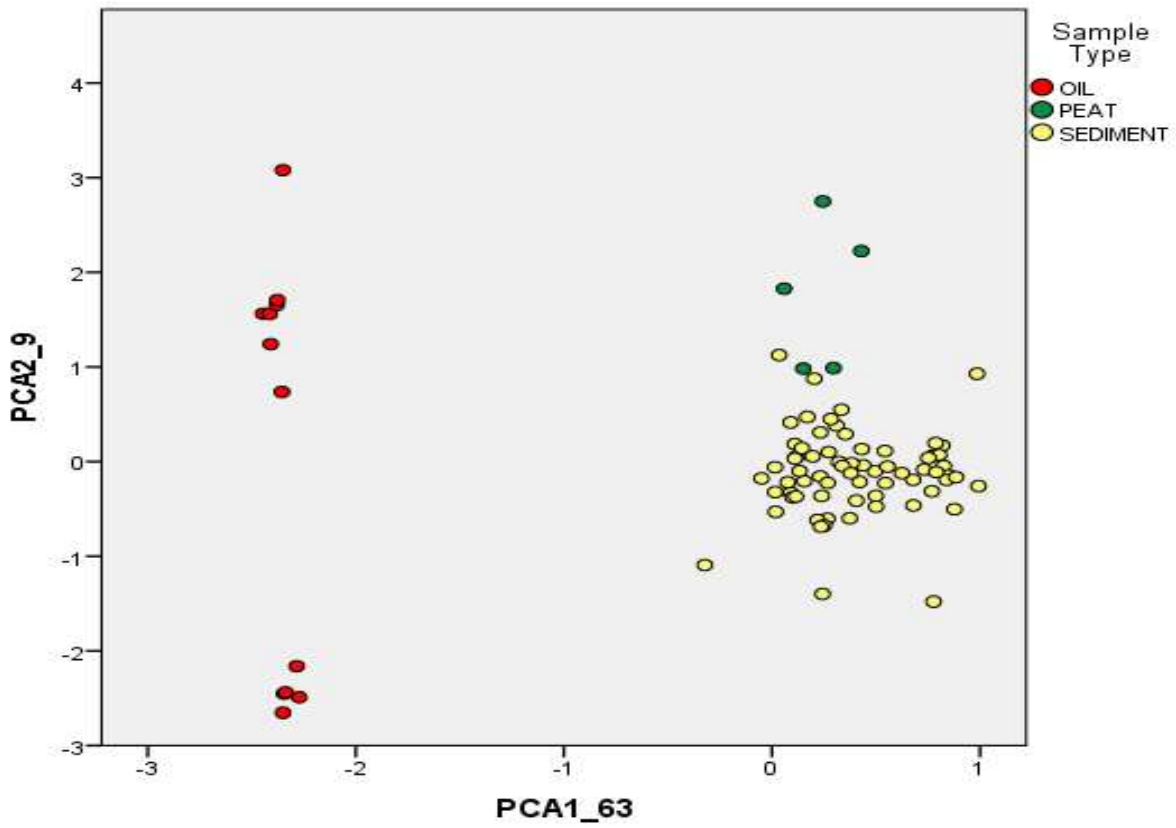


**Figure 81. Principal component analysis (PCA) using the PAH compound data for the ANIMIDA III surface sediment samples, and different North Slope crude oil and river peat samples collected during ANIMIDA I, II, and III.**

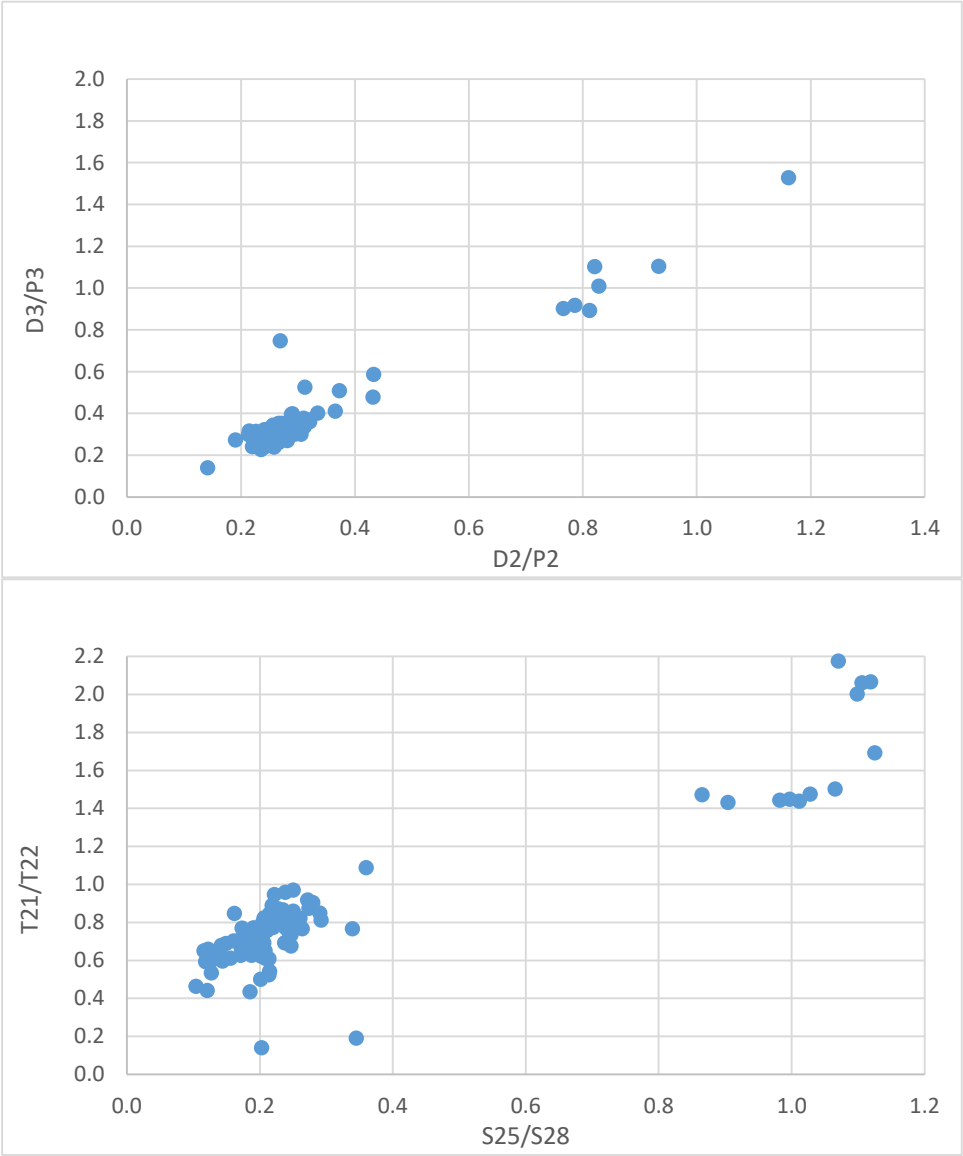


**Figure 82. Ratio analysis using key diagnostic PAH ratios (upper) and petroleum biomarker ratios (lower) data for the ANIMIDA III surface sediment samples, and different North Slope crude oil and river peat samples collected during ANIMIDA I, II, and III.**

#### *4.4.1.1.3 Hydrocarbon Characteristics: Potential Ecological Implications*

One technique of evaluating the significance of the measured sediment hydrocarbons to overall ecological risk of the region involves comparisons to sediment quality guidelines. Sediment quality guidelines have been developed to assess possible adverse biological effects from metals, polychlorinated biphenyls, pesticides, and PAH on benthic organisms. The most commonly utilized guidelines are the Effects Range-Low (ERL) and Effects Range-Median (ERM) values from Long et al. (1995). Threshold effects level (TEL) and probable effects level (PEL) are similar guidelines sometimes used to assess the potential for impact from chemicals in marine sediment (MacDonald et al., 1996). The guidelines can be interpreted to indicate that adverse biological effects are "rarely" (<10% of the time) observed when individual metal or Total PAH concentrations in sediments are lower than the ERL, "occasionally"

observed when present at concentrations between the ERL and ERM, and "frequently" observed when concentrations exceed the ERM. However, O'Connor (2004) demonstrates that the ERL is a poor predictor of the maximum non-toxic concentration of a chemical in marine sediments. Concentrations of PAH usually are higher in fine-grained than coarse sediments, and toxicity of these chemicals also is higher (lower concentrations are associated with toxicity) in fine than coarse sediments. Additionally, in relatively pristine environments, such as the Beaufort Sea, the toxicity of PAH in sediments is dependent on the chemical form of the chemical in the sediments. Chemicals that are tightly bound to sediment particles and POC have a low bioavailability and toxicity compared to the same chemicals in solution or associated with an oil phase in sediment pore water (Neff, 2002).

A comparison of Total PAH concentrations in the sediments to the ERL/TEL and ERM/PEL guidelines shows that none of the samples exceeded the 4,022 ng/g (ERL) 1,684 ng/g (TEL), 44,792 ng/g (ERM), or 416,770 ng/g (PEL) sediment quality guideline values. Similarly, the individual PAH concentrations did not exceed the ERL for the individual 13 PAH with such sediment quality reference values. The concentrations of individual and total PAH are well below concentrations that might be toxic to benthic marine invertebrates inhabiting the sediments.

Potential toxicity of the PAHs present in Beaufort Sea sediments was further evaluated using EPA's Procedures for the Derivation of Equilibrium Partitioning Sediment Benchmarks (ESBs) for the Protection of Benthic Organisms: PAH Mixtures (USEPA, 2003). Based on this approach, if the sum of Equilibrium Partitioning Sediment Benchmark Toxic Units (ΣESBTUFCV) for "total PAHs" is less than or equal to 1.0, the concentration of the mixture of PAHs in the sediment is acceptable for the protection of benthic organisms. ΣESBTUFCV values were calculated for each sediment sample with values ranging from 0.004 to 0.161 (Table 20 and Table A-10), with the majority of values being less than 0.10. The mean ΣESBTUFCV value was 0.065 for the surface sediment samples collected in 2014, and 0.083 for the samples collected in 2015. The ESB approach provides further evidence the concentrations of PAH present in the Beaufort Sea sediments throughout the study area are not toxic to benthic organisms.

**Table 20. Mean and range of equilibrium partitioning sediment benchmarks (ESB), derived as the sum of the equilibrium partitioning sediment benchmark toxic units ($\sum ESBTU_{FCV}$) based on surface sediment PAH concentrations, for samples collected in 2014 and 2015 in ANIMIDA III.**

| Year | Sum Equilibrium Partitioning Sediment Benchmark Toxic Units ($\sum ESBTU_{FCV}$) | | | |
|---|---|---|---|---|
| | Mean | Std Dev (%RSD) | Min | Max |
| ***Surface Sediment*** | | | | |
| 2014 (n=45) | 0.065 | 0.035 (53.4%) | 0.004 | 0.154 |
| 2015 (n=26) | 0.083 | 0.048 (57.5%) | 0.019 | 0.161 |

∑ESBTUFCV = ∑(COC,PAHi)/(COC,PAHi,FCVi), where COC,PAHi (µg/gOC) = [CPAH (ng/g dry wt) x 1/CTOC (%) x 1/10] and COC,PAHi,FCVi values are published effects concentrations (U.S. EPA, 2003).

### 4.4.1.2 Sediment Core

#### *4.4.1.2.1 Hydrocarbon Characteristics: Concentrations and Historical Variations*

Sediment cores are collected, among other reasons, to gain an understanding of the concentrations of chemicals deposited on the seafloor at different times in history. One sediment core was collected during ANIMIDA III and also analyzed for hydrocarbon concentrations. The core was collected at Station 1.2, approximately 40 nautical mi offshore and in approximately 200 m of water. The core was segmented into 2-3 cm segments, representing from the surface sediment (0–2 cm depth) to approximately 80 cm below the sediment surface (78–81 cm segment); segments of the core were analyzed representing deposition that occurred from recent years to several hundreds of years ago, based on a sedimentation rate of approximately 0.14 cm/year determined from isotope dating analysis of the core (Table A-7).

The hydrocarbon concentrations and composition was highly uniform throughout the core. The Total PAH concentrations averaged 1,320 ng/g, and ranged from 1,150 to 1,490 ng/g (Table 15 and Table A-7). The Total PAH concentration was higher than in most ANIMIDA III sediment samples, but consistent with the finding that the concentrations were higher at locations well offshore. The TOC content was also uniform, and was approximately 1.5 %TOC, and the sediment PAH and other hydrocarbon concentrations were, thus, highly uniform whether the data were normalized to % TOC or not (Figure 83). Similar Total PAH concentrations were also measured in subsurface sediments in cores collected in Harrison Bay during ANIMIDA II (Brown et al., 2010). The uniformity in the sediment hydrocarbon concentrations, and composition, indicates that the sources of the hydrocarbons to the Beaufort Sea sediment have been consistent for centuries, are primarily natural, as discussed in Section 4.1.1.2, with no noticeable changes in the type or amount of hydrocarbons deposited; there is no evidence of influence from anthropogenic sources over the past centuries, including in recent years.

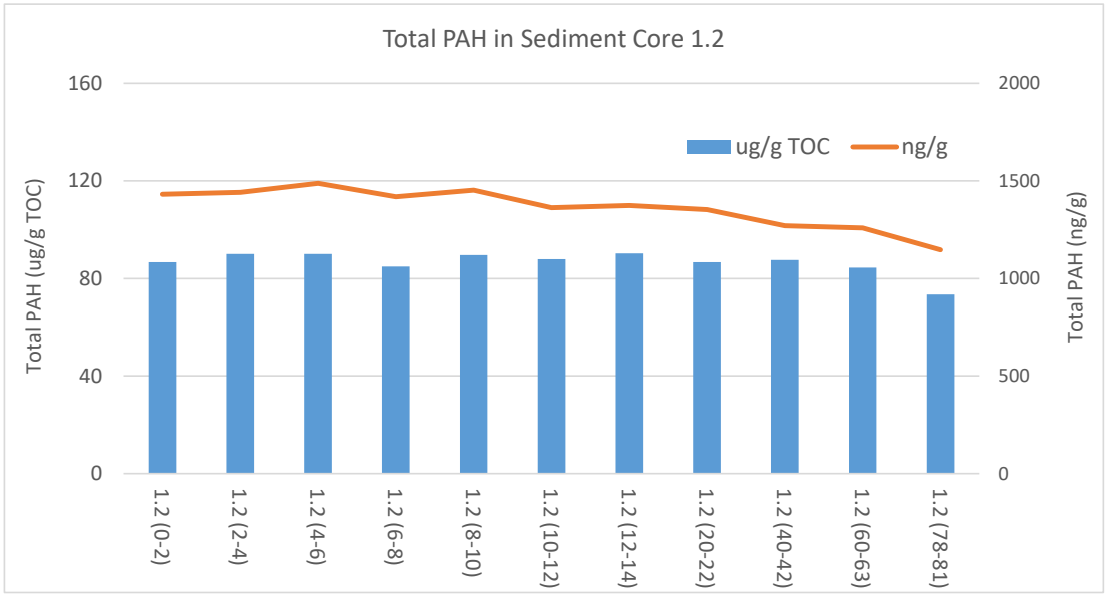


**Figure 83. Sediment Total PAH, normalized to the TOC content and un-normalized, for the 11 segments of the core collected at Station 1.2 in 2014.**

**The segments represent sediment depths from the sediment surface to 81 cm below the surface.**

### 4.4.2 Biota Monitoring

#### 4.4.2.1 Hydrocarbon Tissue Concentrations

The biological tissue hydrocarbon concentrations and summary statistics, represented by the Total PAH and Sum SHC, are summarized in Table 16 for the amphipod (*Anonyx* sp.), clam (*Astarte* sp.), and fish (Arctic cod; *Boreogadus saida*) samples. The data for each individual station by animal species are presented in Tables A-11 and A-12, and the individual compound data have been reported to BOEM and were used to generate the information in this document.

As with the sediments, the PAH concentrations are the class of hydrocarbons that are of greatest interest for studying the accumulation of hydrocarbons in marine animals, because of their potential to cause toxicity and other effects. Total SHC/PHC data are of limited value in biological tissue, both because of analytical challenges resulting in often unreliable data and because they are not useful for assessing potential effects. The S/T chemical biomarkers are so insoluble that they are often not available for accumulation by animals, and they also are not of environmental concern. The focus is therefore on PAH for assessing the accumulation of hydrocarbons by marine animals, and the Sum SHC is also presented as a general assessment of the hydrocarbons.

Hydrophobic organic compounds accumulate in biological tissue bases on many factors, including feeding and metabolic processes, but their accumulation is also often influenced by the lipid content of the animal tissue, much like how organic matter and fine-grained material influences the accumulation of organic compounds in sediment. However, the tissue PAH concentrations correlated rather poorly with the lipid content in the amphipod, clam, and Arctic cod data set as a whole, with only subsets of the data showing a relationship (Figure 84). There was a modest relationship between the PAH and lipid concentration in *Astarte* clams, if two outlier data points are excluded; clams are benthic animals that have shown a relatively good correlation between the accumulation of PAH and the lipid content of the animal in recent studies in the Chukchi Sea. It is difficult to explain the lack of correlation with lipid content in this data set, but the PAH measured for the amphipods may, in part, be from adhered sediment particles and not PAH accumulated in the animal tissue, and the more mobile Arctic cod may be exhibiting some regional differences in their exposure or PAH metabolism/excretion.

The Total PAH concentrations were, for the most part, not greatly different for the different animals, with most measured concentrations ranging between 20 and 100 ng/g, d. wt. The concentrations were lowest for the amphipods and the fish that were collected in 2015, a little higher for the clams (excluding a couple of outliers described below), and a little higher yet for the fish collected in 2014. On a lipid-normalized basis the difference for the Total PAH concentrations in the amphipods and the 2015 fish (the samples with the lowest concentrations) and the other animals was greater, with the clam and 2015 fish samples having clearly higher PAH concentrations but comparable to each other (Figure 85). The saturated hydrocarbon concentrations were, as expected, higher than PAH concentrations because of their natural abundance in this environment, but the concentrations were quite variable and represent a variety of natural sources and materials (as well as likely analytical challenges and interferences, as described earlier).

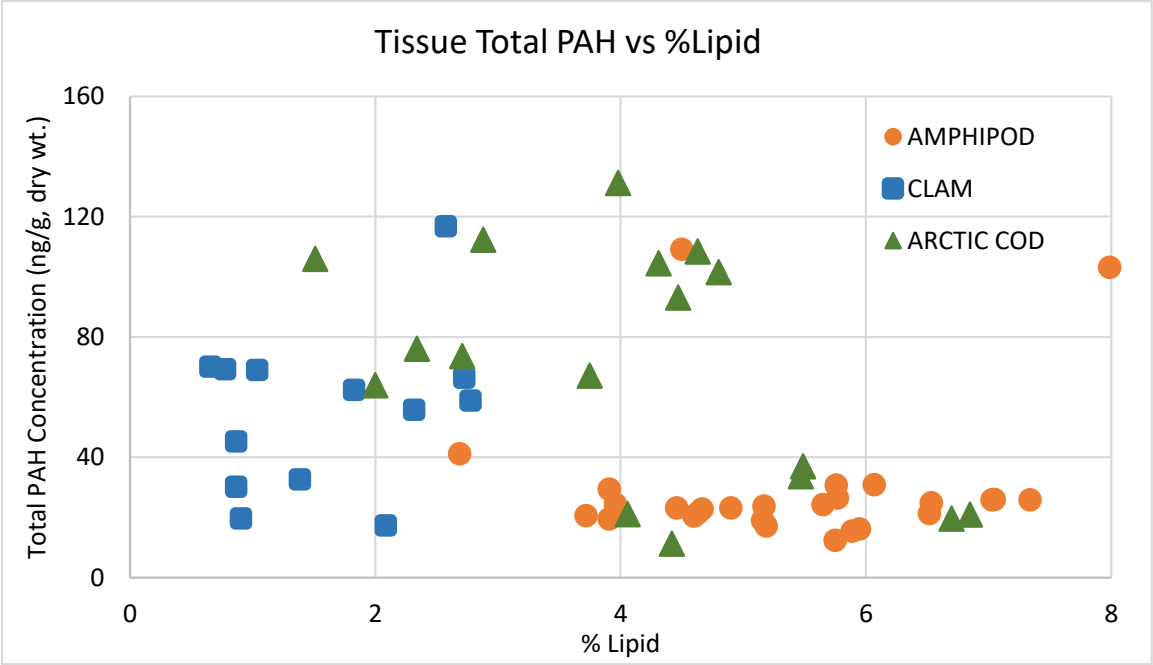


**Figure 84. Total PAH concentrations vs % lipid in the amphipod, clam, and fish tissue samples.**

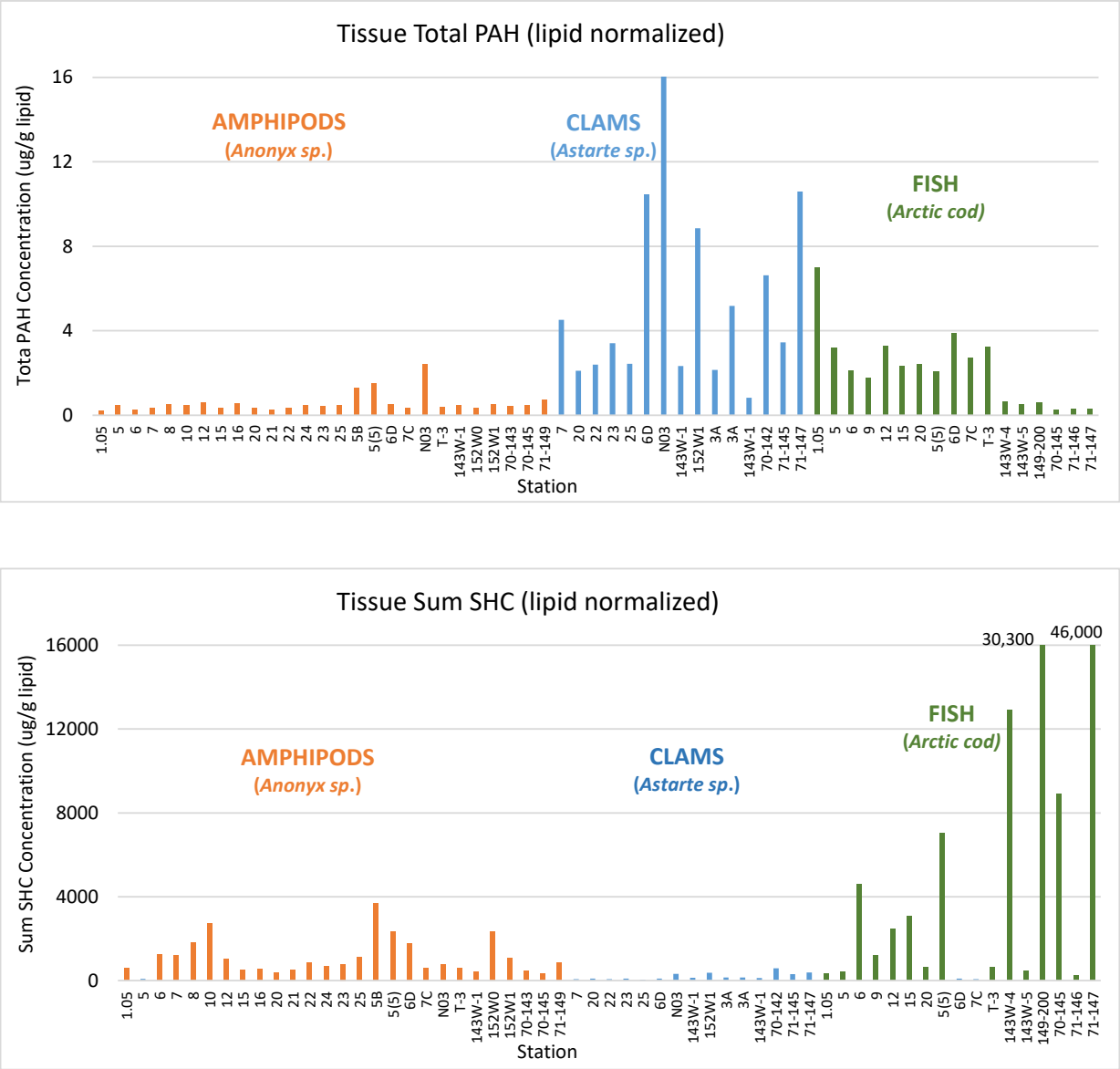


**Figure 85. Lipid-normalized Total PAH (upper) and Sum SHC (lower) concentrations in the amphipod, clam, and fish tissue samples.**

The clams had the highest lipid-normalized PAH concentrations of the three animals, but the lowest lipid-normalized Total SHC concentrations. The higher Total SHC in amphipods and most fish can in large part be attributed to their diets (Neff and Durell, 2012; Neff et al., 2009). Amphipods contain high relative concentrations of pristane, compared to concentrations of other saturated hydrocarbons; pristane is the most abundant alkane in the SHC fraction of amphipods, and alone comprised more than half the SHC in the amphipod samples, and more than 90% of the Total SHC in many samples (elevated n-C17-alkane concentrations was also measured, possibly in large part due to difficulties in resolving that compound from the closely eluting pristane, in the analysis). Amphipods bioaccumulate pristine primarily from their diet of calanoid copepods and phytoplankton/zooplankton detritus. Fish, in turn, feed on amphipods, thus accumulating high relative concentrations of pristane (which comprised more than 95%

of the Total SHC in most fish samples). Without pristane, the SHC concentrations were similar for amphipod and clams and fish. A high relative pristane content indicates that the saturated hydrocarbons in the tissues are primarily from the food. The large differences in pristane concentrations in tissues of the different species of marine invertebrates reflect differences in the contribution of zooplankton or zooplankton detritus in their diets. Virtually all the pristane in the Beaufort Sea is biosynthesized from phytoplankton phytol by calanoid copepods (Avigan and Blumer, 1968).

Total PAH concentrations in amphipods were comparable for the two survey years, as were the concentrations in the clam samples if the few outliers observed in 2014 are excluded (Table 16, A-11 and A-12). The mean Total PAH concentration in amphipods was 30.4 ng/g (d. wt.) in 2014 and 25.1 ng/g in 2015; most amphipod samples had a concentration in the 15 to 30 ng/g range, and two samples had slightly above 100 ng/g (amphipods collected at Stations 5B and N03 in 2014). Though the mean Total PAH concentration in clams collected in 2014 was much higher than for those collected in 2015 (380 vs 44.0 ng/g), the summary statistics were skewed by a few unusually elevated concentration samples in 2015, and particularly by one sample collected at Station N03 with a reported concentration of 1,930 ng/g. Most clam samples had Total PAH concentrations in the 20 to 70 ng/g range. The concentration reported for Station N03 is likely unreliable, and the most likely explanation for this outlier value is the small amount of sample material that was available and used for the analysis; only 0.07 g was available which complicates the analysis and compromises the accuracy of the concentration calculation; for most samples 3–4 g (d. wt.) of material was used for the analysis. The sample for Station 3D also had only a small sample mass available, which probably contributed to that sample having an unusually high reported concentration; 0.39 g was used, which is about a factor of 10 less than most samples. The Arctic cod, on the other hand, had 3–4 times higher concentrations in 2014 than in 2015, possibly due some unidentified differences between the two years (e.g., where the animals spent time, differences in feeding and availability of food). The fish collected in 2014 were, on average, from slightly closer to the shore and coastal development and in slightly shallower waters than those collected in 2015, which could, in part, explain some of the observed differences.

There are additional factors that contribute to seasonal and annual differences in hydrocarbon concentrations in marine animals, some of which influence the lipid content of the tissue. The abundance, size (age), and lipid content of amphipods and other marine animals fluctuates during the year (Nygard et al., 2012; Noyon et al., 2011), factors which contribute to the accumulation of hydrophobic compounds. The lipid content of adult amphipods in the Arctic can fluctuate by as much as a factor of three throughout the year, and can also be different from year-to-year (Nygard et al., 2012; Noyon et al., 2011).

Unlike sediment concentrations, the amphipod and clam hydrocarbon concentrations appear to be lower in the animals collected at the new, farther offshore, stations than closer to the shore (Table 21). This suggests that the surface sediments are not the primary source of the hydrocarbons accumulated by these animals, but possibly hydrocarbons associated with the dissolved organic carbon (DOC) or POC suspended in the water column. The DOC and POC mass and concentrations increase significantly during the late spring and early summer, about two months before the ANIMIDA III surveys, with runoff from the rivers (Rember and Trefry, 2004). However, the proximity to the shore does not seem to influence the tissue hydrocarbon concentrations as clearly as the surface sediment concentrations. There was large variability in the concentrations measured for the historical BSMP and ANIMIDA (nearshore) stations, and a few outlier values greatly influence the summary statistics (e.g., the mean Total PAH in amphipods collected at the new stations was 22.6 ng/g ±19% SD, and for the nearshore stations it was 60.3

±71%RSD), confounding the comparison. The amphipod and clam tissue samples had rather similar hydrocarbon concentrations at most offshore and nearshore stations, and were generally between 15 and 30 ng/g for amphipods and between 20 and 70 ng/g for clams. The tissue PAH concentrations have, historically had some notable year-to-year variability, with the mean Total PAH concentration in amphipods ranging from 25.4 to 95.6 ng/g and from 38.4 to 141 ng/g in clams from ANIMIDA I and II surveys conducted in 2000, 2002, 2004, 2005, and 2006 (Table 21). Total PAH concentrations that were measured during ANIMIDA III were within the range and similar to these historical Beaufort Sea data (Neff et. al., 2009; Neff and Durell, 2012), and also comparable to what has recently been measured in the Chukchi Sea.

**Table 21. Mean and Range of concentrations of TPAH and TSHC in amphipods and clams collected in 2014 and 2015 in ANIMIDA III and between 2000 and 2006 in ANIMIDA I and II. Hydrocarbon concentrations are ng/g dry wt (parts per billion; data for 2000 and 2002 were converted from wet wt. by multiplying by 5, based on ~89% moisture).**

**ANIMIDA I and II data from Neff and Durell (2010).**

| Hydrocarbon | Year | Amphipods | | Clams | |
|---|---|---|---|---|---|
| | | Mean (±SD) | Range | Mean (±SD) | Range |
| ***ANIMIDA III - New Stations (n=24 amphipod and n=11 clam samples)*** | | | | | |
| TotalPAH | 2014/2015 | 22.6 ± 4.39 | 12.4–30.7 | 58.8 ± 26.5 | 17.2–117 |
| TotalSHC | 2014/2015 | 92,900 ± 61,900 | 17,200–208,000 | 86,600 ± 117,000 | 700–295,000 |
| **ANIMIDA III - Historical BSMP and ANIMIDA Stations (n=5 amphipod and n=4 clam samples)** | | | | | |
| TotalPAH | 2014/2015 | 60.3 ± 42.7 | 17.2–109 | 591 ± 909 | 19.5–1,930 |
| TotalSHC | 2014/2015 | 150,000 ± 193,000 | 30,300–489,000 | 3,900,000 ± 6,300,000 | 8,320–13,200,000 |
| **ANIMIDA I and II - Historical BSMP and ANIMIDA Stations** | | | | | |
| TotalPAH | 2000 | 85.8 ± 18.4 | 60.0–115 | 90.4 ± 54.4 | 37.0–195 |
| | 2002 | 95.6 ± 41.6 | 55.0–175 | 80.6 ± 47.8 | 48.0–175 |
| | 2004 | 68.2 ± 33.8 | 39.6–143 | 95.8 ± 52.6 | 42.7–168 |
| | 2005 | 25.4 ± 13.5 | 8.25–50.0 | 38.4 ± 15.1 | 21.8–51.2 |
| | 2006 | 59.6 ± 29.8 | 19.7–123 | 141 ± 40.9 | 100–182 |
| TotalSHC | 2000 | 55,800 ± 45,300 | 0–130,000 | 6000 ± 8580 | 0–22,000 |
| | 2002 | 113,000 ± 71,800 | 23,500–260,000 | 14,100 ± 1390 | 12,500–16,000 |
| | 2004 | 444000 ± 8540 | 29800–54100 | 26,800 ± 14,400 | 678–39,700 |
| | 2005 | 31,600 ± 18,400 | 5171–67,100 | 1510 ± 517 | 1030–2230 |
| | 2006 | 63,000 ± 57,100 | 13,700–249,000 | 12,600 ± 2410 | 10,200–15,000 |

### 4.4.2.2 Potential Ecological Implications of Accumulated Hydrocarbons

One technique of evaluating the ecological and toxicological significance of hydrocarbons accumulated in the tissue of marine animals is to calculate the concentrations of selected PAH on a molar wet weigh basis and compare to the critical body residue (CBR) value. Many nonpolar (unionizable) organic compounds, such as petroleum hydrocarbons, express their toxic effects by accumulating in and swelling lipid-rich biological membranes, causing non-specific narcosis (Abernethy et al., 1988; McCarty et al., 1992). Toxicity occurs when the concentration of total nonpolar organic chemicals in the tissues reaches a critical concentration, the CBR. The CBR for nonpolar organic chemicals in whole tissues of

marine animals is generally between 2 and 8 milliMolar [mM]/kg wet wt., and is widely accepted to be approximately 4.4 mM/kg wet wt (95% confidence interval [C.I.] = 3.7 to 5.2 mM/kg).

Landrum et al. (2003) confirmed and provided additional evidence of the critical body residue principle, including the additivity of toxicity of certain organic contaminants, specifically for PAH. He determined two effects reference values; an effects body residue for 50% mortality (ER50) value of 2.6 mM and a higher lethal body residue for 50% mortality (LR50) value of 7.5 mM, which validates the earlier reported value of 4.4 mM. The effect in the ER was immobility - failure to swim on prodding in 50% of population. As indicated in these documents, the concentration of non-polar organics required to produce severe effects, including acute mortality, in invertebrates and fish is expected to be relatively constant, ranging from between 2 and 8 mM/kg.

The risk to marine animals from bioaccumulation of organic chemicals (PAH, in the case of ANIMIDA III) was estimated by converting all wet-weight tissue concentrations of the individual PAH compounds in the amphipod, clam, and fish samples to millimolar concentrations. The mM concentrations of all analytes in each sample were summed to produce a total concentration of nonpolar organic contaminants in the tissue. This concentration was compared to the CBR value of 4.4 mM. The risk to marine animals from bioaccumulation increases as the resulting concentration approaches 4.4 mM. The CBR value of 4.4 mM is for lethal effects. Sublethal effects may be elicited at lower concentrations of total nonpolar organic chemicals in tissues.

The mean and summary statistics for the mM/kg concentrations, used to compare to the CBR concentrations, were calculated for the ANIMIDA III amphipod, clam, and Arctic cod samples are presented in Table 22. The concentrations for the individual marine animal samples are listed in Table A-13. The tissue body burden concentrations, based on accumulated PAH, was consistently well below the CBR concentrations that may elicit chronic or acute toxicological effects in the animals (approximately 2 to 8 mM/kg). The mean concentration was from 0.037 to 0.040 mM/kg for amphipods, from 0.031 to 0.50 mM/kg for clams, and from 0.031 to 0.12 mM/kg for Arctic cod and the two survey years. All samples had a concentration of less than 0.2 mM/kg, except the clam samples collected at Stations 6D (0.44 nM/kg) and N03 (2.63 mM/kg) which, as discussed earlier, had concentrations of PAH that are deemed unreliable. The marine animals in ANIMIDA III did not have PAH concentrations that would have toxic effects on or cause other harm to the animals. Furthermore, the amphipods, clams, or Arctic cod had not accumulated PAH above the natural background.

**Table 22. Mean and range of critical body residue (CBR) concentrations, based on PAH, in amphipods, clams, and Arctic cod collected in 2014 and 2015 in ANIMIDA III (mM/kg wet weight).**

| Year | Critical Body Residue (based on PAH; mM/kg wet weight) | | | |
|---|---|---|---|---|
| | Mean | Std Dev (%RSD) | Min | Max |
| ***Amphipods*** | | | | |
| 2014 (n=22) | 0.0403 | 0.0320 (74.5%) | 0.0175 | 0.145 |
| 2015 (n=7) | 0.0366 | 0.0048 (13.2%) | 0.0293 | 0.0448 |
| **Clams** | | | | |
| 2014 (n=7) | 0.497 | 0.950 (191%) | 0.0639 | 2.63 |
| 2015 (n=8) | 0.0314 | 0.0123 (39.0%) | 0.0156 | 0.0493 |
| **Arctic Cod** | | | | |
| 2014 (n=11) | 0.121 | 0.0287 (23.8%) | 0.0789 | 0.172 |
| 2015 (n=6) | 0.0314 | 0.0119 (37.9%) | 0.0165 | 0.0484 |
| CBR (mM/kg wet weight) =∑ [CPAH (g/kg wet weight) x 1/PAH molecular weight (g/M) x 1000 mM/M] | | | | |

## Acknowledgments

We thank Dan Holiday and Catherine Coon of BOEM, U.S. Department of Interior, for their interest and enthusiasm for long-term monitoring and studies of hydrocarbons in the Beaufort Sea. We also thank the crew and captains of the *Norseman II* for support and efforts to ensure that the cruises were successful. We also want to thank the scientific colleagues and project team for a most enjoyable team effort. This field and laboratory study was funded by the U.S. Department of the Interior, BOEM, Alaska Outer Continental Shelf Region, Anchorage, Alaska under Contract M13PC00019 as part of the ANIMIDA III project and the BOEM Alaska Environmental Studies Program.

## References


Abernethy S.G., Mackay D., and McCarty L.S. 1988. "Volume fraction" correlation for narcosis in aquatic organisms: the key role of partitioning. Environ. Toxicol. Chem. 7:469-481.

Anders D.E. and Magoon L.B. 1985. Oil-source study in northeastern Alaska. Org. Geochem. 10:407-415.

Anderson D.M., Fukuyo Y., and Matsuoka K. 2003. Cyst methodologies. In: Hallegraeff, G.M., Anderson, D.M., Cembella, A.D. (Eds.), Manual on Harmful Marine Microalgae. Monographs on Oceanographic Methodology 11, UNESCO, pp 165-190.

Avigan J. and Blumer M. 1968. On the origin of pristane in marine organisms. J. Lipid Res. 9:350-352.

Brown J., Boehm P., Cook L., Trefry J., Smith W., and Durell G. 2010. Hydrocarbon and Metal Characterization of Sediments in the cANIMIDA Study Area. cANIMIDA Task Order 2 Final Report. Contract No. M04PC00001, Submitted to U.S. Department of Interior, Anchorage, AK, February, 2010.

Brown J.S., Trefry J.H., Cook L.L., and Boehm P.D. 2004. ANIMIDA Task 2: Hydrocarbon and metal characterization of sediments, bivalves and amphipods in the ANIMIDA study area, Final Report. OCS Study MMS 2004-024, Anchorage, Alaska: Minerals Management Service, Department of Interior.

Gu H., Zeng N., Xie Z., Wang D., Wang W. and Yang W., 2013. Morphology, phylogeny, and toxicity of Atama complex (Dinophyceae) from the Chukchi Sea. Polar biology, 36(3), pp.427-436.

Harvey R.H, Taylor K.A, Pie H.V., and Mitchelmore C.L. 2014. Polycyclic aromatic and aliphatic hydrocarbons in Chukchi Sea biota and sediments and their toxicological response in the Arctic cod, *Boreogadus saida*. Deep-Sea Research II. 102: 32-55.

Landrum P.F., Lotufo G. R., Gossiaux D.C., Gedeon M.L., and Lee J-H. 2003. Bioaccumulation and Critical Body Residue of PAHs in the Amphipod, Diporeia spp.; Additional Evidence to Support Toxicity Additivity for PAH Mixtures. Chemosphere. 51: 481-489.

Long E. R., Macdonald D. D., Smith S.L., and Calder F.D. 1995. Incidence of Adverse Biological Effects Within Ranges of Chemical Concentrations in Marine and Estuarine Sediments. Environ. Management. 19: 81-97.

MacDonald D. D., Carr R.S., Calder F.D., Long E.R., and Ingersoll C.G. 1996. Development and evaluation of sediment quality guidelines for Florida coastal waters. Ecotoxicology. 5:253-278.

McCarthy L.S., Arnot J.A., and Mackay D. 2013. Evaluation of Critical Body Residue Data for Acute Narcosis in Aquatic Organisms. Environmental Toxicology and Chemistry. 32: No. 10, 2301-2314.

McCarty L.S., Mackay D., Smith A.D., Ozburn G.W., and Dixon D.G. 1992. Residue-based interpretation of toxicity and bioconcentration QSARs from aquatic bioassays: neutral narcotic organics. Environ. Toxicol. Chem. 11:917-930.

Natsuike M., Nagai S., Matsuno K., Saito R., Tsukazaki C., Yamaguchi A. and Imai I. 2013. Abundance and distribution of toxic Alexandrium tamarense resting cysts in the sediments of the Chukchi Sea and the eastern Bering Sea. Harmful algae, 27, pp.52-59.

Neff J.M. 1987. Biological effects of drilling fluids, drill cuttings and produced waters. Pages 469-538 In: D.F. Boesch and N.N. Rabalais, Eds., Long Term Effects of Offshore Oil and Gas Development. Elsevier Applied Science Publishers, London.

Neff J.M. 2002. Bioaccumulation in Marine Organisms. Effects of Contaminants from Oil Well Produced Water. Elsevier Science Publishers, Amsterdam. 452 pp.

Neff, J.M. 2010. Fates and Effects of Water Based Drilling Muds and Cuttings in Cold Water Environments. Report to Shell Oil Co., Anchorage, AK. 309 pp.

Neff J.M. and Durell G.S. 2010. Continuation of the Arctic Nearshore Impact Monitoring in the Development Area (cANIMIDA): Synthesis, 1999-2007. cANIMIDA Task Order 1 Final Report. Contract No. M03PC00014, Submitted to U.S. Department of Interior, Anchorage, AK, December, 2010.

Neff J. and Durell G. 2012. Bioaccumulation of natural hydrocarbons in Arctic amphipods in the oil development area of the Alaskan Beaufort Sea. Journal of Integrated Environmental Assessment. 8: No. 2, 301-319.

Neff J.M., Trefry J.H, and Durell G.S. 2009. Integrated Biomonitoring and Bioaccumulation of Contaminants in Biota of the cANIMIDA Study Area. cANIMIDA Task Order 5 Final Report. Contract No. M04PC00020, Submitted to U.S. Department of Interior, Anchorage, AK, October, 2009.

Noyon M., Narcy F., Gasparin S., and Mayzaud P. 2011. Growth and lipid class composition of the Arctic pelagic amphipod Themisto libellula. Marine Biology. 158: 883-892.

Nygard H., Berge J., Soreide J.E., Vihtakari M., and Falk-Petersen S. 2012. The amphipod scavenging guild in two Arctic fjords: seasonal variations, abundance and trophic interactions. Aquatic Biology. 14: 247-264.

O'Connor T.P. 2004. The sediment quality guideline, ERL, is not a chemical concentration at the threshold of sediment toxicity. Mar. Pollut. Bull. 49:383-385.

Olgoonik-Fairweather. 2015. Arctic nearshore impact monitoring in development area III (ANIMIDA III): 2015 field report. Prepared by Olgoonik-Fairweather, Anchorage, AK. October, 2015.

Olgoonik-Fairweather. 2014a. Arctic nearshore impact monitoring in development area III (ANIMIDA III): 2014 field season sampling plan. Prepared by Olgoonik-Fairweather, Anchorage, AK. June, 2014.

Olgoonik-Fairweather. 2014b. Arctic nearshore impact monitoring in development area III (ANIMIDA III): 2014 field report. Prepared by Olgoonik-Fairweather, Anchorage, AK. October, 2014.

Rember R.D. and Trefry J.H. 2004. Increased Concentrations of Dissolved Trace Metals and Organic Carbon During Snowmelt in Rivers of the Alaskan Arctic. Geochim. et Cosmichim. Acta. 68. 3:477-489.

Trefry J.H., Trocine R.P., Alkire M.B., and Semmler C.M. 2009. Continuation of the Arctic Nearshore Impact Monitoring in the Development Area (cANIMIDA) Tasks 3 and 4: Dispersion Pathways for Suspended Sediments and Potential Metals Contaminants in the Coastal Beaufort Sea. Final Report. OCS Study MMS 2009-014. Contract Nos. M04PC00035 and M04PC00036, Submitted to U.S. Department of Interior, Anchorage, AK, March, 2009.

U.S. EPA. 2003. Procedures for the Derivation of Equilibrium Partitioning Benchmarks (ESBs) for Protection of Benthic Organisms: PAH Mixtures. EPA-600-R-02-013. Office of Research and Development. Washington, DC 20460.

Trefry, J.H., Dunton K.H., Trocine R.P., Schonberg S.V., McTigue N.D., Hersh E.S., and McDonald T.J. 2013. Chemical and biological assessment of two offshore drilling sites in the Alaskan Arctic. Marine Environmental Research. 86: 35-45.

Venkatesan M.I. and Kaplan I.R. 1982. Distribution and transport of hydrocarbons in surface sediments of the Alaskan outer continental shelf. Geochim. Cosmochim. Acta 46:2135-2149.

Wang Z., Yang C., Kelly-Hooper F., Hollebone B.P., Peng X., Brown C.E., and Landriault M. 2009. Forensic differentiation of biogenic organic compounds from petroleum hydrocarbons in biogenic and petrogenic compounds cross-contaminated soils and sediments. J. Chromatog. A. 1216:1174-1191.

# Chapter 5 Benthic Infauna, Carbon Resources, and Trophic Structure on the Coast and Shelf of the Beaufort Sea, Alaska


## Abstract

In early August 2014 and 2015, as part of the ANIMIDA III program, we performed a quantitative assessment of the biomass, abundance, and community structure of benthic populations of the Beaufort Sea Shelf along with a detailed characterization of food web dynamics. Our analysis documented a benthic species inventory of 353 taxa collected from 126 individual van Veen grab samples (0.1 $m^2$) at 42 stations. Infaunal abundance was dominated by polychaetes, bivalves, and amphipods while bivalves, echinoderms, and polychaetes constituted the greatest fractions by biomass. Shannon Diversity Index values of the infaunal community at different stations (by abundance) was between 1.5 and 4.1 (mean = 3.3 ± SD 0.02), out of a possible range of 0-5. Thirty of the 42 stations had high diversity values between 3.1 and 3.9 and two stations had higher values, 4.0 and 4.1. Pielou's Evenness Index values ranged from 0.86 to 0.98 (mean = 0.96 ± SD 0.52) out of a range of 0-1, demonstrating balanced contributions from all collected species at many but not all stations. We used a Biota and Environment matching routine to examine the relationships between infaunal distributions of all collected taxa with the physical environment. A combination of water depth, TOC, and salinity correlated with infaunal abundance distribution ($\rho = 0.54$). We also noted that stations exhibiting the highest levels of both pyropheophorbide and pheophorbide *a* (chlorophyll degradation products that are markers for metazoan grazing) were characterized by the highest infaunal abundance. These stations contained polychaetes and benthic crustaceans that constituted >75% of all organisms present and were located in three "hotspots" along the Beaufort shelf. The three hotspots include mid-shelf locations in the western Beaufort in Harrison Bay, the central Beaufort, including Stefansson Sound, and the eastern Beaufort from Barter Island east to Icy Reef.

Our results imply a strong correlation between infaunal abundance and deposited sediment pool that may include ice algae, bacteria, and other benthic microalgae. Preliminary data on the stable nitrogen isotopic composition of benthic organisms reveal complex food webs dominated by decidedly omnivorous consumers that occupy up to four trophic levels. Stable carbon isotopic composition of these benthic organisms, along with isotopic analyses of suspended particulate organic matter and zooplankton, reveal a primary mixture of terrestrial and phytoplankton carbon, but an additional benthic microalgal subsidy appears to play a role at moderate depths that correspond to the three hotspots of infaunal abundance. Half the genera examined also displayed a distinct eastward depletion in $\delta^{13}C$ values that likely reflects the influence of the Mackenzie and other sources of freshwater runoff in the eastern U.S. Beaufort Sea, which transport allochthonous inputs of terrestrial organic carbon that become available as a food source to the benthos. These results provide compelling evidence for the important role of terrestrial carbon in Beaufort Sea food webs. Aside from the nearshore Sagavanirktok and Colville Rivers' deltas, the U.S. Beaufort Sea shelf overall supports a rich benthic infauna community, particularly in the region around Kaktovik where repeated upwelling events have been reported.

## 5.1 Introduction

Our knowledge of the benthic ecosystem of the coast and shelf of the U.S. Beaufort Sea is not as comprehensive when compared to other shelves, largely due to logistical challenges imposed by multi-year ice and an inhospitable climate. Extreme changes in Alaska nearshore environmental conditions have been visible in recent years, particularly since 2007. Recent data indicate that Arctic summer ice extent is declining 13% per decade, relative to the 1979 to 2000 average, with a record low ice cover recorded in 2007 and 2012 (40% lower than the long-term average minimum). Three of the lowest ice extents have been recorded in the past five years (2012, 2015, and 2016) based on data from the National Snow and Ice Date Center. These large losses in summer open-water ice cover are concentrated in the western Arctic, particularly in the Beaufort Sea, which has resulted in considerable areas of open water. The increased fetch has produced record rates of coastal erosion which in turn contributes enormous quantities of sediment into the coastal zone with significant implications for the exchange of carbon, water, and nutrients on the shelf (Mathis et al, 2012; Pickart et al., 2013). Such changes are likely to cause shifts in trophic linkages and faunal diversity. Information on food webs and benthic species composition are therefore critical in delineating ecosystem responses to dramatic physical shifts in ice, circulation and hydrography.

The coast and shelf of the Beaufort Sea extends from Point Barrow in Alaska to Banks Island in Canada, and incorporates three distinct shelf environments (inner, mid, and outer) and two large river systems, the Colville and the Mackenzie. In marked contrast to the Chukchi-Bering ecosystem on the west and the Queen Charlotte Islands on the east, the Beaufort Sea, and the eastern U.S. Beaufort Sea in particular, is decidedly estuarine in character. The combined flows of the Colville and the Mackenzie Rivers annually add nearly 350 cubic kilometers $[km]^3$ of freshwater plus 130 x 106 tons sediment to a relatively broad shelf that ranges in width from 40 km in Alaska to 150 km in Canada (Macdonald et al., 2004). In addition, the U.S. Beaufort Sea coast, from Barrow to Demarcation Bay, is skirted by an irregular and discontinuous chain of barrier islands that enclose numerous shallow (<8 m) lagoons that are fed by many small rivers and streams.

Large scale quantitative studies of Beaufort Sea coastal benthic biota did not begin until relatively recently, following the discovery of oil in Prudhoe Bay. Surveys under the Outer Continental Shelf Environmental Assessment Program (OCSEAP) began in the 1970s and continued into the early 1990s. The two major studies under this program were by led by A.C. Broad who surveyed the nearshore between 1975 and 1980 and A.G. Carey Jr. who sampled from the mid-shelf to the edge of the Arctic Basin (in 1971 and 1975-1978; see Dunton et al., 2005).

The estimates provided by Dunton et al. (2005) for benthic biomass on the U.S. Beaufort Sea shelf are based on historical data from stations that are not evenly distributed across or along the shelf, and consequently, our confidence in predicted values is quite variable. This study provides an excellent opportunity to add an enormous amount of information describing the character of the Beaufort Sea shelf ecosystem, greatly improving our quantitative knowledge of the region. Predicted biomass values, based on the small number of samples collected from this region, range from <25 to 50 $g/m^2$, nearly an order of magnitude less than the northeastern Chukchi shelf. In addition, we have little information on the composition of these benthic communities since earlier work only identified organisms to the level of family, not species. A detailed knowledge of benthic assemblages is required for determination of spatial and temporal patterns in diversity as well as community structure.

Another enigma for this area is the source of carbon that supports the shelf biotic assemblages. We can distinguish terrestrial sources of organic material from marine sources based on their stable isotopic signatures. Terrestrial organic matter is characterized by $\delta^{13}C$ values of -27 to -31‰ and $\delta^{15}N$ values of 0 to 1.5‰. In contrast, marine primary producers are identified by $\delta^{13}C$ values of -22 to -26‰ and $\delta^{15}N$ values of 5 to 7‰. We can use these end-member values in assessing the relative importance of these two sources of carbon to the marine consumers of the Beaufort Sea shelf. Such knowledge provides us with an enhanced understanding of the system that can be used to assess food web structure populations and the dependency of benthic consumers on ultimate carbon sources.

It is widely believed that phytoplankton production provides the ultimate source of food for both the pelagic and benthic components of these communities. However, isotopic data from sediments collected on the Beaufort Sea coast show a strong gradient of increasing terrestrial inputs of POC eastward along the nearshore portion of the eastern Beaufort (Naidu et al., 2000). On the Mackenzie shelf, isotopic evidence led Parsons et al. (1989) to conclude that terrigenous carbon was a significant component of the nearshore food web. The depleted $\delta^{13}C$ values in the organic carbon of Arctic coastal sediments, particularly in regions near the Mackenzie and Colville River Deltas, led Naidu et al. (2000) to conclude that at least 30-50% of the organic matter in nearshore and shelf sediments was of terrigenous origin. The sources of this allochthonous carbon include both river runoff and coastal erosion. Based on calculations made by Reimnitz et al. (1988) for the U.S. Beaufort Sea and Are (1999) for the Laptev Sea, it appears that sediment influx derived from coastal erosion is greater than the riverine influx. However, the hydrological controls on biogeochemical feedbacks and linkages between Arctic watersheds and their receiving basins on the northern Alaskan coast are not well understood.

The fate of this terrigenous carbon in Arctic coastal food webs was at first unknown. Schell (1983) found evidence for the incorporation of ancient (8–12,000 year BP; Schell and Ziemann, 1983) terrestrial peat carbon into freshwater aquatic food webs near the Colville River Delta based on depressed $^{14}C$ abundances in resident fish and ducks. However, $^{14}C$ activities in three marine invertebrate crustaceans were not depressed, leading Schell (1983) to conclude that utilization of terrestrial carbon in the Arctic estuarine environment was very limited. However, DOC is by far the most abundant form of terrigenous carbon exported in Arctic rivers (Gordeev et al., 1996; Lobbes et al., 2000) and, based on $^{14}C$ abundance data, this carbon pool is predominantly young (Benner et al., 2004). This study therefore provides an opportunity to examine the possible incorporation of terrestrial carbon into the food webs of the Beaufort Shelf from the inner shelf (just outside the barrier islands at 20 m water depth) to the shelf edge (ca. 200 m isobath).

Benthic microalgae, another organic matter source hypothesized by the scientific community to exist on the Chukchi Sea benthos, may also supply a $^{13}C$-enriched signal to the benthic food web (Tu et al., 2015; McTigue and Dunton, 2014; Glud et al., 2009; Wulff et al., 2009). Other possible organic matter (OM) sources include microbially degraded detrital material (McConnaughey and McRoy, 1979; Lovvorn et al., 2005; North et al., 2014; McTigue et al., 2015). Benthic microalgae (microphytobenthos, MFB) have eluded stable isotope analysis in the Arctic, but they have been identified in other systems as $^{13}C$-enriched primary producers relative to phytoplankton (France, 1995; Dubois et al., 2009). Benthic microalgae exhibit values that fit within the expected range of an OM source that would explain some $^{13}C$-enriched benthic consumers in the Bering and Chukchi Seas (Lovvorn et al., 2005; North et al., 2014; McTigue et al., 2015; Tu et al., 2015). Stable carbon isotopic composition of these benthic organisms, along with isotopic analyses of SPOM and zooplankton, reveal a primary mixture of terrestrial and

phytoplankton carbon, but an additional subsidy in a deposited sediment pool may include ice algae, bacteria, and other benthic microalgae at moderate depths that correspond to the three hotspots of infaunal abundance. We have no knowledge on the potential importance of microalgal carbon as an additional food resource in the Beaufort Sea.

In early August 2014 and 2015, we collected benthic samples from 43 stations on the Beaufort Sea coast from 153° W to ~141° W in water depths ranging from 6 to 395 m (Figure 86). Our main objectives were to (1) identify the food web patterns of the benthic community in relation to organic carbon supply and (2) assess the natural variability of infauna distribution on the Beaufort Sea shelf. The results of our sampling better defined the trophic structure of the shelf and revealed patterns of benthic species abundance and distribution that appear related to both unique oceanographic features and the presence of alternative carbon sources produced in situ.

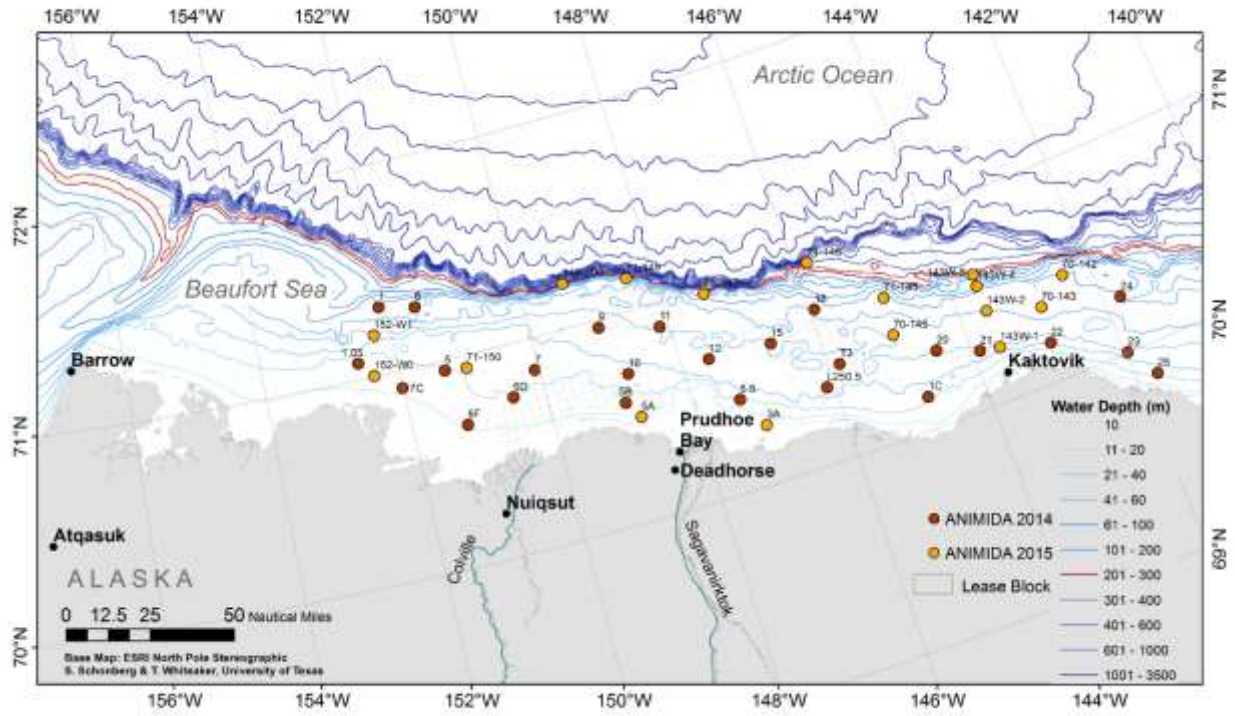


**Figure 86. ANIMIDA III infauna station locations for years 2014 and 2015.**

## 5.2 Materials and Methods

### 5.2.1 Study Region

The U.S. Beaufort Sea portion of the continental shelf averages ~80 km between the coast and the shelf break that follows the 200-m isobath and stretches ~600 km from Point Barrow to the Canadian border located east of Demarcation Bay (Dunton et al., 2006). The U.S. Beaufort Sea coast is bordered by a discontinuous chain of barrier islands that enclose numerous river-fed shallow (<8 m) lagoons that are fed by many small rivers and streams. Landfast ice forms over the shelf waters to the 20-m isobath in the fall where it abuts to drifting polar pack ice resulting in grounded ice ridges and rubble fields that

extended up to 13 m high (the Stamukhi Zone; Reimnitz et al., 1977; Barnes et al., 1984) and persists until early summer when it retreats north due to warmer air temperatures and pulses of freshwater from numerous rivers that drain the Alaskan North Slope. The hydrographic structure on the shelf is driven by a complex interaction between bathymetry, river inflow, coastal erosion, ice cover, wind forcing, and large-scale circulation forces of the Arctic Ocean (Pickart, 2004). Water flow along the continental slope consists of a mixture of water masses derived from Pacific, Atlantic, and Arctic origins (Weingartner, 2003). The shelf flow is topographically steered to produce eastward flow which is in opposition to the prevailing northeast winds (Chapman, 2003). Wind events can generate westward jets over the shelf and also can produce upwelling of deep basin water up the slope and onto the shelf (Hufford, 1975; Mountain, 1975; Chapman, 2003). During summer months, western U.S. Beaufort Sea shelf and slope waters are influenced by an inflow of productive Chukchi Summer Water and Alaskan Coastal Water that flow east from the Barrow Canyon (Pickart, 2004; von Appen and Pickart, 2012) and are thought to enhance pelagic and benthic productivity in the extent of these waters (Carey and Ruff, 1977).

### 5.2.2 Field Collections

We collected benthic infauna and epifauna at 43 stations at depths ranging from 6 to 395 m for isotopic analysis along the coast in August 2014 and 2015 aboard the R/V *Norseman II*. In 2014, stations were selected using two basic criteria: (1) to reoccupy historic BSMP and historic Camden Bay stations, and (2) create new random locations that spanned the Beaufort shelf, including current BOEM oil lease block locations, using a probability-based computation in ArcGIS 10 within 1260 $km^2$ hexagonal tessellated grid cells (White et al., 1992). In 2015, we added the Beaufort Sea DBO lines at 152° W and 143° W. Seven stations were planned for the 152° W DBO line but only two were successfully sampled due to persistent ice cover in the central Beaufort Sea shelf. The 143° W DBO line was ice-free allowing the research team to occupy six stations.

**Infaunal benthos.** Benthic infaunal invertebrates were collected from double van Veen grabs (3 grabs per station) at 25 stations in 2014 and 17 stations in 2015 (Figure 86). Use of a double van Veen grab (0.1 $m^2$) insured that the physical and chemical properties associated with the sediments could be matched to the biological samples obtained from the companion grab. Samples were sieved through a 1 mm mesh using a low-flow sieve table to ensure gentle handling of soft-tissue invertebrates (i.e., polychaetes) to aid in taxonomy. Organisms were preliminarily identified to lowest possible taxonomic level shipboard then preserved in 80% ethanol.

Upon their arrival to the University of Texas Marine Science Institute (UTMSI), infaunal samples were reexamined. Taxonomic specialists were used to verify identifications of dominant groups including crustaceans (Ken Coyle, UAF), mollusks (Nora Foster, UAF) and polychaetes (Leslie Harris, Natural History Museum of Los Angeles County). After identifications were complete, species within each grab sample were blotted and measured for wet weight biomass (including mollusk shells).

### 5.2.3 Community Structure: Species Diversity

An ecological analysis of infaunal species abundance was performed using routines available in the PRIMER v6 software package (Clarke and Gorley, 2006; Primer-e, 2016. Total number of species (S), Shannon Diversity Index (H' loge), and Pielou's Evenness Index (J') were calculated for species abundance data ($m^2$) using the DIVERSE routine in PRIMER (Clarke and Warwick, 2001). The Shannon Diversity routine assumes that individuals are randomly sampled from a large population:

$$H' = -\sum_{i=1}^{R} p_i \ln p_i$$

where pi is the proportion of individuals that belong to species i and R is richness (the number of species in the dataset). Mathematically, the Shannon Diversity value has the potential to range from 0–5 but in practice it usually lies between 1.5 and 3.5 and only rarely is >4 (Magurran, 2004). The higher values indicate greater species diversity. Pielou's Index (J') is constrained between 0 and 1. The less variation between count of species the higher the value of J'.

### 5.2.4 Community Structure:Environmental Variables

Environmental variables were plotted using the PRIMER v6 PCA routine to determine how a set of environmental factors collected at 42 stations related to each other. Environmental variables included: (1) hydrographic characteristics (bottom water temperature and salinity), (2) infauna nutrient sources (sediment TOC, total organic nitrogen [TON], carbon to nitrogen molar ratio [C:N], sediment chlorophyll *a*, and (3) physical habitat (sediment grain size; gravel, sand, mud). Distribution by total water depth, longitude, and latitude were also examined. Sediment grain size data were provided by John Trefry (FIT), and bottom water temperature and salinity data were collected from ship's CTD and made available by Jeremy Kasper (UAF). All other analyses were performed in the UTMSI laboratory.

PCA is a mathematical procedure that uses an orthogonal transformation to convert a set of possibly correlated variable values into a set of values of linearly uncorrelated variables called principal components. The first principal component (PC1, x axis) accounts for as much of the variability in the data as possible, with each succeeding component having the highest variance possible under the constraint that it be uncorrelated with the preceding components. The data were normalized prior to running the PCA function to fulfill the requirement that the data be normally distributed.

The Biota-Environmental (BIO-ENV) routine in PRIMER v6 was used to explore relationships between Chukchi Sea Offshore Monitoring in Development Area (COMIDA) Hanna Shoal species abundance and biomass and selected environmental variables (same variables as listed above for the PCA analysis). The BIO-ENV routine calculates Spearman rank correlations between the similarity matrix derived from infaunal species abundance or biomass data and matrices derived from environmental variables that could explain the biotic structure (Clarke and Warwick, 2001). The statistical significance of the results was tested by the global BIO-ENV match permutation test whereby each set of samples was randomly permuted relative to the other. The null hypothesis was that there is no relationship between the species abundance matrix and any of the possible resemblance matrices subsets of the environmental variables. The real rank correlation coefficient was compared with the permuted null hypothesis values, and if the actual coefficient was larger than any of the permuted coefficients, then the null hypothesis was rejected with a $p < 1\%$. Biota abundance values were square root transformed prior to analysis to meet assumptions of normality, and environmental parameters were log-transformed and normalized prior to analysis in order to derive meaningful Euclidean distances between environmental data variables with different scales.

### 5.2.5 Isotopic Sampling

**Particulate Organic Matter (POM).** Water samples were collected from (CTD) bottles for isotopic analysis of SPOM. CTD bottles were tripped at two depths: at the chlorophyll maximum zone and 2-3 m above the seabed. Approximately 500 mL of seawater from each depth were subsequently

filtered through non-combusted 25 mm glass fiber filters (GFF) in duplicate, then frozen for future High Performance Liquid Chromatography (HPLC) chlorophyll analyses. In addition, 2 L off seawater were filtered onto combusted GFF filters in duplicate, dried, and stored for future POM stable isotope analyses.

**Plankton**. Phytoplankton and zooplankton hand nets (20 and 335 µm mesh; Sea-Gear, Melbourne, FL) were deployed to collect pelagic organisms for stable isotope analyses. A 20 µm phytoplankton net was lowered vertically to 5 m above the sea floor and then slowly retrieved. The collected contents were filtered through a series of three sieves to collect material < 63 µm. The resulting filtrate was filtered onto pre-combusted 25 mm GFF (0.7 µm pore size) under low vacuum in duplicate and dried.

A 335 µm zooplankton net was lowered vertically to 5 m above the sea floor and then slowly retrieved. The sample was filtered through a 1mm mesh sieve. If present, large calanoid copepods, *Calanus hyperboreus* and *Calanus glacialis*, were occasionally collected in the 1 mm mesh sieve and removed for separate stable isotope analysis. The resulting filtrate was filtered onto pre-combusted 25 mm GFF (0.7 µm pore size) under low vacuum in duplicate and dried.

**Surface Sediments**. Sediment organic matter (SOM) was collected from the upper 2-cm of an undisturbed 0.1 $m^2$ van Veen grab with the barrel of a 20 cubic centimeter (cc) syringe (1.8 cm diameter) for three analyses: pigments, stable isotope analysis, and ammonium concentration. Pigment samples were collected in duplicate using a 20 cc syringe, stored in a darkened centrifuge tube and frozen. Sediments for isotopic analysis were also collected with a 20 cc syringe in duplicate and dried. Ammonium samples were collected with a 60 cc syringe, extruded into a pre-labeled Whirl-pac bags and frozen for shipment. Porewater was extracted by centrifuging thawed sediments. The supernatant underwent colorimetric analysis as described by Parsons et al. (1984).

**Benthic Fauna.** Infauna were collected from one of three double van Veen grabs deployed from the ship for biological and chemical analysis. From the first double van Veen grab, one side was sampled for SOM and the other side was used for quantitative infauna collection. The third van Veen grab was used for collection of infauna organisms for stable isotope analyses. Each grab sample was sieved using a low-flow slide table to ensure gentle handling of soft-bodied invertebrates. Infauna were collected from a 1 mm mesh sieve at the base of the table. Animals from quantitative grabs were sorted under a microscope and preserved in 80% ethanol. Specimens for stable isotope analyses were sorted, identified to the lowest taxonomic group possible, and dried. Large samples for isotope analysis were first dissected to remove muscle tissue, and smaller organisms were dried whole.

Benthic epifauna were collected using a 3.05 m plumb-staff beam trawl (PSBT-A) with a 7 mm mesh and a 4 mm cod-end liner. Epifauna samples were sieved over 1 mm mesh and washed with ambient surface water to remove extraneous organic matter and sediment. Invertebrates were keyed to lowest taxonomic level possible, usually species, in the field. When possible, muscle tissue was extracted from the organism for stable isotope analyses. Biota and tissue samples were dried shipboard in aluminum dishes at 60 °C.

**Pigment analyses**. Pigments targeted in the sediments were chlorophyll *a*, the pheopigments pheophytin *a*, pheophorbide *a*, pyropheophorbide *a*, and the accessory pigments chlorophyll b, chlorophyll c (defined as the sum of c1 and c2), fucoxanthin, peridinin, prasinoxanthin, and 19-hex-fucoxanthin. Sediment pigments were extracted using 10 mL of 100% acetone since residual porewater in the sample dilutes the acetone concentration (Sun et al., 1991). Volume of porewater was determined and

accounted for in extract volume. Samples were sonicated in chilled water for 15 min in darkness. After centrifuging samples for 5 min at 4000 revolutions per minute (rpm), supernatant was decanted and filtered through 0.2 μm nylon filters. To ensure the complete extraction of pigments from sediments, each sample was extracted twice and the extracts were combined. If the combined extract was cloudy, the entire 20 mL was re-filtered through a 0.2 μm nylon filter.

The HPLC pigment analysis followed protocol of DHI (DHI Water and Environment, Denmark). Briefly, a binary gradient of 28 milliMolar (mM) tetrabuyl ammonium acetate (TBA) in methanol (30%:30%, v:v) (eluent A) and methanol (eluent B) was used. Eluant B was ramped from 5% to 95% in 22 min, and held for 7 min before falling back to 5% within 2 min. A C8 HPLC column (Agilent Eclipse XDB, 3.5 μm, 4.6 mm x 150 mm) was used, and the eluted pigment was detected by UV-vis absorbance (wavelength = 450 nanometer [nm]). Concentrations were determined by comparing pigment peaks of equal retention time to those of certified commercial standards (DHI, VWR, and Sigma-Aldrich, USA).

**TOC, TN, and stable C and N isotopic analyses.** To remove carbonates that would interfere with stable carbon isotope analysis, a subsample of faunal tissues (particularly calcifying organisms and small, whole organisms) and sediments were soaked in hydrochloric acid (HCl) until bubbling stopped, then rinsed in deionized water and dried at 60 °C to a constant weight. Tissue and sediment subsamples prepared for stable nitrogen isotope analysis were not subjected to acidification. Muscle tissue excised from shell or exoskeleton was not acidified. Samples were not lipid extracted prior to stable isotope analyses so that data could be comparable to other studies from the region (e.g., McTigue and Dunton, 2014; Iken et al., 2010; Tu et al., 2014). Previous work determined a low likelihood that lipids in Arctic consumers influenced $\delta^{13}C$ values (Graeve et al., 1997; Iken et al., 2010, Dunton et al., 2012; Smith et al., 2016).

Dried tissue samples were manually homogenized with a mortar and pestle, and tissue, sediment, and filter samples were weighed in tin capsules to the nearest $10^6$ g. Samples were analyzed on an automated system for coupled $\delta^{13}C$ and $\delta^{15}N$ measurements using a Finnegan MAT Delta Plus mass spectrometer attached to an elemental analyzer (CE Instruments, NC 2500). Samples were combusted at 1,020 °C and injected into the mass spectrometer with continuous flow. Isotopic ratios are denoted in standard δ notation relative to carbon and nitrogen standards of PDB and atmospheric N2, respectively where

$$\delta X=[(Rsample/Rstandard)-1] \times 1000$$

X is either $^{13}C$ or $^{15}N$ of the sample and R corresponds to the $^{13}C/^{12}C$ or $^{15}N/^{14}N$ ratio. Instrumental analytical error was ±0.15‰ and analytical sample error was ±0.20‰, based on internal standards from the NIST and the International Atomic Energy Agency. We reported total nitrogen (TN) instead of TON since inorganic nitrogen, especially ammonium, can bind to clay minerals common to marine sediments and inflate the amount of measured N (Stein and Macdonald, 2004).

**Trophic Level (TL) Determinations.** Trophic levels were determined from isotopic values using the trophic enrichment equation of Iken et al. (2010):

$$TL\ (Phyto) = (\delta^{15}N_{consumer} - \delta^{15}NPhyto)/3.4 + 1$$

where 3.4 is the average ‰ enrichment in $\delta^{15}N$ between successive TLs using 20 μm net phytoplankton as the ultimate trophic carbon source ($\delta^{13}N$=7.7‰; Table 28). We recognize in using 3.4‰ that there is some variation in the appropriate enrichment per trophic level in different ecosystems,

including the ecosystem studied here. For example, in the Antarctic Peninsula, Dunton (2001) used a value of 3.2‰ per trophic level, which is comparable to values of 3.3‰ applied by Wada et al. (1987) to the Southern Ocean and Rau et al. (1992) in the northeast Atlantic. In the U.S. Arctic, Iken et al. (2010) used a 3.4‰ enrichment based on the extensive reviews of the topic by Vander Zanden and Rasmussen (2001) and Post (2002), which identified 3.4‰ as an average isotopic fractionation for aquatic consumers.

In recognition that trophic increases are variable between consumers and their source material, we introduced mixing lines that delimited the isotopic value ranges expected for the transfer of $^{13}C$ or $^{15}N$ through the food web. In recognition of the variability in $^{13}C$ or $^{15}N$ enrichments noted by Dunton et al. (2012), we used two conservative mixing lines to best assess the relative importance and role of terrestrial organic-C, SPOM and MFB sources available to consumers on $\delta^{13}C$ vs $\delta^{15}N$ bi-plots. In this approach, also used by Darnaude et al. (2004), two mixing lines are constructed that potentially correspond to minimum and maximum trophic increases of +1.0‰ and +2.0‰ in $\delta^{13}C$ and maximum and minimum trophic increases of +4.0‰ and +2.5‰ in $\delta^{15}N$ per trophic level. These two potential combinations of the range of trophic level enrichment for both carbon and nitrogen isotope values result in positive slopes of 1.25 and 4 from the source material. These mixing lines provide a boundary and a mechanistic tool to assess the dependence of consumers on the suspected ultimate carbon sources. Our selection of terrestrial organic-C, phytoplankton, and MFB as carbon and nitrogen end-members for shelf biota was largely based on the opportunistic and omnivorous feeding strategies employed by most Arctic fauna (Dunton and Schell, 1987; Iken et al., 2010).

## 5.3 Results

### 5.3.1 Infauna Inventory

A total of 353 taxa were identified from 126 van Veen grab samples (0.1 $m^2$) collected from 42 stations in 2014 and 2015. Species occurrence by abundance included *Polychaeta* (56%) followed by *Crustacea* (20%), *Mollusca* (13%), *Echinodermata* (8%), *Nemertea*, (2%), *Sipunculida* (1%), and other phyla (2%). Species distribution by biomass was dominated by *Mollusca* (37%) followed by *Echinodermata* (20%), *Polychaeta* (19%), *Sipunculida* (5%), *Crustacea* (4%), *Nemertea* (3%), and other phyla (12%). All annelid species belonged to *Polychaeta* (135 species) except for two oligochaete specimens. The dominant mollusc groups were *Bivalvia* (39 species) and *Gastropoda* (29 species). Within the *Arthropoda*, *Malacostraca* represented the most diverse class, including 62 species of *Amphipoda*, 13 *Cumacea* species, and 3 *Decapoda*. The remaining taxa ('Miscellaneous') included *Porifera*, *Bryozoa*, *Hydrozoa*, *Priapulida*, *Alcyonaria*, *Anthozoa*, *Actinaria*, *Scleractinia*, *Hemichordata*, *Brachiopoda*, and *Ascidiacea*. Infaunal abundance and biomass were low in the nearshore area west of the Sagavanirktok River and in the Colville River Delta at 10 to 30 m water depths (Figure 87, Figure 88). The primary species inhabiting this region were small crustaceans (amphipods and cumaceans) and polychaetes. All stations included these three groups except for stations 1.05 and 152-W0, located in the western side of the Colville Delta, which did not have molluscs. In general, abundance values were greater to the east of the 148° W line and notably higher on the shelf north of Kaktovik between 142° W and 144° W (Figure 87). The biomass distribution showed a different pattern with similar values among all stations except for low numbers in the river deltas and two stations located on the shelf break between 146° W and 143° W (Figure 88). Biomass station means are dominated by molluscs, echinoderms, and polychaetes (Figure 88). Large bodied clams, brittle stars, nemerteans, or sipunculids contributed greatly to the overall station

biomass value in the mid shelf stations. Echinoderms and nemerteans did not occur in water <30 m in depth.

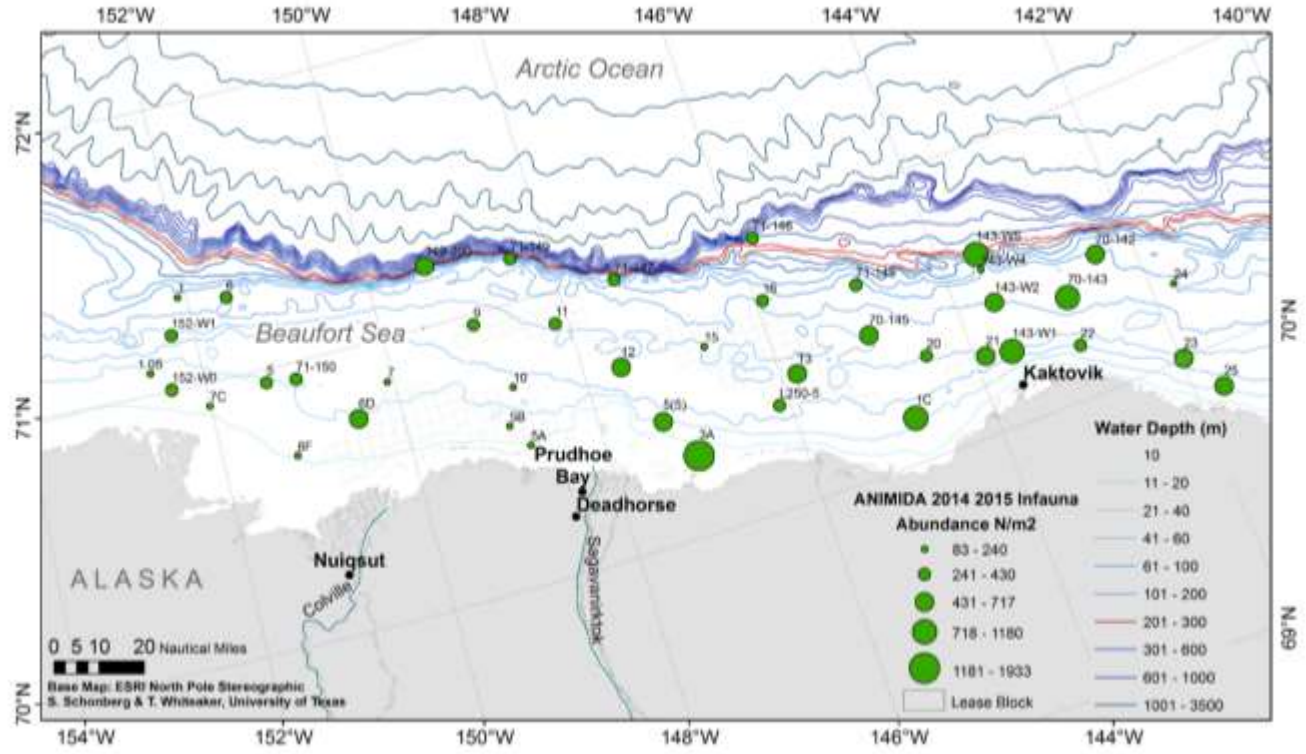


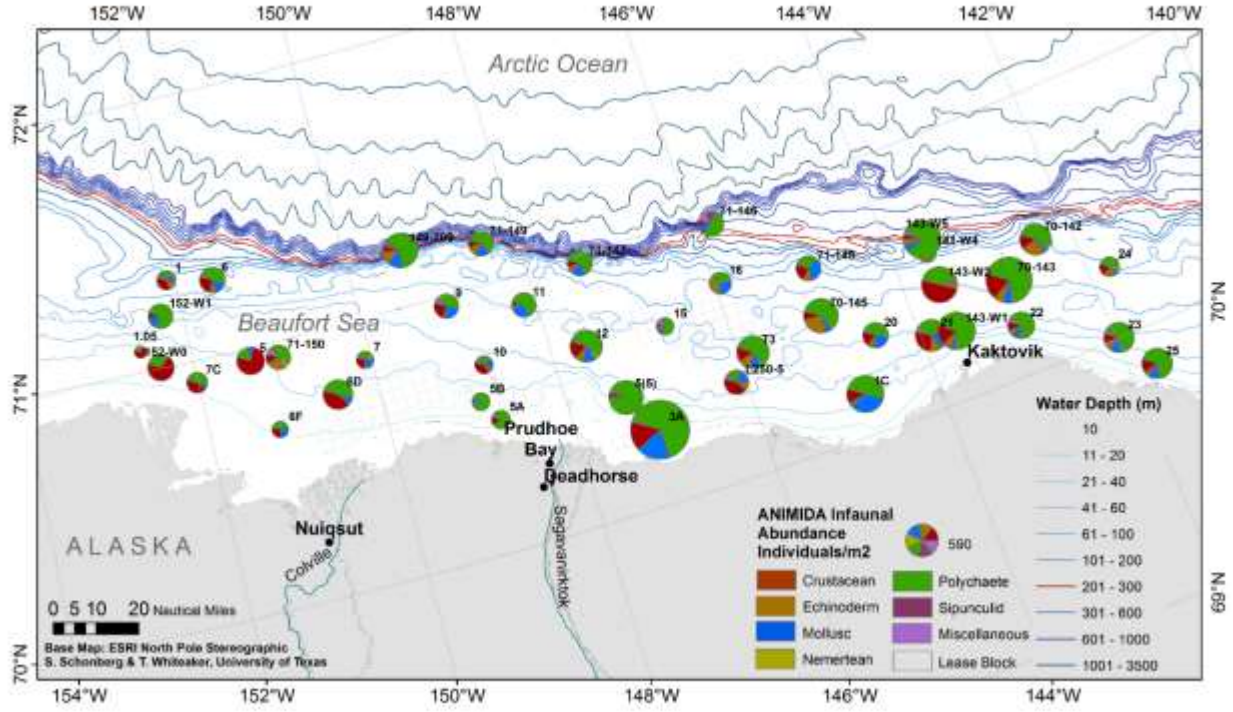

**Figure 87. Total infauna station abundance (N/m$^2$) for 2014 and 2015 (top panel). Infaunal abundance distribution by principle taxonomic group (bottom panel).**

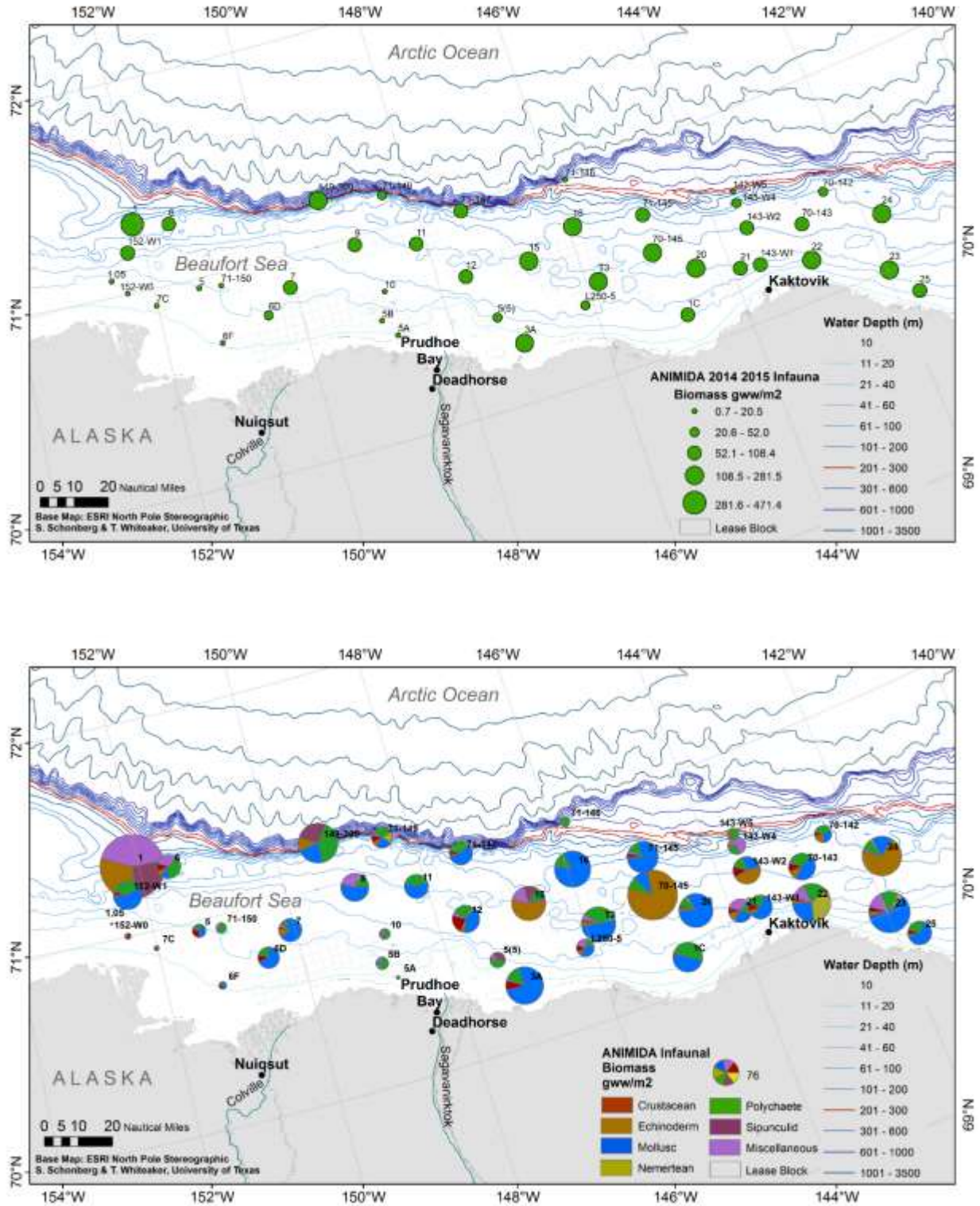

**Figure 88. Total infauna station biomass (grams wet weight (gww)/m$^2$) for 2014 and 2015 (top panel). Infaunal abundance distribution by principle taxonomic group (bottom panel).**

### 5.3.2 Infauna Diversity

Total taxa, and Shannon Diversity and Pielou's Evenness Indexes were calculated to explore trends in infaunal community structure in the study area. Station taxa totals varied between 5 and 77 per station. Stations with fewest species were located nearshore in the Sagavanirktok and Colville River Deltas (Figure 89). The largest taxon count values were concentrated in waters located in the greater Kaktovik region where the shelf break becomes less steep and moves closer to the Alaskan coast resulting in deeper nearshore water (Figure 89). The abundance Shannon Diversity values followed similar distribution patterns as the taxa totals (Figure 89). Station 3A, located just west of Prudhoe Bay, is notable because it is a nearshore station (<10 m) that has high abundance, biomass, taxon count, and diversity. It is the only station in this study situated within the coastal lagoon system created by the discontinuous chain of barrier islands that follow the Alaskan coastline. Beaufort Sea Lagoons and have been shown to be highly productive areas for both benthic and pelagic organisms (Dunton et al., 2006).

Shannon Diversity abundance values ranged from 1.56 (Station 1.05) to 4.14 (Station 70-143) with a mean = 3.3 ± SD 0.02 (Figure 89). Thirty of the 42 stations had diversity values between 3.1 and 3.9 and two stations ranged between 4.0 and 4.1 (out of a maximum of 5) indicating that areas of the seafloor in this study area support a diverse ecosystem. Pielou's Index values ranged from 0.86 (Station 5(5) to 0.98 (Station 15) with a mean = 0.96 ± SD 0.52 indicating that many but not all stations have an even distribution of species. The relationships between infaunal abundance, Shannon Diversity and Pielou's Evenness indicated that low abundance did not necessarily correspond with low species diversity or evenness (Figure 87, Figure 89, Figure 90). Most stations located in the Sagavanirktok and Colville River Delta had low or medium abundance and diversity values but a few of them had high evenness values indicating a balance in the few species that were present. Stations located in the region north of Kaktovik had consistently high abundance, biomass, diversity, and evenness numbers. They are all around robust infaunal stations.

Species diversity is most likely greater than reported because some of the most abundant polychaetes collected in this study require further taxonomic evaluation (Leslie Harris, Natural History Museum of Los Angeles County, pers.comm.). The polychaete groups in question are represented by the genera *Barantolla, Chaetozone, Brada, Bradabyssa, Chone, Eteone, Euchone, Flabelliderma, Heteromastus, Mediomastus, Ophelina, Pholoe, Scoletoma, Sphaerodoropsis, Sternaspis, Syllis*, and *Terebellides*. A limited number of polychaete samples were examined due to budget constraints, so many are identified only to family or genera.

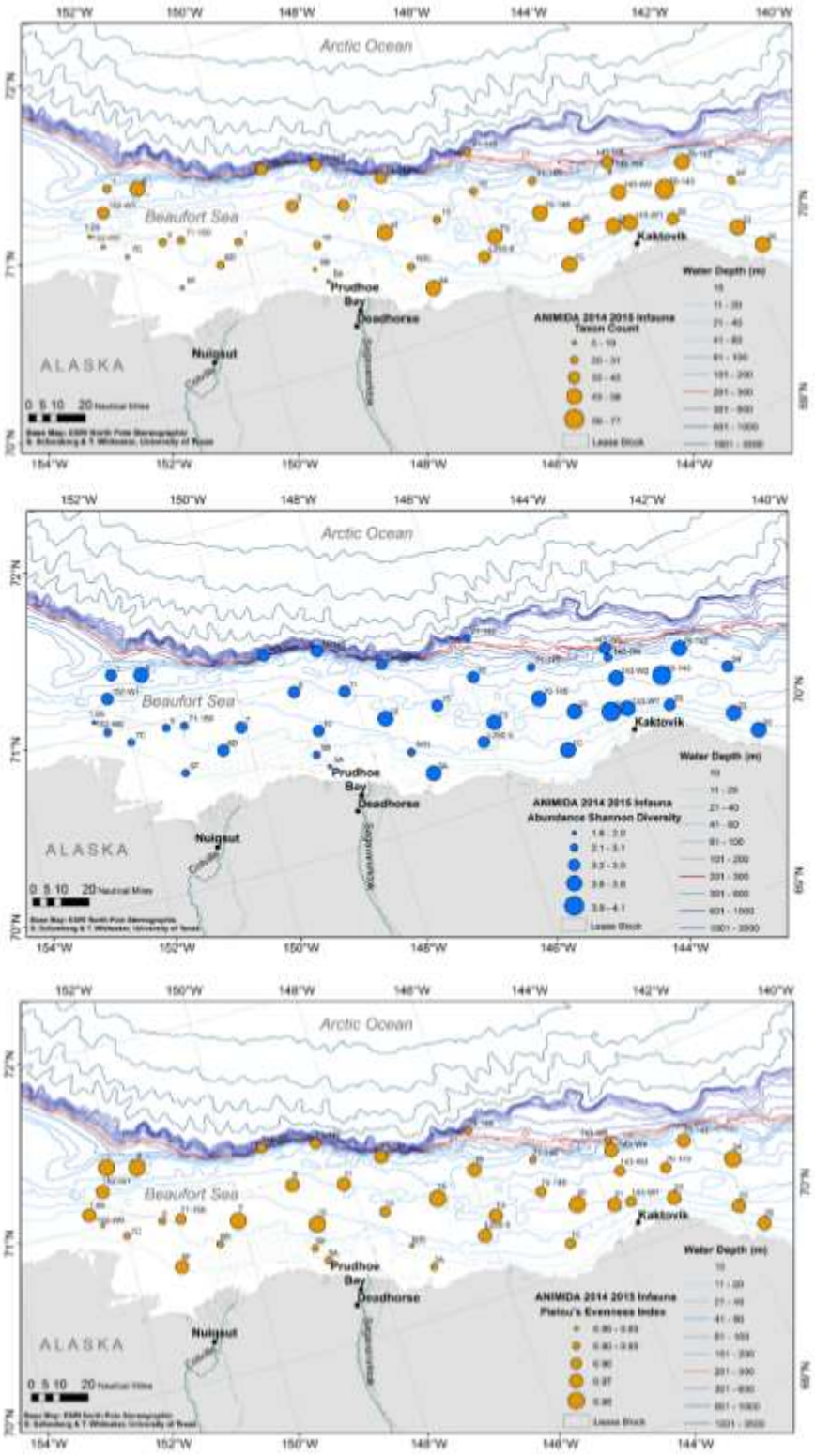


**Figure 89. Total infauna taxonomic count by station for 2014 and 2015 (top panel), Shannon Diversity Index values on the basis of infauna abundance (middle panel), and values of Pielou's Evenness Index (bottom panel).**

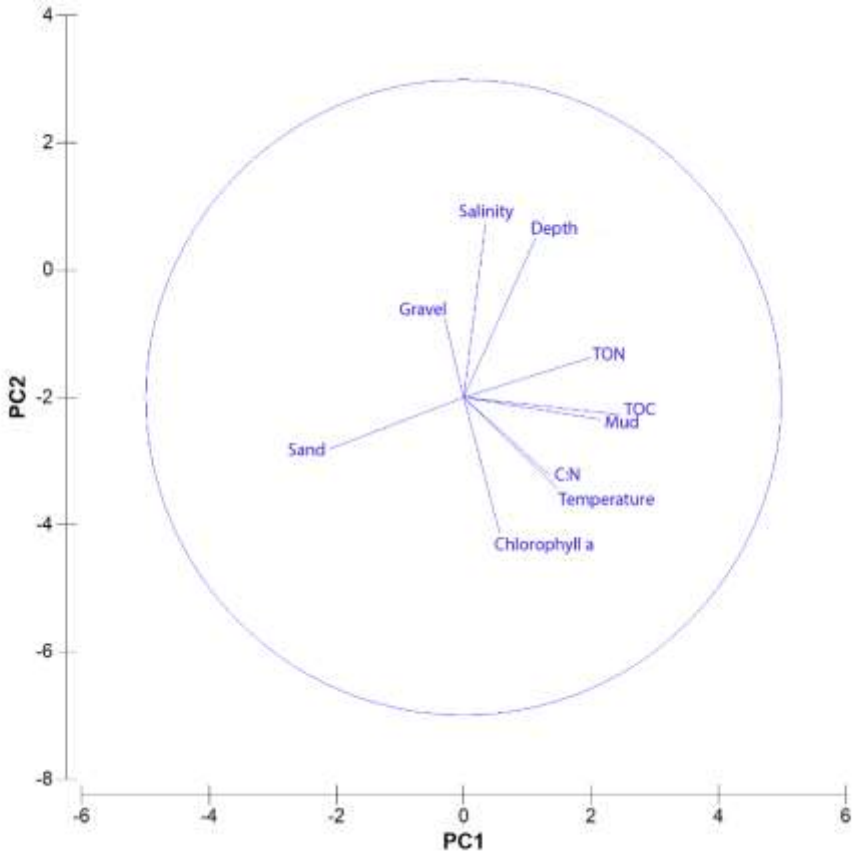


**Figure 90. Relationships between benthic environmental factors determined using a Principal Component Analysis (PCA) routine.**

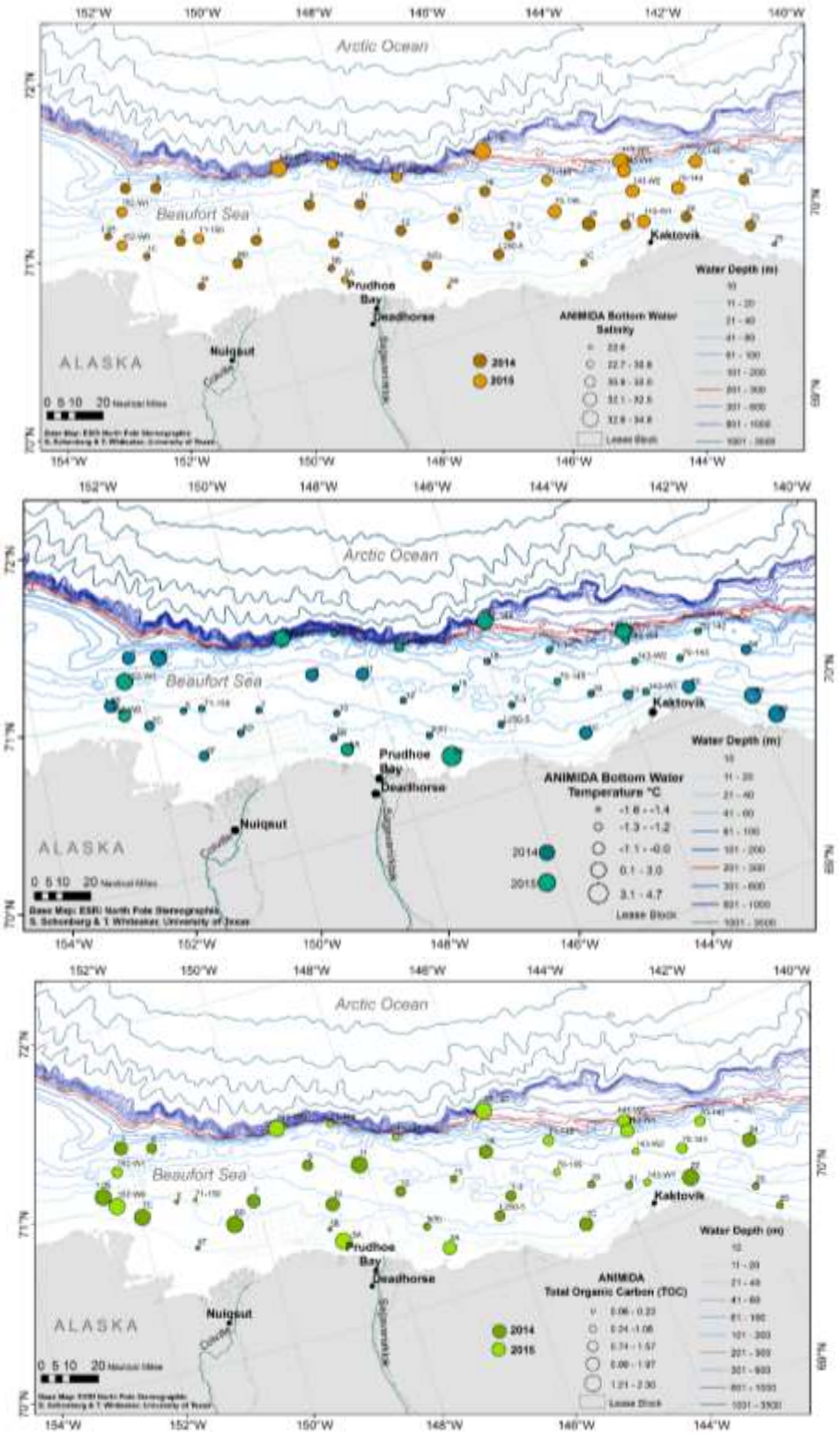


**Figure 91. CTD bottom water salinity (top panel), bottom water temperature (middle panel), and TOC (bottom panel) at infauna stations.**

### 5.3.3 Environmental Factors and Infauna

**Sediment Grain Size.** Shelf sediments, taken from one side of a double van Veen grab that was a companion to the infaunal grab, were analyzed by John Trefry at FIT (sediment grain size and chemistry) and Ken Dunton at UTMSI ($\delta^{13}C$ and $\delta^{15}N$ isotopes, chlorophyll *a*, TOC, TON, and C:N). The sediments on the Beaufort Sea shelf were a mixture of mud (silt/clay) and sand with a gravel fraction at some stations located between 30–100 m depth (see J. Trefry's chapter, this report). The nearshore stations (< 30 m) were a combination of mud and sand, with sand dominating in the Colville River Delta. Three of the sand dominated delta stations (5, 5B, 6F) had such low levels of organic material that the mass spectrometer was unable to detect reliable TON values. Three stations along the shelf break (71-146, 143-W4, and 143-W5) and two stations on the western edge of the Colville River Delta (152-W0 and 152-W1) were 94-100% mud. The majority of the stations were a combination of sand and mud with a gravel fraction in some of the mid shelf stations.

**PCA.** Environmental variables were plotted using PRIMER's PCA to determine how a set environmental factors collected at 42 stations related to each other (Figure 90). The length of the vector lines corresponds with the variable influence or strength of each variable. The results on the PCI axis show that stations with higher measurements of mud substrates (right side) have associated higher levels of TOC, TON, chlorophyll *a* and are in deeper water than sand and gravel areas (left side).

**Biota and environment analysis.** A set of environmental variables including total water depth, bottom water temperature and salinity, sediment chlorophyll *a*, grain size (gravel, sand, mud), TOC, TON, and C:N were incorporated into the BIO-ENV matching routine in PRIMER v6 to determine which environmental factors had the strongest correlations with species abundance (Table 23). According to the highest Spearman correlation ($\sigma$) ranking, water depth, and TOC had the most robust association with species abundance distributions for all collected infaunal invertebrate groups ($\sigma = 0.56$). The addition of salinity to depth and TOC was almost as robust ($\sigma = 0.54$). The combination of depth, TOC, salinity, chlorophyll *a*, and C:N produced Spearman values greater than 0.50 indicating that they are all factors that influence the distribution of infauna. Spearman correlation values range from 0 to 1 with 1 indicating a perfect correlation. Values 0.40 to 0.59 are considered a moderate correlation. Bottom water salinity, temperature, and TOC distribution are mapped (Figure 91).

### 5.3.4 Sediment Pigments, Carbon, and Nitrogen Inventories

We sampled the seabed at 43 stations on the Beaufort Sea coast over both years of this study, 26 stations in 2014 and 19 stations in 2015 (Table 24). To better document spatial differences in isotopic variability along the coast, we classified the stations into three major regions on the basis of longitude: Western (153-148° W), Central (148-144° W), and Eastern <144° W) Beaufort. Bottom water temperatures ranged from -1.6 at depths > 30 m to 4.7 °C at station 3A (6.4 m depth), with most salinities varying from 30 to 32, but with one station at 22.7 (station 3A).

**Table 23. Station environmental data used in the Biota and Environment (BIO-ENV) analysis with respect to mean values of abundance and biomass.**

| Year | Date | Station | Latitude | Longitude | Depth m | Salinity | Temp C | Chla mg m-2 | TON | TOC | C:N | Gravel | Sand | Mud | Abundance m-2 | Biomass g m-2 |
|---|---|---|---|---|---|---|---|---|---|---|---|---|---|---|---|---|
| 2014 | 8/6/2014 | 1 | 71.31985 | -152.0900 | 63.5 | 31.633 | -0.227 | 1.012 | 0.11 | 1.10 | 12.024 | 42.70 | 19.60 | 37.70 | 206.67 | 471.41 |
| 2014 | 8/6/2014 | 1.05 | 71.07183 | -152.5822 | 16.4 | 30.419 | -0.720 | 0.170 | 0.11 | 1.44 | 15.539 | 0.00 | 21.50 | 78.60 | 83.33 | 0.67 |
| 2014 | 8/6/2014 | 5 | 70.95292 | -151.3542 | 19.3 | 31.097 | -1.419 | 0.109 | 0.10 | 0.15 | 8.826 | 0.00 | 93.40 | 6.60 | 430.00 | 20.53 |
| 2014 | 8/6/2014 | 6 | 71.28257 | -151.5597 | 55 | 31.028 | 0.525 | 2.805 | 0.10 | 0.95 | 11.665 | 9.10 | 42.20 | 48.70 | 370.00 | 63.06 |
| 2014 | 7/31/2014 | 7 | 70.84987 | -150.0608 | 26.3 | 31.614 | -1.536 | 0.544 | 0.15 | 1.12 | 8.613 | 0.00 | 9.70 | 90.30 | 170.00 | 59.84 |
| 2014 | 8/5/2014 | 9 | 70.96333 | -148.9953 | 37 | 31.162 | -0.364 | 4.846 | 0.06 | 0.92 | 17.216 | 1.20 | 23.10 | 75.60 | 333.33 | 88.40 |
| 2014 | 8/1/2014 | 10 | 70.71263 | -148.7655 | 24.6 | 31.627 | -1.560 | 3.476 | 0.14 | 1.04 | 8.491 | 9.30 | 16.60 | 74.00 | 183.33 | 13.08 |
| 2014 | 8/5/2014 | 11 | 70.88448 | -148.1355 | 43.7 | 31.455 | -0.904 | 2.374 | 0.13 | 1.30 | 11.744 | 0.40 | 49.40 | 50.10 | 333.33 | 65.09 |
| 2014 | 8/4/2014 | 12 | 70.67172 | -147.5905 | 38.4 | 31.599 | -1.470 | 21.348 | 0.11 | 0.98 | 10.621 | 0.20 | 36.80 | 63.00 | 576.67 | 84.25 |
| 2014 | 8/4/2014 | 15 | 70.64602 | -146.6607 | 36 | 31.740 | -1.466 | 1.849 | 0.08 | 0.68 | 9.677 | 61.90 | 21.60 | 16.50 | 170.00 | 132.63 |
| 2014 | 8/4/2014 | 16 | 70.73417 | -145.9916 | 61 | 31.764 | -1.528 | 0.616 | 0.10 | 1.09 | 12.418 | 17.20 | 48.00 | 34.80 | 270.00 | 149.20 |
| 2014 | 8/2/2014 | 20 | 70.3579 | -144.4952 | 39.8 | 32.001 | -1.608 | 0.716 | 0.07 | 0.51 | 8.059 | 0.50 | 75.20 | 24.30 | 363.33 | 130.43 |
| 2014 | 8/2/2014 | 21 | 70.27523 | -143.9104 | 36 | 31.637 | -1.354 | 0.400 | 0.07 | 0.56 | 9.101 | 8.00 | 47.20 | 44.80 | 566.67 | 62.63 |
| 2014 | 8/2/2014 | 22 | 70.19152 | -142.9047 | 36 | 30.993 | -0.361 | 3.561 | 0.13 | 1.41 | 12.793 | 11.30 | 12.80 | 75.90 | 400.00 | 164.63 |
| 2014 | 8/3/2014 | 23 | 70.00377 | -141.9630 | 35.8 | 30.920 | 0.015 | 4.440 | 0.09 | 0.73 | 9.825 | 0.50 | 52.40 | 47.00 | 510.00 | 190.84 |
| 2014 | 8/3/2014 | 24 | 70.26003 | -141.7631 | 53.5 | 31.849 | -1.372 | 2.368 | 0.15 | 1.20 | 9.148 | 0.50 | 31.80 | 67.70 | 216.67 | 175.22 |
| 2014 | 8/4/2014 | 25 | 69.85098 | -141.7181 | 22.5 | 29.693 | 2.932 | 5.629 | 0.08 | 0.73 | 10.573 | 0.00 | 38.50 | 61.40 | 516.67 | 63.89 |
| 2014 | 8/4/2014 | 1C | 70.15795 | -144.8053 | 24.7 | 30.499 | -0.725 | 0.449 | 0.11 | 1.10 | 11.871 | 0.00 | 26.10 | 73.90 | 760.00 | 100.79 |
| 2014 | 8/1/2014 | 5(5) | 70.43655 | -147.3442 | 19.6 | 31.141 | -1.574 | 0.782 | 0.05 | 0.64 | 13.566 | 1.70 | 53.50 | 44.80 | 650.00 | 26.95 |
| 2014 | 8/7/2014 | 5B | 70.58027 | -148.9327 | 17.4 | 30.347 | -1.471 | 0.286 | 0.05 | 0.06 | 7.096 | 0.00 | 96.30 | 3.70 | 180.00 | 17.82 |
| 2014 | 7/31/2014 | 6D | 70.74947 | -150.4754 | 18.9 | 31.509 | -1.492 | 14.513 | 0.16 | 1.40 | 10.306 | 0.10 | 79.70 | 20.10 | 490.00 | 52.05 |
| 2014 | 8/5/2014 | 6F | 70.67223 | -151.1876 | 13.5 | 30.661 | -1.301 | 0.152 | 0.12 | 0.23 | 14.938 | 0.10 | 91.40 | 8.50 | 150.00 | 6.63 |
| 2014 | 8/6/2014 | 7C | 70.91292 | -151.9948 | 14.4 | 30.511 | -1.332 | 0.152 | 0.12 | 1.44 | 13.633 | 0.90 | 31.30 | 67.90 | 240.00 | 3.15 |
| 2014 | 8/1/2014 | L250-5 | 70.36478 | -146.1182 | 31.5 | 31.548 | -1.620 | 1.386 | 0.11 | 0.89 | 9.436 | 0.00 | 33.75 | 66.25 | 330.00 | 35.00 |
| 2014 | 8/1/2014 | T-3 | 70.45125 | -145.8372 | 38.5 | 31.859 | -1.470 | 2.060 | 0.11 | 0.88 | 9.534 | 4.10 | 43.30 | 52.60 | 590.00 | 132.81 |
| 2015 | 8/3/2015 | 143-W1 | 70.25728 | -143.6066 | 38.8 | 32.244 | -1.425 | 6.355 | 0.08 | 1.08 | 16.100 | 4.10 | 32.90 | 63.10 | 790.00 | 65.34 |
| 2015 | 8/3/2015 | 143-W2 | 70.44248 | -143.5957 | 48 | 32.432 | -1.618 | 3.452 | 0.09 | 0.98 | 12.086 | 15.70 | 51.70 | 32.60 | 716.67 | 84.65 |
| 2015 | 8/3/2015 | 143-W4 | 70.56907 | -143.6001 | 154 | 32.527 | -1.507 | 1.735 | 0.16 | 1.74 | 12.633 | 0.00 | 5.80 | 94.20 | 186.67 | 36.20 |
| 2015 | 8/3/2015 | 143-W5 | 70.62602 | -143.5908 | 303 | 34.741 | 0.450 | 0.425 | 0.18 | 1.89 | 12.256 | 0.00 | 2.10 | 97.90 | 806.67 | 16.69 |
| 2015 | 8/6/2015 | 149-200 | 71.21227 | -149.3430 | 207 | 34.614 | 0.146 | 0.357 | 0.16 | 2.12 | 15.940 | 25.40 | 15.50 | 59.10 | 670.00 | 179.55 |
| 2015 | 8/1/2015 | 152-W0 | 71.00417 | -152.3793 | 15.9 | 31.585 | -0.639 | 10.523 | 0.15 | 2.30 | 18.175 | 0.00 | 23.00 | 97.70 | 386.67 | 4.41 |
| 2015 | 8/1/2015 | 152-W1 | 71.19385 | -152.2531 | 38 | 31.575 | 0.665 | 6.745 | 0.12 | 1.47 | 14.270 | 0.00 | 2.50 | 97.50 | 336.67 | 92.33 |
| 2015 | 8/2/2015 | 3A | 70.28238 | -147.0900 | 6.4 | 22.626 | 4.686 | 68.580 | 0.11 | 1.97 | 20.603 | 0.00 | 19.40 | 80.50 | 1933.33 | 159.83 |
| 2015 | 8/2/2015 | 5A | 70.49468 | -148.7640 | 11.8 | 30.836 | -0.293 | 9.149 | 0.12 | 2.17 | 20.300 | 0.00 | 35.75 | 64.30 | 193.33 | 1.67 |
| 2015 | 8/4/2015 | 70-142 | 70.46577 | -142.4026 | 65.5 | 32.355 | -1.591 | 1.878 | 0.10 | 1.31 | 15.059 | 9.30 | 48.40 | 42.20 | 550.00 | 32.94 |
| 2015 | 8/4/2015 | 70-143 | 70.36135 | -142.8518 | 57 | 32.323 | -1.549 | 5.076 | 0.08 | 1.39 | 21.225 | 4.60 | 41.10 | 54.40 | 1180.00 | 80.84 |
| 2015 | 8/5/2015 | 70-145 | 70.49115 | -144.9682 | 45.8 | 32.124 | -1.605 | 5.839 | 0.11 | 1.08 | 11.945 | 74.80 | 14.50 | 10.60 | 663.33 | 281.46 |
| 2015 | 8/5/2015 | 71-145 | 70.67525 | -144.9170 | 103 | 31.959 | -1.509 | 0.625 | 0.15 | 1.57 | 12.528 | 0.00 | 27.80 | 72.10 | 346.67 | 108.44 |
| 2015 | 8/5/2015 | 71-146 | 70.95688 | -145.8006 | 395 | 34.799 | 0.614 | 0.856 | 0.17 | 2.06 | 13.787 | 0.00 | 0.40 | 99.60 | 366.67 | 10.92 |
| 2015 | 8/6/2015 | 71-147 | 70.9716 | -147.3822 | 100 | 31.803 | -1.184 | 0.456 | 0.08 | 1.05 | 15.072 | 69.80 | 17.60 | 12.50 | 346.67 | 60.35 |
| 2015 | 8/6/2015 | 71-149 | 71.15253 | -148.4144 | 68.4 | 31.411 | -1.471 | 0.768 | 0.07 | 0.77 | 12.556 | 5.40 | 73.60 | 21.00 | 343.33 | 49.28 |
| 2015 | 8/1/2015 | 71-150 | 70.94037 | -151.0301 | 18.2 | 31.794 | -1.463 | 5.496 | 0.02 | 0.22 | 11.696 | 0.00 | 94.10 | 5.90 | 333.33 | 12.53 |

**Table 24. Location, depth, salinity, and temperature for all biological stations sampled in 2014 and 2015.**

| Station | Date | Lat DD | Long DD | Region | Depth (m) | Salinity | Temperature (°C) |
|---|---|---|---|---|---|---|---|
| 1 | 6-Aug-14 | 71.320 | -152.090 | Western | 63.5 | 31.633 | -0.227 |
| 1.05 | 6-Aug-14 | 71.072 | -152.582 | Western | 16.4 | 30.419 | -0.720 |
| 1C | 4-Aug-14 | 70.158 | -144.805 | Central | 24.7 | 30.499 | -0.725 |
| 5 | 6-Aug-14 | 70.953 | -151.354 | Western | 19.3 | 31.097 | -1.419 |
| 5(5) | 1-Aug-14 | 70.437 | -147.344 | Central | 19.6 | 31.141 | -1.574 |
| 5B | 7-Aug-14 | 70.580 | -148.933 | Western | 17.4 | 30.347 | -1.471 |
| 6 | 6-Aug-14 | 71.283 | -151.560 | Western | 55 | 31.028 | 0.525 |
| 6D | 31-Jul-14 | 70.749 | -150.475 | Western | 18.9 | 31.509 | -1.492 |
| 6F | 5-Aug-14 | 70.672 | -151.188 | Western | 13.5 | 30.661 | -1.301 |
| 7C | 6-Aug-14 | 70.913 | -151.995 | Western | 14.4 | 30.511 | -1.332 |
| 7 | 31-Jul-14 | 70.850 | -150.061 | Western | 26.3 | 31.614 | -1.536 |
| 8 | 31-Jul-14 | 70.757 | -149.440 | Western | 19 | | |
| 9 | 5-Aug-14 | 70.963 | -148.995 | Western | 37 | 31.162 | -0.364 |
| 10 | 1-Aug-14 | 70.713 | -148.765 | Western | 24.6 | 31.627 | -1.560 |
| 11 | 5-Aug-14 | 70.884 | -148.135 | Western | 43.7 | 31.455 | -0.904 |
| 12 | 4-Aug-14 | 70.672 | -147.591 | Central | 38.4 | 31.599 | -1.470 |
| 15 | 4-Aug-14 | 70.646 | -146.661 | Central | 36 | 31.740 | -1.466 |
| 16 | 4-Aug-14 | 70.734 | -145.992 | Central | 61 | 31.764 | -1.528 |
| 20 | 2-Aug-14 | 70.358 | -144.495 | Central | 39.8 | 32.001 | -1.608 |
| 21 | 2-Aug-14 | 70.275 | -143.910 | Eastern | 36 | 31.637 | -1.354 |
| 22 | 2-Aug-14 | 70.192 | -142.905 | Eastern | 36 | 30.993 | -0.361 |
| 23 | 3-Aug-14 | 70.004 | -141.963 | Eastern | 35.8 | 30.920 | 0.015 |
| 24 | 3-Aug-14 | 70.260 | -141.763 | Eastern | 53.5 | 31.849 | -1.372 |
| 25 | 4-Aug-14 | 69.851 | -141.718 | Eastern | 22.5 | 29.693 | 2.932 |
| L250-5 | 1-Aug-14 | 70.365 | -146.118 | Central | 31.5 | 31.548 | -1.620 |
| T-3 | 1-Aug-14 | 70.451 | -145.837 | Central | 38.5 | 31.859 | -1.470 |
| 143 W1 | 3-Aug-15 | 70.257 | -143.607 | Eastern | 38.8 | 32.244 | -1.425 |
| 13 W2 | 3-Aug-15 | 70.442 | -143.596 | Eastern | 48 | 32.432 | -1.618 |
| 143 W3 | 3-Aug-15 | 70.548 | -143.538 | Eastern | 103 | | |
| 143 W4 | 3-Aug-15 | 70.569 | -143.600 | Eastern | 154 | 32.527 | -1.507 |
| 143 W5 | 3-Aug-15 | 70.626 | -143.591 | Eastern | 303 | 34.741 | 0.450 |
| 143 W6 | 3-Aug-15 | 70.745 | -143.592 | Eastern | 502 | | |
| 149-200 | 6-Aug-15 | 71.212 | -149.343 | Western | 207 | 34.614 | 0.146 |
| 152-W0 | 1-Aug-15 | 71.004 | -152.379 | Western | 15.9 | 31.585 | -0.639 |
| 152-W1 | 1-Aug-15 | 71.194 | -152.253 | Western | 38 | 31.575 | 0.665 |
| **3A** | 2-Aug-15 | 70.282 | -147.090 | Central | 6.4 | 22.626 | 4.686 |

| Station | Date | Lat DD | Long DD | Region | Depth (m) | Salinity | Temperature (°C) |
|---|---|---|---|---|---|---|---|
| 5A | 2-Aug-15 | 70.495 | -148.764 | Western | 11.8 | 30.836 | -0.293 |
| 70-142 | 4-Aug-15 | 70.466 | -142.403 | Eastern | 65.5 | 32.355 | -1.591 |
| 70-143 | 4-Aug-15 | 70.361 | -142.852 | Eastern | 57 | 32.323 | -1.549 |
| 70-145 | 5-Aug-15 | 70.491 | -144.968 | Central | 45.8 | 32.124 | -1.605 |
| 71-145 | 5-Aug-15 | 70.675 | -144.917 | Central | 103 | 31.959 | -1.509 |
| 71-146 | 5-Aug-15 | 70.957 | -145.801 | Central | 395 | 34.799 | 0.614 |
| 71-147 | 6-Aug-15 | 70.972 | -147.382 | Central | 100 | 31.803 | -1.184 |
| 71-149 | 6-Aug-15 | 71.153 | -148.414 | Western | 68.4 | 31.411 | -1.471 |
| **71-150** | 1-Aug-15 | 70.940 | -151.030 | Western | 18.2 | 31.794 | -1.463 |

**Sediment pigments.** Sediment chlorophyll *a* concentrations ranged from 0.11 to 68.6 mg/m$^2$, 0.01 to 5.7 μg/g (Table 25; Figure 93a). Three defined hotspots containing the highest concentrations of pigments were noted: (1) at stations 152W0 and 6D (12.5 – 44.8 mg/m$^2$, 1.8 – 2.3 μg/g;) in the western Beaufort, (2) stations 5A, 12 and 3A (9.2 – 68.6 mg/m$^2$, 1.6 – 5.7 μg/g;) in the central Beaufort, and, (3) at six stations in the eastern Beaufort (stations 143W1, 7-143, 22, 23, 24, and 25) where chlorophyll *a* values ranged from 3.6 – 6.4 mg/m$^2$ (0.5 – 0.9 μg/g;). The highest chlorophyll *a* concentration was recorded at station 3A (68.6 mg/m$^2$, 5.7 μg/g), located inshore of the Barrier Islands in Stefansson Sound at 6.4 m. The area of moderately high sediment chlorophyll levels east of 143° W, from the inner to mid-shelf (22 to 60 m depths) encompasses a large region in contrast to the patchiness in chlorophyll concentrations observed in the western and central Beaufort.

Pheophytin *a* generally coincided with chlorophyll *a* concentrations (Figure 93b, Figure 94) although there were a few notable exceptions. We found pheophytin *a* in relatively high concentrations at stations where chlorophyll *a* was also highest (stations 152W0, 6D, 12, 3A, and 143W1). Pheophorbide *a*, a marker for metazoan grazing, showed distinctly higher concentrations in the western and eastern Beaufort Sea chlorophyll *a* hotspots (Figure 93c). Pyropheophorbide *a*, the secondary degradation product of pheophorbide *a*, was clearly formed at all three hotspots where chlorophyll *a* was observed in higher concentrations (Figure 93d). In some cases (e.g., stations 7, 23, L250-5, 143W4) the chlorophyll *a*:pyropheophorbide *a* (chl:pyro) ratios were markedly <1 (Figure 94). Total pheopigment concentrations (sum of pheophytin *a*, pheophorbide *a*, and pyropheophorbide *a*) spanned to values that matched the range in chlorophyll *a* concentrations. Despite high pheopigment concentrations at some stations, the ratio of chlorophyll to total pheopigments (chl:pheo) was substantially >1 at 33 of 43 stations (Figure 94).

**Table 25. Concentrations of sedimentary pigments by area at 43 stations on the Beaufort Sea shelf.**

| Station | chl c2 | Pheo-phorbide | peridinin+isomer | Pyropheo-phorbide | 19-but fuxocantin | fuxocanthin | prasinoxanthin | 19-hex fuxocanthin | zeaxanthin | chl b | chl a | Pheo-phytin |
|---|---|---|---|---|---|---|---|---|---|---|---|---|
| | *mg/m²* | *mg/m²* | *mg/m²* | *mg/m²* | *mg/m²* | *mg/m²* | *mg/m²* | *mg/m²* | *mg/m²* | *mg/m²* | *mg/m²* | mg/m² |
| *1* | *0.06* | *1.61* | *0.36* | *9.29* | *0.11* | *0.82* | *0.23* | *0.00* | *0.01* | *0.17* | *1.01* | **0.60** |
| *1.05* | *0.00* | *0.00* | *0.10* | *0.64* | *0.02* | *0.39* | *0.00* | *0.00* | *0.01* | *0.00* | *0.17* | **0.00** |
| *1C* | *0.08* | *0.00* | *0.39* | *5.51* | *0.05* | *1.75* | *0.00* | *0.00* | *0.00* | *0.07* | *0.45* | **0.00** |
| *5* | *0.05* | *0.00* | *0.11* | *0.91* | *0.02* | *1.02* | *0.00* | *0.00* | *0.00* | *0.00* | *0.11* | **0.00** |
| *5(5)* | *0.03* | *0.00* | *0.19* | *1.95* | *0.07* | *3.57* | *0.00* | *0.00* | *0.00* | *0.02* | *0.78* | **0.00** |
| *5B* | *0.04* | *0.00* | *0.00* | *0.36* | *0.00* | *0.83* | *0.00* | *0.00* | *0.00* | *0.02* | *0.29* | **0.32** |
| *6* | *0.14* | *0.37* | *0.32* | *4.30* | *0.07* | *1.46* | *0.02* | *0.01* | *0.00* | *0.18* | *2.81* | **0.19** |
| *6D* | *1.49* | *34.06* | *3.34* | *81.76* | *0.34* | *7.41* | *0.03* | *0.02* | *0.03* | *1.14* | *14.51* | **0.69** |
| *7* | *0.04* | *0.00* | *0.07* | *1.94* | *0.04* | *2.21* | *0.00* | *0.00* | *0.00* | *0.00* | *0.54* | **0.00** |
| *7C* | *0.00* | *0.00* | *0.07* | *0.62* | *0.00* | *0.12* | *0.01* | *0.00* | *0.00* | *0.02* | *0.15* | **0.00** |
| *8* | *0.34* | *25.29* | *1.69* | *33.34* | *1.30* | *4.91* | *0.05* | *0.00* | *0.03* | *0.40* | *3.62* | **1.55** |
| *9* | *0.10* | *6.27* | *0.62* | *16.21* | *0.21* | *2.60* | *0.07* | *0.01* | *0.02* | *0.50* | *4.85* | **1.45** |
| *10* | *0.05* | *0.00* | *0.16* | *3.71* | *0.09* | *2.95* | *0.00* | *0.00* | *0.00* | *0.08* | *3.48* | **0.00** |
| *11* | *0.11* | *0.56* | *0.39* | *3.46* | *0.08* | *1.72* | *0.23* | *0.00* | *0.00* | *0.07* | *2.37* | **0.00** |
| *12* | *0.19* | *1.10* | *0.50* | *13.06* | *0.19* | *6.84* | *0.09* | *0.06* | *0.05* | *1.87* | *21.35* | **2.69** |
| *15* | *0.17* | *0.00* | *0.44* | *7.29* | *0.07* | *2.04* | *0.03* | *0.00* | *0.00* | *0.05* | *1.85* | **0.10** |
| *16* | *0.16* | *0.33* | *0.04* | *0.94* | *0.00* | *1.96* | *0.01* | *0.00* | *0.00* | *0.05* | *0.62* | **0.00** |
| *20* | *0.01* | *0.00* | *0.65* | *2.17* | *0.10* | *1.19* | *0.10* | *0.00* | *0.00* | *0.05* | *0.72* | **0.00** |
| *21* | *0.04* | *0.00* | *0.13* | *1.06* | *0.02* | *1.94* | *0.01* | *0.00* | *0.00* | *0.05* | *0.40* | **0.00** |
| *22* | *0.63* | *12.20* | *0.85* | *22.10* | *0.19* | *2.74* | *0.31* | *0.03* | *0.01* | *0.06* | *3.56* | **0.00** |
| *23* | *0.16* | *2.36* | *0.45* | *11.77* | *0.07* | *3.80* | *0.13* | *0.00* | *0.05* | *0.23* | *4.44* | **0.19** |
| *24* | *0.11* | *1.30* | *0.23* | *1.38* | *0.01* | *2.39* | *0.00* | *0.00* | *0.01* | *0.13* | *2.37* | **0.00** |

| Station | chl c2 | Pheo-phorbide | peridinin+isomer | Pyropheo-phorbide | 19-but fuxocantin | fuxocanthin | prasinoxanthin | 19-hex fuxocanthin | zeaxanthin | chl b | chl a | Pheo-phytin |
|---|---|---|---|---|---|---|---|---|---|---|---|---|
| | mg/m² | mg/m² | mg/m² | mg/m² | mg/m² | mg/m² | mg/m² | mg/m² | mg/m² | mg/m² | mg/m² | mg/m² |
| *25* | *0.23* | *14.77* | *1.27* | *33.18* | *0.72* | *3.53* | *0.10* | *0.02* | *0.05* | *0.89* | *5.63* | **0.00** |
| *L250-5* | *0.03* | *0.00* | *0.17* | *0.38* | *0.02* | *1.12* | *0.02* | *0.00* | *0.01* | *0.01* | *1.39* | **0.00** |
| *T-3* | *0.18* | *3.69* | *0.69* | *12.81* | *0.10* | *2.04* | *0.03* | *0.00* | *0.00* | *0.05* | *2.06* | **0.19** |
| *3A* | *1.37* | *3.86* | *0.68* | *26.17* | *0.71* | *34.79* | *0.10* | *0.05* | *0.51* | *4.48* | *68.58* | **18.91** |
| *5A* | *0.39* | *1.17* | *0.14* | *5.57* | *0.11* | *5.44* | *0.05* | *0.03* | *0.03* | *0.60* | *9.15* | **0.34** |
| *70-142* | *0.14* | *3.45* | *0.11* | *4.93* | *0.12* | *1.24* | *0.06* | *0.01* | *0.00* | *0.06* | *1.88* | **0.22** |
| *70-143* | *0.35* | *1.01* | *0.46* | *9.23* | *0.28* | *3.36* | *0.09* | *0.01* | *0.01* | *0.19* | *5.08* | **0.60** |
| *70-145* | *0.48* | *1.95* | *0.43* | *8.04* | *0.28* | *4.44* | *0.07* | *0.01* | *0.01* | *0.14* | *5.84* | **0.28** |
| *71-145* | *0.02* | *0.00* | *0.10* | *1.34* | *0.03* | *0.42* | *0.04* | *0.00* | *0.00* | *0.00* | *0.63* | **0.00** |
| *71-146* | *0.07* | *1.74* | *0.36* | *7.02* | *0.11* | *0.37* | *0.10* | *0.01* | *0.01* | *0.17* | *0.86* | **0.00** |
| *71-147* | *0.02* | *0.00* | *0.15* | *2.54* | *0.06* | *0.46* | *0.03* | *0.00* | *0.00* | *0.07* | *0.46* | **0.00** |
| *71-149* | *0.06* | *0.00* | *0.12* | *2.31* | *0.06* | *0.60* | *0.03* | *0.00* | *0.01* | *0.00* | *0.77* | **0.00** |
| *71-150* | *0.75* | *1.33* | *0.09* | *4.11* | *0.04* | *4.87* | *0.01* | *0.00* | *0.01* | *0.27* | *5.50* | **0.34** |
| *143 W1* | *0.26* | *5.66* | *0.37* | *14.16* | *0.38* | *3.25* | *0.07* | *0.03* | *0.06* | *0.67* | *6.35* | **0.81** |
| *143 W2* | *0.21* | *0.82* | *0.38* | *7.29* | *0.30* | *2.60* | *0.04* | *0.00* | *0.00* | *0.50* | *3.45* | **0.43** |
| *143 W4* | *0.15* | *6.71* | *0.36* | *21.33* | *0.18* | *0.61* | *0.06* | *0.02* | *0.16* | *0.53* | *1.73* | **1.15** |
| *143 W5* | *0.02* | *0.00* | *0.04* | *1.74* | *0.03* | *0.18* | *0.03* | *0.00* | *0.01* | *0.05* | *0.43* | **0.00** |
| *149-200* | *0.03* | *0.51* | *0.10* | *4.37* | *0.07* | *0.21* | *0.06* | *0.00* | *0.04* | *0.05* | *0.36* | **0.00** |
| *149-350* | *0.17* | *0.24* | *0.24* | *8.14* | *0.22* | *0.66* | *0.15* | *0.02* | *0.20* | *0.61* | *2.04* | **0.00** |
| *152 W0* | *0.20* | *0.56* | *0.53* | *20.59* | *0.55* | *3.77* | *0.16* | *0.04* | *0.13* | *2.28* | *10.52* | **2.51** |
| *152 W1* | *0.23* | *1.03* | *0.17* | *7.36* | *0.14* | *3.06* | *0.09* | *0.01* | *0.03* | *0.79* | *6.75* | **1.90** |

The pigments chlorophyll b, chlorophyll c, prasinoxanthin, and 19-hex-fucoxanthin were found in very low concentrations and displayed no significant trends within the study area. Fucoxanthin, a biomarker for diatoms, predominated other accessory pigments in sediments (Table 25). Its concentration correlates with sedimentary chlorophyll *a* (Table 25), and suggests that diatoms contribute a large proportion of the chlorophyll *a* standing stock in sediments, in addition to sedimentary pheopigments (Table 25). Contrarily, the dinoflagellate marker peridinin was not significantly correlated to chlorophyll *a* or any other benthic parameter measured by this study. At 44 of 47 stations, peridinin concentrations were < 1 mg/m$^2$ (<0.3µg/g).

**Suspended and sedimentary organic matter analyses.** Analysis of sediment organic content (Table 26) showed sediment ammonium values were expectedly variable, from 25 to 200 µM, with one value at 437 µM (station 3A). Sediment stable carbon isotope values ranged from -26.8 to -23.7‰, and $\delta^{15}$N values from 4 to 6.4‰. Percent organic carbon and nitrogen in sediments ranged from 0.2 to 2.2% and 0.02 to 0.18%, respectively.

SPOM stable carbon isotope values in the chlorophyll maximum layer ranged from -27.4 to -17.1‰, compared to -26.4 to -20.3‰ near the seabed (Table 27). At all but six stations, the mean near-bottom SPOM $\delta^{13}$C value was more enriched than the near-surface value (Figure 95). Stable nitrogen isotope values of SPOM in the chlorophyll maximum layer ranged from 1.9 to 8.1‰, compared to 2.0 to 14.4‰ near the seabed (Table 27).

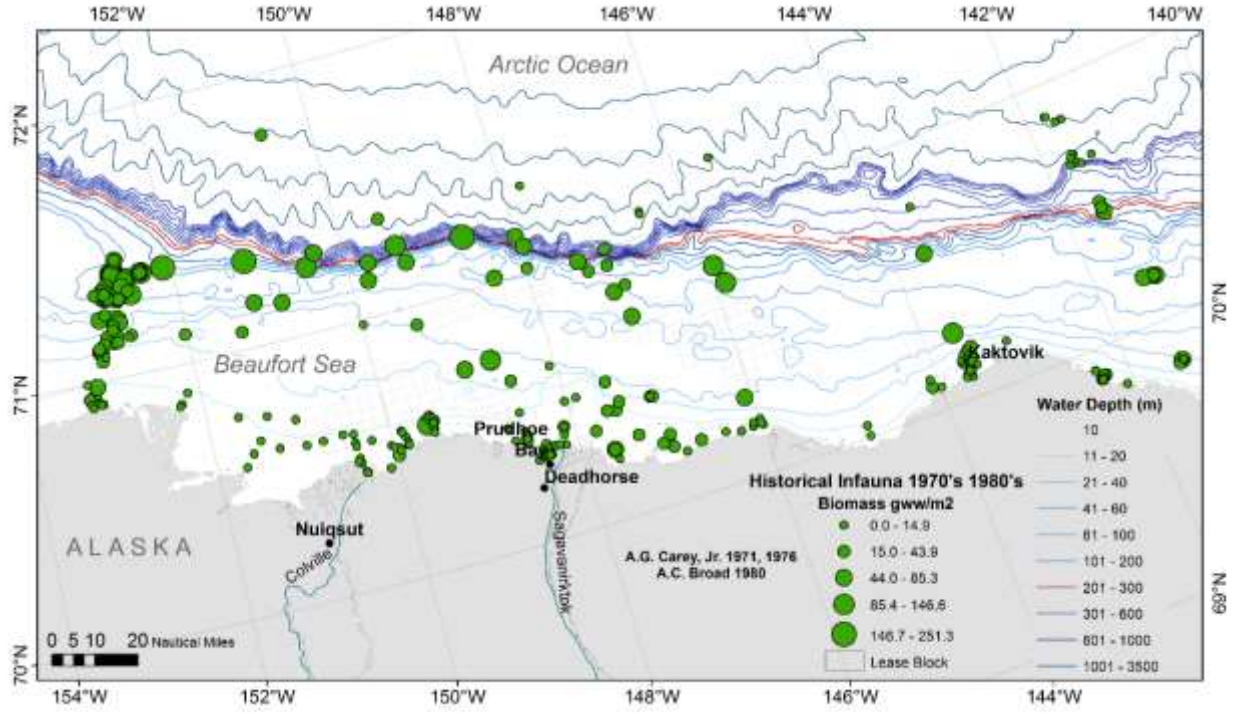


**Figure 92. Patterns of infaunal biomass (gww/m$^2$) collected in the 1970's and 1980's under the WEBSEC and OCSEAP programs.**

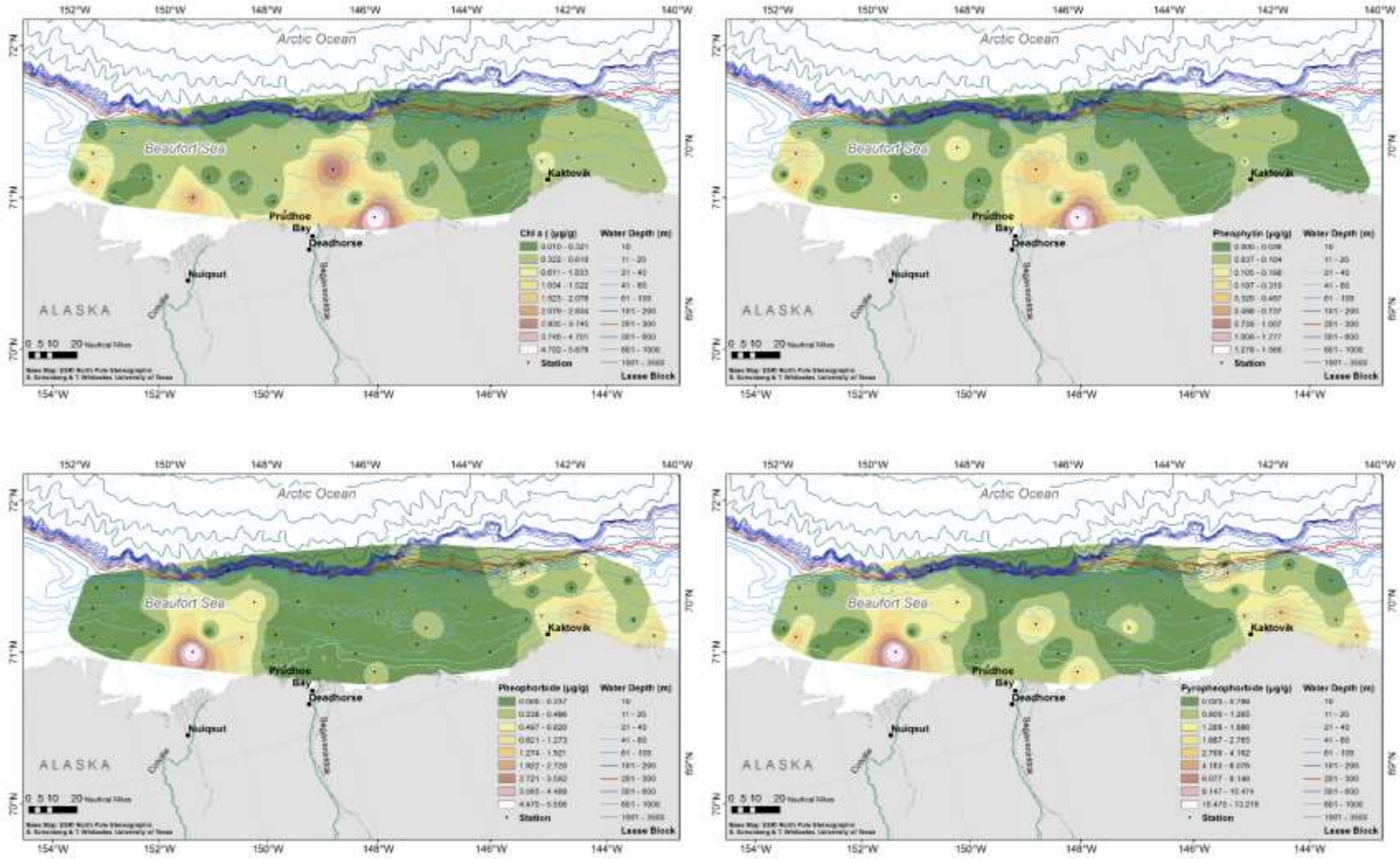


**Figure 93. Interpolation of sedimentary pigments chlorophyll *a* (top left), pheophytin *a* (top right), pheophorbide *a* (bottom left), and pyropheophorbide *(*bottom right). The color scheme represents pigment concentration (µg/g).**

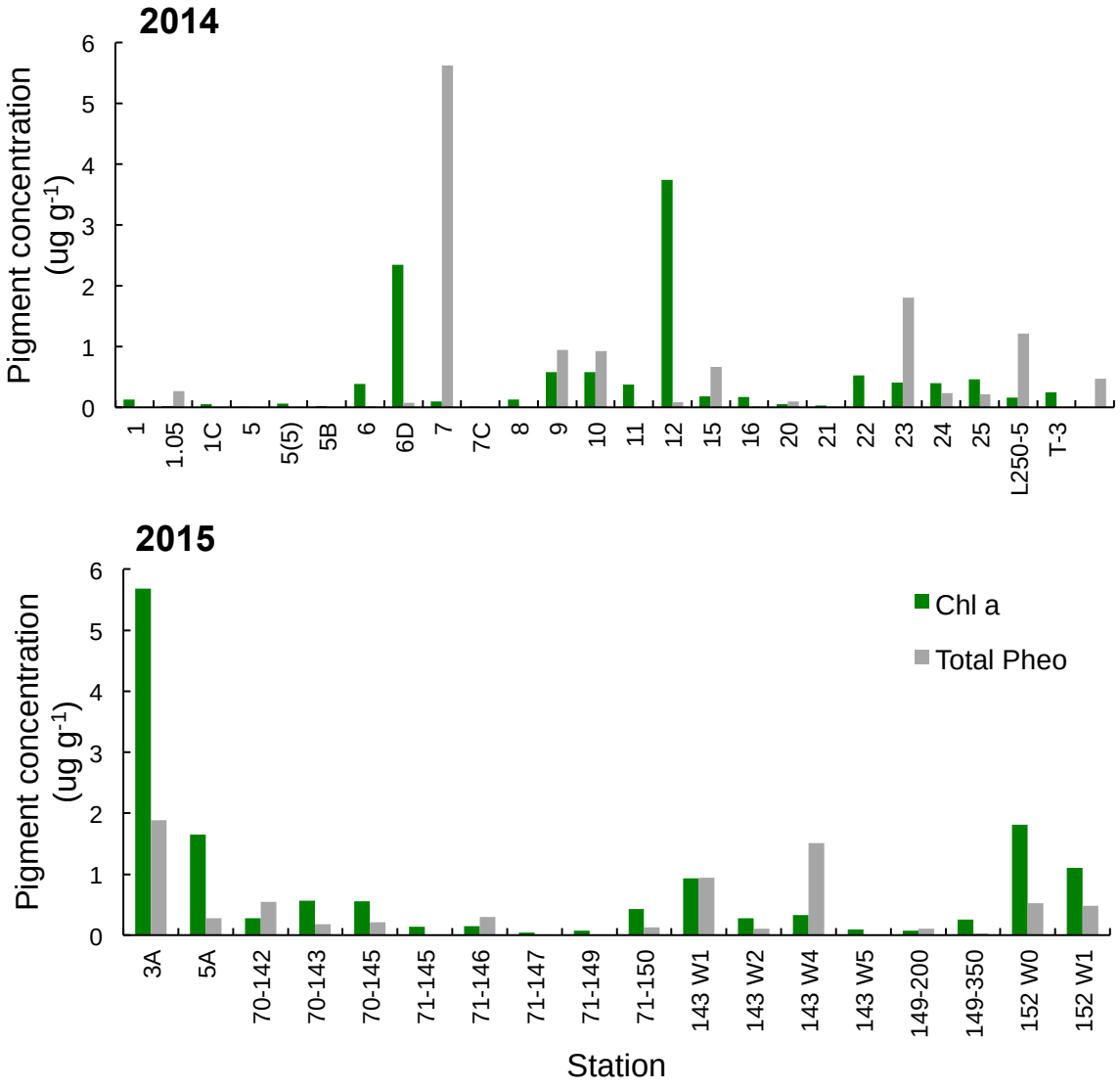


**Figure 94. Concentration of chlorophyll *a* and total pheopigments (sum of pheophytin, pheophorbide, and pyropheophorbide) at each station.**

**Some stations contain less chlorophyll *a* than total pheopigments.**

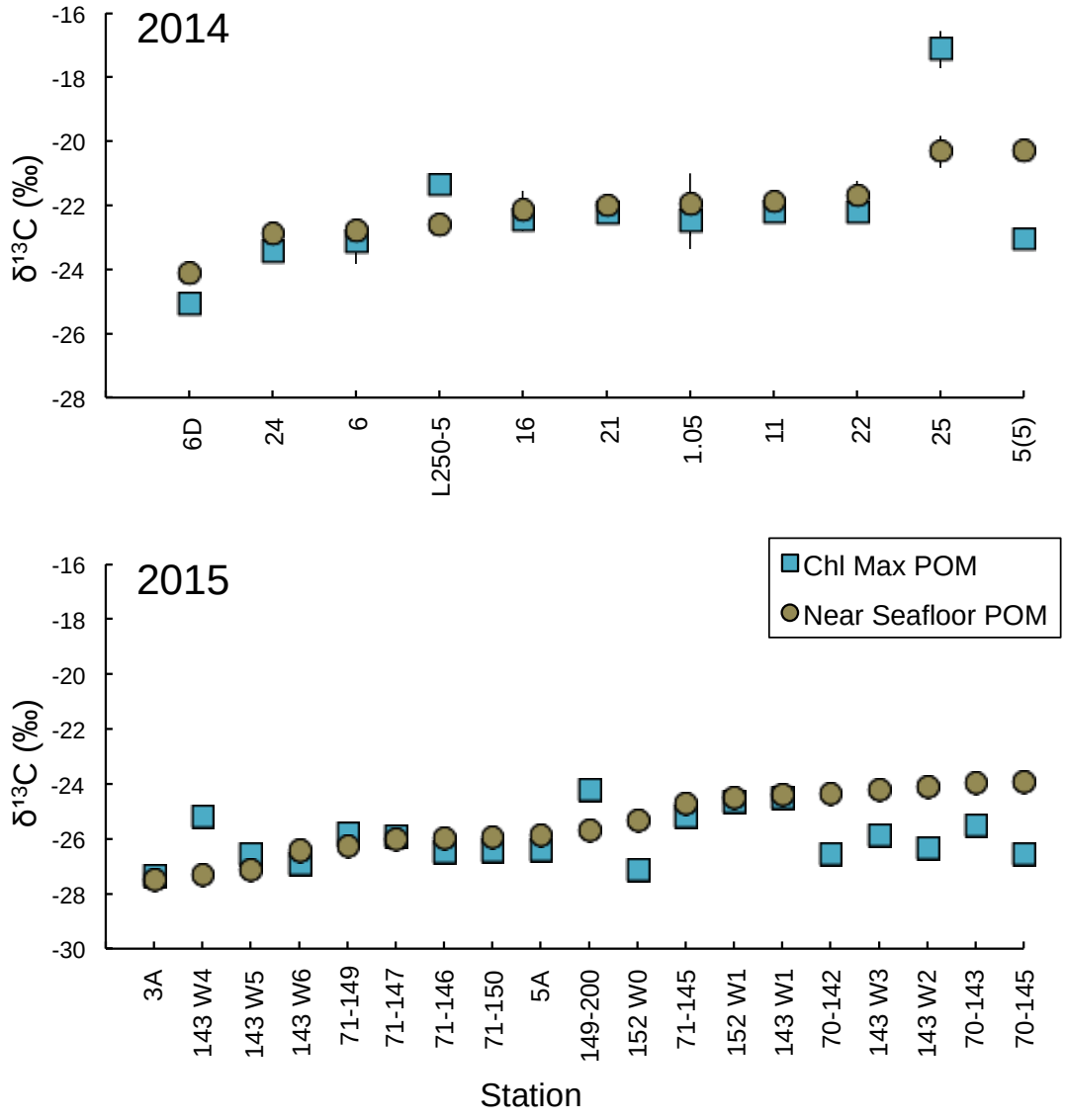


**Figure 95. Mean (±SD) carbon isotope value for SPOM collected within the chlorophyll maximum zone and within 2 m the seabed at each station.**

**Table 26. Sediment chemistry including total chlorophyll *a* and ammonium concentrations, carbon and nitrogen isotope values, and percent carbon and nitrogen. Data are from one replicate or the mean (±SD) of two replicates.**

| Station | Chl a mg/m$^2$ | $NH_4$ µM | $\delta^{13}C$ ‰ | $\delta^{15}N$ ‰ | % C | % N |
|---|---|---|---|---|---|---|
| 1 | 1.01 | 41.3 ± 7.28 | | | | |
| 1.05 | 0.17 | 103.83 ± 7.28 | -23.66 ± 3.01 | 4.24 ± 0.08 | 1.44 ± 0.12 | 0.11 ± 0.00 |
| 1C | 0.45 | 51.98 ± 1.89 | | | | |
| 5 | 0.11 | 35.78 ± 2.16 | | | | |
| 5(5) | 0.78 | 141.57 ± 14.29 | -25.6 ± 0.03 | 4.93 ± 0.79 | 0.64 ± 0.02 | 0.05 ± 0.01 |
| 5B | 0.29 | 24.34 ± 1.08 | | | | |
| 6 | 2.81 | 37.87 ± 12.67 | -24.94 ± 0.03 | 6.03 ± 0.07 | 0.95 ± 0.02 | 0.1 ± 0.00 |
| 6D | 14.51 | 192.08 ± 16.18 | -25.09 ± 0.05 | 6.35 ± 0.74 | 1.4 ± 0.04 | 0.16 ± 0.01 |
| 6F | 0 | 68.18 ± 2.16 | | | | |
| 7 | 0.54 | 107.64 ± 20.75 | | | | |
| 7C | 0.15 | 58.45 ± 4.04 | | | | |
| 8 | 3.62 | 167.68 ± 29.12 | | | | |
| 9 | 4.85 | 80.38 ± 8.08 | | | | |
| 10 | 3.48 | 50.26 ± 11.86 | | | | |
| 11 | 2.37 | 88.39 ± 15.1 | -24.93 ± 0.14 | 5.9 ± 0.14 | 1.3 ± 0.02 | 0.13 ± 0.01 |
| 12 | 21.35 | 35.97 ± 2.43 | | | | |
| 15 | 1.85 | 63.79 ± 11.6 | | | | |
| 16 | 0.62 | 67.23 ± 23.45 | -24.71 ± 0 | 5.91 ± 0.01 | 1.09 ± 0.15 | 0.1 ± 0.00 |
| 20 | 0.72 | 75.99 ± 12.13 | | | | |
| 21 | 0.4 | 71.23 ± 1.08 | -25.69 ± 0.11 | 5.31 ± 1.03 | 0.56 ± 0.15 | 0.07 ± 0.01 |
| 22 | 3.56 | 65.32 ± 8.36 | -25.42 ± 0.74 | 4.25 ± 0.08 | 1.4 ± 0.34 | 0.13 ± 0.02 |
| 23 | 4.44 | 36.34 ± 9.97 | | | | |
| 24 | 2.37 | 41.3 ± 0.27 | -25.14 ± 0.01 | 4.47 ± 0.16 | 1.2 ± 0.1 | 0.15 ± 0.01 |
| 25 | 5.63 | 52.74 ± 8.9 | -26.04 ± 0.12 | 5.18 ± 0.42 | 0.73 ± 0.02 | 0.08 ± 0.01 |
| L250-5 | 1.39 | 37.68 ± 15.1 | -25.6 ± 0.05 | 3.43 ± 0.35 | 0.89 ± 0.08 | 0.11 ± 0.00 |
| T-3 | 2.06 | 94.29 ± 53.1 | | | | |
| 143 W1 | 6.35 | 87.93 ± 3.85 | -26.4 | 5.55 | 1.08 | 0.08 |
| 143 W2 | 3.45 | 94.81 ± 5.43 | -26.05 | 6.24 | 0.98 | 0.09 |
| 143 W4 | 1.73 | 85.85 ± 10.86 | -25.67 | 5.88 | 1.74 | 0.16 |
| 143 W5 | 0.43 | 63.45 ± 16.29 | -25.75 | 6.34 | 1.89 | 0.18 |
| 149-200 | 0.36 | 74.17 ± 5.2 | -25.97 | 6.15 | 2.12 | 0.16 |
| 149-350 | 2.04 | 70.97 ± 16.07 | -25.99 | 5.74 | 1.94 | 0.17 |
| 152 W0 | 10.52 | 116.73 ± 33.72 | -26.65 | 4.72 | 2.3 | 0.15 |
| 152 W1 | 6.75 | 130.81 ± 5.2 | -25.89 | 5.83 | 1.47 | 0.12 |
| 3A | 68.58 | 436.58 ± 77.84 | -26.49 | 4.05 | 1.97 | 0.11 |
| 5A | 9.15 | 131.29 ± 5.43 | -26.6 | 4.72 | 2.17 | 0.12 |
| 70-142 | 1.88 | 64.25 ± 7.47 | -25.89 | 6.13 | 1.31 | 0.1 |
| 70-143 | 5.08 | 75.29 ± 5.88 | -26.37 | 5.15 | 1.38 | 0.08 |
| 70-145 | 5.84 | 84.57 ± 0.45 | -25.96 | 6.44 | 1.08 | 0.11 |
| 71-145 | 0.63 | 136.57 ± 131.46 | -25.33 | 6.23 | 1.57 | 0.15 |
| 71-146 | 0.86 | 55.45 ± 9.05 | -25.64 | 6.19 | 2.06 | 0.17 |
| 71-147 | 0.46 | 177.05 ± 7.24 | -25.64 | 6.88 | 1.05 | 0.08 |
| 71-149 | 0.77 | 77.21 ± 0.91 | -25.91 | 6.11 | 0.77 | 0.07 |
| 71-150 | 5.5 | 152.73 ± 8.15 | -26.8 | 4.05 | 0.22 | 0.02 |

**Table 27. Stable isotopic measurements of SPOM samples collected approximately 2 m above the seabed and within the chlorophyll maximum zone.**

**Data are from one sample or a mean (±SD) from two replicates. n.d. indicates no data**

| | Near Seafloor | | Chl Max | |
|---|---|---|---|---|
| Station | $\delta^{13}C$ ‰ | $\delta^{15}N$ ‰ | $\delta^{13}C$ ‰ | $\delta^{15}N$ ‰ |
| 1.05 | -21.98 ± 0.97 | 7.71 ± 0.33 | -22.5 ± 0.87 | 7.42 ± 0.47 |
| 5(5) | -20.3 ± 0.12 | 7.14 ± 0.16 | -23.06 ± 0.05 | 6.47 ± 0.18 |
| 6 | -22.81 | 7.82 | -23.15 ± 0.67 | n.d. |
| 6D | -24.16 ± 0.27 | 11.85 ± 0.05 | -25.1 ± 0.31 | n.d. |
| 11 | -21.91 ± 0.35 | 7.98 ± 0.49 | -22.22 ± 0.1 | 8.11 ± 0.8 |
| 16 | -22.17 ± 0.64 | 7.15 ± 0.13 | -22.49 ± 0.14 | 6.63 ± 0.36 |
| 21 | -22.03 ± 0.06 | 7.5 ± 0.2 | -22.26 ± 0.19 | 7.35 ± 0.41 |
| 22 | -21.72 ± 0.48 | 7.78 ± 0.18 | -22.25 | 7.61 |
| 24 | -22.9 | 7.14 | -23.46 | 5.09 |
| 25 | -20.34 ± 0.5 | 14.43 ± 0.15 | -17.14 ± 0.58 | n.d. |
| L250-5 | -22.61 | 7.25 | -21.4 ± 0.04 | 7.1 ± 0.27 |
| 143 W1 | -24.41 | 10.17 | -24.52 | 7.77 |
| 143 W2 | -24.14 | 10.78 | -26.36 | 2.97 |
| 143 W3 | -24.26 | 15.22 | -25.89 | 9.67 |
| 143 W4 | -27.35 | 3.45 | -25.22 | 5.79 |
| 143 W5 | -27.16 | 2.48 | -26.55 | 2.31 |
| 143 W6 | -26.45 | 1.97 | -26.94 | 3.06 |
| 149-200 | -25.71 | 3.74 | -24.22 | 6.06 |
| 152 W0 | -25.34 | 8.33 | -27.15 | 3.92 |
| 152 W1 | -24.54 | 4.53 | -24.66 | 6.81 |
| 3A | -27.51 | 3.93 | -27.38 | 3.95 |
| 5A | -25.89 | 7.03 | -26.42 | 5.17 |
| 70-142 | -24.39 | 5.69 | -26.57 | 1.94 |
| 70-143 | -24.01 | 14.14 | -25.53 | 5.42 |
| 70-145 | -23.94 | 5.68 | -26.58 | 2.91 |
| 71-145 | -24.75 | 3.70 | -25.22 | 3.26 |
| 71-146 | -26 | 1.97 | -26.5 | 2.18 |
| 71-147 | -26.04 | 2.49 | -25.91 | 3.25 |
| 71-149 | -26.28 | 4.58 | -25.84 | 2.37 |
| 71-150 | -25.98 | 6.00 | -26.44 | 6.08 |

### 5.3.5 Isotopic Composition of the Pelagic and Benthic Biota

Stable carbon isotopic values of both calanoid copepods and gelatinous zooplankton yielded ranges in $\delta^{13}C$ values from -25.9 to -25.2‰ (Table 28). Similarly, stable nitrogen isotopic values of both calanoid copepods and gelatinous zooplankton yielded similar in $\delta^{15}N$ values that ranged from 9.5 to 11.0‰. For the 20 µm net fraction (denoted phytoplankton), the mean $\delta^{13}C$ and $\delta^{13}N$ values were -24.6‰ and 7.7‰, respectively (Table 28).

We found no significant relationship between bulk $\delta^{13}C$ values and C:N of benthic biota (Figure 96). Based on this lack of correlation, no post-analysis adjustments of the data were applied to account for "lipid bias." Because lipids are important energy reserves for Arctic animals (Møller and Hellgren, 2006), and the process of lipid extraction may also compromise other tissue constituents, no lipid extractions were performed on our samples to avoid the potential loss of critical information and introduction of error into the food web analysis.

We measured the C and N isotopic values of ~300 infaunal organisms from benthic grabs and trawls, with a focus on 20 genera that were common across the Beaufort Sea shelf (Table 29). We observed a distinct depletion in both consumer $\delta^{13}C$ and $\delta^{15}N$ values with decreasing longitude across the Beaufort Sea coast and noted the expected increases in $\delta^{15}N$ content with trophic level. To better illustrate the spatial differences in isotopic composition and examine food web structure without the confounding effects of longitude, we plotted the stable isotope content of phytoplankton, zooplankton, and 13 key genera from stations representing a variety of longitudes and depths in the Beaufort Sea (Figure 97). Data for each genus were averaged and compared to known values of primary producers in the Beaufort Sea to determine the extent to which these carbon sources are assimilated by consumers. For example, primary consumers (e.g., zooplankton, the bryozoan *Alcyonidium*) were more depleted in $^{13}C$ and $^{15}N$ then secondary consumers (the seastar *Leptasterias* and the fish *Lumpenus*).

Across all 15 groups, isotopic values for C and N are generally lower in the eastern Beaufort and higher in the western Beaufort. This trend reflects the predominance of depleted $\delta^{13}C$ and $\delta^{15}N$ organic carbon derived from terrestrial organic matter that is advected from the Mackenzie River on the east, versus marine organic carbon (relatively $\delta^{13}C$ and $\delta^{15}N$ enriched) originating from the northern Chukchi Sea on the west. Superimposed on this trend is the stepwise isotopic enrichment of fauna with increasing trophic level. However, the longitudinal depletion in $^{13}C$ is distinct, and for two genera (the seastar *Leptasterias* and the Arctic cod, *Boreogadus saida*) correlation coefficients were significant and greater than 0.4 (Figure 98). The west to east depletion ranged from 2-4‰ in a variety of fauna, including gastropods, seastars, shrimp, fish, brittle stars, and polychaetes.

The relationship between consumers and their ultimate carbon sources revealed the importance of both terrestrial and phytoplankton sources, although MFB may also be an important carbon source for some genera (Figure 99). Our selection of end-member carbon and nitrogen sources for the Beaufort ecosystem is based on 20 µm net tows for the phytoplankton endmember (Table 28), a $\delta^{13}C$ and $\delta^{15}N$ for the terrestrial endmember (-29.0 and 3.3‰ respectively; Harris, 2015), and a $\delta^{13}C$ MPB value of-17.5 ± 1.5‰, which represents a mean of benthic diatom isotope values reported in the literature (see Harris, 2015).

**Table 28. Stable isotopic values determined for calanoid copepods, 20 µm net tows (designated phytoplankton), 305 µm net zooplankton, and *Calanus spp.* from samples collected across the Beaufort shelf.**

| Species | n | $\delta^{13}C$ (‰) | $\delta^{15}N$ (‰) | Molar C:N |
|---|---|---|---|---|
| Calanus | 22 | -25.49 ± 0.84 | 10.72 ± 0.6 | 6.26 ± 1.36 |
| *Calanus glacialis* | 9 | -25.88 ± 1.05 | 10.53 ± 0.44 | 5.83 ± 1.25 |
| *Calanus hyperboreus* | 9 | -25.24 ± 0.64 | 11.01 ± 0.74 | 6.92 ± 1.52 |
| *Calanus sp.* | 4 | -25.18 ± 0.43 | 10.52 ± 0.32 | 5.75 ± 0.62 |
| Phytoplankton | 22 | -24.63 ± 0.91 | 7.68 ± 1.5 | |
| Zooplankton | 21 | -25.42 ± 0.93 | 9.52 ± 1.38 | |

**Table 29. Stable isotopic composition and molar C:N ratios of 20 common infaunal and epifaunal organisms collected across the Beaufort shelf. TL is the estimated trophic level.**

| Species | n | $\delta^{13}C$ (‰) | $\delta^{15}N$ (‰) | Molar C:N | TL |
|---|---|---|---|---|---|
| Alcyonidium | | | | | |
| *Alcyonidium disciforme* | 3 | -24.57 ± 0.37 | 8.97 ± 2.53 | 12.52 ± 10.5 | 1.4 ± 0.74 |
| *Alcyonidium gelatinosum* | 6 | -24.38 ± 0.32 | 9.94 ± 0.65 | 7.37 ± 1.41 | 1.69 ± 0.19 |
| Anonyx | | | | | |
| *Anonyx nugax* | 2 | -22.71 ± 1.16 | 18.22 ± 0.1 | 7.7 ± 0.18 | 4.12 ± 0.03 |
| *Anonyx sp.* | 36 | -22.79 ± 1.23 | 15.91 ± 1.36 | 6.87 ± 2.18 | 3.44 ± 0.4 |
| Astarte | | | | | |
| *Astarte borealis* | 3 | -18.84 ± 0.89 | 14.48 ± 2.75 | 4.42 ± 0.06 | 3.02 ± 0.81 |
| *Astarte montagui* | 14 | -21.45 ±0.56 | 9.09 ± 0.47 | 4.95 ± 0.33 | 1.44 ± 0.14 |
| *Astarte sp.* | 13 | -20.76 ± 1.44 | 12.51 ± 2.45 | 4.85 ± 0.56 | 2.44 ± 0.72 |
| Boreogadus | | | | | |
| *Boreogadus saida* | 26 | -22.24 ± 1.09 | 13.26 ± 1.12 | 4.29 ± 0.47 | 2.66 ± 0.33 |
| Eualus | | | | | |
| *Eualus gaimardii* | 34 | -19.66 ± 0.33 | 14.4 ± 1.5 | 3.77 ± 0.11 | 3 ± 0.44 |
| Leptasterias | | | | | |
| *Leptasterias arctica* | 3 | -21.45 ± 0.16 | 12.4 ± 0.71 | 7.21 ± 1.84 | 2.41 ± 0.21 |
| *Leptasterias groenlandicus* | 22 | -23.49 ± 0.85 | 12.23 ± 1.03 | 8.76 ± 3.61 | 2.36 ± 0.3 |
| *Leptasterias sp.* | 1 | -23.21 | 11.72 | | 2.21 |
| Lumpenus | | | | | |
| *Lumpenus fabricii* | 4 | -22.59 ± 1.27 | 13.91 ± 1.14 | 4.8 ± 0.38 | 2.85 ± 0.33 |
| Margarites | | | | | |
| *Margarites costalis* | 28 | -20.71 ± 0.96 | 10.69 ± 0.98 | 4.43 ± 0.44 | 1.91 ± 0.29 |
| *Margarites sp.* | 2 | -21.38 ± 0.28 | 10.08 ± 0.18 | 4.48 ± 0.1 | 1.73 ± 0.05 |
| Nephtys | | | | | |
| *Nephtys ciliata* | 5 | -18.41 ± 0.56 | 14.47 ± 1.76 | 4.14 ± 0.24 | 3.02 ± 0.52 |
| *Nephtys sp.* | 22 | -21.24 ± 1.72 | 13.05 ± 3.38 | 5.18 ± 0.96 | 2.25 ± 1.47 |
| Ophiacantha | | | | | |
| *Ophiacantha bidentata* | 18 | -24.4 ± 0.86 | 14.9 ± 1.18 | 7.91 ± 1.18 | 3.15 ± 0.35 |
| Ophiocten | | | | | |
| *Ophiocten sericeum* | 17 | -23.62 ± 1.35 | 10.81 ± 0.9 | 9.59 ± 1.08 | 1.94 ± 0.27 |
| Phyllodoce | | | | | |
| *Phyllodoce groenlandica* | 22 | -21.95 ± 1 | 12.77 ± 0.96 | 5.97 ± 1.03 | 2.52 ± 0.28 |

The benthic food web of the Beaufort includes first level herbivores such as calanoid copepods, bryozoans (*Alcyonidium*), brittle stars (*Ophiocten*), gastropods (*Margarites*), and bivalves (*Astarte*) that have different carbon sources ($\delta^{13}C$ values range from -25 to -21‰) but yet have very similar $\delta^{15}N$ values (10.5‰). Some higher trophic level biota are clearly more dependent on terrestrial carbon sources owing to their depleted $\delta^{13}C$ values (the brittle star *Ophiacantha*, the amphipod *Anonyx*), while others are not

(the seastar *Leptasterias*, the Arctic cod *Boreogadus*, the polychaete *Phyllodoce*). Still others appear to assimilate a more enriched carbon source (the polychaete *Nephtys*, and the shrimp *Eualus*).

Overall, our isotopic data reflect a benthic community dominated by a variety of omnivorous benthic feeders that have intermediate values between the two major end-members (Figure 99). These omnivorous organisms include amphipods, polychaetes, gastropods, and bivalves and occupy up to four trophic levels based on $\delta^{15}N$ values that range from 9 to 18‰ (Table 29; Figure 99).

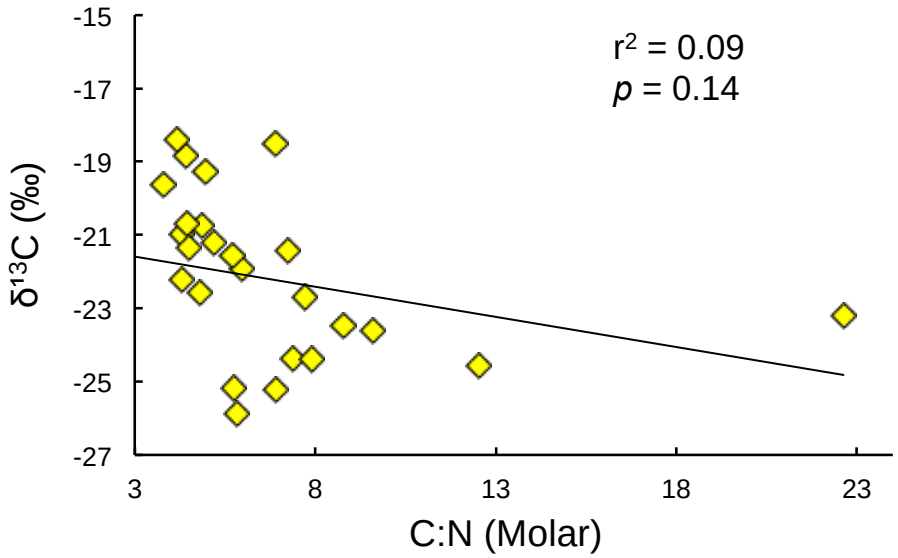


**Figure 96. Relationship between the C:N molar ratio and its corresponding carbon isotopic value. Data points are means for each species analyzed. Linear regression analysis shows the relationship is not significant.**

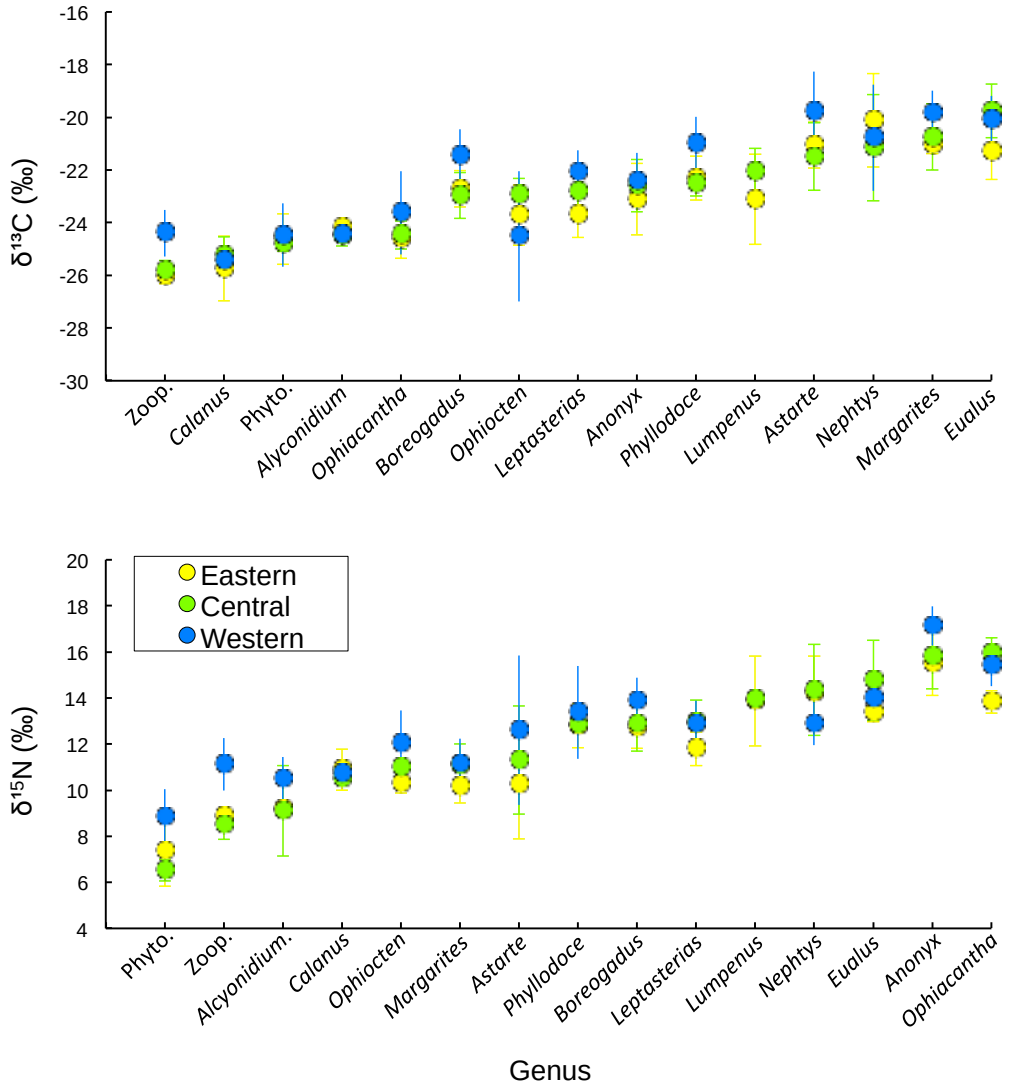


**Figure 97. Mean (±SD) carbon and nitrogen isotope value of genera collected during the 2014 and 2015 ANIMIDA cruises (data for both years are combined) from each geographic region (Eastern, Central, and Western).**

**"Phyto" and "zoop" refer to filtered 20 and 305 µm net samples, respectively.**

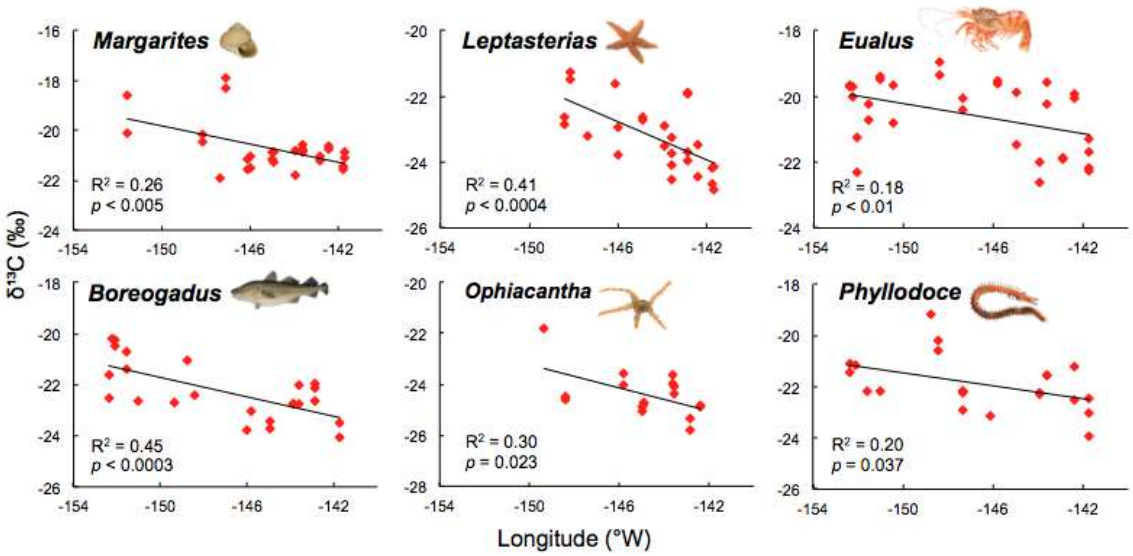


**Figure 98. $\delta^{13}C$ vs. Longitude (°W) for characteristic Arctic benthic fauna. Pearson correlations and p-values of linear regression analyses for each genus are noted within each panel.**

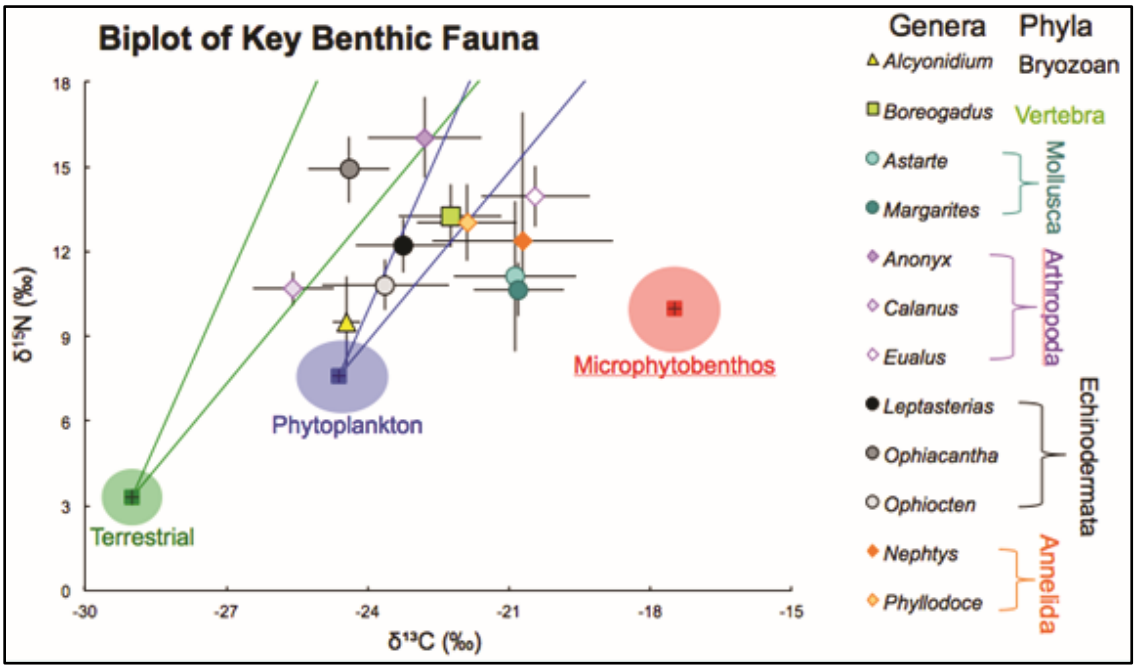


**Figure 99. C and N isotopic biplot (mean ± SD) of 12 characteristic Arctic benthic fauna and three carbon end-members (see Table 23).**

**Data from all sites and all years have been pooled. Lines depict trophic enrichment factors of 0.8 to 2 ‰ for $\delta^{13}C$ and 2 to 4 ‰ for $\delta^{15}N$.**

## 5.4 Discussion

### 5.4.1 Distribution and Diversity of Infauna

Very few infauna data sets exist for the U.S. Beaufort Sea. With the exception of two large programs led by Oregon State and Western Washington from 1971 to 1981 (Dunton et al., 2005), studies have been brief and focused on small defined areas. The only substantial infaunal collections with which to compare the ANIMIDA III data were made from 1971 to 1981 under Western Beaufort Sea Ecological Cruises (WEBSEC) and then continued under the OCSEAP. Physical parameters, such as near bottom temperature, salinity, and sediment grain size were also measured to characterize the in situ environmental conditions at the time of collection.

Several studies that include Beaufort Sea infauna have transpired in the interim years between the historic programs and the present, but are all narrow in scope. In the past 10 years, Shell Exploration sponsored two programs that were focused on specific areas (Harrison Bay and Camden Bay) and BOEM continues to support a field program in the Stefansson Sound Boulder Patch (5–8 m depths) which is located in close proximity to offshore oil and gas exploration and development activities. Consequently, the benthic samples collected at nearly 450 stations under the WEBSEC and OCSEAP programs represent the only large-scale study of Beaufort Shelf infaunal populations. Because these samples were collected prior to the onset of major regional climatic changes on the Beaufort Sea, especially with respect to ice extent, they are a scientific treasure.

Patterns of infaunal biomass based on historical sampling efforts and obtained from station means are available in WEBSEC and OCSEAP summary reports (Figure 92). Stations in much of the middle shelf are lacking, including the region sampled off Kaktovik where ANIMIDA III data indicated the existence of a rich infaunal community with high diversity and abundance values. These available historical biomass data show a general pattern of low biomass means along the nearshore coast and in stations located beyond the 200-m shelf break with higher values in the middle shelf and at some shelf slope stations (Figure 92).

Data from these historic programs were deposited with the National Oceanographic Data Center (NODC) in 1982 and stored in a complex hierarchical file format without programming support to extract usable data records. Therefore, we do not have individual species records from grabs collected under the WEBSEC or OCSEAP programs to analyze for diversity or species richness. Station environmental data were collected but are stored in separate files that must be linked to the infauna data files to enable rigorous analysis of relationships between environmental factors and infaunal distribution patterns. Efforts are underway to secure funding to allow a comprehensive analysis that includes mapping and statistical analysis of these historical datasets of infaunal information. Once these analyses are conducted, the data can be applied to ask questions related to temporal changes in infaunal distribution, composition, diversity, and abundance in response to drivers of regional climatic change.

The ANIMIDA III infauna abundance data collection shows that three major infaunal groups (amphipods, polychaetes and bivalves) are dominant inhabitants on the U.S. Beaufort Sea shelf. Previous Beaufort Sea studies reported the same dominant groups (Carey et al., 1975; Feder and Schamel, 1976; Carey and Ruff, 1977; Broad et al., 1978; Bilyard and Carey, 1979; Griffiths and Dillinger, 1981; Feder and Jewett, 1982; Carey et al., 1984). Schonberg et al. (2014) reported the same three dominant sets for the adjacent northeastern Chukchi Sea. These three invertebrate groups are important because of being

widespread, numerous, and an important prey source for marine mammals and birds (Grebmeier et al., 2006).

Under the ANIMIDA III program, two stations (T3 and L250-5) were selected for benthic sampling that were also sampled in summers 2008 and 2009 during the Shell Exploration sponsored Camden Bay program. From a total of 81 stations sampled during the Camden Bay project, 179 taxa were identified, which is considerable, given the relatively small sampling area. The measurement of biomass at station T3 in 2009 was 57.3 g/$m^2$ and in 2014 it was 132 g/$m^2$. T3 abundance in 2009 was 477 individuals 9ind)/$m^2$ and 590 ind/$m^2$ in 2014. The measurement of biomass at station L250 in 2009 was 45.3 g/$m^2$ and in 2014 it was 35 g/$m^2$. T3 abundance in 2009 was 309 ind/$m^2$ and 330 ind/$m^2$ in 2014. Patchy distribution of infauna and lack of navigational precision makes it difficult to make a direct station comparison, but it is apparent is that these two stations continue to be moderately productive.

In summers 2012 and 2013, infaunal data was collected in the COMIDA Hanna Shoal program from stations located in the northeastern Chukchi Sea, a highly productive region which abuts the western edge of the U.S. Beaufort Sea. A total of 380 taxa were collected in 85 van Veen grabs at 39 stations. The project Shannon Diversity Index mean = 3.7 ± SD 0.36 and Pielou's Evenness mean = 0.94 ± SD 0.02. When compared, these values show that the Beaufort Sea shelf has a less vigorous infaunal population than the northeastern Chukchi Sea.

### 5.4.2 Environmental Influences on Infaunal Distribution

Previous studies described the Beaufort Sea shelf as being blanketed predominantly by patchy silty sands and mud (Barnes and Reimnitz, 1974). The sediments collected during ANIMIDA III were principally composed of sand and silt but small amounts of gravel were also collected in many of the middle shelf stations (see J. Trefry's chapter, this report). Results from analyses of environmental influences on infauna distribution patterns indicated that sediment grain size was not an indicator for infaunal configurations.

BIO-ENV routine results from COMIDA Hanna Shoal data showed that infauna distribution in the northeastern Chukchi Sea was best explained by a combination of water depth, sediment chlorophyll *a*, and the C:N molar ratio. Chlorophyll *a* and the C:N molar ratio are both proxies for sediment nutrients available to infaunal inhabitants. ANIMIDA III BIO-ENV results indicated that water depth and TOC were the strongest two drivers of distribution patterns ($\sigma = 0.56$), but the combination of depth, salinity, TOC, chlorophyll *a*, and C:N molar ratio produced a Spearman value of 0.52 indicating that together they explain more than 50% of the variance in the distribution of infauna. Salinity was not a determining environmental feature in the northeastern Chukchi Sea due to the lack of riverine input but is an important influence on the Beaufort shallow nearshore where depressed salinity levels were measured. The north slope of Alaska has numerous rivers and streams emptying onto the Beaufort Sea shelf including the powerful Mackenzie and Colville Rivers. ANIMIDA sediments in the Colville River Delta tended to be sandy and nutrient poor. Infaunal populations had low diversity and low biomass and were dominated by small crustaceans and polychaetes. Historical data from the WEBSEC and OCSEAP programs also showed small infaunal populations in the Colville River Delta and numerous coastal shallow stations (Figure 92).

Distributional relationships (Figure 91) show that hydrographic (bottom water salinity and temperature) and one nutritional indicator are drivers of infaunal distribution in the BIO-ENV routine. Salinity values > 32 were present at most stations in the region offshore of Kaktovik between 144° W and

146° W and at three stations along the shelf break (149-200, 71-146, and 143-W5). These three shelf break stations also had warm bottom water temperatures and elevated TOC indicating they are waters of Bering-Chukchi origination. The middle shelf waters offshore of Barter Island are saline, but cold. This may indicate that deep Arctic Ocean waters are flowing onto the shelf through upwelling events which have been reported to occur regularly in this area in response to easterly winds (Hufford, 1975; Mountain, 1975).

Bottom waters collected in the western portion of the study area along the 152° W line, had salinities between 31 and 32, were warm and contained higher levels of TOC. They had low infauna abundance values (Figure 87) and low biomass in the three inshore stations but higher biomass in the three middle shelf stations (Figure 88). Species count and Shannon's diversity showed a similar pattern to the biomass (Figure 89). This area is most likely influenced by a combination of freshwater from the Colville River and also by Bering-Chukchi waters that have been reported to inundate the Beaufort shelf, particularly in late summer (Hufford, 1975; Mountain, 1975; see J. Kasper's chapter this report).

### 5.4.3 Sediment Chlorophyll: A Critical Link to Benthic Metazoans?

Sedimentary pigments provide an estimate of the amount of benthic production that is available to the benthic fauna, and can indicate how this organic matter degrades on the seabed (McTigue et al., 2015). Our HPLC results show that the major accessory pigment in the sediment is fucoxanthin, which is a strong biomarker for diatoms. Other accessory pigments included peridinin (a dinoflagellate marker) and prasinoxanthin (a unicellular green algal marker), but neither of these pigments were found consistently in high concentrations. A variety of different chlorophyll *a* derivatives can exist in marine sediments, and these can provide insights into metazoan grazing versus microbial degradation of organic matter in sediments, the latter of which has not been investigated in the Beaufort Sea using pigment biomarkers. Virtually no measurements of benthic chlorophyll for the Beaufort Sea have been reported in the literature. The values reported here are extremely unique, and provide some extraordinary insight into the nature of in situ production on the Beaufort shelf.

The benthic chlorophyll values we recorded for the Beaufort Sea are modest at best compared to the adjacent Chukchi Sea. Overall, concentrations of chlorophyll *a* are an order of magnitude lower than reported by McTigue et al. (2015) in the northeastern Chukchi Sea. The lower values can be attributed to several factors, including the lack of a significant epontic ice algal contributions during spring ice melt, lower light penetration to the seabed, and more frequent disruption and scouring of the seabed by deep draft ice. In contrast, Beaufort Sea lagoon sediments are characterized by sediment chlorophyll concentrations equivalent to the Chukchi Sea benthos (Dunton, unpub. data). Although the winter ice in lagoons is also largely devoid of ice algae, the shallow depths (3-5 m) and protected nature of lagoon sediments promote the continued proliferation of the MFB.

Despite the low sediment chlorophyll concentrations in Beaufort Sea sediments, the distribution of "hotspots" indicates that areas of seabed not only exhibit in situ microalgal production, but that benthic herbivores are actively assimilating this carbon source based on the high levels of pheophorbide *a*, a marker for metazoan grazing, and pyropheophorbide *a*, the secondary degradation product of pheophorbide *a* (Figure 93). **It is interesting to note that the stations exhibiting the highest levels of both pyropheophorbide and pheophorbide *a*, were characterized by the highest infaunal abundance. Polychaetes and benthic crustaceans constituted >75% of all organisms present at these stations (152W0, 6D, 12, 3A, 143W4, 22, and 25).** Consequently, it appears that there exists the

possibility of a strong correlation between infaunal abundance and an in situ benthic microalgal carbon subsidy. Since benthic infauna are stationary and relatively long-lived, such production is likely perennial in nature. Finally, the presence of a viable $^{13}C$ MFB would explain the $^{13}C$ enriched infauna, including crustaceans, polychaetes, brittle stars, and bivalves (Figure 99).

### 5.4.4 The Beaufort Shelf Food Web

Measurements of the stable carbon and nitrogen isotopic composition of the resident fauna provide valuable markers in assessing the role of ultimate carbon sources and in defining trophic structure. Half the genera examined also display a distinct eastward depletion in $\delta^{13}C$ values (Figure 98). This likely reflects the influence of the Mackenzie River and other sources of freshwater runoff in the eastern U.S. Beaufort Sea, which carry allochthonous inputs of terrestrial organic carbon that become available as a food source to the benthos. Our results, along with more recent observations (Divine et al., 2015; Bell et al., 2016), continue to provide compelling evidence for the important role of terrestrial carbon in Beaufort Sea food webs.

Our preliminary data on the stable nitrogen isotopic composition of benthic organisms reveal complex food webs dominated by decidedly omnivorous consumers (Figure 99). Stable carbon isotopic composition of these benthic organisms, along with isotopic analyses of SPOM and zooplankton collected in situ, reveal a primary mixture of terrestrial and phytoplankton carbon, but an additional benthic microalgal subsidy appears to play a role at moderate depths that correspond to hotspots of infaunal abundance. The intermediate $\delta^{13}C$ values of most genera indicate they assimilate organic matter derived from a mix of these carbon sources.

Finally, it is important to note that most consumers in this study exhibited an opportunistic feeding strategy as reflected in their omnivorous behavior as detritovores, similar to other Arctic systems (e.g., McTigue and Dunton, 2014). The distinct $^{13}C$ enrichment with increasing trophic level likely reflects the increasing importance of MFB, microbial degradation, and colonization of buried organic matter that is ingested by deposit feeders, which rapidly results in an enrichment of $\delta^{13}C$ values in the combined microbial-detrital pool. This suggests that there is a strong link between the microbial and metazoan food webs rather than a direct pathway for terrestrial organic matter incorporation into first level consumers since very few organisms can assimilate terrestrial matter directly.

In contrast to the more productive Chukchi Sea shelf ecosystem, the estuarine character of the Beaufort Sea results in a decidedly more complex ecosystem, especially on a spatial scale. Sources of terrestrial carbon are prominent, but not easily assimilated. Contributions by benthic microalgae, although small, are measurable, especially on the inner (shallow) shelf environment. The presence of microalgae at shallower depths is likely attributed to the higher levels of light that reach the seabed. Because irradiance is strongly attenuated with depth, benthic microalgae are more likely to survive and photosynthesize in shallower environments. Unlike the Chukchi shelf, which exhibits a narrow range of depths (30–60 m, exclusive of Barrow Canyon), the bathymetry of the Beaufort Shelf varies from 10 to 200 m. These differences are reflected both in the character of the benthos and the relative importance of carbon sources to omnivorous consumers. The resilience of the system is illustrated in the diversity and longevity of the benthic fauna and their opportunistic feeding strategy, in which carbon is efficiently transferred to the highest trophic levels, with clear benefits to native populations on the Beaufort coast (Figure 100).

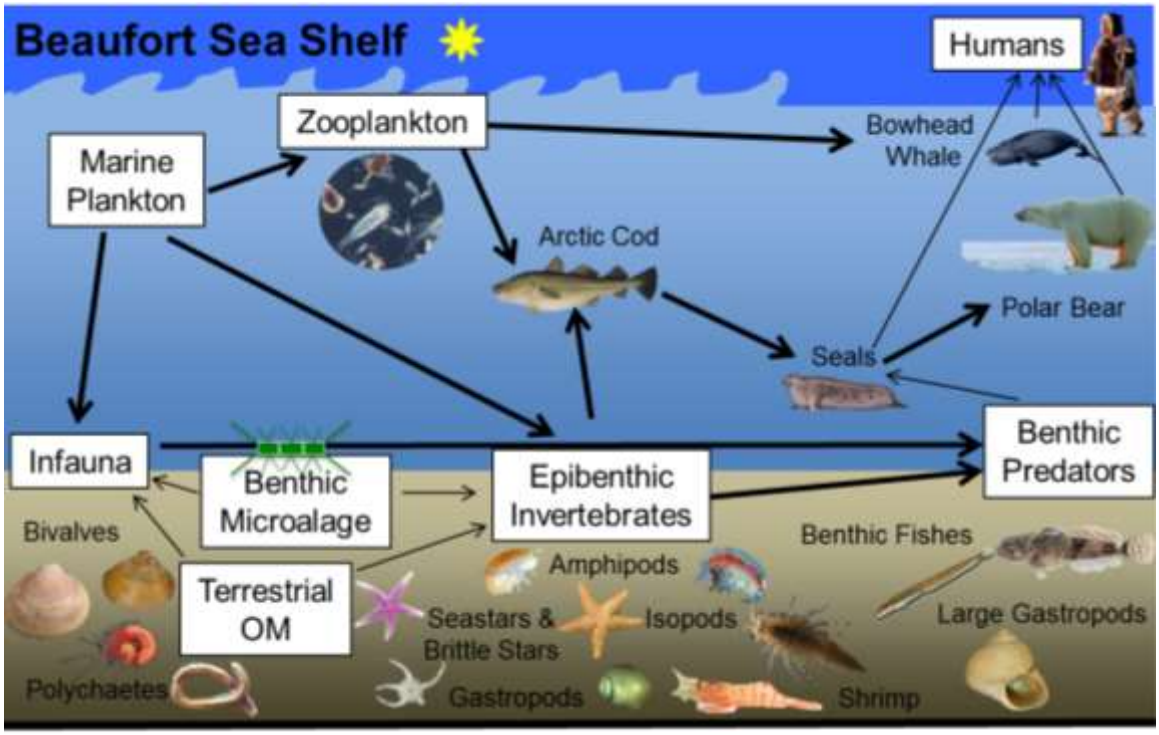


**Figure 100. Conceptual diagram showing hypothesized trophic relationships among consumers in a Beaufort Sea shelf ecosystem. [1]**

[1] Carbon derived from phytoplankton is the major autochthonous carbon source but consumers also assimilate benthic microalgae (MFB) produced in situ and allochthonous (terrestrial) inputs to variable extent. Arrows (light and dark) show the direction and magnitude of energy transfer. The trophic redundancy of the food web is reflected in the strong omnivorous behavior of most consumers. The diversity of the system is a key attribute of its resiliency to physical perturbations. Food web connections are based on isotopic data derived from this study and data from Harris and Dunton (unpublished), and Dunton et al. (2012).

## Acknowldgements

Funding was provided by the BOEM under the capable leadership of our program manager Cathy Coon. We thank the Olgoonik Fairweather staff and the captain and crew of the R/V *Norseman II* on 2014 and 2015 ANIMIDA cruises. We are especially grateful to UTMSI graduate students Christina Bonsell and Carrie Harris who worked diligently with little sleep to expertly process hundreds of samples that arrived on deck on a daily basis. Dan Holiday provided invaluable assistance sieving infauna from benthic grabs on nearly a continuous basis. Our epifauna isotope collection would have been quite sparse without the generous aid from our UAF colleagues including PIs Katrin Iken and Bodil Bluhm and their superb field team, including Lauren Bell, Lorena Edenfield, Tanja Schollmeier, and Kelly Walker. We thank our wonderful staff at UTMSI for processing hundreds of stable isotope samples (Kim Jackson, Madison Becker, Sarah Cunningham, and Patricia Garlough).

## References


Are F.E. 1999. The role of coastal retreat for sedimentation in the Laptev Sea. In: Kassens, H., Bauch, H., Dmitrenko, I., Eicken, H., Hubberten, H.-W., Melles, M., Thiede, J. & Timokhov, L. (eds) Land-Ocean systems in the Siberian Arctic: dynamics and history. Springer, Berlin: 287–299.

Barnes P.W. and Reimnitz. E. 1974. Sedimentary processes on Arctic shelves off the northern coast of Alaska. In: Reed, J.C., Sater, J.E., (eds.), Proceedings of a Symposium on Beaufort Sea Coast and Shelf Research. Arctic Institute of North America 439-476.

Barnes P.W., Rearic D.M., and Reimnitz E. 1984. Ice gouging characteristics and processes. In: Barnes, P., Schell D., Reimnitz, E., (eds.), The Alaskan Beaufort Sea: ecosystems and environments. Academic Press Inc., San Diego 185-212.

Bell L.E., Bluhm B.A., and Iken K. 2016. Influence of terrestrial organic matter in marine food webs of the Beaufort Sea shelf and slope. Marine Ecology Progress Series 550, 1-24.

Benner R., Benitez-Nelson B., Kaiser K., and Amon, R.M.W. 2004. Export of young terrigenous dissolved organic carbon from rivers to the Arctic Ocean. Geophysical Research Letters 31, L05305, doi:10.1029/2003GL019251.

Bilyard G.R. and Carey A.G., Jr. 1980. Distribution of western Beaufort Sea polychaetous annelids. Marine Biology 54, 329-339.

Broad A.C., Koch H., Mason D.T., Petri D.M., Schneider D.E., and Taylor E.J. 1978. Environmental Assessment of selected habitats in the Beaufort Sea littoral system. In: Environmental Assessment of the Alaskan Continental Shelf: Principal Investigators' Reports for the Year Ending March 31, 1978. Boulder, CO: National Oceanic and Atmospheric Administration 5, 1-84.

Carey A.G., Jr., Ruff R.E., Castillo J.G., and Dickinson J.J. 1975. Benthic ecology of the western Beaufort Sea continental margin: preliminary results. In: Reed, J.C., Sater, J.E., (eds.), Proceedings of a Symposium on Beaufort Sea Coast and Shelf Research. Arctic Institute of North America 665-680.

Carey A.G. Jr., and Ruff R.E. 1977. Ecological studies of the benthos in the western Beaufort Sea with special reference to bivalve molluscs. In: Dunbar, M.J., (ed.), Polar Oceans. The Arctic Institute of North America, Calgary, Alberta 505-530.

Carey A.G., Jr., Scott P.H., and Walters K.R. 1984. Distributional ecology of shallow southwestern Beaufort Sea (Arctic Ocean) bivalve Mollusca. Marine Ecology Progress Series 17, 125-134.

Carey A.G., Jr. 1991. Ecology of North American Arctic continental shelf benthos: a review. Continental Shelf Research 11(8-10), 865-883.

Chapman D.C. 2003. Physical Oceanography of the Beaufort Sea – Workshop Proceedings. OCS Study MMS 2003-045. Prepared by MBC Applied Environmental Sciences, Costa Mesa, CA. Prepared for the U.S. Dept. of the Interior, Minerals Management Service, Alaska OCS Region, Anchorage, AK 22 pp.

Clarke K.R. and Gorely R.N. 2006. PRIMER v6: User manual/tutorial, PRIMER-E, Plymouth UK 192 pp.

Clarke K.R. and Warwick R.M. 2001. Change in Marine Communities: An Approach to Statistical Analysis and Interpretation. 2nd ed. PRIMER-E, Plymouth, UK 172 pp.

Darnaude A.M., Salen-Picard C., Polunin N.V.C., and Harmelin-Vivien M.L. 2004. Trophodynamic linkage between river runoff and coastal fishery yield elucidated by stable isotope data in the Gulf of Lions (NW Mediterranean). Oecologia 138, 325-332.

Divine L.M., Iken K., and Bluhm B.A. 2015. Regional benthic food web structure on the Alaska Beaufort Sea shelf. Marine Ecology Progress Series 531, 15-32.

Dubois S., Orvain F., Marin-Leal J.C., Ropert M., and Lefebvre S. 2007. Small-scale spatial variability of food partitioning between cultivated oysters and associated suspension feeding species, as revealed by stable isotopes. Marine Ecology Progress Series 336, 151-160.

Dunton K.H and Schell D.M. 1987. Dependence of consumers on macroalgal (*Laminaria solidungula*) carbon in an arctic kelp community: $\delta^{13}C$ evidence. Marine Biology 93, 615-625.

Dunton K.H. 2001. $\delta^{15}N$ and $\delta^{13}C$ measurements of Antarctic peninsula fauna: trophic relationships and assimilation of benthic seaweeds. American Zoologist 41, 99-112.

Dunton K.H., Goodall J.L., Schonberg S.V., Grebmeier J.M., and Maidment D.R. 2005. Multi-decadal synthesis of benthic-pelagic coupling in the western arctic: role of cross-shelf advective processes. Deep-Sea Research II 52, 3462-3477.

Dunton K.K., Weingartner T., and Carmack E.C. 2006. The nearshore western Beaufort Sea ecosystem: Circulation and importance of terrestrial carbon in arctic coastal food webs. Progress in Oceanography 362-378.

Dunton K.H., Schonberg S.V., and Cooper L.W. 2012. The ecology of coastal waters and estuarine lagoons of the eastern Alaskan Beaufort Sea. Estuaries and Coasts 35, 416-435.

Feder H.M., and Schamel D. 1976. Shallow water benthic fauna of Prudhoe Bay. In: Hood, D.W. and Burrell, D.C., (eds.), Assessment of the Arctic Marine Environment, Selected Topics. University of Alaska, Institute of Marine Science Occasional Publication No. 4, 329-359.

Feder H.M. and Jewett S. 1982. Prudhoe Bay Waterflood Project Infaunal Monitoring Program. Final Report Prepared for ARCO Oil and Gas Co. by Institute of Marine Science, University of Alaska, Fairbanks 148 pp. + appendices.

France R.L., 1995. Carbon$^{13}$ enrichment in benthic compared to planktonic algae: foodweb implications. Marine Ecology Progress Series 124, 307–312.

Glud R.N., Woelfe, J., Karsten U., Kühl M., and Rysgaard S. 2009. Benthic microalgal production in the Arctic: Applied methods and status of the current database. Botanica Marina 52, 559–571.

Gordeev V.V., Martin J.M., Sidorov I.S., and Sidorova M.V. 1996. A reassessment of the Eurasian River input of water, sediment, major elements, and nutrients to the Arctic Ocean. American Journal of Science 296, 664-691.

Graeve M., Kattner G., and Piepenburg D. 1997. Lipids in Arctic benthos: Does the fatty acid and alcohol composition reflect feeding and trophic interactions? Polar Biology 18, 53-61.

Grebmeier J.M., Cooper L.W., Feder H.M., and Sirenko B.I. 2006. Ecosystem dynamics of the Pacific-influenced Northern Bering and Chukchi Seas in the Amerasian Arctic. Progress in Oceanography 71, 331-361.

Griffiths W.B. and Dillinger R.E. 1981. Beaufort Sea barrier island – lagoon ecological process studies: The invertebrates. Environmental Assessment of the Alaskan Continental Shelf 8, 1-359.

Harris C.M., 2015. Hydrological and ecological observations along the eastern Beaufort Sea coast of Alaska. M.S. Thesis, The University of Texas at Austin 112 pp.

Hufford G.L., 1975. Preliminary analysis of Beaufort shelf circulation in the summer. In: Reed, J.C., Sater, J.E., (eds.), Proceedings of a Symposium on Beaufort Sea Coast and Shelf Research. Arctic Institute of North America 567-588.

Iken K., Bluhm B., and Dunton K.H. 2010. Benthic food-web structure under differing water mass properties in the southern Chukchi Sea. Deep-Sea Research II 57, 71-85.

Lobbes J. M., Fitznar H.P, and Kattner G. 2000. Biogeochemical characteristics of dissolved and particulate organic matter in Russian rivers entering the Arctic Ocean. Geochimica et Cosmochimica Acta 64, 2973-2983.

Lovvorn J.R., Cooper L.W., Brooks M.L., De Ruyck C.C. Bump, J.K., and Grebmeier. J.M. 2005. Organic matter pathways to zooplankton and benthos under pack ice in late winter and open water in late summer in the north-central Bering Sea. Marine Ecology Progress Series 291, 135-150.

Macdonald R.W., Naidu A.S., Yunker M.B., and Gobeil C. 2004. The Beaufort Sea: distribution, sources, fluxes and burial of organic carbon. In: Stein R., Macdonald, R.W., (eds.), The Organic Carbon Cycle in the Arctic Ocean. Springer 177-193.

Magurran A.E., 2004. Measuring Biological Diversity. Blackwell Publishing 107-108.

Mathis J.T., Byrne R.H., McNeil C.L., Pickart R.P., Juranek L., Liu S., Ma J., Easley R.A., Elliot M.W., Cross J.N., Reisdorph S.C., Morison S., Lichendorph T., and Feely R.A. 2012. Storm-induced upwelling of high $pCO_2$ waters onto the continental shelf of the Western Arctic Ocean and implications for carbonate mineral saturation states. Geophysical Research Letters, 39, L07606, doi:10.1029/2012GL051574.

McConnaughey T. and McRoy C.P. 1979. Food web structure and the fractionation of carbon isotopes in the Bering Sea. Marine Biology 53, 257-262.

McTigue N.D. and Dunton K.H. 2014. Trophodynamics and organic matter assimilation pathways in the northeast Chukchi Sea, Alaska. Deep-Sea Research II 102, 84-96.

McTigue N.D. Bucolo P., Liu Z., and Dunton K.H. 2015. Pelagic-benthic coupling, food webs, and organic matter degradation in the Chukchi Sea: Insights from sedimentary pigments and stable carbon isotopes. Limnology and Oceanography 60, 429-445.

Mountain D.G. 1975. Preliminary analysis of Beaufort shelf circulation in the summer. In: Reed, J.C., Sater, J.E., (eds.), Proceedings of a Symposium on Beaufort Sea Coast and Shelf Research. Arctic Institute of North America 493-510.

Naidu A.S., Cooper L.W., Finney B.P., Macdonald R.W., Alexander C., and Semiletov I.P. 2000. Organic carbon isotope ratios ($\delta^{13}C$) of Arctic Amerasian continental shelf sediments. International Journal of Earth Sciences 89, 522-532.

North C.A., Lovvorn J.R., Kolts J.M., Brooks M.L., Cooper L.W., and Grebmeier J.M. 2014. Deposit-feeder diets in the Bering Sea: potential effects of climatic loss of sea ice-related microalgal blooms. Ecological Applications 24, 1525-1542.

Parsons T.R., Maita Y., and Lalli C.M. 1984. A Manual of Chemical and Biological Methods for Seawater Analysis. Pergamon Press, Oxford, U.K.

Parsons T.R., Webb D.G., Rokeby B.E., Lawrence M., Hopky G.E., and Chiperzak D.B. 1989. Autotrophic and heterotrophic production in the Mackenzie River/Beaufort Sea estuary. Polar Biology 9, 261-266.

Pickart R.S. 2004. Shelfbreak circulation in the Alaskan Beaufort Sea: Mean structure and variability. Journal of Geophysical Research 109, C04024 14 p.

Pickart R.S, Schulze L.M., Moore G.W.K., Charette A. Arrigo K., van Dijken G., and Danielson S. 2013. Long-term trends of upwelling and impacts on primary productivity in the Alaskan Beaufort Sea. Deep Sea Research I 79, 106-121.

Post D.M. 2002. Using stable isotopes to estimate trophic position: models, methods, and assumptions. Ecology 83,703-718.

Primer-e, 2016. http://www.primer-e.com

Rau G.H., Takahashi T., Des Marais D. J., Repeta D.J., and Martin J.H. 1992. The relationship between $\delta^{13}C$ of organic matter and $[CO_2(aq)]$ in ocean surface water: data from a JGOFS site in the northeast Atlantic Ocean and a model. Geochimica et Cosmochimica Acta 56, 1413-1419.

Reimnitz E., Barnes P.W., Toimil L.J., and Melchior J. 1977. Ice gouge recurrence and rates of sediment reworking, Beaufort Sea, Alaska. Geology 5, 405-408.

Reimnitz E., Graves S.M., and Barnes P.W. 1988. Beaufort Sea coastal erosion, shoreline evolution, and sediment flux. Bureau of Ocean Energy Management, Regulation and Enforcement 78 pp. http://www.gomr.boemre.gov/PI/PDFImages/ESPIS/1/1133.pdf.

Schell D.M. 1983. Carbon-13 and carbon-14 abundances in Alaskan aquatic organisms: delayed production from peat in arctic food webs. Science 219, 1068-1071.

Schell D.M. and Ziemann P.J. 1983. Accumulation of peat carbon in the Alaska Arctic Coastal Plain and its role in biological productivity. In: Permafrost: Fourth International Conference, Proceedings, 17-22 July 1983, Washington, D.C.: National Academy Press, 1105-1110.

Schonberg S.V., Clarke J.T., and Dunton K.H. 2014. Distribution, abundance, biomass and diversity of benthic infauna in the Northeast Chukchi Sea, Alaska: Relation to environmental variables and marine mammals. Deep-Sea Research II 102, 144-163.

Smith S.D., Connelly T.L., Harris C.M., Dunton K.H., and McClelland J.W. 2016. Seasonal trophic linkages in Arctic marine invertebrates assessed via fatty acids and compound-specific stable isotopes. Ecosphere DOI: 10.1002/ecs2.1429.

Stein R., and Macdonald R.W. 2004. Geochemical proxies used for organic carbon source identification in Arctic Ocean sediments. In: Stein, R., Macdonald, R.W., (eds.), The Organic Carbon Cycle in the Arctic Ocean. Berlin: Springer 1, 24-32.

Sun M.Y., Aller R.C., and Lee C. 1991. Early diagenesis of chlorophyll-*a* in Long Island Sound sediments - A measure of carbon flux and particle reworking. Journal of Marine Research 49, 379-401.

Tu K.L., Blanchard A.L., Iken K., and Horstmann-Dehn L. 2015. Small-scale spatial variability in benthic food webs in the northeastern Chukchi Sea. Marine Ecology Progress Series 528, 19-37.

Vander Zanden M.J. and Rasmussen J.B. 2001. Variation in delta N-15 and delta C-13 trophic fractionation: Implications for aquatic food web studies. Limnology and Oceanography 46, 2061-2066.

Von Appen W-J and Pickart R.S. 2012. Two configurations of the Western Arctic Shelfbreak Current in summer. Journal of Physical Oceanography 42, 329-351.

Wada E., Terazaki M., Kabaya Y., and Nemoto T. 1987. $^{15}N$ and $^{13}C$ abundances in the Antarctic Ocean with emphasis on the biogeochemical structure of the food web. Deep-Sea Research 34, 829-841.

Weingartner T. 2003. Physical Oceanography of the Beaufort Sea – Workshop Proceedings. OCS Study MMS 2003-045. Prepared by MBC Applied Environmental Sciences, Costa Mesa, CA. Prepared for the U.S. Dept. of the Interior, Minerals Management Service, Alaska OCS Region, Anchorage, AK 12 pp.

White D., Kimerling J.A., and Overton S.W. 1992. Cartographic and geometric components of a global sampling design for environmental monitoring. Cartography and Geographic Information Science 19, 5-2.

Wulff A., Iken K., Quartino M.L., Al-Handal A., Wiencke C., and Clayton M.N. 2009. Biodiversity, biogeography and zonation of marine benthic micro- and macroalgae in the Arctic and Antarctic. Botanica Marina, 52:491–507. doi: 10.1515/BOT.2009.072.

# Chapter 6 Epibenthic Communities and Demersal Fish Communities


## Abstract

The shelf of the Beaufort Sea is defined by dynamic physical and biological gradients that have a distinctive influence on epibenthic and demersal fish standing stocks. During the ANIMIDA project phase III (2014–2016) we conducted an ecosystem study characterizing parts of the Beaufort Sea nearshore, shelf, and upper slope in terms of its physical oceanography, benthic community and food web structure, and contaminant foot print (hydrocarbons, metals) to identify relationships between human use, physical environment, and ecosystem response. This chapter reports on the findings related to epibenthos and demersal fish community structure which varied both along and across shelf.

Epifaunal communities shallower than 20 m, sampled primarily in the western part of the study area near the Colville and Sagavanirktok Rivers, were relatively depauperate in species richness and abundance/biomass, likely related to a combination of bottom fast ice, scour by deep-draft ice, and extreme salinity changes during spring break-up. Dominant epibenthos in this zone included mobile crustaceans. Shelf areas outside such perturbations were more species rich with largely overlapping character species in several community clusters. Shelf break and upper slope fauna formed distinct clusters, but typical deep-water species were only found at the deepest stations. Dominant fauna on the shelf and upper slope included echinoderms and mollusks. Demersal fish were less abundant and diverse than epibenthic invertebrates, but fish communities were also distinct between nearshore and offshore areas, though less bound to the 20 m isobath and grouped in fewer clusters. Sculpins (*Cottidae*) generally dominated by abundance, while *Liparidae*, *Gadidae,* and *Zoarcidae* also contributed almost equally to the species inventory. Along shelf, the decreasing influence of Pacific-origin water along the continental slope resulted in lower epibenthic stocks east of 150° W compared to previous studies conducted further west. A shift in taxonomic composition also aligned with this longitude.

In summary, the ANIMIDA III results document that epibenthic communities reflected the physically very dynamic nature of the Beaufort Sea shelf, characterized by strong land-ocean interactions in its nearshore zone, and its interaction across a steep slope that reaches into Atlantic-origin waters. The areas off the Colville and Sagavanirktok Rivers contained less rich epibenthic communities than the Chukchi-influenced western Beaufort Sea and also somewhat less rich communities than the shelf region off Barter Island.


## 6.1 Introduction

Arctic shelf ecosystems are often dominated by rich benthic communities as a result of the tight coupling to locally high primary production in the overlying water column (Grebmeier, 2012). Where benthic communities are tightly coupled to water-column processes they can serve as useful indicators of biological response not only of water column processes, but also to climatic variability (Grebmeier et al., 2006). This is because many benthic organisms are long-lived and slow-growing and therefore integrate processes over longer time spans than pelagic systems (Piepenburg et al., 1995). Thus, seasonal and interannual variability are dampened in seabed communities, allowing for observation of longer-term (years-to-decade long) trends in ecosystem function (Dunton et al., 2005; Smith et al., 2006). These Arctic benthic shelf communities play vital roles in remineralization processes and as prey for higher trophic levels such as bottom-feeding fishes, seals, and diving birds (Coyle et al., 1997; Ambrose et al.,

2001; Lovvorn et al., 2003). Within benthic communities, it is ecologically relevant to differentiate between macro-infauna living within the sediments and epifauna living on top of the sediments. These benthic components differ in their mobility, size range of organisms, dominant taxonomic composition, dominant feeding modes, and the mode of collection. This section of the report focuses on epibenthic communities including demersal fishes.

The Beaufort Sea is an interior shelf with a complex hydrography strongly influenced by river inputs and land-ocean interactions (c.f. Carmack and Wassmann, 2006). This is in contrast to the neighboring Chukchi Sea which is an inflow shelf characterized strongly by advective inflow of sub-Arctic waters containing heat, high nutrient, and particle loads. In its western part, the Beaufort Sea experiences the influence of that advective influx of nutrient-rich Pacific waters carried through the Chukchi Sea. This influence decreases towards the east as reflected in the highest epibenthic biomass present on the western Beaufort Sea slope where the Pacific-water inflow is strongest with a decrease towards the east (Rand and Logerwell, 2011; Bluhm et al., 2014; Ravelo et al., 2015). Although the Beaufort Sea is downstream of the Chukchi shelf it differs considerably in water mass characteristics and productivity (Dunton et al., 2005), but also in bathymetry and faunal assemblages. Our recent assessment of large parts of the shelf benthos in the U.S. Beaufort Sea found considerable along-shelf differences in abundance, biomass, and community composition of epibenthos, in addition to depth being a key factor that structures these communities (Ravelo et al., 2015). These key roles of both Pacific water influence and depth were confirmed during the Transboundary project (Norcross et al., 2015) which extensively sampled the steep depth gradients of the Beaufort slope covering all major vertical water masses and confirmed that the west to east gradient in community patterns on the shelf also is present at the slope. The ANIMIDA III study region not only covers previously sampled monitoring stations around historic drilling sites (Trefry et al., 2013), but also further improved the shelf-wide coverage in epifaunal and demersal fish sampling and covered spatial gaps, such as in the nearshore region.

Within the U.S. Arctic, epibenthic research efforts have increased greatly in the last decade related to oil and gas exploration (Day et al., 2013), climate warming (Crane and Ostrovskiy, 2015), and the need to provide information for the Arctic Fisheries Management Plan (NPFMC 2009). Especially the Chukchi Sea shelf has undergone intense study of epibenthic communities in the past decade (Feder et al., 2005; Bluhm et al., 2009; Blanchard et al., 2013; Ravelo et al., 2014). The Beaufort Sea epifauna was poorly studied until the 1970s when a broad but sparsely spaced trawl survey in 1976–77 was conducted (Frost and Lowry, 1983), for which Bluhm et al. (2014) recovered species-level information of invertebrates. During the WEBSEC survey, macrofauna studies were funded (e.g., Carey and Ruff, 1977), but trawl–based work remained unfunded, though unpublished trawl-based epibenthos data were recovered by the PI recently (Bluhm, 2014). Continuous long-term monitoring (1981–present) of fishes has been conducted in the very nearshore shallow waters in the Prudhoe Bay oil development region (Thorsteinson et al., 1992; Fechhelm et al., 2010). In more recent years increased interest in the Beaufort Sea has resulted in several BOEM-supported studies with differing extent and station density including the western Beaufort Sea in 2008 (Rand and Logerwell, 2011; Bluhm et al., 2014), the broad and dense sampling of ~200 km of the Beaufort Sea shelf in 2011 (Ravelo et al., 2015) and the 2012-14 Transboundary study primarily in the eastern Alaskan and Mackenzie River areas (Norcross et al., 2015).

The Beaufort Sea shelf extends from Point Barrow, Alaska, to Banks Island in Canada, and incorporates three distinct shelf environments (inner, mid, and outer; c.f. Ravelo et al., 2015), with numerous small rivers and streams, and two large river systems, the Colville and Mackenzie Rivers. The U.S. Beaufort Sea, especially the eastern sector, is estuarine in character with combined flows from the Colville and Mackenzie Rivers annually adding nearly 350 $km^3$ of freshwater plus 130 x 106 tons sediment to a shelf that ranges in width from only 40 km in Alaska to 150 km in Canada (Macdonald et al., 2004). This freshwater inflow influences the nearshore benthic populations especially during break-up in the spring when a pulse of riverine water causes large changes in temperature, salinity and nutrients (see Chapter 3, Trefry). In addition to these two large inputs of freshwater, the span of coastline from Barrow to Demarcation Bay is skirted by an irregular and discontinuous chain of barrier islands that enclose numerous shallow (<8 m) and productive lagoons that are fed by many small rivers and streams (Dunton et al., 2012). While the nearshore area is influenced by land-ocean interactions as well as landfast ice that persists for over half a year and affects the seabed to about the 20 m isobath (Mahoney et al., 2014), the shelf break interacts with the Canada Basin over a steep slope that has recently experiences increasing frequency of upwelling events (Pickart et al., 2011).

While the ANIMIDA program has historically mostly focused on the nearshore areas, the 2014-2015 sampling included shelf and shelf break stations for two reasons: first, the larger context helped improve interpretation of the nearshore stations and second, we sampled stations related to the recently expanded network of the DBO.. In fact, ANIMIDA PIs played a major role in establishing the Beaufort Sea DBO lines 6 and 7 and - through ANIMIDA field work - were the first to sample them.

### 6.1.1 Objectives

The specific objectives for the epibenthos and fish components of the ANIMIDA III project were to: (1) describe epibenthic and demersal fish community structure based on trawl sampling and (2) identify environmental factors (relating to hydrography, food availability and sediment properties) that influence epibenthic and fish community structure, abundance, and biomass.

## 6.2 Methods

### 6.2.1 Field Sampling and Taxonomic Identifications

A total of 44 successful trawls were sampled for epibenthos in 2014 (26 stations) and 2015 (18 stations) at depths ranging from 3-302 m (Figure 101, Table 30). In both years, a second trawl was collected at eight stations because the first trawl sample collected was deemed non-quantitative (based on the time-depth recorder (TDR)-profile and trawl content) or too small (not representative of the present fauna). Epibenthos and fishes were sampled from trawls using a modified 3-m PSBT-A with 7 mm mesh and 4 mm cod end liner and bottom roller gear to avoid penetration of the foot rope into the typically soft, muddy sediment on the shelf. Start and end time stamps of the bottom trawling were taken to later be matched with specific latitude and longitudes from the ship records. The net was also affixed with a TDR (Star Oddi) that provides a detailed profile of bottom time of the trawl.

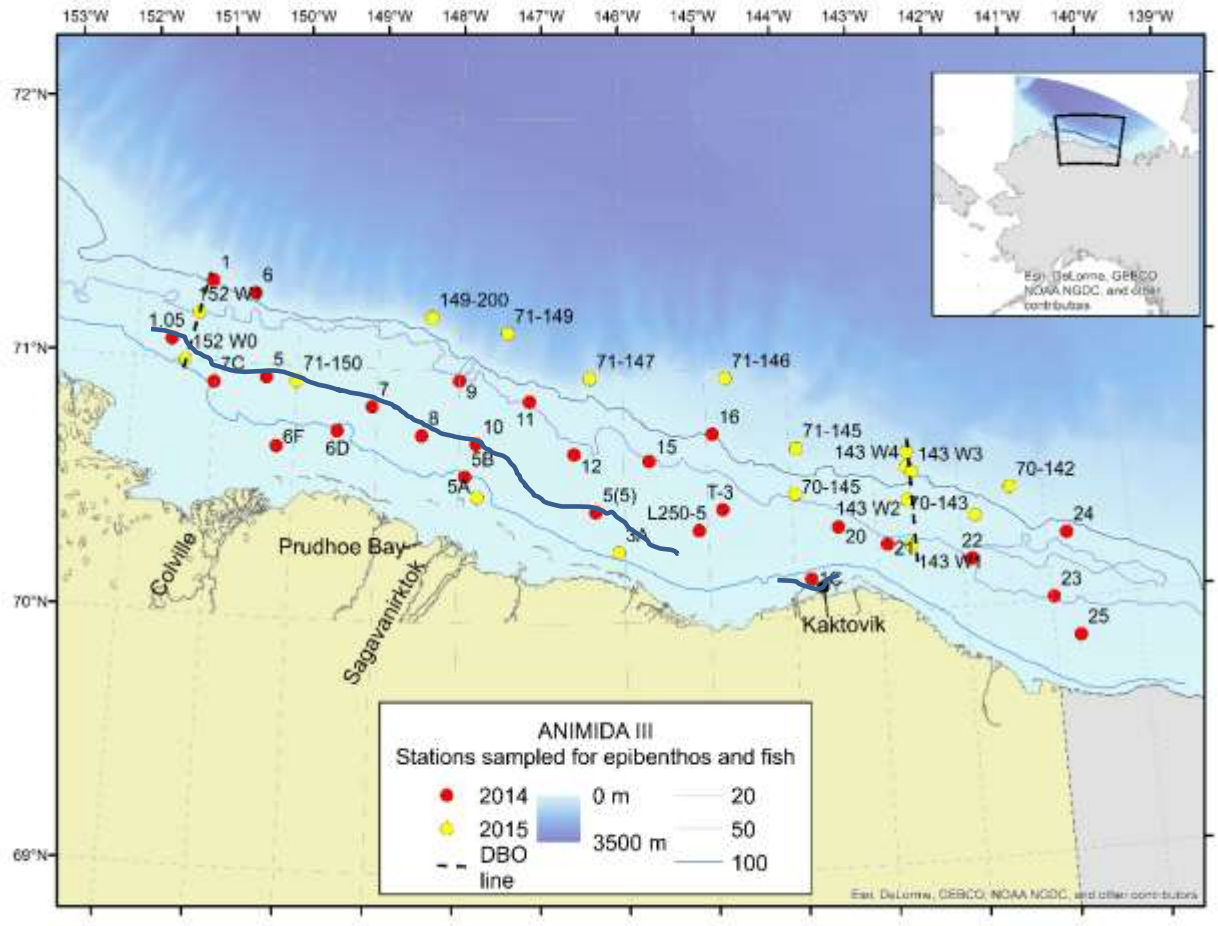


**Figure 101. Stations sampled for epibenthos in 2014 and 2015 during the ANIMIDA III research project. [2]**

[2] DBO lines correspond to Distributed Biological Observatory lines established during the course of ANIMIDA III sampling. Note that the original 20 m isobath mapped does not exactly match the actual depths measured during ANIMIDA III, specifically more stations had actual depths <20 m (see Table 30) and a revised 20 m isobath is therefore suggested (thick blue line). This is relevant for the interpretation of community structure.

**Table 30. Stations sampled for epibenthos and fish during ANIMIDA III.**

**Latitude in decimal degrees North, longitude in decimal degrees West. Depth in meters. Stations within the 20 m isobath are printed in bold. Cluster groups relate to cluster analysis results.**

| Station | Date | Latitude | Longitude | Depth | Cluster groups | |
|---|---|---|---|---|---|---|
| | | | | | Epibenthos | Fish |
| 1 | 6-Aug-14 | 71.32 | -151.10 | 64 | c | c |
| 1.05 | 6-Aug-14 | 71.08 | -151.56 | **16** | m | a |
| 1C | 4-Aug-14 | 70.15 | -143.80 | 24 | d | b |
| 5 | 6-Aug-14 | 70.95 | -150.37 | **19** | o | b |
| 5(5) | 1-Aug-14 | 70.44 | -146.34 | **19** | n | b |
| 5B | 7-Aug-14 | 70.58 | -147.92 | **17** | o | b |
| 6 | 6-Aug-14 | 71.28 | -150.56 | 54 | c | c |
| 6D | 31-Jul-14 | 70.75 | -149.48 | 19 | o | b |
| 6F | 5-Aug-14 | 70.68 | -150.21 | **13** | o | b |
| 7 | 31-Jul-14 | 70.85 | -149.06 | 25 | d | b |
| 8 | 31-Jul-14 | 70.74 | -148.45 | **19** | n | b |
| 9 | 5-Aug-14 | 70.96 | -148.00 | 36 | d | c |
| 10 | 1-Aug-14 | 70.71 | -147.79 | 24 | l | c |
| 11 | 5-Aug-14 | 70.88 | -147.14 | 44 | d | b |
| 12 | 5-Aug-14 | 70.67 | -146.60 | 39 | d | c |
| 15 | 4-Aug-14 | 70.64 | -145.69 | 40 | f | c |
| 16 | 4-Aug-14 | 70.74 | -144.92 | 61 | e | c |
| 20 | 2-Aug-14 | 70.35 | -143.45 | 39 | e | b |
| 21 | 2-Aug-14 | 70.27 | -142.88 | 39 | e | c |
| 22 | 2-Aug-14 | 70.19 | -141.89 | 35 | e | c |
| 23 | 3-Aug-14 | 70.01 | -140.97 | 35 | e | c |
| 24 | 3-Aug-14 | 70.26 | -140.75 | 52 | e | c |
| 25 | 3-Aug-14 | 69.85 | -140.70 | 23 | e | c |
| 143-W1 | 3-Aug-15 | 70.26 | -142.60 | 37 | f | c |
| 143-W2 | 3-Aug-15 | 70.44 | -142.61 | 45 | g | c |
| 143W-3 | 4-Aug-15 | 70.55 | -142.54 | 100 | h | c |
| 143-W4 | 4-Aug-15 | 70.57 | -142.60 | 151 | h | a |
| 143-W5 | 4-Aug-15 | 70.63 | -142.58 | 302 | a | a |
| 149-200 | 6-Aug-15 | 71.21 | -148.35 | 200 | b | a |
| 152-W0 | 1-Aug-15 | 71 | -151.38 | **13** | o | a |
| 152-W1 | 1-Aug-15 | 71.19 | -151.25 | 36 | i | a |
| 3A | 2-Aug-15 | 70.28 | -146.07 | **3** | j | b |
| 5A | 2-Aug-15 | 70.5 | -147.77 | **9** | k | a |

| Station | Date | Latitude | Longitude | Depth | Cluster groups | |
|---|---|---|---|---|---|---|
| | | | | | Epibenthos | Fish |
| 70-142 | 4-Aug-15 | 70.46 | -141.38 | 62 | g | C |
| 70-143 | 4-Aug-15 | 70.36 | -141.82 | 54 | f | c |
| 70-145 | 5-Aug-15 | 70.49 | -143.95 | 43 | g | c |
| 71-145 | 5-Aug-15 | 70.67 | -143.91 | 96 | g | C |
| 71-146 | 5-Aug-15 | 70.96 | -144.74 | 399 | a | a |
| 71-147 | 6-Aug-15 | 70.97 | -146.40 | 107 | g | c |
| 71-149 | 6-Aug-15 | 71.15 | -147.41 | 62 | g | c |
| 71-150 | 1-Aug-15 | 70.94 | -150.00 | **15** | o | b |
| 7C | 6-Aug-14 | 70.92 | -151.01 | **10** | o | b |
| L250-5 | 1-Aug-14 | 70.36 | -145.11 | 30 | d | b |
| T-3 | 2-Aug-14 | 70.44 | -144.82 | 38 | f | c |

Epibenthic invertebrates were sorted from the full catch to lowest taxonomic level practical on board when feasible, or else from a well-mixed subsample of the catch. Fishes were always collected from the entire haul. Counts and wet weight per taxon were determined on board using digital hanging scales. Invertebrate vouchers were preserved in a 4% formalin-seawater solution buffered with hexamethylenetetramine for later confirmation of species identifications with taxonomic specialists. Fishes were frozen. Field identifications were based on the at-sea team's experience of working in the Pacific Arctic for over a decade, and a variety of taxonomic identification literature. The taxon names used were standardized to the World Register of Marine Species, the most widely accepted standard for current names of marine species. The matching was done using the match function available on the WoRMS web site. Individuals with uncertain taxonomic identity were sent to taxonomic experts for improved or corrected identification. The following taxonomists were consulted: Linda Cole for ascidians, Ken Coyle for amphipods (UAF), Nora Foster for mollusks (NRF Taxonomic Services, Fairbanks), Max Hoberg for polychaetes (UAF), Monika Kedra for sipunculans (Institute of Oceanology, Polish Academy of Sciences), and Chris Mah for sea stars (Smithsonian Institution). A few specimens of sea spiders, *Pycnogonida*, were also sent out, but identifications have not been received yet. Several taxa remained at the higher taxa level such as *Nemertea*.

When describing the results, we refer to nearshore stations as those up to 20 m deep, shelf stations as those >20 to 99 m, and shelf break stations as those >100 m deep. We refer to the western study area as covering the area up to the Sagavanirktok River delta. Environmental context data used in our analysis included bottom water temperature and salinity from CTD deployments (see section 2 of the report for details). Sediment chl-*a*, grain size, and sediment isotope and organic content data were obtained from grab samples as available (see section 2 for details).

### 6.2.2 Data Analysis

Approximate faunal densities can be calculated from trawl size, trawling time on the bottom, and trawling speed (Holme and McIntyre, 1984). The coordinates and TDR data together with ship speed during towing allowed us to calculate towed area and calculate abundance and biomass for epibenthic invertebrates and fishes. Patterns in epibenthic biomass is emphasized in this report more than abundance

patterns because biomass data include colonial taxa such as sponges, hydrozoans, bryozoans, ascidians, etc., which cannot be enumerated as individuals and are thus excluded from abundance assessments. Hence, biomass patterns present a more complete picture of the communities and will be the primary focus although most analyses will be presented for both metrics. For all following analyses, we excluded taxa from the haul data that were pelagic (such as jelly fish and euphausiids) or clearly infaunal (i.e., living inside rather than on top of the sediment such as most clams and various polychaetes) because they were neither the target fauna nor caught quantitatively with the trawl. Pelagic taxa occasionally get caught in the trawl while the net gets deployed through the water column and infauna occasionally gets caught when the net digs into the upper sediment layer (which is ideally avoided). In some cases, we combined several species from a genus or closely related genera where field notes or voucher identifications suggested doubtful or inconsistent identifications at the species level. Abundance and biomass data were standardized to 100 $m^2$ for visualization of community patterns and statistical analysis. Mapping of the spatial distribution of total abundance, biomass, number of taxa, and diversity indices per station, relative proportion of representative taxa within each phylum for epibenthos and families for fish, and significant clusters were performed using ArcGIS (ArcMap 13). Total abundance and biomass data were projected onto maps by scaled circles, with breaks determined by Jenks' natural breaks.

For multivariate statistical analysis, a square-root transformation was applied to reduce the influence of taxa with very large abundance or biomass. Community structure analysis for epibenthos and fish were completed primarily using multivariate statistics programs within the software package Primer-e V7 (Clarke and Gorley, 2015). Diversity indices, Shannon-Wiener's diversity ($H' = -\Sigma\ Pi\ \log_e(Pi)$), Margalef's Richness ($d = (S-1)/\log_e N$), and Pielou's Evenness ($J' = H'/\log_e S$), were calculated from biomass (gww/100 $m^2$) for all stations using the DIVERSE routine in Primer-e V7. Pi is the proportion of individuals belonging to the ith species, S is taxon richness (in most cases at species level), and N is the total number of individuals in the sample.

To determine the taxa that best explain the pattern of the epifaunal community across all stations, the Biological Variables Stepwise Procedure (BVSTEP) was used separately on the abundance and biomass data, using a Bray-Curtis resemblance matrix and Spearman rank correlation. The BVSTEP procedure employs a step wise approach, searching for high rank correlations between a faunal data matrix and a Bray-Curtis similarity matrix. Community cluster analysis, calculated with biomass data for epibenthos and abundance data for fish, provided station grouping by similarity, using group averaging based on Bray-Curtis resemblance matrix. The Similarity Profile (SIMPROF) test detected the statistical significance of the internal structure at each node of the dendrogram. Patterns in community structure were visualized in non-metric multidimensional scaling (nMDS) plots. A 2D stress level of up to 0.2 was deemed acceptable. The Similarity Percentages (SIMPER) analysis was used to identify indicator taxa for communities within each significant cluster. Community differences were assessed for pre-determined depth groups using 1-way Analysis of Similarities (ANOSIM) with three levels (<20 m is nearshore highest disturbance area, 21-99 is mid-shelf, and >100 m is shelf break). ANOSIM yields global R values that are a measure of scaled separation between groups and that can be directly compared to assess the relative importance of various factors on community composition. R values range from 0 to 1 with smaller values indicating a factor has little influence and R-values above ~0.45 being considered biologically relevant (Clarke and Gorley, 2015). Standardized biomass, abundance, and diversity measures per station were analyzed for depth and longitudinal trends using linear regressions in R (www.r-project.org, V2.15.0).

Epibenthic and fish community structure were each matched with environmental variables (based on square-root transformed biomass and abundance data) to assess which variable combination was most influential in determining community composition. Analysis was done using the BEST routine, which employs Spearman rank correlations. The following environmental variables were used and kindly provided by ANIMIDA III collaborators: latitude and longitude (as indirect variables indicating geographic location); bottom salinity, bottom temperature, fluorescence, and turbidity (as hydrographic indicators); sediment chl-*a* (µg/g sediment d. wt., log-transformed), C:N ratio, TON, and TOC in the sediment (as indirect indicators of food availability and quality); and % gravel (square-root transformed), % sand, % mud (% silt and % clay combined) of the sediment (as descriptors of sediment type). Additional variables included bottom water nutrient concentrations ($PO_4$, $SiO_4$, $NO_2$, and $NH_4$). Methods for measuring all these variables are described in the respective sections of the ANIMIDA III report. In all analyses, environmental variables were normalized to bring them to the same measurement scale. Combinations of up to five variables were considered, and the combination producing the highest correlation coefficient was considered the best match to the biological matrix.

## 6.3 Results

### 6.3.1 Invertebrates

A total of 44 stations was sampled for invertebrate community structure (Table 30). The total abundance per station ranged from 10 ind/100 $m^2$ (station 152-W0) to 5,063 ind/100 $m^2$ (station 70-142) with a mean of 676 ind/100 $m^2$ (SD: 987) (Figure 102, Table 31). Abundance was lowest in the western part of the study area and at most nearshore stations, except near Kaktovik. Abundance was highest on the middle shelf in the central part of the study area up to Kaktovik and at several shelf break stations. The total biomass per station ranged from 5.0 gww/100 $m^2$ (station 152-W0) to 3,964.3 gww/100 $m^2$ (station 15) with a mean of 375.8 gww/100 $m^2$ (SD: 654.8) (Figure 103). As with abundance, biomass was generally lower in the western part of the study area and at nearshore stations. Biomass was higher at some mid-shelf stations and on the outer shelf northeast of Kaktovik.

The number of taxa per station ranged from five (station 5A) to 53 (station 22) with a mean of 30 (SD: 12) (Figure 104). The number of taxa was generally lowest at nearshore stations, in particular in the western study area. Taxa numbers were highest at some shelf break stations, and at most stations in the eastern part of the study area. Shannon Diversity Index ranged from < 0.1 (station 5A) to 3.1 (station 25) with a mean of 1.9 (SD: 0.7, Figure 105, Table 31). Margalef's Richness Index ranged from 0.7 (station 5A) to 6.6 (station 22) with a mean of 4.9 (SD: 1.4, Figure 106, Table 31). Pielou's Evenness index ranged from 0.1 (station 5A) to 0.8 (station 10) with a mean of 0.6 (SD: 0.2, Figure 107, Table 31). In general, diversity indices had stations with high and low values throughout the study region. Stations with the lowest values for all indices were mostly in the central and western areas (Figure 105 through Figure 107).

**Table 31. Station metrics for epibenthos and fish during ANIMIDA III.**

| Station | Epibenthos | | | | | | Fish | | | | |
|---|---|---|---|---|---|---|---|---|---|---|---|
| | Abu. | Bio. | Taxa | Shan. | Mar. | Piel. | Abu. | Taxa | Shan. | Mar. | Piel. |
| 1 | 60.40 | 204.03 | 45 | 2.55 | 5.77 | 0.67 | 3.26 | 7 | 1.63 | 1.72 | 0.84 |
| 1.05 | 31.82 | 9.44 | 17 | 1.80 | 3.52 | 0.63 | 2.68 | 3 | 0.49 | 0.61 | 0.44 |
| 10 | 1248.33 | 211.47 | 17 | 2.31 | 2.09 | 0.81 | 4.21 | 5 | 1.15 | 1.07 | 0.71 |
| 11 | 308.11 | 234.18 | 41 | 2.25 | 5.16 | 0.61 | 1.99 | 5 | 1.47 | 1.34 | 0.91 |
| 12 | 1488.19 | 445.68 | 41 | 2.49 | 4.76 | 0.67 | 2.71 | 8 | 1.93 | 2.12 | 0.93 |
| 15 | 1297.09 | 3964.26 | 37 | 0.45 | 3.40 | 0.13 | 5.64 | 8 | 1.83 | 1.74 | 0.88 |
| 16 | 1181.82 | 274.89 | 25 | 2.35 | 3.03 | 0.73 | 4.17 | 9 | 1.94 | 2.15 | 0.88 |
| 1C | 712.33 | 371.49 | 31 | 2.11 | 3.65 | 0.62 | 2.34 | 6 | 1.74 | 1.59 | 0.97 |
| 20 | 1416.32 | 318.96 | 26 | 1.98 | 3.10 | 0.61 | 2.84 | 5 | 1.33 | 1.20 | 0.82 |
| 21 | 733.38 | 263.26 | 40 | 2.61 | 4.95 | 0.71 | 4.23 | 10 | 2.03 | 2.40 | 0.88 |
| 22 | 702.00 | 258.07 | 53 | 2.93 | 6.62 | 0.74 | 3.45 | 6 | 1.28 | 1.41 | 0.71 |
| 23 | 644.98 | 459.41 | 35 | 2.54 | 4.03 | 0.71 | 3.10 | 6 | 1.55 | 1.46 | 0.86 |
| 24 | 468.34 | 245.71 | 38 | 2.87 | 4.74 | 0.79 | 1.48 | 4 | 1.28 | 1.11 | 0.92 |
| 25 | 381.60 | 134.62 | 45 | 3.05 | 6.11 | 0.80 | 6.89 | 8 | 1.56 | 1.65 | 0.75 |
| 5 | 66.95 | 53.44 | 30 | 2.12 | 4.62 | 0.62 | 6.17 | 6 | 1.16 | 1.21 | 0.65 |
| 5(5) | 215.90 | 50.20 | 37 | 2.39 | 5.79 | 0.66 | 6.36 | 10 | 1.90 | 2.17 | 0.82 |
| 5B | 65.53 | 34.54 | 31 | 2.63 | 5.13 | 0.76 | 3.51 | 4 | 0.89 | 0.84 | 0.64 |
| 6 | 160.17 | 646.98 | 43 | 1.58 | 4.79 | 0.42 | 6.13 | 8 | 1.85 | 1.70 | 0.89 |
| 6D | 92.96 | 63.79 | 28 | 1.79 | 4.18 | 0.54 | 3.23 | 6 | 1.44 | 1.44 | 0.80 |
| 6F | 99.15 | 290.49 | 14 | 0.49 | 1.63 | 0.18 | 2.60 | 3 | 0.89 | 0.61 | 0.81 |
| 7 | 90.36 | 57.94 | 41 | 2.48 | 6.29 | 0.67 | 2.01 | 6 | 1.58 | 1.67 | 0.88 |
| 7C | 52.57 | 41.75 | 14 | 1.16 | 2.15 | 0.44 | 12.31 | 5 | 0.77 | 0.83 | 0.48 |
| 8 | 80.99 | 19.74 | 28 | 2.49 | 5.11 | 0.75 | 2.71 | 3 | 0.94 | 0.61 | 0.86 |
| 9 | 137.60 | 142.37 | 25 | 0.91 | 3.31 | 0.28 | 3.86 | 7 | 1.81 | 1.64 | 0.93 |
| L250-5 | 380.02 | 146.99 | 46 | 2.18 | 6.17 | 0.57 | 1.36 | 4 | 1.20 | 1.15 | 0.86 |
| T-3 | 1892.19 | 845.75 | 29 | 1.52 | 3.10 | 0.45 | 4.57 | 9 | 1.64 | 2.09 | 0.75 |
| 143-W1 | 876.29 | 775.71 | 49 | 2.15 | 5.36 | 0.55 | 1.92 | 5 | 1.17 | 1.36 | 0.73 |
| 143-W2 | 665.49 | 652.80 | 29 | 1.71 | 3.19 | 0.51 | 7.35 | 9 | 1.44 | 1.86 | 0.65 |
| 143W-3 | 2136.81 | 1886.99 | 37 | 1.85 | 3.66 | 0.51 | 6.17 | 7 | 1.40 | 1.46 | 0.72 |
| 143-W4 | 513.67 | 251.90 | 37 | 2.38 | 4.60 | 0.66 | 2.16 | 6 | 1.66 | 1.63 | 0.93 |
| 143-W5 | 174.96 | 228.72 | 18 | 2.13 | 2.20 | 0.74 | 1.52 | 2 | 0.60 | 0.37 | 0.86 |
| 149-200 | 1896.95 | 848.81 | 26 | 1.58 | 2.76 | 0.49 | 2.38 | 7 | 1.36 | 1.89 | 0.70 |
| 152-W0 | 10.02 | 5.03 | 14 | 1.83 | 3.32 | 0.69 | 0.85 | 3 | 1.04 | 0.93 | 0.95 |
| 152-W1 | 10.97 | 6.47 | 20 | 2.06 | 4.56 | 0.69 | 0.70 | 6 | 1.75 | 2.57 | 0.98 |
| 3A | 56.52 | 12.97 | 24 | 2.04 | 4.73 | 0.64 | 1.22 | 2 | 0.67 | 0.40 | 0.97 |
| 5A | 20.81 | 31.72 | 5 | 0.09 | 0.69 | 0.06 | 0.14 | 1 | 0.00 | 0.00 | NA |

| Station | Epibenthos | | | | | | Fish | | | | |
|---|---|---|---|---|---|---|---|---|---|---|---|
| | Abu. | Bio. | Taxa | Shan. | Mar. | Piel. | Abu. | Taxa | Shan. | Mar. | Piel. |
| 70-142 | 5062.92 | 417.54 | 34 | 2.09 | 3.96 | 0.59 | 4.00 | 6 | 1.65 | 1.36 | 0.92 |
| 70-143 | 3671.57 | 1546.62 | 45 | 2.42 | 4.56 | 0.64 | 5.93 | 8 | 1.82 | 1.71 | 0.88 |
| 70-145 | 277.84 | 206.22 | 35 | 1.36 | 4.46 | 0.38 | 1.32 | 9 | 1.96 | 3.10 | 0.89 |
| 71-145 | 348.33 | 171.66 | 36 | 2.43 | 4.70 | 0.68 | 4.29 | 7 | 1.62 | 1.60 | 0.83 |
| 71-146 | 38.64 | 61.84 | 23 | 1.58 | 3.42 | 0.50 | 0.36 | 3 | 1.08 | 1.56 | 0.98 |
| 71-147 | 515.64 | 339.61 | 32 | 1.76 | 3.81 | 0.51 | 3.37 | 7 | 1.77 | 1.71 | 0.91 |
| 71-149 | 1366.63 | 313.74 | 45 | 1.90 | 5.47 | 0.50 | 2.68 | 5 | 1.15 | 1.22 | 0.72 |
| 71-150 | 19.75 | 19.88 | 20 | 1.98 | 3.59 | 0.66 | 1.15 | 6 | 1.29 | 2.05 | 0.72 |

Abu.: abundance in individuals/100 $m^2$. Bio.: biomass in gram wet weight /100 $m^2$. Taxa: total number of taxa per station. Shan.: Shannon Diversity index. Mar.: Margalef's Richness index. Piel.: Pielou's Evenness index.

Across all stations, a total of 247 taxa were identified in 10 phyla. 69.6% were identified to species level, 17.8% to genus level, and the remaining 12.6% to higher taxonomic levels. *Arthropoda* had the highest number of taxa accounting for 85 taxa (34% of the total taxon number), followed by *Mollusca* with 71 taxa (29% of the total taxon number), and *Echinodermata* with 33 taxa (13% of the total taxon number). All other phyla accounted each for less than 10% of the total taxa (Figure 108). Composition within phyla by abundance and biomass showed a different picture than composition by taxa. In terms of abundance, excluding all colonial organisms, taxa in the phylum *Echinodermata* accounted for 70% of the total abundance, *Arthropoda* accounted for 15% of the total abundance, *Mollusca* accounted for 14% of the total abundance, and the taxa of all other phyla amounted each to less than ≤ 1% of the total abundance (Figure 108). In terms of biomass, *Echinodermata* represented 62%, *Mollusca* to 13%, and *Arthropoda* to 12% of the total biomass across all groups, and all other groups each amounted to less than 10% of the total biomass (Figure 108). Spatially, stations in the east had the three major Phyla (*Arthropoda, Mollusca,* and *Echinodermata*) more evenly represented in terms of number of taxa, while stations in the in the west had a higher proportion of taxa in the Phylum *Arthropoda* (Figure 109). In terms of abundance and biomass, western stations were dominated by arthropods while eastern stations were dominated by echinoderms (Figure 110 and Figure 111).

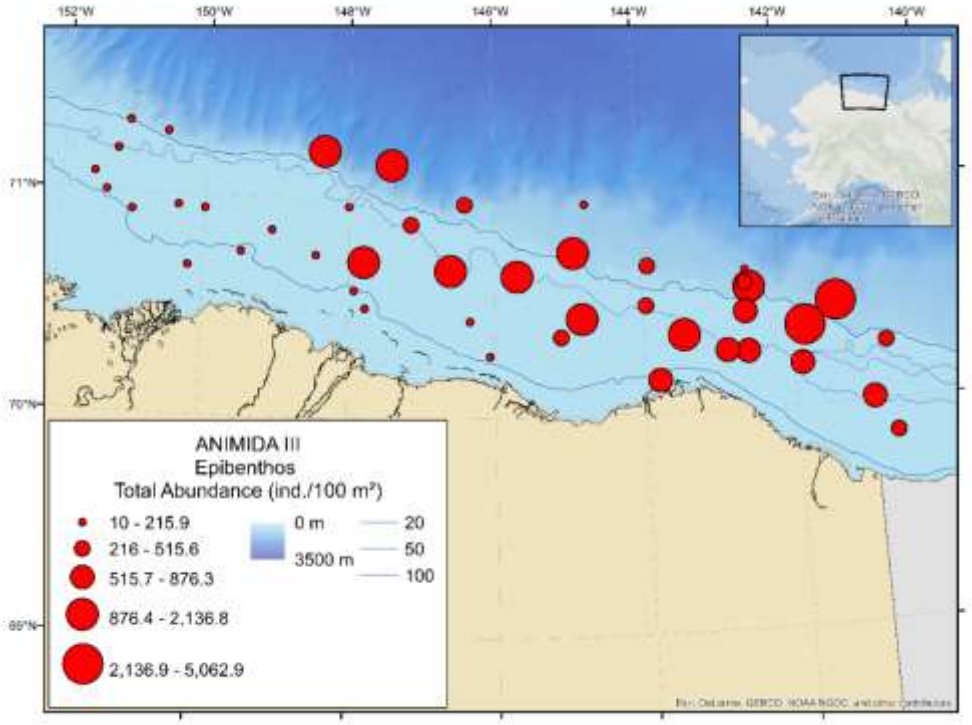


**Figure 102. Total epibenthic abundance per station measured in number of individuals per 100 m$^2$.**

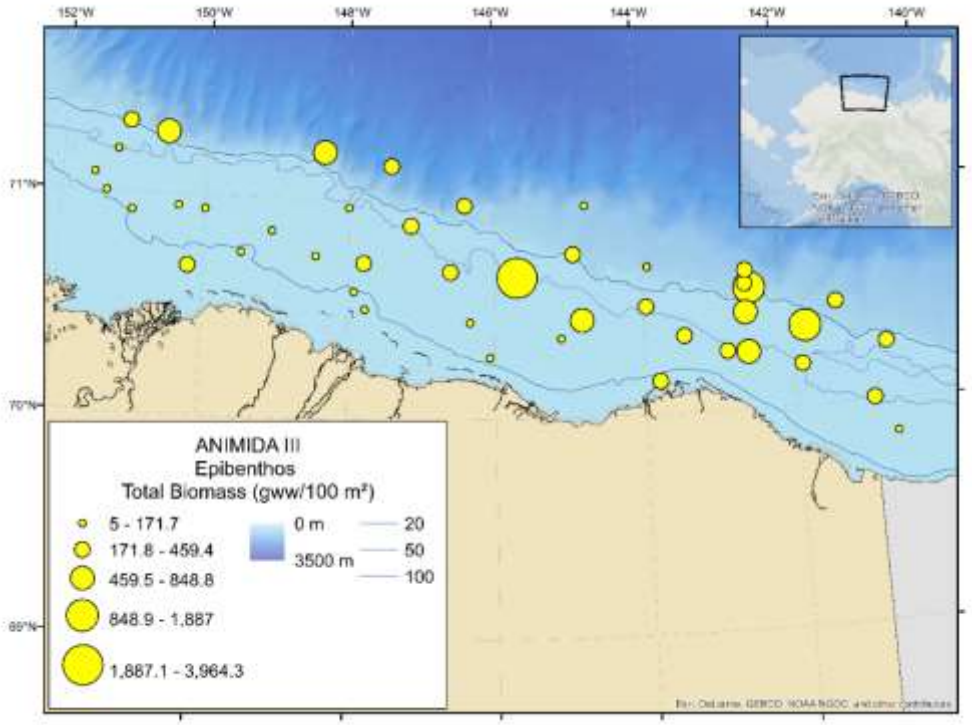


**Figure 103. Total epibenthic biomass per station measured in grams of wet weight per 100 m$^2$.**

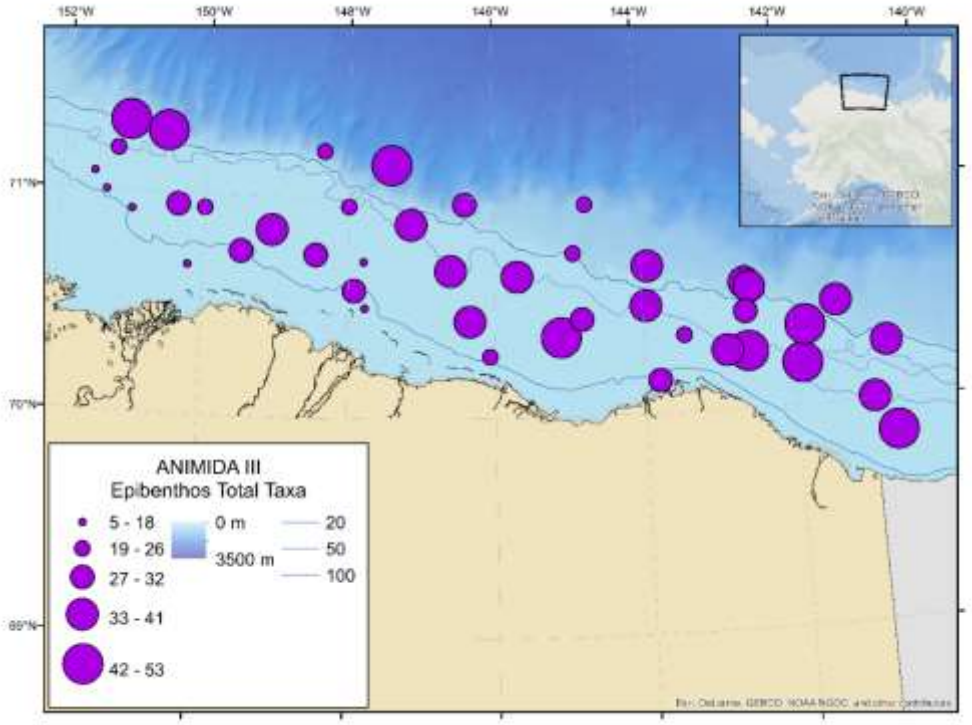


**Figure 104. Total number of epibenthic taxa per station. Most taxa were identified to species level.**

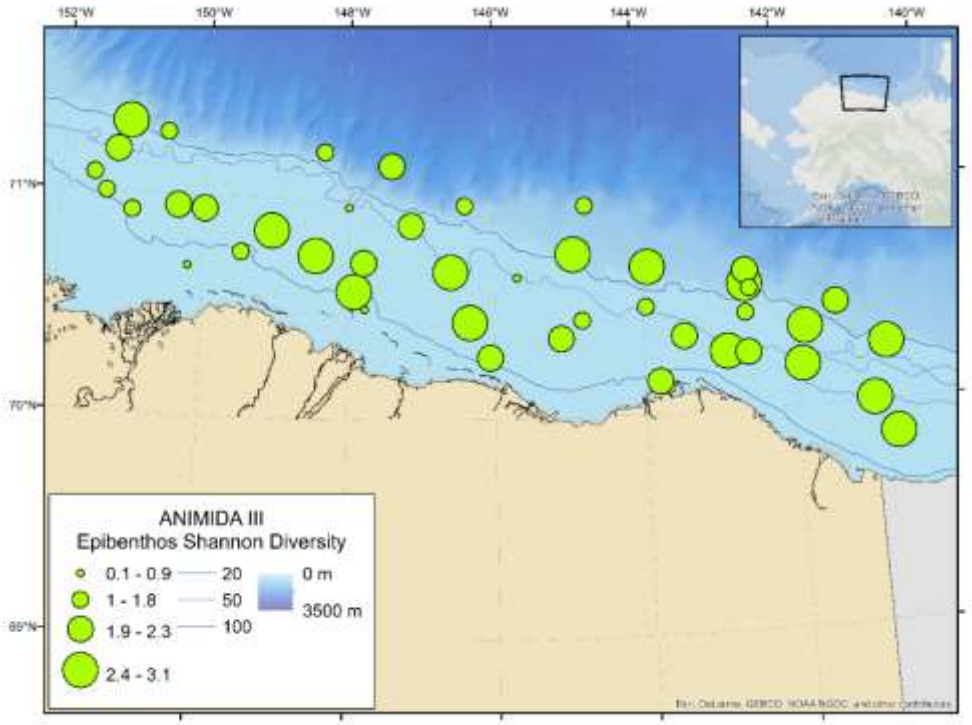


**Figure 105. Epibenthos: Shannon Diversity values per station.**

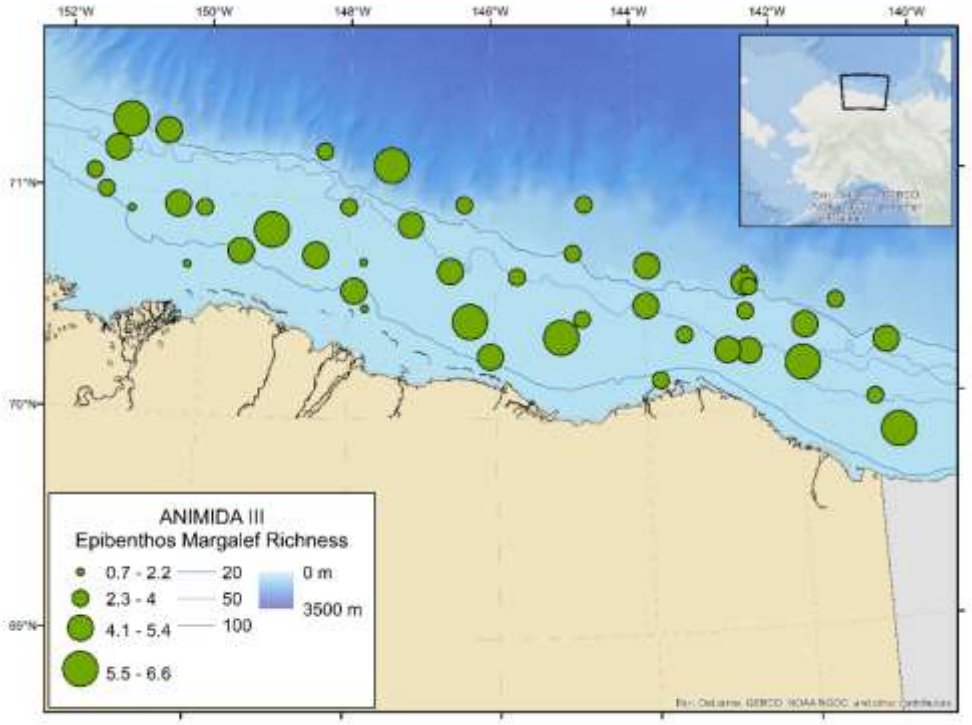


**Figure 106. Epibenthos: Margalef's Richness values per station.**

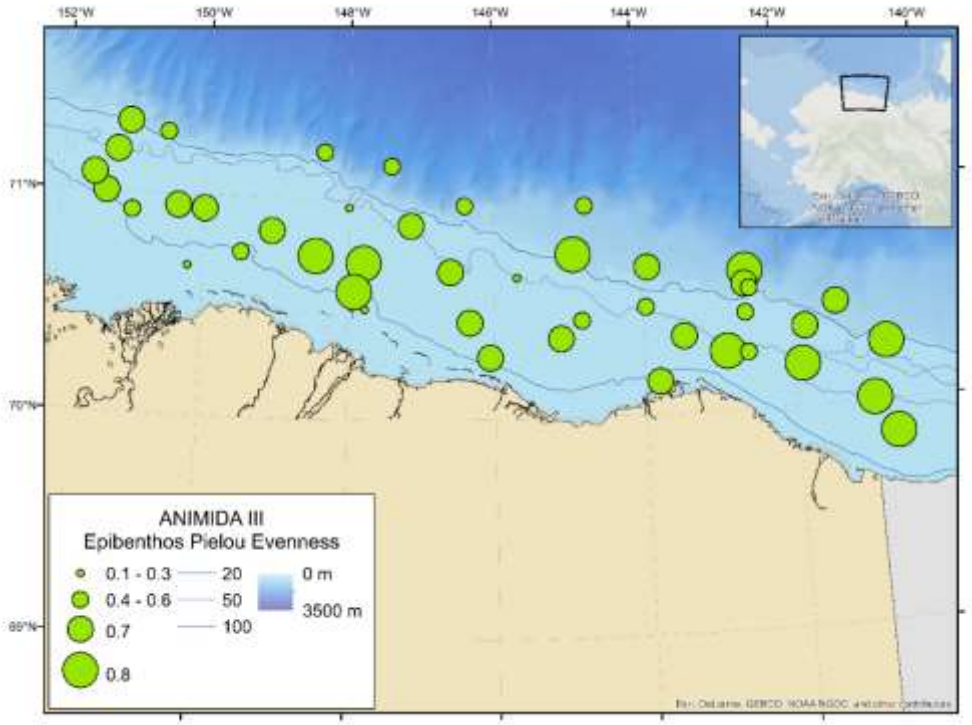


**Figure 107. Epibenthos: Pielou's Evenness values per station.**

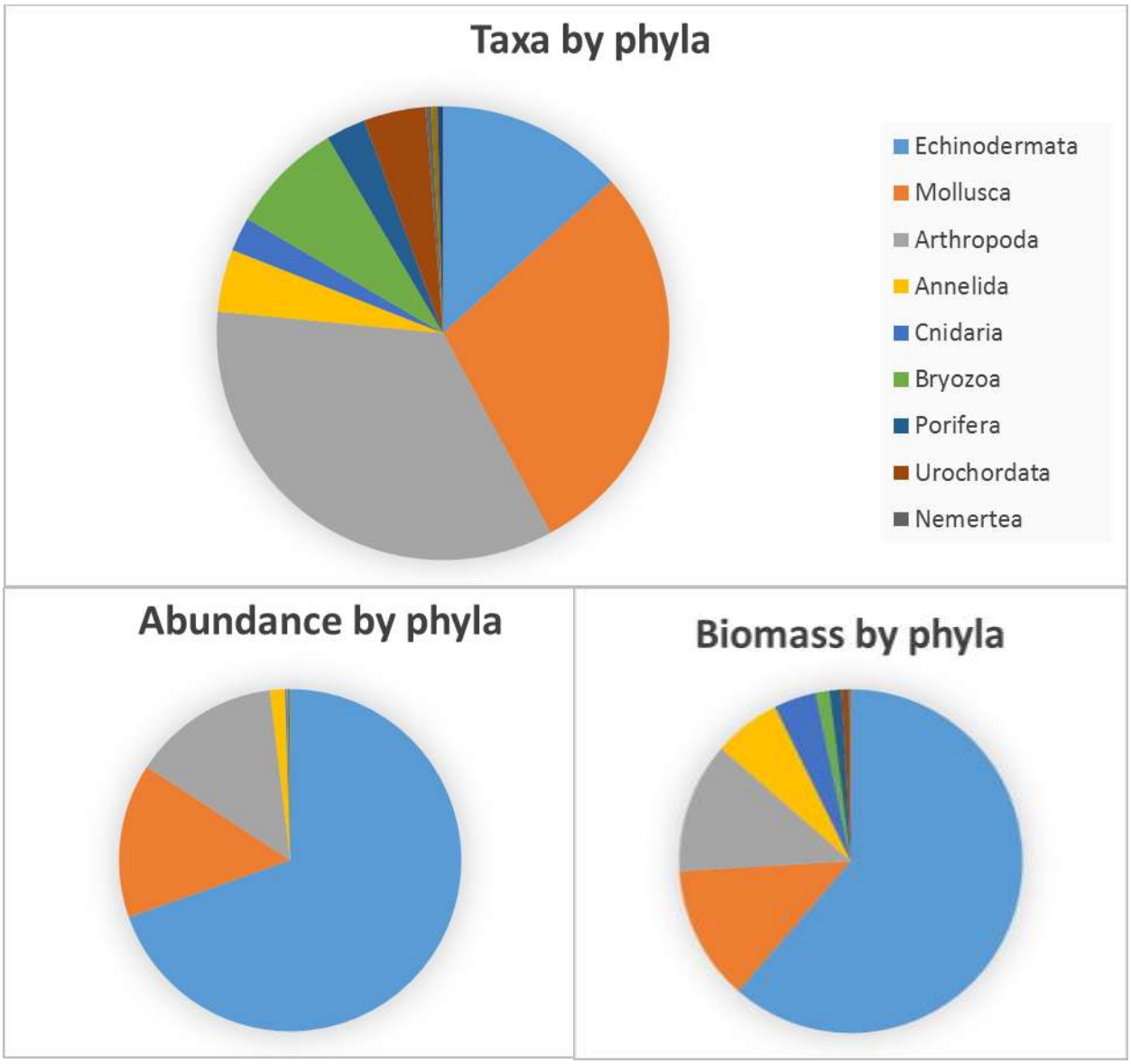


**Figure 108. Relative proportion of the number of epibenthic taxa in each phylum by species number (top panel), total abundance (bottom left), and total biomass (bottom right).**

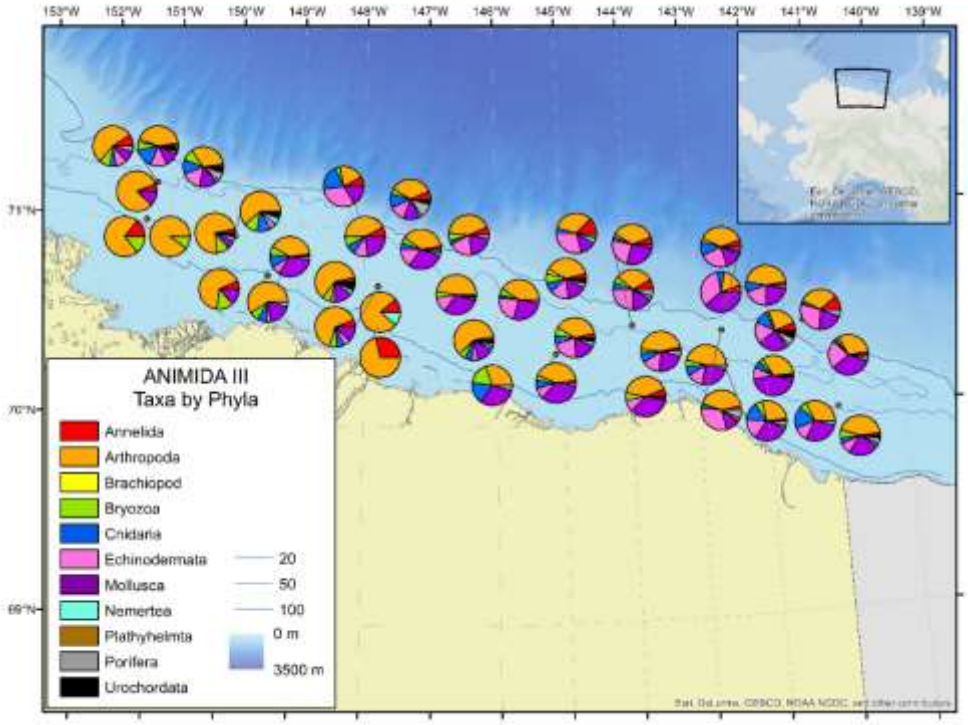


**Figure 109. Proportion of epibenthic taxa by phyla at each station.**

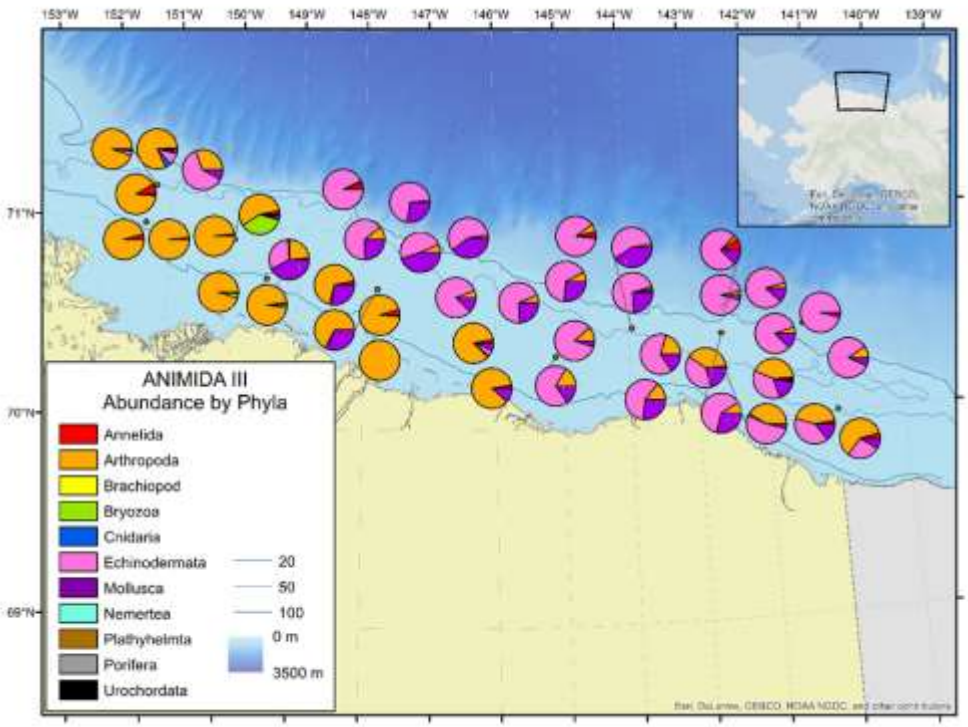


**Figure 110. Proportion of epibenthic abundance by phyla at each station.**

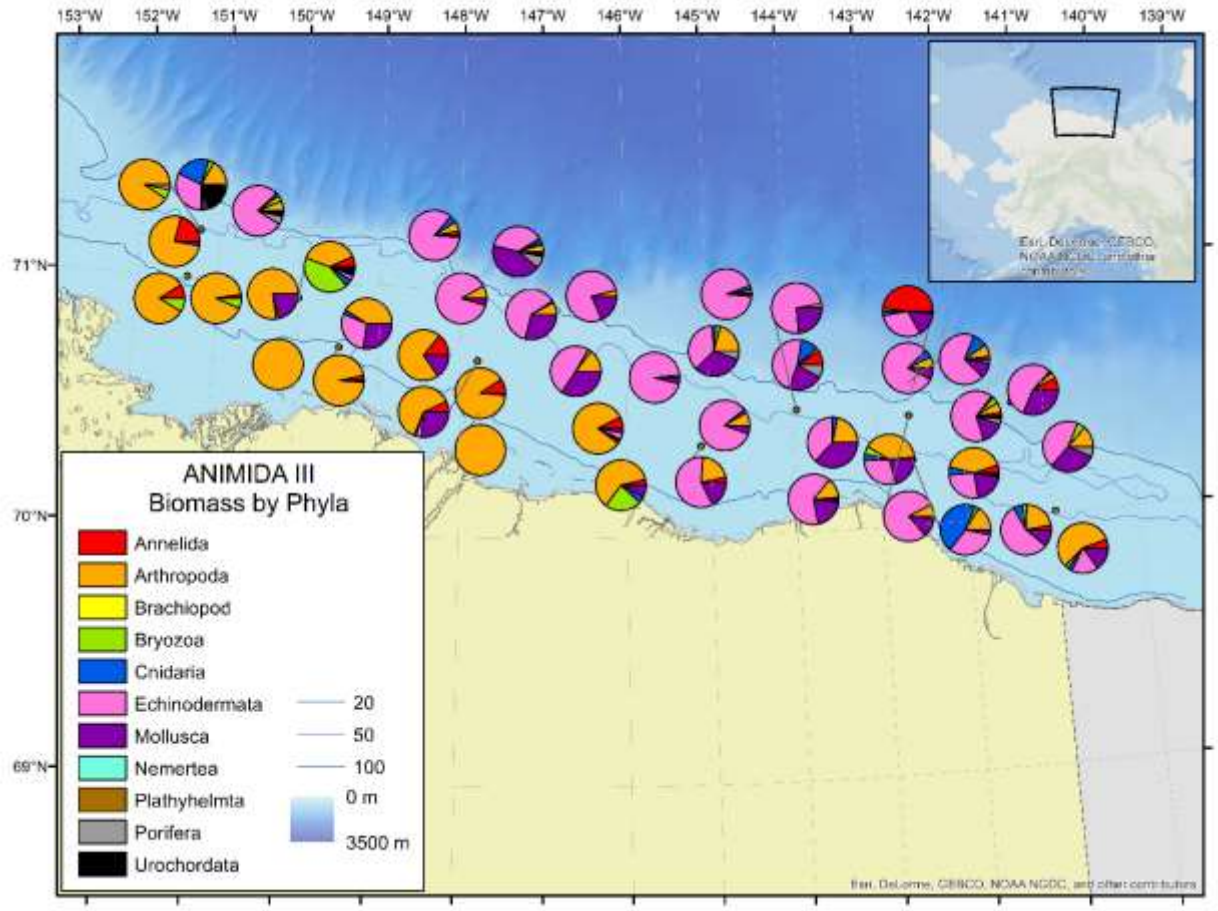


**Figure 111. Proportion of epibenthic biomass by phyla at each station.**

Within each phylum, the proportion of number of taxa, abundance, and biomass were dominated by different classes, respectively. Within the arthropods, amphipods contributed 46% to the total taxa (Figure 112), while cumaceans contributed 46% of the total abundance (Figure 113). Decapods and isopods contributed 35% and 31% of the total biomass, respectively (Figure 114). Within the mollusks, gastropods contributed 80% of all mollusk species and of the total biomass (Figure 115), while bivalves contributed 82% of the total abundance (Figure 116, Figure 117). Within the echinoderms asteroids contributes 43% of the total number of taxa (Figure 118), while ophiuroids contributed 98% of the total abundance (Figure 119), and holothurians contributed 57% of the total biomass (Figure 120). The differences in dominance between abundance and biomass are obviously related to the difference in body size and weight of individuals of a given species.

The nine taxa representing the community for epibenthic abundance were, in order of importance, the amphipod *Acanthostepheia behringiensis*, the cumeaceans *Diastylis alaskensis* and *Diastylis scorpioides*, the shrimp *Eualus gaimardii*, the brittle star *Ophiocten sericeum*, the amphipod *Paroediceros lynceus*, the shrimp *Sabinea septemcarinata*, the isopod *Saduria entomon*, and the bivalve *Similipecten greenlandicus* (Best analysis correlation 0.95, Figure 115). Of these, *Ophiocten sericeum* and S*imilpecten greenlandicus* were the most abundant species in the central and eastern parts of the study area.

*Acanthostepheia behringiensis* and *Saduria entomon* were most abundant at nearshore stations in the western study area. In terms of biomass, the 14 taxa selected as community representatives were, in order of importance, the amphipod *Acanthostepheia behringiensis*, the shrimp *Eualus gaimardii*, the brittle stars *Ophiacantha bidentata* and *Ophiocten sericeum*, the amphipod *Paroediceros lynceus*, the polychaete family *Polynoidae*, the sea cucumber *Psolus peronii*, the shrimp *Sabinea septemcarinata*, the isopod *Saduria entomon*, the bivalve *Similipecten greenlandicus*, the isopod *Synidotea bicuspida*, the sea star *Urasterias lincki*, the polycheate *Pista estevanica*, and the sea star *Pontaster tenuispinus* (Best analysis correlation 0.91, Figure 116). As with abundance, *Acanthostepheia behringiensis* and *Saduria entomon* were most biomass-rich at nearshore stations in the western study area. *Psolus peronii* dominated biomass at several shelf stations in the central and eastern study area, while a variety of stations contributed to the remaining stations.

Cluster analysis, performed on the epibenthic biomass data set, resulted in a large number of nine significant clusters and six independent stations (Figure 117). Cluster groups contained two to seven stations each with an average similarity within clusters of 44.4% (SD: 4.8). Similarity within clusters ranged from 35.6 to 58.6% (Table 32). The most geographically contiguous cluster groups in the MDS plot (cluster o) corresponded to the western shallow stations (light blue in Figure 118). Several other clusters characterized the shelf: mostly western shelf stations (orange cluster), central (dark blue), and eastern (light green) stations grouped together with some geographic overlap. Separate clusters contained deeper stations (purple, pink, red, and yellow in Figure 119). All unique stations, i.e., those that did not cluster with other stations, were in the central and western areas. A total of 35 taxa contributed to a least 70% of the similarity within all clusters. There was much redundancy in species between clusters, with the shrimp *Sabinea septemcarinata* and the bivalve *Similipecten greenlandicus* contributing highly to the similarity within six clusters, the brittle star *Ophiocten sericeum* and the shrimp *Eualus gaimardii* in five clusters, all other taxa contributing to four or less clusters (Table 32). Despite this overlap in species, nearshore, shelf and deep-water clusters also contained species specific to each of those three depth zones. Examples include the isopod *Saduria entomon* and the amphipod *Acanthostepheia behringiensis* for nearshore clusters, the brittle star *Ophiocten sericeum*, the shrimps *Eualus gairmardii* and *Sabinea septemcarinata* for shelf stations, and the sea stars *Pontaster tenuispinus* and *Bathybiaster vexillifer* for deeper stations.

Across the study region, depth (log transformed) was not a significant predictor of total epibenthic abundance (square root transformed), total epibenthic biomass (square root transformed), total number of epibenthic taxa, or any of the epibenthic diversity indices (Figure 120). As a general trend, however, shallow and deep stations had lower abundance, biomass, and number of taxa, while the middle shelf stations showed large variability in these metrics (Figure 121a-c). Diversity indices were lower at shallow stations, intermediate at deeper stations, and had the greatest variability in the shelf stations (Figure 121d-f). Longitude was a significant predictor of total epibenthic abundance (square root transformed), total epibenthic biomass (square root transformed), total number of epibenthic taxa, and Shannon Diversity, though correlation values were very low (Figure 121**,** a-d). Longitude was not a significant predictor of Margalef Richness or Pielou's Evenness (e-f).

Epibenthic community structure by biomass varied significantly with depth (global R: 0.77, sig. level: 0.01% in ANOSIM). Post-hoc test resulted in significant differences across all depth categories, with the largest difference between shallow and deep stations (Table 33).

**Table 32. Epibenthic taxa contributing to at least an accumulated 70% of the within cluster similarity (SIMPER analysis). Clusters are listed in decreasing order of within-cluster similarity.**

| Cluster group | Average similarity (%) | Species | Contrib% | Cum.% |
|---|---|---|---|---|
| n | 58.6 | *Anonyx* sp. | 13.3 | 13.3 |
| | | Polynoidae | 11.9 | 25.1 |
| | | *Paroediceros lynceus* | 11.4 | 36.6 |
| | | *Eualus gaimardii* | 9.0 | 45.5 |
| | | *Sabinea septemcarinata* | 9.0 | 54.5 |
| | | *Similipecten greenlandicus* | 7.7 | 62.2 |
| | | *Diastylis* sp. | 6.7 | 68.9 |
| | | *Acanthostepheia behringiensis* | 6.3 | 75.2 |
| c | 47.3 | *Psolus peronii* | 17.0 | 17.0 |
| | | *Eualus gaimardii* | 8.5 | 25.5 |
| | | *Sabinea septemcarinata* | 8.5 | 33.9 |
| | | *Hyas coarctatus* | 7.4 | 41.3 |
| | | Bryozoan erect hard | 7.1 | 48.4 |
| | | *Strongylocentrotus pallidus* | 6.9 | 55.3 |
| | | Porifera | 5.5 | 60.7 |
| | | *Tubularia* sp. | 4.3 | 65.1 |
| | | *Crossaster papposus* | 4.3 | 69.4 |
| | | *Spirontocaris* sp. | 3.8 | 73.1 |
| e | 45.3 | *Ophiocten sericeum* | 16.0 | 16.0 |
| | | *Psolus peronii* | 9.3 | 25.3 |
| | | *Sabinea septemcarinata* | 9.0 | 34.2 |
| | | *Diastylis goodsiri* | 8.4 | 42.6 |
| | | *Similipecten greenlandicus* | 8.1 | 50.7 |
| | | *Synidotea bicuspida* | 6.2 | 57.0 |
| | | *Eualus gaimardii* | 5.1 | 62.1 |
| | | *Leptasterias groenlandica* | 5.0 | 67.1 |
| | | *Diastylis* cf *scorpioides* | 4.9 | 71.9 |
| d | 45.1 | *Urasterias lincki* | 24.9 | 24.9 |
| | | *Ophiocten sericeum* | 13.7 | 38.5 |
| | | *Similipecten greenlandicus* | 12.5 | 51.0 |
| | | *Sabinea septemcarinata* | 9.1 | 60.2 |
| | | *Eualus gaimardii* | 6.0 | 66.2 |
| | | *Diastylis goodsiri* | 2.9 | 69.0 |
| | | *Anonyx* sp. | 2.6 | 71.6 |

| Cluster group | Average similarity (%) | Species | Contrib% | Cum.% |
|---|---|---|---|---|
| g | 43.5 | *Similipecten greenlandicus* | 25.6 | 25.6 |
| | | *Ophiocten sericeum* | 17.5 | 43.0 |
| | | *Florometra sp.* | 6.7 | 49.8 |
| | | *Strongylocentrotus pallidus* | 5.8 | 55.6 |
| | | *Psolus peronii* | 5.3 | 60.9 |
| | | *Ophiacantha bidentata* | 5.2 | 66.1 |
| | | *Sabinea septemcarinata* | 3.3 | 69.4 |
| | | *Margarites costalis* | 3.0 | 72.3 |
| f | 42.9 | *Psolus peronii* | 29.3 | 29.3 |
| | | *Ophiocten sericeum* | 13.6 | 42.9 |
| | | *Margarites costalis* | 7.6 | 50.5 |
| | | *Similipecten greenlandicus* | 6.6 | 57.1 |
| | | *Sabinea septemcarinata* | 5.7 | 62.9 |
| | | *Pteraster obscurus* | 5.6 | 68.5 |
| | | *Leptasterias groenlandica* | 5.2 | 73.6 |
| a | 39.3 | *Pontaster tenuispinus* | 41.1 | 41.1 |
| | | *Ctenodiscus crispatus* | 16.2 | 57.2 |
| | | *Bathybiaster vexillifer* | 15.2 | 72.5 |
| o | 37 | *Saduria entomon* | 21.5 | 21.5 |
| | | *Acanthostepheia behringiensis* | 20.6 | 42.1 |
| | | *Eualus gaimardii* | 15.7 | 57.8 |
| | | *Saduria sabini* | 8.7 | 66.5 |
| | | *Polynoidae* | 5.9 | 72.4 |
| h | 35.6 | *Ophiocten sericeum* | 17.9 | 17.9 |
| | | *Ophiacantha bidentata* | 15.2 | 33.2 |
| | | *Colus sabini* | 9.0 | 42.1 |
| | | *Allantactis parasitica* | 8.2 | 50.3 |
| | | *Gersemia fruticosa* | 7.6 | 57.9 |
| | | *Similipecten greenlandicus* | 6.9 | 64.8 |
| | | *Argis lar* | 6.0 | 70.8 |

**Table 33. ANOSIM post-hoc test showing significant differences among depth categories for epibenthic community structure based on biomass data (shallow: <20 m, mid-depth: 21-99 m, and deep: >100 m).**

| Groups | R statistic | Significance level (%) | Possible permutations | Actual permutations |
|---|---|---|---|---|
| Shallow vs Mid-depth | 0.82 | 0.01 | Very large | 9999 |
| Shallow vs Deep | 0.91 | 0.02 | 6188 | 6188 |
| Mid-depth vs Deep | 0.60 | 0.08 | 201376 | 9999 |

The environmental variables that best described the epibenthic community structure in terms of abundance and biomass were (in order of importance) TOC, longitude, and bottom water salinity (Correlation coefficients: 0.64 and 0.62, respectively) (Table 34).

**Table 34. Environmental variables selected as epibenthic community drivers (BvSTEP analysis). In bold best combination.**

| Community structure metric | variable | Correlation |
|---|---|---|
| Epibenthic abundance | TOC | 0.41 |
| | TOC + Longitude | 0.59 |
| | **TOC + Longitude + Bottom water salinity** | **0.64** |
| Epibenthic biomass | TOC | 0.43 |
| | TOC + Longitude | 0.54 |
| | **TOC + Longitude + Bottom water salinity** | **0.62** |

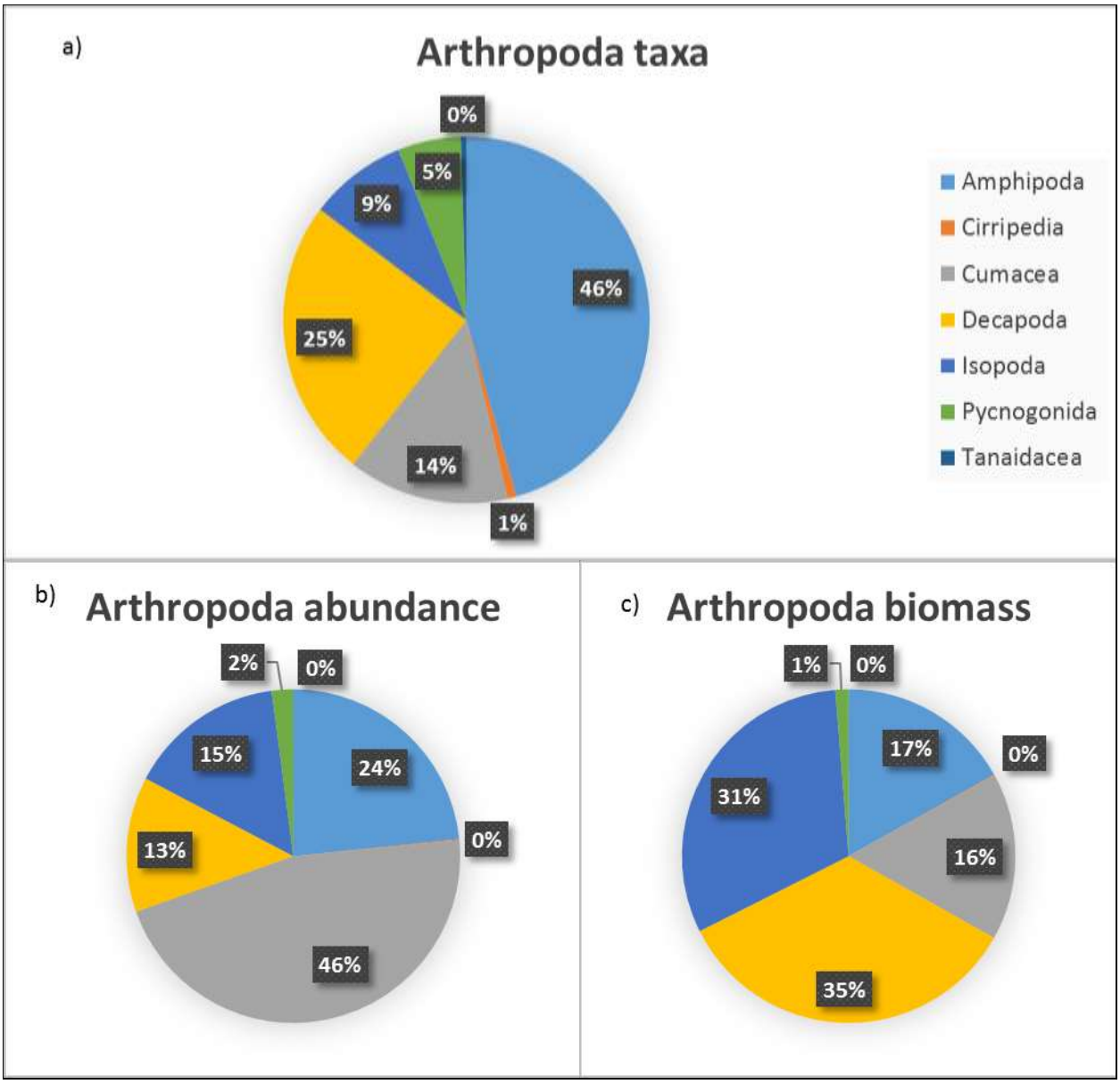


**Figure 112. Proportion of the number of epibenthic taxa (a), total abundance (b), and total biomass (c) per order of the phylum Arthropoda.**

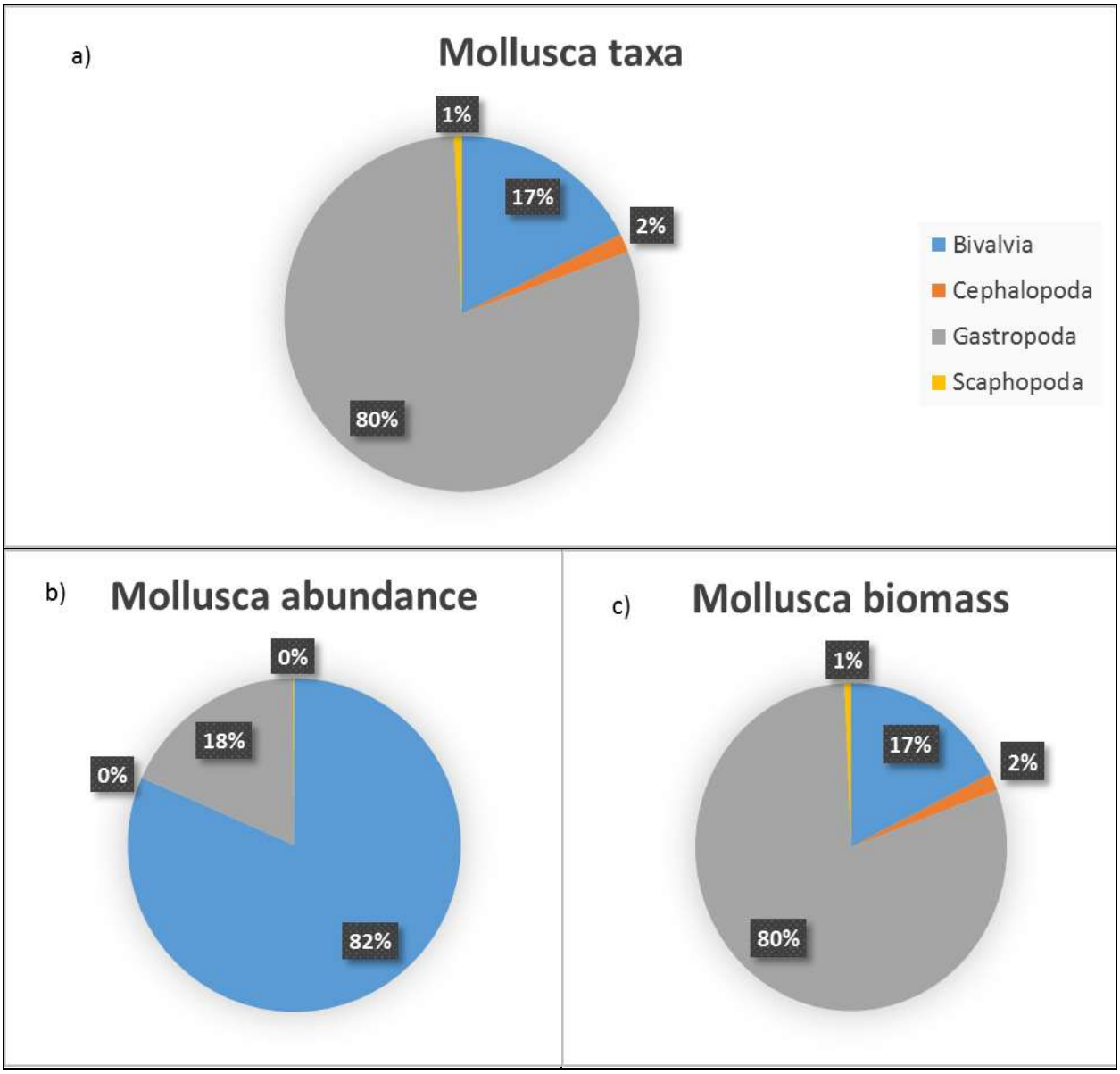


**Figure 113. Proportion of the number of epibenthic taxa (a), total abundance (b), and total biomass (c) per order of the phylum Mollusca.**

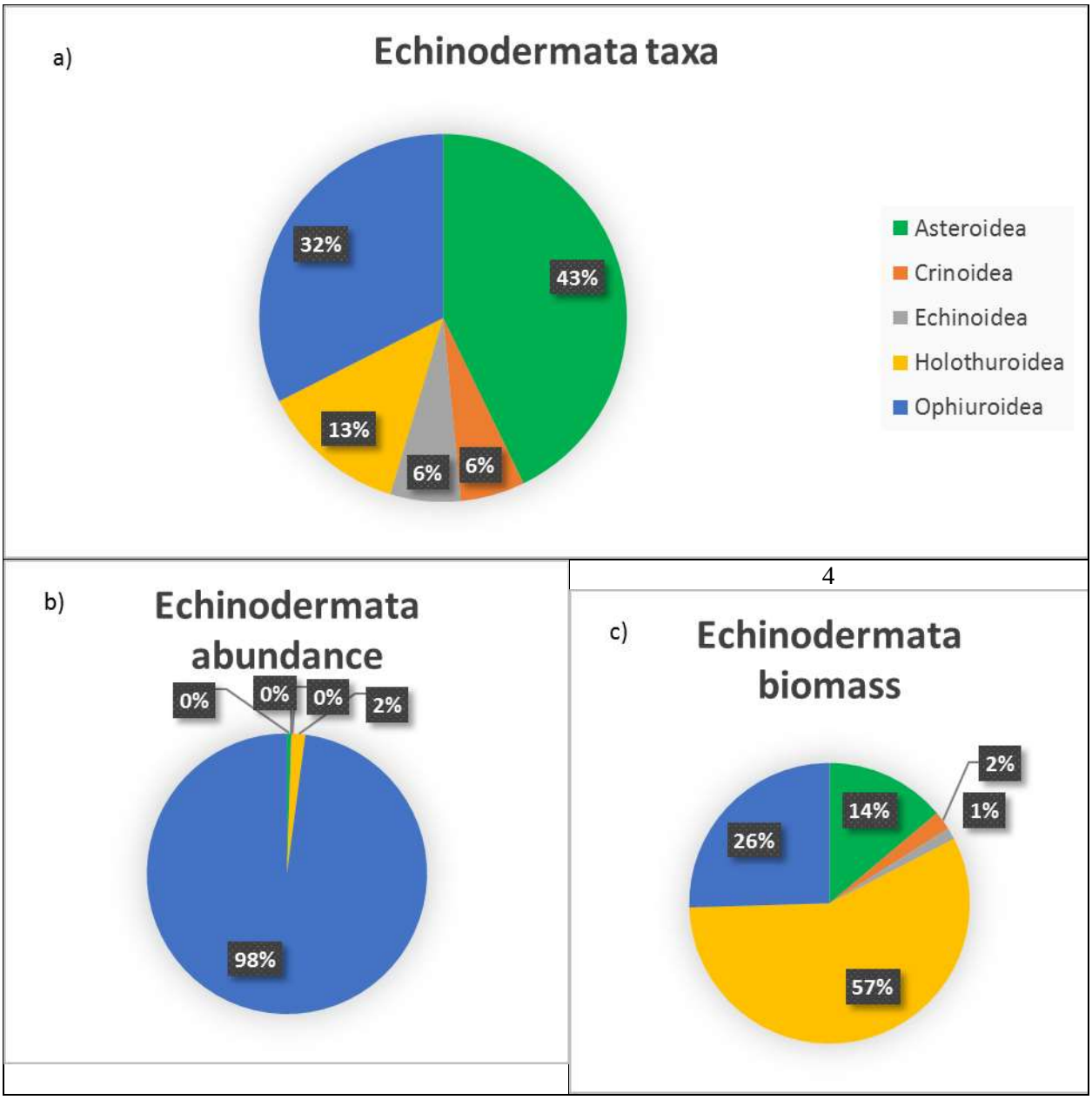


**Figure 114. Proportion of the number of epibenthic taxa (a), total abundance (b), and total biomass (c) per order of the phylum Echinodermata.**

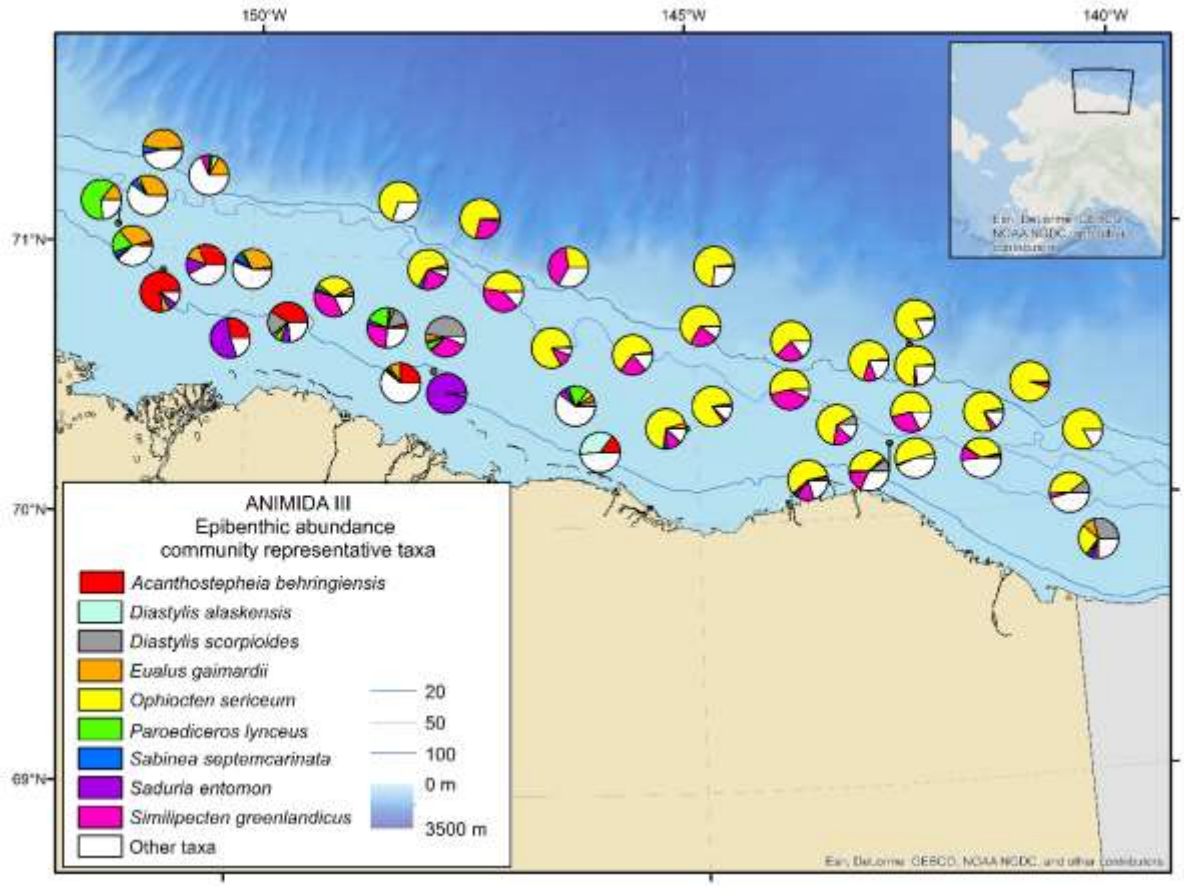


**Figure 115. Proportion of epibenthic abundance for community representative taxa. (Best correlation 0.95; details in methods).**

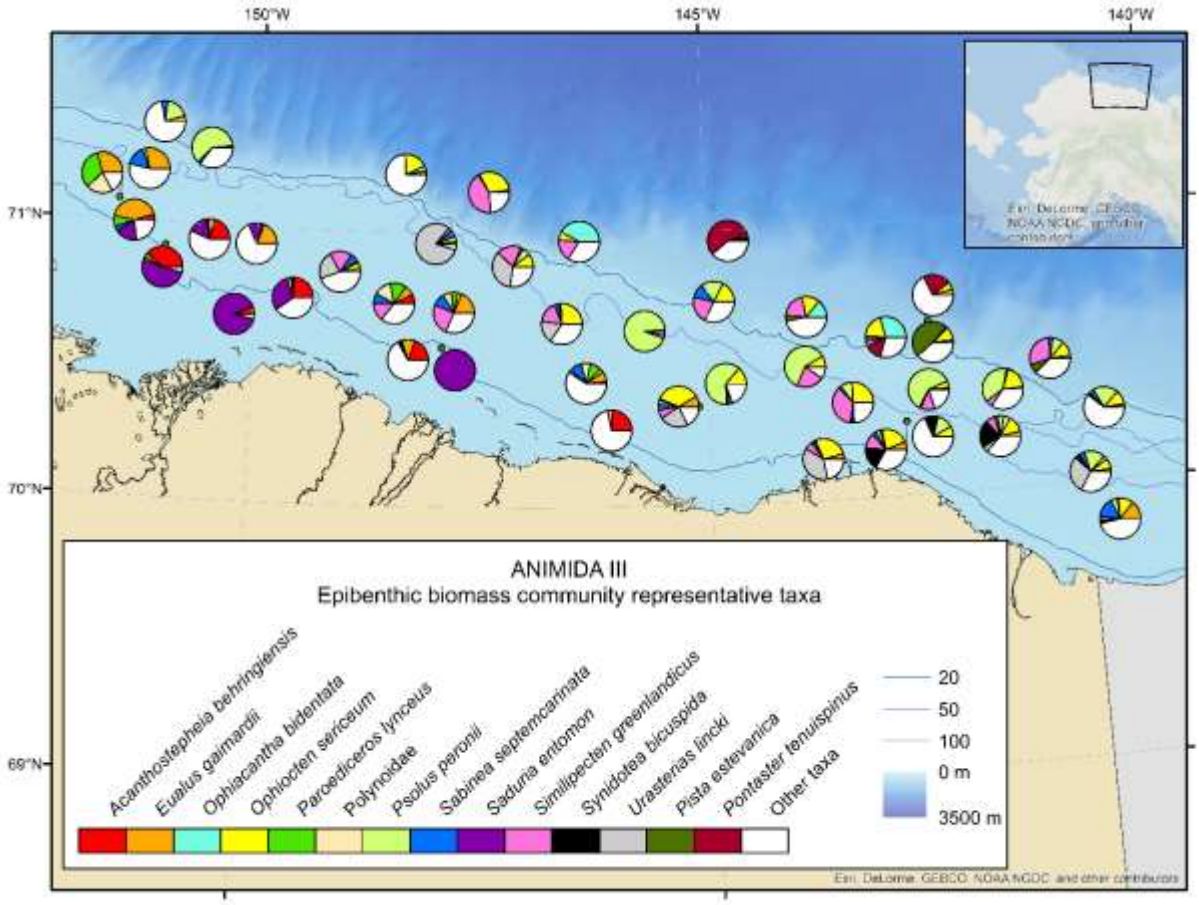


**Figure 116. Proportion of epibenthic biomass for community representative taxa. (Best correlation 0.95; details in methods).**

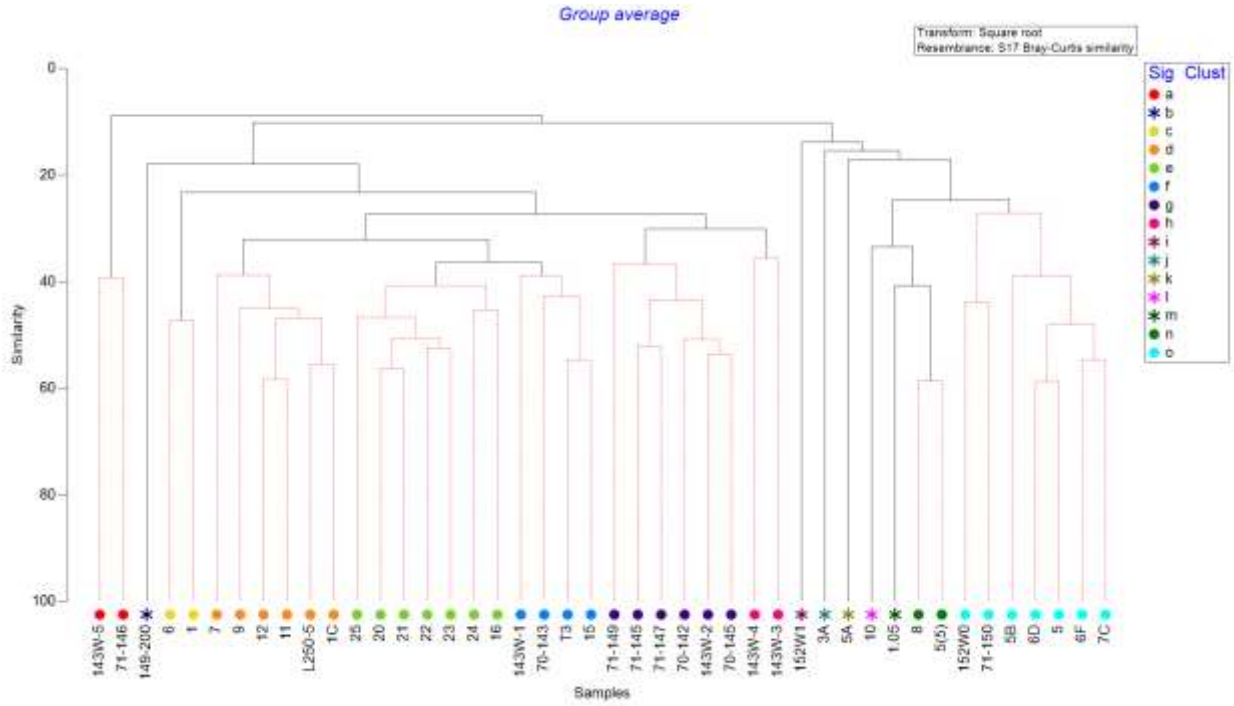


**Figure 117. Cluster analysis based on Bray-Curtis resemblance matrix performed on epibenthic biomass composition data.**

**Significant clusters symbolized with colored circles and independent stations symbolized with colored asterisk.**

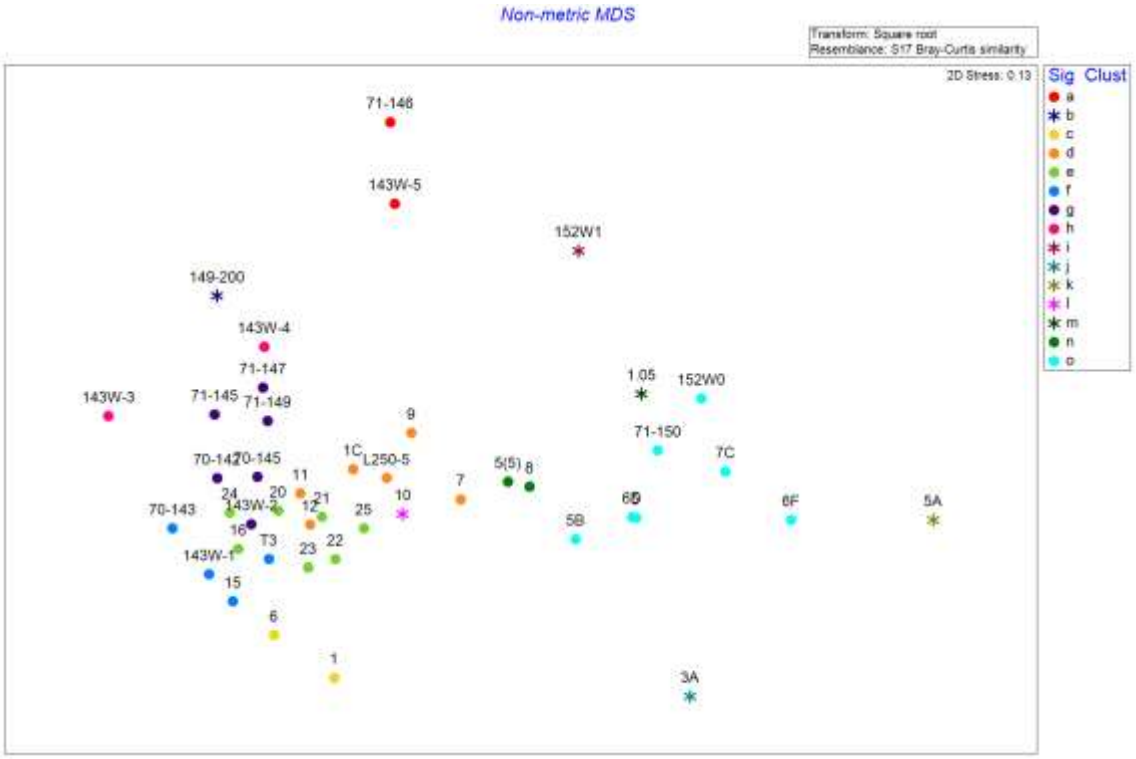


**Figure 118. Multi-dimensional Scaling plot of epibenthic community structure based on biomass composition.**

**Significant station clusters symbolized with colored circles and independent stations symbolized with colored asterisk.**

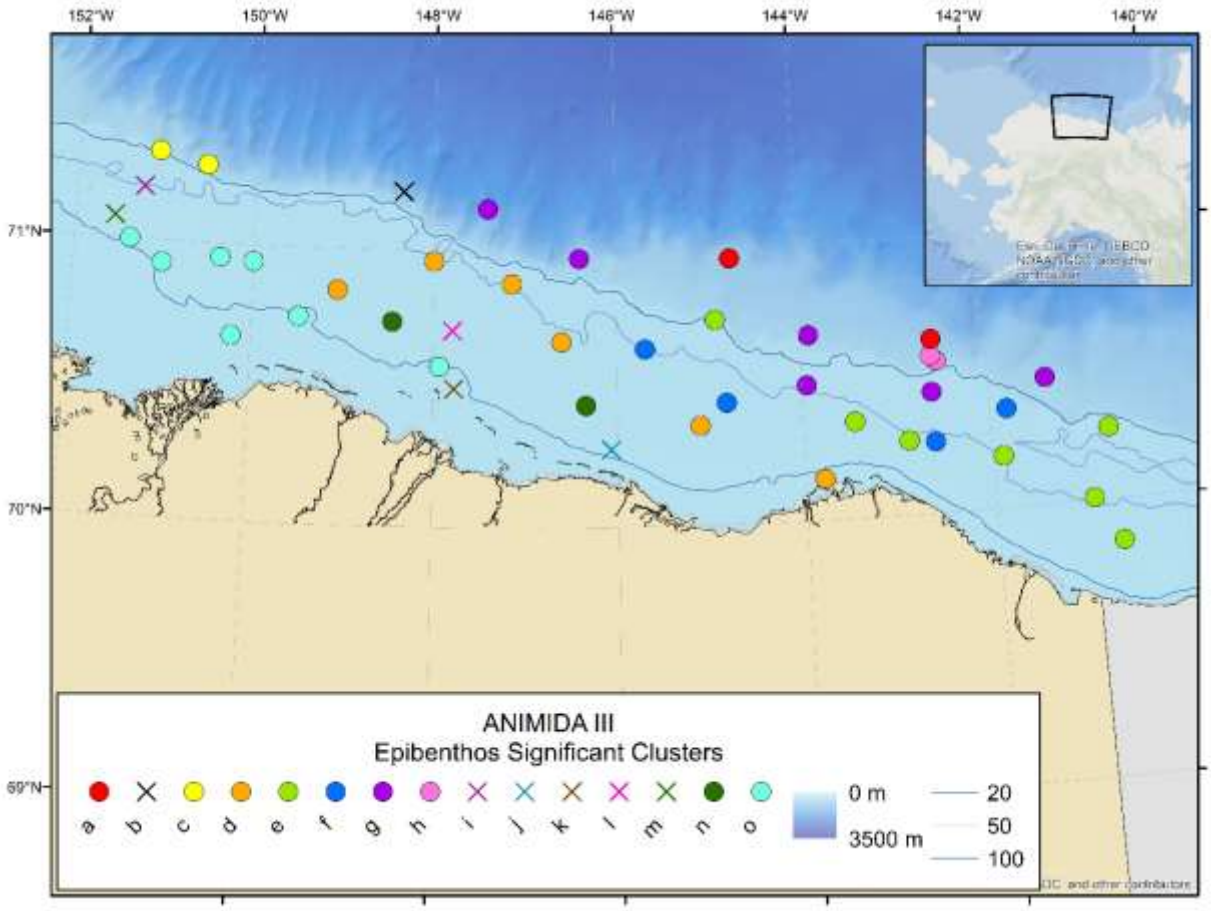


**Figure 119. Spatial distribution of significant clusters based on epibenthic biomass.**

**Significant station clusters symbolized with colored circles and independent stations symbolized with colored asterisk.**

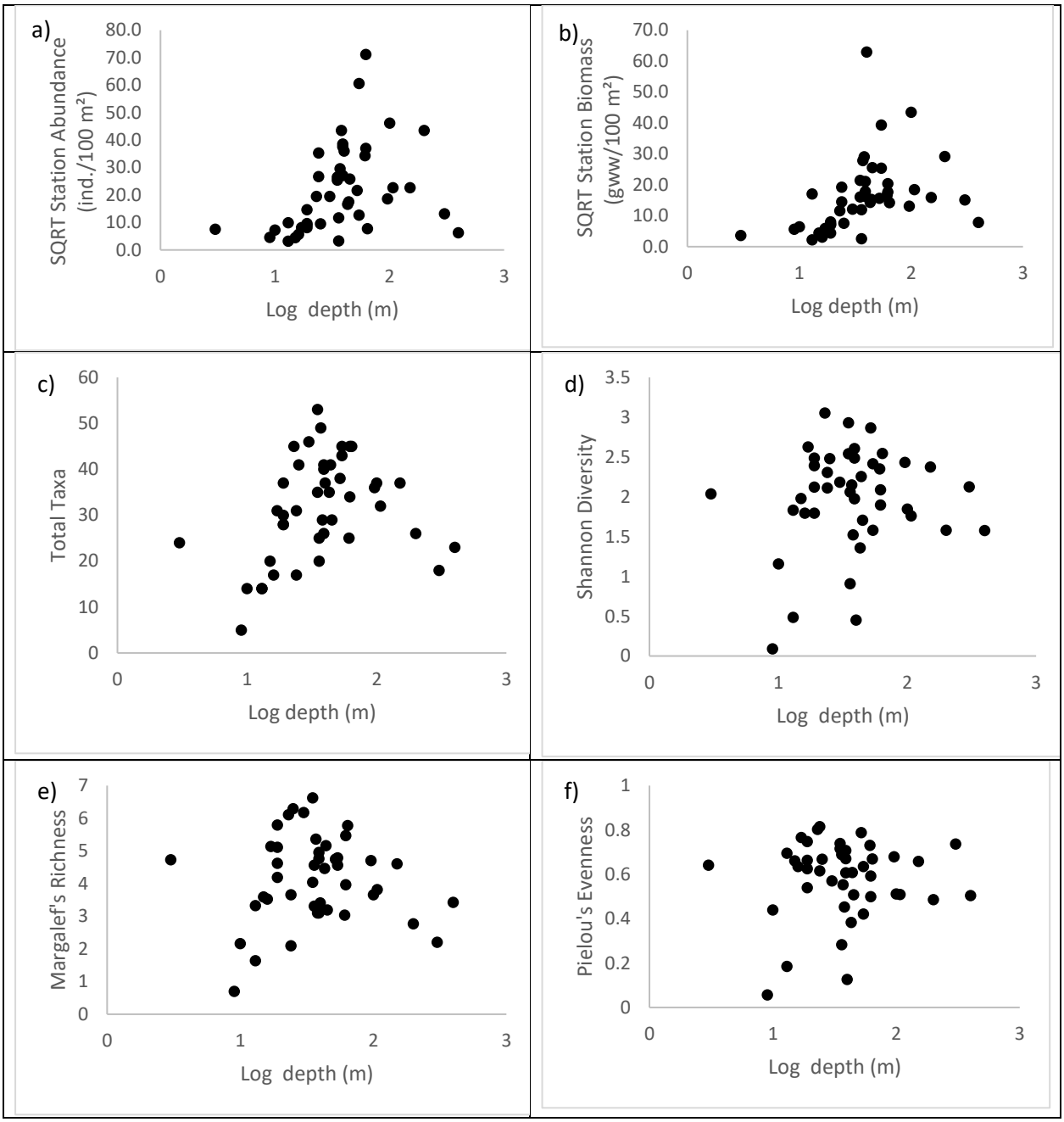


**Figure 120. Depth as a predictor of the square root transformed epibenthic abundance measured in ind/100 m$^2$ (a), square root transformed epibenthic biomass in grams of wet weight/100 m$^2$ (b), epibenthic total taxa (c), epibenthic Shannon Diversity (d), epibenthic Margalef's Richness (e), epibenthic Pielou's Evenness (f).**

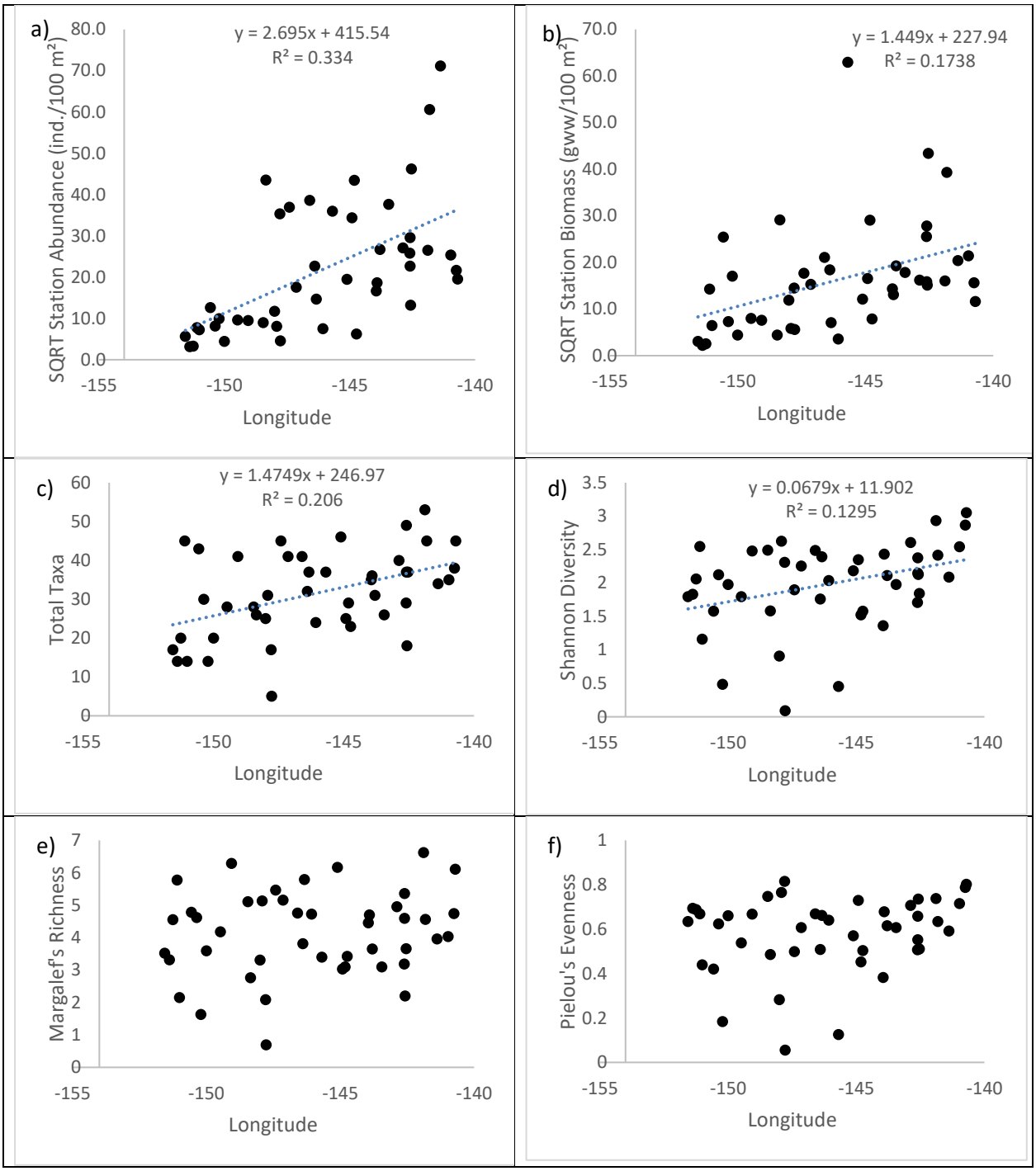


**Figure 121. Longitude as a predictor of square root transformed epibenthic abundance (ind/100 m$^2$)(a), square root transformed epibenthic biomass (grams of wet weight/100 m$^2$)(b), epibenthic total taxa (c), epibenthic Shannon Diversity (d), epibenthic Margalef's Richness (e), epibenthic Pielou's Evenness (f).**

### 6.3.2 Fish

The 44 stations were also sampled successfully for fish in 2014 and 2015 (Figure 101, Table 30). The total abundance per station ranged from less than one ind/100 $m^2$ (stations 5A and 71-145) to 12 ind/100 $m^2$ (station AN14-7C) with a mean of 3.4 ind/100 $m^2$ (SD: 2.3) (Figure 122, Table 31). Stations with high and low abundance were distributed evenly throughout the study region, with a consistently higher abundance on the shelf off of Kaktovik. The number of taxa per station ranged from one (station 5A) to 10 (stations AN14-21 and AN14-5(5)) with a mean of 5.9 (SD:2.2) (Figure 123). In general, a higher number of taxa was found in stations east of Prudhoe Bay. Shannon Diversity Index ranged from 0 (station 5A) to 2.0 (station AN14-21) with a mean of 1.4 (SD: 0.5). Margalef Richness Index ranged from 0 (station 5A) to 3.1 (station 70-145) with a mean of 1.5 (SD: 0.6) and Pielou's Evenness Index ranged from 0.4 (station AN14-1.05) to 0.9 (station 71-146) with a mean of 0.8 (SD: 0.1) (Table 32). All diversity indices generally showed large variability throughout the study region with little spatial pattern, though diversity indices values were lowest in the western nearshore study area (Figure 124 through Figure 126).

Across all stations a total of 29 fish taxa were identified from eight families (Figure 127a). The families sculpin (*Cottidae*) and sand lances (*Ammodytidae*) each accounted for 24% of the total number of taxa, followed by the families snail fishes (*Liparidae*) and pricklebacks or shannies (*Stichaeidae*) each accounting for 17% of the total number of taxa. All other families accounted each for less than 10% of the total number of taxa (Figure 127a). In terms of abundance, the family *Cottidae* accounted for 58% of the total abundance across all groups, the family cods and haddocks (*Gadidae*) accounted for 13% of the total abundance, and the family *Ammodytidae* accounted for 12% of the total abundance across all groups. All other families accounted each for less than 10% of the total abundance (Figure 128b). Throughout the study region most families were represented at each station, though most stations had a large proportion of *Cottidae* (Figure 128). In terms of abundance, most stations showed an even proportion of most classes (Figure 129).

The nine taxa selected as community representatives for fish abundance were, in order of importance, *Icelus spatula* (Spatulate Sculpin), *Gymnocanthus tricuspis* (Arctic Staghorn Sculpin), *Boreogadus saida (*Arctic cod), *Artediellus scaber* (Hamecon), *Triglops pingelii* (ribbed sculpin), *Aspidophoroides olrikii* (Arctic alligatorfish), *Gymnelus hemfasciatus*, and *Lycodes polaris* (Canadian Eelpout) (Figure 130).

Cluster analysis, performed on the fish abundance, grouped the stations into three significant clusters (Figure 131a-c). Cluster groups contained from eight to 22 stations with an average similarity within clusters of 40.3% (SD: 3.1). Of the three cluster groups, one cluster contained stations that were located primarily nearshore, the second cluster contained stations on the shelf and shelf break throughout the study region, and the third cluster consisted of dispersed stations half of which were at the shelf break (Figure 131c). A total of seven taxa contributed to a least 70% of the similarity within clusters. In contrast to the epibenthos, few species characterized similarity within each cluster with only *Boreogadus saida* contained in two clusters and all other taxa contained in only one cluster (Table 35). *Gymnocanthus tricuspis* and *Lycodes polaris* contributed most to station similarity in the nearshore cluster, I*celus spatula*, *Boreogadus saida*, *Gymnelus hemifasciatus,* and *Triglops pingelii* contributed >70% of the similarity to the shelf and shelf break cluster; *Boreogadus saida* and *Lycodes* sp. characterized the geographically non-contiguous cluster.

**Table 35. Fish taxa contributing to at least an accumulated 70% of the within cluster similarity (SIMPER analysis).**

| Cluster group | Average similarity (%) | Species | Contribution (%) | Cumulative (%) |
|---|---|---|---|---|
| c | 42.3 | *Icelus spatula* | 29.7 | 29.7 |
| | | *Boreogadus saida* | 16.3 | 46.0 |
| | | *Gymnelus hemifasciatus* | 14.0 | 60.0 |
| | | *Triglops pingelii* | 10.9 | 71.0 |
| b | 41.9 | *Gymnocanthus tricuspis* | 58.3 | 58.3 |
| | | *Lycodes polaris* | 13.3 | 71.6 |
| a | 36.7 | *Boreogadus saida* | 66.1 | 66.1 |
| | | *Lycodes* sp. | 24.5 | 90.6 |

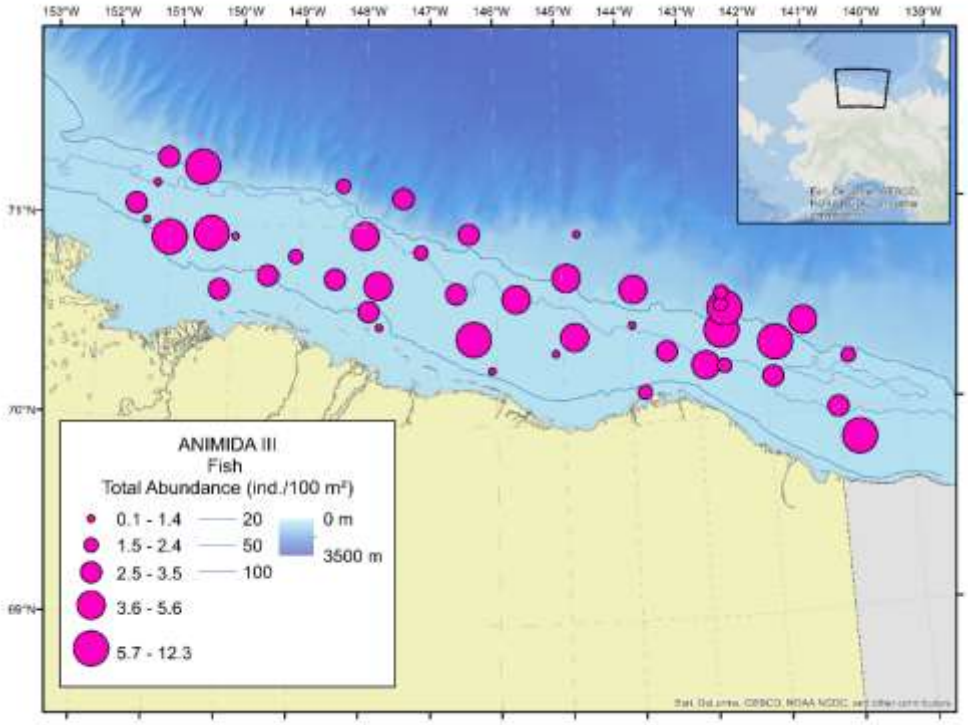


**Figure 122. Total fish abundance per station measured in number of individuals per 100 m$^2$.**

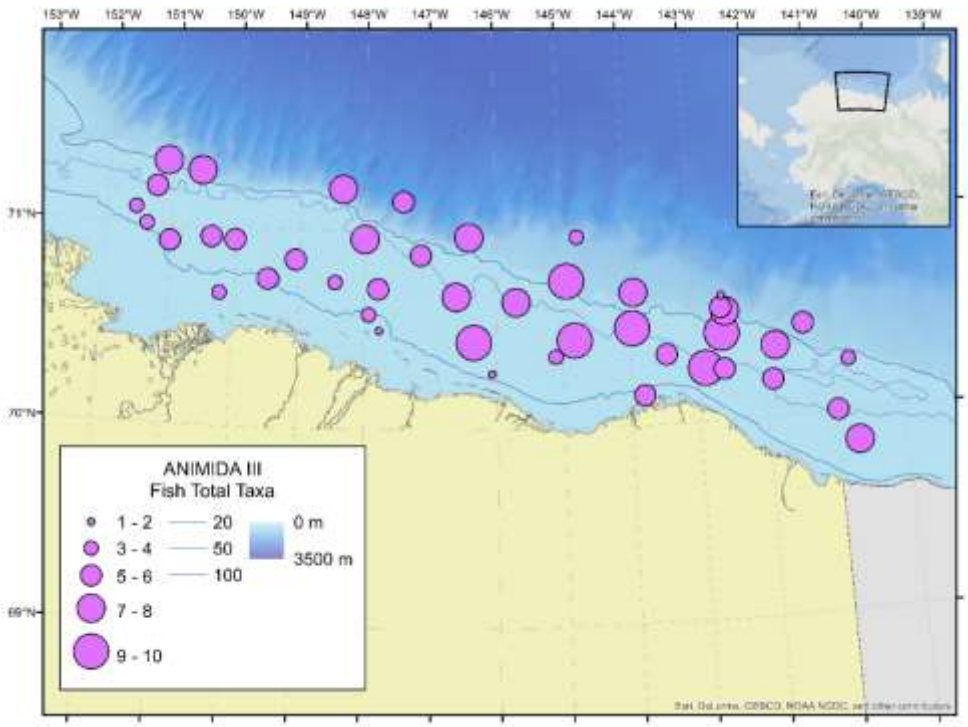


**Figure 123. Total number of fish taxa (mostly species) per station.**

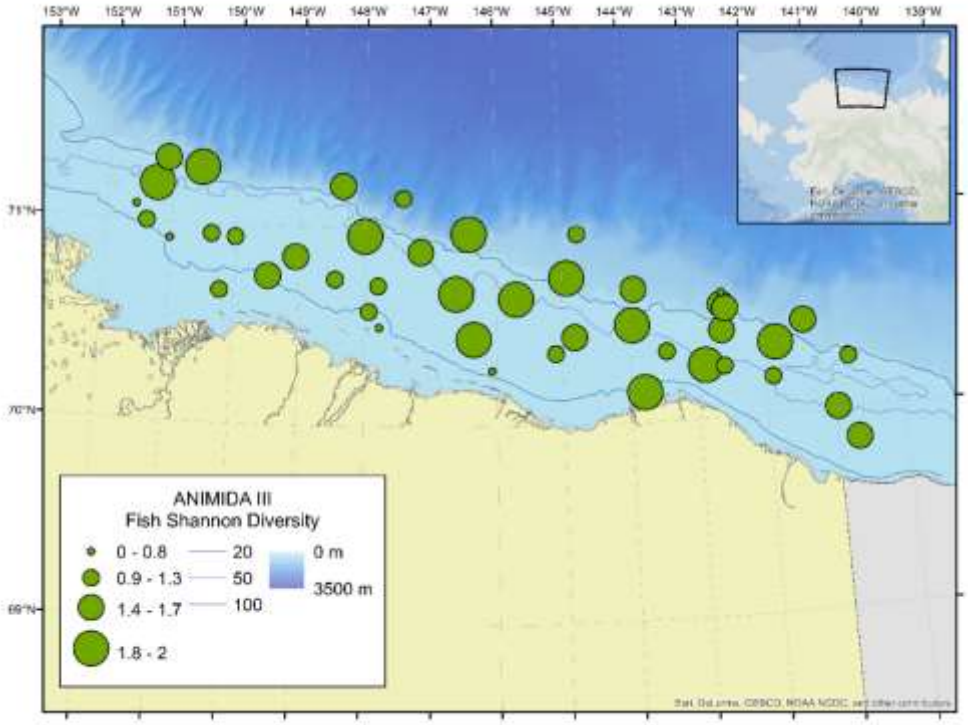


**Figure 124. Fish: Shannon Diversity values per station.**

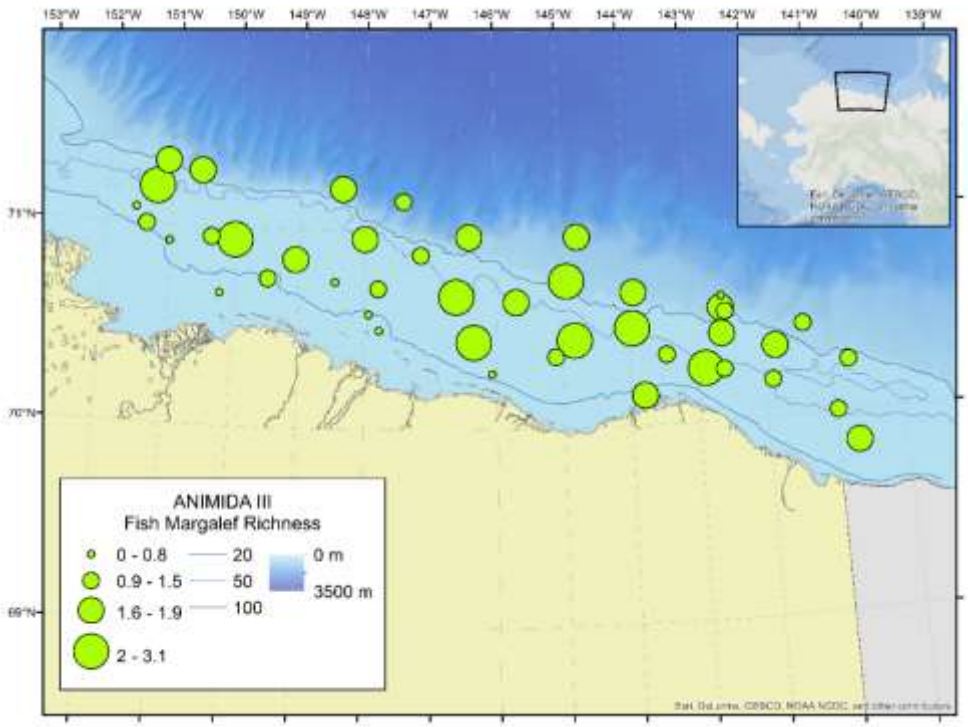


**Figure 125. Fish: Margalef's Richness values per station.**

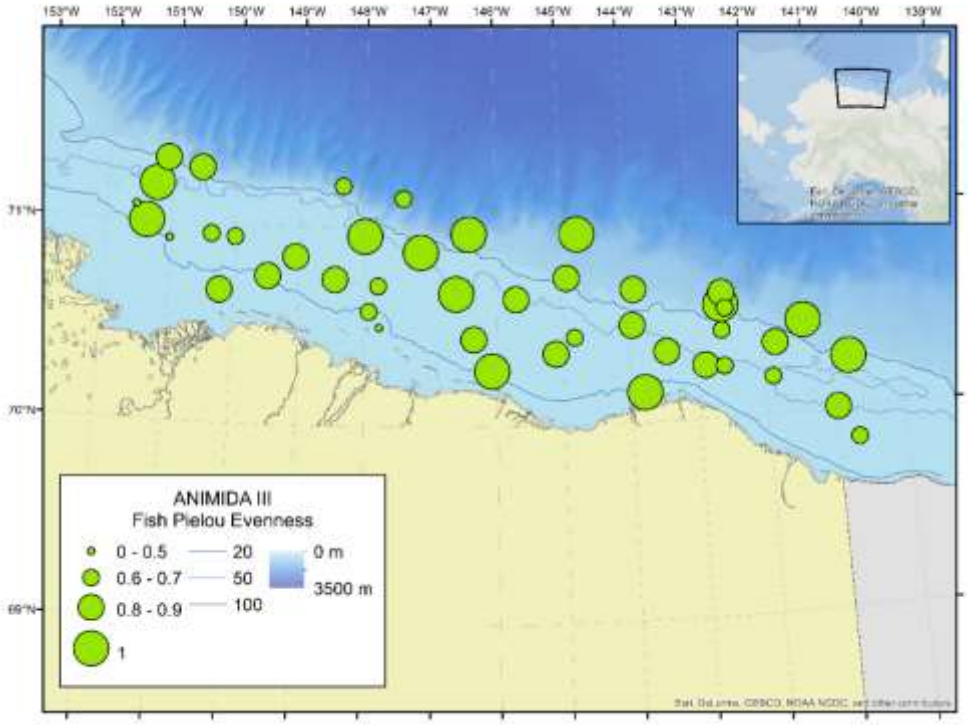


**Figure 126. Fish: Pielou's Evenness values per station.**

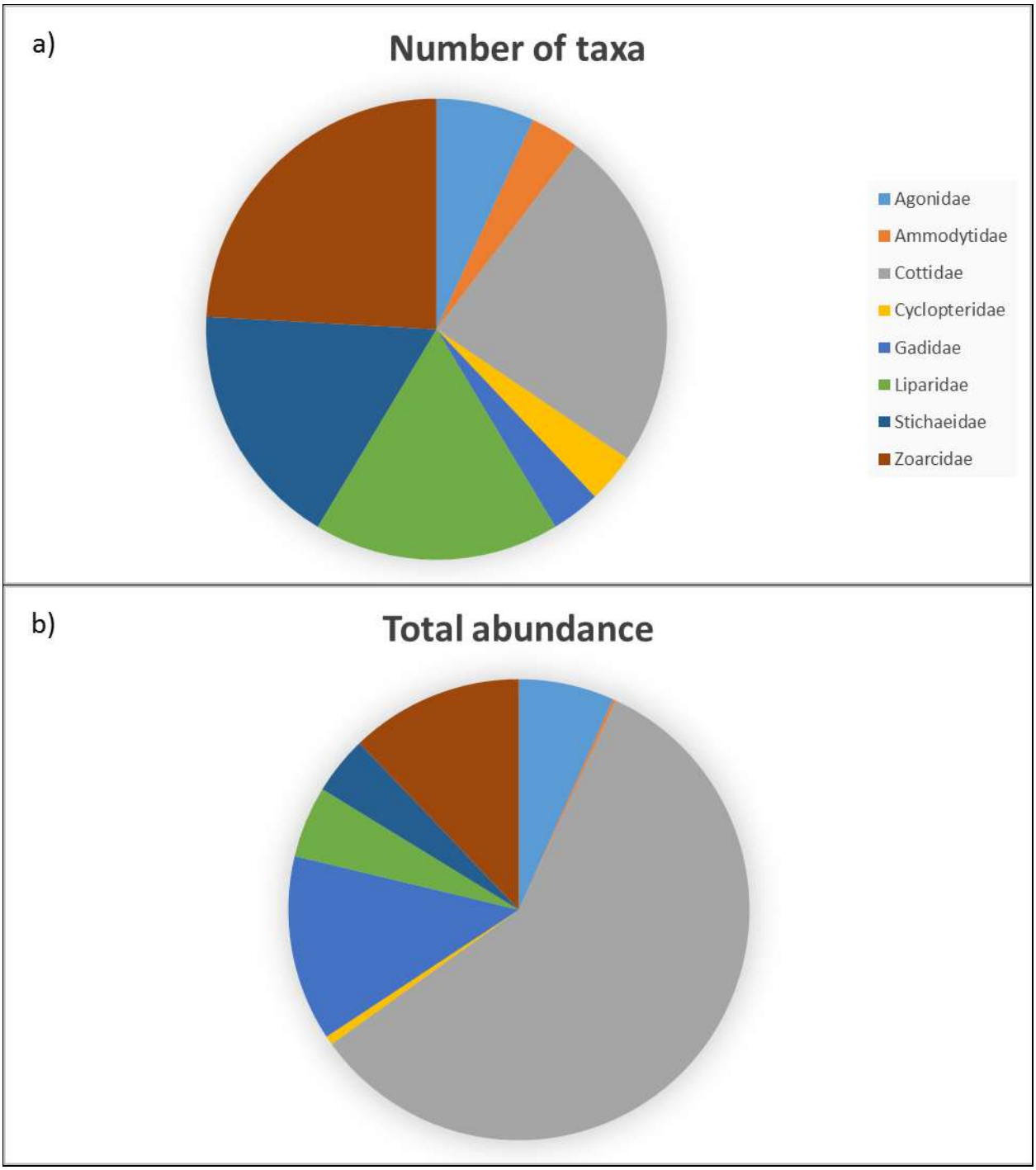


**Figure 127. Proportion of the number of fish taxa (a) and total abundance (b) per family across all stations sampled.**

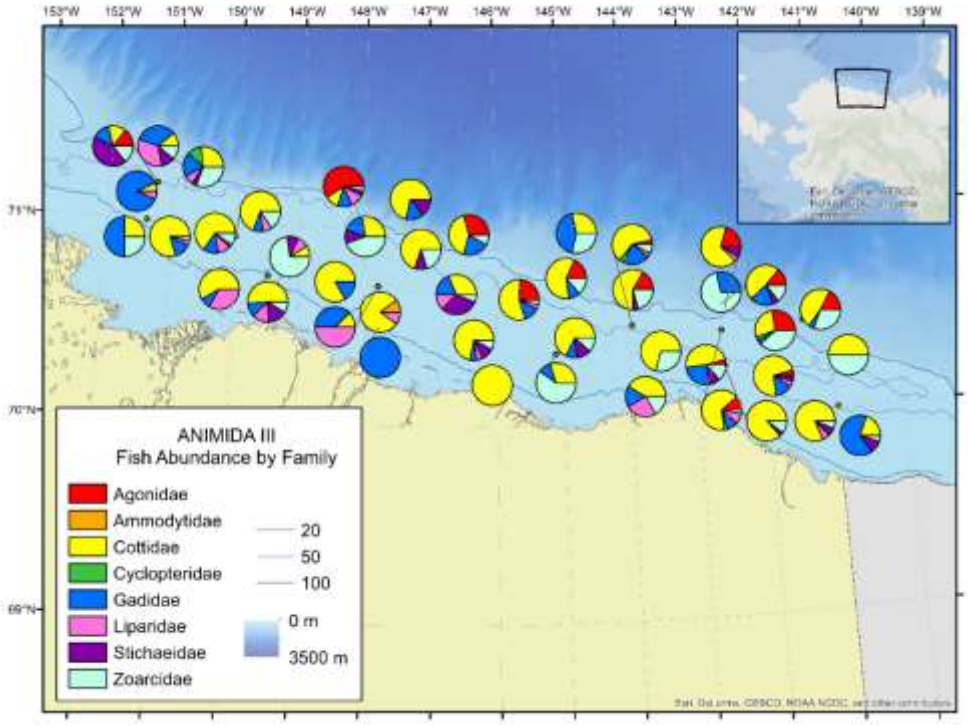


**Figure 128. Proportion of fish families by fish abundance at each station.**

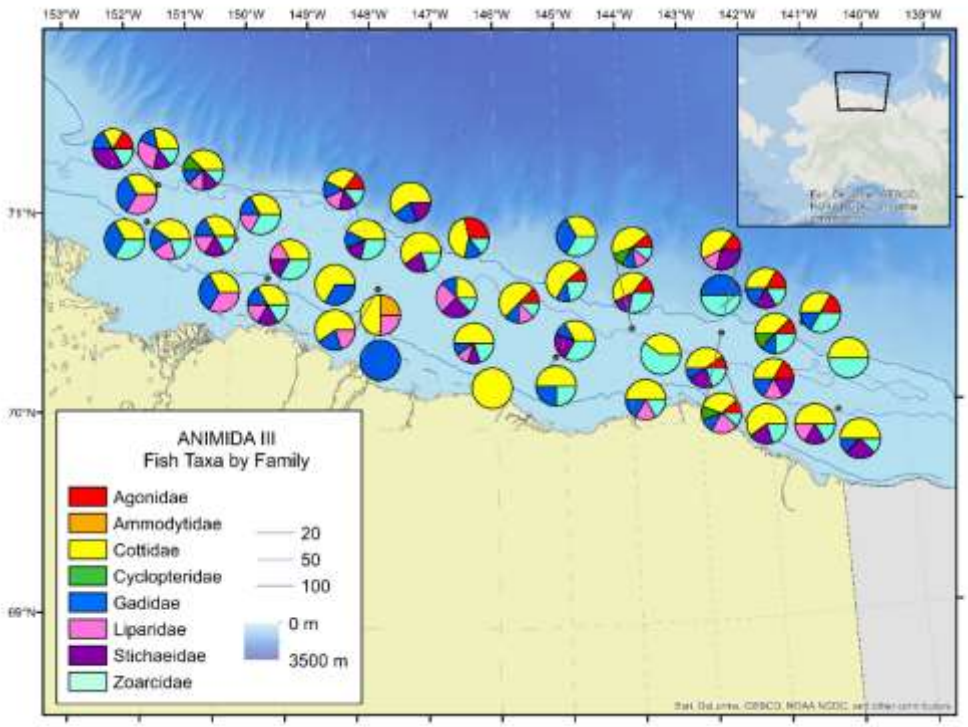


**Figure 129. Proportion of fish families by number of taxa in each family at each station.**

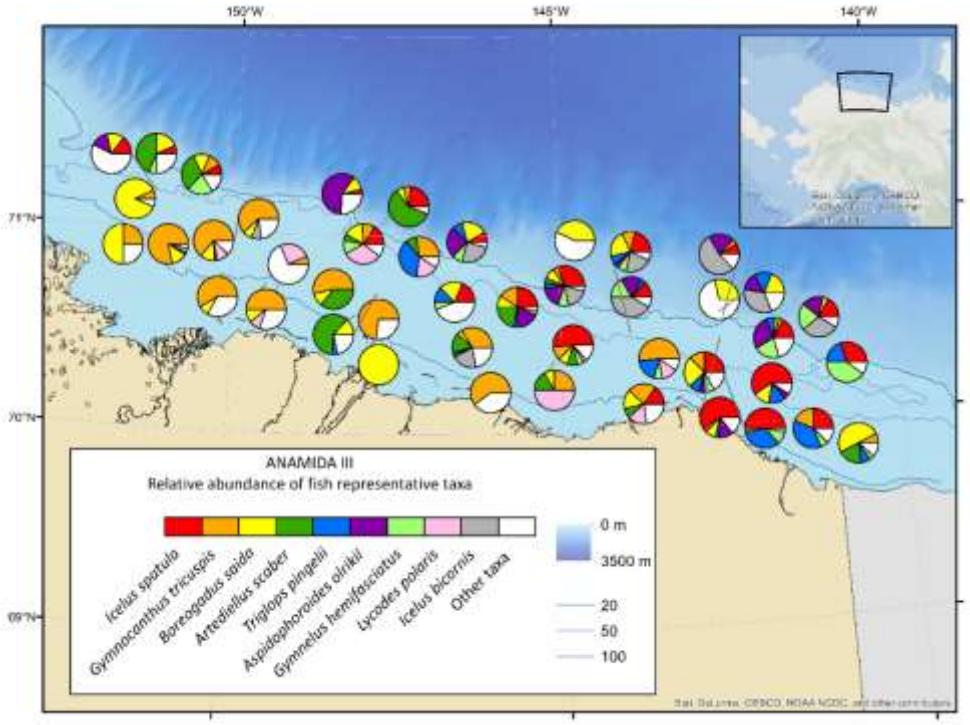


**Figure 130. Proportion of representative fish taxa for the demersal fish community by abundance. (Best correlation 0.95, details in methods).**

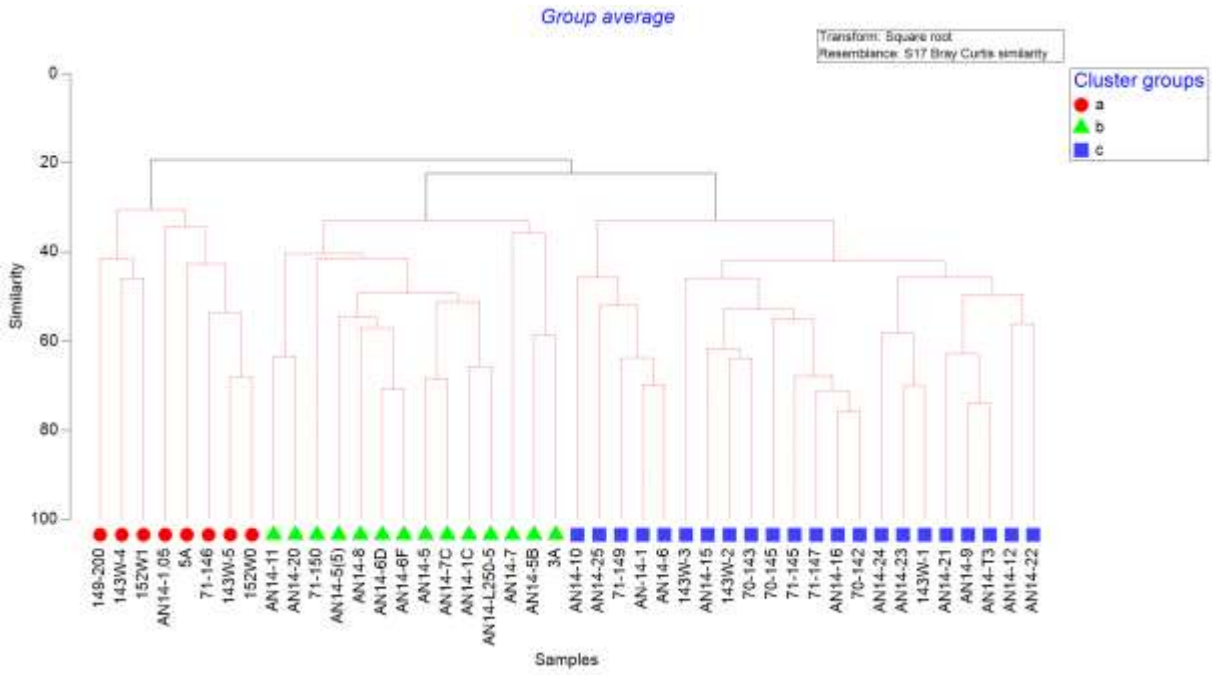


**Figure 131. Community structure of demersal fishes: Cluster analysis based on Bray-Curtis resemblance matrix performed on fish abundance.**

**Significant station clusters symbolized with different color and shape symbols.**

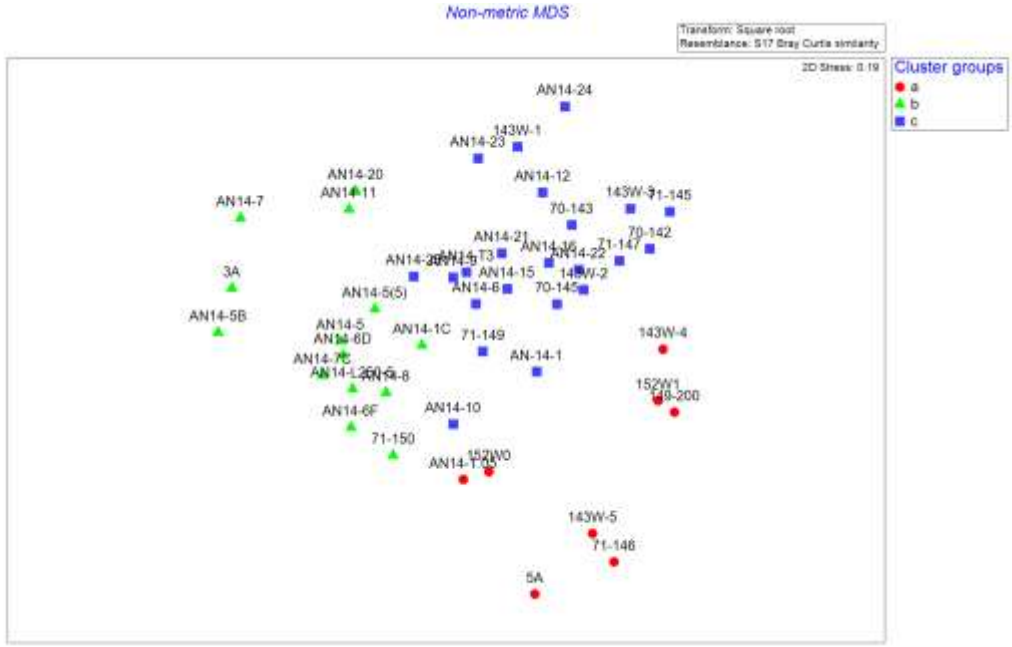


**Figure 132. Community structure of demersal fishes: Multi-dimensional Scaling plot of fish community composition data by abundance.**

**Significant station clusters symbolized with different color and shape symbols.**

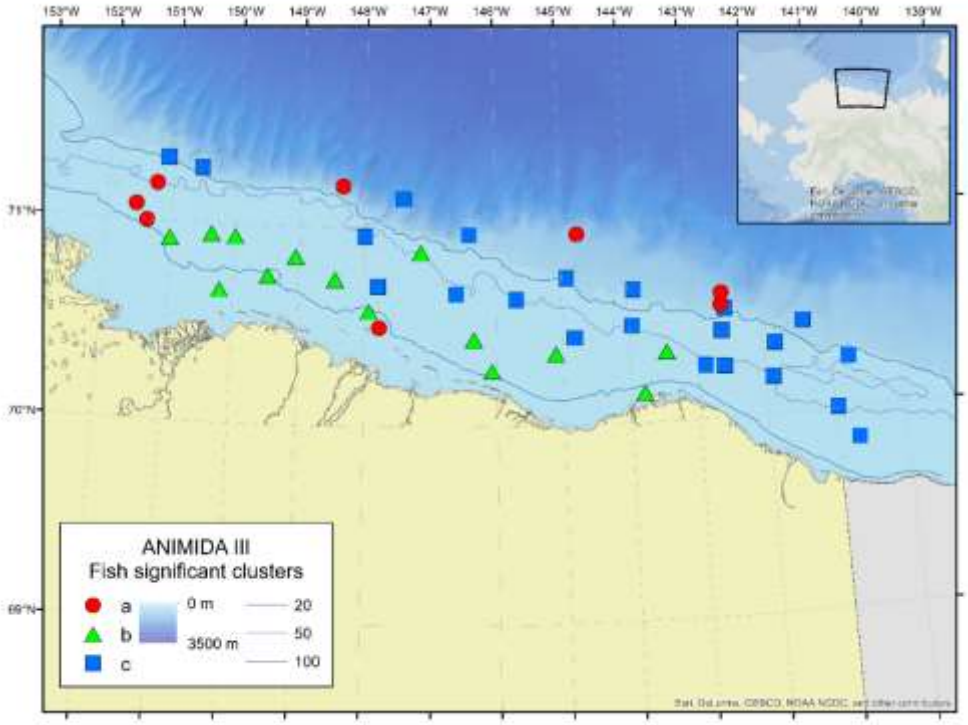


**Figure 133. Spatial distribution of significant fish community clusters based on abundance data. Significant station clusters symbolized with different color and shape symbols.**

Across the study region, depth (log transformed) and longitude were not significant predictors of total fish abundance (square root transformed), total number of fish taxa, or any of the fish diversity indices (Figure 134 and Figure 135). Similar to epibenthic metrics, however, shallow and deep stations had lower abundance, number of taxa and diversity indices Shannon and Margalef, while the middle shelf stations showed large variability in these metrics (Figure 134a-d). Pielou's Evenness had larger variability within similar depths (Figure 134e). Longitude showed a large variability but not clear trend with all metrics (Figure 135a-e).

In contrast, fish community structure (based on abundance data) varied significantly with depth (R: 0.47, sig. level: 0.01%). Post-hoc test documented significant differences across all three depth categories, with the largest difference between shallow and deep stations (Table 36).

The environmental variables that best matched the entire fish community structure were, in order of importance, TOC, bottom water salinity, longitude, % sand, and $PO_4$ (Corr: 0.48) (Table 37). These variables represent location, hydrography, and sediment characteristics.

**Table 36. ANOSIM post-hoc test showing significant differences among depth categories for fish abundance communities**

**(shallow: <20 m, mid-depth: 21-99 m, and deep: >100 m).**

| Groups | R statistic | Significance level (%) | Possible permutations | Actual permutations |
|---|---|---|---|---|
| Shallow vs Mid-depth | 0.46 | 0.01 | 854992152 | 999 |
| Shallow vs Deep | 0.61 | 0.02 | 4368 | 999 |
| Mid-depth vs Deep | 0.44 | 0.2 | 169911 | 999 |

**Table 37. Environmental variables selected as fish community drivers (BvSTEP analysis).**

**In bold combination with highest correlation coefficient. TOC is total organic carbon content of the sediment.**

| Community metric | variable | Correlation |
|---|---|---|
| Fish abundance | TOC | 0.36 |
| | TOC + Bottom water salinity | 0.42 |
| | TOC + Bottom water salinity + Longitude | 0.45 |
| | TOC + Bottom water salinity + Longitude + Sand | 0.46 |
| | **TOC + Bottom water salinity + Longitude + Sand + $PO_4$** | **0.48** |

## 6.4 Discussion

### 6.4.1 Epibenthic Communities

In general, epibenthic communities varied with depth and along the shelf throughout the study region. While not statistically significant in all metrics evaluated, depth and longitudinal trends were demonstrated by the significant difference in epibenthic community structure between three depth categories (nearshore, shelf, shelf break), and by longitude being a significant predictor of total abundance and biomass (i.e., epibenthic standing stock) and among the explanatory variables of epibenthic community structure. Depth invoked by onshore-offshore bathymetric gradients and geographic location (here position along the shelf) act as easily measurable proxies for a combination of environmental drivers that influence epibenthic organisms (Piepenburg, 2005). The importance of these two factors supports previous findings from earlier epifauna studies in the Beaufort Sea region, both from the 1970s and the 2010s (Carey and Ruff, 1977; Roy et al., 2014; Bluhm et al., 2014; Norcross et al., 2015; Ravelo et al., 2015) and will be discussed in the following.

#### 6.4.1.1 Onshore-offshore patterns and environmental influences

This study supports previous work highlighting the strong land-ocean interactions in the nearshore Beaufort Sea. Organisms that inhabit the shallow region of the U.S. Beaufort Sea shelf (<~20 m) are affected by multiple seasonally distinct physical forces. These create a year-round high stress environment (e.g., Macdonald and Carmack, 1991; Mahoney et al., 2014) that helps explain the low abundance, biomass, and taxon richness of epibenthos at shallow stations in this study. Prominent factors include seasonally varying freshwater inflow), ice gouging (though not directly measured in this study), and resulting sediment properties (Table 34 and see Chapter 3 of this report). The formation of ice keels from grounded sea ice pressure ridges in the Stamukhi zone scars the seafloor from about 15 to 45 m depth through deep draft-ice keels, with the largest density of gouging reported around 17 m water depth (Barnes et al., 1982; Mahoney et al., 2014). This recurrent physical disturbance overturns the predominating soft sediments in the study area and reduces diversity of long-lived species, while at the same time opening up patches for early-successional opportunistic species (Conlan et al., 1998 and references therein; this study). In addition to gouging, the ice keels create a barrier for water movement near the seafloor, modifying currents and in turn affecting the distribution of sediments (Barnes et al., 1982; Reimnitz and Kempema, 1984; Macdonald and Carmack, 1991). As rivers start to flow in the spring and early summer the nearshore environment is flooded with fresh inflow water forming the Riverine Coastal Domain (Carmack et al., 2015) and, if trapped behind ice ridges, may pool as a brackish water lake of high turbidity (Carmack and Macdonald, 2002).

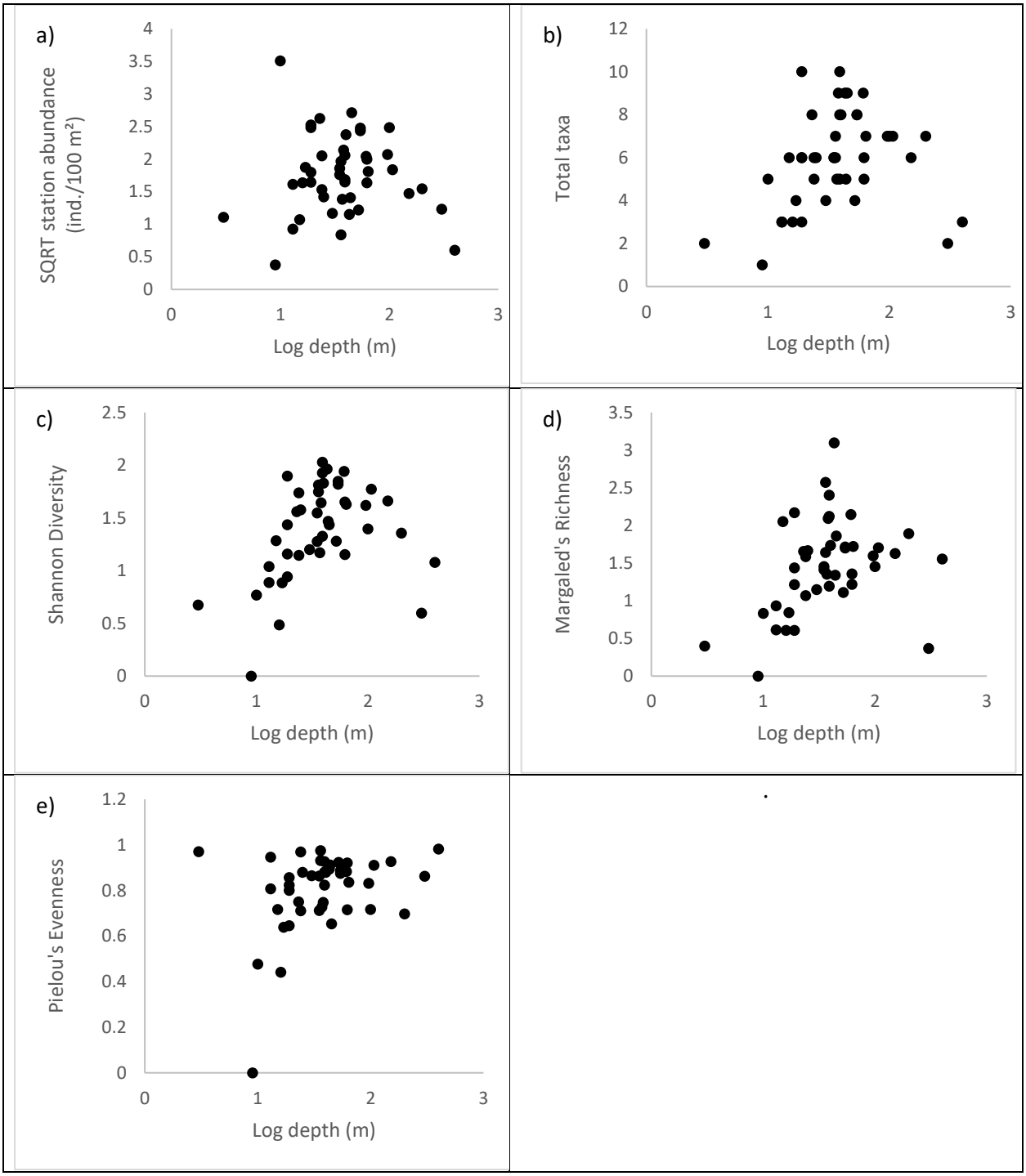


**Figure 134. Depth (log transformed) as a predictor of the square root transformed fish abundance measured in ind/100 m$^2$ (a), fish total taxa (b), fish Shannon Diversity (c), fish Margalef's Richness (d), and fish Pielou's Evenness (e).**

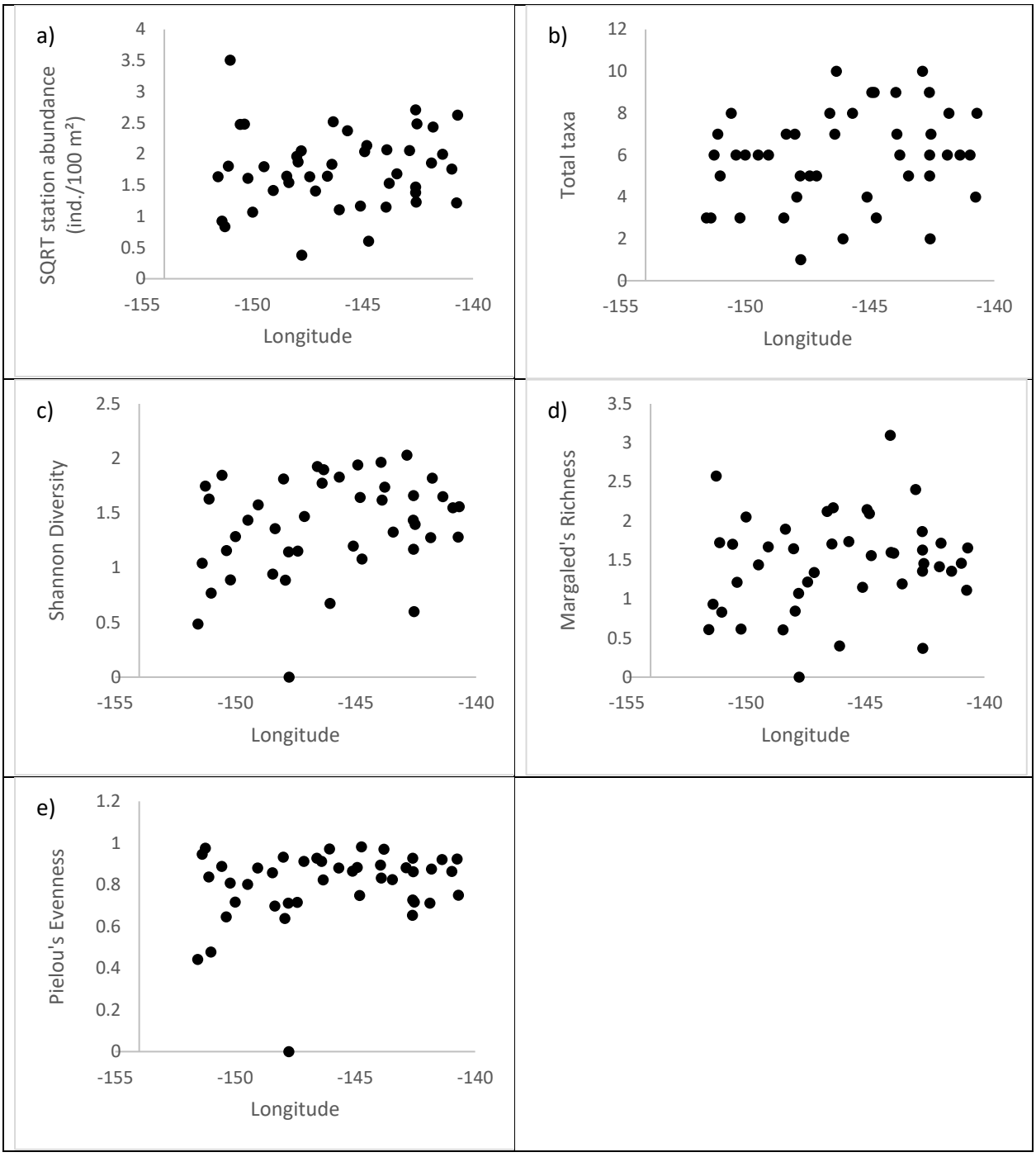


**Figure 135. Longitude as a predictor of the square root transformed fish abundance measured in ind/100 m$^2$ (a), fish total taxa (b), fish Shannon Diversity (c), fish Margalef's Richness (d), and fish Pielou's Evenness (e).**

Salinity increases in the nearshore environment from October through mid-May as a result first of reduced riverine input and later through brine injection from the formation of sea ice (Macdonald and Carmack, 1991; Dunton et al., 2006). On the U.S. Beaufort Sea shelf, after breakup and until late fall, rivers discharging freshwater and terrigenous sediments mix rapidly off the coast (Hearon et al., 2009). In summary, the nearshore environment of the U.S. Beaufort Sea shelf is a highly dynamic environment, with additive extreme changes in salinity, temperature, water movement, and physical disturbance (Barnes, 1999; Mahoney et al., 2014). The combination of characteristic taxa found in this zone during ANIMIDA III and the overall low epibenthic standing stock of the nearshore U.S. Beaufort Sea shelf clearly reflect the environmental disturbances that take place in this region. Our findings confirm that few benthic taxa tolerate these conditions, and those that do – certain crustaceans - are mobile enough to avoid the worst conditions.

In the ANIMIDA region specifically, the combined influences of the Colville and Sagavanirktok Rivers and ice gouging are evident in epibenthic invertebrate community abundance, biomass, and taxonomic composition in the central Beaufort Sea (i.e., the western part of the ANIMIDA III study area) where essentially all shallow stations (<20 m) of the program were sampled. In terms of community composition, stations in the vicinity of the deltas of the two rivers were characterized by a dominance (either in abundance or biomass) of especially the amphipods *Acanthostepheia behringiensis*, *Paroediceros lynceus*, and the isopod *Saduria entomon* (Figure 115 and Figure 116). These crustaceans are mobile generalist predators and scavengers (Graeve et al., 1997; Macdonald et al., 2010; Bell et al., 2016), feeding traits which presumably allow them to inhabit areas with lower food availability, variable environmental conditions and perhaps higher disturbance. Furthermore, *Saduria entomon* tolerates large salinity ranges from 0.2 to 30, possibly allowing this species to remain in the nearshore year-round (Haahtela, 1990; Sandberg and Bonsdorff, 1990). Both S. *entomon* (previously called *Mesidotea entomon*) and *A. behringiensis* were listed among the most common species in the nearshore Beaufort already in the 1970s (Crane, 1974) suggesting a rather stable community of stress tolerant epibenthos. The shrimp *Eualus gaimairdii* was common at a few western nearshore stations and is a very widely distributed epibenthic shrimp with more pelagic feeding habits (Birkely and Gulliksen, 2003) that perhaps opportunistically exploits the nearshore area through its mobility on occasion. In concordance with previous findings from the region (Ravelo et al., 2015), nearshore stations had lowest epibenthic abundance and biomass.

Standing stock increased and community structure changed beyond approximately the 20 m isobath. Most shelf station beyond the 20 m isobath up to the shelf break were sampled in the central and eastern part of the ANIMIDA study area (Figure 101) due to an ice tongue that left us unable to sample more shelf and shelf break stations in the western study area in 2015. As a result of that and less variability in environmental conditions shelf clusters of high epibenthic similarity (d, e, f in Figure 117) had a strong overlap in their characteristic species (Table 32). With the exception of the western area (more detail in section 6.1.2) the shelf stations were primarily dominated by echinoderms and by molluscs (Figure 110 and Figure 115). Echinoderms, in particular brittle stars, generally dominate Arctic shelves (Piepenburg, 2005; Bluhm et al., 2009; Ravelo et al., 2014, 2015) and are generally stenohaline (Russell, 2013), which likely explains their general absence from the nearshore zone though exceptions exist. The central and especially eastern study area may experience the intrusion of comparatively warm and fresh water from the Mackenzie River (Bell et al., 2015) which contributes significantly to the melting of sea ice over the Beaufort Sea shelf, and can delay the onset of freezing in the fall (Carmack et al., 2015).

Recent research has linked an increase in strong easterly wind events over past decades with increased intrusion of Mackenzie River shelf waters further into the U.S. Beaufort Sea shelf and promoting an earlier sea ice retreat (Macdonald et al., 1998; Pickart et al., 2013). The apparent increase in abundance and biomass of epifauna towards the Mackenzie River delta in comparison to stations influenced by the Colville and Sagavanirktok Rivers may be related to gradual changes in sea ice regimes from east to west and perhaps related productivity patterns. Clearly, none of the stations in the central and eastern study area were within the dynamic Stamukhi zone and, hence, presumably were less mechanically disturbed. Also, and perhaps at least locally more important, known upwelling related to the much steeper bathymetric profile has long been documented to occur off Barter Island (Huffort, 1974; Mountain, 1974). In the ANIMIDA III group's proposal for selecting the 143° W line as a DBO line, we argue that this upwelling phenomenon may be linked to a tongue of higher productivity offshore of Barter Island that, as Don Schell in the 1970s argued, led to use of this area as a bowhead feeding area, backed by the long-standing tradition of Inupiat villagers' of Kaktovik to hunt for bowhead whales. The somewhat elevated epibenthic (and fish) stocks may lend support to that notion.

In contrast to previous studies in the region, there was no clear increase in epibenthos organism abundance or biomass on the shelf break or decrease with increasing depth on the slope (Rand and Logerwell, 2011; Norcross et al., 2015; Ravelo et al., 2015) during ANIMIDA sampling. What seems like a difference in findings is in fact related to the differences in spatial coverage between the projects' sampling efforts. The epibenthic abundance and biomass peaks observed during the 2011 sampling at 100-220 m in the central and western U.S. Beaufort Sea was attributed to a combination of inflow of high nutrient waters of Pacific origin and recurrent wind-driven upwelling (Schulze and Pickart, 2012; Ravelo et al., 2015). The western extent of the ANIMIDA III sampling area begins where the Pacific-water influence along the shelf weakens, apparently leaving less particle deposition for epibenthos resulting in lower standing stocks at the shelf break off the Colville area (Figure 103) compared to the area to the west (Ravelo et al., 2015; more in section 6.1.2.). In terms of community composition change even further down the slope, we found a depth-related pattern in the present study, though it was not as marked as in previous surveys. This is not surprising given that the stations sampled on the shelf break (>100 m) were few and scattered in this study (six stations), while the depth-related pattern was very strong in the 2012-2014 sampling that systematically sampled transects from 20-1,000 m down slope (Norcross et al., 2015). Nevertheless, the depth pattern was strong enough in ANIMIDA III sampling to result in clusters a, c, g, and h separate from the shelf clusters, with typical deeper water species only contained in the deepest clusters (a, h), for example the sea stars *Pontaster tenuispinus* and *Bathybiaster vexillifer* (Table 32).

In conclusion, the ANIMIDA III findings regarding nearshore, shelf, and shelf break patterns fit well within the findings of both earlier studies and within the understanding of the Beaufort Sea system, despite somewhat weaker shelf-break patterns found during our 2014-2015 sampling. Using the epibenthos, ANIMIDA III findings clearly document that (1) environmental conditions in the nearshore system are stressful for epibenthos, resulting in low stocks and low biodiversity with the dominance of tolerant mobile crustaceans; (2) the decreasing influence of Pacific-origin water along the continental slope results in lower epibenthic stocks east of 150° W compared to further west; (3) faunal patterns change downslope, though less clear (because this was not an ANIMIDA III focus) than documented in the Transboundary project; and (4) local scale patchiness exists within the nearshore, shelf, and shelf break in epibenthic communities.

#### 6.4.1.2 Along-Shelf Faunal Patterns

An along-shelf shift in community structure accompanies the onshore-offshore pattern. The differences in community structure from east to west in the ANIMIDA III study area are well reflected in the proportional changes in number of taxa, abundance and biomass by phyla. In terms of taxonomic composition, a clear longitudinal trend can be observed, where especially the proportion of Arthropoda decreases towards the east while the proportions of Mollusca and Echinodermata increase (Figure 109). This same longitudinal pattern is even more evident in the relative proportion of abundance and biomass per phylum, with a marked change in proportion from Echinodermata and Mollusca to Arthropoda dominance from east to west (Figure 110 and Figure 111). The large dominance of the phylum Arthropoda, specifically various species of amphipods, shrimps and isopods, offshore of the Colville and Sagavanirktok Rivers reflect the apparently extreme conditions that occur in this area, described in the previous section.

The results from this analysis also coincide with previous findings in that total abundance and biomass varied longitudinally (in addition to varying with depth). Longitude (i.e., location along the shelf) was a significant predictor of total abundance and biomass, even though the correlation values were low. Across the whole U.S. Beaufort Sea shelf, the highest abundances occur on the shelf break in the vicinity of the Chukchi Sea as a result of nutrient-rich Pacific water inflow (Rand and Logerwell, 2011; Ravelo et al., 2015); this far western area was not sampled during ANIMIDA III. During ANIMIDA III, the areas with the lowest abundance and biomass were in the central part of the US Beaufort Sea (i.e., the western part of the study region) offshore of the Colville and Sagavanirktok Rivers, and increased again towards the east in the same range of values as previously reported (Norcross et al., 2015; Ravelo et al., 2015). The increase in epibenthic biomass towards the east was less pronounced than the changes in abundance, mostly due to the type of species that were dominant in the eastern stations. Eastern stations were dominated by small-bodied taxa, such as the brittle star *Ophiocten sericeum*, the bivalve *Similipecten greenlandicus*, and the cumacean *Diastylis scorpioides*. In contrast, the number of taxa and common biodiversity indices did not show a striking longitudinal trend throughout the study region. For these metrics, an overall patchiness was the observed prevailing pattern. This result is important because it emphasizes that common biodiversity measures may not be influenced by or reflect the same large-scale changes in key environmental conditions that affect the standing stock, abundance and the community structure of a region.

Although most taxa had a wide along-shelf distribution throughout the study area, their relative abundance and dominance changed greatly from east to west. This distribution pattern was also observed for infaunal polychaetes in a 1970's survey in the same region (Bilyard and Carey, 1979) and is in part related to the declining influence of Pacific-originated waters towards the east in the U.S. Beaufort Sea. A previous trawl survey described a break point in epibenthic species distribution and a marked reduction in biomass and abundance along the shelf break at ~ 150° W (Ravelo et al., 2015). While ANIMIDA III only sampled eight stations west of 150° W, the results confirm the earlier study, for example in that the brittle star *Ophiura sarsii* was largely absent east of 149° W (while highly dominant on shelfbreak and slope stations west of 150° W; Rand and Logerwell, 2011; Ravelo et al., 2015). More obvious, ANIMIDA III sampling confirmed the dominance of the brittle star species *Ophiocten sericeum* on the central and eastern U.S. Beaufort Sea shelf. *Ophiocten sericeum* is found in small numbers in other areas of the Pacific Arctic, but often dominates in areas highly influenced by riverine input, such as in the Laptev and Kara Seas (Fetzer and Deubel, 2006; Piepenburg and Schmid, 1997), and apparently also the rivers of the

Beaufort Sea. This biogeographic break point around 150° W is important and was in fact one of our arguments during the discussion about where to place the newly established DBO line, since changes in oceanographic patterns in this area would over time will presumably leave a detectable biological imprint at the seafloor.

The community in the western study area was mostly dominated by small crustaceans that are highly mobile and have the potential to rapidly enter areas after a disturbance, such as sea ice scouring and freshet events. These taxa provide a food source for diving ducks, stressing the importance of their presence in the shallow nearshore environment including lagoons (Dunton et al., 2012). Along the whole coast rivers and coastal erosion carry substantial amounts of terrigenous organic matter (OMterr), but the Mackenzie River outflow overwhelms all other sources (Rachold et al., 2004) and there may be a higher level of microbial processing in the eastern part of the study region before material enters the marine benthic food web. A previous analysis found substantial differences in food web length and the proportion of biomass in each trophic level in the epibenthic community found under the influence of the Mackenzie River and communities sampled further west on the Beaufort Sea shelf (Norcross et al., 2015; Bell et al., 2016). The presence of the microbial loop at the lower trophic levels of these OMterr-influenced food webs may be defining the organisms inhabiting the shelf under the influence of the Mackenzie River, leading to a unique epibenthic community and perhaps allowing for higher abundance and biomass. Alternatively or in addition, the above mentioned upwelling off Barter Island (Huffort ,1974; Mountain, 1974) could support the along-shore increase in standing stock compared to the central Beaufort shelf area.

### 6.4.2 Fish Communities

In comparison to epibenthic invertebrates, demersal fishes are less abundant, less species rich and contribute ≤20% to each catch in most cases in terms of standing stock and species richness, though fish tend to receive disproportionally high levels of attention. While this situation appears to be typical for high Arctic shelves (Norcross et al., 2010; Logerwell et al., 2011; Majewski et al., 2016), it is in stark contrast to the southeastern Bering and the Barents Seas where demersal fishes fuel large fisheries (Ingvaldsen et al., 2015). Also, both anadromous fishes and pelagic fishes can sustain subsistence fisheries even in high Arctic regions (Logerwell et al., 2015). ANIMIDA III sampling, however, focuses on demersal marine fish communities. General environmental characteristics of the study area obviously also apply as backdrop for the demersal fish community and are not repeated in this section.

Fish community structure, but not fish total abundance showed a depth dependent spatial pattern (Figure 122), though highest abundance generally occurred at shelf stations (Figure 134). While the low number of stations sampled on the slope in this study limits our ability to further explore the effect of increasing depth to total fish abundance, we did detect significant depth-related differences in fish community structure (Figure 131). The two main cluster of stations divided shelf / shelf break stations from nearshore stations. The delineation of these two cluster groups was not as clearly tied to the 20-m isobath as the benthic communities, which is in agreement with results from the wider Canadian Beaufort shelf where the transition in demersal fish communities was rather around 50 m (Majewski et al., 2015). This difference to the invertebrate fauna may be related to the higher mobility of fishes compared to epibenthos, i.e., the fishes ability to avoid adverse conditions, and to the fact that our sampling occurred during summer when freshet and ice gouging were absent. The Arctic Staghorn Sculpin *Gymnocanthus tricuspis* and Polar Eelpout *Lycodes polaris* characteristic of the nearshore cluster are two very abundant and widespread Arctic fishes typical of shelf and nearshore zones (Mecklenburg et al., 2011, 2016;

Majewski et al., 2016). While the Arctic cod *Boreogadus saida* contributed to the similarity of two clusters, the offshore and scattered clusters, the relative abundance of this species did not show any particular spatial patters in ANIMIDA III catches. More broad sampling, however, has shown this species to be an especially important component of the Beaufort Sea slope (>200-350 m) demersal fish community, but has also been reported to occur across the Beaufort shelf, in brackish lagoons and almost fresh waters of river mouths (Cohen et al., 1990; Norcross et al. 2015; Majewski et al., 2015). The Halfbarred Pout, *Gymnelus hemifasciatus*, the Spatulate Sculpin, *Icelus spatula* and the Ribbed Sculpin, *Triglops pingelii* characteristic of the shelf and upper slope cluster beside *B. saida* are all common and widely distributed Arctic shelf fishes (Mecklenburg et al., 2016). The third smaller cluster consisted of stations unexpectedly scattered throughout the study region which may be related to the fact that one of its characteristics taxa, *Lycodes* sp., was not identified to species and could have comprised several species. The ANIMIDA III depth-related patterns support findings by the Transboundary and Beaufort Regional Environmental Assessment (BREA) studies in the central and eastern Beaufort regions that demonstrate clear spatial trends in demersal fish abundance from shelf to slope, but sampled down to 1,000 m (Norcross et al., 2015; Majewski et al., 2016). These two studies found a suite of eelpout species to dominate deeper hauls starting at about 500 m, a depth range not covered by ANIMDA III. This finding may explain the absence of a more distinct slope fish community in the ANIMIDA III station set.

In the more spatially expansive Transboundary study, pelagic fish abundance and biomass was lower in areas nearing the Mackenzie River; however, this difference was not observed for demersal fish abundance or biomass (Norcross et al., 2015). Furthermore, they also found that the observed shelf-slope difference in abundance was consistent longitudinally as there was no evidence of an along-shore gradient in either biomass or abundance. Two possible explanations were given for these differences; for pelagic fish, in addition to the influence of the Mackenzie River plume, the timing of sampling was in the late open-water season, which could bias the results as there may be more or different small midwater fishes present at other times in the year. For the demersal fishes, perhaps the increase in easterly winds that drives the plume offshore and causes stratification of the shelf waters (Wood et al., 2013) does not affect the bottom waters, and, thus, does not affect demersal fishes. Visible indications of the plume extent are seen in satellite photos of chlorophyll and temperature in the surface. More mixing for prolonged periods of time is likely needed for the effects of the plume to reach the bottom to influence demersal fishes.

In terms of total abundance across the study area, the family *Cottidae* was more abundant than all other families. In terms of number of taxa, however, four families dominated the taxonomic inventory with nearly the same number of taxa (Figure 127). Spatially, the abundance of three of the dominant families, *Cottidae*, *Gadidae*, and *Zoarcidae*, had an even distribution throughout the study region, while the family *Liparidae* was found mostly nearshore or in western stations (Figure 127 and Figure 129). These results coincide with findings from previous studies in the same region and expanding further east (Norcross et al., 2015). In contrast to epibenthic diversity per station, fish diversity did show a spatial trend of reduced number of taxa, lower Shannon Diversity, Margalef's Richness, and Pielou's Evenness in the vicinity of the Colville and Sagavanirktok Rivers (Figure 123 through Figure 125). The influence of the two rivers could also be seen in the relative abundance of community representative taxa, which varied longitudinally similar to epibenthic representative taxa (Figure 130). As previously reported, the sculpin *Triglops pingelii* was characteristic of the shelf area under the influence of the Mackenzie River in this analysis while the Arctic Staghorn Sculpin *Gymnocanthus tricuspis* was dominant at many stations in the Colville and Sagavanirktok River influence areas. The community representative Arctic alligatorfish,

*Aspidophoroides olrikii*, Twohorn and Spatulate Sculpin, *Icelus spatula* and *I. bicornis*, in contrast were essentially absent from most freshwater-influenced stations in the vicinity of the Colville and Sagavanirktok Rivers. While these species apparently tolerate salinities down to 23-25 (Mecklenburg et al., 2016), they seem to avoid the riverine shallow areas of the Colville and Sagavanirktok deltas and shelf sections. These patterns highlight the important influence of freshwater inputs for the community composition of the Beaufort Sea shelf even for mobile organisms.

## Acknowledgments

This study was made possible in part by samples collected under a BOEM Contract Number M13PC00019 US Department of the Interior, BOEM. We thank Dan Holiday and Cathy Coon for their roles as Project Officers. Project management and field support through OF is gratefully acknowledged, with thanks especially to Justin Blank, Sheyna Wisdom, Willow Hetrick and initially Waverly Thorsen. Invaluable help on deck was provided by the *Norseman II* crew, and tireless support in trawl sorting was provided by Dan Holiday (BOEM), Nathan Wolf (OF), Katrin Iken, Lauren Bell, Kyle Dilliplaine, Lorena Edenfield, Kelly Walker, and Tanja Schollmeier (all UAF). A big thanks goes to the ANIMIDA III team for fruitful discussion and support: Ken Dunton and Susan Schonberg (UTA), Scott Libby and Greg Durell (Battelle), Jeremy Kasper (UAF), and John Trefry (FIT). We thank our taxonomic experts listed in the methods section for their expertise and time. Fish were collected under IACUC permit numbers 601331-2 and 601331-3, and ADF&G permit numbers CF-14-099 and CF-15-113. A letter of acknowledgement (2014-07) was provided by the National Marine Fisheries Service, and the North Slope Borough approved ANIMIDA III field activities (NSF 14-757).

## References


Ambrose W., Clough L., Tilney P., and Beer L. 2001. Role of echinoderms in benthic remineralization in the Chukchi Sea. Mar Biol 139:937–949.

Barnes D.K. 1999. The influence of ice on polar nearshore benthos. J Mar Biol Assoc UK 79:401-407

Barnes P.W., Reimnitz E., and Fox D. 1982. Ice rafting of fine-grained sediment, a sorting and transport mechanism, Beaufort Sea, Alaska. J Sediment Petrol 52:493-502

Bell L.E., Bluhm B.A., and Iken K. 2016. Influence of terrestrial organic matter in marine food webs of the Beaufort Sea shelf and slope. Mar Ecol Prog Ser. 550:1-24.

Bilyard G.R., Carey J.A.G. 1979. Distribution of western Beaufort Sea polychaetous annelids. Mar Biol 54:329-339. Birkely S.R. and Gulliksen B. 2003. Feeding ecology in five shrimp species (*Decapoda*, *Caridea*) from an Arctic fjord (Isfjorden, Svalbard), with emphasis on *Sclerocrangon boreas* (Phipps, 1774). Crustaceana 76(6):699-715

Blanchard A.L., Parris C.L., Knowlton A.L., and Wade N.R. 2013. Benthic ecology of the northeastern Chukchi Sea. Part II. Spatial variation of megafaunal community structure, 2009–2010. Cont Shelf Res 67:67–76.

Bluhm B.A., Iken K., Mincks S.L., Sirenko B.I., and Holladay B.A. 2009. Community structure of epibenthic megafauna in the Chukchi Sea. Aquat Biol 7:269–293.

Bluhm B.A., Huettmann F., and Norcross B.L. 2014. Ecological analyses of western Beaufort Sea data. OCS Study BOEM 2014-014, Anchorage, AK: USDOI, MMS, Alaska OCS Region, 46 pp

Carey A.G. Jr. and Ruff R.E. 1977. Ecological studies of the benthos in the western Beaufort Sea with special reference to bivalve mollusks. In: Dunbar, M. L. (ed) Polar Oceans. Calgary: Arctic Institute of North American, pp 505–530.

Carmack E.C. and Macdonald R.W. 2002. Oceanography of the Canadian Shelf of the Beaufort Sea: a setting for marine life. Arctic 55:29-45.

Carmack E. and Wassmann P. 2006. Food webs and physical–biological coupling on pan-Arctic shelves: unifying concepts and comprehensive perspectives. Progr Oceanogr 71(2), 446-477.

Carmack E.C., McLaughlin F.A., Vagle S., Melling H., and Williams W.J. 2010. Structures and property distributions in the three oceans surrounding Canada in 2007: A basis for a long-term ocean climate monitoring strategy. Atmos Ocean 48:211-224

Carmack E.C., Winsor P., and Williams W. 2015. The contiguous panarctic riverine coastal domain: a unifying concept. Prog Oceanogr. 139, 13-23. doi:10.1016/j.pocean.2015.07.014

Clarke K.R. and Gorley R.N. 2015. PRIMER v7: User Manual/Tutorial. PRIMER-E Ltd., Plymouth. 296 pp.

Cohen D.M., Inada T., Iwamoto T., and Scialabba N. 1990. FAO species catalogue. Vol. 10. Gadiform fishes of the world (Order Gadiformes). An annotated and illustrated catalogue of cods, hakes, grenadiers and other gadiform fishes known to date. FAO Fish Synop. 125(10). Rome: FAO. 442 p.

Conlan K.E., Lenihan H.S., Kvitek R.G., and Oliver J.S. 1998. Ice scour disturbance to benthic communities in the Canadian High Arctic. Mar Ecol Prog Ser 166:1-16.

Coyle K.O., Gillispie J.A., Smith R.L., and Barber W.E. 1997. Food habits of four demersal Chukchi Sea fishes. Am Fish Soc Symp 19:310–318.

Crane K. and Ostrovskiy A. 2015. Russian-American Long-term Census of the Arctic: RUSALCA. Oceanography, 28(3), 18-23.

Crane, J.J. 1974. Ecological studies of the benthic fauna in an arctic estuary. M.S. thesis. University of Alaska Fairbanks.

Day R. H., Weingartner T. J., Hopcroft R. R., Aerts L. A., Blanchard A. L., Gall A. E., Gallaway B. J., Hannay D. E., Holladay B. H., Mathis J. T., Norcross B. L., Questel J. M., and Wisdom S. S. 2013. The offshore northeastern Chukchi Sea, Alaska: a complex high-latitude ecosystem. Cont Shelf Res 67:147-165.

Dunton K.H., Goodall J.L., Schonberg S.V., Grebmeier J.M., and Maidment D.R. 2005. Multi-decadal synthesis of benthic–pelagic coupling in the western Arctic: role of cross-shelf advective processes. Deep-Sea Res Pt II 52(24–26):3462–3477.

Dunton K.H., Weingartner T., and Carmack E.C. 2006. The nearshore western Beaufort Sea ecosystem: Circulation and importance of terrestrial carbon in arctic coastal food webs. Prog Oceanog 71(2–4):362–378.

Dunton K.H., Schonberg S.V., and Cooper L.W. 2012. Food web structure of the Alaskan nearshore shelf and estuarine lagoons of the Beaufort Sea. Estuaries Coasts 35:416-435

Feder H.M., Jewett S.C., and Blanchard A. 2005. Southeastern Chukchi Sea (Alaska) epibenthos. Polar Biol 28:402–421.

Fechhelm R.G., Dillinger Jr R.E., Gallaway B.J., and Griffiths W.B. 1992. Modeling of in situ temperature and growth relationships for yearling broad whitefish in Prudhoe Bay, Alaska. Amer Fish Soc 121(1):1-12

Fetzer I. and Deubel H. 2006. Effect of river run-off on the distribution of marine invertebrate larvae in the southern Kara Sea (Russian Arctic). J Mar Syst 60:98-114

Frost K.J. and Lowry L.F. 1983. Demersal fishes and invertebrates trawled in the northeastern Chukchi and western Beaufort Seas 1976-1977. U.S. Department of Commerce NOAA Tech Rep NMFS-SSRF-764

Graeve M., Kattner G., and Piepenburg D. 1997. Lipids in Arctic benthos: does the fatty acid and alcohol composition reflect feeding and trophic interactions? Polar Biol 18:53-61

Grebmeier J.M. 2012. Shifting patterns of life in the Pacific Arctic and Sub-Arctic seas. Annu Rev Mar Sci 4:63–78.

Grebmeier J.M., Cooper L.W., Feder H.M.., and Sirenko B.I. 2006. Ecosystem dynamics of the Pacific-influenced Northern Bering and Chukchi Seas in the Amerasian Arctic. Prog Oceanogr 71:331–361

Haahtela I. 1990. What do Baltic studies tell us about the isopod *Saduria entomon* (L.)? Ann Zool Fennici 27:269-278

Hearon G., Dickins D., Ambrosius K., and Morris K. 2009. Mapping sea ice overflood using remote sensing: Smith Bay to Camden Bay. DF Dickins Associates, Coastal Frontiers Corporation, Aerometric, and The Geophysical Institute, University of Alaska, Alaska

Holme N.A. and McIntyre A.D. 1984. Methods for the study of marine benthos. 2nd edition. Blackwell Scientific Publ., Oxford, London, 387 pp.

Hufford G.L. 1974. Warm water advection in the Southern Beaufort Sea August-September 1971. J Geophys Res 78:2702-2707

Ingvaldsen,R. B., Bogstad B., Dolgov A.V., Ellingsen K.E., Gjøsæter H., Gradinger R., Johannesen E., Tveraaa T., and Yoccoz N. G. 2015. Sources of uncertainties in cod distribution models. Nature Climate Change 5(9):788-789

Logerwell,E., Rand K., and Weingartner T.J. 2011. Oceanographic characteristics of the habitat of benthic fish and invertebrates in the Beaufort Sea. Polar Biol 34:1783–1796.

Logerwell E., Busby M., Carothers C., Cotton S., Duffy-Anderson J., and Farley E. 2015. Fish communities across a spectrum of habitats in the western Beaufort Sea and Chukchi Sea. Progr Oceanography136:115-132.

Lovvorn J.R., Richman S.E., Grebmeier J.M., and Cooper L.W. 2003. Diet and body condition of spectacled eiders wintering in pack ice of the Bering Sea. Polar Biol 26:259–267.

Macdonald R.W. and Carmack E.C. 1991. The role of large-scale under-ice topography in separating estuary and ocean on an arctic shelf. Atmosphere-Ocean, 29(1):37-53

Macdonald R.W., Solomon S.M., Cranston R.E., Welch H.E., Yunker M.B., and Gobeil C. 1998. A sediment and organic carbon budget for the Canadian Beaufort Shelf. Mar Geol 144:255-273

Macdonald R.W., Naidu A.S., Yunker M.B., and Gobeil C. 2004. The Beaufort Sea: distribution, sources, fluxes, and burial rates of organic carbon. In: Stein R, Macdonald RW (eds.) The organic carbon cycle in the Arctic Ocean. Springer: Heidelberg, pp. 177–192.

Macdonald T.A., Burd B.J., Macdonald V.I., and van Roodselaar A. 2010. Taxonomic and feeding guild classification for the marine benthic macroinvertebrates of the Strait of Georgia, British Columbia.

Mahoney A.R., Eicken H., Gaylord A.G., and Gens R. 2014. Landfast sea ice extent in the Chukchi and Beaufort Seas: The annual cycle and decadal variability. Cold Reg Sci Technol 103:41-56

Majewski A. R., Walkusz W., Lynn B.R., Atchison S., Eert J., and Reist J.D. 2015. Distribution and diet of demersal Arctic Cod, *Boreogadus saida*, in relation to habitat characteristics in the Canadian Beaufort Sea. Polar Biol 39:1-12

Majewski A.R, Suchy K.D., Atchison S.P., Henry J., MacPhee S.A., Walkusz W., Eert J., Dempsey M., Niemi A., de Montety L., Geoffroy M., Giraldo C., Michel C., Archambault P., Williams W.J., Fortier L., and Reist J.D. 2016. Uniqueness of Fishes and Habitat Utilization in Oil & Gas Lease

Blocks Relative to Non-Lease Areas in the Canadian Beaufort Sea. Environmental Studies Revolving Funds Report Series, No. XXX, Ottawa. xi + 90 p.

Mountain,D. G. 1974. Preliminary analysis of Beaufort shelf circulation in summer. The coast and shelf of the Beaufort Sea, Arlington VA: Arctic Inst of N America, 27-48.

Mecklenburg C. W., Møller P.R., and Steinke D. 2011. Biodiversity of arctic marine fishes: taxonomy and zoogeography. Mar Biodiv 41(1):109-140

Mecklenburg C., Mecklenburg T.A., Sheiko B.A., and Steinke D. 2016. Pacific Arctic marine fishes. Conservation of Arctic Flora and Fauna, Akureyri, Iceland. ISBN: 978-9935-431-55-4

Møller, P., and L. Hellgren. 2006. Lipids and stable isotopes in marine food webs in West Greenland: trophic relations and health implications. Technical University of DenmarkDanmarks Tekniske Universitet, Department of Biochemistry and NutritionInstitut for Biokemi og Ern{æ}ring.Norcross B. L., Holladay B.A., Busby M.S., and Mier K.L. 2010. Demersal and larval fish assemblages in the Chukchi Sea. Deep Sea Res II 57(1):57-70

Norcross B., Bluhm B., Hardy S., Hopcroft R., and Iken K. 2015. US-Canada Transboundary Fish and Lower Trophic Communities: Abundance, Distribution, Habitat and Community Analysis. BOEM Agreement Number M12AC00011. Draft final report.

NPFMC. 2009. Fishery Management Plan for fish resources of the Arctic Management Area. North Pacific Fishery Management Council, 146 p.

Pickart R.S., Spall M.A., Moore G., Weingartner T.J., Woodgate R.A., Aagaard K., and Shimada K. 2011. Upwelling in Alaskan Beaufort Sea: Atmospheric forcing and local versus non-local response. Prog Oceanogr 88:78-100

Pickart R.S., Schulze L.M., Moore G., Charette M.A., Arrigo K.R., van Dijken G., and Danielson S. 2013. Long–term trends of upwelling and impacts on primary productivity in the Alaskan Beaufort Sea. Deep Sea Res Part I. doi: doi:10.1016/j.dsr.2013.05.003

Piepenburg D. 2005. Recent research on Arctic benthos: common notions need to be revised. Polar Biol 28:733–755.

Piepenburg D. and Schmid M.K. 1997. A photographic survey of the epibenthic megafauna of the Arctic Laptev Sea shelf: Distribution, abundance, and estimates of biomass and organic carbon demand. Mar Ecol Ser 147, 63–75.

Piepenburg D., Blackburn T.H., von Dorrien C.F., Gutt J., Hall P.O.J., Hulth S., Kendall M.A., Opalinski K.W., Rachor E., and Schmid M.K. 1995. Partitioning of benthic community respiration in the Arctic (northwest Barents Sea). Mar Ecol Prog Ser 118:119–213.

R Development Core Team. 2014. R: A language and environment for statistical computing. R Foundation for Statistical Computing, Vienna, Austria. Retrieved from <http://www.R-project.org/>

Rachold V., Eicken H., Gordeev V.V., Grigoriev M.N., Hubberten H.W., Lisitzin A.P., Shevchenko V.P., and Shcirrmeister L. 2004. Modern terrigenous organic carbon input to the Arctic Ocean. In: Stein R, Macdonald RW (eds) The organic carbon cycle in the Arctic Ocean. Springer, Heidelberg, p 33−55

Rand K.M. and Logerwell E.A. 2011. The first demersal trawl survey of benthic fish and invertebrates in the Beaufort Sea since the late 1970s. Polar Biol 34:475–488; doi 10.1007/s00300-010-0900-2

Ravelo A.M., Konar B., and Bluhm B.A. 2015. Spatial variability of epibenthic communities on the Alaska Beaufort Shelf. Polar Biol doi: 10.1007/s00300-015-1741-9

Ravelo A.M., Konar B., Trefry J.H., and Grebmeier J.M. 2014. Epibenthic community variability in the northeastern Chukchi Sea. Deep-Sea Res II 102:119–131.

Reimnitz E. and Kempema E. 1984. Pack ice interaction with Stamukhi Shoal, Beaufort Sea, Alaska. In: Barnes P, Schell D, Reimnitz E (eds) The Alaskan Beaufort Sea. Academic Press Inc., Orlando, pp 159-181

Russell M.P. 2013. Echinoderm responses to variation in salinity. Adv Mar Biol 66:171-212.

Roy V., Iken K., and Archambault P. 2014. Environmental drivers of the Canadian Arctic mega-epibenthic communities. PLoS ONE 9(7):e100900.

Sandberg E. and Bonsdorff E. 1990. On the structuring role of *Saduria entomon* (L.) on shallow water zoobenthos. Ann Ann Zool Fennici 27:279-284

Schulze L.M. and Pickart R.S. 2012. Seasonal variation of upwelling in the Alaskan Beaufort Sea: Impact of sea ice cover. J Geophys Res 117, C06022. doi:10.1029/2012JC007985

Smith C.R., Mincks S., and DeMaster D.J. 2006. A synthesis of bentho-pelagic coupling on the Antarctic shelf: Food banks, ecosystem inertia and global climate change. Deep-Sea Research II 53:875–894.

Thorsteinson L.K., Jarvela L.E., and Hale D.A. 1991. Arctic fish habitat use investigations: Nearshore studies in the Alaskan Beaufort Sea, summer 1990. National Oceanic and Atmospheric Administration, National Ocean Service, Office of Ocean Resources Conservation and Assessment.

Trefry J.H., Dunton K.H., Trocine R.P., SchonbergS.V., McTigue, N.D., Hersh E., and McDonald T.J. 2013. Chemical and biological assessment of two offshore drilling sites in the Alaskan Arctic. Mar Env Res 86, 35-45. DOI: 10.1016/j.marenvres.2013.02.008

Wood K.R., Overland J.E., Salo S.A., Bond N.A., Williams W.J., and Dong X. 2013. Is there a ‘‘new normal’’ climate in the Beaufort Sea? Polar Research 32, 19552. doi.org/10.3402/polar.v32i0.19552

# APPENDIX A: Characteristics of Petroleum Hydrocarbons in the Sediments and Benthic Organisms of the Beaufort Sea Continental Shelf

**Table A-1. PAH and alkyl PAH target analytes with approximate reporting and method detection limits.**

| Compound Names | Sediment (ng/g dry) | | Tissue (ng/g dry) | |
|---|---|---|---|---|
| | RL | MDL[1] | RL | MDL[1] |
| **Naphthalene[2]** | 1.2 | 0.531 | 2.9 | 2.98 |
| C1-Naphthalenes | 1.2 | 0.531 | 2.9 | 2.98 |
| C2-Naphthalenes | 1.2 | 0.531 | 2.9 | 2.98 |
| C3-Naphthalenes | 1.2 | 0.531 | 2.9 | 2.98 |
| C4-Naphthalenes | 1.2 | 0.531 | 2.9 | 2.98 |
| Biphenyl[3] | 1.2 | 0.162 | 2.9 | 1.25 |
| **Acenaphthylene** | 1.2 | 0.186 | 2.9 | 1.04 |
| **Acenaphthene** | 1.2 | 0.150 | 2.9 | 1.06 |
| Dibenzofuran[3] | 1.2 | 0.201 | 2.9 | 2.29 |
| **Fluorene** | 1.2 | 0.138 | 2.9 | 3.02 |
| C1-Fluorenes | 1.2 | 0.138 | 2.9 | 3.02 |
| C2-Fluorenes | 1.2 | 0.138 | 2.9 | 3.02 |
| C3-Fluorenes | 1.2 | 0.138 | 2.9 | 3.02 |
| **Anthracene** | 1.2 | 0.225 | 2.9 | 0.726 |
| **Phenanthrene** | 1.2 | 0.246 | 2.9 | 2.62 |
| C1-Phenanthrenes/Anthracenes | 1.2 | 0.246 | 2.9 | 2.62 |
| C2-Phenanthrenes/Anthracenes | 1.2 | 0.246 | 2.9 | 2.62 |
| C3-Phenanthrenes/Anthracenes | 1.2 | 0.246 | 2.9 | 2.62 |
| C4-Phenanthrenes/Anthracenes | 1.2 | 0.246 | 2.9 | 2.62 |
| Retene[3] | 1.2 | 0.174 | 2.9 | 0.600 |
| Dibenzothiophene[3] | 1.2 | 0.144 | 2.9 | 1.28 |
| C1-Dibenzothiophene[3] | 1.2 | 0.144 | 2.9 | 1.28 |
| C2-Dibenzothiophene[3] | 1.2 | 0.144 | 2.9 | 1.28 |
| C3-Dibenzothiophene[3] | 1.2 | 0.144 | 2.9 | 1.28 |
| C4-Dibenzothiophene[3] | 1.2 | 0.144 | 2.9 | 1.28 |
| **Fluoranthene** | 1.2 | 0.444 | 2.9 | 0.944 |
| **Pyrene** | 1.2 | 0.537 | 2.9 | 0.848 |
| C1-Fluoranthenes/Pyrenes | 1.2 | 0.537 | 2.9 | 0.848 |
| C2-Fluoranthenes/Pyrenes | 1.2 | 0.537 | 2.9 | 0.848 |
| C3-Fluoranthenes/Pyrenes | 1.2 | 0.537 | 2.9 | 0.848 |
| **Benzo(a)anthracene** | 1.2 | 0.369 | 2.9 | 0.752 |
| **Chrysene** | 1.2 | 0.333 | 2.9 | 0.606 |
| C1-Chrysenes | 1.2 | 0.333 | 2.9 | 0.606 |
| C2-Chrysenes | 1.2 | 0.333 | 2.9 | 0.606 |
| C3-Chrysenes | 1.2 | 0.333 | 2.9 | 0.606 |
| C4-Chrysenes | 1.2 | 0.333 | 2.9 | 0.606 |
| **Benzo(b)fluoranthene** | 1.2 | 0.390 | 2.9 | 0.723 |
| **Benzo(k)fluoranthene** | 1.2 | 0.201 | 2.9 | 0.663 |
| Benzo(e)pyrene | 1.2 | 0.303 | 2.9 | 0.642 |
| **Benzo(a)pyrene** | 1.2 | 0.411 | 2.9 | 0.468 |

| Compound Names | Sediment (ng/g dry) | | Tissue (ng/g dry) | |
|---|---|---|---|---|
| | RL | MDL[1] | RL | MDL[1] |
| Perylene | 1.2 | 0.354 | 2.9 | 0.612 |
| **Indeno(1,2,3-cd)pyrene** | 1.2 | 0.462 | 2.9 | 0.543 |
| **Dibenz(a,h)anthracene** | 1.2 | 0.285 | 2.9 | 0.279 |
| **Benzo(g,h,i)perylene** | 1.2 | 0.450 | 2.9 | 0.417 |
| Sum PAH16 (∑16 EPA priority PAH | NA | NA | NA | NA |
| Total PAH | NA | NA | NA | NA |

[1] Sediment MDL based on a 20g sample size (wet weight; 16.63 g d. wt.) with a dilution factor of 2 and PIV=1000uL. Tissue MDL based on 20 g sample size (wet weight; 3.58 g d. wt.) with a dilution factor of 2.051 and PIV=500uL

[2] Bolded compounds are the 16 priority PAH pollutants.

[3] Compounds (eight in total) ***not*** included in the sediment ESB calculations because published $C_{OC,PAHi,FCVi}$ values are not available.

**Table A-2. 2015 Petroleum biomarker (S/T) target analytes with approximate reporting and method detection limits.**

| Compound Names Used | Sediment (ng/g dry) | | Tissue (ng/g dry) | |
|---|---|---|---|---|
| | RL | MDL[1] | RL | MDL |
| ***Base 15 Compounds*** | | | | |
| C23 Tricyclic Terpane (T4) | 1.8 | 0.318 | 7.6 | 1.39 |
| C29 Tricyclic Terpane -22S (T9) | 1.8 | 0.318 | 7.6 | 1.39 |
| C29 Tricyclic Terpane -22R (T10) | 1.8 | 0.318 | 7.6 | 1.39 |
| Ts-18a(H)-22,29,30-Trisnorneohopane | 1.8 | 0.318 | 7.6 | 1.39 |
| Tm-17a(H)-22,29,30-Trisnorhopane | 1.8 | 0.318 | 7.6 | 1.39 |
| 30-Norhopane (T15) | 1.8 | 0.318 | 7.6 | 1.39 |
| 18a(H) & 18b(H)-Oleananes (T18) | 1.8 | 0.318 | 7.6 | 1.39 |
| 17a(H),21b(H)-hopane (Hopane; T19) | 1.8 | 0.318 | 7.6 | 1.39 |
| 30-Homohopane -22S (T21) | 1.8 | 0.318 | 7.6 | 1.39 |
| 30-Homohopane -22R (T22) | 1.8 | 0.318 | 7.6 | 1.39 |
| 13b(H),17a(H)-20S-Diacholestane (S4) | 0.60 | 0.114 | 2.5 | 0.402 |
| 13b(H),17a(H)-20R-Diacholestane (S5) | 0.60 | 0.114 | 2.5 | 0.402 |
| 14a(H),17a(H)-20R-Methylcholestane | 0.60 | 0.114 | 2.5 | 0.402 |
| 14a(H),17a(H)-20S-Ethylcholestane | 0.60 | 0.114 | 2.5 | 0.402 |
| 14a(H),17a(H)-20R-Ethylcholestane | 0.60 | 0.114 | 2.5 | 0.402 |
| ***Additional Compounds Analyzed*** | | | | |
| C24 Tricyclic Terpane (T5) | 1.8 | 0.318 | 7.6 | 1.39 |
| C25 Tricyclic Terpane (T6) | 1.8 | 0.318 | 7.6 | 1.39 |
| C24 Tetracyclic Terpane (T6a) | 1.8 | 0.318 | 7.6 | 1.39 |
| C26 Tricyclic Terpane -22S (T6b) | 1.8 | 0.318 | 7.6 | 1.39 |
| C26 Tricyclic Terpane -22R (T6c) | 1.8 | 0.318 | 7.6 | 1.39 |
| C28 Tricyclic Terpane -22S (T7) | 1.8 | 0.318 | 7.6 | 1.39 |
| C28 Tricyclic Terpane -22R (T8) | 1.8 | 0.318 | 7.6 | 1.39 |
| 17a(H),21b(H)-28,30-Bisnorhopane | 1.8 | 0.318 | 7.6 | 1.39 |
| 17a(H),21b(H)-25-Norhopane (T14b) | 1.8 | 0.318 | 7.6 | 1.39 |
| 18a(H)-30-Norneohopane -C29Ts (T16) | 1.8 | 0.318 | 7.6 | 1.39 |
| 17a(H)-Diahopane (X) | 1.8 | 0.318 | 7.6 | 1.39 |
| 30-Normoretane (T17) | 1.8 | 0.318 | 7.6 | 1.39 |
| Moretane (T20) | 1.8 | 0.318 | 7.6 | 1.39 |
| 30-Bishomohopane -22S (T26) | 1.8 | 0.318 | 7.6 | 1.39 |
| 30,31-Bishomohopane -22R (T27) | 1.8 | 0.318 | 7.6 | 1.39 |
| 30,31-Trishomohopane -22S (T30) | 1.8 | 0.318 | 7.6 | 1.39 |
| 30,31-Trishomohopane -22R (T31) | 1.8 | 0.318 | 7.6 | 1.39 |
| Tetrakishomohopane -22S (T32) | 1.8 | 0.318 | 7.6 | 1.39 |
| Tetrakishomohopane -22R (T33) | 1.8 | 0.318 | 7.6 | 1.39 |
| Pentakishomohopane -22S (T34) | 1.8 | 0.318 | 7.6 | 1.39 |
| Pentakishomohopane -22R (T35) | 1.8 | 0.318 | 7.6 | 1.39 |
| 13b(H),17a(H)-20S- | 0.60 | 0.114 | 2.5 | 0.402 |
| 14a(H),17a(H)-20S-Cholestane (S12) | 0.60 | 0.114 | 2.5 | 0.402 |

| Compound Names Used | Sediment (ng/g dry) | | Tissue (ng/g dry) | |
|---|---|---|---|---|
| | RL | MDL[1] | RL | MDL |
| 14a(H),17a(H)-20R-Cholestane (S17) | 0.60 | 0.114 | 2.5 | 0.402 |
| 14a(H),17a(H)-20S-Methylcholestane | 0.60 | 0.114 | 2.5 | 0.402 |
| 14b(H),17b(H)-20R-Cholestane (S14) | 0.60 | 0.114 | 2.5 | 0.402 |
| 14b(H),17b(H)-20S-Cholestane (S15) | 0.60 | 0.114 | 2.5 | 0.402 |
| 14b(H),17b(H)-20R-Methylcholestane | 0.60 | 0.114 | 2.5 | 0.402 |
| 14b(H),17b(H)-20S-Methylcholestane | 0.60 | 0.114 | 2.5 | 0.402 |
| 14b(H),17b(H)-20R-Ethylcholestane | 0.60 | 0.114 | 2.5 | 0.402 |
| 14b(H),17b(H)-20S-Ethylcholestane | 0.60 | 0.114 | 2.5 | 0.402 |
| 14a(H),17a(H)-20R-Cholestane (S17)[2] | 0.06 | 0.114 | 2.5 | 0.402 |
| 17b(H),21b(H)-Hopane [2] | 1.8 | 0.318 | 7.6 | 1.39 |

[1] Sediment MDL based on a 20g sample size (wet weight; 16.64 g d. wt.) with a dilution factor of 1 and PIV=1000uL. Tissue RL was estimated based on a 20g sample size (wet weight; 4.03 g d. wt.) with a dilution factor of 2.051 and PIV=500uL.

[2] Compounds used for response factor generation in the calibration. The hopane compound is used to generate the RF to quantify the hopanes; the cholestane compound is used to generate the RF to quantify all other compounds.

**Table A-3. 2015 SHC target analytes with approximate reporting and method detection limits.**

| Compound Names | Common Abbreviation | Sediment (ng/g dry) | | Tissue (ng/g dry) | |
|---|---|---|---|---|---|
| | | RL | MDL | RL | MDL |
| n-Nonane | n-C9 | 120 | 7.46 | 305 | 28.7 |
| n-Decane | n-C10 | 120 | 5.70 | 305 | 90.2 |
| n-Undecane | n-C11 | 120 | 5.93 | 305 | 35.8 |
| n-Dodecane | n-C12 | 120 | 6.42 | 305 | 30.4 |
| n-Tridecane | n-C13 | 120 | 7.57 | 305 | 21.5 |
| Isoprenoid RRT 1380 [2] | IP1380 | NA | NA | 305 | NA |
| n-Tetradecane | n-C14 | 120 | 5.66 | 305 | 29.6 |
| Isoprenoid RRT 1470 [2] | IP1470 | NA | NA | 305 | NA |
| n-Pentadecane | n-C15 | 120 | 5.49 | 305 | 56.3 |
| n-Hexadecane | n-C16 | 120 | 12.9 | 305 | 30.1 |
| Norpristane (1650) [2] | IP1650 | NA | NA | 305 | NA |
| n-Heptadecane | n-C17 | 120 | 5.71 | 305 | 48.0 |
| Pristane | Pristane | 120 | 25.0 | 305 | 95.3 |
| n-Octadecane | n-C18 | 120 | 8.06 | 305 | 23.9 |
| Phytane | Phytane | 120 | 9.23 | 305 | 24.9 |
| n-Nonadecane | n-C19 | 120 | 4.91 | 305 | 26.9 |
| n-Eicosane | n-C20 | 120 | 10.1 | 305 | 30.6 |
| n-Heneicosane | n-C21 | 120 | 3.07 | 305 | 29.3 |
| n-Docosane | n-C22 | 120 | 17.6 | 305 | 36.3 |
| n-Tricosane | n-C23 | 120 | 6.97 | 305 | 25.8 |
| n-Tetracosane | n-C24 | 120 | 17.4 | 305 | 25.1 |
| n-Pentacosane | n-C25 | 120 | 15.4 | 305 | 16.2 |
| n-Hexacosane | n-C26 | 120 | 10.2 | 305 | 15.4 |
| n-Heptacosane | n-C27 | 120 | 8.97 | 305 | 25.9 |
| n-Octacosane | n-C28 | 120 | 9.62 | 305 | 19.7 |
| n-Nonacosane | n-C29 | 120 | 6.26 | 305 | 23.0 |
| n-Triacontane | n-C30 | 120 | 6.85 | 305 | 21.1 |
| n-Hentriacontane | n-C31 | 120 | 4.05 | 305 | 40.0 |
| n-Dotriacontane | n-C32 | 120 | 5.74 | 305 | 25.7 |
| n-Tritriacontane | n-C33 | 120 | 2.87 | 305 | 23.9 |
| n-Tetratriacontane | n-C34 | 120 | 4.99 | 305 | 30.6 |
| n-Pentatriacontane | n-C35 | 120 | 5.19 | 305 | 26.8 |
| n-Hexatriacontane | n-C36 | 120 | 4.44 | 305 | 31.1 |
| n-Heptatriacontane | n-C37 | 120 | 9.92 | 305 | 40.0 |
| n-Octatriacontane | n-C38 | 120 | 5.65 | 305 | 44.3 |
| n-Nonatriacontane | n-C39 | 120 | 9.26 | 305 | 52.6 |
| n-Tetracontane | n-C40 | 120 | 10.0 | 305 | 60.6 |

| Compound Names | Common Abbreviation | Sediment (ng/g dry) | | Tissue (ng/g dry) | |
|---|---|---|---|---|---|
| | | RL | MDL | RL | MDL |
| Sum SHC (C9-C40) | ∑SHC | NA | NA | NA | NA |
| SHC Total (C9-C40) | TotSHC | NA | 694 | NA | 267,000 |

[1] Water MDL based on 1L sample with a dilution factor of 1 and PIV=500uL. Sediment MDL based on a 20g sample size (wet weight; 16.64 g d. wt.) with a dilution factor of 2 and PIV=1000uL. Tissue RL is estimated based on 20 g sample size (wet weight; 3.36g d. wt.) with a dilution factor of 2.051 and PIV=500uL.

[2] Standards are not available for this compound. The RL and MDL of the compound which elutes prior to the isoprenoid compound is applied.

**Table A-4. Quality control sample measurement quality objectives (MQOs).**

| QC Sample Type | Measurement Quality Objective (MQO) | Corrective Action |
|---|---|---|
| Hydrocarbons (PAH/SHC/Biomarker)[a] | | |
| Method Blank (MB) | Target analyte concentration in MB <5x the MDL, or MB result is N-qualified.<br>Data are acceptable if field sample concentration >5x MB; however, field sample data <5x the MB will be B-qualified regardless of MB concentration. | Review with PM, possibly re-analyze and/or re-extract and reanalyze. If data fail MQO, report data with qualifiers. |
| Laboratory Control Sample (LCS) | Target analyte recoveries:70-130%;<br>50-130% for nonane. | Review with PM, possibly re-analyze and/or re-extract and reanalyze. If data fail MQO, report data with qualifiers. |
| Matrix Spike (MS) | Target analyte recoveries:70-130%;<br>50-130% for nonane.<br>Spike concentration must be >5x unspiked field sample concentration for MQO to apply. | Compare with LCS. If the MS results are outside the LCS, review with the PM to determine if difference is due to matrix effects or analytical. Review sample prep records, re-analyze as directed by the PM. If data fail MQO, report data with qualifiers. |
| Matrix Spike Duplicates (MSD) | RPD ≤ 30%.<br>Spike concentration must be >5x unspiked field sample concentration for MQO to apply. | Review with PM, possibly re-analyze and/or re-extract and reanalyze. If data fail MQO, report data with qualifiers. |
| North Slope Crude (NSC) | RPD ≤ 30%.<br>Concentration must be >5x the MDL for MQO to apply. | Review with PM, possibly re-analyze and/or re-extract and reanalyze. If data fail MQO, report data with qualifiers. |
| Standard Reference Material (SRM) | PD ≤ 30% from target concentration and the 95% confidence level.<br>Analyte concentration must be certified and >5x the MDL for MQO to apply. | Review with PM, possibly re-analyze and/or re-extract and reanalyze. If data fail MQO, report data with qualifiers. |
| Surrogate Internal Standard (SIS) | Recoveries: 40-120%. | Review with PM, possibly re-analyze and/or re-extract and reanalyze. If data fail MQO, report data with qualifiers. |

[a] Hydrocarbon MQOs are based on the use of surrogate recovery corrected data.

**Table A-5. Analytical chemistry data qualifiers/flags.**

| **Laboratory Data Qualifiers** – Hydrocarbon Analysis | |
|---|---|
| N | The QC result does not meet the accuracy, precision, or method blank MQO. The quality control result, not the related sample compound, is qualified. |
| n | The QC result does not meet the base accuracy or precision MQO, but meets the contingency criteria.<br>Spiked sample (MS/MSD) and SRM result is less than 5X the native sample concentration or less than 5X the MDL (field sample replicate). |
| B | Blank contamination. The analyte was detected in the field sample at <5X the Method Blank concentration; the qualifier is applied the field sample. The B qualifier is not applied if the sample data is J-qualified. |
| J | Estimated value: The analyte was positively identified but at a concentration less than the sample-specific RL. |
| U | Analyte was not detected at a 3-5:1 signal:noise ratio. The reported data value is the sample-specific MDL. |
| D | Dilution analysis value. The initial analysis was outside the calibration range of the instrument. |
| E | Estimated value. Result is greater than the highest calibration concentration. |
| ME | Estimated value. Significant matrix interference. |
| MI | Significant matrix interference. Value could not be determined or estimated. |
| T | Holding time (HT) exceeded. |
| H | Surrogate compound was diluted out. Qualifier used when surrogate recovery is affected by dilution of sample extract. |
| NA | Not applicable. |

**Table A-6. Surface Sediment Hydrocarbon Concentrations ANIMIDA III 2014**

**(PAH and S/T in ng/g d. wt. and SHC in ug/g, d. wt.)**

| Station | Station Type | Total PAH | Sum S/T | Sum SHC (C9-C40) | SHC Total (C9-C40) | % TOC |
|---|---|---|---|---|---|---|
| 1 | Random | 791 | 89.5 | 3.45 | 6.79 | 1.33 |
| 1.05 | Random | 1,120 | 134 | 5.92 | 9.48 | 1.08 |
| 1.2 | Random | 1,220 | 126 | 7.95 | 10.3 | 1.75 |
| 4 | Random | 51.1 | 9.68 | 0.36 | 0.49 | 0.68 |
| 5 | Random | 103 | 13.0 | 0.55 | 1.62 | 0.29 |
| 6 | Random | 646 | 75.2 | 2.85 | 4.48 | 0.83 |
| 6.1 | Random | 1,190 | 122 | 7.03 | 8.12 | 1.44 |
| 7 | Random | 879 | 107 | 5.19 | 9.22 | 1.20 |
| 8 | Random | 633 | 64.7 | 3.91 | 4.94 | 1.09 |
| 9 | Random | 1,030 | 150 | 4.20 | 9.25 | 1.18 |
| 9-DUP | Random | 1,030 | 140 | 3.93 | 4.12 | 1.38 |
| 9A | Random | 1,300 | 154 | 6.41 | 6.23 | 1.13 |
| 10 | Random | 485 | 69.6 | 3.67 | 5.31 | 1.32 |
| 11 | Random | 595 | 89.9 | 2.49 | 4.18 | 1.16 |
| 11A | Random | 730 | 80.3 | 3.42 | 2.84 | 1.07 |
| 12 | Random | 777 | 131 | 3.46 | 4.39 | 0.79 |
| 15 | Random | 463 | 80.3 | 2.00 | 1.74 | 1.53 |
| 16 | Random | 525 | 90.1 | 2.23 | 3.72 | 1.22 |
| 18 | Random | 409 | 92.5 | 2.26 | 5.54 | 0.86 |
| 20 | Random | 195 | 40.8 | 1.01 | 1.10 | 0.37 |
| 21 | Random | 277 | 69.7 | 1.68 | 2.56 | 0.82 |
| 22 | Random | 414 | 109 | 3.66 | 12.6 | 1.16 |
| 23 | Random | 436 | 84.3 | 2.42 | 5.37 | 0.64 |
| 24 | Random | 568 | 125 | 2.55 | 8.23 | 1.16 |
| 25 | Random | 607 | 119 | 4.48 | 6.53 | 1.05 |
| 1B | BSMP/ANIMIDA | 65.7 | 14.8 | 0.73 | 0.52 | 0.72 |
| 1C | BSMP/ANIMIDA | 548 | 111 | 3.34 | 6.41 | 1.12 |
| 2C | BSMP/ANIMIDA | 464 | 87.0 | 3.17 | 5.02 | 1.39 |
| 5B | BSMP/ANIMIDA | 22.6 | 8.41 | 0.20 | 0.61 | 0.82 |
| 5E | BSMP/ANIMIDA | 27.8 | 8.71 | 0.28 | 0.50 | 0.25 |
| 5(5) | BSMP/ANIMIDA | 248 | 47.3 | 2.08 | 0.65 | 1.66 |
| 6D | BSMP/ANIMIDA | 233 | 29.8 | 1.53 | 3.12 | 0.77 |
| 6F | BSMP/ANIMIDA | 151 | 16.0 | 0.87 | 0.53 | 1.95 |
| 7C | BSMP/ANIMIDA | 1,060 | 115 | 6.59 | 8.87 | 1.35 |
| N03 | BSMP/ANIMIDA | 540 | 74.1 | 4.71 | 3.66 | 2.28 |
| HEX-1 | Camden Bay | 347 | 95.3 | 2.75 | 12.1 | 0.90 |
| L250-5 | Camden Bay | 418 | 101 | 2.63 | 10.9 | 0.90 |

| Station | Station Type | Total PAH | Sum S/T | Sum SHC (C9-C40) | SHC Total (C9-C40) | % TOC |
|---|---|---|---|---|---|---|
| L250-5-DUP | Camden Bay | 523 | 127 | 3.00 | 11.2 | 0.83 |
| HEX-12 | Camden Bay | 497 | 111 | 2.86 | 6.73 | 0.92 |
| HEX-17 | Camden Bay | 451 | 119 | 3.32 | 13.7 | 1.04 |
| HH1-5 | Camden Bay | 415 | 86.4 | 2.50 | 5.67 | 0.88 |
| S-XA | Camden Bay | 252 | 50.3 | 1.54 | 0.66 | 0.59 |
| T-3 | Camden Bay | 386 | 78.3 | 2.13 | 4.48 | 0.96 |
| T-XA | Camden Bay | 439 | 99.4 | 2.31 | 8.75 | 1.07 |
| M-4 | Camden Bay | 369 | 82.5 | 1.85 | 4.73 | 1.28 |
| | | | | | | |
| | Mean | 532 | 85.1 | 3.01 | 5.51 | 1.07 |
| | Min | 22.6 | 8.41 | 0.20 | 0.49 | 0.25 |
| | Max | 1,300 | 154 | 7.95 | 13.7 | 2.28 |
| | STD | 331 | 39.9 | 1.80 | 3.65 | 0.40 |
| | RSD | 62% | 47% | 60% | 66% | 37% |

**Table A-7. Sediment Core Hydrocarbon Concentrations ANIMIDA III 2014**

**(PAH and S/T in ng/g d. wt.and SHC in ug/g, d. wt.)**

| Station | Core Segment Depth (cm) | Age of Sediment (~yrs)[a] | Total PAH | Sum S/T | Sum SHC (C9-C40) | SHC Total (C9-C40) | % TOC |
|---|---|---|---|---|---|---|---|
| 1.2 | 0-2 | 7 | 1,430 | 176 | 8.47 | 18.2 | 1.65 |
| 1.2 | 2-4 | 21 | 1,440 | 167 | 8.33 | 13.0 | 1.60 |
| 1.2 | 4-6 | 36 | 1,490 | 173 | 8.33 | 14.8 | 1.65 |
| 1.2 | 6-8 | 50 | 1,420 | 169 | 8.24 | 18.8 | 1.67 |
| 1.2 | 8-10 | 64 | 1,450 | 171 | 8.27 | 15.0 | 1.62 |
| 1.2 | 10-12 | 79 | 1,360 | 179 | 8.04 | 23.5 | 1.55 |
| 1.2 | 12-14 | 93 | 1,370 | 172 | 7.72 | 11.5 | 1.52 |
| 1.2 | 20-22 | 150 | 1,350 | 155 | 7.40 | 11.4 | 1.56 |
| 1.2 | 40-42 | 307 | 1,270 | 155 | 6.49 | 12.7 | 1.45 |
| 1.2 | 60-63 | 439 | 1,260 | 154 | 6.45 | 13.4 | 1.49 |
| 1.2 | 78-81 | 568 | 1,150 | 141 | 6.19 | 10.2 | 1.56 |
| | | | | | | | |
| Mean | | | 1,360 | 165 | 7.63 | 14.8 | 1.57 |
| Min | | | 1,150 | 141 | 6.19 | 10.2 | 1.45 |
| Max | | | 1,490 | 179 | 8.47 | 23.5 | 1.67 |
| STD | | | 102 | 11.7 | 0.87 | 3.96 | 0.07 |
| RSD | | | 7.5% | 7.1% | 11% | 27% | 4.5% |

[a] The age of the sediments in the core segment is approximate, and is based on $^{137}Cs$ and $^{210}Pb$ isotope dating, which produced a sedimentation rate of approximately 0.14 cm/yr. The mid-depth of the core segment was used to estimate the number of years since that sediment had been deposited.

**Table A-8. Surface Sediment Hydrocarbon Concentrations ANIMIDA III 2015**

**(PAH and S/T in ng/g d. wt. and SHC in ug/g, d. wt.)**

| Station | Station Type | Total PAH | Sum S/T | Sum SHC (C9-C40) | SHC Total (C9-C40) | % TOC |
|---|---|---|---|---|---|---|
| 70-142 | Offshore BIO | 476 | 96.9 | 1.92 | 5.61 | 0.82 |
| 70-143 | Offshore BIO | 547 | 150 | 2.36 | 7.44 | 0.76 |
| 70-145 | Offshore BIO | 305 | 61.1 | 1.33 | 2.73 | 1.05 |
| 71-145 | Offshore BIO | 871 | 161 | 3.50 | 7.89 | 1.17 |
| 71-146 | Offshore BIO | 1,410 | 159 | 5.07 | 12.3 | 1.32 |
| 71-147 | Offshore BIO | 436 | 56.9 | 1.71 | 2.53 | 0.84 |
| 71-147A | Offshore BIO (core) | 1,470 | 192 | 5.73 | 17.7 | 1.27 |
| 71-149 | Offshore BIO | 324 | 41.1 | 1.19 | 1.93 | 0.67 |
| 71-150 | Offshore BIO | 96.0 | 16.2 | 0.41 | 0.48 | 0.30 |
| 149-200 | Offshore BIO | 782 | 96.8 | 3.65 | 6.39 | 0.83 |
| 149-350 | Offshore BIO | 1,380 | 160 | 6.46 | 12.7 | 1.35 |
| 3A | BSMP/ANIMIDA | 427 | 69.4 | 3.79 | 9.42 | 2.36 |
| 4A | BSMP/ANIMIDA | 333 | 30.0 | 2.11 | 2.89 | 0.93 |
| 4B | BSMP/ANIMIDA | 122 | 17.3 | 0.85 | 0.13 | 0.84 |
| 5A | BSMP/ANIMIDA | 514 | 84.5 | 3.82 | 7.31 | 1.92 |
| BP01 | BSMP/ANIMIDA | 348 | 50.1 | 2.28 | 3.12 | 1.23 |
| L08 | BSMP/ANIMIDA | 310 | 43.7 | 2.77 | 5.50 | 1.10 |
| N03 | BSMP/ANIMIDA | 407 | 71.7 | 2.96 | 5.21 | 1.93 |
| N06 | BSMP/ANIMIDA | 629 | 100 | 4.95 | 9.29 | 1.85 |
| 143W-1 | DBO-East | 616 | 166 | 2.45 | 16.1 | 1.00 |
| 143W-2 | DBO-East | 321 | 69.2 | 1.31 | 3.44 | 0.84 |
| 143W-4 | DBO-East | 1,200 | 212 | 4.62 | 16.7 | 1.22 |
| 143W-5 | DBO-East | 1,250 | 183 | 4.77 | 17.1 | 1.21 |
| 143-W6 | DBO-East | 1,380 | 205 | 4.80 | 14.3 | 1.17 |
| 152W0 | DBO-West | 1,320 | 179 | 7.34 | 15.6 | 1.52 |
| 152W1 | DBO-West | 1,120 | 145 | 4.77 | 11.9 | 0.99 |
| Kup[1] (peat) | Kuparuk River | 161 | 102 | 15.6 | 14.7 | NA[2] |
| Sag (peat) | Sagavanirktok River | 501 | 131 | 4.13 | 7.73 | NA |
| | Mean[3] | 707 | 108 | 3.34 | 8.30 | 1.17 |
| | Min | 96.0 | 16.2 | 0.41 | 0.13 | 0.30 |
| | Max | 1,470 | 212 | 7.34 | 17.7 | 2.36 |
| | STD | 450 | 62.3 | 1.82 | 5.58 | 0.45 |
| | RSD | 64% | 58% | 54% | 67% | 38% |

[1] Peat samples collected in 2006 from Kuparuk, Sagavanirktok, and Colville Rivers as well as from Pingok Island (a Jones Island off Oliktok Point between Colville and Kuparuk Rivers) and Eskimo Island (in western Harrison Bay, near stations 7A and 7G).

[2] NA: Not available.

[3] The summary statistics are for the surface sediments and do not include the river peat samples.

**Table A-9. Hydrocarbon Diagnostic Measures for Sediment, Peat, and Oil Samples Analyzed During ANIMIDA III in 2014 and 2015**

| Station | Pyro/Petro PAH | Retene+ Perylene /TPAH | LALK/ TALK | Pristane/ Phytane | CPI |
|---|---|---|---|---|---|
| Surface Sediment - 2014 | | | | | |
| 1 | 0.147 | 0.093 | 0.318 | 2.49 | 3.72 |
| 1.05 | 0.140 | 0.105 | 0.265 | 2.19 | 4.32 |
| 1.2 | 0.129 | 0.099 | 0.218 | 2.35 | 4.75 |
| 4 | 0.100 | 0.101 | 0.309 | 2.00 | 4.27 |
| 5 | 0.137 | 0.083 | 0.346 | 1.90 | 3.09 |
| 6 | 0.154 | 0.087 | 0.348 | 2.27 | 3.38 |
| 6.1 | 0.139 | 0.098 | 0.239 | 2.39 | 4.39 |
| 7 | 0.142 | 0.104 | 0.312 | 2.11 | 4.09 |
| 8 | 0.142 | 0.167 | 0.259 | 1.97 | 4.40 |
| 9 | 0.164 | 0.087 | 0.372 | 2.00 | 3.10 |
| 9-DUP | 0.163 | 0.087 | 0.371 | 2.04 | 3.10 |
| 9A | 0.151 | 0.098 | 0.281 | 2.20 | 3.87 |
| 10 | 0.154 | 0.106 | 0.269 | 1.97 | 4.09 |
| 11 | 0.162 | 0.084 | 0.381 | 2.44 | 3.04 |
| 11A | 0.149 | 0.094 | 0.294 | 2.48 | 4.00 |
| 12 | 0.172 | 0.102 | 0.339 | 2.59 | 3.44 |
| 15 | 0.173 | 0.092 | 0.368 | 1.92 | 3.13 |
| 16 | 0.178 | 0.088 | 0.402 | 2.81 | 2.70 |
| 18 | 0.196 | 0.139 | 0.332 | 1.63 | 3.42 |
| 20 | 0.184 | 0.132 | 0.361 | 1.85 | 3.18 |
| 21 | 0.212 | 0.175 | 0.293 | 1.74 | 3.54 |
| 22 | 0.206 | 0.174 | 0.224 | 1.68 | 4.84 |
| 23 | 0.197 | 0.117 | 0.415 | 1.69 | 2.72 |
| 24 | 0.177 | 0.116 | 0.259 | 1.88 | 4.42 |
| 25 | 0.187 | 0.123 | 0.207 | 1.84 | 5.03 |
| 1B | 0.147 | 0.118 | 0.165 | 2.14 | 6.26 |
| 1C | 0.177 | 0.125 | 0.239 | 1.82 | 4.53 |
| 2C | 0.167 | 0.121 | 0.215 | 2.07 | 4.95 |
| 5B | 0.112 | 0.092 | 0.255 | 2.50 | 4.17 |
| 5E | 0.111 | 0.121 | 0.298 | 2.33 | 4.56 |
| 5(5) | 0.161 | 0.131 | 0.254 | 2.18 | 4.21 |
| 6D | 0.131 | 0.142 | 0.284 | 1.94 | 4.10 |
| 6F | 0.113 | 0.095 | 0.252 | 2.57 | 4.34 |
| 7C | 0.134 | 0.108 | 0.204 | 2.23 | 4.83 |
| N03 | 0.123 | 0.128 | 0.185 | 2.21 | 5.37 |
| HEX-1 | 0.234 | 0.149 | 0.336 | 1.72 | 3.55 |

| Station | Pyro/Petro PAH | Retene+ Perylene /TPAH | LALK/ TALK | Pristane/ Phytane | CPI |
|---|---|---|---|---|---|
| L250-5 | 0.198 | 0.145 | 0.331 | 1.62 | 3.41 |
| L250-5-DUP | 0.200 | 0.143 | 0.312 | 1.55 | 3.49 |
| HEX-12 | 0.198 | 0.139 | 0.333 | 1.78 | 3.60 |
| HEX-17 | 0.202 | 0.135 | 0.268 | 1.50 | 3.94 |
| HH1-5 | 0.184 | 0.136 | 0.315 | 1.75 | 3.82 |
| S-XA | 0.194 | 0.137 | 0.338 | 1.94 | 3.70 |
| T-3 | 0.191 | 0.125 | 0.360 | 1.87 | 3.10 |
| T-XA | 0.201 | 0.138 | 0.357 | 1.52 | 3.23 |
| M-4 | 0.177 | 0.099 | 0.365 | 1.79 | 2.99 |
| ***Sediment Core - 2014*** | | | | | |
| 1.2 (0-2 cm) | 0.133 | 0.121 | 0.213 | 2.02 | 5.39 |
| 1.2 (2-4 cm) | 0.133 | 0.119 | 0.220 | 1.89 | 5.26 |
| 1.2 (4-6 cm) | 0.133 | 0.121 | 0.212 | 1.82 | 5.29 |
| 1.2 (6-8 cm) | 0.137 | 0.123 | 0.210 | 1.64 | 5.16 |
| 1.2 (8-10 cm) | 0.136 | 0.122 | 0.214 | 1.86 | 5.27 |
| 1.2 (10-12 cm) | 0.136 | 0.123 | 0.212 | 1.40 | 4.95 |
| 1.2 (12-14 cm) | 0.138 | 0.125 | 0.212 | 1.90 | 5.11 |
| 1.2 (20-22 cm) | 0.136 | 0.125 | 0.203 | 1.82 | 5.15 |
| 1.2 (40-42 cm) | 0.147 | 0.132 | 0.213 | 2.02 | 4.93 |
| 1.2 (60-63 cm) | 0.144 | 0.131 | 0.200 | 2.02 | 4.56 |
| 1.2 (78-81 cm) | 0.140 | 0.129 | 0.207 | 2.10 | 4.95 |
| ***Surface Sediment - 2015*** | | | | | |
| 70-142 | 0.176 | 0.085 | 0.439 | 1.70 | 2.50 |
| 70-143 | 0.182 | 0.115 | 0.375 | 1.54 | 3.07 |
| 70-145 | 0.174 | 0.098 | 0.386 | 2.03 | 2.92 |
| 71-145 | 0.166 | 0.093 | 0.392 | 1.68 | 2.88 |
| 71-146 | 0.139 | 0.087 | 0.376 | 1.83 | 3.40 |
| 71-147 | 0.149 | 0.093 | 0.367 | 2.03 | 3.58 |
| 71-147A | 0.148 | 0.098 | 0.332 | 1.68 | 3.54 |
| 71-149 | 0.134 | 0.094 | 0.402 | 2.48 | 3.27 |
| 71-150 | 0.200 | 0.104 | 0.366 | 2.14 | 3.46 |
| 149-200 | 0.138 | 0.101 | 0.296 | 2.09 | 4.33 |
| 149-350 | 0.135 | 0.103 | 0.276 | 2.16 | 4.82 |
| 3A | 0.148 | 0.147 | 0.183 | 1.66 | 7.01 |
| 4A | 0.135 | 0.085 | 0.252 | 2.00 | 6.10 |
| 4B | 0.140 | 0.130 | 0.252 | 1.63 | 5.52 |
| 5A | 0.148 | 0.135 | 0.202 | 1.86 | 6.00 |
| BP01 | 0.146 | 0.129 | 0.226 | 1.83 | 6.03 |
| L08 | 0.127 | 0.146 | 0.169 | 2.00 | 7.88 |

| Station | Pyro/Petro PAH | Retene+ Perylene /TPAH | LALK/ TALK | Pristane/ Phytane | CPI |
|---|---|---|---|---|---|
| N03 | 0.147 | 0.126 | 0.217 | 1.88 | 6.12 |
| N06 | 0.142 | 0.134 | 0.190 | 1.95 | 6.36 |
| 143W-1 | 0.220 | 0.130 | 0.335 | 1.37 | 3.21 |
| 143W-2 | 0.194 | 0.092 | 0.400 | 1.57 | 2.83 |
| 143W-4 | 0.164 | 0.089 | 0.394 | 1.58 | 3.06 |
| 143W-5 | 0.145 | 0.085 | 0.410 | 1.65 | 2.97 |
| 143-W6 | 0.155 | 0.076 | 0.432 | 1.59 | 2.51 |
| 152W0 | 0.145 | 0.127 | 0.229 | 1.94 | 5.63 |
| 152W1 | 0.142 | 0.099 | 0.312 | 2.21 | 4.36 |
| ***River Peat*** | | | | | |
| Kuparuk River | 0.232 | 0.327 | 0.044 | 1.58 | 8.67 |
| Sagavanirktok River | 0.133 | 0.191 | 0.228 | 1.93 | 5.92 |
| ***Crude Oil*** | | | | | |
| Alaska North Slope Oil | 0.007 | 0.001 | 0.710 | 1.64 | 0.86 |
| Alaska North Slope Oil | 0.008 | 0.002 | 0.709 | 1.74 | 0.82 |
| Alaska North Slope Oil | 0.007 | 0.003 | 0.713 | 1.52 | 0.80 |
| Alaska North Slope Oil | 0.008 | 0.002 | 0.713 | 1.45 | 0.82 |
| Northstar Oil | 0.006 | 0.000 | 0.799 | 1.77 | 0.93 |
| Northstar Oil | 0.007 | 0.000 | 0.803 | 1.78 | 0.91 |
| Northstar Oil | 0.007 | 0.002 | 0.802 | 1.67 | 0.88 |
| Northstar Oil | 0.006 | 0.000 | 0.805 | 1.68 | 0.87 |

**Table A-10. Equilibrium partitioning sediment benchmarks (ESB), derived as the sum of the equilibrium partitioning sediment benchmark toxic units (∑ESBTUFCV) based on surface sediment PAH concentrations, for samples collected in 2014 and 2015 in ANIMIDA III.**

| 2014 | |
|---|---|
| **Station** | **$\sum ESBTU_{FCV}$** |
| 1 | 0.080 |
| 1.05 | 0.138 |
| 1.2 | 0.095 |
| 4 | 0.011 |
| 5 | 0.046 |
| 6 | 0.104 |
| 6.1 | 0.112 |
| 7 | 0.097 |
| 8 | 0.075 |
| 9 | 0.116 |
| 9-DUP | 0.098 |
| 9A | 0.154 |
| 10 | 0.048 |
| 11 | 0.069 |
| 11A | 0.092 |
| 12 | 0.129 |
| 15 | 0.040 |
| 16 | 0.058 |
| 18 | 0.061 |
| 20 | 0.069 |
| 21 | 0.043 |
| 22 | 0.045 |
| 23 | 0.090 |
| 24 | 0.064 |
| 25 | 0.076 |
| 1B | 0.012 |
| 1C | 0.064 |
| 2C | 0.045 |
| 5B | 0.004 |
| 5E | 0.016 |
| 5(5) | 0.020 |
| 6D | 0.040 |
| 6F | 0.011 |
| 7C | 0.106 |
| N03 | 0.032 |
| HEX-1 | 0.050 |

| 2015 | |
|---|---|
| **Station** | **$\sum ESBTU_{FCV}$** |
| 70-142 | 0.078 |
| 70-143 | 0.094 |
| 70-145 | 0.038 |
| 71-145 | 0.100 |
| 71-146 | 0.146 |
| 71-147 | 0.070 |
| 71-147A | 0.156 |
| 71-149 | 0.065 |
| 71-150 | 0.041 |
| 149-200 | 0.127 |
| 149-350 | 0.138 |
| 3A | 0.024 |
| 4A | 0.049 |
| 4B | 0.019 |
| 5A | 0.035 |
| BP01 | 0.038 |
| L08 | 0.037 |
| N03 | 0.028 |
| N06 | 0.045 |
| 143W-1 | 0.077 |
| 143W-2 | 0.050 |
| 143W-4 | 0.132 |
| 143W-5 | 0.141 |
| 143-W6 | 0.161 |
| 152W0 | 0.115 |
| 152W1 | 0.150 |
| | |
| | |
| | |
| | |
| | |
| | |
| | |
| | |
| | |

| 2014 | |
|---|---|
| **Station** | **$\sum$ESBTU$_{FCV}$** |
| L250-5 | 0.059 |
| L250-5-DUP | 0.081 |
| HEX-12 | 0.070 |
| HEX-17 | 0.055 |
| HH1-5 | 0.061 |
| S-XA | 0.055 |
| T-3 | 0.052 |
| T-XA | 0.052 |
| M-4 | 0.038 |
| | |
| Mean | 0.065 |
| STD | 0.035 |
| Min | 0.004 |
| Max | 0.154 |

| 2015 | |
|---|---|
| **Station** | **$\sum$ESBTU$_{FCV}$** |
| | |
| | |
| | |
| | |
| | |
| | |
| | |
| | |
| | |
| | |
| | 0.083 |
| | 0.048 |
| | 0.019 |
| | 0.161 |

**Table A-11. Biological Tissue Hydrocarbon Concentrations ANIMIDA III 2014**

**(PAH in ng/g d. wt. and SHC in ug/g, d. wt.)**

| Station | Matrix/Animal | Total PAH | Sum SHC (C9-C40) | SHC Total (C9-C40) | % Lipid |
|---|---|---|---|---|---|
| 1.05 | Amphipod | 12.4 | 34.4 | 53.0 | 5.75 |
| 5 | Amphipod | 23.1 | 4.02 | 199 | 4.90 |
| 6 | Amphipod | 16.1 | 74.7 | 107 | 5.95 |
| 7 | Amphipod | 25.8 | 87.4 | 118 | 7.34 |
| 8 | Amphipod | 23.1 | 80.5 | 151 | 4.46 |
| 10 | Amphipod | 21.4 | 127 | 179 | 4.63 |
| 12 | Amphipod | 24.4 | 40.4 | 44.1 | 3.96 |
| 15 | Amphipod | 19.0 | 26.3 | 25.6 | 5.16 |
| 16 | Amphipod | 20.5 | 20.4 | 17.2 | 3.72 |
| 20 | Amphipod | 21.3 | 25.4 | 27.9 | 6.52 |
| 21 | Amphipod | 15.4 | 29.7 | 31.6 | 5.89 |
| 22 | Amphipod | 25.9 | 59.4 | 80.8 | 7.05 |
| 24 | Amphipod | 26.4 | 38.3 | 40.2 | 5.77 |
| 23 | Amphipod | 24.3 | 44.2 | 51.6 | 5.65 |
| 25 | Amphipod | 19.5 | 44.4 | 52.0 | 3.91 |
| 5B | Amphipod | 103 | 296 | 489 | 7.99 |
| 5(5) | Amphipod | 41.1 | 62.9 | 64.2 | 2.69 |
| 6D | Amphipod | 30.9 | 108 | 133 | 6.07 |
| 7C | Amphipod | 17.2 | 31.2 | 35.5 | 5.19 |
| N03 | Amphipod | 109 | 33.5 | 30.3 | 4.50 |
| T-3 | Amphipod | 28.8 | 42.1 | 54.6 | 7.71 |
| T-3 | Amphipod | 20.8 | 32.3 | 34.3 | 5.36 |
| 7 | Clam (*Astarte sp.)* | 117 | 1.95 | 6.35 | 2.58 |
| 20 | Clam (*Astarte sp.)* | 58.7 | 2.83 | 0.70 | 2.78 |
| 22 | Clam (*Astarte sp.)* | 55.6 | 1.70 | 236 | 2.32 |
| 23 | Clam (*Astarte sp.)* | 62.3 | 1.74 | 268 | 1.83 |
| 25 | Clam (*Astarte sp.)* | 66.3 | 1.13 | 295 | 2.73 |
| 6D | Clam (*Astarte sp.)* | 366 | 3.59 | 2,370 | 3.50 |
| N03 | Clam (*Astarte sp.)* | 1,930 | 12.9 | 13,200 | 4.00 |
| 1.05 | Arctic Cod | 106 | 5.32 | 571 | 1.51 |
| 5 | Arctic Cod | 63.9 | 7.94 | 604 | 2.00 |
| 6 | Arctic Cod | 102 | 221 | 293 | 4.80 |
| 9 | Arctic Cod | 67.1 | 45.3 | 55.1 | 3.75 |
| 12 | Arctic Cod | 131 | 98.6 | 115 | 3.98 |
| 15 | Arctic Cod | 108 | 142 | 167 | 4.63 |
| 20 | Arctic Cod | 104 | 27.2 | 15.1 | 4.31 |
| 5(5) | Arctic Cod | 93.1 | 314 | 442 | 4.47 |
| 6D | Arctic Cod | 112 | 2.68 | 906 | 2.88 |

| Station | Matrix/Animal | Total PAH | Sum SHC (C9-C40) | SHC Total (C9-C40) | % Lipid |
|---|---|---|---|---|---|
| 7C | Arctic Cod | 73.6 | 1.93 | 848 | 2.71 |
| T-3 | Arctic Cod | 76.1 | 15.2 | 7.01 | 2.34 |
| | | | | | |
| | Mean - amphipod | 30.4 | 61.0 | 91.8 | 5.46 |
| | Mean - clam | 380 | 3.69 | 2,340 | 2.82 |
| | Mean - Arctic cod | 94.3 | 80.1 | 366 | 3.40 |

**Table A-12. Biological Tissue Hydrocarbon Concentrations ANIMIDA III 2015**

**(PAH in ng/g d. wt. and SHC in ug/g, d. wt.)**

| Station | Matrix/Animal | Total PAH | Sum SHC (C9-C40) | SHC Total (C9-C40) | % Lipid |
|---|---|---|---|---|---|
| 143W-1 | Amphipod | 23.7 | 22.4 | 87.5 | 5.17 |
| 152W0 | Amphipod | 25.8 | 164 | 208 | 7.03 |
| 152W1 | Amphipod | 30.7 | 61.5 | 114 | 5.76 |
| 70-143 | Amphipod | 20.4 | 20.5 | 188 | 4.60 |
| 70-145 | Amphipod | 22.1 | 16.3 | 140 | 4.64 |
| 70-145 | Amphipod | 23.5 | 15.5 | 160 | 4.69 |
| 71-149 | Amphipod | 29.4 | 33.5 | 72.9 | 3.91 |
| 143W-1 | Clam (*Astarte borealis*) | 32.5 | 1.99 | 13.9 | 1.39 |
| 152W1 | Clam (*Astarte borealis*) | 69.1 | 2.92 | 17.2 | 0.78 |
| 3A | Clam (*Astarte borealis*) | 19.5 | 1.32 | 8.32 | 0.91 |
| 3A | Clam (*Astarte borealis*) | 45.1 | 1.32 | 8.58 | 0.87 |
| 143W-1 | Clam (*Astarte crenata*) | 17.2 | 2.64 | 19.2 | 2.09 |
| 70-142 | Clam (*Astarte crenata*) | 68.9 | 6.10 | 49.1 | 1.04 |
| 71-145 | Clam (*Astarte crenata*) | 30.0 | 2.67 | 24.4 | 0.87 |
| 71-147 | Clam (*Astarte crenata*) | 69.9 | 2.60 | 21.6 | 0.66 |
| 143W-4 | Arctic Cod | 37.0 | 708 | 453 | 5.49 |
| 143W-5 | Arctic Cod | 21.1 | 18.9 | 83.6 | 4.06 |
| 149-200 | Arctic Cod | 33.6 | 1,660 | 1,170 | 5.47 |
| 70-145 | Arctic Cod | 11.3 | 393 | 286 | 4.42 |
| 71-146 | Arctic Cod | 21.0 | 15.6 | 93.6 | 6.85 |
| 71-147 | Arctic Cod | 19.5 | 3,080 | 1,720 | 6.70 |
| | | | | | |
| | Mean - amphipod | 25.1 | 47.6 | 139 | 5.11 |
| | Mean - clam | 44.0 | 2.70 | 20.3 | 1.08 |
| | Mean - Arctic cod | 23.9 | 978 | 634 | 5.50 |

**Table A-13. Critical body residue (CBR) concentrations, based on PAH, in the Amphipods, Clams, and Arctic Cod collected in 2014 and 2015 in ANIMIDA III (mM/kg wet weight).**

| 2014 | | | 2015 | | |
|---|---|---|---|---|---|
| **Station** | **Matrix/Animal** | **CBR (mM/kg wet wt)** | **Station** | **Matrix/Animal** | **CBR (mM/kg wet wt)** |
| 1.05 | Amphipod | 0.0175 | 143W-1 | Amphipod | 0.0363 |
| 5 | Amphipod | 0.0341 | 152W0 | Amphipod | 0.0448 |
| 6 | Amphipod | 0.0250 | 152W1 | Amphipod | 0.0398 |
| 7 | Amphipod | 0.0373 | 70-143 | Amphipod | 0.0293 |
| 8 | Amphipod | 0.0351 | 70-145 | Amphipod | 0.0337 |
| 10 | Amphipod | 0.0328 | 70-145 | Amphipod | 0.0353 |
| 12 | Amphipod | 0.0320 | 71-149 | Amphipod | 0.0368 |
| 15 | Amphipod | 0.0289 | | | |
| 16 | Amphipod | 0.0288 | | | |
| 20 | Amphipod | 0.0329 | | | |
| 21 | Amphipod | 0.0244 | | | |
| 22 | Amphipod | 0.0371 | | | |
| 24 | Amphipod | 0.0333 | | | |
| 23 | Amphipod | 0.0373 | | | |
| 25 | Amphipod | 0.0319 | | | |
| 5B | Amphipod | 0.134 | | | |
| 5(5) | Amphipod | 0.0477 | | | |
| 6D | Amphipod | 0.0482 | | | |
| 7C | Amphipod | 0.0276 | | | |
| N03 | Amphipod | 0.145 | | | |
| T-3 | Amphipod | 0.0441 | | | |
| T-3 | Amphipod | 0.0311 | | | |
| | | | | | |
| 7 | Clam (*Astarte sp.)* | 0.131 | 143W-1 | Clam (*A. borealis*) | 0.0312 |
| 20 | Clam (*Astarte sp.)* | 0.0666 | 152W1 | Clam (*A. borealis*) | 0.0462 |
| 22 | Clam (*Astarte sp.)* | 0.0639 | 3A | Clam (*A. borealis*) | 0.0156 |
| 23 | Clam (*Astarte sp.)* | 0.0649 | 3A | Clam (*A. borealis*) | 0.0345 |
| 25 | Clam (*Astarte sp.)* | 0.0840 | 143W-1 | Clam (*A. crenata*) | 0.0206 |
| 6D | Clam (*Astarte sp.)* | 0.441 | 70-142 | Clam (*A. crenata*) | 0.0493 |
| N03 | Clam (*Astarte sp.)* | 2.63 | 71-145 | Clam (*A. crenata*) | 0.0201 |
| | | | 71-147 | Clam (*A. crenata*) | 0.0341 |
| | | | | | |
| 1.05 | Arctic Cod | 0.127 | 143W-4 | Arctic Cod | 0.0484 |
| 5 | Arctic Cod | 0.0825 | 143W-5 | Arctic Cod | 0.0253 |
| 6 | Arctic Cod | 0.134 | 149-200 | Arctic Cod | 0.0426 |
| 9 | Arctic Cod | 0.0789 | 70-145 | Arctic Cod | 0.0165 |
| 12 | Arctic Cod | 0.172 | 71-146 | Arctic Cod | 0.0296 |

| 2014 | | | 2015 | | |
|---|---|---|---|---|---|
| **Station** | **Matrix/Animal** | **CBR (mM/kg wet wt)** | **Station** | **Matrix/Animal** | **CBR (mM/kg wet wt)** |
| 15 | Arctic Cod | 0.141 | 71-147 | Arctic Cod | 0.0259 |
| 20 | Arctic Cod | 0.139 | | | |
| 5(5) | Arctic Cod | 0.119 | | | |
| 6D | Arctic Cod | 0.141 | | | |
| 7C | Arctic Cod | 0.0957 | | | |
| T-3 | Arctic Cod | 0.100 | | | |

| | ***Amphipods*** | ***Clams*** | ***Arctic cod*** |
|---|---|---|---|
| Mean | 0.0414 | 0.249 | 0.0893 |
| STD | 0.0280 | 0.667 | 0.0501 |
| Min | 0.0175 | 0.0156 | 0.0165 |
| Max | 0.145 | 2.63 | 0.172 |

# APPENDIX B: Benthic Infauna, Carbon Resources, and Trophic Structure on the Coast and Shelf of the Beaufort Sea, Alaska

**Appendix Table 1: Lots of close to 60 species collected during the ANIMIDA 2014 cruise and archived at the Smithsonian Institutions in Washington, DC.**

| Genus | Species | Subspecies | Phylum | Voucher # | Station |
|---|---|---|---|---|---|
| *Brada* | *villosa* | | Annelida | V131 | AN14-20 |
| *Acanthostepheia* | *beringiensis* | | Arthropoda | V281 | AN14-6F |
| *Atylus* | *smitti* | | Arthropoda | V228 | AN14-16 |
| *Diastylis* | *goodsiri* | | Arthropoda | V144 | AN14-21 |
| *Diastylis* | *scorpioides* | | Arthropoda | V145 | AN14-21 |
| *Diastylis* | *spinulosa* | | Arthropoda | V178 | AN14-24 |
| *Diastylis* | *alaskensis* | | Arthropoda | V361 | AN14-1 |
| *Eualus* | *gaimardii* | *gaimardii* | Arthropoda | V16, V38 | AN14-6D, AN14-7 |
| *Eualus* | *gaimardii* | *belcheri* | Arthropoda | V17, V37 | AN14-6D, AN14-7 |
| *Gammeracanthus* | *loricatus* | | Arthropoda | V287 | AN14-6F |
| *Lembos* | *arcticus* | | Arthropoda | V149, V254 | AN14-21, AN14-12 |
| *Melita* | *quadrispinosa* | | Arthropoda | V90 | AN14-5(5) |
| *Onisimus* | c.f. *derjugini* | | Arthropoda | V311 | AN14-5 |
| *Pagurus* | *trigonocheirus* | | Arthropoda | V132, V165 | AN14-20, AN14-22 |
| *Pagurus* | *capillatus* | | Arthropoda | V166 | AN14-22 |
| *Paroediceros* | *lynceus* | | Arthropoda | V55 | AN14-7 |
| *Rhachotropis* | *aculeata* | | Arthropoda | V148 | AN14-21 |
| *Sabinea* | *septemcarinata* | | Arthropoda | V3, V42(use) | AN14-6D, AN14-7 |
| *Saduria* | *sabini* | | Arthropoda | V1 | AN14-6D |
| *Saduria* | *entomon* | | Arthropoda | V2, V21 | AN14-6D |
| *Stegocephalus* | *ampulla* | | Arthropoda | V147 | AN14-21 |
| *Synidotea* | *bicuspida* | | Arthropoda | V12 | AN14-6D |
| *Alcyonidium* | *disciforme* | | Bryozoa | V7, V46 | AN14-6D, AN14-7 |
| *Alcyonidium* | *gelatinosum* | *andersoni* | Bryozoa | V9, V146 | AN14-6D |
| *Eucratea* | *loricata* | | Bryozoa | V39 | AN14-7 |
| *Allantactis* | *parasitica* | | Cnidaria | V225 | AN14-16 |
| *Gersemia* | *rubiformis* | | CNIDARIA | V102, V284, V233, V354 | AN14-5(5), AN14-25, AN14-16, AN14-1 |
| *Hormathia* | *nodosa* | | Cnidaria | V187 | AN14-23 |
| *Leptasterias* | *arctica* | | Echinodermata | V119 | AN14-T3 |

| | | | | |
|---|---|---|---|---|
| *Leptasterias* | *groenlandica* | Echinodermata | V239 | AN14-15 |
| *Myriotrochus* | *rinkii* | Echinodermata | V4, V53(use) | AN14-6D, AN14-7 |
| *Ocnus* | *glacialis* | Echinodermata | V182 | AN14-24 |
| *Ophiocten* | *sericeum* | Echinodermata | V13, V36 | AN14-6D, AN14-7 |
| *Ophiura* | *sarsii* | Echinodermata | V312 | AN14-6 |
| *Psolus* | *peronii* | Echinodermata | V122 | AN14-T3 |
| *Pteraster* | *obscurus* | Echinodermata | V121 | AN14-T3 |
| *Pteraster* | *jordani* | Echinodermata | V349 | AN14-1 |
| *Rhegaster* | *tumidus* | Echinodermata | V224 | AN14-16 |
| *Stegophiura* | *nodosa* | Echinodermata | V313 | AN14-6 |
| *Urasterias* | *linckii* | Echinodermata | V211 | AN14-16 |
| *Admete* | *solida* | Mollusca | V217 | AN14-16 |
| *Amicula* | *vestita* | Mollusca | V355 | AN14-1 |
| *Astarte* | *montagui* | Mollusca | V64 | AN14-7 |
| *Astarte* | *borealis* | Mollusca | V45 | AN14-7 |
| *Buccinum* | *angulosum* | Mollusca | V168 | AN14-22 |
| *Buccinum* | *scalariforme* | Mollusca | V253 | AN14-12 |
| *Cylichna* | *alba* | Mollusca | V214 | AN14-16 |
| *Cylichna* | *occulta* | Mollusca | V215 | AN14-16 |
| *Margarites* | *costalis* | Mollusca | V5 | AN14-6D |
| *Onchidiopsis* | sp. | Mollusca | V127 | AN14-T3 |
| *Pandora* | *glacialis* | Mollusca | V105 | AN14-5(5) |
| *Similipecten* | *greenlandicus* | Mollusca | V6 | AN14-6D |
| *Stenosemus* | *albus* | Mollusca | V356, V369 | AN14-1, AN14-1.05 |
| *Tachyrhynchus* | *erosus* | Mollusca | V174 | AN14-22 |
| *Trichotropis* | *bicarinata* | Mollusca | V175 | AN14-22 |
| *Margarites* | *beringensis* | Mollusca | V40 | AN14-7 |
| *Polymastia* | sp. | Porifera | V180 | AN14-24 |
| *Boltemia* | *ovifera* | Urochordata | V346 | AN14-1 |